Jeffrey Meyer
Tracey E. Schefter
Editors

Radiation Therapy for Liver Tumors

Fundamentals and Clinical Practice

Springer

Radiation Therapy for Liver Tumors

Jeffrey Meyer · Tracey E. Schefter
Editors

Radiation Therapy for Liver Tumors

Fundamentals and Clinical Practice

Springer

Editors
Jeffrey Meyer, MD, MS
Department of Radiation Oncology
University of Texas Southwestern Medical Center
Dallas, TX, USA

Tracey E. Schefter, MD
Department of Radiation Oncology
University of Colorado Comprehensive Cancer Center
Aurora, CO, USA

ISBN 978-3-319-54530-1 ISBN 978-3-319-54531-8 (eBook)
DOI 10.1007/978-3-319-54531-8

Library of Congress Control Number: 2017936465

Printed on acid-free paper

This Springer imprint is published by Springer Nature
The registered company is Springer International Publishing AG
The registered company address is: Gewerbestrasse 11, 6330 Cham, Switzerland

Foreword

A first-year resident in radiation oncology who opens up *Radiation Therapy for Liver Tumors* might reasonably assume that as with any textbook, the knowledge contained therein is long-established received wisdom, passed down for generations, just some old stuff we need to know. He or she would be mistaken.

As recently as one generation ago, let us say in the mid-1990s, a comprehensive summary of the full spectrum of noninvasive methods for treating primary and metastatic liver tumors might have required a few paragraphs nested within a chapter covering a grab bag of miscellaneous topics that did not fit in the main chapters. Even just a decade ago, in one major text, the entire world of radiation for liver and hepatobiliary tumors was addressed in a single 17-page chapter, and even that was probably generous treatment [1]. But here we are now, in 2017, and a full textbook can barely contain the burgeoning wealth of information presently available in this area and steadily growing.

Drs. Schefter, Meyer, and colleagues are to be congratulated for assembling a large team of experts representing the many specialists who are, ideally, involved in the management of hepatic malignancies. The writing is clear and offers thorough coverage of radiobiological and clinical data that inform our modern practice. It takes a village to care for a single cancer patient nowadays, with so much nuance and sophistication involved in all of the diagnostic and therapeutic modalities at our disposal, and the value of multidisciplinary input cannot be overstated.

That same neophyte resident who might not know how much recent progress has been made in the area of radiotherapy for liver tumors may be forgiven, of course, for assuming it took maybe a half century for so much basic and translational science to develop, rather than maybe a decade and a little bit more. The only unforgivable act on his or her part, or for that matter on the part of any practicing radiation oncologist, would be to ignore the important information contained within the pages. There are now safe and effective ways of using radiotherapy in a variety of forms to offer patients

with liver malignancies extended disease-free survivorship with high quality of life, a distinct advance of high value to patients. And so my advice to the new resident or practicing radiation oncologist who has not yet had a chance to absorb this knowledge is simple: just read this book ☺.

Brian D. Kavanagh MD, MPH
University of Colorado, Denver, USA

Reference

1. E. Halperin et al. (eds.), *Perez and Brady's Principles and Practice of Radiation Oncology*, Chapter 57, 5th edn. (Lippincott Williams & Wilkins, 2007)

Preface

The application of radiation therapy in the treatment of liver neoplasms presents multiple challenges. Treatment technique and dose prescription, the risk of normal tissue injury, and motion management represent some of the challenges for the radiation oncologist. Equally important, however, is patient selection within the context of the multidisciplinary approach. Appropriate treatment of liver tumors typically involves a true nexus of interactions amongst hepatologists, medical, surgical, and radiation oncologists, transplant surgeons, and diagnostic and interventional radiologists.

The purpose of this book is to address the details of radiation therapy for primary and secondary tumors of the liver as well as issues related to multidisciplinary management and the various treatment options offered by other specialties. To that end, in addition to chapters describing the details of radiation treatment planning, from external beam to brachytherapy, from photons to particles, there are also chapters written by expert surgeons, hepatologists, and radiologists. This approach is intended to familiarize the practitioner with the unique aspects of liver irradiation and also create a common understanding and language for fruitful interactions between the radiation oncologist and other specialists. The contents of this book reflect the multidisciplinary interactions seen at a liver tumor board.

A special emphasis of this book is the "how-to" or "nuts-and-bolts" aspects of radiation treatment for liver tumors. The goal is not only to provide information for the practitioner on the evidence that broadly drives our practice, but also to discuss practical details that arise in the day-to-day management. Finally, the authors also address the shortcomings of our present-day knowledge and look forward to future directions.

Treatment of liver tumors is a complex and dynamic area of oncology, and radiation therapy is playing an increasingly prominent role. Radiation oncologists can play an important role in the multidisciplinary care of liver cancer patients and also expand the frontiers of liver tumor management, and this book is intended as a foundational guide.

Dallas, TX, USA — Jeffrey Meyer
Aurora, CO, USA — Tracey E. Schefter

Note Regarding Radiation Dose Constraints

One of the most important practical considerations in radiation treatment planning for liver malignancies or other types of tumors is sparing of normal tissues. To this point, various guidelines are in place to aid the radiation oncologist, medical dosimetrist, and physicist. The renowned paper by Emami et al. published in 1991 compiled available information, including clinician experience, regarding dose–volume relationships for various normal tissue injuries [1]. The Quantitative Analyses of Normal Tissue Effects in the Clinic (QUANTEC) effort, published in 2010, reported on and analyzed updated available literature on normal tissue toxicities and gave recommendations to physicians and the team of planners [2].

There are three tables in this textbook reporting on radiation dose constraints (Tables 4.2, 9.1 and 12.2), and further discussion of constraints in these and other chapters. Pathophysiology of radiation-induced injury to the normal liver is discussed in the text as well. In addition to information culled from the liver-specific QUANTEC paper, planning constraints from ongoing cooperative group trials, as well as institutional preferences, are presented [3]. *With specific respect to the liver*, the reader will see that both mean dose constraints as well as critical volume-based constraints, different conceptualizations of normal tissue sparing, are reported.

We emphasize to the reader that much remains to be known about normal tissue injury, and that the available dose–volume constraints, although grounded in clinical data and rational consideration, are incomplete, and thus, dose constraints should be used judiciously in the clinic. It should be noted that the dose constraints are largely derived from data that are not personalized for individual patients but rather across a population of patients. Patient-specific considerations will likely be further integrated in planning constraints in the future.

References

1. B. Emami, J. Lyman, A. Brown et al., Tolerance of normal tissue to therapeutic irradiation. Int. J. Radiat. Oncol. Biol. Phys. **21**, 109–122 (1991)
2. L.B. Marks, R.K. Ten Haken, M.K. Martel, Guest editor's introduction to QUANTEC: a users guide. Int. J. Radiat. Oncol. Biol. Phys. **76**(3 Suppl), S1–2 (2010)
3. C.C. Pan, B.D. Kavanagh, L.A. Dawson et al., Radiation-associated liver injury. Int. J. Radiat. Oncol. Biol. Phys. **76**(3 Suppl), S94–100 (2010)

Contents

Contributors

Sarah Berhane, PhD Department of Molecular and Clinical Cancer Medicine, University of Liverpool, Liverpool, UK

Scott W. Biggins, MD, MAS Division of Gastroenterology and Hepatology, University of Washington, Seattle, WA, USA

Daniel T. Chang, MD Department of Radiation Oncology, Stanford Healthcare, Stanford, CA, USA

Michael A. Choti, MD Department of Surgery, University of Texas Southwestern Medical Center, Dallas, TX, USA

Kyle Cuneo, MD Department of Radiation Oncology, University of Michigan Health System, Ann Arbor, MI, USA

Barish H. Edil, MD Department of Surgery, University of Colorado Hospital, Aurora, CO, USA

Issam El Naqa, MA, MS, PhD, DABR Department of Radiation Oncology, University of Michigan Health System, Ann Arbor, MI, USA

Michael R. Folkert, MD, PhD Department of Radiation Oncology, Southwestern Medical Center, The University of Texas, Dallas, TX, USA

Ana Luiza Mandelli Gleisner, MD, PhD Department of Surgery, University of Colorado, Aurora, CO, USA

Karyn A. Goodman, MD, MS Radiation Oncology, University of Colorado Cancer Center, Aurora, CO, USA

Purva Gopal, MD, MS Department of Pathology, UT Southwestern Medical Center, Dallas, TX, USA

Ali A. Haydar, MD, MRCP, FRCR Department of Radiology, American University of Beirut Medical Centre, Beirut, Lebanon

Sarah E. Hoffe, MD Department of Radiation Oncology, Moffitt Cancer Center, Tampa, FL, USA

Theodore S. Hong, MD Department of Radiation Oncology, Massachusetts General Hospital, Boston, MA, USA

Brian Hrycushko, PhD Department of Radiation Oncology, Southwestern Medical Center, The University of Texas, Dallas, TX, USA

Hero K. Hussain, MD, FRCR, FACR Department of Radiology, University of Michigan Health System, Ann Arbor, MI, USA

Morten Høyer, MD, PhD Danish Center for Particle Therapy, Aarhus University Hospital, Aarhus N, Denmark

D. Thor Johnson, MD, PhD Department of Radiology, University of Colorado Denver, Centennial, CO, USA

Philip J. Johnson, MD, FRCP Department of Molecular and Clinical Cancer Medicine, University of Liverpool, Liverpool, UK

Avash Kalra, MD Department of Gastroenterology and Hepatology, University of Colorado, Denver, CO, USA

Jeffrey B. Kaplan, MD Department of Pathology, University of Colorado, Aurora, CO, USA

Florence K. Keane, MD Department of Radiation Oncology, Massachusetts General Hospital, Boston, MA, USA

Adam Leon Kesner, PhD Department of Radiology, University of Colorado, Aurora, CO, USA

Harun Khan, MBBS School of Medicine, Imperial College, London, UK

Ankaj Khosla, MD Department of Radiology, UT Southwestern, Dallas, TX, USA

Matthew Knecht, MD Department of Radiation Medicine, Loma Linda University Health, Loma Linda, CA, USA

Julie L. Koenig, BS Stanford University School of Medicine, Stanford, CA, USA

Albert C. Koong, MD, PhD Radiation Oncology, Stanford University, Stanford, CA, USA

Theodore S. Lawrence, MD, PhD Department of Radiation Oncology, University of Michigan Health System, Ann Arbor, MI, USA

S. Lindsey Davis, MD Division of Medical Oncology, Department of Medicine, University of Colorado Anschutz Medical Campus, Aurora, CO, USA

Cheryl Meguid, DNP Department of Surgical Oncology, University of Colorado Hospital, Aurora, CO, USA

Eric A. Mellon, MD, PhD Department of Radiation Oncology, University of Miami Miller School of Medicine Sylvester Comprehensive Cancer Center, Miami, FL, USA

Keshav M. Menon, MD Department of Radiology, University of Texas Southwestern Medical Center, Dallas, TX, USA

Jeffrey Meyer, MD, MS Department of Radiation Oncology, University of Texas Southwestern Medical Center, Dallas, TX, USA

Gilbert Murimwa, MSc University of South Florida Morsani College of Medicine, Tampa, FL, USA

Layla Antoine Nasr, MD Department of Diagnostic Radiology, American University of Beirut Medical Center, Toledo, OH, USA

Dawn Owen, MD, PhD Department of Radiation Oncology, University of Michigan Health System, Ann Arbor, MI, USA

Sagar A. Patel, MD Harvard Radiation Oncology Program, Harvard Medical School, Boston, MA, USA

Erqi L. Pollom, MD Department of Radiation Oncology, Stanford Healthcare, Stanford, CA, USA

Matthew R. Porembka, MD Department of Surgery, University of Texas Southwestern Medical Center, Dallas, TX, USA

Yushen Qian, MD Department of Radiation Oncology, Stanford Healthcare, Stanford, CA, USA

M. Reza Rajebi, MD Radiology, University of Colorado, Aurora, CO, USA

Robert K. Ryu, MD, FSIR Division of Interventional Radiology, University of Colorado Anschutz Medical Campus, Aurora, CO, USA

Tracey E. Schefter, MD Department of Radiation Oncology, University of Colorado, Aurora, CO, USA

Amit G. Singal, MD, MS Department of Internal Medicine, UT Southwestern Medical Center, Dallas, TX, USA

Camille L. Stewart, MD Department of Surgery, University of Colorado School of Medicine, Aurora, CO, USA

Randall K. Ten Haken, PhD Department of Radiation Oncology, University of Michigan Health System, Ann Arbor, MI, USA

Clayton K. Trimmer, DO Department of Interventional Radiology, University of Texas Southwestern Medical Center, Dallas, TX, USA

David C. Westerly, PhD Department of Radiation Oncology, University of Colorado School of Medicine, Aurora, CO, USA

Andrew Wroe, PhD Department of Radiation Medicine, Loma Linda University Health, Loma Linda, CA, USA

Gary Y. Yang, MD Department of Radiation Medicine, Loma Linda University Health, Loma Linda, CA, USA

Adam C. Yopp, MD Department of Surgery, UT Southwestern Medical Center, Dallas, TX, USA

Abbreviations

AASLD	American Association for the Study of Liver Disease
ADC	Apparent diffusion coefficient
ALT	Alanine aminotransferase
AST	Aspartate aminotransferase
BCLC	Barcelona Clinic Liver Cancer
BED	Biological effective dose
CASH	Chemotherapy-associated steatohepatitis
CRC	Colorectal Cancer
CT	Computed tomography
CTP	Child–Turcotte–Pugh
DWI	Diffusion weighted imaging
EBRT	External beam radiotherapy
ERCP	Endoscopic retrograde cholangiopancreatography
FACT-Hep	Functional Assessment of Cancer Therapy Hepatobiliary
FDG-PET	Fluorodeoxyglucose positron-emission tomography
FFLP	Freedom from local progression
FLR	Future liver remnant
GI	Gastrointestinal
GRE	Gradient recalled echo
GTV	Gross tumor volume
HCC	Hepatocellular carcinoma
HDR	High-dose rate
iBR	Interstitial brachytherapy
ICG	Indocyanine green
IHCC	Intrahepatic cholangiocarcinoma
INR	International normalized ratio
IVC	Inferior vena cava
LI-RADS	Liver Imaging Reporting and Data System
MDCT	Multidetector computed tomography
MELD	Model for end-stage liver disease
miRNA	MicroRNA
MRCP	Magnetic resonance cholangiopancreatography
MRI	Magnetic resonance imaging
MTD	Maximum tolerated dose
NAFLD	Nonalcoholic fatty liver disease
NASH	Nonalcoholic steatohepatitis
NTCP	Normal tissue complication probability
OPTN	Organ Procurement Transplantation Network

OS	Overall survival
PFS	Progression-free survival
PMH	Princess Margaret Hospital
PVT	Portal vein thrombus
RBE	Relative biological effectiveness
REILD	TARE-induced liver disease
RES	Reticuloendothelial system
RFA	Radiofrequency ablation
RILD	Radiation-induced liver disease
RSI	Radiosensitivity index
RT	Radiotherapy
SABR	Stereotactic ablative radiation therapy
SABR	Stereotactic ablative radiotherapy
SBRT	Stereotactic body radiation therapy
SBRT	Stereotactic body radiotherapy
SIRT	Selective internal radiation therapy
SPECT	Single-photon emission computed tomography
TACE	Transarterial chemoembolization
TARE	Transarterial radioembolization
TIPS	Transjugular intrahepatic portosystemic shunt
TTP	Time to progression
UNOS	United Network for Organ Sharing
US	Ultrasound
VTR	Virtual tumor resection

Part I
Fundamentals

Liver Anatomy and Function

1

Jeffrey B. Kaplan, MD, Avash Kalra, MD
and Scott W. Biggins, MD, MAS

List of abbreviations

TIPS	Transjugular Intrahepatic Portosystemic Shunt
MELD	Model for End-Stage Liver Disease
INR	International Normalized Ratio
TACE	Transarterial chemoembolization
AST	Aspartate aminotransferase
ALT	Alanine aminotransferase
CTP	Child-Turcotte-Pugh
OPTN	Organ Procurement Transplantation Network
UNOS	United Network for Organ Sharing

1.1 Introduction

The liver is the central clearing house for most metabolic functions in the body [1]. These functions include lipid, carbohydrate, and protein metabolism; coagulation factor production; albumin production; detoxification of xenobiotics; storage of vitamins and glycogen; and bile processing and secretion. The liver is situated at the receiving end, via the portal circulation, of the intestines, which provide metabolic substrates to the liver. Blood flows out of the liver, carrying away the fruits of its metabolic labor, into the inferior vena cava. Bile flows out of the liver via the bile ducts to aid in digestion and dispose of certain waste products. The liver is for the most part composed of hepatocytes, bile ducts, and blood vessels. Diseases typically target one of these principal components. But, as this is a

J.B. Kaplan
Department of Pathology, University of Colorado, 12605 E 16th Ave, Room 3018 Mail Stop F768, 80045 Aurora, CO, USA
e-mail: Jeffrey.kaplan@ucdenver.edu

A. Kalra
Department of Gastroenterology and Hepatology, University of Colorado, 12631 E. 17th Ave. B158 Aurora, 80045 Denver, CO, USA
e-mail: Avash.kalra@ucdenver.edu

S.W. Biggins (✉)
Division of Gastroenterology and Hepatology, University of Washington, 1959 NE Pacific Street, Box 356175, 98195 Seattle, WA, USA
e-mail: bigginss@medicine.washington.edu

J. Meyer and T.E. Schefter (eds.), *Radiation Therapy for Liver Tumors*,
DOI 10.1007/978-3-319-54531-8_1

functional system, injury to one component generally affects other components of the system.

The liver has an enormous functional reserve: approximately 80–90% of the liver needs to be destroyed before its essential functions can no longer be adequately performed. Fortunately, the liver is one of the few organs with a high regenerative capacity; this is seen in the ancient Greek story of Prometheus, the giver of fire to humans, who was punished with an endless cycle of having his newly regenerated liver eaten by a bird each day.

As the liver is involved in many functions, injury to the liver disturbs these functions to various extents, leading to various signs and symptoms. Thus, when the liver fails, some of the problems include deranged nutrient metabolism, clotting defects, toxicities from detoxification abnormalities, bile processing and secretion abnormalities, and low albumin production, among others.

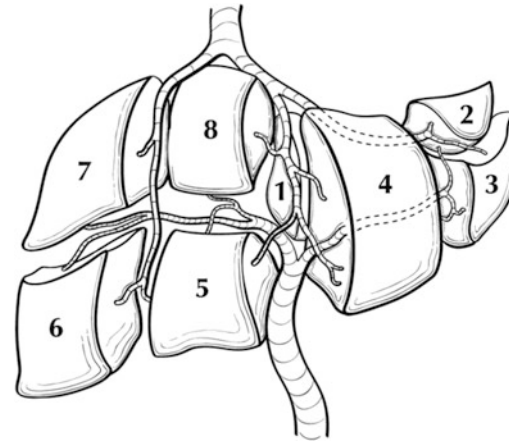

Fig. 1.1 Schematic picture of the segments of the liver. The liver can be divided into eight segments based on first and second order divisions of the hepatic artery, portal vein, and bile duct [Reprinted from Compton CC, Byrd DR, Garcia-Aguilar J, et al. Liver. In: Compton CC, Byrd DR, Garcia-Aguilar J, et al. (eds). AJCC Cancer Staging Atlas. New York, NY: Springer Science 2012: 241–249. With permission from Springer Science+ Business Media]

1.2 Normal Gross Anatomy

The liver is predominately located in the right upper portion of the abdominal cavity [2]. It normally has a smooth surface contour, is tan-brown in color, and has a weight of 1.4–1.6 kg in an adult. Some of the notable surface landmarks include: from the perspective of the anterior/superior surface, the right lobe and the smaller left lobe of the liver; and from the perspective of the posterior/inferior surface, the quadrate lobe, caudate lobe, gallbladder bed, and porta hepatis (also known as the liver hilum) [3].

Blood flows into the liver through the portal vein and hepatic artery at the porta hepatis. Blood flows out of the liver through the three major hepatic veins, the left, right, and intermediate (middle), at the superior/inferior surface. Bile flows out of the liver through the common hepatic duct at the liver hilum. Anatomic variants exist in the branching and location of blood vessels and bile ducts. The liver can be divided into eight segments based on first and second order divisions of the hepatic artery, portal vein, and bile duct (Fig. 1.1). After approximately twenty, not necessarily symmetrical, orders of branching, the portal veins, hepatic arteries, and bile ducts terminate in the hepatocellular parenchyma.

1.3 Normal Microscopic Anatomy

The liver is composed of three principal components: hepatocytes, blood vessels, and bile ducts. The microscopic anatomy is fairly basic, especially in light of the liver's plethora of functions (Figs. 1.2, 1.3 and 1.4). Hepatocytes form the bulk of the organ and are arranged in interconnecting trabeculae. Blood vessels perfuse the organ. Blood flows into the liver through ramifications of the hepatic artery and portal vein, then courses through the sinusoids in between the hepatocyte trabeculae, and finally drains into central veins which eventually merge into the hepatic veins. Bile flows out of the liver through bile canaliculi between hepatocytes. These drain into bile ducts which eventually empty into the duodenum. The hepatic artery, portal vein, and bile duct branches course through the liver together in structures called portal tracts (also known as portal triads).

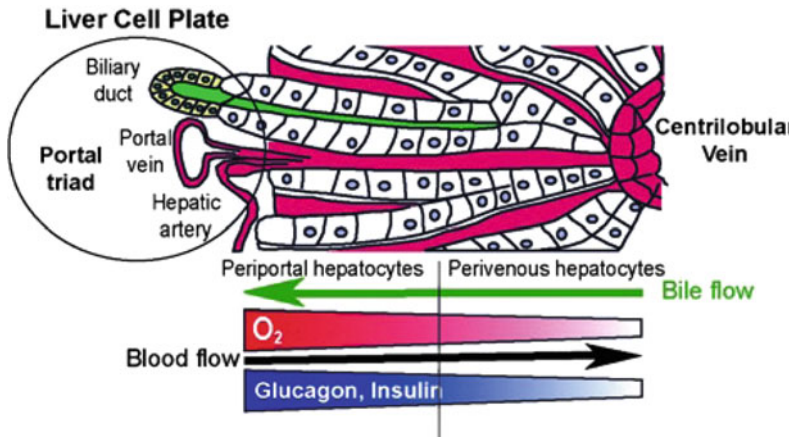

Fig. 1.2 Cartoon schematic of liver lobule. Schematic representation of a portion of a liver lobule. Hepatocytes (*white boxes*) radiate in thin trabeculae between the portal triad (*left*) and central vein (*right*). Blood (*red*) from branches of the portal vein and hepatic artery flows from the portal triad through sinusoids between hepatocellular trabeculae to the central vein. Bile (*green*) flows in bile canaliculi in the middle of hepatoceullar trabeculae from the perivenular region (*right*) to the portal triad (*left*) [Reprinted from Colnet S, Perret C. Liver Zonation. In: Monga SPS (ed). Molecular Pathology of Liver Diseases, Part I. New York, NY: Springer Science 2011: 7-16. With permission from Springer Science+Business Media]

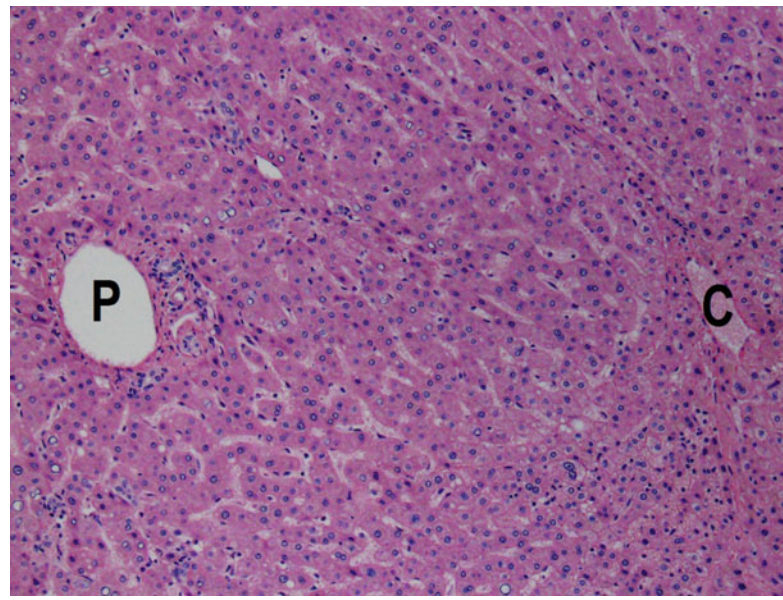

Fig. 1.3 Histologic picture of liver lobule/acinus. Histologic appearance of a liver lobule (H&E; approximately 200×). Hepatocytes form the bulk of the organ and are arranged in radiating trabeculae between the portal triad (*P*) and central vein (*C*)

The theoretical microscopic functional unit of the liver can be viewed as the hexagonal lobule or the triangular acinus. These smallest units of blood and bile flow are not rigid anatomic constructs in the actual liver but serve as a useful framework in understanding the liver in health and disease. In either conception, portal tracts are at one end and central venules are at the other end. Variations in blood flow, oxygen and nutrient tension, and hepatocellular metabolic machinery exist across the lobule or acinus. These variations are the basis for many of the microscopic topographic manifestations of liver disease.

Several specialized cells are present in the sinusoids or below the sinusoids (also known as the space of Disse). Kupffer cells are resident

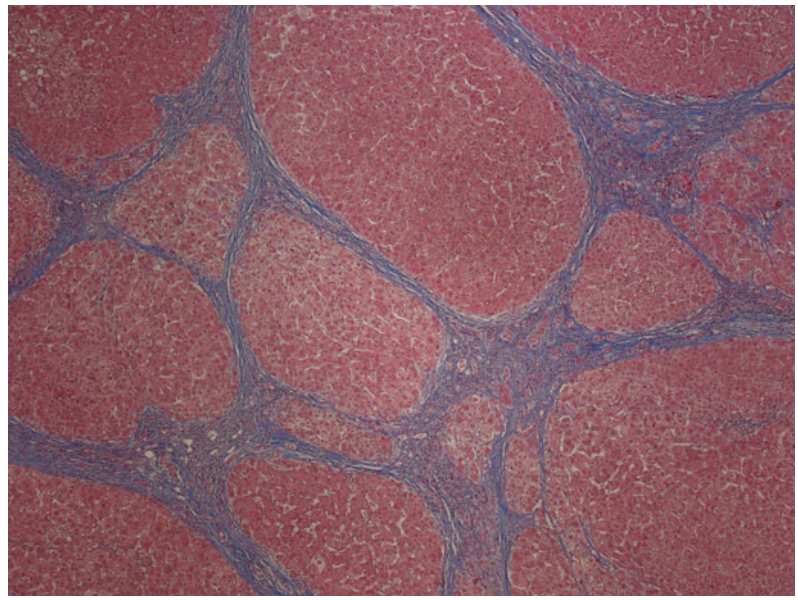

Fig. 1.4 Histologic picture of a cirrhotic liver. Histologic appearance of a cirrhotic liver (Masson's trichrome; approximately 40×). Regenerative parenchymal nodules (*red*) are demarcated by fibrous septa (*blue*) that bridge from portal tract portal tract and portal tract to central vein

macrophages within the liver and are part of the body's reticulo-endothelial system. Stellate cells (also known as Ito cells) are resident mesenchymal cells involved in storage of vitamin A and maintaining the liver's architectural framework.

1.4 Basic Physiologic Concepts

The liver has a dual blood supply: approximately 25% of the blood is supplied by the hepatic artery and approximately 75% of the blood is supplied by the portal vein. These vessels bring various materials to the liver, such as oxygen, nutrients, and toxins. Highly oxygenated blood from the hepatic artery is especially important for maintaining the integrity of the bile ducts. The dual blood supply mixes at the level of the sinusoids in the periportal region.

The sinusoids are a low-pressure system; the pressure gradient across the sinusoids is generally 0–5 mm Hg. The sinusoids are lined by fenestrated endothelium, under which lies the microvillous surface of the hepatocyte in the space of Disse. This is the principal metabolic interface of the liver. Oxygen tension, nutrient load, and toxin concentration varies across the hepatic acinus as blood flows from zone 1 (in the periportal region) to zone 3 (in the pericentral region).

The major, often interrelated, functions of the hepatocyte include nutrient metabolism, detoxification of xenobiotics, and bile processing and secretion. Not all hepatocytes perform the same functions to the same extent. The function of hepatocytes varies from region to region in the acinus due to variation in some of the hepatocyte's metabolic machinery across the hepatic acinus, typically along a portal-to-central axis.

1.5 Basic Pathologic Concepts

Injury is usually directed at one of the three principal structures comprising the liver: hepatocytes, blood vessels, or bile ducts. Because of the close anatomic and functional proximity to one another, injury to one of these compartments often leads to some degree of injury to another of the compartments. Injury to the liver covers a spectrum from minimal, subclinical injury to massive, fulminant liver failure. Liver injury can occur abruptly over a short course or it can be sustained over the long term. In general, acute injury, while it may be severe, leads to resolution in most cases. That said, in some cases the acute

injury can be so severe that it leads to liver failure. Sustained liver injury, on the other hand, is perhaps the more pernicious problem in liver disease, as this leads to liver scarring which erodes liver function and can ultimately lead to Advanced liver disease.

Liver failure is marked by several signs and symptoms. Patients are generally jaundiced from the systemic accumulation of bilirubin. Ascites and peripheral edema are the accumulation of body cavity and tissue fluid due to hypoalbuminemia. Fetor hepaticus is a musty odor that results from sulfur-containing substances entering the systemic circulation. Estrogen metabolism is disrupted and results in physical examination findings such as spider angiomata, palmar erythema, and hypogonadism and gynecomastia in men. A coagulopathy results from the lack of production and secretion of coagulation factors. Hepatic encephalopathy, characterized by a spectrum of disturbances in consciousness, is partly caused by hyperammonemia that results from liver failure. Hepatorenal syndrome is renal failure in the setting of liver failure due to a number of vascular perfusion abnormalities.

As previously discussed, the liver has a high functional reserve in that about 80–90% of the functional capacity of the liver needs to be eroded before liver failure ensues. There are three basic morphologic appearances of the failed liver: massive hepatic necrosis, chronic liver disease resulting in cirrhosis, and hepatic dysfunction without overt necrosis. Of these, cirrhosis is the most common cause of liver related deaths and is the twelfth leading cause of death in the United States.

Cirrhosis is the common end point of a variety of chronic liver diseases. It is essentially a scarred liver that cannot perform its functions optimally. It can be clinically divided into compensated and decompensated forms, depending on whether or not the cirrhotic liver can still perform many of its functions. As discussed later in this chapter, the presence of decompensated cirrhosis worsens prognosis and increases the urgency of clinical management.

Cirrhosis is characterized by the presence of fibrous septations throughout the liver that results in parenchymal nodularity. The central pathophysiologic mechanisms that occur in most diseases that lead to cirrhosis are chronic, continued death and regeneration of hepatocytes that leads to the deposition of extracellular matrix and a gradual architectural and vascular reorganization of the liver. This reorganized liver no longer functions as well as the original.

One of the consequences of cirrhosis is portal hypertension. Portal hypertension is increased blood pressure in the portal circulation. Recall that the portal circulation drains the intestinal tract. In cirrhosis, this increased blood pressure is a result of the vascular reorganization of the cirrhotic liver–the vascular resistance through the sinusoids is increased and there are abnormal connections between the portal and arterial systems. The principal clinical consequences of portal hypertension are ascites, the formation of portosystemic shunts, congestive splenomegaly, and hepatic encephalopathy.

Jaundice is the yellow discoloration of the skin that results from disturbances in bilirubin metabolism. Icterus is the corresponding yellow color seen in the sclera. Cholestasis describes the systemic retention of bilirubin and the solutes normally excreted in bile. This occurs when bilirubin production exceeds bilirubin clearance. It commonly results from disturbances in bile excretion due to mechanical blockages but can occur via many other mechanisms, such as excessive bilirubin production as in hemolytic diseases, reduced hepatocyte uptake or conjugation as occurs in hepatitides, or decreased hepatocellular excretion as in some genetic metabolic diseases.

1.6 General Classes of Liver Disease

We can divide liver disease into categories by etiology. Some of these broad categories include metabolic, toxic, infectious, circulatory, and neoplastic diseases. We can also divide liver disease by time frame into acute and chronic diseases (or even acute on chronic disease). And we can divide it by the compartment primarily targeted by the disease, into hepatocyte,

Table 1.1 Classifications of adult liver disease

Etiology	Timeframe	Compartmental
Metabolic	Acute	Hepatocyte
Toxic	Chronic	Bile Duct
Infectious		Vasculature
Circulatory		
Neoplastic		

bile duct, and vascular diseases (Table 1.1). The initial goal of the clinicopathologic examination is to classify the disease process into as few of these general categories as possible. Our final goal is to arrive at a single best diagnosis or narrowed differential diagnosis. Several common laboratory, procedural, and imaging studies are used to assess for the presence and degree of liver injury, as well as the functional status of the liver.

Clinicians use readily available blood tests to assess liver injury, and these tests provide practical information regarding the potential etiology as well as severity of the injury. Laboratory markers used in this assessment include liver enzyme levels (e.g. alkaline phosphatase, gamma glutamyl transferase, aspartate aminotransferase, or AST, and alanine aminotransferase, or ALT), tests of synthetic function (e.g. prothrombin time, albumin), and the serum bilirubin level. Though overlapping, or mixed, abnormalities are common, the pattern of laboratory derangements helps clinicians classify liver injury as either hepatocellular or cholestatic in nature.

For example, predominantly elevated aminotransferases—AST and ALT—reflects hepatocyte injury caused by a number of potential insults, and the magnitude of elevation can help delineate the cause. Markedly elevated AST and ALT levels may be seen, for instance, in acute viral hepatitis or a toxin exposure, while less elevated levels, classically with an AST to ALT ratio of 2–1, are often seen in patients with alcoholic liver disease [4, 5]. In contrast, a predominantly elevated alkaline phosphatase in the setting of liver injury is suggestive of cholestatic disease, i.e. biliary obstruction from either an intrahepatic (e.g. primary sclerosing cholangitis) or extrahepatic (e.g. choledocholithiasis) process.

1.7 Decompensated Cirrhosis, Portal Hypertension, and Disease Severity

Just as the distinction between hepatocellular and cholestatic injury provides meaningful clinical information, so too does the histologic distinction between mild fibrotic disease and cirrhosis. Progression of liver disease to its most advanced and irreversible stage, cirrhosis, is clinically significant and associated with increased morbidity and mortality (Table 1.2). Patients who develop cirrhosis typically experience a natural history that includes an initial period of "compensated" disease, during which reported median survival rates are in the range of 10–12 years [6, 7]. However, cirrhotic patients are prone to decompensating events—gastrointestinal bleeding, or development of ascites, jaundice, or hepatic encephalopathy—that increase mortality dramatically. For example, the development of esophageal varices alone has been associated with mortality rates of up to 25% at 5 years [8].

The primary pathophysiologic influence behind the vast majority of complications, or decompensating events, in cirrhotic patients is portal hypertension, i.e. the increased resistance to portal blood flow that creates an increased gradient of pressure between the portal vein and the inferior vena cava. When the portal pressure increases beyond 12 mm Hg, patients develop ascites, the most common complication of cirrhosis that increases susceptibility to infection and carries with it a 50% independent mortality risk within 2 years [9]. Additional consequences of portal hypertension include the formation of varices, thereby increasing the risk for fatal hemorrhage, and the development of

Table 1.2 Common complications of cirrhosis

Type of Complication	Complication
Portal Hypertensive	Ascites Varices Hepatorenal syndrome Hepatic hydrothorax Portopulmonary hypertension Hepatopulmonary syndrome Hepatic encephalopathy
Malignant	Hepatocellular carcinoma
Systemic	Sarcopenia Cachexia Fatigue Anxiety Depression

encephalopathy. In the latter, neurotoxins normally cleared by healthy livers are shunted into portal hypertension-induced portosystemic collaterals, affecting the central nervous system and resulting in a spectrum of neuropsychiatric disturbances [10].

Transjugular intrahepatic portosystemic shunts (TIPS) alleviate portal hypertension, and therefore its complications, by lowering the portal pressure below the threshold of 12 mm Hg. As a result, TIPS is often utilized for patients experiencing recurrent variceal hemorrhage, or active hemorrhage despite endoscopic therapy, as well as for patients with refractory or diuretic-resistant ascites [11].

Severity of liver disease is commonly estimated by a clinical scoring system utilizing the Model for End-Stage Liver Disease (MELD) score. Using a patient's serum creatinine, total bilirubin, and international normalized ratio (INR), the MELD score—a value ranging from 6 to 40—is predictive of mortality in patients on the transplant waiting list and independently predicts survival in patients with a variety of liver disease [12, 13]. Since 2002, though originally validated to predict mortality in patients undergoing TIPS for complications of portal hypertension [14], the MELD score has formed the backbone of the liver transplant allocation system [15–18]. Prior to this, clinicians utilized the Child-Turcotte-Pugh (CTP) score—using serum bilirubin, serum albumin, and INR in addition to subjective grades of ascites and encephalopathy (Table 1.3)—as the primary tool to predict mortality in cirrhotic patients [19]. CTP was originally designed to predict mortality in patients with liver disease and bleeding esophageal varices. Its role was subsequently broadened to predict risk of other operations in cirrhotic

Table 1.3 Child-Turcotte-Pugh (CTP) scoring calculator

Points	1	2	3
Total Bilirubin (mg/dL)	<2.0	2–3	>3
Albumin (g/dL)	>3.5	2.8–3.5	<2.8
INR	<1.7	1.7–2.2	>2.2
Ascites	Absent	Mild	Severe
Encephalopathy	Absent	Grade I–II	Grade III–IV

Class A = 5–6 points
Class B = 7–9 points
Class C = 10–15 points

patients and to stage patients with hepatocellular cancer by way of it reflecting the competing risk of cirrhosis-associated death in patients with this type of cancer. Further discussion of this topic is found in Chap. 3.

In 2014, the Organ Procurement Transplantation Network (OPTN) approved a proposal by the United Network for Organ Sharing (UNOS) to incorporate a patient's serum sodium into the MELD score calculation. This revolutionary implementation of "MELD-Na," which formally began in January 2016, is supported by data that hyponatremia is predictive of mortality for patients listed for liver transplantation, particularly among patients with a low MELD score, and its incorporation into the calculation predicts waiting list mortality better than MELD alone [17, 20–23]. The most up-to-date calculator for the MELD score can be found on the OPTN website: https://optn.transplant.hrsa.gov/resources/allocation-calculators/meld-calculator/.

The MELD-Na score is calculated as follows: MELD-Na = MELD + 1.32 × (137-Na) − [0.033× MELD*(137-Na)].

Importantly, the MELD score, in addition to the aforementioned laboratory abnormalities and portal hypertensive complications, can have important prognostic information for interventional radiologists and oncologists tasked with managing hepatocellular carcinoma, a common malignant complication of cirrhosis. Transarterial chemoembolization (TACE) in patients with poor hepatic reserve—elevated baseline serum bilirubin, INR, or creatinine; decreased serum albumin; presence of ascites or encephalopathy; MELD score above 20—has been associated with a statistically significant risk of irreversible hepatotoxicity resulting in death or the need for urgent liver transplantation [24]. These findings underscore the importance of understanding the clinical assessment of patients with liver disease, as well as the intricacies of the liver transplant allocation process.

References

1. Theise ND. Liver and gallbladder. In: Kumar V, Abbas AK, Aster JC, editors. Robbins and Cotran pathologic basis of disease. Philadelphia: Elsevier Saunders; 2015. p. 821–81.
2. Crawford JM, Burt AD. Anatomy, pathophysiology, and basic mechanisms of disease. In: Burt AD, Portmann BC, Ferrell LD, editors. MacSween's pathology of the liver. Edinburgh: Churchill Livingstone Elsevier; 2012. p. 1–77.
3. U.S. Department of Health & Human Services. Organ Procurement and Transplantation Network. http://optn.transplant.hrsa.gov. Accessed 13 May 2014.
4. Pratt DS, Kaplan MM. Evaluation of abnormal liver-enzyme results in asymptomatic patients. N Engl J Med. 2000;342(17):1266–71.
5. Dutta A, Saha C, Johnson CS, Chalasani N. Variability in the upper limit of normal for serum alanine aminotransferase levels: a statewide study. Hepatology. 2009;50(6):1957–62.
6. D'Amico G, Garcia-Tsao G, Pagliaro L. Natural history and prognostic indicators of survival in cirrhosis: a systematic review of 118 studies. J Hepatol. 2006;44(1):217–31.
7. D'Amico G, Pasta L, Morabito A, D'Amico M, Caltagirone M, Malizia G, et al. Competing risks and prognostic stages of cirrhosis: a 25-year inception cohort study of 494 patients. Aliment Pharmacol Ther. 2014;39(10):1180–93.
8. Zipprich A, Garcia-Tsao G, Rogowski S, Fleig WE, Seufferlein T, Dollinger MM. Prognostic indicators of survival in patients with compensated and decompensated cirrhosis. Liver Int: Official J Int Assoc Study Liver. 2012;32(9):1407–14.
9. Gines P, Fernandez-Esparrach G, Arroyo V. Ascites and renal functional abnormalities in cirrhosis. Pathogenesis and treatment. Baillieres Clin Gastroenterol. 1997;11(2):365–85.
10. Bustamante J, Rimola A, Ventura PJ, Navasa M, Cirera I, Reggiardo V, et al. Prognostic significance of hepatic encephalopathy in patients with cirrhosis. J Hepatol. 1999;30(5):890–5.
11. Boyer TD, Haskal ZJ. American Association for the Study of Liver D. The Role of Transjugular Intrahepatic Portosystemic Shunt (TIPS) in the Management of Portal Hypertension: update 2009. Hepatology. 2010;51(1):306.
12. Wiesner R, Edwards E, Freeman R, Harper A, Kim R, Kamath P, et al. Model for end-stage liver disease (MELD) and allocation of donor livers. Gastroenterology. 2003;124(1):91–6.

13. Said A, Williams J, Holden J, Remington P, Gangnon R, Musat A, et al. Model for end stage liver disease score predicts mortality across a broad spectrum of liver disease. J Hepatol. 2004;40(6):897–903.
14. Malinchoc M, Kamath PS, Gordon FD, Peine CJ, Rank J, ter Borg PC. A model to predict poor survival in patients undergoing transjugular intrahepatic portosystemic shunts. Hepatology. 2000; 31(4):864–71.
15. Kamath PS, Wiesner RH, Malinchoc M, Kremers W, Therneau TM, Kosberg CL, et al. A model to predict survival in patients with end-stage liver disease. Hepatology. 2001;33(2):464–70.
16. Biggins SW, Bambha K. MELD-based liver allocation: who is underserved? Semin Liver Dis. 2006; 26(3):211–20.
17. Kalra A, Wedd JP, Biggins SW. Changing prioritization for transplantation: MELD-Na, hepatocellular carcinoma exceptions, and more. Curr Opin Organ Transplant. 2016;21(2):120–6.
18. Smith JM, Biggins SW, Haselby DG, Kim WR, Wedd J, Lamb K, et al. Kidney, pancreas and liver allocation and distribution in the United States. Am J Transpl: Official J Am Soc Transpl Am Soc Transplant Surg. 2012;12(12):3191–212.
19. Biggins SW. Beyond the numbers: rational and ethical application of outcome models for organ allocation in liver transplantation. Liver Transpl: Official Publ Am Assoc Study Liver Dis Int Liver Transpl Soc. 2007;13(8):1080–3.
20. Biggins SW, Rodriguez HJ, Bacchetti P, Bass NM, Roberts JP, Terrault NA. Serum sodium predicts mortality in patients listed for liver transplantation. Hepatology. 2005;41(1):32–9.
21. Biggins SW, Kim WR, Terrault NA, Saab S, Balan V, Schiano T, et al. Evidence-based incorporation of serum sodium concentration into MELD. Gastroenterology. 2006;130(6):1652–60.
22. Kim WR, Biggins SW, Kremers WK, Wiesner RH, Kamath PS, Benson JT, et al. Hyponatremia and mortality among patients on the liver-transplant waiting list. N Engl J Med. 2008;359(10):1018–26.
23. Biggins SW. Use of serum sodium for liver transplant graft allocation: a decade in the making, now is it ready for primetime? Liver Transpl: Official Publ Am Assoc Study Liver Dis Int Liver Transpl Soc. 2015;21(3):279–81.
24. Garwood ER, Fidelman N, Hoch SE, Kerlan RK Jr, Yao FY. Morbidity and mortality following transarterial liver chemoembolization in patients with hepatocellular carcinoma and synthetic hepatic dysfunction. Liver Transpl: Official Publ Am Assoc Study Liver Dis Int Liver Transpl Soc. 2013; 19(2):164–73.

Imaging Characteristics of Normal Liver and Liver Tumors

2

Ali A. Haydar, MD, MRCP, FRCR, Layla Antoine Nasr, MD and Hero K. Hussain, MD, FRCR, FACR

Abbreviations

US	Ultrasound
CT	Computed tomography
MRI	Magnetic resonance imaging
FDG-PET	Fluorodeoxyglucose, positron emission tomography
MDCT	Multidetector computed tomography
MRCP	Magnetic resonance cholangiopancreatography
ERCP	Endoscopic retrograde cholangiopancreatography
GRE	Gradient recalled echo
DWI	Diffusion-weighted imaging
ADC	Apparent diffusion coefficient
HCC	Hepatocellular carcinoma
IVC	Inferior vena cava
RES	Reticuloendothelial system
TIPS	Transjugular intrahepatic portosystemic shunt
GI	Gastrointestinal
AASLD	American Association for the Study of Liver Disease
LI-RADS	Liver imaging reporting and data system

A.A. Haydar (✉)
Department of Radiology, American University of Beirut Medical Centre, Bliss Street, Beirut 1107 2020, Lebanon
e-mail: ah24@aub.edu.lb

L.A. Nasr
Department of Diagnostic Radiology, American University of Beirut Medical Center, 2139 Orchard Lakes Pl E, Apt 31, Toledo, OH 43615, USA
e-mail: lan03@mail.aub.edu

H.K. Hussain
Department of Radiology, University of Michigan Health System, Ann Arbor, MI, USA

2.1 Anatomy

2.1.1 Gross Anatomy and Landmarks

The liver lies in the upper abdomen and extends from the epigastrium medially to fill the right hypochondrium. Its superior surface is dome-shaped and follows the contour of the diaphragm lying approximately at the level of the fifth rib. Its anterior surface extends down to the right costal margin.

J. Meyer and T.E. Schefter (eds.), *Radiation Therapy for Liver Tumors*,
DOI 10.1007/978-3-319-54531-8_2

The major landmark of the superior surface of the liver is the sagittal groove, which is the notch for ligamentum teres (formerly the umbilical vein), and lies at the free edge of the falciform ligament. The major landmark of the inferior or visceral surface is the porta hepatis, which is a central depression that accommodates the portal vein, hepatic artery and common bile duct [1, 2].

2.1.2 Liver Size

The weight of a normal liver is approximately 2% that of total adult body weight [3]. CT Liver volumetric measurements are useful to assess the functional residue of the liver prior to resection and the volume of the liver in transplant donors. Using commercially available software, measurements may be done manually, or by semi-automated or automated programs, the latter requiring significantly less time. Individual lobar and segmental volumes can also be measured. Enhanced CT in the venous phase is the preferred phase to measure and segment the liver due to better delineation of blood vessels [4].

2.1.3 Segments and Vascular Supply

The liver receives approximately 75% of its blood supply from the portal vein and 25% from the hepatic artery, while blood drains via three main hepatic veins into the IVC. The pressure difference between measurements in the wedged (occluded) hepatic vein and the IVC (also known as the corrected sinusoidal pressure) is normally between 4 and 8 mmHg. This pressure measurement can be used to evaluate liver disease, namely cirrhosis [5].

The liver is divided into eight functional segments according to the Couinaud classification. Each of these segments receives a branch of the portal vein, is bounded by a hepatic vein [6], and has its separate hepatic arterial branch and bile duct [3]. The major landmarks used to divide the liver into its functional segments are the portal and the hepatic veins. The main portal vein divides the liver axially into two virtual superior (segments VII, VIII, IVa, and II) and inferior parts (VI, V, IVb, and III). The middle hepatic vein divides the liver into left and right lobes. The left hepatic vein runs vertically and separates the left lateral and left medial segments of the liver. The plane of the left portal vein divides the lateral segment into superior segment II and inferior segment III, and the left medial segment into superior segment IVa and inferior segment IVb. The right hepatic vein divides the right lobe into anterior segments V/VIII and posterior segments VI/VII. The plane of the right portal vein divides the right lobe into superior segments VII and VIII, and inferior segments V and VI. Segment I (caudate lobe) receives portal supply from both lobes and drains directly to the IVC [2, 7].

2.2 Liver Imaging Techniques and Imaging of the Normal Liver

2.2.1 Plain Radiography

The complex shape of the liver and limited soft tissue contrast of plain radiographs makes reliable identification of the liver boundaries difficult. Even though significant findings such as gross hepatomegaly, hepatic calcification, and pneumobilia may be detected on plain films [8], further evaluation with other modalities would most likely be needed.

2.2.2 Ultrasound

Ultrasound (US) of the liver is performed using a phased array transducer operating between 3 and 5 MHz Doppler capabilities [9]. The normal echotexture of the liver parenchyma is homogeneous and slightly more reflective than the adjacent renal cortex. Scanning the liver in all directions in deep inspiration is essential to cover its entire span and detect inconspicuous lesions. In case a lesion is found, intravenous injection of a microbubble intravascular contrast agent can improve its characterization by observing the arterial and portal phases of enhancement.

The gallbladder, intra- and extrahepatic bile ducts are also routinely assessed by US for dilatation and presence of stones. In addition, Doppler interrogation of the liver vasculature is routinely performed to visualize the portal flow phasicity and measure its velocity. Portal vein branches may be identified by their radiating pattern from the hilum and the increased reflectivity of their walls. In contrast, hepatic veins radiate from the inferior vena cava and their walls are not distinguishable from the adjacent parenchyma. On Doppler examination, the normal hepatic vein trace reflects the transmitted right-heart pressure changes with reversal of flow during the cardiac cycle. Ultrasound is also used to assess the patency and flow velocity of the hepatic artery and its branches [10].

2.2.3 Computed Tomography

The liver appears homogeneous on non-contrast computed tomography (CT) with attenuation values of 55–65 HU, approximately 8 HU greater than the spleen. The vascular structures of the liver, the common bile, common hepatic, and right and left hepatic ducts are easily identified on contrast-enhanced CT, while the peripheral intrahepatic ducts are not. Multiphasic, multidetector CT (MDCT) scan is commonly used to assess the liver and characterize liver lesions. This technique typically includes an arterial-dominant phase at 10–30 s post contrast injection, a portal or venous phase at 60–90 s post contrast injection, and a delayed phase at 5–10 min post contrast injection. An unenhanced scan is optional and not routinely performed at all centers. The minimum requirement is an arterial phase and a portal/venous phase; however, the delayed phase is of great value in the characterization some benign and malignant lesions (e.g., hemangioma and cholangiocarcinoma) [2]. Optimizing the protocols and timing of these phases are important to maximize lesion-to-liver contrast. For this purpose, a method known as automatic bolus tracking is used to time the arterial phase; scanning is triggered when contrast is, for example, detected in the celiac axis or hepatic artery. This technique gives more consistent results and accounts for the variation in cardiac output and intravascular volume [11].

Cone beam CT is basically a CT scan performed with catheter injection into the hepatic artery in the angiography suite to detect subtle liver lesions or to guide treatment used mainly in oncology liver directed therapies such as transarterial chemoembolization [12].

2.2.4 Magnetic Resonance Imaging

Magnetic resonance imaging (MRI) has several advantages over CT and US for imaging the liver. First, it lacks ionizing radiation. Second, it has excellent soft tissue contrast and is therefore preferred for lesion detection and characterization. Third, it clearly delineates the biliary system and the hepatic vascular anatomy and patency. MRI has a wider range of tissue contrast and contrast media compared to other imaging techniques due to a combination of field strength, pulse sequences, interdependent sequence parameters, and the availability of liver-specific contrast agents. All of these factors serve to strengthen image quality [13, 14].

Multichannel phased array coils are routinely used for imaging the liver. When performing MR sequences, there is always a trade-off between image resolution and scan time. Shortening scan time can compromise intrinsic contrast and spatial resolution and limit the usefulness of MRI for lesion detection and characterization. Comprehensive liver MR imaging includes breath-hold T1-weighted (T1W) in-phase and out-of-phase gradient-recalled echo (GRE) imaging sequences for lipid detection and lesion characterization, and breath-hold T2-weighted (T2W) imaging using a turbo spin-echo sequence, usually single shot. Higher quality T2W images are acquired with respiratory-triggered multishot sequences. Also, quantitative diffusion-weighted imaging (DWI) and apparent diffusion coefficient (ADC) calculations are increasingly being studied for their role in lesion detection and characterization [15]. Multiphasic contrast-enhanced

T1W GRE imaging is routinely performed in all MRI studies of the liver.

The intensity of normal liver parenchyma is the same as, or slightly higher than, that of adjacent muscle on T1- and T2-weighted imaging. The liver–spleen differences may serve as a simple guide to the efficacy of intrinsic T1 and T2 weighting. Generally, the spleen should be lower signal (darker) than liver on T1W images and higher signal (brighter) on T2W imaging. The appearance of vessels varies widely on MRI depending on pulse sequence and on the use of artifact suppression techniques or contrast media. In particular, intravascular signal on conventional spin-echo sequences may occur normally and should not be interpreted as thrombus without confirming on other sequences. Finally, the bile ducts are best imaged using a dedicated magnetic resonance cholangiopancreatography (MRCP) technique with fluid-sensitive, heavily T2-weighted imaging [16].

For contrast-enhanced images, Gadolinium-based non-specific extracellular contrast agents are injected intravenously and provide enhancement on T1W images in a similar fashion to iodinated contrast media at CT examination. For example, breath-hold T1W sequences allow the acquisition of multiphasic (arterial, portal/venous, delayed) images. The enhancement characteristics of many focal lesions are similar to CT. Several liver-specific contrast agents are increasingly being used but have not yet made it to the guidelines for liver lesion characterization. Hepatocyte-specific gadolinium-based agents accumulate in hepatocyte and are excreted in bile via specific receptors on the hepatocytes. They result in enhancement of the normal liver parenchyma and biliary system on T1W imaging and serve as an indicator of the presence of and the function of hepatocytes. Liver-specific agents that are taken up by Kupffer cells, which represent the reticuloendothelial system (RES) of the liver, have also been developed [17].

2.2.5 Nuclear Imaging

Radionuclide imaging of the liver is performed using ^{99m}Technetium-sulfur colloid or albumin colloid, which are taken up by the reticuloendothelial system. Liver scintigraphy is seldom used as a primary diagnostic investigation but can help characterize focal lesions when MRI and CT are not available [18]. PET and PET/CT are not frequently used to identify malignant liver lesions. Their main role in imaging primary liver neoplasms, particularly hepatocellular carcinoma, is for the assessment of extrahepatic metastasis. For cholangiocarcinoma, PET-CT offers no added benefit compared to CT and MRI/MRCP in detecting the primary tumor. In fact, it is inferior to MRI especially in detecting primaries of the extrahepatic biliary duct. The only instance where nuclear imaging would be more reliable is in detecting distant metastatic disease from cholangiocarcinoma [19].

2.2.6 Invasive Liver Imaging

The hepatic arteries are best visualized by selective catheterization.

The hepatic veins can be routinely seen on digital subtraction angiography. However, for direct visualization, they are catheterized retrogradely, using a femoral or jugular approach and venography is obtained with the catheter free in the veins. Wedged hepatic venous pressure measurement is performed following impaction of an end-hole catheter in a small branch of a hepatic vein. The catheter position is confirmed by the injection of contrast medium, which produces parenchymal staining [20].

The portal system is not normally visualized on a selective hepatic arteriogram unless there has been flow reversal or an arterioportal shunt. Therefore, it is accessed directly by a catheter or needle inserted into a portal vessel percutaneously under ultrasound guidance, or indirectly by selective injections into the celiac, splenic, superior mesenteric, or inferior mesenteric arteries. Direct methods (including percutaneous splenic, transhepatic and transjugular approaches) are now used only when therapeutic procedures [e.g., Transjugular Intrahepatic Portosystemic Shunt (TIPS)] or sampling techniques (e.g., direct portal venous pressure measurement) are needed.

Cholangiography can be performed retrogradely via an endoscopic approach [Endoscopic Retrograde Cholangiopancreatography (ERCP)] or percutaneously by placing a needle or catheter through the liver parenchyma into the bile ducts. Diagnostic MRCP has largely replaced the invasive diagnostic methods for imaging the biliary system. These invasive methods are now performed as part of therapeutic interventions to drain an obstructed biliary tree [21].

2.3 Imaging of Liver Cirrhosis (Table 2.1)

2.3.1 General Imaging Features of Cirrhosis

Regardless of etiology, gross morphologic changes of advanced cirrhosis are well recognized by any cross-sectional technique such as US, CT, or MRI. These encompass hepatomegaly in the early stages, shrinkage of the right lobe with enlargement of the lateral segment of the left lobe and caudate lobe, and nodularity of the surface contour [22].

On US examination, the liver contour may appear nodular with coarse echotexture. Flow dynamics of the hepatic vasculature may also be altered. These alterations are evaluated with Doppler sonography. In the hepatic artery, the resistive index is either increased due to compression by cirrhotic liver parenchyma, or decreased due to spontaneous arteriovenous shunt formation. The latter is more specific for cirrhosis [10]. Changes also occur in the portal flow in the setting of portal hypertension (see the next section). The portal flow slows down (velocity less than 15 cm/sec), becomes stagnant, or is reversed; this reversal is termed "hepatofugal flow" [23]. Finally, the hepatic venous circulation loses its phasicity and ceases to reflect right atrial pressure changes [10].

On CT imaging (Fig. 2.1), the cirrhotic liver appears enlarged in the early stages and shrunken in severe cirrhosis. As cirrhosis advances, the liver margins appear nodular, and the organ becomes diffusely heterogeneous because of the fibrotic changes in its parenchyma [24]. Regenerative nodules are difficult to see on non-contrast CT, unless they contain iron (siderotic nodules) which makes them hyperdense relative to the

Table 2.1 Imaging findings of liver cirrhosis

Ultrasound	CT	MRI	Angiography
– Hepatomegaly (early) – Irregular contour – Right lobe and medial left lobe atrophy; lateral left lobe and caudate lobe enlargement – Coarsened echotexture – Arteriovenous shunts – Hepatic arteries: increased or decreased resistive index; dilation and tortuosity – Portal veins: slow flow, stagnancy, or hepatofugal flow – Hepatic veins: loss of phasicity – Splenomegaly – Ascites – Portovenous collaterals	– Hepatomegaly (early) – Irregular contour – Right lobe and medial left lobe atrophy; lateral left lobe and caudate lobe enlargement – RN/SN/fibrosis – Arteriovenous shunts – Splenomegaly – Ascites	– Hepatomegaly (early) – Irregular contour – Right lobe and medial left lobe atrophy; lateral left lobe and caudate lobe enlargement – RN/SN/fibrosis – Arteriovenous shunts – Splenomegaly – Ascites	– Early: mildly stretched hepatic arteries – Advanced: tortuosity and "corkscrew" appearance of arteries with sudden loss in caliber; arteriovenous shunts – Portosystemic collaterals – Hepatofugal flow

Abbreviations: *RN* Regenerative Nodules; *SN* Siderotic Nodules

surrounding parenchyma. Enhanced CT may or may not reveal RNs since they do not typically enhance in the arterial phase [25]. Arterioportal shunts are often seen after contrast administration. They typically have a linear or wedge-shaped appearance and are subcapsular in location with no visible mass effect [26].

Findings on MRI (Fig. 2.2) are similar to those of CT. Additionally, fibrosis is of high signal on T2W imaging [24], and RNs have a non-specific appearance on T1W and T2W images, but sometimes contain lipid or iron. The iron-containing (siderotic) nodules show low signal on both T1W and T2W images [27].

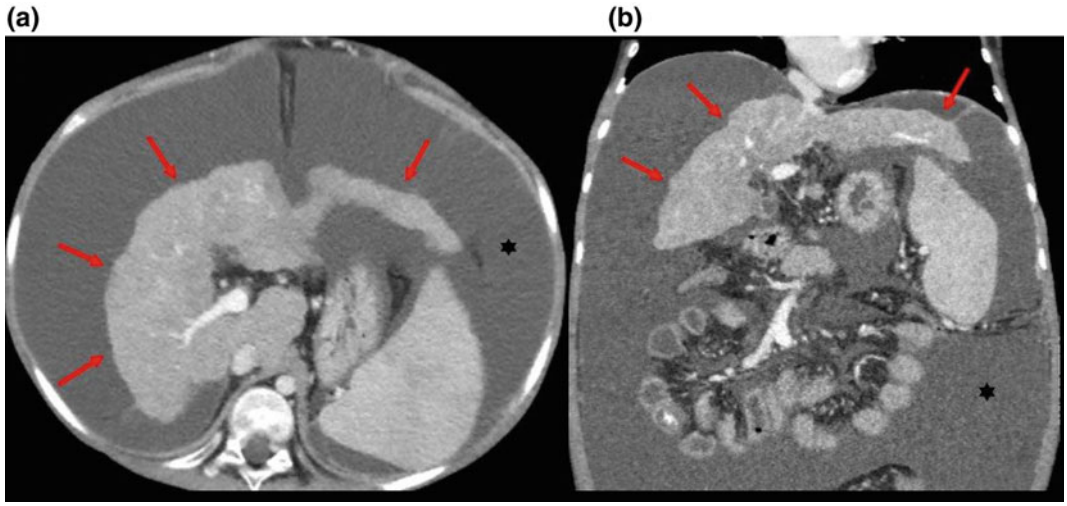

Fig. 2.1 Gross changes of liver cirrhosis seen on an axial (**a**) and coronal (**b**) images from an enhanced CT scan. The liver is shrunken with an irregular nodular contour (*arrows*) and surrounding ascitic fluid (*asterisks*)

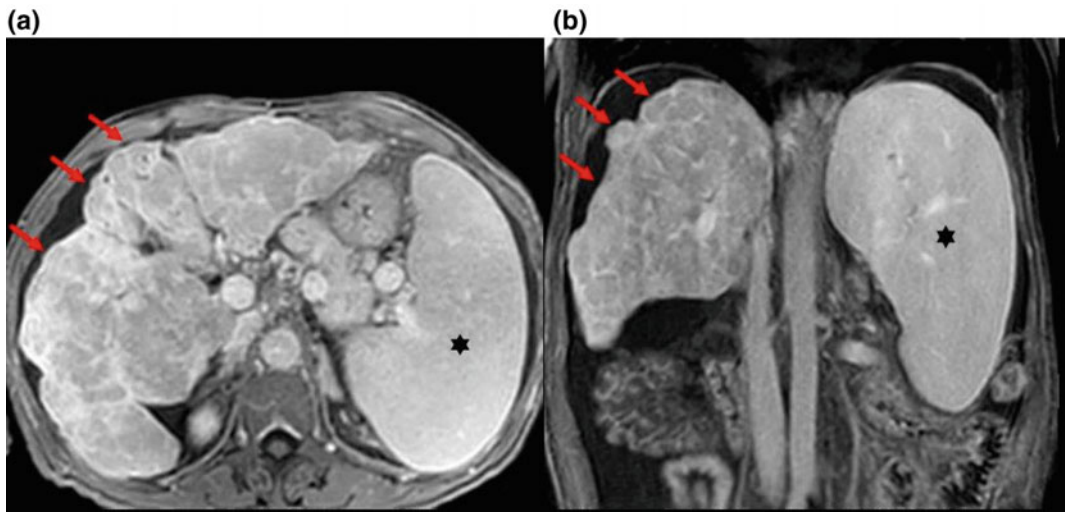

Fig. 2.2 Gross changes of liver cirrhosis seen on axial (**a**) and coronal (**b**) images from MR with gadolinium. The liver shows an irregular nodular contour (*arrows*). There is also splenomegaly secondary to portal hypertension (*asterisks*)

2.3.2 Imaging of the Effects of Portal Hypertension

The normal portal pressure measures between 4 and 11 mmHg [5]. PH is responsible for many extrahepatic manifestations of cirrhosis. It leads to splenomegaly (Fig. 2.2) with or without small nodular iron deposits within the spleen (Gamna-Gandy bodies). These deposits are related to foci of chronic hemorrhage in longstanding portal hypertension and are readily seen on MRI as foci of susceptibility artifact on GRE imaging [28]. The most specific finding of PH is the development of collateral portal venous anastomoses (varices) (Fig. 2.3). These occur in the gastroesophageal, perirectal, and retroperitoneal, with recanalization of the paraumbilical vein. When these varices develop, it is usually an indicator that the portal vein pressure exceeds 12 mm Hg. They may bleed, and the bleeding can be life-threatening. Noninvasive diagnostic imaging methods, such as color flow Doppler US, contrast-enhanced CT, and MRI can be used to identify collaterals. The major limitation of all imaging modalities is the inability to measure variceal pressure, which correlates directly with the risk of hemorrhage. Portal vein flow is altered by PH and may become stagnant. This stagnancy increases the risk of portal vein thrombosis. It is important to note that long-standing thrombosis may be associated with periportal collateral formation which re-establishes flow to the liver. This is also known as "cavernous transformation" and is a strong indication of bland thrombus in the portal vein [25]. Invasive imaging with angiography can also show the collateral flow as well as hepatofugal flow in the portal circulation [29].

2.4 Imaging of Liver Malignancies

2.4.1 Hepatocellular Carcinoma (Table 2.2)

2.4.1.1 Overview

Hepatocellular carcinoma (HCC) is the most common primary malignant neoplasm of the liver. Liver cirrhosis of any etiology is a major predisposing factor for development of HCC. HCC can be solitary, multifocal, or diffuse. The five-year survival of patients with HCC is approximately 30% [30].

On ultrasound, small HCC (<3cm) may be of increased or decreased reflectivity in relation to the adjacent parenchyma. An outer margin with a reduced reflectivity is present in some cases and thought to represent the thin fibrous capsule. Larger lesions may show internal heterogeneity, due to hemorrhagic, necrotic, or fatty components [9]. HCC may also be associated with portal vein thrombosis or intravascular tumor. Doppler examination can help distinguish tumor thrombus from bland thrombus in the portal vein:

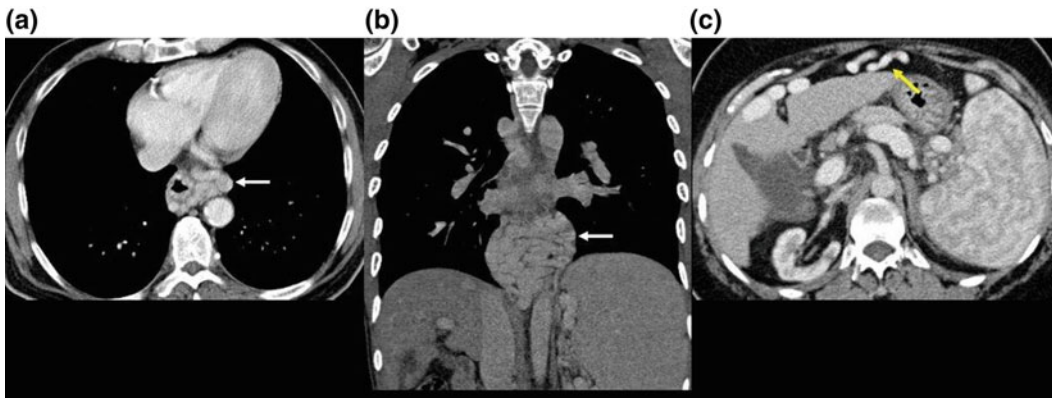

Fig. 2.3 Axial and coronal images from an enhanced CT scan (**a**, **b**) showing esophageal varices (*white arrow*). Axial image from an enhanced CT scan (**c**) showing a recanalized umbilical vein (*yellow arrow*)

Table 2.2 Imaging findings of hepatocellular carcinoma

Ultrasound	CT	MRI	Angiography
• Lesion with increased or decreased reflexivity[a] • May show thin fibrous capsule with reduced reflexivity (target sign) • Tumor thrombus in portal vein	• Non-enhanced: Ill-defined hypoattenuating; may have focal internal calcifications • Enhanced: Arterial hyperenhancement; portal venous/delayed washout and capsular appearance; tumor thrombus in portal vein	• Non-enhanced: Low T1W signal[b]; heterogeneous hyperintense T2W signal • Enhanced: Arterial hyperenhancement; portal venous/delayed washout and capsular appearance; tumor thrombus in portal vein	• Dilated feeding arteries; abundant abnormal vessels ('tumor stains')[c]; arteriovenous shunting • Translucent rim (<10% of cases) • "Threads and streaks" appearance in portal vein invasion

[a]Large lesions (≥3 cm) may show internal heterogeneity due to hemorrhagic, necrotic, or fatty components
[b]May show high T1W signal due to fat or glycogen accumulation
[c]May be hypovascular or avascular

the presence of arterial signal within the occluding material is indicative of tumor thrombus. This distinction is extremely important as tumor thrombus renders patients ineligible for liver transplantation [31]. High-velocity Doppler signals are often seen in HCC and are the result of arterioportal shunting, which is common in HCC [9].

On unenhanced CT, focal or multifocal HCC appears as ill-defined low-attenuation lesion(s). Focal areas of internal calcification have been described in up to 7.5% of lesions. Most HCCs hyperenhance relative to the liver parenchyma in the arterial phase, because they are supplied by the hepatic artery (Fig. 2.4). Some lesions enhance in a peripheral pattern around a central area of lower attenuation. Enhancement of HCC is better seen in the late arterial phase (i.e., when the portal vein becomes visible) than in the early arterial phase. The arterial phase also distinguishes tumor thrombus from bland thrombus (Fig. 2.5), because tumor thrombus enhances. In the portal venous or delayed phases, HCCs usually have lower attenuation than background liver tissue; this is known as the "washout appearance" [32]. Portal venous invasion and expansion is thought to be a specific feature of HCC. The CT features of portal venous invasion by HCC include arterioportal fistulae, periportal streaks of high attenuation, and dilatation of the main portal vein or its major branches [33].

On non-contrast MRI, HCC is typically of decreased signal on T1W images and of increased to heterogeneous signal on T2W images, depending on the size [34]. However, some lesions are of increased signal on T1W probably due to fat or glycogen accumulation. On contrast-enhanced T1W images, the enhancement patterns with gadolinium parallel those for enhanced CT examination, with most lesions hyperenhancing in the arterial phase, and becoming hypointense or washing out in the portal venous and/or delayed phases (Fig. 2.6). A delayed enhancing rim (capsule or pseudocapsule) is often seen around HCCs. Atypical regenerative and dysplastic nodules can mimic the pattern of HCC enhancement in the arterial phase and prompt uncertainty in the diagnosis.

Radionuclide imaging, including FDG-PET, is relatively non-specific for HCC and is not recommended for detecting or characterizing lesions but useful for the detection of metastatic HCC outside the liver.

Angiography shows dilated feeding arteries to the HCC, abundant abnormal vessels ("tumor stains") (Fig. 2.7), and arteriovenous shunting. Some HCC may have a surrounding capsule, and some may appear hypo- or avascular portal vein invasion produces a "threads and streaks" appearance highly suggestive of but not specific for HCC (Fig. 2.5). Angiography is used infrequently for the diagnosis of HCC because of its

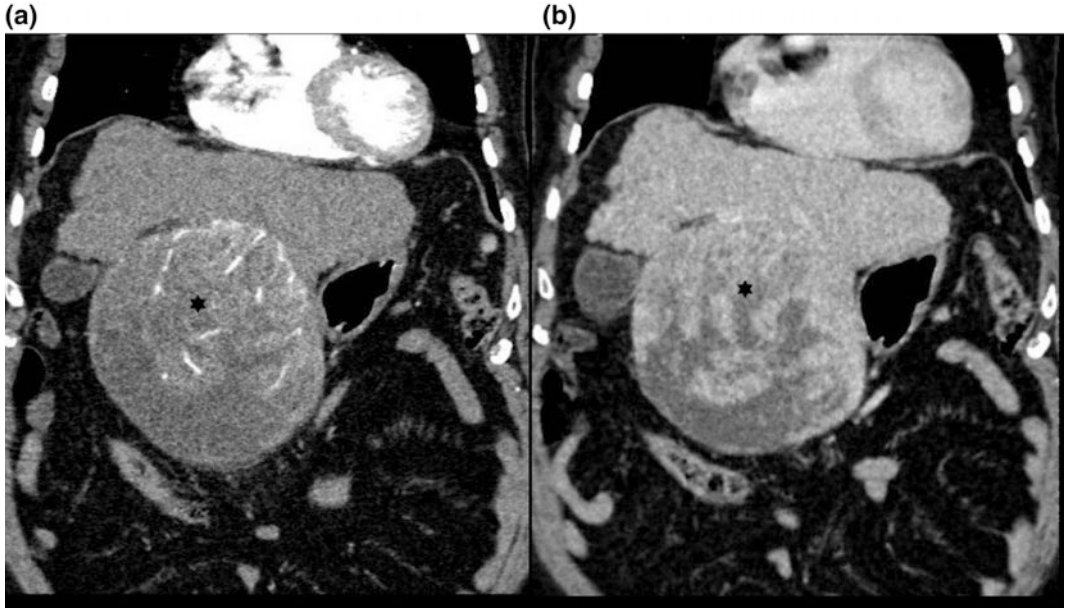

Fig. 2.4 Coronal images from a triphasic CT scan showing a large hepatocellular carcinoma (*asterisks*) with heterogeneous hyperenhancement in the arterial phase (**a**) and heterogeneous washout appearance in the portal venous phase (**b**)

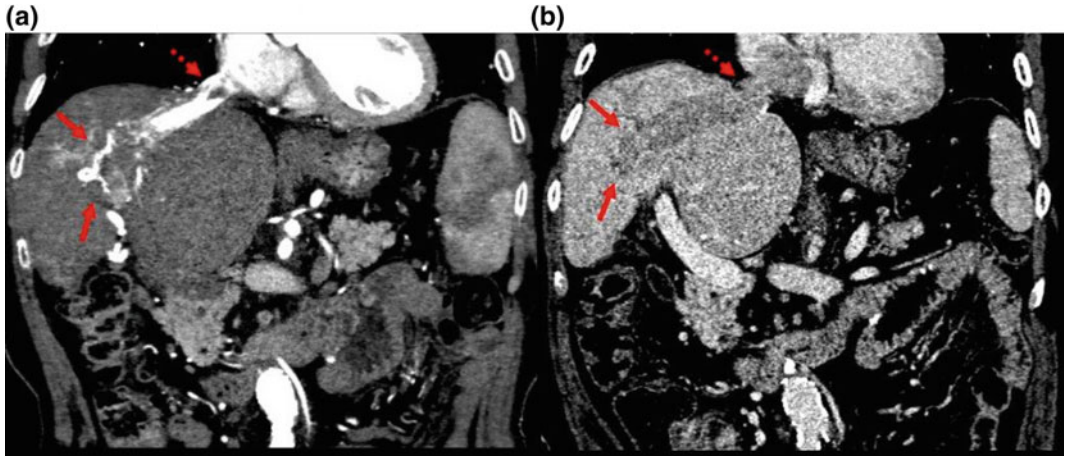

Fig. 2.5 Coronal images from a triphasic CT scan showing an HCC (*arrows*) invading the hepatic vein and extending to the right atrium (*dashed arrow*). The invading tumor exhibits a classic "threads and streaks" appearance in the arterial phase (**a**) and washout appearance in the portal phase (**b**)

invasive nature. However, it can be helpful for preoperative assessment by defining the arterial and venous anatomy and by evaluating the site and extent of portal or caval involvement when other techniques are unavailable or equivocal [35].

2.4.1.2 Detection of HCC in Cirrhotic Patients

Several guidelines and recommendations exist for this purpose. The American Association for the Study of Liver Diseases (AASLD) [36] recommends that patients with chronic hepatitis

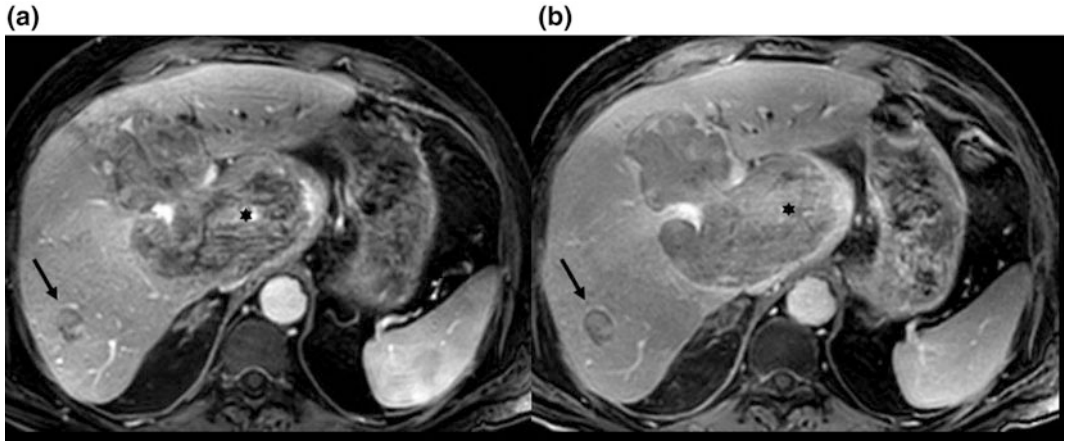

Fig. 2.6 Axial images from an MRI with gadolinium showing a large hepatocellular carcinoma (*asterisks*) and a small HCC (*arrows*) with enhancement in the arterial phase (**a**) and washout appearance in the portal venous phase (**b**)

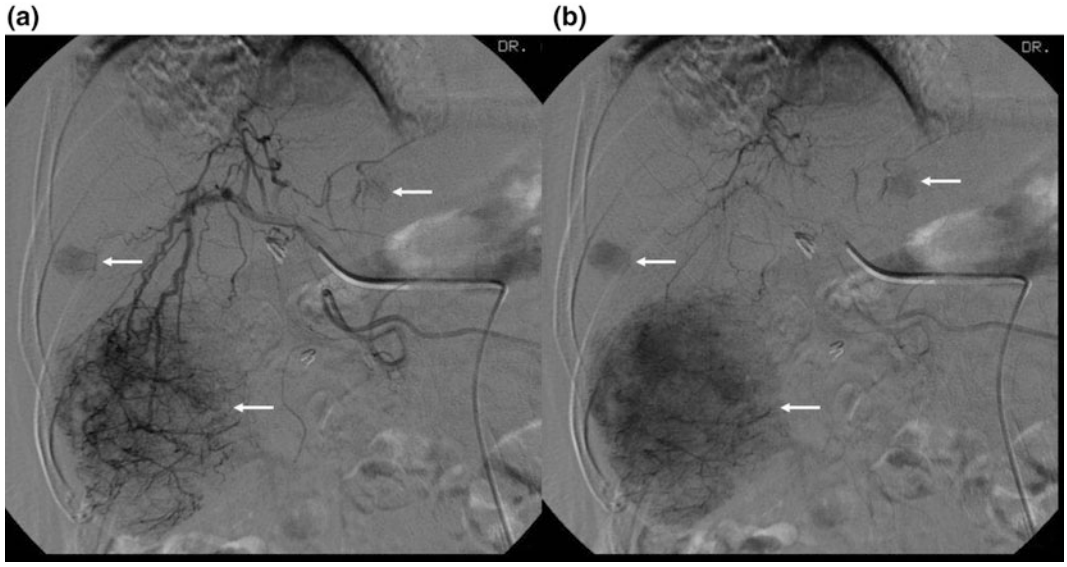

Fig. 2.7 Digital subtraction angiogram of the hepatic artery in the early (**a**) and late (**b**) arterial phases showing "tumor stains" (*arrows*) which represent multiple hepatocellular carcinomas

and/or biopsy-documented cirrhosis be screened for hepatocellular carcinoma (HCC) by ultrasound (US) at six-month intervals. CT and MRI, however, are not recommended for screening and are reserved for evaluation of certain lesions already detected on US or if an US study is equivocal or technically limited. Nodules smaller than 1 cm detected on US screening should be followed up with further US at three- to six-month intervals for two years. If no growth occurs during that interval, return to routine surveillance is recommended. However, nodules $\geq$1 cm should be investigated further with either four-phase multidetector CT or dynamic contrast-enhanced (MRI). Masses with appearances typical of HCC (e.g., hypervascular in the arterial phase with washout appearance in the portal venous or delayed phase) should be treated

as such. However, if they display an atypical behavior, they should be biopsied or imaged again with a different modalities for confirmation. If a biopsy with tumor markers proves inconclusive, they should be followed up by imaging at three- to six-month intervals until the nodule disappears, enlarges, or displays diagnostic characteristics of HCC. If they enlarge, they should be biopsied again.

The American College of Radiology (ACR) has recently supported an initiative that has helped standardize imaging in end-stage liver disease. This is known as the Liver Imaging–Reporting and Data System (LI-RADS) (see Algorithm, Fig. 2.8). The LI-RADS relies on objective criteria that are based solely on enhanced CT and/or MR imaging findings and classifies lesions in at-high-risk individuals into categories according to *probability* of malignancy. The features that are suggestive of HCC and used in the categorization are the following: (1) Mass-like appearance, (2) Arterial phase hyperenhancement (3) Washout of contrast in later phases after hyperenhancement, (4) Presence of a capsule, (5) Size of at least one cm and/or increase in one cm within one year, and (6) Tumor invasion of the portal vein. At the extreme ends of the spectrum are LR-1 and LR-5. LR-1 is a lesion that is benign with 100% certainty, such as a cyst or a hemangioma. LR-5, on the other hand, is a lesion that has a 100% chance of being HCC and satisfies at least four of the above criteria. For the other categories, LR-2 means the lesion is most probably benign with an atypical form of lesions otherwise classified in LR-1. LR-3 and LR-4, respectively, indicate an

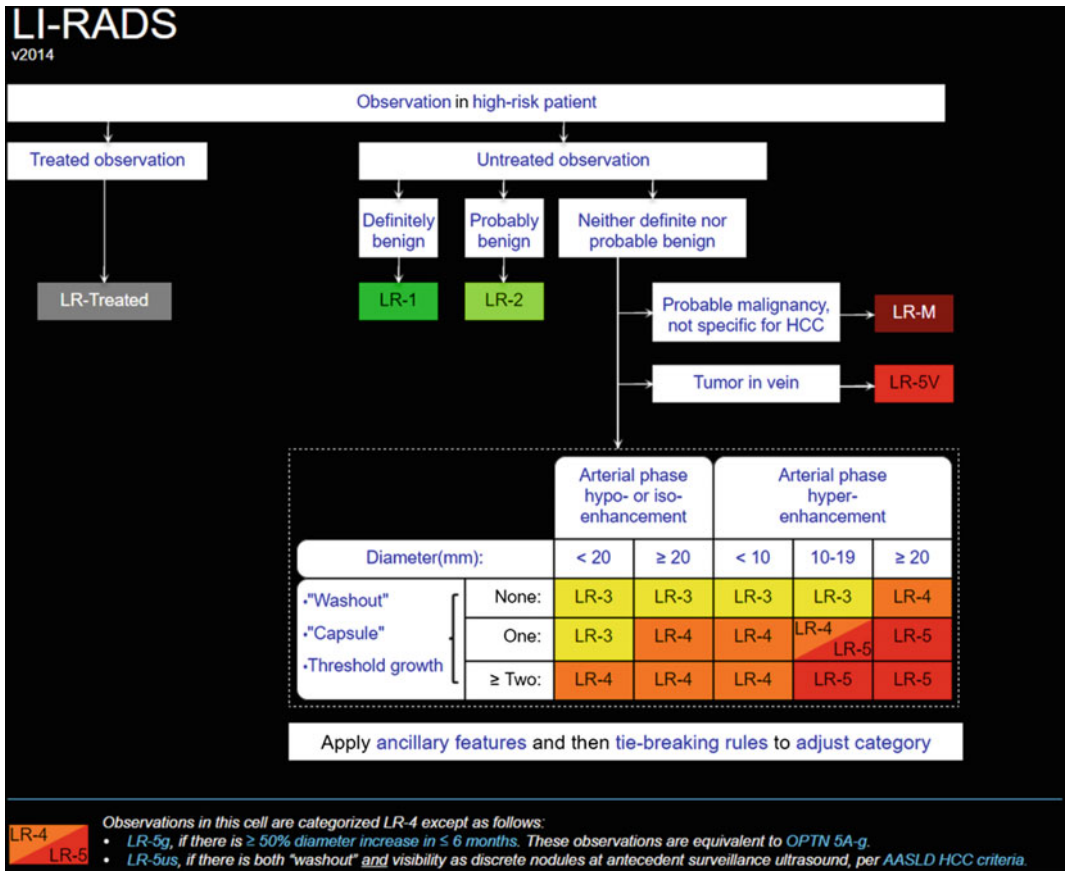

Fig. 2.8 LI-RADS algorithm [Reprinted from LI-RADS algorithm, atlas, and Lexicon, 2014. © ACR Press]

intermediate probability of HCC and a high probability of HCC; they satisfy the stated criteria to different extents. Also to note, LI-RADS includes a LR-M category which suggests the presence of a malignancy other than HCC (e.g., intrahepatic cholangiocarcinoma) [37, 38].

2.4.2 Cholangiocarcinoma

Cholangiocarcinoma is an uncommon tumor that arises from the bile duct epithelium and that tends to spread by local infiltration. Approximately 80–90% are extrahepatic (in the perihilar region (Klatskin tumors) or the distal common duct) and the rest are classified as intrahepatic or peripheral, arising within the liver and presenting as a hepatic mass [39]. The majority of tumors present with malignant hilar biliary obstruction (Fig. 2.9). Grossly, cholangiocarcinomas are classified into periductal or "infiltrating stenotic" (most common), exophytic or intraductal, or mass-forming [40]. Their appearance on imaging varies with size and pathological type [41]. Most of the infiltrating stenotic tumors are less than one–two cm in diameter, and the exophytic tumors are less than 5 cm.

On US, intrahepatic cholangiocarcinomas appear as nodules or focal bile duct wall thickening and are usually slightly hyperechoic [9]. However, in the extrahepatic types, US is much more specific in detecting bile duct dilation, an indirect imaging finding related to obstruction by the tumor [42].

On CT, the tumor nodules are usually isodense or slightly hypodense compared with liver and are more easily seen on dual-phase contrast-enhanced imaging; the infiltrating stenotic type tends to enhance in the arterial phase. The exophytic are more conspicuous on portal phase contrast-enhanced imaging, where they appear less dense than the liver. Delayed-phase imaging to 10–20 min may show late tumor enhancement. The mass-forming type shows peripheral

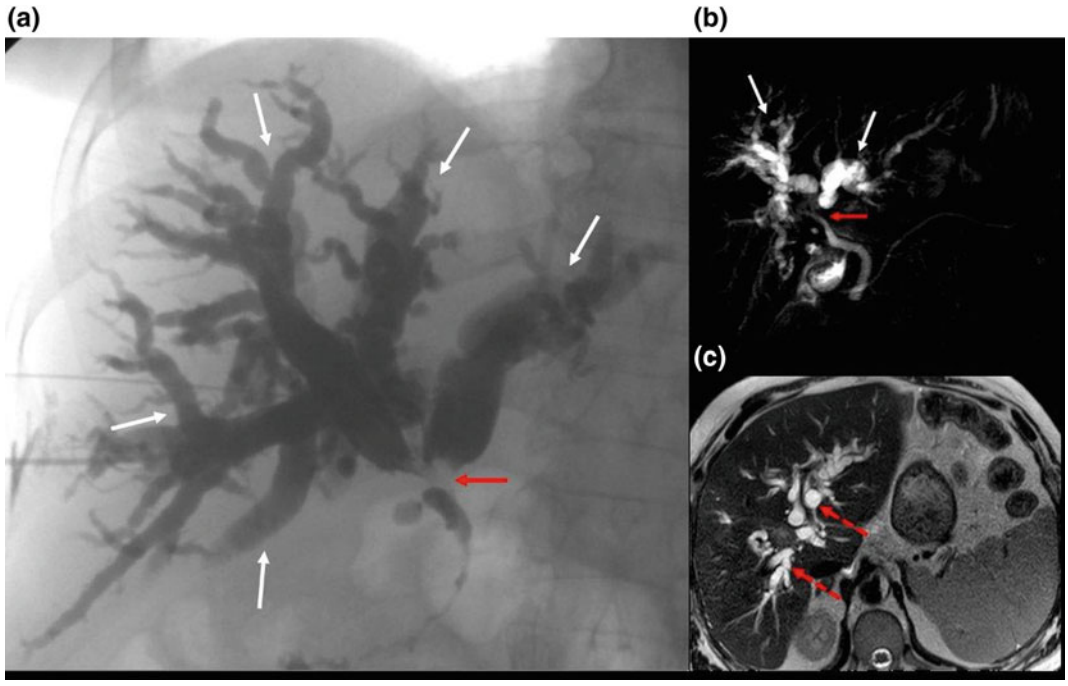

Fig. 2.9 Percutaneous Cholangiogram (**a**) and MRCP (**b**) showing a hilar obstructive lesion (*solid red arrows*) with resultant proximal biliary tree dilatation (*white arrows*). Axial T2W MR image (**c**) showing the dilated intrahepatic biliary ducts (*dashed red arrows*) with no apparent hilar lesion

enhancement on arterial phase with gradual filling in the portal and delayed phases [41].

On MRI, the tumors are hypointense on T1- and hyperintense on T2-weighted imaging and show some progressive enhancement on dynamic imaging. The most specific noninvasive modality that depicts the proximal extent of the obstruction, which critically affects treatment options, is magnetic resonance cholangiopancreatography (MRCP). In fact, it is comparable in specificity to direct cholangiography and ERCP [21].

Cholangiocarcinomas are usually hypo- or avascular, and angiography plays a minimal to no role in the diagnosis [43].

2.4.3 Metastases

The liver is one of the most common organs to which many primary malignancies from different organ systems metastasize. Hepatic metastases occur hematogenously; gastrointestinal tract tumors metastasize to the liver via the portal vein, and tumors elsewhere to the liver via the hepatic artery.

Metastases have a wide range of appearances on imaging (Fig. 2.10) but usually share the features of growth on serial imaging, multiplicity, and variation of size. Although hepatic metastases generally derive their blood supply from the hepatic artery, they can either be hypo- or hypervascular compared to the surrounding liver parenchyma. Hypervascular metastatic deposits include those from breast, kidney, thyroid, neuroendocrine, and melanoma primaries, while hypovascular deposits most commonly arise from lung, gastric, breast, and colorectal carcinoma [14, 22]. Metastatic lesions with central necrosis may have a partly cystic appearance. Mucin-secreting metastases from the GI tract may demonstrate calcifications [13]. On US, metastases appear non-specific. They may be homogeneous, have a target-sign appearance, show cystic and/or calcified components, and be of increased or decreased reflectivity [9].

On CT, most metastatic lesions are hypoattenuating on unenhanced images and remain so on portal phase images. Hypervascular tumors are often visible as low-attenuation lesions on unenhanced images, enhance avidly in the arterial phase, then fade to isointensity or wash out to hypodensity in the portal or delayed phases. CT is the most sensitive method for detecting the subtle calcifications that may occur within mucin-secreting metastases of GI tract origin.

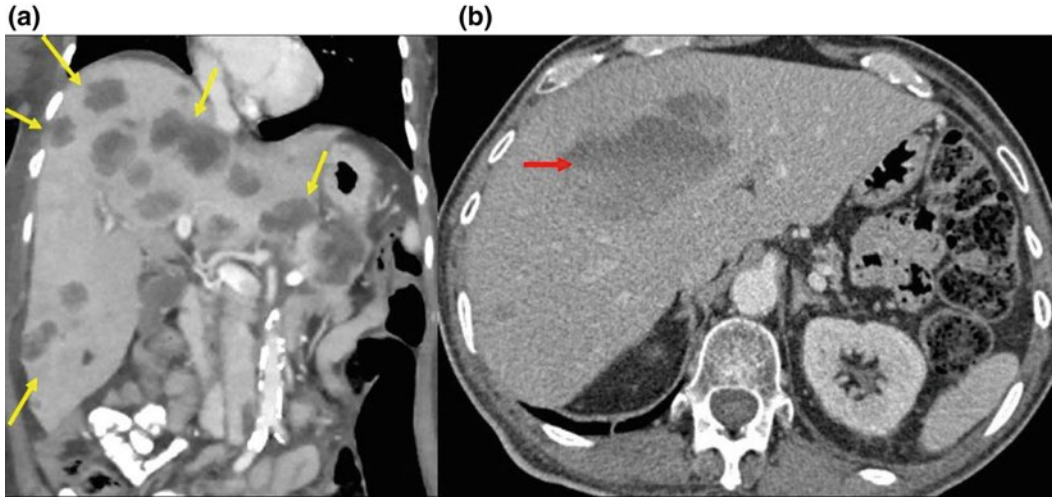

Fig. 2.10 Coronal image from an enhanced CT scan showing multiple, scattered hypodense metastatic liver lesions from colon cancer (*yellow arrows*) (**a**). Axial image from an enhanced CT scan showing a hemorrhagic metastatic lesion with dense blood layering in the lesion (*red arrow*) (**b**)

Central necrosis and rim enhancement can also be clearly demonstrated on CT [13].

On MRI, the majority of metastases are of low signal on T1W and high signal on T2W images. However, lesions with hemorrage or melanoma may have a high signal on T1-weighted imaging. Lesions with a hyperintense viable rim on T2-weighted imaging and hypointense necrotic center have a characteristic "target-sign" appearance [14]. Contrast-enhanced MR studies give similar appearances to CT for the detection and demonstration of lesions in the unenhanced, arterial, and portal phases. Hepatobiliary-specific contrast serves to increase the signal difference between metastatic lesions and background parenchyma thereby increasing their detection [14, 44]. On colloid radionuclide imaging, the majority of metastases appear as areas of reduced activity due to a lack of Kupffer cells.

Studies comparing the relative sensitivity and specificity of cross-sectional imaging techniques in the detection of hepatic metastases can be difficult to evaluate because of variations of technique, methods of validation, and the rapid evolution of imaging technology. For example, in one systematic review, the sensitivities of MRI (after 2004), CT, and PET/CT in detecting colorectal cancer (CRC) liver metastasis in patients without prior chemotherapy treatment were 85, 74, and 66%, respectively [45]. The sensitivities dropped for MRI and CT to 60 and 47%, respectively, for lesions less than one cm.

Post neoadjuvant chemotherapy, the sensitivities were 86, 70, and 52% for MRI, CT, and PET/CT, respectively [46]. In clinical practice, the choice of imaging technique is usually influenced by the likely management implications and local availability and expertise [13].

2.5 Imaging of Irradiated Liver and Liver Tumors

2.5.1 Imaging of Irradiated Normal Liver

Radiographic characterization of irradiated liver tumors and normal liver parenchyma is challenging and can require close collaboration between the diagnostic radiologist and treating radiation oncologist. Herfarth and colleagues described three types of focal radiographic appearances (on CT scan with multiphase contrast) in patients with liver tumors irradiated with high single-fraction radiation doses [47]. In the type I reaction, the liver parenchyma irradiated past a threshold dose appeared hypodense in portal venous phase imaging, and isodense in late-phase imaging; in the type II reaction, the liver parenchyma was hypodense in portal venous phase imaging and hyperdense in late-phase imaging; in the type III reaction, the liver parenchyma was isodense or hyperdense in portal venous phage imaging and hyperdense in late-phase imaging. The reactions appeared to follow a temporal pattern, with the type III reaction following type I and II reactions in sequence. The authors postulated that the type II reaction appearance is related to the veno-occlusive histopathologic findings seen in irradiated liver tissue. Obstruction of venous inflow of contrast to damaged liver tissue would make it hypodense relative to undamaged liver tissue that is well perfused during the portal venous phase of imaging. In late-phase imaging, contrast would now be presented in the damaged liver tissue and it would appear hyperdense relative to the rest of the liver parenchyma. Olsen and colleagues provided support for this model in a study with both radiographic and histopathologic imaging of high-dose irradiated liver [48]. Figure 2.11 shows early (3 months) post-imaging changes consistent with a type II reaction in a patient with hepatocellular carcinoma treated with stereotactic radiation therapy.

2.5.2 Imaging of Irradiated Liver Tumors

Arterial phase contrast enhancement is a hallmark of hypervascular liver tumors such as hepatocellular carcinoma. Embolization and radiofrequency ablation can directly affect blood vessels through occlusion and/or direct ablation. Thus, eradicated tumors that have been treated with these

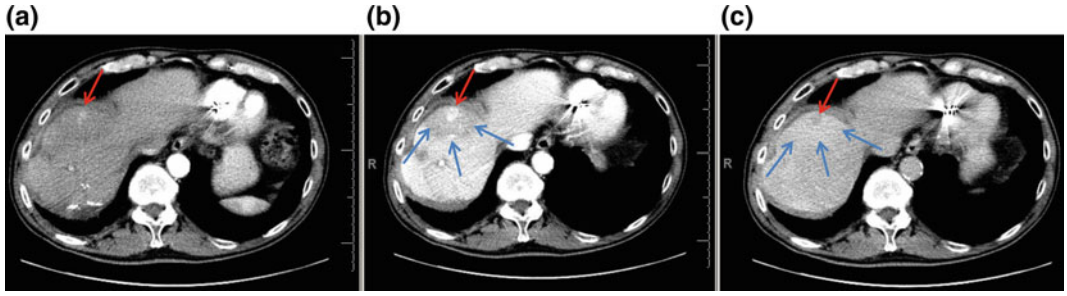

Fig. 2.11 Axial images of a segment eight hepatocellular carcinoma lesion treated with stereotactic radiation therapy. **a** Arterial phase imaging showing contrast enhancement (*red arrow*), **b** portal venous phase imaging showing continuing enhancement (*red arrow*) with a surrounding rim of injured, hypodense liver (*blue arrows*), **c** delayed-phase imaging with washout of contrast from the tumor and subtle hyperenhancement of the immediately surrounding liver (*blue arrows*)

approaches will lose contrast enhancement, and this is considered to be associated with induction of tumor necrosis. The European Association for the Study of the Liver (EASL) guidelines call for post-treatment measurement of the enhancing area of treated tumors, distinct from traditional RECIST criteria, which measures overall tumor size. The AASLD adopted the assessment of tumor necrosis (loss of contrast enhancement), as opposed to assessment of tumor size, in what is known as modified RECIST (mRECIST) criteria, and recommended that this be used in future studies of novel therapies for the treatment of hepatocellular cancer [49]. As discussed elsewhere in this book, radiation therapy differs from embolization and thermal ablations with respect to the manner and kinetics of tumor cell kill, as well as effects on blood vessels. Thus, changes in enhancement patterns, and overall tumor size, may differ post-radiation as compared with interventional approaches. Price et al. reported on the time course of contrast and tumor size changes following high-dose stereotactic radiation therapy for hepatocellular carcinoma. There was a gradual and progressive loss of contrast enhancement which paralleled a decrease in tumor size (with tumor size reduction less pronounced), continuing to 12 months following the completion of radiation [50].

PET and various sequences on MRI may also be helpful in determining the response of treated liver tumors to radiation as well. A sustained decrease in the maximum SUV value following treatment indicates tumor response, whereas an increase in FDG avidity is suspicious for residual cancer [51]. On MR imaging, changes in diffusion-weighted signal intensity as well as T2 signal hyperintensity can be followed to assess lesion response [51].

References

1. Kekis P, Kekis B. Surgical anatomy of the liver. In: Liver and Biliary Tract Surg. Vienna: Springer; 2006. pp. 17–33.
2. Webb WR, Brant WE, Major NM. Fundamentals of body CT. Elsevier Health Sciences. 5 Sep 2014. pp. 188–213.
3. Sibulesky L. Normal liver anatomy. Clin Liver Dis. 2013 Mar 1;2(S1).
4. Lim MC, Tan CH, Cai J, Zheng J, Kow AW. CT volumetry of the liver: where does it stand in clinical practice? Clin Radiol. 2014;69(9):887–95.
5. L'Herminé C. Normal hepatic circulation—anatomy and physiology. In: Radiol of Liver Circ. Netherlands: Springer;1985. pp. 1–3.
6. Lafortune M, Madore F, Patriquin H, Breton G. Segmental anatomy of the liver: a sonographic approach to the Couinaud nomenclature. Radiology. 1991;181(2):443–8.
7. O'Neil M, Damjanov I, Taylor RM. Normal liver. In: Liver Pathology for Clinicians. Springer International Publishing;2015. pp. 1–9.
8. Gelfand DW. The liver: plain film diagnosis. Semin Roentgenol. 1975;10(3):177–85. WB Saunders.
9. Nisenbaum HL, Rowling SE. Ultrasound of focal hepatic lesions. Semin Roentgenol. 1995;30(4): 324–46. WB Saunders.

10. McNaughton DA, Abu-Yousef MM. Doppler US of the liver made simple 1. Radiographics. 2011;31 (1):161–88.
11. Sandstede JJ, Tschammler A, Beer M, Vogelsang C, Wittenberg G, Hahn D. Optimization of automatic bolus tracking for timing of the arterial phase of helical liver CT. Eur Radiol. 2001;11(8):1396–400.
12. Sahani DV, Singh AH. Dual-phase liver MDCT. In: MDCT: a pract approach. Milan: Springer; 2006. pp. 39–48.
13. Sica GT, Ji H, Ros PR. CT and MR imaging of hepatic metastases. Am J Roentgenol. 2000;174 (3):691–8.
14. Namasivayam S, Martin DR, Saini S. Imaging of liver metastases: MRI. Cancer Imaging. 2007;7(1):2.
15. Liu PS, Hussain HK. Contemporary and emerging technologies in abdominal magnetic resonance imaging. Semin Roentgenol. 2013;48(3):203–13. Elsevier.
16. Katabathina VS, Dasyam AK, Dasyam N, Hosseinzadeh K. Adult bile duct strictures: role of MR imaging and MR cholangiopancreatography in characterization. Radiographics. 2014;34(3):565–86.
17. Seale MK, Catalano OA, Saini S, Hahn PF, Sahani DV. Hepatobiliary-specific MR contrast agents: role in imaging the liver and biliary tree 1. Radiographics. 2009;29(6):1725–48.
18. Kinnard MF, Alavi A, Rubin RA, Lichtenstein GR. Nuclear imaging of solid hepatic masses. Semin Roentgenol. 1995;30(4)375–95. WB: Saunders.
19. Kim JY, Kim MH, Lee TY, Hwang CY, Kim JS, Yun SC, Lee SS, Seo DW, Lee SK. Clinical role of 18F-FDG PET-CT in suspected and potentially operable cholangiocarcinoma: a prospective study compared with conventional imaging. Am L Gastroenterol. 2008;103(5):1145–51.
20. Schlant RC, Galambos JT, Shuford WH, Rawls WJ, Winter TS, Edwards FK. The clinical usefulness of wedge hepatic venography. Am J Med. 1963;35 (3):343–9.
21. Halefoglu AM. Magnetic resonance cholangiopancreatography. Semin Roentgenol. 2008;43(4):282–9. WB: Saunders.
22. Maniam S, Szklaruk J. WJR. World. 2010;2(8): 309–22.
23. Wachsberg RH, Bahramipour P, Sofocleous CT, Barone A. Hepatofugal flow in the portal venous system: pathophysiology, imaging findings, and diagnostic pitfalls 1. Radiographics. 2002;22 (1):123–40.
24. Gupta AA, Kim DC, Krinsky GA, Lee VS. CT and MRI of cirrhosis and its mimics. Am J Roentgenol. 2004;183(6):1595–601.
25. Sangster GP, Previgliano CH, Nader M, Chwoschtschinsky E, Heldmann MG. MDCT imaging findings of liver cirrhosis: spectrum of hepatic and extrahepatic abdominal complications. HPB Surg. 2013;6:2013.
26. Tappouni R, Sakala MD, Hosseinzadeh K. Mimics of Hepatic Neoplasms. Semin Roentgenol. 2015;50 (4):305–19. Elsevier.
27. Watanabe A, Ramalho M, AlObaidy M, Kim HJ, Velloni FG, Semelka RC. Magnetic resonance imaging of the cirrhotic liver: an update. World J Hepatol. 2015;7(3):468.
28. Yilmaz S, Yekeler E, Rozanes I. Hepatobiliary and pancreatic: Gamna–Gandy bodies of the spleen. J Gastroen Hepatol. 2007;22(5):758.
29. Aspestrand F, Kolmannskog F. CT and angiography in chronic liver disease. Acta Radiol. 1992;33 (3):251–4.
30. Clark HP, Carson WF, Kavanagh PV, Ho CP, Shen P, Zagoria RJ. Staging and current treatment of hepatocellular carcinoma 1. Radiographics. 2005;25(suppl_1):S3–23.
31. Hanna RF, Aguirre DA, Kased N, Emery SC, Peterson MR, Sirlin CB. Cirrhosis-associated hepatocellular nodules: correlation of histopathologic and MR imaging features 1. Radiographics. 2008;28 (3):747–69.
32. ACR (American College of Radiology). Liver imaging reporting and data system. http://www.acr.org/Quality-Safety/Resources/LIRADS.
33. Tublin ME, Dodd GD 3rd, Baron RL. Benign and malignant portal vein thrombosis: differentiation by CT characteristics. Am J Roemtgenol. 1997;168 (3):719–23.
34. Hussain SM, Reinhold C, Mitchell DG. Cirrhosis and lesion characterization at MR imaging 1. Radiographics. 2009;29(6):1637–52.
35. Yamashita Y, Takahashi M, Baba Y, Kanazawa S, Charnsangavej C, Yang D, Wallace S. Hepatocellular carcinoma with or without cirrhosis: a comparison of CT and angiographic presentations in the United States and Japan. Abdom Imaging. 1993;18(2):168–75.
36. McEvoy SH, McCarthy CJ, Lavelle LP, Moran DE, Cantwell CP, Skehan SJ, Gibney RG, Malone DE. Hepatocellular carcinoma: illustrated guide to systematic radiologic diagnosis and staging according to guidelines of the American Association for the Study of Liver Diseases. Radiographics. 2013;33(6):1653–68.
37. Purysko AS, Remer EM, Coppa CP. Leão Filho HM, Thupili CR, Veniero JC. LI-RADS: a case-based review of the new categorization of liver findings in patients with end-stage liver disease. Radiographics. 2012;32(7):1977–95.
38. Mitchell DG, Bruix J, Sherman M, Sirlin CB. LI-RADS (liver imaging reporting and data system): summary, discussion, and consensus of the LI-RADS management working group and future directions. Hepatology. 2015;61(3):1056–65.
39. Blechacz BR, Gores GJ. Cholangiocarcinoma. Clin Liver Dis. 2008;12(1):131–50.
40. Engelbrecht MR, Katz SS, van Gulik TM, Laméris JS, van Delden OM. Imaging of perihilar cholangiocarcinoma. Am J Roentgenol. 2015;204(4):782–91.

41. Chung YE, Kim MJ, Park YN, Choi JY, Pyo JY, Kim YC, Cho HJ, Kim KA, Choi SY. Varying appearances of cholangiocarcinoma: radiologic-pathologic correlation 1. Radiographics. 2009;29 (3):683–700.
42. Sainani NI, Catalano OA, Holalkere NS, Zhu AX, Hahn PF, Sahani DV. Cholangiocarcinoma: current and novel imaging techniques 1. Radiographics. 2008;28(5):1263–87.
43. Soulen MC. Angiographic evaluation of focal liver masses. In Semin Roentgenol. 1995;30(4):362–74.
44. Oliva MR, Saini S. Liver cancer imaging: role of CT, MRI, US and PET. Cancer Imaging. 2004.4 Spec No A:S42.
45. Niekel MC, Bipat S, Stoker J. Diagnostic imaging of colorectal liver metastases with CT, MR imaging, FDG PET, and/or FDG PET/CT: a meta-analysis of prospective studies including patients who have not previously undergone treatment 1. Radiology. 2010;257(3):674–84.
46. van Kessel CS, Buckens CF, van den Bosch MA, van Leeuwen MS, van Hillegersberg R, Verkooijen HM. Preoperative imaging of colorectal liver metastases after neoadjuvant chemotherapy: a meta-analysis. Ann Surg Oncol. 2012;19(9):2805–13.
47. Herfarth KK, Hof H, Bahner ML, et al. Assessment of focal liver reaction by multiphasic CT after stereotactic single-dose radiotherapy of liver tumors. Int J Radiat Oncol Biol Phys. 2003;57:444–51.
48. Olsen CC, Welsh J, Kavanagh BD, et al. Microscopic and macroscopic tumor and parenchymal effects of liver stereotactic body radiotherapy. Int J Radiat Oncol Biol Phys. 2009;73:1414–24.
49. Lencioni R, Llovet JM. Modified RECIST (mRECIST) assessment for hepatocellular carcinoma. Semin Liver Dis. 2010;30(1):52–60.
50. Price TR, Perkins SM, Sandrasegaran K, et al. Evaluation of response after stereotactic body radiotherapy for hepatocellular carcinoma. Cancer. 2012;118:3191–8.
51. Haddad MM, Merrell KW, Hallemeier CL, et al. Stereotactic body radiation therapy of liver tumors: post-treatment appearances and evaluation of treatment response: a pictorial review. Abdom Radiol (NY). 2016;41:2061–77.

Assessment of Liver Function: Focus on the ALBI Score

3

Philip J. Johnson, MD, FRCP, Harun Khan, MBBS and Sarah Berhane, PhD

3.1 Introduction

Most patients with hepatocellular carcinoma (HCC) have two distinct, but related, diseases, a chronic liver disease (CLD) and the tumour, i.e. the HCC itself. The former may be attributable to one of numerous well-recognised aetiologies ranging from the common, such as chronic viral hepatitis types B and/or C, alcohol-related and non-alcoholic fatty liver disease (NAFLD) to the rarer types such as primary biliary cirrhosis, hemochromatosis and autoimmune hepatitis. By the time HCC is diagnosed, the fibrosis associated with one of these liver diseases has often, but not always, reached the stage of 'cirrhosis', defined histologically as the presence of regenerative nodules of hepatocytes surrounded by fibrotic connective tissue that bridges between portal tracts.

This associated liver disease impinges on all aspects of HCC management. Diagnosis is made more complicated, since it is easy to confuse nodular regeneration with HCC, on radiological examination, both in the primary diagnostic setting and whilst undertaking screening/surveillance. Liver biopsy may be complicated by haemorrhage. The prognosis is also intimately related to the underlying liver disease, as death and morbidity may be associated with all the complications of CLD including variceal haemorrhage and liver failure rather than the actual HCC. Indeed, the underlying liver disease and the HCC can be seen as 'competing' causes of death in HCC.

Herein we discuss the various systems that have been developed to quantify and monitor the severity of the CLD in patients with HCC.

3.2 The Child-Pugh Score/Class and Its Limitations

The Child-Pugh classification is the most widely used system for assessing the severity of chronic liver disease. It involves five components. These include two discrete variables: presence or absence of ascites and encephalopathy; and three continuous variables: prothrombin time (PT), serum albumin and bilirubin level. Each component is scored individually (1, 2 or 3 points—3 being the most severe) using empirically selected cut-off values. The total score for each patient determines their Child-Pugh class (A, B or C—C having the worst prognosis) and hence the severity of their chronic liver disease.

Despite its wide use, there are several limitations to the Child-Pugh scoring system. Although each variable has a statistically significant effect on the severity of liver disease, there is

P.J. Johnson (✉) · S. Berhane
Department of Molecular and Clinical Cancer Medicine, University of Liverpool, The Sherrington Building, 2nd floor, Ashton Street, Liverpool L69 3GE, UK
e-mail: Philip.Johnson@liverpool.ac.uk

H. Khan
School of Medicine, Imperial College, London, UK

J. Meyer and T.E. Schefter (eds.), *Radiation Therapy for Liver Tumors*,
DOI 10.1007/978-3-319-54531-8_3

interdependence amongst some of the parameters. For example, albumin levels and PT have a strong correlation, as both are dependent upon the hepatic synthesis of proteins (albumin and coagulation factors, respectively). The inclusion of both of these variables in one scoring system may lead to their overemphasis [1].

Second, the cut-off values for the continuous variables are not based on clear evidence in relation to the prognosis of chronic liver disease. Specifically, different cut-off scores do not clearly correspond to significant changes in disease prognosis, such as mortality risk [1]. Moreover, the discrete variables suffer from a 'ceiling effect', as values that correspond to a score of 3 may vary significantly. For example, patients with scores of 3 may have bilirubin levels just above 51 μmol/l or significantly above this threshold [1].

Each variable in the CPS is equally weighted [2]. In practice, the variables may impact disease prognosis to differing extents. They may not be equally important when reviewing the prognosis of chronic liver disease. For example, the newer scoring system that assesses chronic liver disease severity, the model for end-stage liver disease (MELD) score, places differing emphasis on its constituent variables based on their impact upon disease prognosis [2] (and see MELD section).

Another commonly criticised feature is the ambiguity of the formal descriptors of each discrete variable. They may be interpreted differently by different clinicians. For example, ascites is classified as mild, moderate or severe, which may be a subjective score—ultimately leading to differences in individual scores for the same patient. The ambiguous language used to describe the cut-offs has also led to slight alterations in the descriptions across literature sources. For example, some resources score "moderate ascites" with 2 points, whilst others score "moderate ascites" with 3 points.

Moreover, many factors that are regarded very important in chronic liver disease prognosis have been excluded by the Child-Pugh system. A widely cited example includes renal function assessment [3, 4]. Additional variables include markers of portal hypertension, such as oesophageal varices, age and serum creatinine [2]—the latter of which is included in the MELD score with twice the emphasis as bilirubin levels [1]. Finally, the cause of cirrhosis is also not considered in the Child-Pugh scoring system nor is co-existent risk factors, which may influence the morbidity attributable to cirrhosis. These include viral infections, such as hepatitis B, high-risk behaviours, such as chronic alcohol abuse and inflammatory processes as in autoimmune hepatitis [5]. Overall, although still widely used, there are many limitations of the Child-Pugh score, which are becoming increasingly criticised. Nonetheless, as shown in Fig. 3.1, AASLD (American Association of the Study of Liver Disease) Guidelines for staging and treatment of HCC are in part a function of the CPS.

3.3 Alternatives to CPS—The Model for End-Stage Liver Disease (MELD)

MELD is, like the ALBI score, described below, a validated statistically based model that predicts mortality in patients with cirrhosis. It is based on three variables—serum bilirubin, serum creatinine and the international normalised ratio (INR). Although originally developed in the field of portal hypertension management [4] it has, since 2002, been adopted by the United Network for Organ Sharing (UNOS) for prioritisation of patients awaiting liver transplantation in the United States [7]. Subsequent analyses have shown it to be a reliable prognostic model in many other forms of chronic liver disease; aetiology appears to have only a minor influence on its utility [8].

The formula is as follows:

$$\begin{aligned}\text{MELD} = 3.78 &\times \ln[\text{serum bilirubin } (\text{mg/d}L)] + 11.2 \\ &\times \ln[\text{INR}] + 9.57 \\ &\times \ln[\text{serum creatinine } (\text{mg/dL})] + 6.43.\end{aligned}$$

The result is presented as a continuous variable ranging from 6 to 40. The higher the MELD

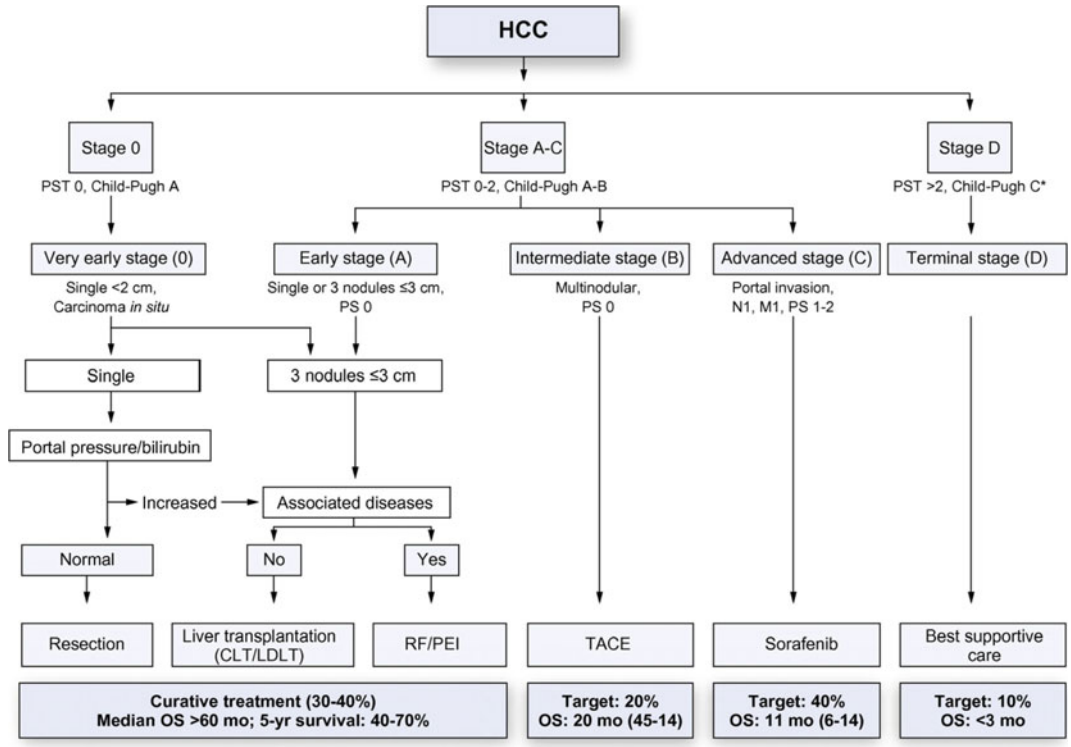

Fig. 3.1 The BCLC staging system. Note the central role of CPS in deciding stage and hence therapeutic options. Reprinted from [6]. With permission from Elsevier

score, the worse the mortality. Approximate figures for 3-month mortality in patients with 'end-stage liver disease' are 71.3, 52.5, 6 and 1.9% at scores of 30–39, 20–29, 10–19 and <9, respectively.

Although the three variables in MELD are apparently 'objective', it is now recognised that there is methodology-related inter-laboratory variation in INR (in the order of 25%) and creatinine (particularly in those undergoing paracentesis or receiving diuretics) and these variations may have a significant impact on the final score [9, 10]. Furthermore, serum creatinine is influenced by body mass [11] a particularly important factor in patients with malignant disease such as HCC [11]. Finally, the MELD score is, strictly speaking, like the CPS, designed and developed to be applied to patients with cirrhosis, rather than chronic liver disease in general. The MELD-Na score is discussed in detail in Chap. 1.

3.4 Alternatives to CPS—The Albumin–Bilirubin (ALBI) Score

Recognising the limitations of the CPS we have developed a new approach to the estimation of 'liver function' specifically for application in the setting of HCC [12]. We used a large dataset of patients with HCC from which to identify those liver-related factors that most closely influence prognosis. In the event these were identified as serum albumin and bilirubin. We then used a rigorous statistical modelling approach to develop the 'ALBI score' which can easily be characterised by a grade from 1 to 3, 1 being the best and 3 the worst. In all clinical situations the ALBI score appears to be at least as good as CPS in predicting prognosis and in some scenarios, better. Given that it only involves two of the five variables within the CPS and excludes the two

subjective variables of ascites and encephalopathy, it is likely that it can be applied consistently across a wide spectrum of liver disease. The ALBI score also has the specific strength that it is, unlike the CPS, applicable to patients with chronic liver disease (rather than just 'cirrhosis').

The score is calculated from the formula

$$\text{ALBI score} = (\log_{10}\ \text{bilirubin} \times 0.66) + (\text{Albumin} \times -0.085),$$

where bilirubin is in μmol/l and albumin in g/L.

Specific cut-offs are then applied to generate three prognostic groups, ALBI score ≤ -2.60 (ALBI grade 1), > -2.60 to ≤ -1.39 (ALBI grade 2) and > -1.39 (ALBI grade 3).

Although superficially it appears complex, it is simple to derive a grade from a 'heat map' (Fig. 3.2).

Below we illustrate the application of the ALBI score to various clinical scenarios and comment on its strengths in these particular situations.

3.5 ALBI in Early, Potentially, Curative Disease

ALBI predicts post-operative liver failure better that CPS [13] although many surgeons will use a specific test of liver function prior to resection, such as indocyanine green (ICG) [14] clearance or follow Makuchi criteria [15]. Of particular

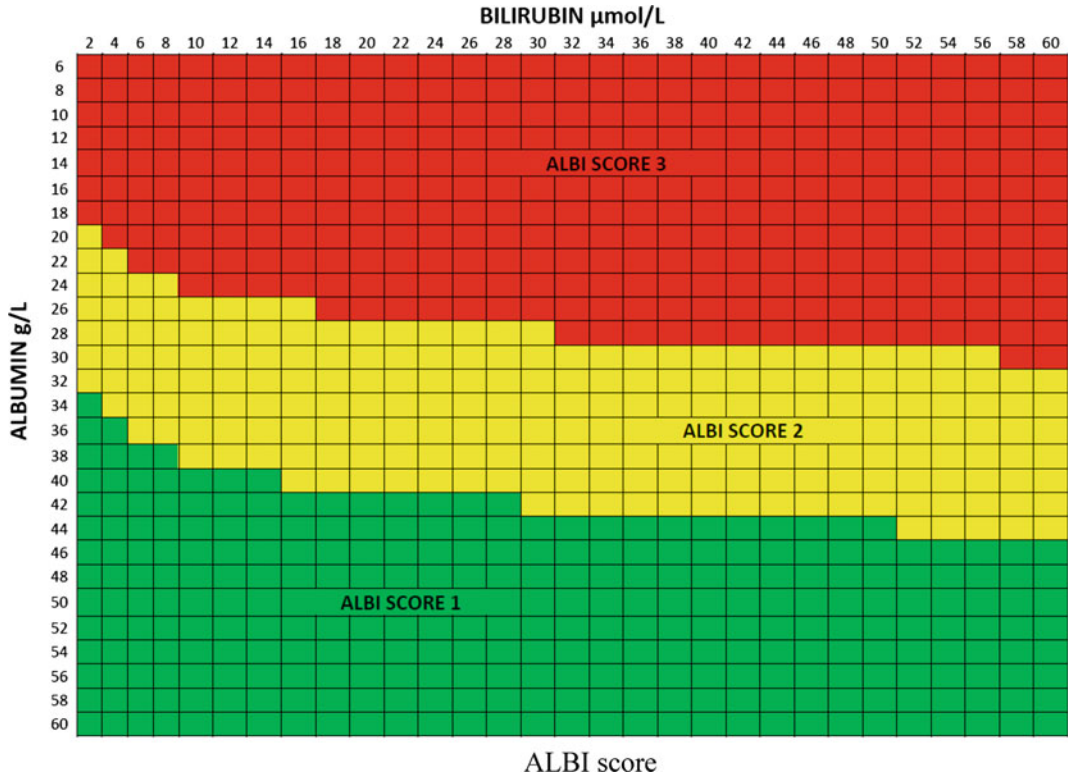

Fig. 3.2 A 'heat map' for calculation of the ALBI score/grade. The score and grade are identified as the points at which the albumin (*vertical axis*) and bilirubin (*horizontal axis*) cross. Reprinted from [12]. With permission from American Society of Clinical Oncology

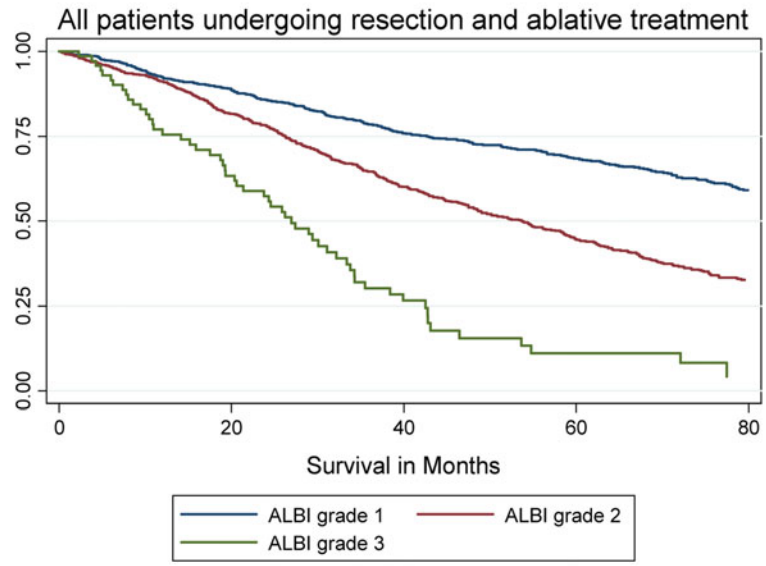

Fig. 3.3 Survival according to ALBI score in an international cohort of 2556 patients undergoing potentially curative therapy (mainly resection or radio-frequency ablation). Reprinted from [16]. Note the clarity of discrimination

ALBI grade	N	Median survival in months (95% C.I.)	5-year survival, % (95% C.I.)	Hazard ratio (95% C.I.)
1	1142	105.6 (95.6, 122.7)	67.8 (64.4, 70.9)	1
2	1032	53.6 (48.1, 58.5)	44.7 (41.1, 48.3)	2.0 (1.8, 2.3)
3	82	26.9 (20.4, 32.4)	14.6 (7.1, 24.6)	4.7 (3.7, 6.2)

note, ICG clearance correlates well with the ALBI score. In patients undergoing ablative therapies or resection administered with curative intent, the ALBI score clearly distinguishes three distinct prognostic groups [16] (Fig. 3.3). The major clinical implication is that liver function has a major impact on long-term survival even when there is no HCC recurrence.

3.6 ALBI in Intermediate HCC

Among patients with intermediate HCC receiving intra-arterial treatment such as transarterial chemo-embolisation (TACE) or selective internal radiation (SIR), ALBI grade appears to outperform CPS classification in terms of discriminating survival [17]. Figure 3.4 shows our own study comparing ALBI to CPS in patients receiving TACE [18].

3.7 ALBI in Advanced HCC and the Palliative Setting

The standard of treatment for patients with advanced, unresectable HCC is Sorafenib. In general, such treatment is confined to patients with CPS grade 'A' disease. Figure 3.5a is based on data from patients receiving Sorafenib in clinical trials and clearly demonstrates that CPS grade 'A' disease is not homogenous; patients with CPS 'A' disease have quite different prognoses when their ALBI score is 1 or 2 versus 3. The ALBI score is equally discriminatory in the palliative setting where patients receive no active treatment (Fig. 3.5b).

The benefits of Sorafenib, as shown in Fig. 3.5a, are very modest, improving survival for only around 3 months. It is becoming apparent that equally significant improvements

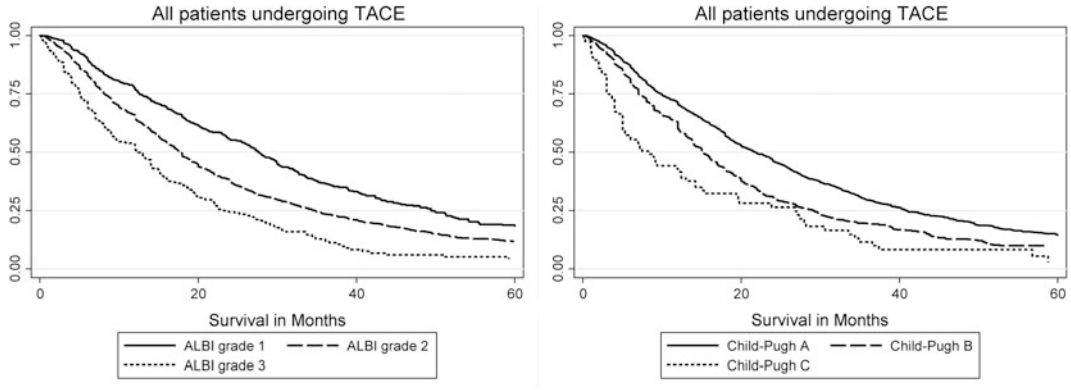

Classification system	N	Median survival in months (95% C.I.)
ALBI grade 1	659	27.60 (25.53, 29.90)
ALBI grade 2	1981	17.76 (16.94, 18.62)
ALBI grade 3	351	12.40 (9.61, 14.18)
C-P A	1791	21.78 (20.00, 23.65)
C-P B	1055	15.20 (14.00, 16.28)
C-P C	118	8.26 (5.00, 12.40)

Fig. 3.4 Comparison of ALBI and CPS in an international cohort of 2991 patients undergoing TACE. From a formal statistical standpoint, both systems are equally discriminatory. Reprinted from [18]

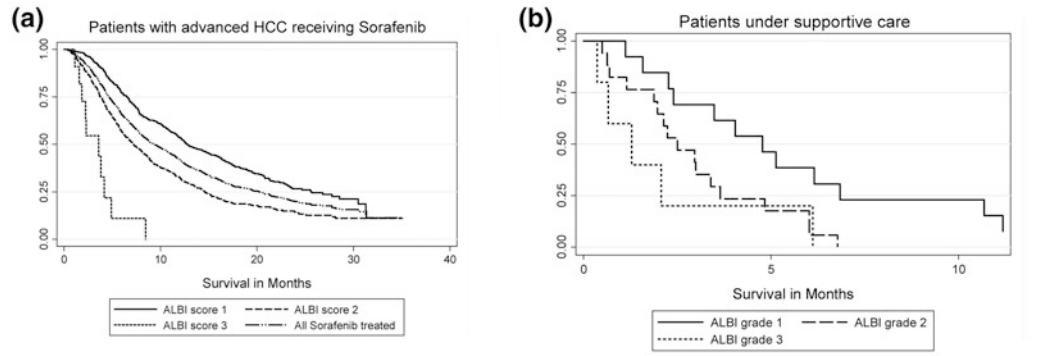

ALBI grade	N	Median survival, months (95% Conf. Interval)
1	475	12.7 (11.7, 14.9)
2	542	7.2 (6.4, 8.2)
3	11	3.6 (1.6, 4.9)
All Sorafenib treated	1028	9.3 (8.5, 10.5)

ALBI grade	N	Median survival, months (95% Conf. Interval)
1	13	4.8 (2.3, 6.8)
2	17	2.5 (1.2, 3.7)
3	5	1.3 (0.4)

Fig. 3.5 ALBI in advanced HCC and the palliative setting. In (**a**) all patients were receiving sorafenib. In (**b**) patients were receiving best supportive therapy only. Reprinted from [12]. With permission from American Society of Clinical Oncology

Table 3.1 Comparison of prognostic performance among nine staging systems

Staging system	Homogeneity likelihood ratio chi-square test	C-index	95% CI	AIC
AJCC TNM	466.201	0.675	0.659–0.691	16920.88
BCLC	996.704	0.757	0.741–0.773	16390.38
ALBI-BCLC[a]	995.797	0.760	0.744–0.777	16391.29
CLIP	1190.446	0.786	0.769–0.803	16196.64
ALBI-CLIP[a]	1229.148	0.789	0.772–0.806	16157.94
JIS	781.938	0.734	0.717–0.750	16605.15
LCSGJ TNM	471.965	0.686	0.670–0.702	16915.12
Okuda	908.873	0.728	0.714–0.743	16146.39
Tokyo	482.069	0.701	0.684–0.718	16905.01

Based on data from Ref. [19]

[a]Refers to the system performance when CPS is replaced by ALBI. The higher the homogeneity likelihood ratio and C-index, the better the discriminatory performance. *AICc* corrected Akaike information criterion; *AJCC* American Joint Committee on Cancer; *ALBI* Albumin–bilirubin; *BCLC* Barcelona Clinic Liver Cancer; *CI* Confidence interval; *CLIP* Cancer of the Liver Italian Program; *JIS* Japan Integrated Staging; *LCSGJ* Liver Cancer Study Group of Japan; *TNM* Tumour–Node–Metastasis

can be obtained by improving underlying liver function for example by treating chronic viral hepatitis. ALBI is particularly useful for documenting changes in liver function over time (being far more 'granular' than CPS) such as occurs in the process of treating viral hepatitis; this application of ALBI is of considerable current research interest. Also, of interest, is that ALBI seems to be of similar utility in assessing survival in patients with advanced HCC who receive best supportive care only (Fig. 3.5b).

3.8 Substituting ALBI for CPS in Current Staging Systems

It must be emphasised that ALBI is not an HCC staging system—rather it is a liver function staging system. However, most current HCC staging (BCLC, JIS and CLIP) integrate the CPS to account for liver function. Recent research has demonstrated that substituting ALBI [18–23] for CPS either improves or has no detrimental effect on the system's performance (Table 3.1). Given the advantage of ALBI, listed above, it is reasonable to expect that these staging systems might be amended to involve ALBI rather CPS.

3.9 Conclusion

The CPS is the most widely used system for grading the severity of chronic liver disease. MELD is used predominantly for prioritising liver grafts for patients awaiting liver transplantation. ALBI offers numerous benefits over CPS, the limitations of which are widely acknowledged.

References

1. Durand F, Valla D. Assessment of prognosis of cirrhosis. Semin Liver Dis. 2008;28:110–22.
2. Christensen E. Prognostic models including the Child-Pugh, MELD and Mayo risk scores–where are we and where should we go? J Hepatol. 2004;41:344–50.
3. Angermayr B, Cejna M, Karnel F, et al. Child-Pugh versus MELD score in predicting survival in patients undergoing transjugular intrahepatic portosystemic shunt. Gut. 2003;52:879–85.
4. Malinchoc M, Kamath PS, Gordon FD, et al. A model to predict poor survival in patients undergoing transjugular intrahepatic portosystemic shunts. Hepatology. 2000;31:864–71.
5. Pessione F, Ramond MJ, Peters L, et al. Five-year survival predictive factors in patients with excessive

alcohol intake and cirrhosis. Effect of alcoholic hepatitis, smoking and abstinence. Liver Int. 2003;23:45–53.
6. European Association for the Study of the Liver. European Organisation for Research and Treatment of Cancer. EASL–EORTC Clinical Practice Guidelines: Management of hepatocellular carcinoma. J Hepatol. 2012;56(4):908–43.
7. Wiesner R, Edwards E, Freeman R, et al. Model for end-stage liver disease (MELD) and allocation of donor livers. Gastroenterology. 2003;124:91–6.
8. Durand F, Valla D. Assessment of the prognosis of cirrhosis: Child-Pugh versus MELD. J Hepatol. 2005;42(Suppl):S100–7.
9. Trotter JF, Olson J, Lefkowitz J, et al. Changes in international normalized ratio (INR) and model for endstage liver disease (MELD) based on selection of clinical laboratory. Am J Transplant. 2007;7:1624–8.
10. Cholongitas E, Marelli L, Kerry A, et al. Different methods of creatinine measurement significantly affect MELD scores. Liver Transpl. 2007;13:523–9.
11. Nankivell BJ. Creatinine clearance and the assessment of renal function. Aust Prescr. 2001;24:15–7.
12. Johnson PJ, Berhane S, Kagebayashi C, et al. Assessment of liver function in patients with hepatocellular carcinoma: A new evidence-based approach-the ALBI grade. J Clin Oncol. 2015;33:550–8.
13. Zou D, Qi X, Zhu C, et al. Albumin-bilirubin score for predicting the in-hospital mortality of acute upper gastrointestinal bleeding in liver cirrhosis: A retrospective study. Turk J Gastroenterol. 2016;27:180–6.
14. Hemming AW, Scudamore CH, Shackleton CR, et al. Indocyanine green clearance as a predictor of successful hepatic resection in cirrhotic patients. Am J Surg. 1992;163:515–8.
15. Makuuchi M, Kosuge T, Takayama T, et al. Surgery for small liver cancers. Semin Surg Oncol. 1993;9:298–304.
16. Toyoda H, Lai PB, O'Beirne J, et al. Long-term impact of liver function on curative therapy for hepatocellular carcinoma: application of the ALBI grade. Br J Cancer. 2016;114:744–50.
17. Hickey R, Mouli S, Kulik L, et al. Independent Analysis of Albumin-Bilirubin Grade in a 765-Patient Cohort Treated with Transarterial Locoregional Therapy for Hepatocellular Carcinoma. J Vasc Interv Radiol. 27(6):795–802. doi:10.1016/j.jvir.2016.03.005. Epub 2016 Mar 31.
18. Waked I, Berhane S, Toyoda H, et al. Transarterial chemo-embolisation of hepatocellular carcinoma: impact of liver function and vascular invasion. Br J Cancer. 2017;116(4):448–54. doi:10.1038/bjc.2016.423. Epub 2017 Jan 26. [PubMed PMID: 28125820; PubMed Central PMCID: PMC5318968].
19. Chan AW, Kumada T, Toyoda H, et al. Integration of albumin-bilirubin (ALBI) score into Barcelona clinic liver cancer (BCLC) system for hepatocellular carcinoma. J Gastroenterol Hepatol 2016;31(7):1300–6. doi:10.1111/jgh.13291.
20. Chan AW, Chong CC, Mo FK, et al. Applicability of albumin-bilirubin-based Japan integrated staging score in hepatitis B-associated hepatocellular carcinoma. J Gastroenterol Hepatol. 2016;31(10):1766–72. doi:10.1111/jgh.13339. [PubMed PMID: 26992142].
21. Chan AW, Chong CC, Mo FK, et al. Incorporating albumin-bilirubin grade into the cancer of the liver Italian program system for hepatocellular carcinoma. J Gastroenterol Hepatol. 2017;32(1):221–8. doi:10.1111/jgh.13457. [PubMed PMID: 27257086].
22. Shao YY, Liu TH, Lee YH, et al. Modified CLIP with objective liver reserve assessment retains prognosis prediction for patients with advanced hepatocellular carcinoma. J Gastroenterol Hepatol. 2016;31(7):1336–41. doi:10.1111/jgh.13312.
23. Hiraoka A, Kumada T, Michitaka K, et al. Usefulness of albumin-bilirubin (ALBI) grade for evaluation of prognosis of 2584 Japanese patients with hepatocellular carcinoma. J Gastroenterol Hepatol. 2016;31(5):1031–6. doi:10.1111/jgh.13250.

Radiation Sensitivity of the Liver: Models and Clinical Data

4

Issam El Naqa, MA, MS, PhD, DABR, Kyle Cuneo, MD, Dawn Owen, MD, PhD, Theodore S. Lawrence, MD, PhD and Randall K. Ten Haken, PhD

4.1 Introduction

Liver radiation exposure commonly occurs during radiotherapy treatment of gastrointestinal (GI) malignancies. A variety of descriptions of liver toxicity are in use. Historically, the phenomenon of radiation-induced liver disease (RILD) was reported as early as the 1920s but its pathophysiology was not characterized until 1966 in the seminal work by Reed and Cox [1]. RILD is divided into classical and nonclassical types. In classical RILD, the patients present with fatigue, weight gain, increased abdominal girth, hepatomegaly, anicteric ascites, and high elevation in alkaline phosphatase (ALP) [2]. In nonclassical RILD, patients with underlying chronic hepatic disease such as cirrhosis and viral hepatitis present with jaundice and elevated serum transaminases (ALT/AST) [3]. Clinically, RILD typically occurs between 4 and 8 weeks after irradiation but could happen as early as 2 weeks and as late as 7 months after completion of treatment [4]. RILD is a major limiting factor to dose escalation or re-irradiation for GI cancers.

Other toxicity metrics are also in use. The CTCAE version 4.0 [5] defines liver toxicity of grade ≥ 3 clinically as mild to severe encephalopathy (i.e., loss of brain function due to increased toxins in the blood) that would interfere with activities of daily living (ADL), or enzymatically by elevated levels of alkaline phosphatase (ALP), alanine aminotransferase (ALT), aspartate aminotransferase (AST), or gamma-glutamyl transpeptidase (GGT) as summarized in Table 4.1.

4.2 Histopathology of Radiation Liver Injury

It has been long recognized that the pathological lesion in classical RILD is veno-occlusive disease (VOD), which is characterized by congestion in the central portion of each liver lobule formed by trapped erythrocytes in a dense network of reticulin and collagen fibers [2]. It is believed that elevated levels of transforming growth factor beta (TGF-β) mediate this process by stimulating migration of fibroblasts that proliferate and deposit collagen in areas of RILD; likely in a similar fashion to other liver fibrotic diseases [6]. Radiologically, RILD is characterized on computed tomography (CT) imaging as a hypodense region in the liver parenchyma within the target volume. This was first reported by Yamasaki et al. [7] as shown in Fig. 4.1. Hypodensity in the portal venous phase likely reflects impaired inflow of venous blood, and hyperdensity seen in delayed phase likely is a result of impaired outflow of contrast related to the venous obstruction.

I. El Naqa (✉) · K. Cuneo · D. Owen · T.S. Lawrence · R.K. Ten Haken
Department of Radiation Oncology, University of Michigan Health System, Argus Building I, 519 W. William, Ann Arbor, MI 48103, USA
e-mail: ielnaqa@med.umich.edu

J. Meyer and T.E. Schefter (eds.), *Radiation Therapy for Liver Tumors*,
DOI 10.1007/978-3-319-54531-8_4

Table 4.1 NCI CTCAE (Common Terminology Criteria for Adverse Events) v4.0 liver toxicity

Adverse event	Grade 1	Grade 2	Grade 3	Grade 4	Grade 5
ALP increased	>ULN–2.5 × ULN	>2.5–5 × ULN	>5–20 × ULN	>20 × ULN	
Total bilirubin increased	>ULN–1.5 × ULN	>1.5–3 × ULN	>3–10 × ULN	>10 × ULN	
GGT increased	>ULN–2.5 × ULN	>2.5–5 × ULN	>5–20 × ULN	>20 × ULN	
AST increased	>ULN–3 × ULN	>3–5 × ULN	>5–20 × ULN	>20 × ULN	
ALT increased	>ULN–3 × ULN	>3–5 × ULN	>5–20 × ULN	>20 × ULN	
Liver failure (clinical)			Asterixis; mild encephalopath; limiting self-care ADL	Moderate to severe encephalopathy; coma; life-threatening consequences	Death
Portal hypertension		Decreased portal vein flow	Reversal/retrograde portal vein flow associated with varices and/or ascites	Life-threatening consequences; urgent operative intervention needed	Death

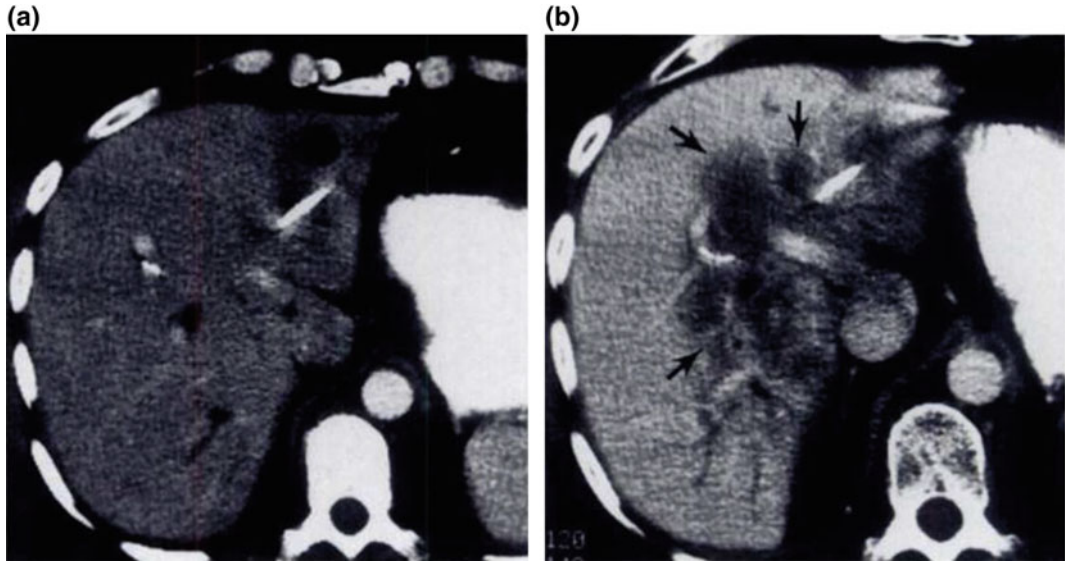

Fig. 4.1 Classical RILD on CT images. **a** Pretreatment CT scan showing baseline homogeneous hepatic parenchymal density **b** Posttreatment CT showing a geographic region of RILD with irregular decreased attenuation pointed by the *arrows* [7]. (Reprinted with permission from the American Journal of Roentgenology)

In nonclassical RILD, hepatocyte loss and dysfunction along with hepatic sinusoidal endothelial death and stellate cell activation are observed [8]. As noted earlier, these patients develop elevated ALT/AST indicating severe damage to the hepatocytes. It has been shown that patients who are hepatitis B carriers or had CP class B cirrhosis are at a higher risk of RILD [9]. Other clinical risk factors for RILD include prior transcatheter arterial chemoembolization

(TACE), concurrent chemotherapy, portal vein tumor thrombosis, tumor stage, and male sex [3, 8, 10, 11].

4.3 Normal Tissue Complication Probability (NTCP) Modeling

4.3.1 Overview

Radiation-induced injuries and toxicities involve a complex cascade of radiobiological processes that can begin within a few hours after irradiation and can progress over weeks, months, and years. According to the onset time of these toxicities, they are clinically classified into early and late effects. Early effects are typically transient and manifest during treatment or within a few weeks of the completion of a fractionated radiotherapy schedule [12, 13]. The mathematical modeling of such effects can be carried out using *bottom-up* and/or *top-down* approaches [14]. Bottom-up approaches use first principles of physics, chemistry, and biology to model cellular damage temporally and spatially in response to treatment [15, 16]. Top-down approaches are typically phenomenological models and depend on parameters available from the collected clinical, dosimetric, and/or biological data [17]. These approaches in turn are subdivided into data-driven or analytical models, which will be the main subject of this chapter.

4.3.2 NTCP Modeling

In an NTCP model, the relationship between risk variables (x) and observed toxicity probability (NTCP) could be generally represented by a mapping of the form $\mathrm{NTCP} = f(x; w)$, where w is a set of modeling parameters that need to be estimated. If the form structure $f(\cdot)$ has a finite number of parameters then the model is considered parametric (e.g., Probit, Logit, Poisson, etc.). If the form structure does not have a finite number of parameters then the model is considered to be nonparametric (e.g., Logistic regression, Cox regression, Neural network, etc.); more specifically, the model in this case is characterized as being data-driven.

4.4 NTCP Modeling of the Irradiated Liver

The most commonly used model for liver NTCP has been the Lyman model and its variants [18, 19]. The basic Lyman model is Probit-based (integral of a standard normal Gaussian distribution), which is characterized by a sigmoidal shape and is mathematically given by

$$\mathrm{NTCP}\,(D; \mathrm{TD}_{50}, m, n) = \frac{1}{\sqrt{2\pi}} \int_{-\infty}^{t} \exp\left(-u^2/2\right) \mathrm{d}u, \tag{4.1}$$

where $t = \frac{D - \mathrm{TD}_{50}}{m\mathrm{TD}_{50}}$, D is the dose damage metric; TD_{50} is the position of the 50% probability tolerance dose (TD) point; and m is a parameter to control the slope of the dose-response curve. Note that TD_{50} is expressed as function of the liver partial volume (V)

$$\mathrm{TD}_{50}(V) = \frac{\mathrm{TD}_{50}(1)}{V^n}, \tag{4.2}$$

where $\mathrm{TD}_{50}(1)$ is TD_{50} for the whole volume and n is a volume dependence parameter. The parameters of the model are calculated using maximum likelihood estimation approaches [20]. To account for inhomogeneous dose distributions, different power law methods are typically applied to Eq. (4.2) such as the effective volume (Veff) and the generalized equivalent uniform dose (gEUD) [21]. To correct for various dose-fractionations regimens, physical doses are typically converted into biologically equivalent dose in 2 Gy fraction (EQD_2) using the Linear-quadratic (LQ) model [22]:

$$\mathrm{EQD}_2 = D\frac{d + \alpha/\beta}{2 + \alpha/\beta}, \tag{4.3}$$

where D, d are the total dose and the dose per fraction, respectively. The parameter α/β with

values 2–3 has been typically used for RILD [10, 11].

4.4.1 Conventionally Fractionated Radiation Therapy

The Emami paper estimated the liver TD50/5 (50% probability of RILD at 5 years) for one-third partial liver irradiation, two-thirds partial liver irradiation, and whole liver irradiation to be 55, 45, and 40 Gy, respectively, while the TD5/5 (5% probability of RILD at 5 years) was estimate to be 50, 35, and 30 Gy, respectively for these same volumes [13]. The corresponding fit to the Lyman model yielded these values: TD_{50} = 45 Gy; m = 0.15, and n = 0.32 [23].

Quantitative efforts to estimate RILD risk using 3D-CT imaging and dose-volume histogram (DVH) have been pioneered by the University of Michigan group [11, 24, 25]. In a population of about 200 patients with primary and metastatic cancers, the Michigan model estimates for classical RILD suggested a large volume effect ($n \approx 1$) and strong correlation with mean liver dose. The TD_{50} for primary and metastatic liver cancers was 35.4 and 40.7 in EQD2 Gy, respectively. These results were adopted by the Quantitative Assessment of Normal Tissue Effects in the Clinic (QUANTEC) consortium and are summarized in Fig. 4.2 [10].

Other investigators have shown that liver tolerance dose interestingly varied according to whether the patients were hepatitis B carriers (TD_{50} = 50 Gy) [9] or had C-P class B status (TD_{50} = 23 Gy) [26].

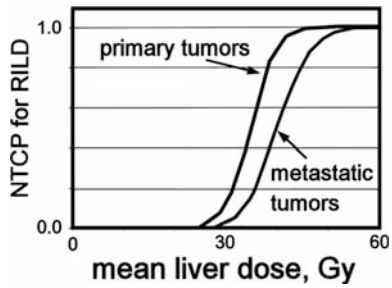

Fig. 4.2 Classical RILD NTCP for primary and metastatic liver using the Michigan Lyman model with mean liver dose expressed in EQD2. The plots suggest higher tolerance in patients with liver metastases compared to primary liver cancer (Reprinted from [27] with permission from © Elsevier)

4.4.2 Stereotactic Body Radiation Therapy and Critical Volumes

The utilization of steretotactic body radiotherapy (SBRT) for liver tumors has recently been widely adopted due to clinical effectiveness seen in several studies for early cancer stages (including primary and metastatic liver) [28–32] and the socioeconomic benefits of shortened courses [33]. The local control in these studies with carefully preselected populations can exceed 90% after 1 year with an RILD event rate <5% using $\geq$ 10 Gy per fraction [10]. At first, these results may seem inconsistent with the classical understanding of radiobiology wherein tumors with higher $\alpha/\beta \approx 10$ (e.g., liver and lung cancer), in which the LQ model would predict that hyperfractionation would give a therapeutic gain while hypofractionation would yield a therapeutic loss [34]. However, it should be noted that the liver is a parallel functioning organ composed of parenchymal tissues in which subdivisions are able to perform similar and independent functions. This is coupled with advances in image guidance and radiation delivery technologies that would create a wider geometrical window of opportunity to exploit for dose escalation [35]. Moreover, available clinical data mainly support LQ application in the range of 1–5 Gy; at higher doses, its applicability is currently a subject of intense debate [35–39]. In any case, it is widely recognized that the LQ model is an approximation to more sophisticated kinetic reaction models [40]. Therefore, several modifications have been introduced to the LQ model to allow better fit to higher doses per fraction. These modifications to the LQ model effectively aim to straighten the survival curve at higher doses. This could be achieved by simply having higher α/β values in cases of rapidly proliferating and hypoxic tumors [36, 41] or by developing alternate models such as the modified LQ (MLQ), the

linear–quadratic–linear (LQL) [42–44], linear–quadratic–cubic (LQC) [45], the universal survival curve (USC) [46], and the generalized LQ (gLQ) [47] among others.

QUANTEC recommended mean liver dose constraints (physical dose) for SBRT are summarized in Table 4.2 [10]. In addition, QUANTEC recommended that a critical volume of 700 cc, estimated from partial hepatectomy series, of uninvolved liver to receive <15 Gy in three fractions following the University of Colorado experience in metastatic liver cancer [48]. The concept of critical volume follows from the idea that an organ is composed of functional subunits [49]. In case of parallel-arranged organs such as the liver, this concept entails that a proportion of the organ can be destroyed without clinically relevant loss of the organ function as a whole. NTCP modeling with the input foundations of a parallel arrangement of the liver and thresholds for induction of clinically evident damage has found utility in matching clinical results [50].

4.5 Discussion and Future Directions

NTCP modeling of the liver has been an important companion for designing clinical trials and the management of primary and metastatic liver cancer. However, in some instances clinical intuition has preceded any modeling prediction as in the case of SBRT indicating limitations of our current modeling schemes and the necessity to adopt approaches that do not only confirm our current understanding but also allow us to exploit emerging knowledge and explore new horizons. Modifications to the classical Lyman model allow incorporation of clinical [51, 52] and biological information [53, 54]. However, biological markers of RILD have not been systematically investigated, and several studied biomarkers of VOD have been suggested for RILD including serum levels of hyaluronic acid, plasminogen activator inhibitor, thrombomodulin, *P*- and *E*-selectin, TGF-β, von Willebrand factor-cleaving protease, and many others [8].

Imaging provides another useful resource of information not only for assessment [55] but also for prediction of radiation-induced toxicity. An approach that has been successfully applied to studying RILD and liver function is using portal venous perfusion imaging by dynamic contrast enhanced CT [56] or MRI [57, 58]. These studies have shown that mean liver portal venous perfusion is associated with ICG-R15 retention and further that mean venous perfusion in the liver is reduced by about 1%/Gy with hepatic irradiation. In addition, several single-photon emission computed tomography (SPECT) tracers have been proposed to image liver fibrosis. These include using SPECT with Asialoglycoprotein receptor (ASGPR) [59] or albumin [60] Technetium-99 m tagged tracers. However, the incorporation of such valuable imaging information into NTCP modeling remains limited.

There are several limitations and pitfalls that can occur when developing NTCP models for liver toxicities. A common limitation in applying NTCP models to toxicity endpoints is the variability in normal tissue contouring (e.g., whole liver contouring, subtraction of the tumor volume, bile duct,

Table 4.2 QUANTEC Recommendations: SBRT mean liver dose (MLD) (for liver volume minus the gross tumor volume) and volume constraints

Liver tumor type	MLD constraints	Critical volume constraint
Metastatic	<15 Gy/3 fractions	≥700 cc receives ≤15 Gy/3–5 fractions
	<20 Gy/6 fractions	
Primary	<13 Gy/3 fractions	
	<18 Gy/6 fractions	
Primary: Child-Pugh B	<6 Gy (at 4–6 Gy per fraction)	

etc.) that could result in varying values for dose-volume metrics. Normal tissue atlases could aid in alleviating this problem [61]. Another common pitfall is related to the process of LQ-based EQD dose conversion to account for varying fractionation schedules, where the conversion needs to be done on a voxel-by-voxel basis of 3D dose distribution, and then DVH reduction and/or dose-volume metrics estimations could be carried out because of the inherent nonlinearity in the EQD transformation. Another problematic issue is overlooking the impact of the time factor; ironically, this was one of the earliest criticisms of the basic LQ model as pointed out by Fowler [62]. This is particularly important when comparing long and short treatment durations. This time factor in the modified LQ model is given by $\frac{\ln(2)(T-T_k)}{\alpha T_p}$, where T is scheduled treatment time, T_k is treatment delayed tumor repopulation time, and T_p is the tissue doubling time, all given in days. Further complicating the time issue is the variability in total elapsed time for delivery, which could vary from treatments in consecutive days to 1–3 fractions per week. However, a practical challenge of applying the time factor is the lack of knowledge of these parameters in a standard clinical setting. Another less pronounced issue is that increasing the intra-fraction time as experienced in hypofractionation treatments (e.g., SRS or SBRT) would allow for sublethal damage repair in both the tumor and normal tissue, which would particularly impact the protraction factor of the LQ model and the resulting therapeutic gain.

It should be also noted that despite the fact that there have been several useful modifications to the LQ model for hypofractionated treatments (e.g., SRS or SBRT), trying to account for newly recognized biological effects such as vascular damage, effects on stem cells, and immune-mediated effects remains challenging [39].

Besides incorporating new radiobiological knowledge into current models, NTCP modeling could also benefit from recent advances in data science and the use of advanced computational techniques that are able to accommodate complex and potentially nonlinear relationships in the data and have the potential to generalize better to unseen data compared to traditional statistical methods [63, 64].

4.6 Conclusions

NTCP models are necessary to predict treatment risks and aid in optimizing radiotherapy planning in the era of personalized/precision medicine. Liver cancer has been a hotbed for the development of NTCP models that have contributed significantly to our understanding of partial volume irradiation effects, metastatic versus primary tolerance doses, and the impact of baseline liver function on observed RILD limiting its incidence and in turn allowing for safe escalation of radiation dose. However, the widespread use of SBRT will require similar efforts in developing accurate NTCP models to ensure optimized utilization of this new promising modality. Moreover, NTCP modeling can also benefit from advances in biotechnology and computational modeling to go beyond simplified dosimetric models into more advanced top-down or bottom-up systems-based approaches in radiobiology. These advances may improve the interfacing of radiation physics, imaging and molecular biology in the era of the big '-omics' revolution. Progress in NTCP modeling can only be achieved via collective efforts among all the stake holders (clinicians, biologists, physicists, modelers, etc.) while recognizing what Sir R.A. Fisher, one of the founding fathers of modern modeling and statistics, once said "I believe that no one who is familiar, either with mathematical advances in other fields, or with the range of special biological conditions to be considered, would ever conceive that everything could be summed up in a single mathematical formula, however complex" [65]. The caveat here is that modern developments should be geared towards systems-based models and not individual formulae.

Acknowledgements This work was by part supported by NIH P01 CA59827 and the University of Michigan Cancer Center fund G017459.

References

1. Reed GB Jr, Cox AJ Jr. The human liver after radiation injury. A form of veno-occlusive disease. Am J Pathol. 1966;48(4):597–611.
2. Lawrence TS, Robertson JM, Anscher MS, Jirtle RL, Ensminger WD, Fajardo LF. Hepatic toxicity resulting from cancer treatment. Int J Radiat Oncol Biol Phys. 1995;31(5):1237–48.
3. Liang S-X, Zhu X-D, Xu Z-Y, et al. Radiation-induced liver disease in three-dimensional conformal radiation therapy for primary liver carcinoma: The risk factors and hepatic radiation tolerance. Int J Radiat Oncol Biol Phys. 65(2): 426–34.
4. Westover KD, Hong TS. Liver. In: Shrieve DC, Loeffler J, eds. Human Radiation Injury Philadelphia, PA Lippincott Williams & Wilkins; 2010.
5. NCI. CTCAE ver 4.0. 2010. http://evs.nci.nih.gov/ftp1/CTCAE/About.html
6. Dooley S, ten Dijke P. TGF-β in progression of liver disease. Cell Tissue Res. 2012;347(1):245–56.
7. Yamasaki SA, Marn CS, Francis IR, Robertson JM, Lawrence TS. High-dose localized radiation therapy for treatment of hepatic malignant tumors: CT findings and their relation to radiation hepatitis. Am J Roentgenol. 1995;165(1):79–84.
8. Guha C, Kavanagh BD. Hepatic radiation toxicity: Avoidance and Amelioration. Semin Radiat Oncol. 2011;21(4):256–63.
9. Cheng JC, Wu JK, Lee PC, et al. Biologic susceptibility of hepatocellular carcinoma patients treated with radiotherapy to radiation-induced liver disease. Int J Radiat Oncol Biol Phys. 2004;60(5):1502–9.
10. Pan CC, Kavanagh BD, Dawson LA, et al. Radiation-Associated liver injury. Int J Radiat Oncol, Biol, phys 2010;76(30):S94–100.
11. Dawson LA, Normolle D, Balter JM, McGinn CJ, Lawrence TS, Ten Haken RK. Analysis of radiation-induced liver disease using the Lyman NTCP model. Int J Radiat Oncol Biol Phys 2002;53.
12. Bentzen SM. Preventing or reducing late side effects of radiation therapy: radiobiology Meets molecular pathology. Nat Rev Cancer. 2006;6(9):702–13.
13. Emami B, Lyman J, Brown A, et al. Tolerance of normal tissue to therapeutic irradiation. Int J Radiat Oncol Biol Phys; 21(1):109–22.
14. El Naqa I. Biomedical informatics and panomics for evidence-based radiation therapy. Wiley Interdisc Rev: Data Min Knowl Discovery. 2014;4(4):327–40.
15. El Naqa I, Pater P, Seuntjens J. Monte Carlo role in radiobiological modelling of radiotherapy outcomes. Phys Med Biol. 2012;57(11):R75–97.
16. Pater P, Backstom G, Villegas F, et al. Proton and light ion RBE for the induction of direct DNA double strand breaks. Med Phys. 2016;43(5):2131.
17. El Naqa I. Outcomes Modeling. In: Starkschall G, Siochi C, eds. Informatics in radiation oncology. Boca Raton, FL: CRC Press, Taylor and Francis; 2013: 257–75.
18. Lyman JT. Complication probability as assessed from dose-volume histograms. Radiat Res Suppl. 1985;8:S13–9.
19. Kutcher GJ, Burman C. Calculation of complication probability factors for non-uniform normal tissue irradiation: The effective volume method gerald. Int J Radiat Oncol Biol Phys 1989;16(6):1623–30.
20. Harris J, Stöcker H. Handbook of mathematics and computational science. New York: Springer; 1998.
21. Niemierko. A generalized concept of equivalent uniform dose (EUD). Med Phys 1999; 26:1101.
22. Bentzen SM, Dörr W, Gahbauer R, et al. Bioeffect modeling and equieffective dose concepts in radiation oncology—Terminology, quantities and units. Radiother Oncol. 2012;105(2):266–8.
23. Burman C, Kutcher GJ, Emami B, Goitein M. Fitting of normal tissue tolerance data to an analytic function. Int J Radiat Oncol Biol Phys. 1991;21 (1):123–35.
24. Dawson LA, Ten Haken RK. Partial Volume Tolerance of the Liver to Radiation. Semin Radiat Oncol. 2005;15(4):279–83.
25. Lawrence TS, Ten Haken RK, Kessler ML, et al. The use of 3-D dose volume analysis to predict radiation hepatitis. Int J Radiat Oncol Biol Phys; 23(4):781–8.
26. Xu Z-Y, Liang S-X, Zhu J, et al. Prediction of radiation-induced liver disease by Lyman normal-tissue complication probability model in three-dimensional conformal radiation therapy for primary liver carcinoma. Int J Radiat Oncol Biol Phys 2006;65(1):189–95.
27. Pan CC, et al. Radiation-associated liver injury. Int J Radiat Oncol Biol Phys. 2010;76(3):S94–100.
28. Chang JY, Senan S, Paul MA, et al. Stereotactic ablative radiotherapy versus lobectomy for operable stage I non-small-cell lung cancer: a pooled analysis of two randomised trials. Lancet Oncol; 16(6):630–7.
29. Liu E, Stenmark MH, Schipper MJ, et al. Stereotactic body radiation therapy for primary and metastatic liver tumors. Transl Oncol. 2013;6(4):442–6.
30. Goodman KA, Wiegner EA, Maturen KE, et al. Dose-escalation study of single-fraction stereotactic body radiotherapy for liver malignancies. Int J Radiat Oncol Biol Phys; 78(2):486–93.
31. Herman JM, Chang DT, Goodman KA, et al. Phase 2 multi-institutional trial evaluating gemcitabine and stereotactic body radiotherapy for patients with

locally advanced unresectable pancreatic adenocarcinoma. Cancer. 2015;121(7):1128–37.
32. Timmerman RD, Herman J, Cho LC. Emergence of stereotactic body radiation therapy and its impact on current and future clinical practice. J Clin Oncol. 2014;32(26):2847–54.
33. Timmerman R, Paulus R, Galvin J, et al. Stereotactic body radiation therapy for inoperable early stage lung cancer. JAMA, J Am Med Assoc. 2010;303 (11):1070–6.
34. Hall EJ, Giaccia AJ. Radiobiology for the radiologist. 6th ed. Philadelphia: Lippincott Williams & Wilkins; 2006.
35. Orton C. Fractionation: raduibiological principles and clinical practice. In: Khan F, Gerbi B, eds. Treatment planning in radiation oncology 3rd ed. Philadelphia, PA: Treatment planning in radiation oncology 2012.
36. Brown JM, Carlson DJ, Brenner DJ. The tumor radiobiology of SRS and SBRT: Are more than the 5 Rs involved? Int J Radiat Oncol Biol Phys 2014;88 (2):254–62.
37. Kirkpatrick JP, Meyer JJ, Marks LB. The linear-quadratic model is inappropriate to model high dose per fraction effects in radiosurgery. Semin Radiat Oncol. 2008;18(4):240–3.
38. Sheu T, Molkentine J, Transtrum MK, et al. Use of the LQ model with large fraction sizes results in underestimation of isoeffect doses. Radiother Oncol: J Eur Soc Ther Radiol Oncol. 2013;109(1):21–5.
39. Song CW, Cho LC, Yuan J, Dusenbery KE, Griffin RJ, Levitt SH. Radiobiology of stereotactic body radiation therapy/stereotactic radiosurgery and the linear-quadratic model. Int J Radiat Oncol Biol Phys. 2013;87(1):18–9.
40. Curtis SB. Lethal and potentially lethal lesions induced by radiation–A unified repair model. Radiat Res. 1986;106(2):252–70.
41. Fowler JF. Development of radiobiology for oncology-a personal view. Phys Med Biol. 2006;51 (13):R263–86.
42. Guerrero M, Carlone M. Mechanistic formulation of a lineal-quadratic-linear (LQL) model: Split-dose experiments and exponentially decaying sources. Med Phys. 2010;37(8):4173–81.
43. Guerrero M, Li XA. Extending the linear-quadratic model for large fraction doses pertinent to stereotactic radiotherapy. Phys Med Biol. 2004;49(20):4825–35.
44. Astrahan M. Some implications of linear-quadratic-linear radiation dose-response with regard to hypofractionation. Med Phys. 2008;35 (9):4161–72.
45. Joiner M, Kogel Avd. Basic clinical radiobiology. 4th ed. London: Hodder Arnold; 2009.
46. Park C, Papiez L, Zhang S, Story M, Timmerman RD. Universal survival curve and single fraction equivalent dose: useful tools in understanding potency of ablative radiotherapy. Int J Radiat Oncol Biol Phys. 2008;70(3):847–52.
47. Wang JZ, Huang Z, Lo SS, Yuh WT, Mayr NA. A generalized linear-quadratic model for radiosurgery, stereotactic body radiation therapy, and high-dose rate brachytherapy. Sci transl med 2010; 2(39): 39ra48.
48. Schefter TE, Kavanagh BD, Timmerman RD, Cardenes HR, Baron A, Gaspar LE. A phase I trial of stereotactic body radiation therapy (SBRT) for liver metastases. Int J Radiat Oncol Biol Phys. 2005;62 (5):1371–8.
49. Withers HR, Taylor JM, Maciejewski B. Treatment volume and tissue tolerance. Int J Radiat Oncol Biol Phys. 1988;14(4):751–9.
50. Jackson A, Ten Haken RK, Robertson JM, Kessler ML, Kutcher GJ, Lawrence TS. Analysis of clinical complication data for radiation hepatitis using a parallel architecture model. Int J Radiat Oncol Biol Phys; 31(4):883–91.
51. Defraene G, Van den Bergh L, Al-Mamgani A, et al. The Benefits of Including Clinical Factors in Rectal Normal Tissue Complication Probability Modeling After Radiotherapy for Prostate Cancer. Int J Radiat Oncol Biol Phys 2012; 82(3):1233–42.
52. Rancati T, Fiorino C, Fellin G, et al. Inclusion of clinical risk factors into NTCP modelling of late rectal toxicity after high dose radiotherapy for prostate cancer. Radiother Oncol. 2011;100(1):124–30.
53. Coates J, Jeyaseelan AK, Ybarra N, et al. Contrasting analytical and data-driven frameworks for radiogenomic modeling of normal tissue toxicities in prostate cancer. Radiother Oncol. 2015;115(1):107–13.
54. Tucker SL, Li M, Xu T, et al. Incorporating Single-nucleotide Polymorphisms Into the Lyman Model to Improve Prediction of Radiation Pneumonitis. Int J Radiat Oncol Biol Phys 2013;85 (1):251–7.
55. Jeraj R, Cao Y, Ten Haken RK, Hahn C, Marks L. Imaging for assessment of radiation-induced normal tissue effects. Int J Radiat Oncol Biol Phys 2010; 76 (3, Supplement): S140–S4.
56. Cao Y, Pan C, Balter JM, et al. Liver function after irradiation based on computed tomographic portal vein perfusion imaging. Int J Radiat Oncol Biol Phys 2008;70(1):154–60.
57. Wang H, Feng M, Jackson A, Ten Haken RK, Lawrence TS, Cao Y. Local and Global function model of the liver. Int J Radiat Oncol Biol Phys 2016;94(1):181–8.
58. Cao Y, Wang H, Johnson TD, et al. Prediction of liver function by using magnetic resonance-based portal venous perfusion imaging. Int J Radiat Oncol Biol Phys 2013;85(1):258–63.
59. Iguchi T, Sato S, Kouno Y, et al. Comparison of Tc-99 m-GSA scintigraphy with hepatic fibrosis and

regeneration in patients with hepatectomy. Ann Nucl Med. 2003;17(3):227–33.
60. Yoshida M, Shiraishi S, Sakaguchi F, et al. A quantitative index measured on 99mTc GSA SPECT/CT 3D fused images to evaluate severe fibrosis in patients with chronic liver disease. Japan J Radiol. 2012;30(5):435–41.
61. Jabbour SK, Hashem SA, Bosch W, et al. Upper abdominal normal organ contouring guidelines and atlas: a Radiation Therapy Oncology Group consensus. Pract Radiat Oncol. 2014;4(2):82–9.
62. Fowler JF. 21 years of biologically effective dose. Br J Radiol. 2010;83(991):554–68.
63. El Naqa I, Bradley JD, Lindsay PE, Hope AJ, Deasy JO. Predicting radiotherapy outcomes using statistical learning techniques. Phys Med Biol. 2009;54(18):S9–30.
64. El Naqa I, Li R, Murphy MJ, editors. Machine learning in radiation oncology: Theory and application. Switzerland: Springer; 2015.
65. Fisher RA. The evolutionary modification of genetic phenomena. 6th International Congress of Genetics 1; 1932. p. 165–72.

Radiation Oncology: Fundamentals and Controversies

5

Jeffrey Meyer, MD, MS and Tracey E. Schefter, MD

5.1 Introduction

Clinical investigation and basic science research complement and inspire each other. The intent of this chapter is not to provide a broad overview of the practice of radiation oncology but rather to discuss in brief specific evolving concepts and ongoing controversies. Some of these controversies have not coincidentally developed in parallel with the recent burgeoning use of high-dose, hypofractionated radiation therapy for liver tumors (as well as tumors in other sites). In keeping with one of the main themes of this book, the concepts and controversies will be framed within the context of integrated multidisciplinary care. The following interrelated topics will be addressed:

(1) fractionation in the history of clinical radiation oncology,
(2) similarities and differences between hypofractionated "ablative" radiation therapy and other ablation modalities,
(3) the principles of spatial cooperation and the oligometastatic disease state, and
(4) the abscopal effect: local therapies and their systemic manifestations.

5.2 Fractionation in the History of Clinical Radiation Oncology

Debates about "optimal" fractionation for radiation treatment courses form a significant and contentious chapter in the history of clinical radiation oncology [1]. These debates have been informed over decades by both clinical experience and laboratory investigation but remain unresolved for a variety of reasons, not the least of which are the heterogeneity of cancer in its locations and intrinsic sensitivity to radiation. When radiation was used to treat tumors in the earliest practice of radiation oncology, short courses of what has been termed "caustic" radiation administration were common [2]. The normal tissue sparing effects of fractionation were appreciated through animal studies in the early 20th century, and steep isoeffect curves plotting total dose versus decreasing dose per fraction for various forms of normal tissue injury are established and understood by students of radiation biology [3]. In general, the therapeutic ratio has since long been thought to favor fractionated treatment, allowing for elimination of tumor cells and concomitant "repair," and thus minimized injury, of normal tissues.

J. Meyer (✉)
Department of Radiation Oncology, University of Texas Southwestern Medical Center, 5801 Forest Park Road, 75214 Dallas, TX, USA
e-mail: Jeffrey.Meyer@UTSouthwestern.edu

T.E. Schefter
Department of Radiation Oncology, University of Colorado, Aurora, CO, USA

J. Meyer and T.E. Schefter (eds.), *Radiation Therapy for Liver Tumors*,
DOI 10.1007/978-3-319-54531-8_5

Renewed interest in single-fraction and high-dose radiation treatments has emerged at various times in the last several decades. Two particular examples—radiosurgery and intraoperative radiation therapy (IORT)—deserve special mention. Classical radiosurgery, pioneered by the neurosurgeon Leksell and others, entails a single high-dose administration of radiation to discrete targeted foci with stereotactic localization [4]. Leksell was seeking a means of noninvasively ablating portions of the brain. At face value, the concept of radiosurgery as applied to the treatment of malignancies runs counter to most of the conventional wisdom of classical radiobiology. IORT similarly treats tumors with very high single doses as part of a surgical exposure procedure, which allows for direct irradiation of a tumor target with shielding of surrounding normal structures [5].

The application of radiosurgery or any high-dose single-fraction or hypofractionated radiation treatment course is in large part predicated on the use of advanced technology to limit the exposure of normal tissue to the high doses of radiation, and it is indeed this concept of limited volumes of high-dose normal tissue irradiation that is not typically considered in the "4Rs" of classical radiobiology which serve as the foundation of conventionally fractionated radiation courses. Gamma knife radiosurgery achieves high doses in focal volumes, with a steep gradient of dose outside of the target. Beam arrangements spread a low dose of radiation around a targeted core of extreme high dose. This same concept can be applied to extracranial targets and is complemented by other emerging technologies such as conformal beam shaping and intensity modulation, as well as the use of image guidance. With these principles in mind, the era of extracranial high-dose hypofractionated radiation therapy, or stereotactic body radiation therapy (SBRT), also referred to as stereotactic ablative radiation therapy (SABR), began in earnest in the 1990s [6, 7]. The adoption of SABR has also required significant changes in the approach of the radiation oncologist to treatment planning issues. Traditional large volume irradiation fields such as AP/PA or 4-field box treatments are generally not compatible with high-dose hypofractionated radiotherapy. Similarly, prophylactic treatment of regional areas "at risk" for cancer involvement, such as draining lymph node regions, common in conventional radiation treatment courses, is also generally not compatible with SABR.

The experiences with intracranial radiosurgery and IORT can and should inform SABR with respect to both normal tissue injury/tolerance doses and tumor response. For example, Abe and colleagues at Kyoto University reported on their experience of treating patients with upper abdominal tumors with single-dose IORT delivered with electrons [8]. Doses required to eradicate both gross and microscopic deposits of cancer with single-fraction treatment were elucidated. In the treatment of gastric cancer, a single-fraction dose of 40 Gy was required to eradicate macroscopic tumors (unresectable lymph nodes) of up to 3 cm, whereas doses of 28–35 Gy were sufficient to treat microscopic tumor deposits. In their experience, 40 Gy was insufficient to eradicate larger primary gastric tumors. These results are in keeping with prior studies of single-fraction intraoperative electron irradiation of unresectable pancreatic adenocarcinomas, in which doses of 25 Gy did not lead to total sterilization of macroscopic disease [9]. Other studies on normal tissue tolerance to single-fraction IORT, and combined conventional irradiation plus single-fraction IORT, both in humans and in animal models, also yielded information for future use in high-dose hypofractionated external beam irradiation courses [10].

Over the past decades, numerous clinical studies have investigated altered fractionation schedules for the treatment of human tumors [11]. For the most part, however, we lack fundamental knowledge of dose–fractionation effects for given tumors in the effort for personalized radiation therapy. We lack robust knowledge of oxygenation and reoxygenation kinetics, tumor growth kinetics, and tumor microenvironmental effects, and how to best integrate this information into appropriate dose–fractionation selection. The importance of these issues in the

context of high-dose hypofractionated radiation therapy remains to be determined, especially for the treatment of bulky tumors. We have the capabilities with our advanced technologies to safely deliver high doses of radiation and to fractionate not only in time but in space as well [12, 13]. Dose–fractionation studies moving forward will involve the translational merging of tumor biology and technology.

5.3 Similarities and Differences Between Hypofractionated "Ablative" Radiation Therapy and Other Ablation Modalities

SABR shares similarities with, but also in some ways contrasts sharply from, the tumor-ablative treatments employed by interventional radiologists (the field of interventional oncology). Most tumor-ablative treatments used in interventional oncology make use of extreme temperatures. Radiofrequency ablation (RFA) is a probe-based ablation technology which employs an alternating current in the probe, which leads to charge agitation within adjacent tissues, causing a rapid rise in temperature [14]. Cell death is increasingly likely and rapid as the temperature rises. At the highest temperatures within the heated tumor ($\geq$50–60 °C), there is onset of protein denaturation, mitochondrial damage, and loss of plasma membrane integrity which leads to coagulative necrosis of the tumor. Cryoablation is also a probe-based therapy [14]. Freeze-thaw cycles injure cells directly through intracellular ice crystal formation and osmotic dehydration, as well as indirectly through deleterious effects on the tumor-supporting vasculature.

The actual mechanism of cell death induced by radiation, both by protracted/fractionated and hypofractionated courses, remains incompletely understood and likely varies as a function of each individual tumor, its microenvironment, the state of the tumor cell in the cell cycle (interphase or cycling), and the radiation dose delivered. Classically, "cell death" induced by radiation is any state in which the irradiated and damaged tumor cell is no longer clonogenically active [15]. Radiation can yield a variety of clonogenically inactive states, including apoptosis, (classical) necrosis, autophagy, and senescence [16]. Students of radiobiology learn about the chromosomal insults that can arise following radiation-induced DNA strand breaks, which may result in the formation of deranged chromosomes, and subsequent mitotic catastrophe leading to cell inactivation [17]. Mitotic catastrophe may lead to cell inactivation by one of the aforementioned pathways [18].

The effects of radiation on the tumor-supporting stroma, and direct or indirect impact of these responses on the tumor, are an active area of investigation and controversy. Budach et al. investigated the stromal component of the tumor radiation response [19]. The authors used tumors grown in SCID mice, which have defective DNA repair. These studies showed minimal impact of the radiosensitive SCID-based surrounding stroma on the radiosensitivity of the tumor. However, other macromolecules in a cell, apart from DNA, may also be affected by radiation with subsequent influence on tumor cell death. Investigators have shown a link between the endothelial cell response to radiation and subsequent tumor cell death, which is mediated by acid sphingomyelinase within the endothelium in the setting of high-dose, but now low-dose, radiation therapy [20–22]. Sphingomyelinase activity generates ceramide, a mediator of apoptosis [22]. In animal models, endothelial apoptosis has been shown to be linked to tumor cell death [20–22]. This vascular component of the tumor cell response to high-dose irradiation, and ways to further exploit it, remains an active area of investigation.

Thus, thermal ablations as practiced by radiologists and surgeons can be seen to differ in their effects on tumor cells and mechanism of cell kill relative to high-dose hypofractionated radiation therapy, although much remains to be learned. These differences are important to understand for several reasons. First, the kinetics of cell death within treated tumor masses may differ markedly between thermal ablation and radiation (see discussion above), and this has implications for the subsequent radiological

appearance of treated lesions for patients undergoing follow-up imaging, as well as, potentially, the risks inherent in treatment of very bulky tumor masses [23]. Second, the variables that are associated with successful ablation have some common ground between the two treatments, but also many differences. The efficacy of thermal ablation treatments is limited by the presence of large-caliber vessels which produce a "heat sink" effect and decrease the likelihood of reaching tumoricidal temperatures [24]. Third, as will be discussed later in this chapter, as local therapies, thermal ablation and radiation therapy may induce differing systemic effects to include different interactions with systemic therapies and the host immune system.

5.4 The Principles of Spatial Cooperation and the Oligometastatic Disease State

Steel and Peckham described multiple ways in which chemotherapy, a systemic therapy, could interact with radiation therapy, a local therapy [25]. In a general sense, the principle of spatial cooperation holds that different therapies can be used to complement each other on the local and systemic levels. For example, a local treatment may be used to eradicate radiographically evident disease, with subsequent delivery of chemotherapy to treat spatially remote and radiographically occult micrometastatic disease. This paradigm is commonly used in the treatment of many different cancer types, especially for local-regionally advanced and high-risk tumors. Ideally, the separate treatments do not have overlapping toxicities, especially when the treatments are given concurrently or in close succession to each other [25].

Local therapies have usually been reserved for palliation only when solid tumors have already demonstrated clear evidence for spread of cancer (distant metastases or M1 disease state). There are important exceptions to this general rule, however. Resection of liver metastases from colorectal tumors in selected patients is a well-established practice, with clinical series showing long-term disease-free survival in a substantial proportion of patients [26]. Critics of this practice of metastasectomy, or any local therapy used to treat metastatic disease with curative intent, such as SABR or thermal ablation, bring attention to possible selection biases in these series and the lack of high-level randomized evidence supporting the practice [27, 28]. Clinical trials evaluating SABR in the treatment of selected patients with metastatic cancer are underway and are a topic of significant scrutiny [29].

Part of the interest in use of local therapies in patients with M1 disease is the concept of the oligometastatic disease state. Weichselbaum and Hellman discussed the notion of patients with "limited" metastatic disease outside of the primary tumor, brought about by the inefficiencies of the metastatic process [30, 31]. In this special situation, eradication of these limited sites in addition to the primary tumor by local therapies would be curative. A second type of oligometastatic disease state may exist when effective systemic therapy eliminates the majority of widespread distant sites of cancer, with remaining bulky sites of disease. Again, in this situation, successful use of local therapies, including SABR, would lead to cure. This latter situation is a good example of the spatial cooperation principle.

The existence of oligometastatic disease states, or more properly how to select patients in these states, is controversial. Nonetheless, the long-term disease-free survival of selected patients with liver-only metastases from colorectal cancer treated with surgery does indicate that not all patients with M1 solid tumors have truly systemically spread disease and cannot achieve long-term disease-free survival [26, 30].

As mentioned, clinical investigation is indeed underway to define the role of aggressive SABR treatments in patients with M1 disease. Two recent studies in patients with metastatic non-small cell lung cancer provide optimism for

this approach. A single-arm phase II study showed a suggestion of improvement in progression-free survival to the use of SABR to sites of metastatic disease compared to expected results with systemic therapy alone [32]. A recent randomized phase II studies in patients with non-small cell lung cancer showed an improvement in progression-free survival with the use of consolidation radiation therapy to patients with limited metastatic sites (following initial systemic therapy) compared to systemic therapy alone [33]. Disease-free survival or "cure" need not be the only acceptable goal, as prolongation of overall survival and prolongation of sustained quality of life are also important outcomes. Minimally invasive treatments such as SABR and thermal ablation may be particularly important moving forward as they are usually associated with relatively minimal toxicities, and thus integrate well with systemic therapies, exemplifying spatial cooperation.

5.5 The Abscopal Effect: Local Therapies and Their Systemic Manifestations

Throughout this chapter, I have distinguished between "systemic" treatment approaches, such as chemotherapy, and "local" treatment approaches such as surgery, radiation therapy, and thermal ablation treatments. The "local" tumor and treatments addressing it are classically thought to be segregated from the distant. However, there is evidence that locally applied cancer treatments can yield systemic manifestations, including anti-tumor effects, challenging this model. This absocopal effect is a recognized phenomenon, and regression of untreated distant sites of cancer have been reported, albeit rarely and usually as case reports, following surgery, radiation therapy, and thermal ablation [34–36]. A number of hypotheses have been generated to explain this phenomenon; among them is the idea that local cancer treatments can stimulate an immune response against treated tumors [37].

This hypothesis of an immunologic basis for abscopal effects following radiation has been investigated in the laboratory, with supportive findings [38, 39]. Radiation has numerous pleiotropic effects on the innate and adaptive immune systems. It can modulate antigen presentation with improved priming of T cells against tumor antigens, enhance leukocyte trafficking to tumors, and alter the cellular content of the tumor microenvironment, potentially reversing immunosuppression [39–42]. Lee et al. found that $CD8^+$ T cells played an important role in the tumor-eradicating effects of high-dose radiation in an animal model [39].

The abscopal effect is, however, a rare phenomenon in the clinic. This is probably related to various overwhelming and multilayered immunosuppressive effects induced by tumors. Because of this, there is great interest in combining radiation therapy with immunostimulating cytokines and drug agents, including interleukin 2, anti-CTLA-4 antibody therapy, and anti-PD-1 and anti-PD-L1 antibody therapies [43]. Such combination therapies have been shown to synergize in preclinical tumor models, and there are encouraging reports of efficacy emerging in human patients as well [44–46]. The influence of particular dose–fractionation regimens as well as treatment volumes on optimized induction of anti-tumor immune responses needs further exploration [39, 47, 48].

Of note, thermal ablation therapies can also synergize with immunostimulating treatments [49, 50] to amplify systemic anti-tumor immunity. It is possible that the "best" combination therapies, with respect to the goal of inducing an abscopal effect, may depend on the tumor type, its anatomical location(s), and specific ablative treatments—be they radiation-based or thermally based.

Special mention should also be made of the potential toxicities of these treatments. Controlled induction of anti-tumor responses without the collateral induction of autoimmunity may be especially challenging. Preclinical work suggests the safety of combination treatments, but this will be an important endpoint in human studies [46, 51]. In some situations, limited autoimmune phenomenon may be an acceptable toxicity, especially if the anti-tumor response is strong

and does not need to be sustained for long periods of time for life prolongation or cure.

References

1. Fowler JF, Denekamp J, Sheldon PW, et al. Optimum fractionation in X-ray treatment of C_3H mouse mammary tumours. Br J Radiol. 1974;47:781–9.
2. Bernier J, Hall EJ, Giaccia A. Radiation oncology: a century of achievements. Nat Rev Cancer. 2004;4:737–47.
3. Hall EJ, Giaccia AJ. Time, dose, and fractionation in radiotherapy. In: Hall EJ, Giaccia AJ, editors. Radiobiology for the radiologist. 6th ed. Philadelphia, PA: Lippincott Williams & Wilkins; 2006. p. 378–97.
4. Leksell L. Stereotactic radiosurgery. J Neurol Neurosurg Psychiatry. 1983;46:797–803.
5. Willett CG, Czito BG, Tyler DS. Intraoperative radiation therapy. J Clin Oncol. 2007;25:971–7.
6. Hamilton AJ, Lulu BA, Fosmire H, et al. Preliminary clinical experience with linear accelerator-based spinal stereotactic radiosurgery. Neurosurgery. 1995;36:311–9.
7. Blomgren H, Lax I, Näslund I, et al. Stereotactic high dose fraction radiation therapy of extracranial tumors using an accelerator. Clinical experience of the first thirty-one patients. Acta Oncol. 1995;34:861–70.
8. Abe M, Takahashi M, Ono K, et al. Japan gastric trials in intraoperative radiation therapy. Int J Radiat Oncol Biol Phys. 1988;15:1431–3.
9. Goldson AL, Ashaveri E, Espinoza MC, et al. Single high dose intraoperative electrons for advanced stage pancreatic cancer: phase I pilot study. Int J Radiat Oncol Biol Phys. 1981;7:869–74.
10. Sindelar WF, Kinsella TJ. Normal tissue tolerance to intraoperative radiotherapy. Surg Oncol Clin N Am. 2003;12:925–42.
11. Bourhis J, Overgaard J, Audry H, et al. Hyperfractionated or accelerated radiotherapy in head and neck cancer: a meta-analysis. Lancet. 2006;368:843–54.
12. Wu Q, Manning M, Schmidt-Ullrich R, et al. The potential for sparing of parotids and escalation of biologically effective dose with intensity-modulated radiation treatments of head and neck cancers: a treatment design study. Int J Radiat Oncol Biol Phys. 2000;46(1):195–205.
13. Zhang X, Penagaricano J, Yan Y, et al. Application of spatially fractionated radiation (GRID) to helical tomotherapy using a novel TOMOGRID template. Technol Cancer Res Treat. 2016;15:91–100.
14. Chu KF, Dupuy DE. Thermal ablation of tumours: biological mechanisms and advances in therapy. Nat Rev Cancer. 2014;14:199–208.
15. Hall EJ, Giaccia AJ. Cell survival curves. In: Hall EJ, Giaccia AJ, editors. Radiobiology for the radiologist. 6th ed. Philadelphia, PA: Lippincott Williams & Wilkins; 2006. p. 30–46.
16. Wouters BG. Cell death after irradiation: how, when, and why cells die. Basic Clin Radiobiol. 2009;27–40 (4th ed. London, England: Hodder Arnold).
17. Hall EJ, Giaccia AJ. DNA strand breaks and chromosomal aberrations. In: Hall EJ, Giaccia AJ, editors. Radiobiology for the radiologist. 6th ed. Philadelphia, PA: Lippincott Williams & Wilkins; 2006. p. 16–29.
18. Vakifahmetoglu H, Olsson M, Zhivotovsky B. Death through a tragedy: mitotic catastrophe. Cell Death Differ. 2008;15:1153–62.
19. Budach W, Taghian A, Freeman J, et al. Impact of stromal sensitivity on radiation response of tumors. J Natl Cancer Inst. 1993;85:988–93.
20. Garcia-Barros M, Paris F, Cordon-Cardo C, et al. Tumor response to radiotherapy regulated by endothelial cell apoptosis. Science. 2003;300(5622):1155–9.
21. García-Barros M, Thin TH, Maj J, et al. Impact of stromal sensitivity on radiation response of tumors implanted in SCID hosts revisited. Cancer Res. 2010;70:8179–86.
22. Fuks Z, Kolesnick R. Engaging the vascular component of the tumor response. Cancer cell. 2005;89–91.
23. Ng KK, Lam CM, Poon RT, et al. Safety limit of large-volume hepatic radiofrequency ablation in a rat model. Arch Surg. 2006;141:252–8.
24. Patterson EJ, Scudamore CH, Owen DA, et al. Radiofrequency ablation of porcine liver in vivo: effects of blood flow and treatment time on lesion size. Ann Surg. 1998;227:559–65.
25. Steel GG, Peckham MJ. Exploitable mechanisms in combined radiotherapy-chemotherapy: the concept of additivity. Int J Radiat Oncol Biol Phys. 1979;5:85–91.
26. Tomlinson JS, Jarnagin WR, DeMatteo RP, et al. Actual 10-year survival after resection of colorectal liver metastases defines cure. J Clin Oncol. 2007;25:4575–80.
27. Treasure T, Macbeth F. Stereotactic body radiotherapy (SBRT) is as yet of unproven benefit for patients with lung metastases. Am J Clin Oncol. 2016;39:423–4.
28. Treasure T, Macbeth F. Is surgery warranted for oligometastatic disease? Thorac Surg Clin. 2016;26:79–90.
29. Palma DA, Salama JK, Lo SS, et al. The oligometastatic state—separating truth from wishful thinking. Nat Rev Clin Oncol. 2014;11:549–57.
30. Hellman S, Weichselbaum RR. Oligometastases. J Clin Oncol. 1995;13:8–10.
31. Weichselbaum RR, Hellman S. Oligometastases revisited. Nat Rev Clin Oncol. 2011;8:378–82.
32. Iyengar P, Kavanagh BD, Wardak Z, et al. Phase II trial of stereotactic body radiation therapy combined with erlotinib for patients with limited but progressive metastatic non-small-cell lung cancer. J Clin Oncol. 2014;32:3824–30.

33. Gomez DR, Blumenschein GR Jr, Lee JJ, et al. Local consolidative therapy versus maintenance therapy or observation for patients with oligometastatic non-small-cell lung cancer without progression after first-line systemic therapy: a multicentre, randomised, controlled, phase 2 study. Lancet Oncol. 2016;17:1672–82.
34. Lokich J. Spontaneous regression of metastatic renal cancer. Case report and literature review. Am J Clin Oncol. 1997;20:416–8.
35. Rao P, Escudier B, de Baere T. Spontaneous regression of multiple pulmonary metastases after radiofrequency ablation of a single metastasis. Cardiovasc Intervent Radiol. 2011;34:424–30.
36. Wersäll PJ, Blomgren H, Pisa P, et al. Regression of non-irradiated metastases after extracranial stereotactic radiotherapy in metastatic renal cell carcinoma. Acta Oncol. 2006;45:493–7.
37. Kaminski JM, Shinohara E, Summers JB, et al. The controversial abscopal effect. Cancer Treat Rev. 2005;31:159–72.
38. Demaria S, Ng B, Devitt ML, et al. Ionizing radiation inhibition of distant untreated tumors (abscopal effect) is immune mediated. Int J Radiat Oncol Biol Phys. 2004;58:862–70.
39. Lee Y, Auh SL, Wang Y, et al. Therapeutic effects of ablative radiation on local tumor require $CD8^+$ T cells: changing strategies for cancer treatment. Blood. 2009;114:589–95.
40. Reits EA, Hodge JW, Herberts CA, et al. Radiation modulates the peptide repertoire, enhances MHC class I expression, and induces successful antitumor immunotherapy. J Exp Med. 2006;203:1259–71.
41. Matsumura S, Wang B, Kawashima N, et al. Radiation-induced CXCL16 release by breast cancer cells attracts effector T cells. J Immunol. 2008;181:3099–107.
42. Filatenkov A, Baker J, Mueller AM, et al. Ablative tumor radiation can change the tumor immune cell microenvironment to induce durable complete remissions. Clin Cancer Res. 2015;21:3727–39.
43. Kang J, Demaria S, Formenti S. Current clinical trials testing the combination of immunotherapy with radiotherapy. J Immunother Cancer. 2016;20(4):51.
44. Deng L, Liang H, Burnette B, et al. Irradiation and anti–PD-L1 treatment synergistically promote antitumor immunity in mice. J Clin Invest. 2014;124:687–95.
45. Zeng J, See AP, Phallen J, et al. Anti–PD-1 blockade and stereotactic radiation produce long-term survival in mice with intracranial gliomas. Int J Radiat Oncol Biol Phys. 2013;86:343–9.
46. Demaria S, Kawashima N, Yang AM, et al. Immune-mediated inhibition of metastases after treatment with local radiation and CTLA-4 blockade in a mouse model of breast cancer. Clin Cancer Res. 2005;11(2 Pt 1):728–34.
47. Dewan MZ, Galloway AE, Kawashima N, et al. Fractionated but not single-dose radiotherapy induces an immune-mediated abscopal effect when combined with anti-CTLA-4 antibody. Clin Cancer Res. 2009;15:5379–88.
48. Kanagavelu S, Gupta S, Wu X, et al. In vivo effects of lattice radiation therapy on local and distant lung cancer: potential role of immunomodulation. Radiat Res. 2014;182:149–62.
49. den Brok MH, Sutmuller RP, Nierkens S, et al. Efficient loading of dendritic cells following cryo and radiofrequency ablation in combination with immune modulation induces anti-tumour immunity. Br J Cancer. 2006;95:896–905.
50. Waitz R, Solomon SB, Petre EN, et al. Potent induction of tumor immunity by combining tumor cryoablation with anti-CTLA-4 therapy. Cancer Res. 2012;72:430–9.
51. Ma S, Richardson JA, Bitmansour A, et al. Partial depletion of regulatory T cells does not influence the inflammation caused by high dose hemi-body irradiation. PLoS ONE. 2013;8(2):e56607.

Part II

Principles of Surgery, Intra-arterial Therapies, and Thermal Ablation

Surgical Considerations

6

Ana Luiza Mandelli Gleisner, MD, PhD

6.1 Introduction

Surgery remains the mainstay of treatment for liver tumors in appropriately selected patients. Advancements in surgical technique and perioperative management have led to a significant improvement in perioperative outcomes for patients undergoing liver resection in the last 50 years, resulting in contemporary perioperative mortality rates of less than 5% in tertiary centers [1]. Recent advances in imaging technology, surgical instruments, and surgical techniques have expanded the application of the laparoscopic approach to complex liver resections, with substantial improvements in the postoperative course for these patients [2].

6.2 Indications

Liver resections are indicated for the management of primary and metastatic liver tumors (Table 6.1) when: (1) oncologically appropriate; (2) technically feasible (resectability); (3) the planned procedure can be performed with acceptable morbidity and mortality given the patient's comorbidities.

The oncologic appropriateness of surgical resection varies according to the tumor biology. The presence of multiple lesions or extrahepatic disease in patients with hepatocellular carcinoma (HCC) or cholangiocarcinoma rarely justifies a liver resection. The presence of major vascular invasion or grossly positive portal lymph nodes in these patients are relative contraindications to resection, as the long-term prognosis is poor [3]. In contrast, favorable outcomes can be achieved in patients with metastatic colorectal cancer (mCRC) and multiple liver lesions, including those with lesions in both the right and left hemilivers (bilobar disease), or extrahepatic disease [4]. Nevertheless, the extrahepatic disease should be limited and resectable [5], and all the liver lesions should be amenable to treatment with resection and/or ablation.

The resectability of the lesions is determined with high-quality imaging. Computed tomography (CT) scan is usually the method of choice, but magnetic resonance imaging (MRI) is emerging as a very useful imaging adjunct, especially in patients with steatosis or lesions that cannot be visualized after preoperative chemotherapy [6]. The location of the hepatic lesions and their relationship to the main hepatic vessels and the biliary tree will ultimately determine the extent of the hepatic resection and lesion resectability (Fig. 6.1). The goal of resection is to obtain negative margins, while leaving adequate functional liver with an intact hepatic arterial and portal venous inflow, venous outflow, and biliary drainage in continuity with the small bowel. For metastatic disease, the number and size of the lesions are no longer determinants of resection as long as the aforementioned requirement is met. While large lesions may involve

A.L.M. Gleisner (✉)
Department of Surgery, University of Colorado,
12631 E 17th Ave, C-313, 80045 Aurora, CO, USA
e-mail: ana.gleisner@ucdenver.edu

J. Meyer and T.E. Schefter (eds.), *Radiation Therapy for Liver Tumors*,
DOI 10.1007/978-3-319-54531-8_6

Table 6.1 Primary and metastatic tumors that may require a major hepatic resection

Primary liver tumors
Hepatocellular carcinoma
Cholangiocarcinoma
Hilar cholangiocarcinoma
Gallbladder cancer
Metastatic liver disease
Colorectal cancer
Neuroendocrine tumors
Non-colorectal non-neuroendocrine tumors

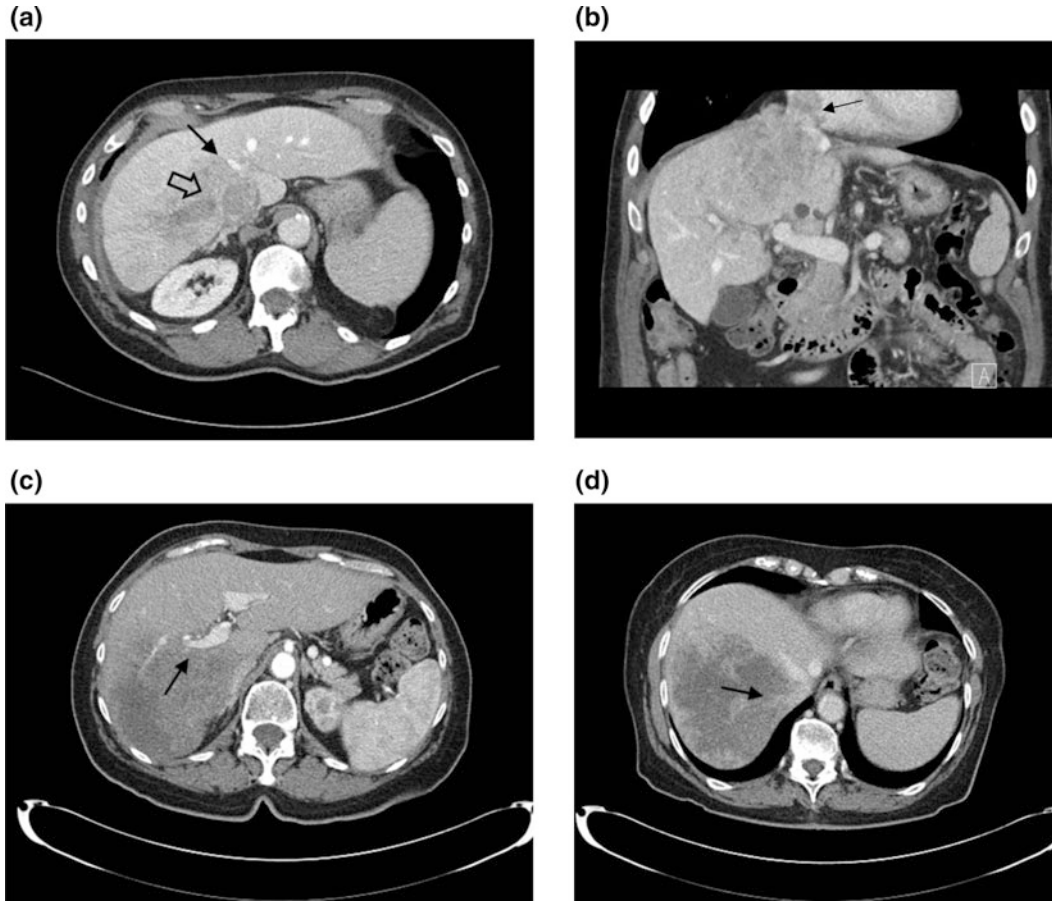

Fig. 6.1 Hepatic lesions and their relationship with hepatic vessels. **a** a lesion on the right liver encases the right hepatic vein (*thick arrow*) and abuts the middle hepatic vein (*thin arrow*); **b** coronal reconstruction shows invasion of the tumor into the IVC, extending to the right atrium (*arrow*); **c** a lesion on the right liver encases the right portal vein (*arrow*); and **d** the right hepatic vein (*arrow*)

several segments of the liver, centrally located lesions, even if small, often cannot be removed without compromising biliary drainage, vascular inflow, or the venous outflow of several liver segments. Consequently, removal of these small, central lesions may require resection of a large amount of functional liver parenchyma, thereby increasing the risk of postoperative liver failure. The adequate volume of the remnant liver is dependent on its function (see Sect. 6.3).

The risk for postoperative liver failure and death is most pronounced in patients with chronic liver dysfunction, especially when there is evidence of cirrhosis. Even minor liver resections can result in rapid liver decompensation following surgery in these patients. Therefore, surgical resection is typically limited to cirrhotic patients with Child-Turcotte-Pugh (CTP) class A and no evidence of significant portal hypertension [7]. The presence of portal hypertension is based on a history of variceal bleed, the presence of thrombocytopenia or evidence of esophageal varices, and splenomegaly on imaging. When in doubt, the hepatic venous pressure gradient can be measured. A pressure gradient greater than or equal to 10 mmHg is associated with an increased risk of decompensation after surgery [8]. Patients with HCC and cirrhosis CTP B or C or with evidence of portal hypertension should be treated with liver transplantation or other modalities if transplantation is contraindicated.

6.3 Preoperative Assessment

Patients considered for surgical resection should have a perioperative risk assessment with clinical optimization of the patient's medical comorbidities and functional status. Complete staging should be performed with CT of the chest and tumor markers as indicated. Positron emission tomography (PET) should be used selectively in patients with mCRC at high risk for extrahepatic metastasis, as higher rates of false negative findings limit its use in patients undergoing chemotherapy or when lesions are smaller than 1 cm. In fact, the use of PET prior to liver resection has been shown to results in changes in the surgical management of less than 10% of the patients and no differences in long-term survival [9].

The function of the liver is typically estimated through liver function tests such as total bilirubin, prothrombin time, and albumin. Imaging-based liver function tests are frequently used in Europe and Asia to determine the extension of the liver parenchyma that can be safely removed [10]. The indocyanine green (ICG) test is the most commonly used method, but new techniques such as 99mTc galactosyl and the 99mTc mebrofenin scintigraphy with single-photon emission computer tomography (SEPCT-CT) [11] and the Gd-EOB-enhanced MRI [12] have been recently introduced and may have an increasing role in the preoperative evaluation of these patients, as they add spatial information [13].

If a major liver resection is planned, the volume of the postoperative liver, or future liver remnant (FLR), is estimated. The volume of the FLR needed to minimize the chances of postoperative liver insufficiency is dependent on the liver remnant's function. Liver dysfunction is common in patients presenting for resection of hepatic malignancies. For example, hepatocellular carcinoma and cholangiocarcinoma are often associated with chronic liver disease, and prolonged modern chemotherapy is associated with significant injury to the liver, as discussed later. For patients with no liver dysfunction, the FLR should be at least 20% of the total liver volume (i.e., one can remove up to 80% of the liver) [14]. Patients with abnormal background liver (i.e., following preoperative chemotherapy) should have a FLR of at least 30% of the total liver volume, while those with cirrhosis should have a FLR of at least 40% [15]. When questionable, formal calculation of the FLR should be performed. The volume of the expected remnant liver and the total liver volume are measured using either CT scan or MRI. The volume of the non-functional liver (parenchyma, i.e., either non-perfused or replaced by tumor) is subtracted from the total liver volume, which is especially important for patients with large lesions. Alternatively, the total liver volume can be estimated

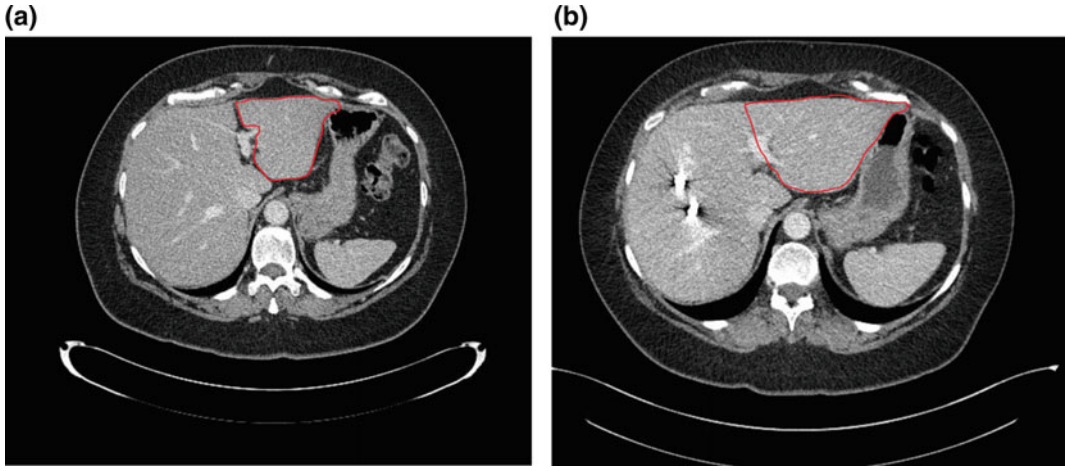

Fig. 6.2 Future liver remnant (FLR) before (**a**) and after portal vein embolization (**b**). The volume of the FLR (in *red*) increased by 30% four weeks after portal vein embolization

with different formulas based on the patient's weight or body surface area [16]. Portal vein embolization should be considered for patients with insufficient FLR. Portal vein embolization involves selective occlusion of the branches of the portal vein feeding the segments planned for resection, which stimulates contralateral hypertrophy (Fig. 6.2). The FLR volume increases significantly within the first 3–4 weeks after the procedure. Liver volumetry is then repeated to assure a minimal FLR volume has been achieved. Otherwise, imaging is repeated in another 4 weeks, as liver regeneration may continue to occur, albeit at a slower rate [17]. The degree of hypertrophy of the remnant (at least 5% increase in volume or a rate of at least 2% increase per week) has been associated with decreased rates of postoperative liver insufficiency [17, 18].

6.4 Effect of Chemotherapy and Radiation

Preoperative chemotherapy is typically administered to patients with mCRC and, at times, cholangiocarcinoma to assess tumor response, convert unresectable tumors to resectable and to address micrometastatic disease that is not seen on imaging. Nevertheless, preoperative chemotherapy has not been shown to improve survival in patients for hepatic resection for mCRC [19]. Moreover, prolonged modern chemotherapy for colorectal cancer may be associated with significant injury to the liver, with increased risk of postoperative complications following liver resection. Specifically, irinotecan-based treatment is associated with steatohepatitis, while oxaliplatin-based chemotherapy is associated with sinusoidal congestion [20]. Also, small (<2 cm) lesions may disappear on imaging with chemotherapy. If not surgically resected, these lesions will recur in up to 80% of the patients [21]. Surgeons and the medical oncologists need to work closely to determine optimal duration of preoperative chemotherapy and the timing for liver resection. In general, if preoperative chemotherapy is used, the duration should be limited to 2–3 months.

Selective internal radiation therapy (SIRT) with Yttrium-90 has been increasingly used in the treatment of liver primary and secondary malignancies, mostly in the palliative setting. Recent studies have been shown that SIRT to one hemiliver often results in significant hypertrophy of the contralateral side [22]. Such findings motivated the use of SIRT as a substitute to portal vein embolization prior to liver resection, with the advantage of providing tumor control in the involved segments while the uninvolved liver

Table 6.2 Nomenclature of major hepatic resections based on the Brisbane 2000 nomenclature of hepatic anatomy and resections

Major hepatic resection	Liver segments resected[a]
Right hepatectomy	5, 6, 7, 8
Extended right hepatectomy	4, 5, 6, 7, 8
Left hepatectomy	2, 3, 4
Extended left hepatectomy	2, 3, 4, 5, 8

[a]Any of these resections may also involve removal of segment 1, which is also referred to as the caudate lobe

grows. Clinical experience is limited with this approach, with some reports describing increases in the technical complexity of the operation, as the liver parenchyma becomes fibrotic and inflexible [23]. There are inconsistent data on the impact of these findings in terms of perioperative outcomes [24, 25].

6.5 Types of Liver Resection

Liver resections can be categorized into anatomic and nonanatomic (wedge resections). Anatomic resections involve the resection of portal territories and include segmentectomies, sectionectomies, hemihepatectomies, and extended hepatectomies. If feasible, anatomic resections should be performed for the treatment of HCC, as HCC tends to spread via portal venous tributaries. In fact, anatomic resections have been associated with improved survival in patients with HCC in observational studies [26]. In contrast, when treating mCRC, superficial resection can be performed nonanatomically, with the goal of achieving microscopically negative margins. The width of the negative surgical margins has not been shown to be associated with increased risk of local recurrence. This strategy, referred to as parenchyma-sparing hepatectomies, is preferred over major hepatectomies for mCRC, when applicable, as these procedures are associated with decreased morbidity and increased rates of salvage ability in cases of recurrence—with no increase in recurrence rate or decrease in overall survival [27].

Liver resections are also defined based on the extension of the resection into minor and major resections. Major hepatic resection involves three or more liver segments based on Couinaud's classification. According to the Brisbane 2000 Nomenclature of Hepatic Anatomy and Resections, proposed by the International Hepato-Pancreato-Biliary Association in an effort to standardize the terminology in the field, the anatomic division of the liver is based on the vascular watershed—the plane intersecting the gallbladder fossa and the inferior vena cava (IVC), described by Cantlie in 1897 and not seen from the surface of the liver [28]. This nomenclature rendered use of the term *liver lobe* obsolete, as this implies the presence of a visible anatomic demarcation (i.e., the umbilical fissure). Such principles were used to define the current terminology for liver resections (Table 6.2), which should no longer be referred to as lobectomies.

Minimally invasive (laparoscopic or robotic) liver resection can be performed in selected patients. Observational data suggest that laparoscopic liver resection is associated with decreased wound complications, intraoperative blood loss, postoperative pain, and length of stay while being associated with similar mortality, positive margin rates, and long-term outcomes in patients with mCRC or HCC [29–31]. Because laparoscopic liver resections are often applied to small, peripheral tumors, there is certainly potential for selection bias. Randomized trials comparing laparoscopic versus open liver resection are currently ongoing.

6.6 Combined Procedures

Liver resection can be done in combination with other procedures such as ablation of liver lesions or resection of the primary tumor in metastatic disease.

Liver resection can be combined with intraoperative ablation of lesions, consistent with the goal of sparing of liver parenchyma. For bilobar metastases, a major liver resection can be performed on the side with the highest disease burden, while ablation is performed on the contralateral side. These procedures may be performed at the same time if the anticipated volume of the FLR is adequate. Otherwise, separate, staged operations should be considered. Ablation can also be used intraoperatively to treat centrally located lesions that would otherwise require a major liver resection in combination with wedge or segmental resection of more superficial lesions in patients with multiple metastases. Ablation is typically thermal, using heat (radiofrequency and microwave ablation) or cold (cryoablation), with the latter rarely used nowadays. Irreversible electroporation, a newer technology based on the short-duration, high-voltage pulses that result in defects in the lipid bilayer—and, ultimately, cell necrosis—is emerging as an attractive substitute to thermal ablation, especially near major vessels, as it is not associated with deflection in the ablation zone due to heat loss near adjacent vascular structures.

In patients with synchronous hepatic metastases, the primary tumor and the liver disease can be addressed at the same time or separately. Concomitant resection of the liver and the primary tumor should be strongly considered when only a minor liver resection is required or when the resection of the primary is straightforward, such as in patients requiring a distal pancreatectomy or a right hemicolectomy. Major liver resections should, however, be avoided when complex procedures are performed for the treatment of the primary tumor, such as extensive pelvic dissections, a low rectal anastomosis, or a duodenopancreatectomy. In these situations, the hepatic metastases can be addressed first or after resection of the primary tumor. Because the liver is often the determinant factor for complete disease resection, the "liver first" approach (or reversed approach) is an attractive option since resectability of the liver metastases will influence the need or extent of the resection of the primary tumor. Besides, the liver disease can progress to unresectable if the primary tumor is addressed first. Occasionally, however, the primary tumor is symptomatic and needs to be resected first. Despite the potential advantages of the reversed approach, retrospective studies have shown no difference in outcomes when this approach is compared to the traditional approaches (combined resection and resection of the primary first) [32, 33].

For primary tumor in the mid and distal rectum, radiation can be given prior to the liver resection, immediately afterward or after the completion of the systemic chemotherapy. Patients can then fully recover from the liver procedure while awaiting for the mandated 6–10 week interval between radiation and rectal resection. Short course radiation should be considered if radiation is to be given prior to liver resection to avoid an extended period when the liver lesion is not being addressed [34]. Selective exclusion of radiotherapy can be considered when the primary tumor has an adequate response to the systemic chemotherapy, as distant recurrence is overwhelmingly more common than local recurrence in patients with synchronous disease [35].

6.7 Surgical Technique

In the open technique, a right subcostal incision with an upper midline extension provides adequate exposure for most tumors. The xyphoid should be removed to facilitate visualization of the suprahepatic IVC. An upper midline incision is usually adequate for resections of the left liver and may suffice for resection of the right liver in a thin patient. Intraoperative ultrasound is performed to identify all known lesions—as well as any new lesions—and their relationship with vascular and biliary structures, as well as the position of the main hepatic vessels relative to the transection plane.

For major hepatic resections, arterial and portal vein inflow vessels can be dissected and controlled in the hilum of the liver or

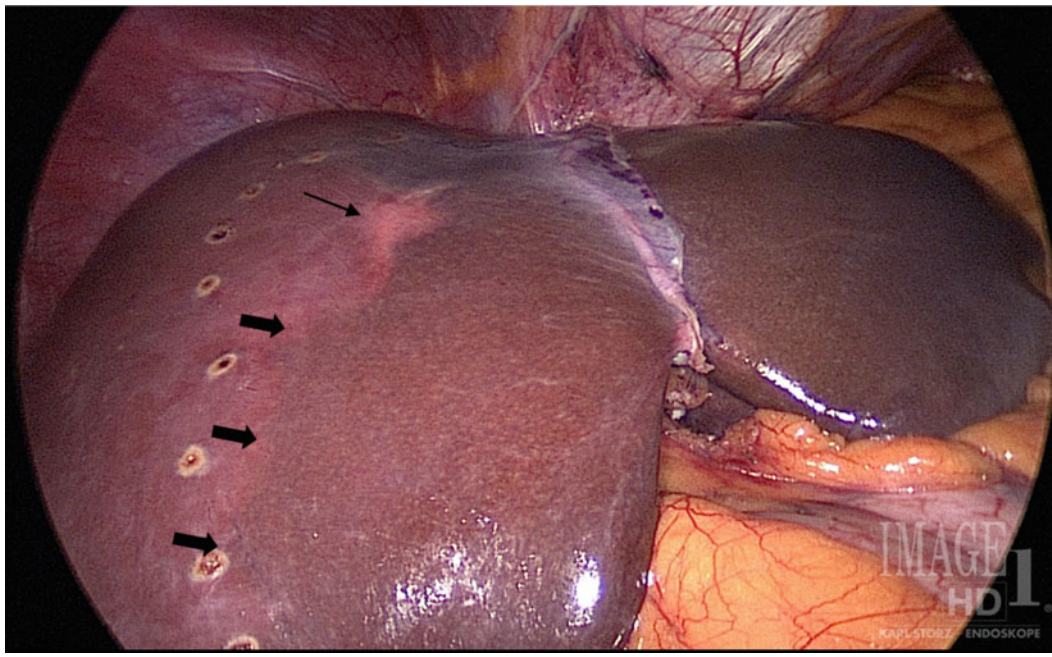

Fig. 6.3 Vascular demarcation line between the right and left hemilivers after ligation of the left hepatic artery and the left branch of the portal vein during a laparoscopic left hepatectomy (*thick arrows*). The transection plane was shifted laterally to assure negative margins for the lesion seen in segment 4 (*thin arrow*)

intraparenchimally, through small hepatotomies. Selective inflow control prior to the transection will result in a vascular demarcation line that will guide the correct transection plane (Fig. 6.3). After inflow has been controlled, control of the hepatic venous outflow is performed. This can also be done outside the liver or within the parenchyma, during the transection.

Occlusion of the portal triad (Pringle maneuver) can be performed in major and minor liver resections during the transection of the parenchyma to decrease blood loss. The liver can tolerate up to 1 h of ischemia, but intermittent vascular occlusion with cycles of 15–20 min on and 5 min off will decrease the ischemia/reperfusion injury, which is especially important in cirrhotic livers. Total ischemic time should always be limited as much as possible. If proper transection planes are selected, a Pringle maneuver is often unnecessary, especially if inflow vascular control has been obtained.

6.8 Parenchymal Transection

Transection of the liver parenchyma can be performed with multiple techniques—most often a combination of techniques—according to the surgeon's experience and preference. Finger fracture (digitoclasy), clamp crushing, water jet devices, and ultrasound energy devices (i.e., CUSA or Cavitron Ultrasonic Surgical Aspirator) gently fracture the parenchyma while preserving vessels and bile ducts crossing the transection plane. These structures are then controlled with ties, clips, energy devices, or staplers for larger structures. Bipolar (i.e., LigaSure) and ultrasonic (Harmonic Scalpel) vessel-sealing devices can be used for control of vessels up to 7–8 mm—decreasing the need for ties and clips and, thereby, resulting in faster transection. Hemostatic devices such as the argon beam coagulator and the radiofrequency sealer devices (i.e., TissueLink

and Aquamantis) are very useful to control bleeding from the cut edge of the liver. Finally, staple devices can be employed for the division of large vessels.

Mobilization of the liver starts with transection of the falciform ligament to the anterior surface of the hepatic veins. For a right liver resection, the right coronary and triangular ligaments are then divided, exposing the bare area of the liver as the right liver is mobilized and rotated to the left and the short hepatic veins draining directly to the IVC are ligated until the right hepatic vein is identify and encircled. Attention is turned to the hilum, where the right hepatic artery and right portal vein are dissected and ligated. The parenchyma is transected at vascular demarcation, and the right hepatic duct is identified and ligated near the left base of the gallbladder fossa. When indicated, segment 4 can be resected along with the right liver. The initial steps are the same, but the transection plane is along the right side of the falciform ligament toward the medial aspect of the right hilar plate. Inflow control to segment 4 and identification and ligation of the middle hepatic vein are performed as the parenchyma is transected.

For a left hepatectomy, the left triangular ligament is divided, exposing the IVC and the left hepatic vein. The round ligament is elevated and the parenchymal bridge between segments 3 and 4B is divided exposing the left hilum at the base of the umbilical fissure. The left hepatic artery, portal vein, and hepatic duct are individually identified and ligated. The common trunk of the middle and the left hepatic veins is encircled as a clamp is passed between the left hepatic vein and the IVC, emerging between the right and middle hepatic veins or ligated intraparenchymally, during transection, which follows the demarcated line. When indicated, the right anterior section (segments 5 and 8) can be resected along with the left hemiliver. The initial steps are the same as those for a left hepatectomy. The main challenge is to define the transection plane, which is horizontal—extending from the right of the gallbladder fossa and anterior to the right hepatic vein toward the base of segment 4—without injuring the inflow to the posterior sector (segments 6 and 7). The pedicle to the right anterior sector will be identified and ligated as transection of the parenchyma approaches the hilum.

6.9 Complications

Although mortality with modern liver resection is low in tertiary centers, morbidity is still significant. While overall morbidity is 40–60%, complications requiring interventions or resulting in death are around 20% [2, 36, 37]. Pulmonary complications are the most common complications in open surgery, occurring in approximately 20% of the patients. Ascites develops in 10–20% of the patients and in up to a third of the patients operated for HCC [37]. Ascites can result in the disruption of the incision and major fluid and electrolyte losses.

Intra-abdominal collections at the transected edge of the liver are common after major liver resections. These collections should be percutaneously drained if the patient becomes symptomatic or if there are clinical signs of infection. Biliary leaks from the transected liver edge are seen in 7% of the cases [36, 37]. If persistent bilious drainage exists, ERCP with sphincterotomy can be performed to diagnose the site of the biliary leakage and decrease the output.

Posthepatectomy liver failure is a rare complication (2%), but it is associated with high mortality (up to 50% of the patients) [38]. Liver insufficiency may present in the early postoperative period with hypotension refractory to vasopressors, respiratory failure, acute renal insufficiency, hypoglycemia, and coagulopathy. Other patients may develop a more protracted course with progressive hyperbilirubinemia, encephalopathy, massive ascites, anasarca, and renal insufficiency. While some of these patients will never recover their liver function and eventually succumb to infection, others will regenerate to sufficient size with appropriate support.

Factors associated with increased risk of postoperative liver failure include the size and function of the liver remnant (especially in cirrhotic patients), intraoperative blood loss, and postoperative complications, most commonly infectious [39, 40]. Treatment is supportive while the liver regenerates, regaining both volume and function.

References

1. Jarnagin WR, Gonen M, Fong Y, et al. Improvement in perioperative outcome after hepatic resection: analysis of 1,803 consecutive cases over the past decade. Ann Surg. 2002;236:397–407.
2. Karagkounis G, Seicean A, Berber E. The impact of laparoscopic approaches on short-term outcomes in patients undergoing liver surgery for metastatic tumors. Surg Laparosc Endosc Percutaneous Tech. 2015;25:229–34.
3. Dixon E, Abdalla E, Schwarz RE, Vauthey JN. AHPBA/SSO/SSAT sponsored consensus conference on multidisciplinary treatment of hepatocellular carcinoma. HPB Official J Int Hepato Pancreato Biliary Assoc. 2010;12:287–8.
4. Schwarz RE, Abdalla EK, Aloia TA, Vauthey JN. AHPBA/SSO/SSAT sponsored consensus conference on the multidisciplinary treatment of colorectal cancer metastases. HPB Official J Int Hepato Pancreato Biliary Assoc. 2013;15:89–90.
5. Pulitano C, Bodingbauer M, Aldrighetti L, et al. Liver resection for colorectal metastases in presence of extrahepatic disease: results from an international multi-institutional analysis. Ann Surg Oncol. 2011;18:1380–8.
6. Zech CJ, Korpraphong P, Huppertz A, et al. Randomized multicentre trial of gadoxetic acid-enhanced MRI versus conventional MRI or CT in the staging of colorectal cancer liver metastases. Br J Surg. 2014;101:613–21.
7. Jarnagin W, Chapman WC, Curley S, et al. Surgical treatment of hepatocellular carcinoma: expert consensus statement. HPB Official J Int Hepato Pancreato Biliary Assoc. 2010;12:302–10.
8. Berzigotti A, Seijo S, Reverter E, Bosch J. Assessing portal hypertension in liver diseases. Exp Rev Gastroenterol Hepatol. 2013;7:141–55.
9. Moulton CA, Gu CS, Law CH, et al. Effect of PET before liver resection on surgical management for colorectal adenocarcinoma metastases: a randomized clinical trial. JAMA. 2014;311:1863–9.
10. Kubota K, Makuuchi M, Kusaka K, et al. Measurement of liver volume and hepatic functional reserve as a guide to decision-making in resectional surgery for hepatic tumors. Hepatology. 1997;26:1176–81.
11. Hayashi H, Beppu T, Okabe H, et al. Functional assessment versus conventional volumetric assessment in the prediction of operative outcomes after major hepatectomy. Surgery. 2015;157:20–6.
12. Akiba A, Murata S, Mine T, et al. Volume change and liver parenchymal signal intensity in Gd-EOB-DTPA-enhanced magnetic resonance imaging after portal vein embolization prior to hepatectomy. Biomed Res Int. 2014;2014:684754.
13. Geisel D, Ludemann L, Hamm B, Denecke T. Imaging-based liver function tests-past, present and future. Rofo. 2015;187:863–71.
14. Abdalla EK, Barnett CC, Doherty D, Curley SA, Vauthey JN. Extended hepatectomy in patients with hepatobiliary malignancies with and without preoperative portal vein embolization. Arch Surg. 2002;137:675–80; discussion 80–1.
15. Asencio JM, Garcia Sabrido JL, Olmedilla L. How to expand the safe limits in hepatic resections? J Hepato-Biliary-Pancreatic Sci. 2014;21:399–404.
16. Ribero D, Amisano M, Bertuzzo F, et al. Measured versus estimated total liver volume to preoperatively assess the adequacy of the future liver remnant: which method should we use? Ann Surg. 2013;258:801–6; discussion 6–7.
17. Ribero D, Abdalla EK, Madoff DC, Donadon M, Loyer EM, Vauthey JN. Portal vein embolization before major hepatectomy and its effects on regeneration, resectability and outcome. Br J Surg. 2007;94:1386–94.
18. Shindoh J, Truty MJ, Aloia TA, et al. Kinetic growth rate after portal vein embolization predicts posthepatectomy outcomes: toward zero liver-related mortality in patients with colorectal liver metastases and small future liver remnant. J Am Coll Surg. 2013;216:201–9.
19. Nordlinger B, Sorbye H, Glimelius B, et al. Perioperative FOLFOX4 chemotherapy and surgery versus surgery alone for resectable liver metastases from colorectal cancer (EORTC 40983): long-term results of a randomised, controlled, phase 3 trial. Lancet Oncol. 2013;14:1208–15.
20. Pawlik TM, Olino K, Gleisner AL, Torbenson M, Schulick R, Choti MA. Preoperative chemotherapy for colorectal liver metastases: impact on hepatic histology and postoperative outcome. J Gastrointest Surg Official J Soc Surg Aliment Tract. 2007;11:860–8.
21. Bischof DA, Clary BM, Maithel SK, Pawlik TM. Surgical management of disappearing colorectal liver metastases. Br J Surg. 2013;100:1414–20.
22. Teo JY, Allen JC Jr, Ng DC, et al. A systematic review of contralateral liver lobe hypertrophy after unilobar selective internal radiation therapy with

Y90. HPB Official J Int Hepato Pancreato Biliary Assoc. 2016;18:7–12.
23. Maker AV, August C, Maker VK, Weisenberg E. Hepatectomy after yttrium-90 (Y90) radioembolization-induced liver fibrosis. J Gastrointest Surg Official J Soc Surg Aliment Tract. 2016;20:869–70.
24. Lewandowski RJ, Donahue L, Chokechanachaisakul A, et al. Y radiation lobectomy: outcomes following surgical resection in patients with hepatic tumors and small future liver remnant volumes. J Surg Oncol. 2016;114:99–105.
25. Henry LR, Hostetter RB, Ressler B, et al. Liver resection for metastatic disease after y90 radioembolization: a case series with long-term follow-up. Ann Surg Oncol. 2015;22:467–74.
26. Zhou Y, Xu D, Wu L, Li B. Meta-analysis of anatomic resection versus nonanatomic resection for hepatocellular carcinoma. Langenbeck's Arch Surg Deut Ges Chirurgie. 2011;396:1109–17.
27. Mise Y, Aloia TA, Brudvik KW, Schwarz L, Vauthey JN, Conrad C. Parenchymal-sparing hepatectomy in colorectal liver metastasis improves salvageability and survival. Ann Surg. 2016;263:146–52.
28. Strasberg SM. Nomenclature of hepatic anatomy and resections: a review of the Brisbane 2000 system. J Hepato-Biliary-Pancreatic Surg. 2005;12:351–5.
29. Schiffman SC, Kim KH, Tsung A, Marsh JW, Geller DA. Laparoscopic versus open liver resection for metastatic colorectal cancer: a metaanalysis of 610 patients. Surgery. 2015;157:211–22.
30. Wei M, He Y, Wang J, Chen N, Zhou Z, Wang Z. Laparoscopic versus open hepatectomy with or without synchronous colectomy for colorectal liver metastasis: a meta-analysis. PLoS ONE. 2014;9:e87461.
31. Yin Z, Fan X, Ye H, Yin D, Wang J. Short- and long-term outcomes after laparoscopic and open hepatectomy for hepatocellular carcinoma: a global systematic review and meta-analysis. Ann Surg Oncol. 2013;20:1203–15.
32. Brouquet A, Mortenson MM, Vauthey JN, et al. Surgical strategies for synchronous colorectal liver metastases in 156 consecutive patients: classic, combined or reverse strategy? J Am Coll Surg. 2010;210:934–41.
33. Kelly ME, Spolverato G, Le GN, et al. Synchronous colorectal liver metastasis: a network meta-analysis review comparing classical, combined, and liver-first surgical strategies. J Surg Oncol. 2015;111:341–51.
34. Adam R, de Gramont A, Figueras J, et al. Managing synchronous liver metastases from colorectal cancer: a multidisciplinary international consensus. Cancer Treat Rev. 2015;41:729–41.
35. Butte JM, Gonen M, Ding P, et al. Patterns of failure in patients with early onset (synchronous) resectable liver metastases from rectal cancer. Cancer. 2012;118:5414–23.
36. Spolverato G, Ejaz A, Kim Y, et al. Patterns of care among patients undergoing hepatic resection: a query of the national surgical quality improvement program-targeted hepatectomy database. J Surg Res. 2015;196:221–8.
37. Dokmak S, Fteriche FS, Borscheid R, Cauchy F, Farges O, Belghiti J. 2012 Liver resections in the 21st century: we are far from zero mortality. HPB Official J Int Hepato Pancreato Biliary Assoc. 2013;15:908–15.
38. Rahbari NN, Garden OJ, Padbury R, et al. Posthepatectomy liver failure: a definition and grading by the international study group of liver surgery (ISGLS). Surgery. 2011;149:713–24.
39. Kooby DA, Fong Y, Suriawinata A, et al. Impact of steatosis on perioperative outcome following hepatic resection. J Gastrointest Surg Official J Soc Surg Aliment Tract. 2003;7:1034–44.
40. Kooby DA, Stockman J, Ben-Porat L, et al. Influence of transfusions on perioperative and long-term outcome in patients following hepatic resection for colorectal metastases. Ann Surg. 2003;237:860–9; discussion 9–70.

Principles of Intra-Arterial Therapies

7

Keshav M. Menon, MD, Ankaj Khosla, MD
and Clayton K. Trimmer, DO

7.1 Introduction

Embolization represents selective intra-arterial delivery of micron-sized embolic particles that can be combined with radioisotopes or chemotherapeutic agents for the treatment of primary or metastatic hepatic malignancies. Bland embolization involves the restriction of vascular supply to the tumor without radioisotope or chemotherapeutic agents. Transarterial chemoembolization (TACE) and radioembolization (TARE) combine embolic particles with cytotoxic agents or with ^{90}Y microspheres, respectively, to treat a variety of hepatic lesions with minimal associated clinical complications.

K.M. Menon
Department of Radiology, University of Texas Southwestern Medical Center, 5323 Harry Hines Blvd., Dallas, TX 75390-8896, USA
e-mail: Keshav.Menon@phhs.org

A. Khosla
Department of Radiology, UT Southwestern, 5323 Harry Hines Blvd., Dallas, TX 75390, USA
e-mail: Ankaj.khosla@phhs.org

C.K. Trimmer (✉)
Department of Interventional Radiology, University of Texas Southwestern Medical Center, 5323 Harry Hines Blvd., Dallas TX 75390-8834, USA
e-mail: Trimmer2005@gmail.com

7.2 Hepatic Vasculature and the Anatomic Basis of Intra-Arterial Therapies

The unique dual vascular supply of the liver allows for selective tumor-based therapy. Hepatic tumors greater than 3 mm in size are estimated to derive 80–100% of vascular supply from the arterial system while normal hepatic parenchyma is predominantly supplied by the portal venous system [1]. The common hepatic artery arises from the celiac trunk and terminates in the gastroduodenal artery (GDA) and the proper hepatic artery. The proper hepatic artery is estimated to supply the entire liver in approximately 55% of patients. Terminal branches may include the right gastric artery in addition to the right and left hepatic arteries. Figure 7.1 demonstrates typical hepatic anatomy.

Approximately 45% of patients demonstrate altered hepatic anatomy (Table 7.1). The common hepatic artery may arise from the aorta or SMA in <5% of cases. The right hepatic artery may commonly originate from the SMA in 15% of cases, and may rarely arise from the celiac trunk. An accessory right hepatic artery may arise from the SMA in approximately 6% of cases and is typically seen to supply Couinaud segments 6 and 7. Both replaced and accessory left hepatic arteries have an estimated incidence of 10–15% and almost exclusively arise from the left gastric artery. Although not considered altered hepatic anatomy, the arterial supply to segment 4 is variable and may be derived from

J. Meyer and T.E. Schefter (eds.), *Radiation Therapy for Liver Tumors*,
DOI 10.1007/978-3-319-54531-8_7

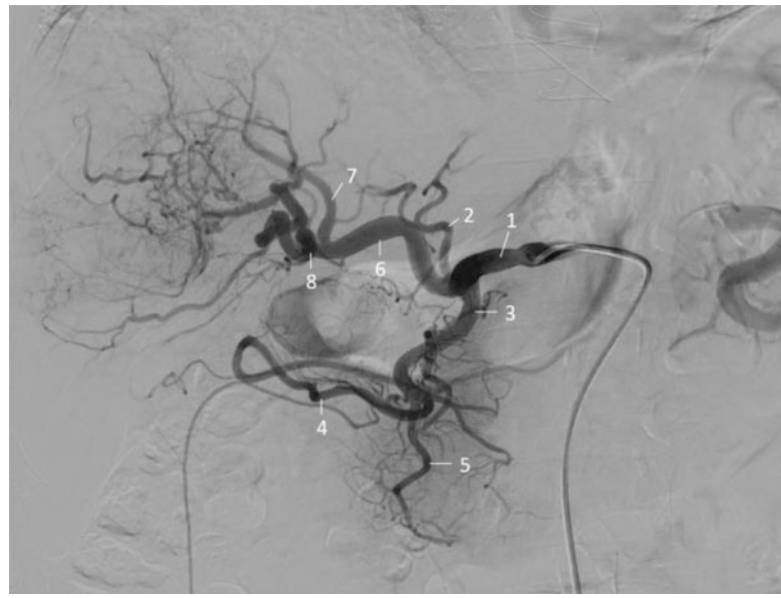

Fig. 7.1 Normal hepatic arterial supply. Digital subtracted angiogram of the common hepatic artery.
1. Common Hepatic Artery.
2. Left Gastric Artery.
3. Gastroduodenal Artery.
4. Right gastroepiploic artery.
5. Superior pancreaticoduodenal.
6. Common Hepatic Artery.
7. Right Hepatic Artery.
8. Left Hepatic Artery

Table 7.1 Hepatic Arterial Anatomy

All branches from common hepatic artery	55–65%
Right hepatic artery from SMA	10–12%
Left hepatic from left gastric artery	4–11%
Accessory left hepatic from left gastric artery	8–11%
Right hepatic from SMA and left hepatic from left gastric artery	2–3%
Right hepatic artery from right phrenic	4–5%
Accessory right hepatic artery	2–3%
Common hepatic artery from aorta	2%
Right hepatic artery from celiac trunk	<1%

Based on data from Refs. [2, 3]

the either the right or left hepatic arteries [2, 3]. Figure 7.2 demonstrates common hepatic arterial variants. The term used to denote aberrant arterial anatomy is "replaced". For instance, if the right hepatic artery arises from the SMA, it is called a replaced right hepatic artery.

7.3 Patient Selection

Pretreatment assessment is based on initial imaging assessment, burden of disease, laboratory markers, patient performance status, hepatopulmonary shunt assessment, and pre-procedure angiography. Diagnosis of HCC can be made through noninvasive findings including an elevated serum alpha-fetoprotein level or characteristic imaging findings on dedicated multiphase CT or MRI (Fig. 7.3). Patients with liver metastases may require biopsy sampling for pathological confirmation. Imaging should evaluate disease burden and assess for portal vein patency, biliary obstruction, and malignant ascites. For TACE, absolute exclusion criteria include greater than 50% involvement of the liver by tumor, extrahepatic metastases, as well as reduced main portal vein flow (from thrombus or stenosis) and renal insufficiency. Patients with poor clinical prognosis including hepatic encephalopathy and jaundice should be

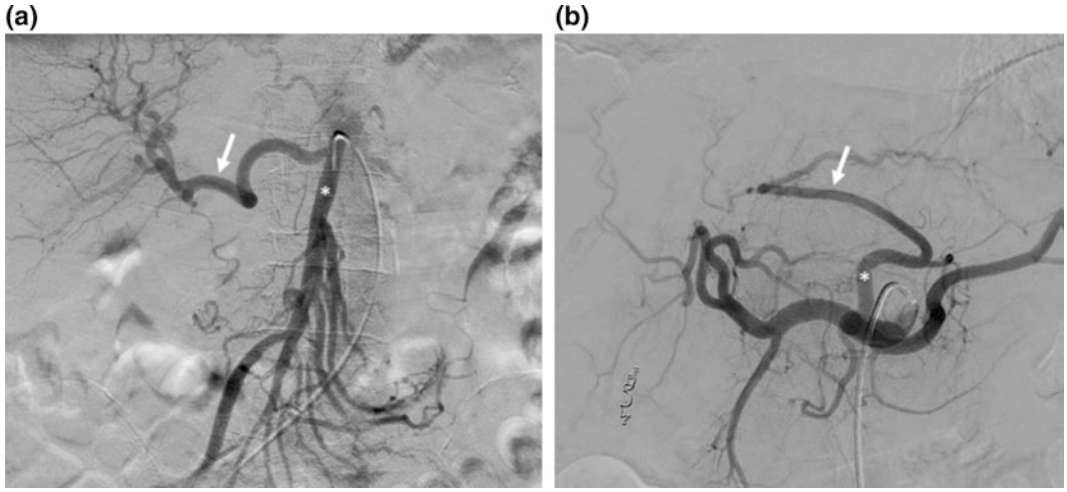

Fig. 7.2 Hepatic Arterial Anatomy Variants: **a** Digital subtracted SMA angiogram demonstrates a replaced right hepatic artery (*arrow*) from the SMA (*). **b** Accessory left hepatic artery (*arrow*) from the left gastric artery (*). Left hepatic artery is visualized

excluded from either treatment [4]. A relative threshold of a bilirubin of <= 2−3 mg/dL has been suggested. In the setting of secondary hepatic malignancy, TACE or TARE should only be considered if patient clinical outcome is dependent on the hepatic metastatic burden [5–8].

7.3.1 Pretreatment Angiographic Assessment

Assessment of the vascular anatomy for TACE procedures can be performed at the time of procedure. Angiographic identification of arteries that may lead to inadvertent injury to nontargeted parenchyma is of critical importance. The hepatic arterial supply is highly variable, as previously discussed, and HCC may co-opt adjacent vasculature including parasitized phrenic and omental arteries (Fig. 7.4). Thorough investigation of the celiac axis and SMA is required for appropriate evaluation of all relevant feeding hepatic arteries. Reflux of embolic particles into the feeding vessels of the gastrointestinal system may lead to injury of the stomach, small bowel, and esophagus [4]. The GDA, right gastric, and left gastric arteries in addition to prominent esophageal and duodenal branch arteries should be clearly identified. Prophylactic coil embolization of these arteries should be performed if the origins of the arteries are close to the site of expected infusion, but prophylactic coil embolization is no longer considered an absolute requirement prior to treatment [9].

The cystic artery should be clearly identified given the variability of origin. Either the infusion catheter must be placed distal to the cystic artery at the time of embolization or the artery should be prophylactically coil embolized during planning angiography to minimize risk of cystitis. Multiple small feeding vessels perfuse the gallbladder and prophylactic coil embolization to the gallbladder is typically well tolerated. There is a theoretical risk of damage to the anterior abdominal wall and a patent falciform artery should be prophylactically embolized to avoid undue patient pain.

7.4 TACE Preparation and Procedure

TACE involves the delivery of cytotoxic agents in conjunction with embolic materials to induce necrosis in the tumor. Microspheres are the most

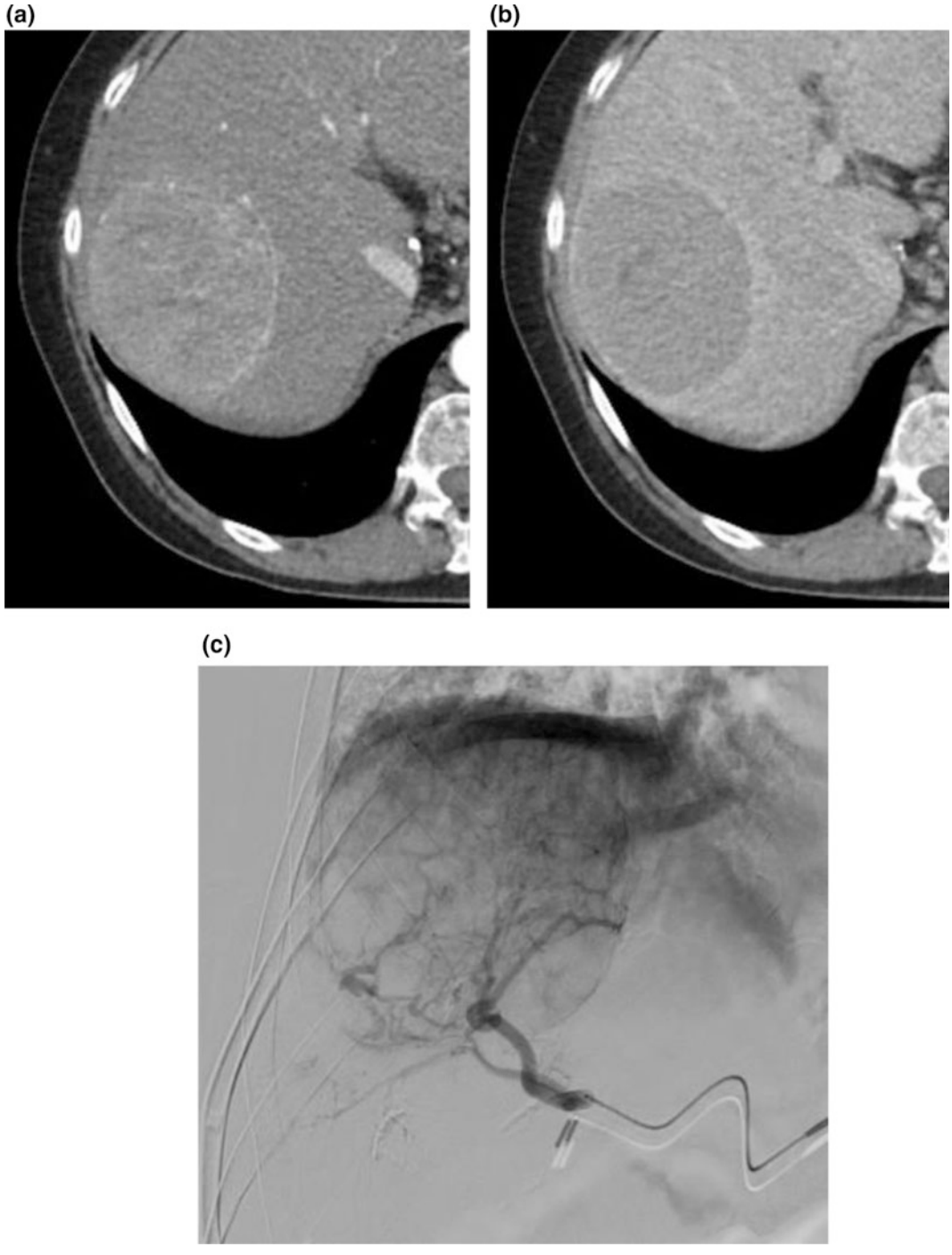

Fig. 7.3 Imaging findings of HCC: **a** Arterial phase CT scan demonstrates arterial enhancement with **b** characteristic tumor washout on delayed phase. **c** Corresponding angiogram demonstrates the typical tumor blush of HCC

Fig. 7.4 Parasitization of the vasculature by hepatocellular carcinoma: Digital subtracted angiogram of the celiac trunk demonstrates a left inferior phrenic artery (*arrow*) characteristically tracking along the diaphragm and supplying the tumor (*)

common embolic agent in TACE. Microspheres may be made from a multitude of compounds including glass, acrylics, and resins to name a few and may vary in size, shape, and the mechanism by which they bind to additional compounds including chemotherapeutics. No consensus exists in the choice of chemotherapeutic agent; however, doxorubicin is the most commonly used chemotherapeutic agent [10, 11]. Alternative chemotherapeutic regimens may utilize irinotecan or combination of doxorubicin, mitomycin-C, and cisplatin. Doxorubicin is usually mixed with lipiodiol in a variety of formulations depending on tumor location and burden to optimize dose to the targeted tumors. The emulsion of lipiodiol and the chemotherapy agent also has a small amount of iodinated contrast added to allow for visualization of the agents on radiographic equipment. This entire mixture is then suspended with 100–300 μm beads and injected to the target site of embolization. Alternatively, the emulsion can be injected and followed by embolization with beads or Gelfoam particles. Injection is usually performed with a microcatheter in subselected arterial segment to prevent nontarget embolization. The emulsion is injected slowly to ensure embolization is as targeted as possible and stasis occurs in the target site [4, 12]. TACE methodologies vary widely between practitioners and institutions. Bland embolization utilizes the same technique with ischemic inducing embolic particles in order to treat conditions including bleeding tumors.

Drug-eluting beads (DEB) are embolic particles impregnated with a chemotherapeutic, typically doxorubicin, that provide higher chemotherapeutic doses with prolonged administration at the targeted tumor. Particles range from 100–700 μm and are administered similar to conventional TACE without the need for lipiodol intermixing. Studies have demonstrated DEB TACE administration to be more reproducible with fewer post-therapeutic side effects.

Superiority of DEB-TACE to conventional TACE remains a matter of investigation. TARE preparation and treatment is discussed in detail in Chap. 11.

7.5 Posttreatment Follow-up

TACE is performed as an outpatient procedure with discharge on the same day. Patients should be monitored for complications associated with any arterial procedure including entry site injury, iatrogenic arterial injuries (including dissection), and nontarget embolization. These complications are usually evident either intraprocedurally or immediately in the post-procedure setting.

For TACE, no risks exist for those in contact with treated patients. Materials that come in contact with chemotherapy should be treated as contaminated and disposed of in a safe manner to avoid risking exposure.

Clinic follow-up one month after therapy should include a full evaluation of liver functional markers and multiphase imaging to assess for tumor necrosis and treatment success. Subsequent imaging 2–3 months after TACE or TARE may be necessary for evaluation for residual tumor or mass growth [13]. Treatment success in TACE or TARE can usually be assessed using modified Response Evaluation Criteria in Solid Tumors (mRECIST). Multiple studies have demonstrated that these criteria correspond to survival outcomes. The clearest determinant of residual or recurrent tumor is usually arterial enhancement of any kind in the tumor bed. Repeat therapy can be performed on demand when residual or recurrent tumor is visualized on follow-up imaging or rising alpha-fetoprotein levels are noted.

7.6 Side Effects and Complications

TACE is a fairly well-tolerated procedure. Postembolization syndrome is frequently seen after TACE and represents a constellation of symptoms that include abdominal pain, nausea, fever, and cachexia. The symptoms are thought to be in proportion to increased embolic effects. Symptomatic management with antiemetics and steroids may be needed, but hospitalization is exceedingly rare [14].

Complications of biliary tree damage typically present as incidental findings of focal dilation or biloma formation [9, 12]. Hepatic abscesses rarely develop but drainage is required if present. Of note, colonization of the biliary system may require prophylactic antibiotics prior to treatment [7]. Finally patients should be monitored for development of hepatic failure, variceal bleeding or renal failure, as these are rare but noted complications of TACE.

References

1. Kennedy A, Nag S, Salem R, Murthy R, McEwan AJ, Nutting C, Benson A 3rd, Espat J, Bilbao JI, Sharma RA, Thomas JP, Coldwell D. Recommendations for radioembolization of hepatic malignancies using yttrium-90 microsphere brachytherapy: a consensus panel report from the radioembolization brachytherapy oncology consortium. Int J Radiat Oncol Biol Phys. 2007;68(1):13–23. doi:10.1016/j.ijrobp.2006.11.060.
2. Michels NA, editor. Blood supply and anatomy of the upper abdominal organs with a descriptive atlas. Philadelphia, PA: Lippincott; 1955.
3. Covey AM, Brody LA, Maluccio MA, Getrajdman GI, Brown KT. Variant hepatic arterial anatomy revisited: digital subtraction angiography performed in 600 patients. Radiology. 2002;224(2):542–7. doi:10.1148/radiol.2242011283.
4. Lencioni R, Petruzzi P, Crocetti L. Chemoembolization of Hepatocellular Carcinoma. Semin Intervent Radiol. 2013;30(1):3–11. doi:10.1055/s-0033-1333648.
5. El-Serag HB. Hepatocellular carcinoma. New Engl J Med. 2011;365(12):1118–27. doi:10.1056/NEJMra1001683.
6. Mahnken AH, Pereira PL, de Baere T. Interventional oncologic approaches to liver metastases. Radiology. 2013;266(2):407–30. doi:10.1148/radiol.12112544.
7. Kaufman JA, Lee MJ editors. Vascular and Interventional Radiology. The Requisites, 2 ed. Philadelphia, PA:Elsevier, Saunders; 2014.
8. Habib A, Desai K, Hickey R, Thornburg B, Lewandowski R, Salem R. Transarterial approaches to primary and secondary hepatic malignancies. Nat Rev Clin Oncol. 2015;12(8):481–9. doi:10.1038/nrclinonc.2015.78.
9. Riaz A, Lewandowski RJ, Kulik LM, Mulcahy MF, Sato KT, Ryu RK, Omary RA, Salem R. Complications following radioembolization with yttrium-90

microspheres: a comprehensive literature review. Journal of vascular and interventional radiology: JVIR. 2009;20 (9):1121–1130; quiz 1131. doi:10.1016/j.jvir.2009.05.030.

10. Lammer J, Malagari K, Vogl T, Pilleul F, Denys A, Watkinson A, Pitton M, Sergent G, Pfammatter T, Terraz S, Benhamou Y, Avajon Y, Gruenberger T, Pomoni M, Langenberger H, Schuchmann M, Dumortier J, Mueller C, Chevallier P, Lencioni R, Investigators PV. Prospective randomized study of doxorubicin-eluting-bead embolization in the treatment of hepatocellular carcinoma: results of the PRECISION V study. Cardiovasc Intervent Radiol. 2010;33(1):41–52. doi:10.1007/s00270-009-9711-7.
11. Pinter M, Hucke F, Graziadei I, Vogel W, Maieron A, Konigsberg R, Stauber R, Grunberger B, Muller C, Kolblinger C, Peck-Radosavljevic M, Sieghart W. Advanced-stage hepatocellular carcinoma: transarterial chemoembolization versus sorafenib. Radiology. 2012;263(2):590–9. doi:10.1148/radiol.12111550.
12. Shah RP, Brown KT, Sofocleous CT. Arterially directed therapies for hepatocellular carcinoma. AJR Am J Roentgenol. 2011;197(4):W590–602. doi:10.2214/AJR.11.7554.
13. Minocha J, Lewandowski RJ. Assessing Imaging Response to Therapy. Radiol Clin North Am. 2015;53(5):1077–88. doi:10.1016/j.rcl.2015.05.010.
14. Clark TWI. Complications of Hepatic Chemoembolization. Semin Intervent Radiol. 2006;23(2):119–25. doi:10.1055/s-2006-941442.

Principles of Thermal Ablation

8

Camille L. Stewart, MD, Barish H. Edil, MD, Robert K. Ryu, MD, FSIR and M. Reza Rajebi, MD

8.1 Introduction

Within the field of local–regional hepatic therapies, the area of thermal ablation plays an important role. First conceptualized in the 1840s, thermal ablation greatly expanded after the advent of cross-sectional imaging. Techniques are generally used for patients with unresectable and borderline resectable disease, which may be due to the size, number, or location of the liver tumors, or for patients judged inoperable due to the patient's poor health. These methods have thus become an integral part of the treatment armamentarium for liver-directed therapy. All techniques presented in this chapter can be used for either primary or metastatic hepatic malignancies, and can also be used in combination with other therapies to maximize effectiveness.

Thermal ablation methods are divided into hyper- and hypothermic techniques, depending on the temperature delivered (Fig. 8.1). In this chapter, we discuss each of thermal ablation methods, mechanisms of tumor ablation, and review of the technical and clinical considerations that must be made when deciding to employ one of these modalities.

8.2 Hyperthermic Techniques

Hyperthermic ablation techniques function by applying supraphysiological temperatures (>40 °C) to tissues, causing changes at the cellular and molecular levels that ultimately result in coagulative necrosis and cell death [1]. Irreversible tissue damage occurs at temperatures in the 45 °C range when applied uniformly for 30–60 min. When temperatures rise above 50–60 °C, protein denaturation, enzyme dysfunction, and membrane cell collapse all rapidly occur, leading to irreversible damage and cell death in seconds [2]. At 100 °C, cell death is instantaneous with evaporation. Coagulative necrosis occurs in the zone of tissue closest to the focus of energy delivery, which is the hottest. Surrounding this necrotic core, energy conduction outward results in a cooler zone of sub-lethal hyperthermic tissue damage [2]. Data primarily from animal studies suggest that tumors have a decreased ability to augment blood flow in response to hyperthermic insults,

C.L. Stewart (✉)
Department of Surgery, University of Colorado School of Medicine, 12605 E. 16th Ave, Aurora, CO 80045, USA
e-mail: Camille.Stewart@ucdenver.edu

B.H. Edil
Department of Surgery, University of Colorado Hospital, 12631 E. 17th Ave, 6th Floor MS-C313, Aurora, CO 80045, USA

R.K. Ryu
Division of Interventional Radiology, University of Colorado Anschutz Medical Campus, 12401 E. 17th Avenue, Leprino 954, Suite 526, Aurora, CO 80045, USA
e-mail: Robert.Ryu@ucdenver.edu

M. Reza Rajebi
Radiology, University of Colorado, 12605 E 16th Ave, Aurora, CO 80045, USA
e-mail: reza.rajebi@ucdenver.edu

J. Meyer and T.E. Schefter (eds.), *Radiation Therapy for Liver Tumors*,
DOI 10.1007/978-3-319-54531-8_8

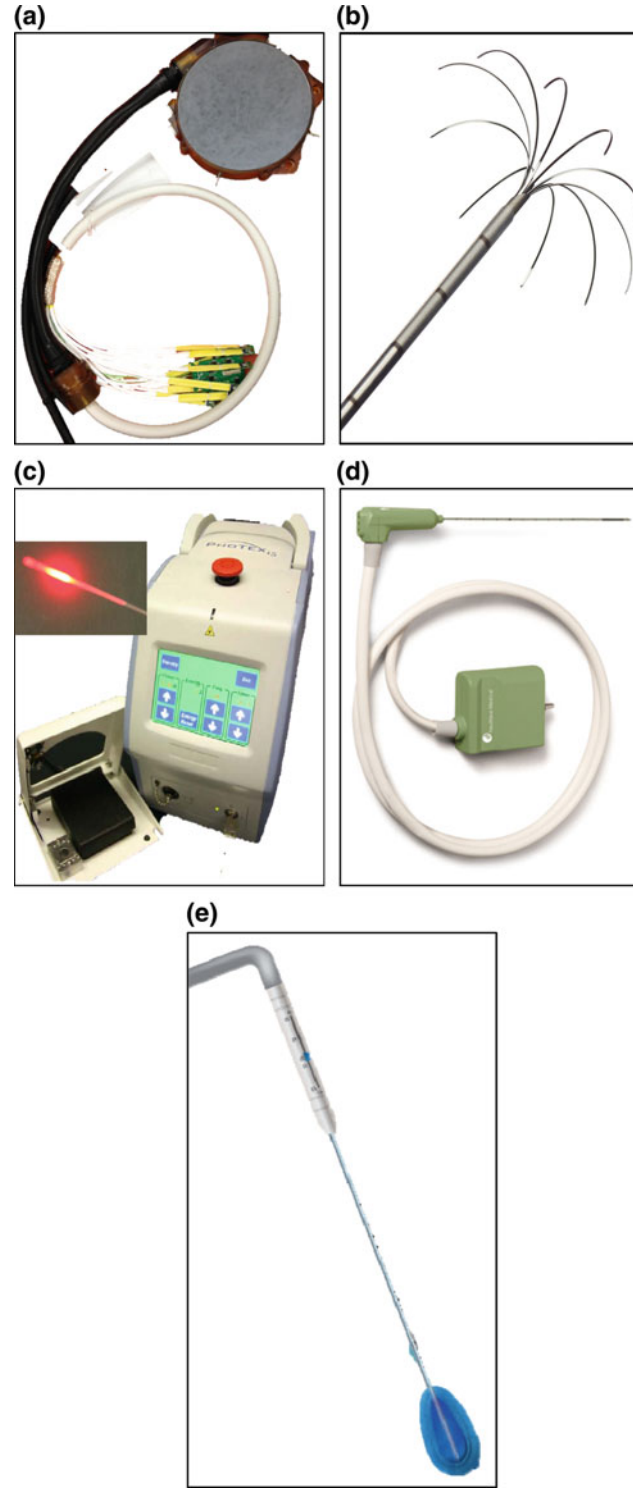

Fig. 8.1 Device images. **a** Philips high-intensity ultrasound transducer. **b** LaVeen radiofrequency ablation probe. **c** Visualase diode laser ablation system. **d** NuWave Certus140 microwave ablation device. **e** Endocare right angle cryoprobe with approximate ablation zone

thus permitting heat to linger longer and promote tissue injury more specifically in these abnormal tissues [1]. Conversely, the peripheral, cooler zone becomes hyperemic. This phenomenon can be used advantageously, by promoting the accumulation of liposomally delivered chemotherapeutic agents, which can be given concurrently to improve effect [2]. All hyperthermic ablation modalities are associated with low but real risks for complications, necessitating routine post-operative observation. If lesions are adjacent to other critical organs or structures, patients can be observed overnight to monitor for hemodynamic changes and ensure pain control.

8.3 Radiofrequency Ablation (RFA)

The application of radiofrequency (RF) energy for parenchymal destruction was first described by d'Arsonval in 1891 [3], and was subsequently broadly introduced into the modern medical world with the advent of electrocautery in the operating room. In 1990, McGahan et al. [4] and Rossi et al. [5] independently reported the use of RF energy for liver tumor ablation. Despite the introduction of multiple new ablative techniques, RFA remains the most investigated modality to date.

8.3.1 Mechanism of Action

Radiofrequency ablation (RFA) utilizes an alternating 500 kHz radiowave current that can be delivered either through a monopolar or bipolar device probe, causing frictional heat up to 100 °C [2]. When these waves are conducted through the liver parenchyma, intrinsically dipolar molecules such as water adjacent to the RFA probe vibrate as they attempt to remain aligned with current. Friction between adjacent molecules causes hyperthermia, leading to coagulative necrosis [6, 7]. Tissue/cell death with RFA is a function of both power (which increases parenchymal temperature) and time. If the generator power is increased too high too fast, it can cause tissue desiccation and charring. This can produce an insulating sleeve around the probe that limits the conduction of energy [6]. A slower increase in temperature avoids charring and is more desirable for creating a larger ablation zone [8].

8.3.2 Technical Considerations

RFA can be performed percutaneously, laparoscopically, or via laparotomy [9]. The percutaneous approach can be guided by ultrasound, CT, or MRI, while the operative approach is generally guided by intra-operative ultrasound [9]. Monopolar probes deliver energy circumferentially around the probe. They penetrate <1 cm around the active electrode [2], and require grounding dispersing pads elsewhere on the patient's body to complete the electrical circuit. A known issue with monopolar RFA is heat loss through adjacent high flow blood vessels (generally >3 mm) through convective heat transfer [1]. This "heat sink" effect decreases energy delivered, lowers the maximum heat applied to the tumor [10], and thus decreases the efficacy of RFA, increasing the chance of residual tumor in the ablation zone. To address this issue, bipolar devices have been created that deliver energy between two probes, allowing for improved, faster energy concentration along a specific line of tissue (Fig. 8.2) [10]. Since bipolar RFA does not require grounding pads, it also eliminates the risk of burn at the site of grounding.

There are multiple RFA systems available with different generators and probe configurations; however, no data exists proving superiority of one system over another. Most variations exist in an attempt to increase the size and homogeneity of the ablation zone, using either multiple electrodes or modifications in technique. Placing up to three probes 1 cm apart has shown to be effective in increasing ablation size. Increased distance >1 cm, however, can lead to dumbbell shaped or entirely separate ablation zones potentially leading to incomplete ablation and thus residual viable tumor. Multi-tined expandable arrays were introduced by LeVeen [11] in

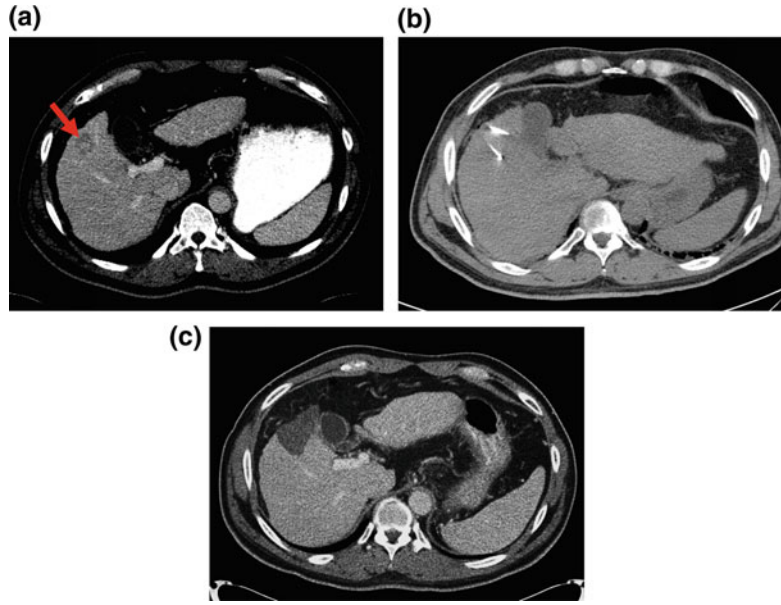

Fig. 8.2 Successful treatment of a hepatocellular carcinoma with radiofrequency ablation under CT guidance. **a** Axial image of the mass with internal enhancement *(arrow)* in portal venous phase. **b** Axial image during radiofrequency ablation with two probes in the lesion. **c** Axial image one month post-procedure demonstrating ablation zone with no evidence of enhancement

order to increase the ablation size. Each tine produces a separate zone of coagulative necrosis that coalesces with the other tine zones at the center of the probe. This leads to a larger and more predictable ablation zone. Goldberg [12] also described internally cooled probes using chilled saline pumped through the shaft to decrease charring.

8.3.3 Patient Considerations and Risks

RFA is most effective for treating tumors that are <3 cm [13] that are located away from major hepatic vessels, because of the heat sink effect referenced above [14, 15]. A 1 cm margin between the zone of ablation and adjacent bowel is also recommended. There are reports of RFA used to treat hepatocellular carcinoma (HCC) with tumor sizes up to 5 cm [16].

Risks for liver RFA are low, with an associated morbidity rate of 2–6% [17]. Most complications are vascular in nature, including bleeding, arteriovenous fistulas, pseudoaneurysms, thrombosis, and infarctions. These complications are more common in cirrhotic patients who already have compromised hemostasis and often have ascites preventing tamponade of blood in the abdominal cavity. As such, some recommend peri-procedural paracentesis [18]. Vascular complications are also more common in patients with superficial, subcapsular tumors and in patients with HCC, since these tumors are hypervascular. Biloma, hepatic abscess, injury to associated organs, and seeding of the needle tract have also been reported. Needle track seeding may be more common in cholangiocarcinoma; as such, some specifically cauterize the needle track for this particular patient population [18]. Percutaneous treatments may preclude subsequent liver transplantation and therefore multidisciplinary evaluation is of utmost importance. A "post-ablation syndrome" has also been described, consisting of a flu-like illness post-procedurally that is self-resolving. For large or multiple ablations, separate sessions can reduce the severity of the post-ablation syndrome. RFA is associated with a mortality rate of 0–2%. Causes of death related to RFA include intestinal perforation, sequelae from portal vein thrombosis, hepatic insufficiency, septic shock from peritonitis, and massive hepatic hemorrhage [17].

8.4 Microwave Ablation (MWA)

Microwaves were initially investigated in the treatment of myocardial arrhythmias in early 1990s [19]. Unpredictable ablation zones, overheating problems, and skin burns hampered the initial experience with microwave ablation of liver tumors. Recent advances in devices and technique, however, have now made MWA a popular ablation modality.

8.4.1 Mechanism of Action

MWA utilizes an alternating 915 MHz to 2.45 GHz microwave current that causes oscillation of intrinsically dipolar molecules such as water. The continuous realignment of the water molecules with the oscillating current results in frictional heat, and subsequent coagulative necrosis [7, 13]. Unlike RFA, which requires conductive tissue to create an ablation zone, MWA only requires polar molecules to create frictional heat, and thus can be used in low conductive tissues, and without grounding pads, to achieve very high temperatures, often in excess of 100 °C [20, 21]. The heat sink effect that occurs adjacent to high flow blood vessels with RFA does also occur with MWA but to a much smaller extent. MWA can therefore be used adjacent to hepatic vessels as large as 10 mm [22]. Charring of adjacent tissue does not occur with MWA, permitting ablation of larger tumors (>3 cm) [23]. MWA is also faster, with ablation times often as low as 2–5 min [21].

8.4.2 Technical Considerations

Like RFA, MWA can be performed percutaneously or with an open technique, using an antenna to deliver microwaves that propagate through the tissue. Percutaneous methods can be guided by ultrasound, CT, or MRI, and open techniques are usually guided by intra-operative ultrasound [9]. The MWA system consists of a generator, a power distribution system, and one or multiple antennae. The antenna becomes heated during ablation and thus most systems require cooling, often with chilled water, saline, or compressed carbon dioxide gas around the antenna shaft [21]. Non-cooled systems do exist, but take longer (25 min) for ablation, and create a "tail" of hyperthermia along the shaft [20, 21]. Some have reported intentionally creating this tail by gradually withdrawing the antenna to cauterize the needle tract and prevent tumor seeding [24].

Different systems deliver various wavelengths of microwaves and power produced by the generator. Lower frequencies (915 MHz) may create larger ablative zones compared to higher frequencies (2.45 GHz), but this has more recently been questioned [25]. Higher power systems (up to 180 W) also create larger and more spherical ablative zones [20]. Multiple antennae can be used during MWA. The use of up to three antennae in an array creates thermally synergistic interactions, which increase the ablative zone more than the total of the individual ablative zones, up to 5–6 cm [20, 26, 27]. Multiple antennae, however, are generally more expensive, require more pre-procedural planning, and have a theoretically higher bleeding risk [20]. Antennas are also available straight or looped (generally using multiple antennae), without a significant difference in the size of ablative zone [26].

8.4.3 Patient Considerations and Risks

This technology can be used on patients with tumors up to 6 cm if a multi-antenna MWA delivery system is used. One study specifically looking at use of MWA in patients with tumors >6 cm showed complete ablation in 3 out of 4 patients, in 2–3 applications [28]. Disadvantages of MWA are generally related to the fact that microwaves are inherently more difficult to generate and deliver safely. MWA requires coaxial cables to prevent power loss and overheating, which are thicker and less flexible compared to the thinner wires used to deliver RFA. Compared to RFA, probes are also larger

diameter and the shape of the ablative zone is less predictable. Ablative zones can be long (up to 6 cm) and oblong in shape, risking burns to the body wall or adjacent structures [25]. Thermocouplers and temperature monitoring can be used in scenarios where MWA is used adjacent to susceptible areas, such as the liver hilum and at the interface of the liver edge and bowel, to reduce heat. Hydrodissection can also be performed with sterile water or 5% dextrose with dilute contrast to create more space between the ablation zone and critical structures [29]. Hydrodissection with saline is avoided to minimize the possibility of ionic interactions with the induced electrical current [30].

Complications from MWA occur rarely. In a series of more than 1100 patients, the frequency of major complications was reported at 2.6% [24]. The most common complication was pleural effusion requiring thoracentesis, all in patients with tumors near the diaphragm. There were two deaths attributed to MWA in this series, both due to pulmonary complications. Other complications that occurred related to MWA included infarction, liver abscesses (Fig. 8.3), bile duct injuries with biloma, bleeding requiring embolization, colonic perforations, and skin burns. Factors associated with complications included using non-cooled shafts and a higher number of treatment sessions [24].

8.5 Interstitial Laser Photocoagulation (ILP)

Interstitial laser photocoagulation (ILP) of liver tumors was first described by Bown in 1983 [31], and is referred by several names in the literature, including laser thermotherapy, laser-induced thermotherapy, laser ablation, and interstitial laser coagulation. Since its introduction, ILP has been used for ablation of tumors in a variety of tissues, including liver, lung, brain, thyroid, and prostate.

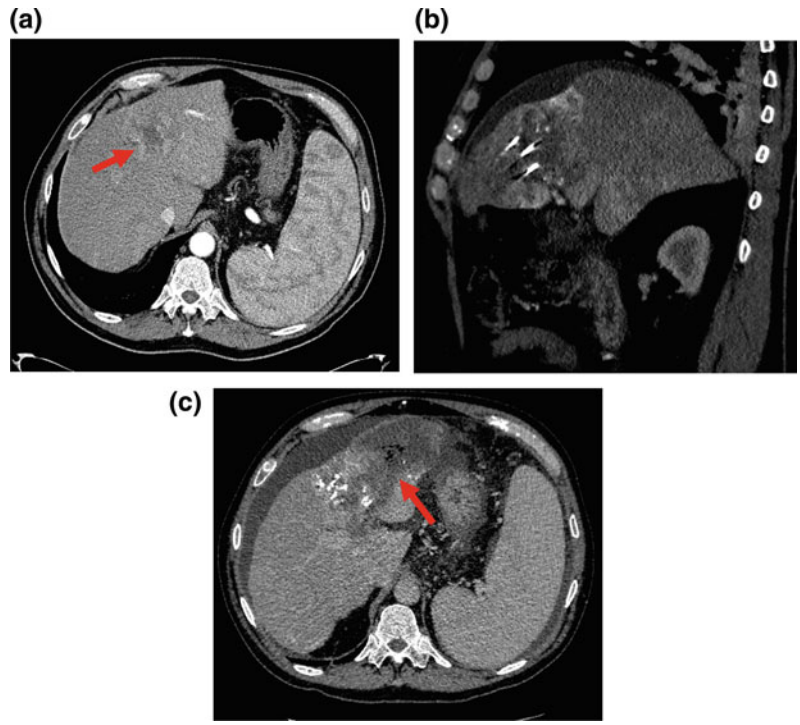

Fig. 8.3 Treatment of hepatocellular carcinoma with microwave ablation under CT guidance, complicated by liver infarction and abscess. **a** Axial image of the mass with enhancement *(arrow)*. **b** Sagittal image during ablation with three antennae **c** Axial image 2 weeks post-procedure with wedge-shaped hypodense area and foci of air in the ablation zone, consistent with liver infarction and abscess formation *(arrow)*

8.5.1 Mechanism of Action

The word laser is an acronym for light amplification by stimulated emission of radiation. With ILP, infrared light is delivered via flexible quartz fibers that are 300–600 μm in diameter. Parenchymal destruction occurs when absorbed infrared light is converted into heat. The heat itself is also conducted further to create a larger ablation zone [32]. Two wavelengths are used for ILP, Neodymium-doped yttrium aluminum garnet (Nd:YAG) (wavelength 1064 nm) and diode (800–980 nm). ILP is generally used at low power (3–15 W) for exposure times ranging from 3 to 20 min. Like other methods of thermal ablation, the volume of the ablation zone is determined by power and duration of exposure.

8.5.2 Technical Considerations

ILP is generally only performed percutaneously, and can be guided by ultrasound, CT, or MRI [9]. Real-time MRI provides excellent resolution for the ablated tissue, and is the preferred method of image guidance for ILP. The laser fiber tips can either be bare or light diffusing. Conventional bare tip fibers produce a near-spherical ablation zone of 1.5 cm, but tend to cause carbonization (i.e., charring) of affected tissue. The resulting black discoloration of the tissue impedes further light penetration [32]. Interstitial light diffusing fibers have largely replaced bare tips and can produce an ablation zone up to 5 cm. Beam-splitting devices can also be applied to use multiple fibers at once. Similar to MWA, a synergistic effect occurs with multiple probes, leading to a four- to sixfold increase in ablation volume [33]. Ablation volumes are also larger with increasing power, but this comes with increasing temperature that can lead to carbonization. Water-cooled laser ablation sheathes have been used to address this issue and enable higher power output with ablation zones up to 8 cm [32, 34]. It should be noted that ILP is also susceptible to a heat sink effect when it is applied adjacent to high flow vessels since laser light is absorbed by hemoglobin. ILP can be used in concert with embolization techniques to help limit hemoglobin laser light absorption [32, 35].

8.5.3 Patient Considerations and Risks

ILP is most effective for patients with tumors <3 cm, away from high flow vascular structures [36]. Like other hyperthermic ablation techniques, the risks for complications with ILP are low, occurring in 1.5% of treatments. Complications from this therapy include pleural effusions, intra-abdominal bleeding, liver abscesses, bile duct injuries, and segmental infarctions [37, 38]. Complications are more likely to occur when ILP is used for tumors deeper than 5 cm from the liver capsule, and when energy delivered exceeds 7200 J. It has been suggested, however, that the risk of complications with ILP may be lower compared with RFA, since devices are thin and the exact location of the device and ablation area are improved with MRI [39]. Deaths have been attributed to ILP, and generally occur in patients with large tumors (>5 cm) who also have decompensated cirrhosis [36].

8.6 High-Intensity Focused Ultrasound (HIFU)

High-intensity focused ultrasound (HIFU) is the only noninvasive thermal ablation modality in use for liver tumors. Ultrasound waves are transmitted extracorporeally through tissue and focused on the liver lesion. This technique is the least well studied of the thermal ablation modalities, and has mostly been used in Asia and Europe. It is not approved by the United States Food and Drug Administration for treatment of liver malignancies at this time [40].

8.6.1 Mechanism of Action

Similar to diagnostic ultrasound imaging, HIFU uses ultrasound waves that are targeted to a desired depth. The waves, however, are

transmitted at a much higher intensity, up to 10,000 Watts/cm^2 for HIFU, compared to a maximum of 720 mW/cm^2 for diagnostic ultrasound [41]. Cellular death is via two different mechanisms, thermal and mechanical. Thermal damage is caused by absorption of acoustic energy in tumor tissue creating temperatures up to 60 °C over a small area. In addition, mechanical cavitation, microstreaming, and radiation forces damage the target tissue further [42]. These effects are caused by alternating compression and expansion of tissues as ultrasound waves propagate through, creating rapidly oscillating gas cavities [41].

8.6.2 Technical Considerations

HIFU can be performed under ultrasound or temperature-sensitive MRI guidance (MR thermometry), but requires a wide aperture with a large angle of convergence of the ultrasound beams to avoid damage to the skin and adjacent normal tissue. Several types of transducers are available depending on the target tissue. Both percutaneous and extracorporeal methods can be used for liver tumors, and interstitial devices have been evaluated for biliary tumors. Acoustic lenses focus waves on a small area, from 1 × 15 mm to 10 × 16 mm, depending on the lens type. Similar to diagnostic ultrasound, the presence of intervening low conductive structures, such as bones and air, however, produce echoes. This can significantly limit the penetration of the waves during the application of HIFU [40]. Thus, if it cannot be visualized in a diagnostic ultrasound, then it is unlikely that treatment with HIFU will be successful [41]. Respiratory motion that causes target motion can also result in incomplete ablation.

8.6.3 Patient Considerations and Risks

Proponents of HIFU assert that the procedure is well tolerated without anesthesia and point to its noninvasiveness. Drawbacks include the multiple contraindications to use, difficulty in obtaining a suitable window without intervening low conductance structures, difficulty in keeping the target tissue motionless, and the time required per treatment session, which can last several hours. Patient-specific contraindications to use include women who are pregnant or nursing, a tumor ablation zone <5 mm from vital structures, tumors with irregular margins, targets >10 cm from the HIFU transducer, and those with known significant intra-abdominal adhesions. The site where HIFU is transduced must also be hair- and scar-free. Removal of ribs has been reported to improve the window for intervention [40]. Accidental patient movement can be suppressed with anxiolytics, and intestinal peristaltic movement can be suppressed using antispasmodics such as tiemonium methylsulfate [41]. Reported complications related to HIFU include diaphragmatic and gastric perforations, osteonecrosis of intervening bones, and skin burns. One technique to decrease the frequency of skin burns is to inject normal saline into the subcutaneous tissues or into the peritoneal cavity to increase the depth of superficial liver tumors from the abdominal wall [40]. It has been recommended that patients undergo repeat imaging of the liver, preferably with MRI, one week after HIFU treatment to evaluate treatment effect [41].

8.7 Cryoablation

The term cryoablation is used to describe all methods that use hypothermia for tissue destruction. First described in 1850 using salt and ice solutions for the treatment of malignancies [43], there are now more sophisticated tools available to cool target tissues using rapidly expanding gas.

8.7.1 Mechanism of Action

Cryoablation initiates tissue cooling by rapid expansion of high-pressure argon gas through the

lumen of a probe. This causes the tissue temperature to drop as low as −160 °C and forms an iceball in the targeted tissue at the end of the probe. Freezing tissue results in the formation of intra- and extracellular ice crystals, cellular dehydration, and cell membrane and organelle damage. Helium gas is then circulated through the probe causing thawing. This induces additional cellular damage from ice crystals and cellular re-expansion, causing cellular apoptosis [44–48]. Repeated freeze–thaw cycles induce occlusion of blood vessels. The release of cellular antigens during apoptosis can also trigger an anti-tumor immune response that results in cellular death beyond the ablation zone [44, 49, 50].

8.7.2 Technical Considerations

Cryoablation can be performed open or percutaneously with image guided insertion of the probe into the tumor. Subsequent iceball formation can be monitored with ultrasound, CT, or MRI. Laparoscopic cryoablation is rarely performed since the probe and transducer are rarely truly transverse or longitudinal to the target, making probe insertion and iceball monitoring a challenge [51]. Freeze times are 10–20 min long, and the desired iceball size is 1 cm greater than the margin of the tumor. Iceball size is increased with freeze time (until a balance of temperature exchange has been reached) and with increasing the number of freeze cycles. Freeze cycles are typically repeated 2–3 times [44]. Multiple cryoprobes can also be used simultaneously and can create large zones of ablation, up to 10 cm in diameter. Multiple probes are recommended for tumors >2 cm in diameter; they should be placed <2 cm apart and within 1 cm of the tumor edge [51]. The heat sink (or conversely, cool sink) effect of high flow vessels also occurs with cryoablation. If multiple probes are used for a tumor that may be subject to this effect because of its proximity to high flow vessels, it is recommended that probes be placed <1 cm apart, and 5 mm from the edge of the tissue target [51].

8.7.3 Patient Considerations and Risks

A benefit to cryoablation is that it is less painful compared to hyperthermic ablation techniques due to the anesthetic effect of cooling. It can usually be performed with conscious sedation, as opposed to RFA and MWA, both which routinely require general anesthesia. Complication rates, however, were reported as high as 40% [52], when liquid nitrogen was used. More recent reviews report major complication rates around 6%. Cryoshock, also known as cold shock, is a rare but feared complication after cryoablation that is related to cytokine release. Symptoms of cryoshock can include hypotension, renal failure, disseminated intravascular coagulation, and acute respiratory distress syndrome. This occurs in 0.3–2% of patients, with greater risk for larger ablation zones, especially those >6 cm [44, 53]. Up to a third of patients also experience minor complications, such as fever and post-procedural pain [53, 54]. Other complications include liver abscesses, biliary fistulas, bleeding (which can be related to iceball fracture), liver failure, renal insufficiency, and thrombocytopenia. Bleeding complications tend to be more frequent compared to hyperthermic techniques since tract ablation cannot be performed with cryoablation probes. To prevent renal complications, some have suggested that patients receive diuretics and mannitol [44]. Some also advocate for overnight observation of patients to ensure pain control and for monitoring for post-procedural complications [51]. Risk of complications and the severity of potential complications, along with less research to support its use, has made this technique less popular compared to hyperthermic ablation techniques.

8.8 Conclusions

Thermal ablation is a popular method of treatment for patients with liver tumors who are poor candidates for surgical resection. There are a number of modalities available to the clinician to choose from that either burn or freeze the tumor

Table 8.1 Comparison of thermal ablation modalities

Ablation modality	Mechanism of action	Advantages	Disadvantages
RFA	Alternating 500 kHz radiowave current via monopolar or bipolar device, causing frictional heat	Well studied, no grounding pad with bipolar devices, multiple probes can be used at once, ablation complete in minutes	Best for masses <3 cm within conductive tissue, heat sink effect when used adjacent to high flow vessels
MWA	Alternating 915 MHz to 2.45 GHz microwave current, causes oscillation of intrinsically dipolar molecules, causing frictional heat	Well studied, can be used in low conductance tissues, no grounding pad, diminished heat sink effect, less adjacent charring than RFA, multiple probes can be used at once for ablation zones up to 6 cm, ablation complete in minutes	Antenna becomes heated requiring a cooling system for faster treatment, ablative zone less predictable than RFA, requires coaxial cables
ILP	Absorbed infrared light converted into heat	Beam splitting permits multiple fibers to be used at once for ablation zones up to 8 cm, well-monitored intra-procedurally with MRI	Less well studied, heat sink effect when used adjacent to high flow vessels, requires up to 20 min of ablation time
HIFU	High-intensity ultrasound waves converted into heat, plus mechanical disruption of tissue	Noninvasive, potentially less painful	Less well studied, difficult to obtain suitable window, multiple contraindications, can require >1 h of ablation time
Cryoablation	Freezing tissue by rapid expansion of high-pressure gas, plus damage from repeat freeze–thaw cycles	Multiple probes can be used at once for ablation zones up to 10 cm, potentially less painful	Cool sink effect occurs adjacent to high flow vessels, high rate of minor complications, potential for cryoshock, and iceball fracture

tissue, each with their advantages and drawbacks (Table 8.1). A number of variables must be considered when selecting a method for tumor ablation, including the desired size of the ablation, the risks to which a particular patient may be susceptible, the equipment available, and the operator's comfort with the modality.

References

1. Rossmanna C, Haemmerich D. Review of temperature dependence of thermal properties, dielectric properties, and perfusion of biological tissues at hyperthermic and ablation temperatures. Crit Rev Biomed Eng. 2014;42(6):467–92.
2. Chu KF, Dupuy DE. Thermal ablation of tumours: biological mechanisms and advances in therapy. Nat Rev Cancer. 2014;14(3):199–208.
3. d'Arsonval M. Action physiologique des courants alternatives. C R Soc Biol. 1891;(43):283–6.
4. McGahan JP, Browning PD, Brock JM, Tesluk H. Hepatic ablation using radiofrequency electrocautery. Invest Radiol. 1990;25(3):267–70.
5. Rossi S, Fornari F, Pathies C, Buscarini L. Thermal lesions induced by 480 KHz localized current field in guinea pig and pig liver. Tumori. 1990;76(1):54–7.
6. Organ LW. Electrophysiologic principles of radiofrequency lesion making. Appl Neurophysiol. 1976–1977;39(2):69–76.
7. Saied A, Katz SC, Espat NJ. Regional hepatic therapies: an important component in the management of colorectal cancer liver metastases. Hepatobiliary Surg Nutr. 2013;2(2):97–107.
8. Goldberg SN, Gazelle GS, Compton CC, Mueller PR, Tanabe KK. Treatment of intrahepatic malignancy with radiofrequency ablation: radiologic-pathologic correlation. Cancer. 2000;88(11):2452–63.
9. Haen SP, Pereira PL, Salih HR, Rammensee HG, Gouttefangeas C. More than just tumor destruction:

immunomodulation by thermal ablation of cancer. Clin Dev Immunol. 2011;2011:160250.
10. Yi B, Somasundar P, Espat NJ. Novel laparoscopic bipolar radiofrequency energy technology for expedited hepatic tumour ablation. HPB (Oxford). 2009;11(2):135–9.
11. LeVeen RF. Laser hyperthermia and radiofrequency ablation of hepatic lesions. Semin Interv Radiol. 1997;14:313–24.
12. Goldberg SN, Gazelle GS, Solbiati L, Rittman WJ, Mueller PR. Radiofrequency tissue ablation: increased lesion diameter with a perfusion electrode. Acad Radiol. 1996;3(8):636–44.
13. Eisele RM. Advances in local ablation of malignant liver lesions. World J Gastroenterol. 2016;22 (15):3885–91.
14. Ueno S, Sakoda M, Kubo F, Hiwatashi K, Tateno T, Baba Y, et al. Surgical resection versus radiofrequency ablation for small hepatocellular carcinomas within the Milan criteria. J Hepatobiliary Pancreat Surg. 2009;16(3):359–66.
15. Huang J, Yan L, Cheng Z, Wu H, Du L, Wang J, et al. A randomized trial comparing radiofrequency ablation and surgical resection for HCC conforming to the Milan criteria. Ann Surg. 2010;252(6):903–12.
16. Chen MS, Li JQ, Zheng Y, Guo RP, Liang HH, Zhang YQ, et al. A prospective randomized trial comparing percutaneous local ablative therapy and partial hepatectomy for small hepatocellular carcinoma. Ann Surg. 2006;243(3):321–8.
17. Howenstein MJ, Sato KT. Complications of radiofrequency ablation of hepatic, pulmonary, and renal neoplasms. Semin Intervent Radiol. 2010;27(3):285–95.
18. Mendiratta-Lala M, Brook OR, Midkiff BD, Brennan DD, Thornton E, Faintuch S, et al. Quality initiatives: strategies for anticipating and reducing complications and treatment failures in hepatic radiofrequency ablation. Radiographics. 2010 Jul–Aug;30(4):1107–22.
19. Langberg JJ, Wonnell T, Chin MC, Finkbeiner W, Scheinman M, Stauffer P. Catheter ablation of the atrioventricular junction using a helical microwave antenna: a novel means of coupling energy to the endocardium. Pacing Clin Electrophysiol PACE. 1991;14(12):2105–13.
20. Hoffmann R, Rempp H, Erhard L, Blumenstock G, Pereira PL, Claussen CD, Clasen S. Comparison of four microwave ablation devices: an experimental study in ex vivo bovine liver. Radiology. 2013;268 (1):89–97.
21. Lubner MG, Brace CL, Hinshaw JL, Lee FT Jr. Microwave tumor ablation: mechanism of action, clinical results, and devices. J Vasc Interv Radiol. 2010;21(8 Suppl):S192–203.
22. Yu NC, Raman SS, Kim YJ, Lassman C, Chang X, Lu DSK. Microwave liver ablation: influence of hepatic vein size on heat-sink effect in a porcine model. J Vasc Interv Radiol JVIR. 2008;19(7):1087–92.
23. Brace CL, Laeseke PF, Sampson LA, Frey TM, van der Weide DW, Lee FT. Microwave ablation with multiple simultaneously powered small-gauge triaxial antennas: results from an in vivo swine liver model. Radiology. 2007;244(1):151–6.
24. Liang P, Wang Y, Yu X, Dong B. Malignant liver tumors: treatment with percutaneous microwave ablation–complications among cohort of 1136 patients. Radiology. 2009;251(3):933–40.
25. Hinshaw JL, Lubner MG, Ziemlewicz TJ, Lee FT Jr, Brace CL. Percutaneous tumor ablation tools: microwave, radiofrequency, or cryoablation–what should you use and why? Radiographics. 2014 Sep-Oct;34(5):1344–62.
26. Yu NC, Lu DS, Raman SS, Dupuy DE, Simon CJ, Lassman C, et al. Hepatocellular carcinoma: microwave ablation with multiple straight and loop antenna clusters–pilot comparison with pathologic findings. Radiology. 2006;239(1):269–75.
27. Trembly BS, Douple EB, Ryan TP, Hoopes PJ. Effect of phase modulation on the temperature distribution of a microwave hyperthermia antenna array in vivo. Int J Hyperth Off J Eur Soc Hyperthermic Oncol North Am Hyperth Group. 1994;10(5):691–705.
28. Yu Z, Liu W, Fan L, Shao J, Huang Y, Si X. The efficacy and safety of percutaneous microwave coagulation by a new microwave delivery system in large hepatocellular carcinomas: four case studies. Int J Hyperth. 2009;25(5):392–8.
29. DeBenedectis CM, Beland MD, Dupuy DE, Mayo-Smith WW. Utility of iodinated contrast medium in hydrodissection fluid when performing renal tumor ablation. J Vasc Interv Radiol. 2010;21 (5):745–7.
30. Goldberg SN, Ahmed M, Gazelle GS, Kruskal JB, Huertas JC, Halpern EF, et al. Radiofrequency thermal ablation with NaCl solution injection: effect of electrical conductivity on tissue heating and coagulation–-phantom and porcine liver study. Radiology. 2001;219(1):157–65.
31. Bown SG. Phototherapy in tumors. World J Surg. 1983;7(6):700–9.
32. Gough-Palmer AL, Gedroyc WM. Laser ablation of hepatocellular carcinoma–a review. World J Gastroenterol. 2008;14(47):7170–4.
33. Ivarsson K, Olsrud J, Sturesson C, Möller PH, Persson BR, Tranberg KG. Feedback interstitial diode laser (805 nm) thermotherapy system: ex vivo evaluation and mathematical modeling with one and four-fibers. Lasers Surg Med. 1998;22 (2):86–96.
34. Roggan A, Mesecke-von Rheinbaben I, Knappe V, Vogl T, Mack MG, Germer C, et al. Applicator development and irradiation planning in laser-induced thermotherapy (LITT). Biomed Tech (Berl). 1997;42(Suppl):332–3.
35. Heisterkamp J, van Hillegersberg R, Mulder PG, Sinofsky EL, IJzermans JN. Importance of eliminating portal flow to produce large intrahepatic lesions

with interstitial laser coagulation. Br J Surg. 1997 Sep;84(9):1245–8.
36. Arienti V, Pretolani S, Pacella CM, Magnolfi F, Caspani B, Francica G, et al. Complications of laser ablation for hepatocellular carcinoma: a multicenter study. Radiology. 2008;246(3):947–55.
37. Vogl TJ, Straub R, Eichler K, Söllner O, Mack MG. Colorectal carcinoma metastases in liver: laser-induced interstitial thermotherapy–local tumor control rate and survival data. Radiology. 2004;230 (2):450–8.
38. Vogl TJ, Straub R, Eichler K, Woitaschek D, Mack MG. Malignant liver tumors treated with MR imaging-guided laser-induced thermotherapy: experience with complications in 899 patients (2,520 lesions). Radiology. 2002;225(2):367–77.
39. Di Costanzo GG, Francica G, Pacella CM. Laser ablation for small hepatocellular carcinoma: state of the art and future perspectives. World J Hepatol. 2014;6(10):704–15.
40. Diana M, Schiraldi L, Liu YY, Memeo R, Mutter D, Pessaux P, Marescaux J. High intensity focused ultrasound (HIFU) applied to hepato-bilio-pancreatic and the digestive system—current state of the art and future perspectives. Hepatobiliary Surg Nutr 2015, Epub ahead of print.
41. Zhou YF. High intensity focused ultrasound in clinical tumor ablation. World J Clin Oncol. 2011;2 (1):8–27.
42. Dubinsky TJ, Cuevas C, Dighe MK, Kolokythas O, Hwang JH. High-intensity focused ultrasound: current potential and oncologic applications. AJR Am J Roentgenol. 2008;190(1):191–9.
43. Arnott J. Practical illustrations of the remedial efficacy of a very low or anesthetic temperature in cancer. Lancet. 1850;2:257–9.
44. Niu LZ, Li JL, Xu KC. Percutaneous cryoablation for liver cancer. J Clin Transl Hepatol. 2014;2(3): 182–8.
45. Mazur P. Freezing of living cells: mechanisms and implications. Am J Physiol. 1984;247(3 Pt 1):C125–42.
46. Mazur P, Rall WF, Leibo SP. Kinetics of water loss and the likelihood of intracellular freezing in mouse ova. Influence of the method of calculating the temperature dependence of water permeability. Cell Biophys. 1984;6(3):197–213.
47. Baust JG, Gage AA. The molecular basis of cryosurgery. BJU Int. 2005;95(9):1187–91.
48. Weber SM, Lee FT, Chinn DO, Warner T, Chosy SG, Mahvi DM. Perivascular and intralesional tissue necrosis after hepatic cryoablation: results in a porcine model. Surgery. 1997;122(4):742–7.
49. Sabel MS. Cryo-immunology: a review of the literature and proposed mechanisms for stimulatory versus suppressive immune responses. Cryobiology. 2009;58(1):1–11.
50. den Brok MHMGM, Sutmuller RPM, Nierkens S, Bennink EJ, Frielink C, Toonen LWJ, et al. Efficient loading of dendritic cells following cryo and radiofrequency ablation in combination with immune modulation induces anti-tumour immunity. Br J Cancer. 2006;95(7):896–905.
51. Hinsaw JL, Lee FT Jr. Cryoablation for liver cancer. Tech Vasc Interv Radiol. 2007;10(1):47–57.
52. Pearson AS, Izzo F, Fleming RY, Ellis LM, Delrio P, Roh MS, et al. Intraoperative radiofrequency ablation or cryoablation for hepatic malignancies. Am J Surg. 1999;178(6):592–9.
53. Xu KC, Niu LZ, He WB, Hu YZ, Zuo JS. Percutaneous cryosurgery for the treatment of hepatic colorectal metastases. World J Gastroenterol. 2008;14(9):1430–6.
54. Littrup PJ, Aoun HD, Adam B, Krycia M, Prus M, Shields A. Percutaneous cryoablation of hepatic tumors: long-term experience of a large U.S. series. Abdom Radiol (NY). 2016 Apr;41(4):767–80.

Part III
Principles of Radiation Therapy

9 External Beam Radiation Therapy for Liver Tumors: Simulation, Treatment Planning, and Advanced Delivery Techniques

David C. Westerly, PhD and Karyn A. Goodman, MD, MS

9.1 Introduction

Historically, the efficacy of radiation therapy (RT) in the setting of primary or metastatic liver disease has been limited by the low liver tolerance to whole liver irradiation. Thus, until relatively recently, RT played a minor role in the management of liver tumors. With the emergence of more conformal RT techniques and sophisticated treatment planning software, more focal treatment fields are now possible, allowing for delivery of higher doses to intrahepatic tumors while sparing the uninvolved liver. In addition, the ability of enhanced diagnostic imaging to identify focal liver lesions allows for more targeted treatments. Finally, prospective collection of quantitative data on toxicities seen after partial liver irradiation delivered with three-dimensional conformal RT techniques (3DCRT) has allowed a better understanding of partial liver radiation tolerance, thereby allowing for safe dose escalation to parts of the liver. Stereotactic body radiation therapy (SBRT) is the most recent advancement in the delivery of a highly conformal, hypofractionated dose and has allowed for safer delivery of ablative radiotherapy doses with the potential to achieve enhanced local control of intrahepatic malignancies.

Dose escalation with fractionated RT has shown a clear dose response for intrahepatic tumors including liver metastases [1], and patients with unresectable focal liver malignancies treated with higher rather than lower doses of radiation have been found to sustain improved symptoms, response rates, and survivals [2, 3]. However, accurate delivery of such targeted treatment is hampered by the significant degree of abdominal organ motion due to respiration and variations in luminal filling of the hollow viscera. The recent emergence of novel imaging and motion management techniques is allowed for more targeted therapy of these tumors and new attempts to escalate RT doses using SBRT. The parallel arrangement of functional subunits in the liver allows for the ability to safely use the focal ablative doses of radiation with SBRT, as long as an adequate proportion of the normally functioning liver is preserved.

9.2 Patient Selection

Patient selection for SBRT treatment to the liver should be based on a multidisciplinary evaluation since surgery remains the gold standard for resectable tumors in patients who have adequate hepatic function. Generally, patients considered for SBRT should typically have 5 or fewer

D.C. Westerly (✉)
Department of Radiation Oncology, University of Colorado School of Medicine, 1665 Aurora Court, Suite 1032, Aurora, CO 80045, USA
e-mail: david.westerly@ucdenver.edu

K.A. Goodman
Radiation Oncology, University of Colorado Cancer Center, 1665 Aurora Court, Suite 1032, Aurora, CO 80045, USA
e-mail: Karyn.goodman@ucdenver.edu

J. Meyer and T.E. Schefter (eds.), *Radiation Therapy for Liver Tumors*,
DOI 10.1007/978-3-319-54531-8_9

lesions. Lesion size restrictions should be based on whether there is adequate baseline liver function and whether or not there is sufficient uninvolved liver volume which can be spared should be established prior to treatment. Central liver tumors which are in close proximity to the liver hilum or in the left lobe of the liver and/or tumors which are adjacent to radiosensitive structures can potentially be treated with SBRT, but the total dose and fractionation scheme may need to be adjusted to meet the dose constraints of the adjacent organs.

9.3 Simulation

Simulation establishes the reference conditions for a patient's radiation treatment. This includes generation and collection of all data related to the patient's setup including imaging datasets needed for treatment planning, patient positioning information, immobilization devices, setup points, and straightening marks, as well as any photos, diagrams, and detailed setup instructions. For liver SBRT, special care must be taken to ensure that a patient's setup at the time of simulation is reproducible to within the accuracy requirements of the planned treatment (typically less than 5–10 mm). This in turn requires careful consideration of various aspects of the patient setup that contribute to inter- and intra-fractional setup uncertainties including imaging technique and respiratory motion.

9.3.1 Patient Setup and Immobilization

In order to allow for appropriate image guidance at the time of treatment delivery, implantation of 3–5 fiducial seeds adjacent to the liver tumor(s) is performed prior to simulation, typically by CT guidance by an interventional radiologist [4]. Preferably, 100% gold seeds should be employed as these are radiographically visualized by kilo-voltage X-rays. Because these seeds can migrate several mm in the first few days after implantation, the simulation should be performed several days after the implantation procedure. The use of fiducial markers as a surrogate for the tumor location is particularly important for liver tumors because they are not well visualized without intravenous contrast, which is not used routinely at the time of treatment. While fiducials allow for better localization and fewer uncertainties at the time of setup, in some cases it is not feasible to place them and other surrogates, such as the liver edge or dome of the diaphragm, can be used.

At simulation, patients are generally placed supine; the treatment position should be reproducible, ideally through an immobilization device, with the arms placed at the side of the head in order to allow for lateral beam angles or arcs. Immobilization is typically achieved using either an alpha cradle or vacloc bag placed over a wing board (see Fig. 9.1), though commercially available SBRT immobilization systems are also available [5]. In cases where the patient cannot hold their arms above their head for an extended period of time, arms akimbo may be acceptable; however, this will depend on the patient's specific anatomy and the possibility of using arm blocking techniques during treatment planning.

9.3.2 Motion Management

One of the major concerns with liver SBRT is the presence of intra-fraction liver motion caused by the patient's breathing. Liver motion is complex due to organ deformation and rotation with respiration. With more targeted approaches to treating liver lesions, such as SBRT, novel methods of accounting for target motion have been developed to improve the accuracy of treatment delivery. There are many approaches to motion management including respiratory gating [6–8], abdominal compression [9], active breathing control (ABC) [10], and tumor tracking [11]. Motion management strategies seek to reduce respiratory motion and improve the accuracy of treatment planning/delivery. These motion management techniques can be categorized as motion compensating or motion restricting.

Fig. 9.1 Setup photo acquired at simulation for a patient receiving liver SBRT. The patient is positioned in an alpha cradle with arms raised overhead and an inflatable compression belt placed around the abdomen

9.3.2.1 Motion-Compensating Techniques

Respiratory gating is a technique in which the radiation beam is turned on and off depending on where the tumor is with respect to the respiratory cycle [8]. The beam is generally turned on during expiration when there is the least amount of motion. Respiratory gating is achieved using software to correlate the motion of the chest wall to the phase of respiration. The tumor motion can be assessed at the time of simulation as described below. Respiratory gating requires the ability to monitor the motion of the tumor on a daily basis to evaluate the degree of respiratory motion of the tumor versus the chest wall motion. Using fluoroscopy, the fiducials can be followed throughout the respiratory cycle to confirm that the treatment beam is turned on at the appropriate time during the respiratory cycle.

For patients treated on the CyberKnife, the Synchrony® system is used for real-time targeting of tumors. A series of light-emitting diodes (LEDs) are placed on the chest wall and movement is detected by wall-mounted cameras in the treatment room. Using motion-tracking software, the Synchrony system identifies, updates, and then correlates external body surface movement with movement of the internal tumor fiducials. Throughout the procedure, the Synchrony system monitors the target and modifies the correlation model as needed to follow changes in tumor motion [12].

9.3.2.2 Motion-Restricting Techniques

Abdominal compression devices such as compression paddles, bands, and pressurized compression belts seek to restrict diaphragm motion, thus limiting the degree of respiratory excursion of the abdominal contents, and have demonstrated the ability to reduce the target motion amplitude to less than 10 mm [13–16]. Active Breathing Control (ABC) is a method to facilitate reproducible controlled breath-hold (typically in maximal inspiration) that also limits the ventilatory motion while the beam is on.

9.3.3 Imaging Studies

Various imaging modalities are used for staging and planning liver SBRT patients. In particular, contrast-enhanced CT is essential for target localization. A CT scan is also required for 3D treatment planning as it provides information

about the electron density of different tissues, which is necessary for accurate dose calculation. While some centers choose to perform a separate non-contrast CT scan for treatment planning, studies performed in our department have shown minimal impact on dose calculation accuracy when using a contrast-enhanced CT scan.

At our institution, we commonly treat patients with respiratory gating. With patients in the treatment position, a liver protocol CT scan (1–2 mm cuts) is first performed for high-resolution delineation of the tumor and surrounding structures. CT images should be obtained from at least 2 cm above the dome of the diaphragm to the bottom of the kidneys. Intravenous contrast is administered in a rapid bolus such that either the arterial phase or portal venous phase is obtained when the patient is being coached to hold his/her breath while in end expiration.

For most hepatic metastases, lesions are best seen in the portal venous phase. They appear hypodense in relation to the liver parenchyma. Hypervascular tumors, such as hepatocellular carcinoma (HCC) and metastatic breast, renal cell, thyroid, and neuroendocrine cancers, may be better imaged in the arterial phase. Review of available diagnostic imaging to determine the best phase for delineating the tumor should be performed prior to simulation and scan timing with respect to the contrast administration should be based on diagnostic radiology algorithms or on discussion with the diagnostic radiologists. Oral contrast can be given approximately one half hour before simulation to allow for visualization of the small bowel and stomach.

An FDG-PET scan can be performed in some institutions with a PET-CT simulator, so there is accurate co-registration of the tumor with the areas of hypermetabolic activity. Otherwise, a diagnostic PET-CT scan can be registered to the simulation CT and a fusion overlay can be visualized in the treatment planning software. The latter technique can be problematic as PET-CT is acquired with free breathing and co-registering with a breath-hold planning CT for example can be inaccurate. An example of this is shown in Fig. 9.2.

To evaluate the extent of respiratory-related liver tumor motion, a four-dimensional (4D)CT scan is also performed in which CT data are

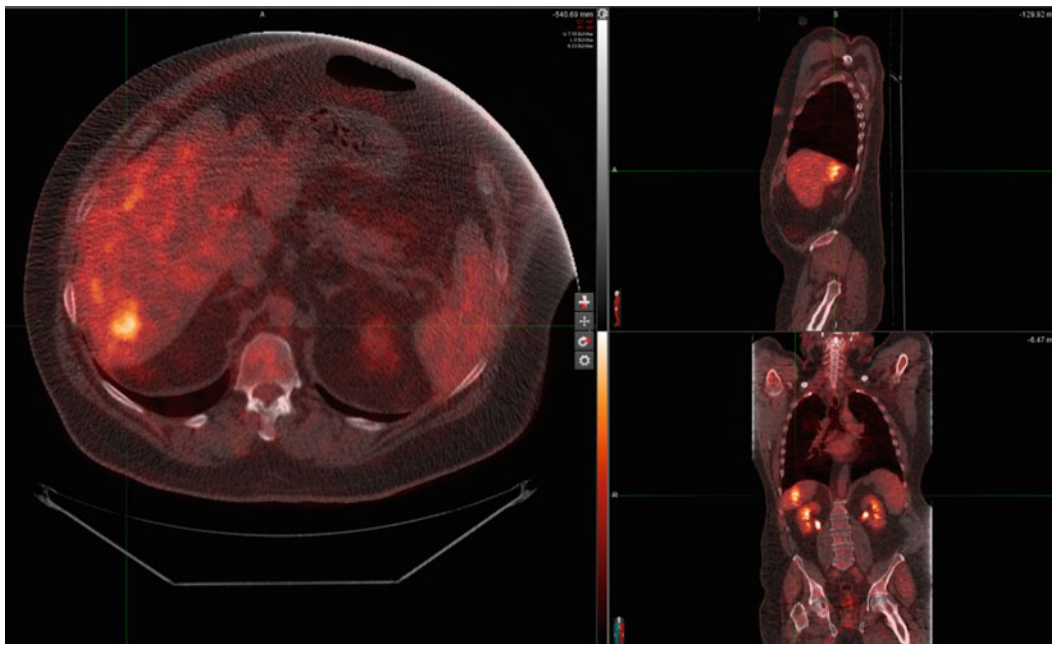

Fig. 9.2 Fusion overlay of a FDG-PET CT scan for a patient undergoing liver SBRT. The hypermetabolic region is clearly visible in the liver and is useful for delineating the gross tumor volume (GTV) on the planning CT scan

acquired during the entire respiratory cycle at each table position. Binning of this data into 10–20 datasets based on either respiratory phase or amplitude as determined by a breathing surrogate such as a spirometer, chest block, or abdominal bellows allows for visualization of the breathing motion and allows one to evaluate temporal changes of the anatomy as a function of the respiratory phase during imaging. At our center, patients are given an audio coaching CD to review prior to the setup procedure to determine an individualized comfortable breathing rhythm. This can increase patient comfort and improved duty cycle (beam-on time as a function of total time) while at the same time help to reduce image artifacts. After binning the 4DCT datasets, the physician can review the tumor motion, to correlate fiducial and tumor motion and to generate an internal target volume (ITV). For patients being treated with respiratory gating, the 4DCT is used to determine the appropriate gating window. Typically, this will be during the expiratory phase which is around the end-expiration phase (phase 50%) and should be a long-enough interval to allow for a reasonable beam-on time. We typically use the 30–70% phases out of the arbitrary 10 binned phases where phase 0% is end-inspiration and phase 50% is end-expiration. We compare the 50% phase with an end-expiration breath-hold CT for concordance. Occasionally, simulation has to be redone in cases where erratic breathing is observed on the reconstructed images that were not detected at the time of simulation. Treatment delivery can be phase based or amplitude based, the latter in our experience is more reproducible. 4D CT scans are also used for patients being treated with motion-restricting techniques.

9.4 Treatment Planning

The application of ultra-hypofractionated dose schedules with SBRT is predicated on the ability to conform the high-dose region to the target volume while controlling the dose fall-off into the surrounding normal tissues. Such conformity is necessary to avoid adverse late effects observed with higher dose-per-fraction regimens. Various planning techniques are used with SBRT to enhance the dose distribution conformity including the use of large numbers of radially distributed treatment beams—either static gantry fields or arcs, the incorporation of non-coplanar beam angles, and the allowance of large (>25% of prescription) hotspots inside the target [17–20]. Additionally, inverse planning techniques can be used to determine the optimal beam fluence required to achieve a certain level of target coverage and normal tissue avoidance. Details of the various techniques used in planning liver SBRT are described in the following sections.

9.4.1 Target and Normal Tissue Delineation

If respiratory gating is used, the gross tumor volume (GTV) is defined on an end-expiratory breath-hold CT image ideally with IV contrast. Additional diagnostic images, such as PET-CT or MRI, are also used if available (with the caveat that one has to be cognizant of different techniques used in diagnostic radiology and resultant issues with accurate co-registration/fusion). No additional margin is added to account for subclinical disease. When respiratory gating is used at our institution, an ITV is created after inspection of the gating window from the 4DCT (usually an expansion of 3–10 mm). With the use of image guidance, accounting for internal motion with the 4D-CT, and intra-fractional motion assessment, usually little to no additional margin is added to generate a final planning target volume (PTV) in our practice. This is in contrast to conventionally fractionated radiotherapy, where the GTV, clinical treatment volume (CTV) including the areas of subclinical disease, and PTV are separately defined [21].

Alternatively, if motion restriction techniques are used, a minimum-intensity-projection (MINIP) image can be generated from a simulation 4DCT to help define the ITV, which encompasses the full range of target motion. A PTV is then defined by adding an expansion of

typically 5–10 mm [22]. The MINIP is reconstructed from low attenuation projections of the 4DCT scan at each table position and can be useful for liver SBRT because it aids in the identification of lesions which are hypodense compared to the surrounding normal liver, especially when IV contrast has been given. Caution is advised when using a MINIP to identify lesions located near the dome of the liver. In such cases, the boundary of the liver and low-density lung tissue can result in significant underestimation of the tumor volume. For these cases, it is advised to assess the extent of the target motion from a cine view of the 4DCT directly.

Critical structures to be identified include the kidneys, liver, stomach, duodenum, and spinal cord. A free-breathing PET-CT may also be registered with the exhalation IV contrast CT scan to confirm the tumor position and aid in the delineation of normal liver and adjacent tissues.

9.4.2 Beam Arrangements

Once the target volume and adjacent normal tissues have been defined in the planning system, appropriate treatment fields must be chosen. This requires the selection of both incident beam angles and the beam ports in cases where static fields are used for treatment. To achieve the high-dose conformity required with SBRT, treatment from a large number of incident beam angles is required. This is accomplished through the use of typically 7–13 non-opposed, static gantry beams or with multiple arcs [23]. While early implementations relied more on the former, as technology used to plan and deliver SBRT treatments has advanced, there has been a gradual shift toward the latter since it is much easier to plan with a few arcs compared to setting the angles and ports for a large number treatment beams. Figure 9.3 illustrates two liver SBRT plans utilizing nine static treatment fields (A) and two coplanar arcs (B). The plan conformity is similar in the two cases; however, the arc plan was considerably easier to generate.

When selecting beam angles, one is faced with the decision of using coplanar or non-coplanar beam arrangements. This choice represents a tradeoff between further distribution of the low-dose region to anatomy located inferior and superior to the target volume in exchange for slightly improved conformity of the higher iso-dose lines to the target. The improvements observed with non-coplanar beam arrangements for SBRT are usually limited by the machine clearance that can be obtained when treating lesions in the thorax and abdomen.

9.4.3 Three-Dimensional Conformal Radiation Therapy

Three-dimensional conformal radiation therapy (3DCRT) uses multi-leaf collimators (MLCs) or Cerrobend blocks to define fixed beam apertures so that they conform to the projection of the target volume from each static gantry angle. The conformance of the calculated dose distribution depends on the resolution of the apertures; for MLC-defined fields, leaf widths of 2.5–10 mm are commonly used with the smaller leaf widths allowing for better conformality [24]. Wedges are also sometimes used to help compensate for variations in patient thickness across the target region. 3DCRT treatments are usually forward planned, though some software applications allow for the use of inverse planning methods to determine beam angles and/or beam weights [25].

3DCRT is well suited for SBRT; the confluence of multiple beams at the center of a smaller lesion with 3DCRT results in a high degree of dose heterogeneity which can result in steeper dose gradients at the target edge. This is desirable for SBRT treatments as it allows for improved normal tissue sparing as well as dose escalation to the GTV. This effect can be enhanced by reducing the block margins. Typically, with 3DCRT, field apertures are expanded 7–12 mm beyond the edge of the target volume to provide lateral electronic equilibrium at the target edge. This allows for adequate target

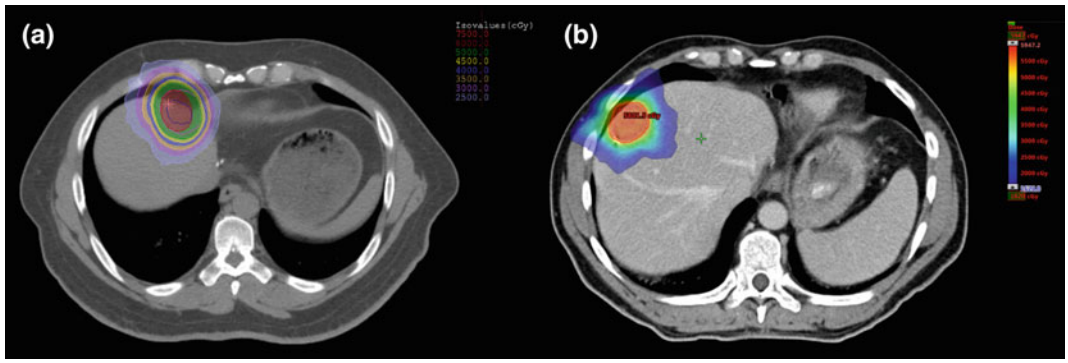

Fig. 9.3 Isodose plan comparison of two liver SBRT patients treated with nine static 3D conformal treatment beams (**a**) and two 360° VMAT arcs (**b**). Both plans exhibit similar dose conformity; however, the planning time required to generate the VMAT plan is considerably less due to automated nature of the VMAT optimization process

coverage without exceeding the global maximum dose by more than 10–20% of prescription. With SBRT, block margins can be reduced or eliminated altogether to further increase the dose gradient at the target edge, simultaneously increasing the dose within the tumor. At our institution, a block margin of 0–3 mm is added for 3DCRT liver SBRT treatments planned using 10 MV photon beams. The margin used depends on the desired hotspot (which may exceed 30% of the prescription dose) as well as the patient's anatomy and normal tissue dose constraints.

For lesions located close to the liver dome, intra-fraction motion may be a serious concern.

9.4.4 Intensity-Modulated Radiation Therapy

With intensity-modulated radiation therapy (IMRT), the spatial fluence distribution is modulated so as to produce the desired dose distribution in the patient. IMRT is usually employed using inverse planning techniques, with plan objectives and constraints specified by the treatment planner and the subsequent fluence distribution calculated by the planning software [26]. This is not always true; the use of field-in-field techniques for breast cancer treatments is an example of forward-planned IMRT. IMRT can be used with static gantry fields or arcs. In this section we focus on static gantry techniques and leave the discussion of arcs to the following section on rotational therapies.

Because very few scenarios allow for a direct solution of the fluence required to generate a desired dose distribution, the fluence maps for IMRT plans are usually determined from iterative optimization [27]. This involves dividing the fluence for each beam into a large number of discrete elements (beamlets). The dose from these beamlets is calculated and the relative weights of all beamlets are optimized until the desired dose distribution (corresponding to the weighted superposition of all beamlets) is obtained.

After determining the optimal fluence distribution, a conversion process is used to generate either a physical compensator or MLC leaf sequences for each treatment beam. The use of stationary compensators for IMRT eliminates MLC/target motion interplay effects; however, the additional cost and effort associated with creating separate compensators for each treatment field has resulted in most centers opting to use MLCs for IMRT delivery. MLC leaf sequences generated for IMRT can be step-and-shoot, where the beam is turned off while the leaves move between static positions, or dynamic, where the MLC motion occurs while the beam is on. The main advantage of fixed-gantry IMRT for liver SBRT treatments is the improved ability to shape the dose distribution to improve target coverage and/or avoid

critical normal tissues, such as the ipsilateral kidney, small bowel, or stomach.

Unwanted perturbation of the dose distribution can arise from interplay between the moving target and moving MLC leaves with intensity-modulated treatments. This interplay effect can result in under- or over-dosing of the target by more than 15% for a single fraction, as was shown in the experimental study performed by Bortfeld et al. [28]. While the magnitude of dose deviations produced by interplay effects decreases rapidly with increasing numbers of fractions, this may still be a concern for SBRT treatments delivered in 5 or fewer fractions.

As described by Yu et al. [29], the magnitude of interplay effects depends on the spatial-temporal characteristics of the patient's breathing motion relative to the temporal gradients in the fluence modulation pattern. In cases where small beam apertures move parallel to the target at a frequency and amplitude similar to the patient's respiratory cycle, large dose discrepancies can result if the delivery occurs over the course of only a few respiratory cycles.

With SBRT the large doses per fraction result in longer treatment delivery times, which helps to average the dose over more breathing cycles. Use of collimator angles where the MLC motion is perpendicular to the primary axis of tumor motion can also help to reduce the interplay effect. Ecclestone and Pierce [30] performed a modeling study to determine the impact of interplay effects on liver SBRT treatments having modulation factors (defined as the ratio of monitor units to dose) ranging from 1.5 to 3.5 and respiratory periods ranging from 3 to 20s, and found the interplay effect in all cases to be clinically negligible. This agrees with the experimental results found by Stambaugh et al. [31], who used a motion phantom with real and simulated motion traces to measure the interplay effect resulting from lung SBRT plans delivered with intensity-modulated arcs. Results of their study showed that interplay effects for realistic motion amplitudes and breathing periods were negligible (<0.2%). Even with increased motion amplitudes of 2–3 cm, dose deviations caused by interplay effects were <3%.

9.4.5 Rotational Therapies

Another approach to SBRT that is gaining in popularity is the use of rotational treatment techniques, including dynamic conformal arc (DCA) therapy, volumetric-modulated arc therapy (VMAT) [32–34], and helical tomotherapy [35, 36]. With DCA therapy, the gantry rotates through a given arc while the MLC dynamically conforms the radiation field to the projection of the target volume at each gantry angle. Typically, the dose rate of the treatment machine is fixed for a given arc and multiple arcs can be used. Similar to 3DCRT, DCAs are usually forward planned.

VMAT also rotates the gantry through a given arc while simultaneously moving the MLC to shape the treatment field, though with VMAT the dose rate and gantry speed may also be modulated. In contrast to DCAs, with VMAT the MLC may not always conform to the projected target contour from each angle. This is due to the fact that VMAT treatments are usually inverse planned so that MLC positions are determined based on the optimizer rather than the geometric properties of the target contour.

Helical tomotherapy is another rotational platform that can be used to plan and deliver liver SBRT. Tomotherapy combines the features of a 6-MV linear accelerator with a CT scanner. A binary, pneumatic MLC is used to modulate a fan beam of radiation that rotates around the patient as they are translated through the bore of the machine on the treatment couch. With tomotherapy, treatments are intensity modulated and inversely planned. Planning parameters include the longitudinal size of the treatment field along with the helical pitch used for the delivery. While the delivery is continuous in nature, planning assumes 51 static beam angles per gantry rotation.

The large number of gantry angles used for planning tomotherapy allows for highly conformal treatment plans. However, a major drawback to using tomotherapy for liver SBRT is the lack of soft tissue contrast with the onboard MVCT imaging system [37]. Also, the relatively large extent of the field in the cranial–caudal direction results in lower dose conformity, though the

introduction of a dynamic jaw that will open and close at the beginning and end of the treatment, respectively, has mitigated this issue to some extent [38].

Rotational SBRT plans delivered with a conventional linear accelerator typically use 1–7 coplanar or non-coplanar arcs. Arcs may subtend less than 360° in order to avoid critical structures adjacent to the target region(s). The main advantages of rotational therapy compared to fixed-gantry techniques are improved conformality of the dose distribution in the high-dose region as well as possible reduction of the treatment time compared to fixed-gantry IMRT. The former stems from the use of more treatment angles, which allows for the dose fall-off at any point on the edge of the target to be defined more equally by the field edge (penumbra) as well as the depth dose. The reduction in treatment time stems from greater efficiency in the delivery of arc treatments as well as avoidance of unnecessarily complicated leaf sequences with fixed-field IMRT [39].

When considering rotational vs. fixed-gantry treatments, one often must choose between giving low doses to a larger volume of normal tissue with rotational therapy compared to giving smaller volumes of normal tissue higher doses with fixed-gantry techniques. In cases where the PTV is located far away from high-risk structures, as is true for many liver SBRT cases, the improved dose conformality and/or reduced treatment time is preferable. However, in certain cases where high-risk critical structures are located directly adjacent to the PTV, fixed-gantry IMRT could allow for improved sparing of these critical structures.

9.5 Daily Image Guidance

Liver tumors are not well visualized on kV cone-beam CT scans due to limitations in resolution and lack of contrast as well as artifacts introduced by respiratory motion and gas in adjacent bowel space. Thus, fiducial markers have been introduced to help identify the tumor and allow for better visualization and improved setup for both conventionally fractionated treatments and more importantly, for SBRT. Gold fiducial markers can be placed as described above, or post-operative clips can also be used to help evaluate the post-operative bed on kV images. Lipiodol from TACE and intra-hepatic stents/drains can also be used as fiducials in selected cases.

For daily treatment, patients are set up on the machine based on the tattoos from their simulation. For respiratory gating patients, the positioning of the fiducials is verified using fluoroscopic images. At our institution, we use audio coaching for both simulation and treatment to ensure that patients are breathing regularly during treatment with respiratory gating. If patients are being treated using an abdominal compression belt for motion management, the fluoroscopy can be used to verify that the motion with the belt is less the 5–10 mm. A CBCT is then obtained and the position of the patient is adjusted to match the position of the fiducials at the time of simulation.

For respiratory gating, the CBCT is also performed during an end-expiration breath-hold and compared to the simulation end-expiration BHCT. As previously mentioned, breath-hold CT affords significantly better imaging quality by reducing respiratory motion artifact and this is especially helpful for CBCT where imaging quality is more limited.

Intra-fraction motion assessment can be performed using triggered (with each breath cycle for gating or every 20° for abdominal compression) KV images taken during treatment delivery. Importantly, there can be drift in the relationship between chest wall motions (surrogate for respiratory motion) with respect to fiducial (tumor) motion, requiring periodic treatment breaks (turning off and on respiratory coaching) in order to re-establish respiratory cycle stability. When respiratory gating is used, the overlay of the contour of the fiducials at the entry of the gating interval (usually the 30% phase) is used to match with the position of the fiducials on the intra-fraction kV image (see Fig. 9.4). This intra-fractional monitoring is key to verifying tumor position. Fiducial auto-detection/beam

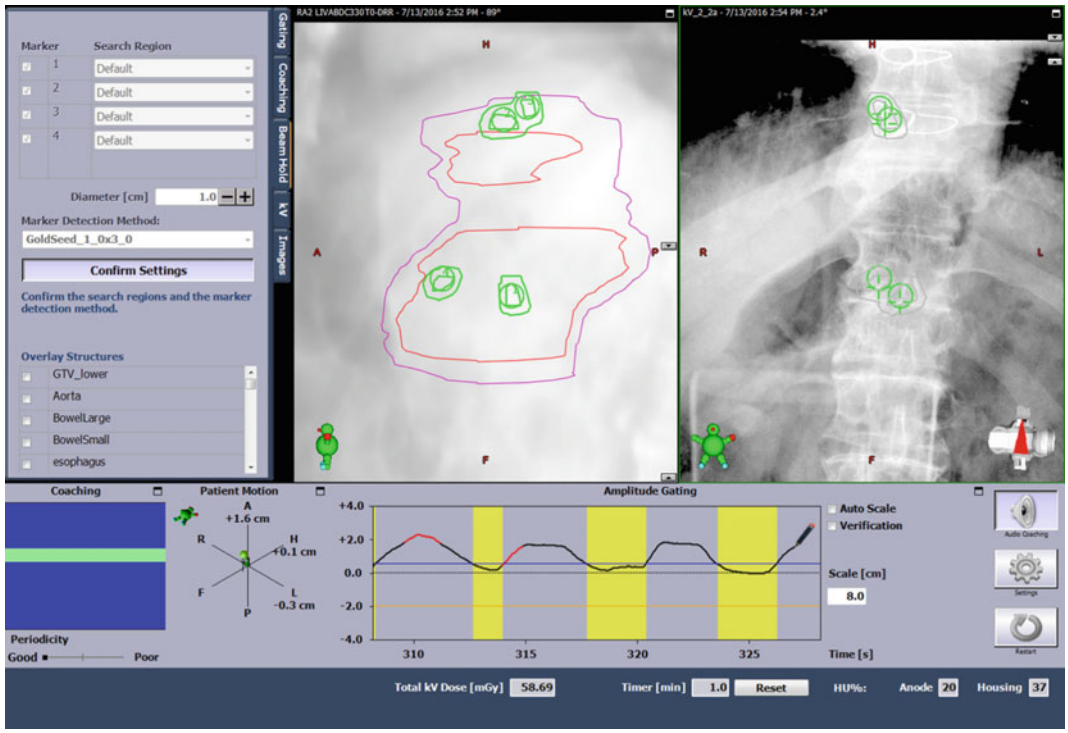

Fig. 9.4 kV projection image acquired during respiratory-gated delivery of liver SBRT treatment. The green contours indicate the acceptable location of fiducial markers that are automatically identified in the image. Beam delivery commences when breathing trace measured by chest block surrogate is in appropriate phase/amplitude and when markers are identified as being within the acceptable contour region

hold software is available on some treatment machines but further discussion is beyond the scope of this chapter.

9.6 Plan Evaluation Criteria

9.6.1 Liver Dose-Limiting Toxicities and Dose Constraints

The most concerning and dose-limiting toxicity of liver radiation is radiation-induced liver disease (RILD). RILD is a clinical syndrome of fatigue, elevated liver enzymes (particularly alkaline phosphatase over liver transaminases), tender anicteric hepatomegaly, and ascites. Pathologic changes consist of pronounced hyperemia acutely, and then veno-occlusive disease, marked central venous congestion, sparing of large veins, and atrophy of adjacent hepatocytes chronically, similar to changes seen following bone marrow transplant or high-dose chemotherapy [40].

Pathophysiologically, deposition of fibrin within the central veins, TGF-beta [41] and TNF-alpha activation [42], has been observed, postulating that injury occurs in the endothelial cells rather than hepatocytes [43]. RILD can be seen 2 weeks to 8 months following the completion of radiation, however, usually occurs within the first 3 months after treatment [44]. The treatment for RILD is largely supportive. Although most patients can recover with diuretic and steroid treatment, RILD has the potential to lead to liver failure and death [43].

Over the last two decades, several models have been developed to establish dose constraints to minimize the risk of RILD in patients receiving hypofractionated radiotherapy. The Quantitative Analyses of Normal Tissue Effects in the

Clinic (QUANTEC) publication on "Radiation associated liver injury" reports dose constraints for SBRT based on their analyses of the literature. The most common liver constraint is based on the surgical literature which required sparing of at least one-third of the liver after a liver resection to maintain reasonable liver function. This translates to approximately 700 cc and thus, the constraint of maintaining $\geq$ 700 cc of normal liver receiving $\leq$ 15 Gy in three to five fractions [45]. In addition, mean dose should be <15 Gy for liver metastases, in three fractions and <20 Gy for liver metastases, in six fractions.

The effective liver volume (Veff) irradiated is a model based on the normal liver volume and the volume irradiated. The Veff is defined as the normal liver volume minus all GTVs, which if homogenously irradiated to the maximum dose would be associated with the same estimated risk of RILD as the delivered heterogeneous treatment plan [46]. A lower Veff correlated with significantly lower risks of RILD, demonstrating in the setting of dose escalation, high doses can be delivered as long as the mean dose to the liver is taken into account [46].

Abiding by certain dosimetric guidelines derived from the studies of high-dose focal radiation to liver metastases may help minimize radiation injury to the normal surrounding liver parenchyma. Strategies include keeping the mean dose for uninvolved liver <32 Gy in 2 Gy per fraction equivalent [46] or the total dose to 700 mL of non-tumorous liver to <15 Gy in 3 fractions. Additionally, one can ensure that <30% of the liver receives 21 Gy in three fractions or 12 Gy in a single fraction [47]. With careful patient selection and by maintaining the appropriate dose constraints, RILD after SBRT occurs in fewer than 5% of cases [45]. The QUANTEC dose constraints for liver SBRT are summarized in Table 9.1.

It is important to keep in mind that patient-related factor such as underlying liver disease that can subsequently compromise normal liver function is also an important predictor of RILD. Patients with abnormal liver function may develop different types of radiation toxicity [48] and may have a different dose–volume relationship for RILD than those characterized in the models by Dawson et al. [46]. Therefore, care must be taken before extrapolating these described tolerances to different patient populations.

Other acute toxicities include transient increase in liver enzymes, reactivation of hepatitis B or a general decline in liver function. Notably, these toxicities are more commonly seen in patients with HCC [48] but are rare in patients with liver metastases, unless a history of prior liver radiation or underlying liver disease is present, which can increase the risk of RILD.

Table 9.1 Liver SBRT normal tissue dose constraints

Organ at risk	Dose constraints (QUANTEC) (conventional fractionation unless otherwise noted)	Dose constraints from [60] (5 fractions)
Liver	$\geq$ 700 cc of normal liver receives $\leq$ 15 Gy in 3–5 fractions Mean normal liver dose: <15 Gy in 3 fractions or <20 Gy in 6 fractions	Liver—GTV mean dose $\leq$ 13 Gy (based on Child–Pugh a cirrhosis patients with HCC)
Spinal cord	Max dose <50 Gy (0.2% risk myelopathy)	Max dose $\leq$ 25 Gy to 0.5 cc
Stomach	D_{100} <45 Gy (<7% risk ulceration)	Max dose $\leq$ 30 Gy to 0.5 cc
Small bowel	V_{45} <195 cc (<10% risk grade 3 + toxicity) (peritoneal cavity)	Max dose $\leq$ 30 Gy to 0.5 cc
Large bowel/Esophagus		Max dose $\leq$ 32 Gy to 0.5 cc
Bilateral kidneys	Mean dose <15–18 Gy (< 5% risk clinical dysfunction)	Mean dose $\leq$ 10 Gy
Chest wall		Max dose $\leq$ 50 Gy to 0.5 cc

Additional potential late toxicities after liver irradiation include biliary sclerosis, hepatic subcapsular injury, gastrointestinal bleeding, small bowel obstruction, gastric outlet obstruction, and fistula formation, depending on whether or not normal tissues such as esophagus, stomach, duodenum, or large bowel are within the high-dose regions of the radiation treatment.

9.6.2 Gastrointestinal Toxicities and Dose Constraints

Due to the radiosensitivity of the stomach, small bowel, and colon, gastrointestinal (GI) toxicity, including ulceration, GI bleeding, stricture, and perforation small bowel obstruction, can be a potential effect of higher dose-per-fraction used for SBRT. GI toxicities have been reported in several studies of liver SBRT, especially when treating central or hilar liver tumors which are often adjacent to the duodenum or stomach [22, 49, 50]. Minimal data exist evaluating the appropriate dose constraints for the esophagus; however, there is a retrospective analysis of risk factors for esophageal toxicity among patients treated with single-fraction spine SBRT at Memorial Sloan Kettering Cancer Center. There was a correlation between high esophageal mucosal dose and esophageal toxicity, in particular ulceration and stricture, with a sharp increase in $\geq$ Grade 3 toxicity at doses above 15 Gy delivered in a single fraction [51]. More recent trials using conservative dose constraints have reported minimal GI toxicity [52]. The dose constraints for the GI organs from the Radiation Therapy and Oncology Group (RTOG) 1112 Study, entitled, Randomized Phase III Study of Sorafenib versus Stereotactic Body Radiation Therapy followed by Sorafenib in Hepatocellular Carcinoma, are listed in Table 9.1.

9.6.3 Chest Wall Dose Constraints

Skin ulceration and rib fractures from high-dose SBRT for lung and liver tumors has been reported, particularly when doses exceeded 30 Gy to 30 cc of the chest wall [53, 54]. Based on these findings, the most commonly used metric is the volume of chest wall receiving ≥ 30 Gy (V_{30}).

9.7 Practical Considerations

In addition to simulation and treatment planning, there are a number of practical issues that must be considered when developing a liver SBRT program. First and foremost is the commissioning of all systems and devices that are used for SBRT delivery. This includes verifying the mechanical and dosimetric accuracy of the treatment machines, as well as verification of the treatment planning model for treatment fields smaller than 4×4 cm^2. Field sizes in this regime are commonly used for SBRT and small errors in commissioning data measurements can have a large impact on the dose delivered to the patient [55].

Ancillary systems should also be commissioned. This includes verifying the accuracy of onboard or in-room imaging systems, the stability of any abdominal compression devices, and the functionality and accuracy of any respiratory gating systems. The American Association of Physicists in Medicine (AAPM) have published Task Group Report 101 [56], which contains useful information about the types of tests that are typically performed as well as the accuracy that one can expect for various systems when developing an SBRT program.

After commissioning is complete, it is also important to establish a comprehensive quality assurance program with baseline data obtained from commissioning measurements to ensure the constancy of system performance. This will include daily tests, such as the Winston-Lutz test to verify the iso-centricity of the treatment machine [57], as well as more in-depth monthly and annual testing. Many of these tests are similar to those performed regularly for standard fractionation treatments; however, the accuracy requirements are usually more stringent for systems used to deliver SBRT [58].

Another practical consideration for SBRT treatments is the increased treatment time

compared to standard fractionation treatments. This is exacerbated if respiratory gating is used since only a portion of the respiratory cycle is utilized for treatment delivery. To mitigate this, flattening filter free (FFF) X-ray beams can be used for treatment; FFF beams can achieve up to four times the dose rate of conventional treatment beams due to the decreased attenuation that results when the flattening filter is removed [59]. This comes at the expense of a field profile that is peaked in the center; however, for SBRT treatments this is typically not a concern (and in fact is desirable) since plans are usually generated to give higher doses to the center of the tumor in order to increase the dose gradient at the target edge. Also, the benefits of FFF beams will be reduced somewhat if the treatment fields are highly modulated; however, this is usually less of an issue with SBRT since the smaller target size and large doses per fraction tend to result in lower modulation factors.

Last but certainly not least, the implementation of a successful SBRT program requires proper education and training of all staff involved in the delivery of SBRT treatments. Given the reduced margin for error that results from delivering large doses in only a few fractions, it is critical for the various team members involved in the planning and delivery of SBRT to understand the role of various setup devices, plan parameters, and delivery protocols so that uncertainties can be minimized at every stage of the process. This training should be performed whenever a new staff member is going to participate in the SBRT program, and also on a continuing basis (e.g., annually) as a refresher to existing staff and also to allow for changes and improvements to the SBRT process.

References

1. Dawson LA, McGinn CJ, Normolle D, Ten Haken RK, Walker S, Ensminger W, Lawrence TS. Escalated focal liver radiation and concurrent hepatic artery fluorodeoxyuridine for unresectable intrahepatic malignancies. J Clin Oncol. 2000;18:2210–8.
2. Mohiuddin M, Chen E, Ahmad N. Combined liver radiation and chemotherapy for palliation of hepatic metastases from colorectal cancer. J Clin Oncol. 1996;14:722–8.
3. Robertson JM, Lawrence TS, Andrews JC, Walker S, Kessler ML, Ensminger WD. Long-term results of hepatic artery fluorodeoxyuridine and conformal radiation therapy for primary hepatobiliary cancers. Int J Radiat Oncol Biol Phys. 1997;37:325–30.
4. Kothary N, Heit JJ, Louie JD, Kuo WT, Loo BW Jr, Koong A, Chang DT, Hovsepian D, Sze DY, Hofmann LV. Safety and efficacy of percutaneous fiducial marker implantation for image-guided radiation therapy. J Vasc Interv Radiol. 2009;20:235–9. doi:10.1016/j.jvir.2008.09.026.
5. Fuss M, Salter BJ, Rassiah P, Cheek D, Cavanaugh SX, Herman TS. Repositioning accuracy of a commercially available double-vacuum whole body immobilization system for stereotactic body radiation therapy. Technol Cancer Res Treat. 2004;3:59–67. doi:10.1177/153303460400300107.
6. Hara R, Itami J, Aruga T, Kozuka T, Yamashita H, Abe Y, Fuse M, Kondo T, Shinohara D, Nagaoka T, Kobiki T. Development of stereotactic irradiation system of body tumors under respiratory gating. Nihon Igaku Hoshasen Gakkai Zasshi. 2002;62:156–60.
7. Kini VR, Vedam SS, Keall PJ, Patil S, Chen C, Mohan R. Patient training in respiratory-gated radiotherapy. Med Dosim. 2003;28:7–11. doi:10.1016/S0958-3947(02)00136-X.
8. Vedam SS, Keall PJ, Kini VR, Mohan R. Determining parameters for respiration-gated radiotherapy. Med Phys. 2001;28:2139–46. doi:10.1118/1.1406524.
9. Heinzerling JH, Anderson JF, Papiez L, Boike T, Chien S, Zhang G, Abdulrahman R, Timmerman R. Four-Dimensional computed tomography scan analysis of tumor and organ motion at varying levels of abdominal compression during stereotactic treatment of lung and liver. Int J Radiat Oncol Biol Phy 2008;70:1571–1578. doi:10.1016/j.ijrobp.2007.12.023.
10. Dawson LA, Eccles C, Bissonnette JP, Brock KK. Accuracy of daily image guidance for hypofractionated liver radiotherapy with active breathing control. Int J Radiat Oncol Biol Phys. 2005;62:1247–52. doi:10.1016/j.ijrobp.2005.03.072.
11. Depuydt T, Verellen D, Haas O, Gevaert T, Linthout N, Duchateau M, Tournel K, Reynders T, Leysen K, Hoogeman M, Storme G, Ridder MD. Geometric accuracy of a novel gimbals based radiation therapy tumor tracking system. Radiother Oncol. 2011;98:365–72. doi:10.1016/j.radonc.2011.01.015.
12. Ozhasoglu C, Saw CB, Chen H, Burton S, Komanduri K, Yue, NJ, Huq SM, Heron DE. Synchrony—Cyberknife respiratory compensation technology. Med Dosim, Image-Guided Radiation Therapy:Part 4–Focal Irradiation and Image Fusion Techniques 2008;33:117–123. doi:10.1016/j.meddos.2008.02.004.

13. Herfarth KK, Debus J, Lohr F, Bahner ML, Fritz P, Höss A, Schlegel W, Wannenmacher MF. Extracranial stereotactic radiation therapy: set-up accuracy of patients treated for liver metastases. Int J Radiat Oncol Biol Phys. 2000;46(2):329–35.
14. Lax I, Blomgren H, Näslund I, Svanström R. Stereotactic radiotherapy of malignancies in the abdomen. Methodol Aspects Acta Oncol. 1994;33 (6):677–83.
15. Lovelock DM, Zatcky J, Goodman K, Yamada Y. The effectiveness of a pneumatic compression belt in reducing respiratory motion of abdominal tumors in patients undergoing stereotactic body radiotherapy. Technol Cancer Res Treat. 2014;13(3):259–67.
16. Wulf J, Hädinger U, Oppitz U, Olshausen B, Flentje M. Stereotactic radiotherapy of extracranial targets: CT-simulation and accuracy of treatment in the stereotactic body frame. Radiother Oncol. 2000;57(2):225–36.
17. de Pooter JA, Wunderink W, Méndez Romero A, Storchi PRM, Heijmen BJM. PTV dose prescription strategies for SBRT of metastatic liver tumours. Radiother Oncol. 2007;85:260–6. doi:10.1016/j.radonc.2007.08.004.
18. Kavanagh BD, Schefter TE, Cardenes HR, Stieber VW, Raben D, Timmerman RD, McCarter MD, Burri S, Nedzi LA, Sawyer TE, Gaspar LE. Interim analysis of a prospective phase I/II trial of SBRT for liver metastases. Acta Oncol. 2006;2006(45):848–55. doi:10.1080/02841860600904870.
19. Rusthoven KE, Kavanagh BD, Cardenes H, Stieber VW, Burri SH, Feigenberg SJ, Chidel MA, Pugh TJ, Franklin W, Kane M, Gaspar LE, Schefter TE. Multi-Institutional phase I/II trial of stereotactic body radiation therapy for liver metastases. JCO. 2009;27:1572–8. doi:10.1200/JCO.2008.19.6329.
20. van der Pool AEM, Méndez Romero A, Wunderink W, Heijmen BJ, Levendag PC, Verhoef C, IJzermans JNM. Stereotactic body radiation therapy for colorectal liver metastases. Br J Surg 2010;97:377–382. doi:10.1002/bjs.6895.
21. Wambersie A, Landberg T. International commission on radiation units and measurements; Supplement to ICRU Report 50; 1999.
22. Goodman KA, Wiegner EA, Maturen KE, Zhang Z, Mo Q, Yang G, Gibbs IC, Fisher GA, Koong AC. Dose-escalation study of single-fraction stereotactic body radiotherapy for liver malignancies. Int J Radiat Oncol Biol Phys. 2010;78(2):486–9.
23. Liu R, Buatti JM, Howes TL, Dill J, Modrick JM, Meeks SL, Optimal number of beams for stereotactic body radiotherapy of lung and liver lesions. Int J Radiat Oncol Biol Phys 2006;66:906–912. doi:10.1016/j.ijrobp.2006.05.014.
24. Tanyi JA, Summers PA, McCracken CL, Chen Y, Ku L-C, Fuss M. Implications of a high-definition multileaf collimator (HD-MLC) on treatment planning techniques for stereotactic body radiation therapy (SBRT): a planning study. Radiat Oncol. 2009;4:22. doi:10.1186/1748-717X-4-22.
25. de Pooter JA, Romero AM, Wunderink W, Storchi PRM, Heijmen BJM. Automated non-coplanar beam direction optimization improves IMRT in SBRT of liver metastasis. Radiother Oncol. 2008;88:376–81. doi:10.1016/j.radonc.2008.06.001.
26. Webb S. Intensity-Modulated Radiation Therapy. CRC Press; 2001
27. Bortfeld T. IMRT: a review and preview. Phys Med Biol. 2006;51:R363. doi:10.1088/0031-9155/51/13/R21.
28. Bortfeld T, Jokivarsi K, Goitein M, Kung J, Jiang SB. Effects of intra-fraction motion on IMRT dose delivery: statistical analysis and simulation. Phys Med Biol. 2002;47:2203. doi:10.1088/0031-9155/47/13/302.
29. Yu CX, Jaffray DA, Wong JW. The effects of intra-fraction organ motion on the delivery of dynamic intensity modulation. Phys Med Biol. 1998;43:91–104.
30. Ecclestone G, Pierce G. The role of VMAT interplay effects for liver stereotactic body radiation therapy. In: Jaffray AD, editor. World Congress on Medical Physics and Biomedical Engineering, June 7-12, 2015, Toronto, Canada. Cham: Springer International Publishing; 2015. p. 409–12.
31. Stambaugh C, Nelms BE, Dilling T, Stevens C, Latifi K, Zhang G, Moros E, Feygelman V. Experimentally studied dynamic dose interplay does not meaningfully affect target dose in VMAT SBRT lung treatments. Med Phys. 2013;40:91710. doi:10.1118/1.4818255.
32. Otto K. Volumetric modulated arc therapy: IMRT in a single gantry arc. Med Phys. 2008;35:310–7. doi:10.1118/1.2818738.
33. Solberg TD, Boedeker KL, Fogg R, Selch MT, DeSalles AAF. Dynamic arc radiosurgery field shaping: a comparison with static field conformal and noncoplanar circular arcs. Int J Radiat Oncol Biol Phys 2001;49:1481–1491. doi:10.1016/S0360-3016(00)01537-6.
34. Yu CX. Intensity-modulated arc therapy with dynamic multileaf collimation: an alternative to tomotherapy. Phys Med Biol. 1995;40:1435. doi:10.1088/0031-9155/40/9/004.
35. Mackie TR, Holmes T, Swerdloff S, Reckwerdt P, Deasy JO, Yang J, Paliwal B, Kinsella T. Tomotherapy: a new concept for the delivery of dynamic conformal radiotherapy. Med Phys. 1993;20:1709–19. doi:10.1118/1.596958.
36. Mackie TR, Balog J, Ruchala K, Shepard D, Aldridge S, Fitchard E, Reckwerdt P, Olivera G, McNutt T, Mehta M. Radiation therapy treatment optimization tomotherapy. Semin Radiat Oncol. 1999;9:108–17. doi:10.1016/S1053-4296(99)80058-7.
37. Westerly DC, Schefter TE, Kavanagh BD, Chao E, Lucas D, Flynn RT, Miften M. High-dose MVCT image guidance for stereotactic body radiation

therapy. Med Phys. 2012;39:4812–9. doi:10.1118/1.4736416.
38. Sterzing F, Uhl M, Hauswald H, Schubert K, Sroka-Perez G, Chen Y, Lu W, Mackie R, Debus J, Herfarth K, Oliveira G. Dynamic jaws and dynamic couch in helical tomotherapy. Int J Radiat Oncol Biol Phys 2010;76:1266–1273. doi:10.1016/j.ijrobp.2009.07.1686.
39. Bortfeld T, Webb S. Single-Arc IMRT? Phys Med Biol. 2009;54:N9. doi:10.1088/0031-9155/54/1/N02.
40. Reed GB Jr, Cox AJ Jr. The human liver after radiation injury. A form of veno-occlusive disease. Am J Pathol. 1966;48(4):597–611.
41. Seong J, Kim SH, Chung EJ, Lee WJ, Suh CO. Early alteration in TGF-beta mRNA expression in irradiated rat liver. Int J Radiat Oncol Biol Phys. 2000;46:639–43.
42. Christiansen H, Saile B, Neubauer-Saile K, Tippelt S, Rave-Frank M, Hermann RM, Dudas J, Hess CF, Schmidberger H, Ramadori G. Irradiation leads to susceptibility of hepatocytes to TNF-alpha mediated apoptosis. Radiother Oncol. 2004;72:291–6.
43. Dawson LA, Ten Haken RK. Partial volume tolerance of the liver to radiation. Semin Radiat Oncol. 2005;15:279–83.
44. Lawrence TS, Robertson JM, Anscher MS, Jirtle RL, Ensminger WD, Fajardo LF. Hepatic toxicity resulting from cancer treatment. Int J Radiat Oncol Biol Phys. 1995;31:1237–48.
45. Pan CC, Kavanagh BD, Dawson LA, et al. Radiation-associated liver injury. Int J Radiat Oncol Biol Phys. 2010;76:S94–100.
46. Dawson LA, Normolle D, Balter JM, McGinn CJ, Lawrence TS, Ten Haken RK. Analysis of radiation-induced liver disease using the Lyman NTCP model. Int J Radiat Oncol Biol Phys. 2002;53:810–21.
47. Wulf J, Guckenberger M, Haedinger U, Oppitz U, Mueller G, Baier K, Flentje M. Stereotactic radiotherapy of primary liver cancer and hepatic metastases. Acta Oncol. 2006;45(7):838–47.
48. Cheng JC, Liu HS, Wu JK, Chung HW, Jan GJ. Inclusion of biological factors in parallel-architecture normal-tissue complication probability model for radiation-induced liver disease. Int J Radiat Oncol Biol Phys. 2005;62:1150–6.
49. Hoyer M, Roed H, Traberg Hansen A, et al. Phase II study on stereotactic body radiotherapy of colorectal metastases. Acta Oncol. 2006;45:823–30.
50. Schefter TE, Kavanagh BD, Timmerman RD, et al. A phase I trial of stereotactic body radiation therapy (SBRT) for liver metastases. Int J Radiat Oncol Biol Phys. 2005;62:1371–8.
51. Cox BW, Jackson A, Hunt M, et al. Esophageal toxicity from high-dose, single-fraction paraspinal stereotactic radiosurgery. Int J Radiat Oncol Biol Phys. 2012;83:e661–7.
52. Rule W, Timmerman R, Tong L, Abdulrahman R, Meyer J, Boike T, Schwarz RE, Weatherall P, Chinsoo CL. Phase I dose-escalation study of stereotactic body radiotherapy in patients with hepatic metastases. Ann Surg Oncol. 2011;18(4):1081–7.
53. Dunlap NE, Cai J, Biedermann GB, et al. Chest wall volume receiving >30 Gy predicts risk of severe pain and/or rib fracture after lung stereotactic body radiotherapy. Int J Radiat Oncol Biol Phys. 2010;76:796–801.
54. Mutter RW, Liu F, Abreu A, et al. Dose–volume parameters predict for the development of chest wall pain after stereotactic body radiation for lung cancer. Int J Radiat Oncol Biol Phys. 2012;82:1783–90.
55. Solberg TD, Balter JM, Benedict SH, Fraass BA, Kavanagh B, Miyamoto C, Pawlicki T, Potters L, Yamada Y. Quality and safety considerations in stereotactic radiosurgery and stereotactic body radiation therapy: executive summary. Pract Radiat Oncol. 2012;2:2–9. doi:10.1016/j.prro.2011.06.014.
56. Benedict SH, Yenice KM, Followill D, Galvin JM, Hinson W, Kavanagh B, Keall P, Lovelock M, Meeks S, Papiez L, Purdie T, Sadagopan R, Schell MC, Salter B, Schlesinger DJ, Shiu AS, Solberg T, Song DY, Stieber V, Timmerman R, Tomé WA, Verellen D, Wang L, Yin F-F. Stereotactic body radiation therapy: The report of AAPM Task Group 101. Med Phys. 2010;37:4078–101. doi:10.1118/1.3438081.
57. Lutz W, Winston KR, Maleki N, A system for stereotactic radiosurgery with a linear accelerator. Int J Radiat Oncol Biol Phys 1988;14:373–381. doi:10.1016/0360-3016(88)90446-4.
58. Klein EE, Hanley J, Bayouth J, Yin F-F, Simon W, Dresser S, Serago C, Aguirre F, Ma L, Arjomandy B, Liu C, Sandin C, Holmes T. Task Group 142 report: Quality assurance of medical acceleratorsa). Med Phys. 2009;36:4197–212. doi:10.1118/1.3190392.
59. Prendergast BM, Fiveash JB, Popple RA, Clark GM, Thomas EM, Minnich DJ, Jacob R, Spencer SA, Bonner JA, Dobelbower MC. Flattening filter-free linac improves treatment delivery efficiency in stereotactic body radiation therapy. J Appl Clin Med Phys. 2013;14(3):4126.
60. RTOG 1112: Randomized Phase III Study of Sorafenib versus Stereotactic Body Radiation Therapy followed by Sorafenib in Hepatocellular Carcinoma. 2016. Website: https://www.rtog.org/ClinicalTrials/ProtocolTable/StudyDetails.aspx?study=1112.

Particle Radiation Therapy for Liver Tumors: Simulation and Treatment Planning

10

Matthew Knecht, MD, Andrew Wroe, PhD
and Gary Y. Yang, MD

10.1 Introduction

After discovery of X-rays in 1895 and their subsequent therapeutic use in skin lesions shortly thereafter in 1896, research has been undertaken to understand and minimize the risks of radiation therapy to normal tissues, while still maintaining tumoricidal doses. As a part of the progression toward improving the therapeutic window, Dr. Ernest Lawrence developed the ability to accelerate ions, and one of his students, Dr. Robert Wilson, wrote the seminal paper hypothesizing the medical use of ion beam therapy in 1946 [1]. In that paper, he showed the graph indicating the Bragg Peak, and discussed the improved penumbra offered by protons over electrons.

Heavy charged particles (i.e., protons and heavier ions) deposit energy primarily through coulombic interactions with orbital electrons and to a small degree through nuclear collisions. As described by Wilson, heavy charged particles deposit significantly more energy in the final portion of their path length in a region called the Bragg peak, which for protons is of the order of a few millimeters at the 90% dose level. This leads to lower entrance doses than photon-based techniques, which allows for fewer beams to be used than with photon techniques, and no primary proton dose beyond the Bragg peak. Other advantageous physical properties of charged particle beams include tighter penumbra at depths less than 15 cm [2, 3] and uniform dose delivery across the target volume with the use of a spread out Bragg peak (SOBP) (Fig. 10.1).

The first clinical use of an ion beam was undertaken by investigators at Berkeley in 1954. Further research included pituitary adenoma treatments at Harvard in 1963, and the first hospital-based proton facility opened at Loma Linda in 1990. These proton centers were developed utilizing passively scattered proton beams that treat the entire tumor volume with a uniform dose at a given time. Subsequent advances in beam delivery techniques have led to the development of proton pencil beam scanning systems that utilize a narrow proton beam and scanning magnets to paint a dose over the desired target. Beyond protons, other particles, such as carbon, are in medical use and showing encouraging initial clinical outcomes.

External beam radiation therapy for liver tumors was initially limited by the high risk of radiation-induced liver disease (RILD) especially since many primary liver tumors occur in the setting of an already cirrhotic liver. As technologic improvements allowed for increasingly

M. Knecht · A. Wroe
Department of Radiation Medicine, Loma Linda University Health, 11234 Anderson St, Suite A-875, Loma Linda, CA 92354, USA
e-mail: mknecht@llu.edu

A. Wroe
e-mail: awroe@llu.edu

G.Y. Yang (✉)
Department of Radiation Medicine, Loma Linda University Health, 11234 Anderson St, Suite B-121, Loma Linda, CA 92354, USA
e-mail: gyang@llu.edu

J. Meyer and T.E. Schefter (eds.), *Radiation Therapy for Liver Tumors*,
DOI 10.1007/978-3-319-54531-8_10

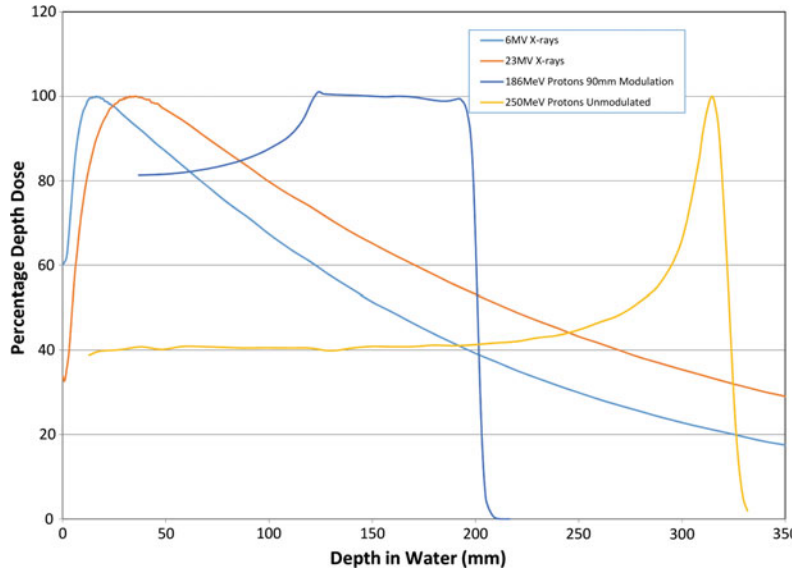

Fig. 10.1 Depth dose profiles for 6 and 23 MV X-rays for comparison with a 90-mm modulated 186 MeV proton beam and an unmodulated 250 MeV proton beam

conformal radiation delivery, photon-based techniques became a viable treatment modality for liver tumors. Particle therapy allows for sparing of low and intermediate radiation dose relative to photon therapy with lower integral dose, an ability to avoid critical structures altogether through the use of fewer beams, no exit dose, and potentially tighter penumbra, thus providing an even wider therapeutic window when treating liver tumors.

The goal of this chapter will be to familiarize the reader with the pertinent practical aspects of ion beam therapy in the treatment of liver patients. The primary particle discussed will be protons, with mention of carbon ions, and the issues surrounding clinical deployment of these ions.

10.2 Patient Selection

When considering particle therapy for liver tumors, many of the selection criteria are disease- and liver function-specific and are thus similar to photon techniques; however, the lower integral dose provided by particle therapy is theorized to expand the therapeutic window, and thus expand patient selection. Basic eligibility for local treatment and thus criteria for the reported phase II trials evaluating particle therapy for hepatocellular carcinoma (HCC) include histologic or imaging diagnosis of HCC limited to the liver (including patients with vessel thrombus), adequate hepatic function, Child-Turcotte-Pugh (CTP) class A or B cirrhosis, Eastern Cooperative Oncology Group (ECOG) performance status 0–2, with three or fewer lesions, who were not eligible at that time for resection or transplant [4–8].

Further considerations which favor selecting radiation therapy over other treatment modalities include the tumor size, tumor thrombus, and central location within the liver. Other modalities used to ablate liver neoplasms, discussed elsewhere in this text, have difficulty treating tumors for a number of different technical factors (thermoablation due to heat sink effect of large vessels and larger tumor size, transarterial chemoembolization [TACE] due to tumor thrombus and blood flow). However, ablative radiation can deliver tumorcidal treatment in these areas and need only meet the dose constraints of the normal organs, thus making it a good treatment option in such cases.

The utility of selecting particle therapy over photon-based techniques comes as particle therapy can allow for further sparing of liver tissue due to reduced low- and intermediate -dose regions (see Fig. 10.2). Thus far, these issues have been explored by retrospective reviews and mathematical modeling showing that for larger tumors

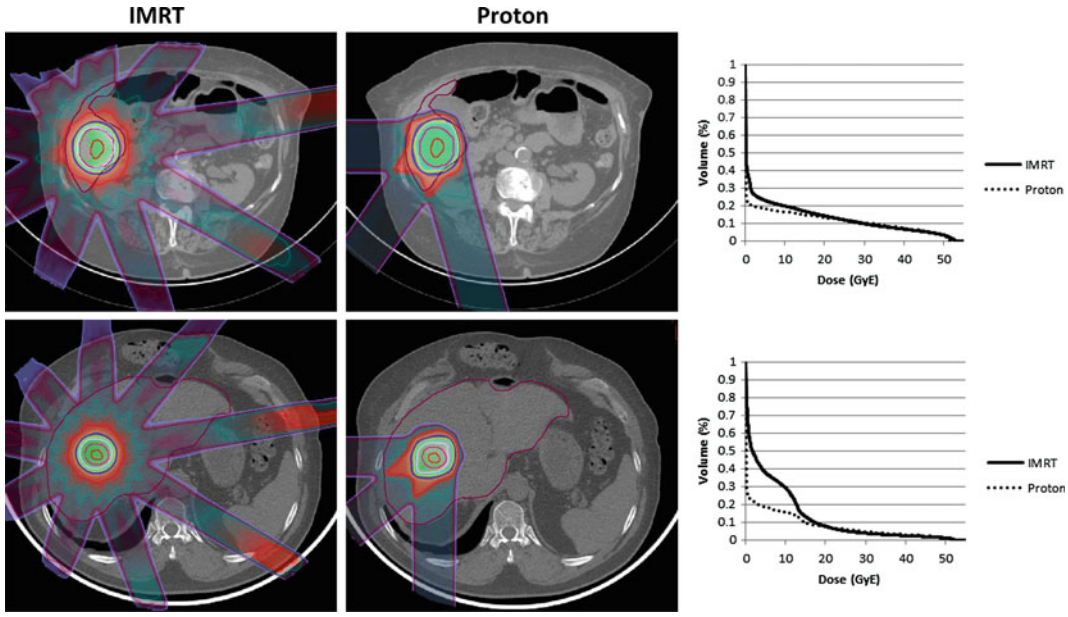

Fig. 10.2 This figure shows nine beam IMRT plans and three beam, passively scattered proton plans for an inferior liver lesion, *upper row*, and a dome lesion, *lower row*. Low and intermediate dose sparing is shown in the liver dose volume histograms, corresponding to the treatment plans in each row

(>5 cm) and for tumors in the central locations larger than 3 cm there is significant sparing of liver tissue with proton therapy [9]. Furthermore, retrospective reviews treating patients with tumors larger than 10 cm [10], CTP class C [11], and portal vein thrombosis [12] provide initial evidence for proton therapy as a treatment modality for these challenging scenarios.

There are several conditions which led to patients being excluded from the reported phase II studies. These included unstable ascites and proximity to gastrointestinal (GI) structures. As ascitic fluid volume changes, the proton path length to the target changes as well which, if unaccounted for, can lead to proton range errors and unacceptable dose coverage of the target.

10.3 Immobilization and Simulation

The goal of immobilization is to provide a stable system by which the patient can be reproducibly set up for treatment on a daily basis. For liver tumors the reproducibility of setup is reflected in the magnitude of the combination an internal target volume (ITV) and planning target volume (PTV) expansions. The ITV expansion reflects the estimated intrafractional motion and the PTV accounts for daily patient setup variability [13] and in the case of protons, beam-specific uncertainties, including range uncertainty.

At Loma Linda University James M. Slater, MD Proton Treatment and Research Center (JMSPTRC), a cylindrical whole body immobilizer or pod system was adapted from 1980s Switzerland's Paul Scherrer Institute (**PSI**) immobilization for pion beam treatments [14] (see Fig. 10.3). Initially developed as a patient-specific polyvinyl chloride pod, it has been upgraded to utilize a generic carbon fiber pod with a patient-specific insert [14, 15]. During simulation the patient lies in the patient-specific insert (which is indexed to the carbon fiber pod) while self-expanding foam is poured around the patient to create the external portion of patient immobilization. This methodology provides a customized whole body immobilization of the

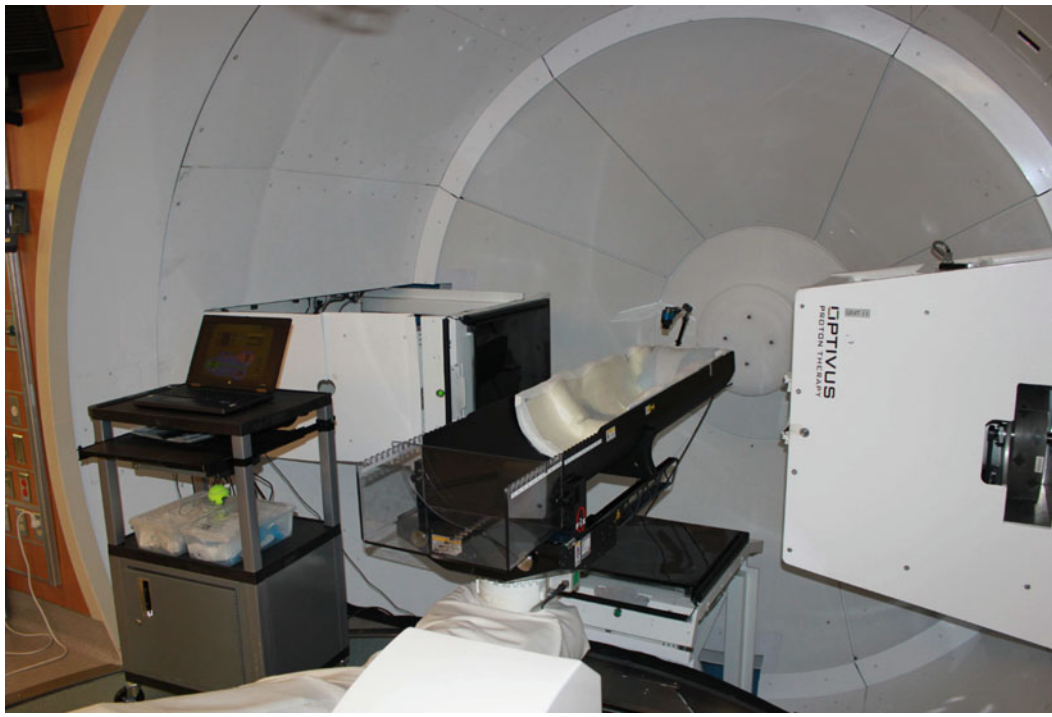

Fig. 10.3 Patient setup at Loma Linda utilizing pod immobilization and SDX for active breath management for treatment of liver tumors

patient allowing for improved stability and reproducibility of setup. Additionally for proton and ion therapy, this system also produces a reproducible external contour of the patient ensuring a reproducible water equivalent path length (WPL) for beams that traverse the immobilization system. Other immobilization options include alpha cradles, vac-lock bags and stereotactic vac-lock bags, however, such systems generally do not ensure a reproducible patient external contour and WPL.

For targets in the abdomen, it is also important to consider respiratory motion in treatment planning and delivery, and thus address this matter during the simulation process. While motion can be tracked and gated with the use of implanted fiducials and external camera systems, the implementation of this can be difficult in proton and ion therapy. This is because while tracking can ensure accurate placement of the target relative to the beam central axis, respiratory motion can result in changes to the water equivalent depth of the target, leading to errors in Bragg peak positioning and underdosing of the target and/or overdosing of surrounding structures. Another option is to reduce target motion using active breathing control, voluntary breath hold, belt systems and spirometric devices. At the JMSPTRC target motion is reduced with a spirometry device (SDX^{TM} available from Qfix) which ensures a reproducible breath hold. The SDX unit differs from active breathing control systems in that while it monitors the patient's inspiration volume, it does not control it. Rather the patient participates in their treatment via feedback from a video screen representation of their level of inspiration. The patient breathes into a predetermined level of inspiration and then a countdown timer displayed to the patient instructs them on the duration of the breath hold for the given treatment or imaging cycle.

Following immobilization simulation proceeds with a non-contrast CT for treatment planning and a contrast CT for tumor localization, both of which

are taken under deep inspiration breath hold. Fiducials are not employed due to the requirement for an invasive procedure and the dose shadow which results from the use of metallic fiducials [16]. Carbon-coated ceramic and stainless steel fiducials are under investigation as an option to address the dose shadow [17], and currently liquid fiducials are becoming clinically available which can be placed with minimally invasive techniques [18]. If a patient cannot tolerate the use of spirometry device the patient is imaged and treated under free breathing conditions and a 4DCT is utilized to define the extent of tumor motion. This approach is possible for passive scattering proton/ion beam delivery as the beam dimensions are static and can be constructed to encompass the target during all phases of the respiration cycle.

10.4 Treatment Planning and Dosimetry

After patient immobilization and imaging, the goal of treatment planning and dosimetry is to define a target and develop a robust plan to deliver a tumoricidal dose to that volume. The target is defined by the gross tumor volume (GTV), with expansions for the clinical tumor volume (CTV), ITV (for mobile tumors), and PTV. A tumoricidal dose then can be planned with beam number and angle selection, addressing proton-specific treatment planning characteristics and patient setup uncertainty.

As mentioned above, target delineation for proton therapy at JMSPTRC utilizes a planning CT scan under breath hold if tolerated by the patient or free breathing conditions if not, without intravenous contrast. A second CT scan under the same conditions with intravenous contrast is performed to guide target delineation, but is not used for dose calculation. The GTV is then defined as the tumor volume seen on the contrast study with reference to prior diagnostic four-phase CT scans or MRIs.

Beyond the GTV, the CTV is added to encompass subclinical disease. The expansion to create the CTV varies between 0 and 1 cm in the reported phase II trials [4–8], and is added at the discretion of the treating physician. In Radiation Therapy Oncology Group (RTOG) 1112, the CTV is defined as being equal to the GTV except in the following situations where an appropriate expansion is added: non-tumor thrombi, prior TACE cavity, or other prior ablation site. Currently at Loma Linda, trials addressing hepatocellular carcinoma include a 1-cm CTV expansion limited to the liver parenchyma, while there is no GTV-to-CTV expansion on the liver metastasis protocol.

The GTV and CTV are assigned based upon tumor characteristics, while the ITV and PTV are added to account for physical uncertainties during treatment. The concept of an ITV, an additional margin to account for intrafractional, physiologic variation (usually relating to respiration-induced motion), was not widely implemented in the current protocols [4–8] and was often included in the overall PTV expansion. Methods described above are used to quantify or limit the amount of physiologic variation, and as recommended by RTOG 1112, breathing motion management is used if the motion is greater than 5 mm on 4DCT. At Loma Linda, when the SDX spirometry device is used for immobilization, no additional margin is added for ITV.

The concept of a PTV in proton therapy is a combination of the familiar physical setup uncertainty as well as beam-specific considerations. Physical setup uncertainty includes the known daily variation of the setup, immobilization, and daily imaging. At JMSPTRC the combination of full body pod and daily orthogonal kV imaging results in a 5 mm daily setup uncertainty. The second component of the PTV in proton planning is a beam-specific range uncertainty (Fig. 10.4). The PTV is related to the stopping power ratio along the beam path during dose calculation including uncertainties in the patient CT image, uncertainty in the parameterized stoichiometric formula to calculate theoretical CT numbers, deviation in human tissue from ICRU standard tissue, uncertainty in mean excitation energy, and uncertainty due to energy dependence of the stopping power ratio not accounted for by the dose calculation algorithm [19]. Additionally, beam-specific uncertainties

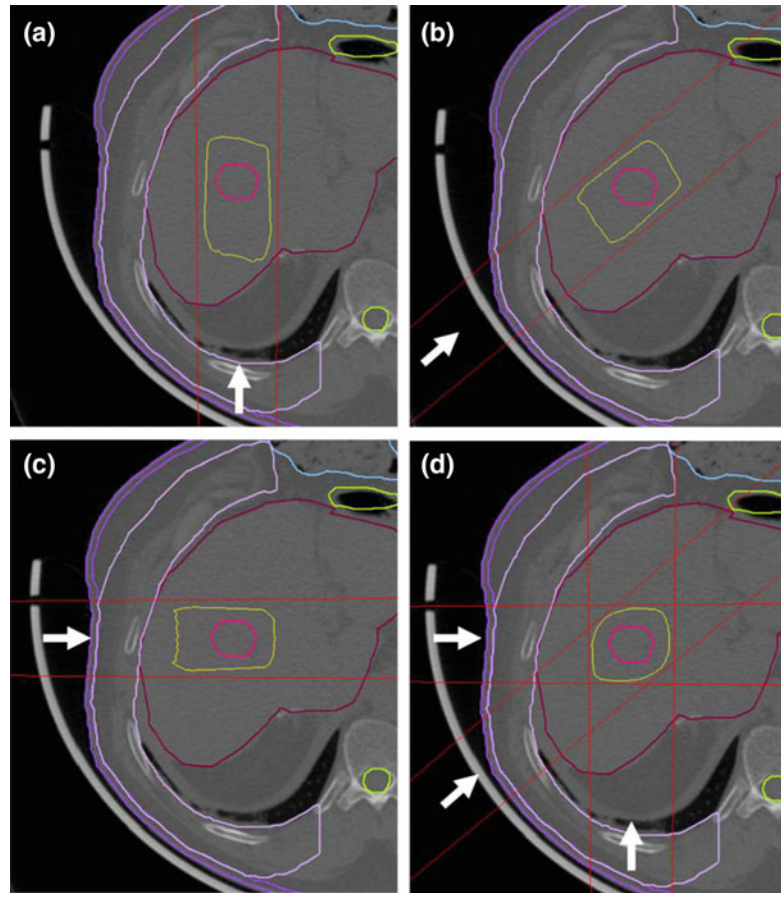

Fig. 10.4 *Panels* **a**, **b,** and **c** show the proton beam-specific PTV as represented by the 90% isodose line, and *panel* **d** shows the combined PTV, *arrows* indicate beam direction

not related to the dose calculation include: commissioning measurement uncertainty, error in compensator design, beam reproducibility, and patient setup [20] also need to be considered. An excellent overview table for range uncertainties and their sources can be found in the Paganetti article [20]. Beam-specific range uncertainty is specified as 3.0–3.5% of the proton range applied to the distal and proximal margins of the target volume to generate a beam-specific PTV. The beam-specific PTV governs the planning for that specific beam with parameters such as beam energy, modulation, compensator design, spot pattern, etc., optimized to ensure coverage of the beam-specific PTV with the prescribed isodose contour.

With regards to proton specific dose constraints there is a significant amount of heterogeneity seen on the current phase II trials though the following constraints can act as a guide: mean liver dose of 13 GyE with a dose of 50 GyE, in 10 fractions per RTOG 1112, V25 < 33% for a prescription of 70.2 GyE in 15 fractions [4], and a mean liver dose of less than or equal to 24 GyE with a prescription of 67.5 GyE in 15 fractions [6]. Currently at Loma Linda, the following constraints are used: for HCC treatment with 70.2 GyE in 15 fractions, liver V25 < 33%; for HCC treatment with GyE in 5 fractions, mean liver dose <13 GyE, and for liver metastasis treatment with 60 GyE in 3 fractions, liver constraints of V27 < 30%, V24 < 50%, and 700

ml receiving <15 GyE. Further evaluation is underway utilizing the equivalent uniform dose model to provide more accurate dose constraints.

Beam selection is critical in proton and heavy ion therapy as one must consider the stability of the WPL the particle will pass through to reach the target and distal edge placement. First, when considering the stability of the WPL, factors such as the edge of the immobilization device, abdominal motion, lung excursion, and bowel gas must be considered. Choosing beams that enter either entirely through the immobilization device or enter entirely avoiding the device are preferable. Beams that traverse the edge of the immobilization device can incur further range uncertainty due to daily shifts of the immobilization device relative to the target, placing more or less of the immobilization device in the beam path. Anterior beams are also avoided where possible, as abdominal motion creates an unstable external contour, and anterior beams tend to pass through abdominal gas creating WPL instability. At the JMSPTRC treatment plans are generated using two to three beams oriented through approximately a 90° arc between the right lateral and posterior positions that when combined with our immobilization techniques (i.e., POD) minimize variations in WPL, which minimize these variables (see Fig. 10.2).

Dome lesions also present a challenge in that respiratory motion can create large differences in WPL due to varying amount of lung in the field, however, reports show that this can be addressed through active breathing management or smearing techniques [22]. Smearing is a technique used to account for uncertainty in WPL due to target motion relative to other anatomy by smoothing out the proton distal edge profile. This is achieved by applying a smear radius to each point on the distal edge surface, with the larger the radius giving a greater level of smoothing. This method impacts the design of the compensator (or beam spot pattern in IMPT) resulting in a broadening and smoothing of the proton distal edge reducing conformity in this region. The goal of this is to ensure that errors involving inadequate distal range caused by shifts in WPL are minimized and target coverage is maintained.

Additionally, when choosing beam angles one must consider the relative biological effectiveness (RBE) of the distal edge of the proton beam. Proton therapy centers employ an RBE correction factor approximated to be 1.1 to dose delivered to the patient, however, near the distal edge of the Bragg peak LET increases markedly which can lead to increased biological damage in this region and even shift in the distal edge of the dose delivery [23]. The extent of biological enhancement in this region is uncertain as it depends on a number of factors including incident energy, LET distribution, cell type, biological endpoint, etc. This uncertainty is managed clinically by using beams that are largely orthogonal to avoid overlap of the distal portion of the Bragg peak, or by avoiding beams that stop on or near critical structures (GI structures in the case of targets in the liver) as these are most at risk from biological enhancement.

10.5 Beam Delivery

Proton and carbon ion beam depth dose distributions are characterized by a low entrance dose, followed by a high-dose peak (Bragg peak) at a predetermined depth governed by their initial energy and a sharp distal falloff (see Fig. 10.1) after which no primary particle dose is deposited. The superposition on multiple Bragg peaks of varying energy allows for the creation of a uniform dose area known as the spread out Bragg peak (SOBP) whose width can be customized to the target. This unique depth dose profile allows for conformal and homogeneous dose delivery to the target with fewer treatment beams (typically 2–3) and a lower integral dose to surrounding normal tissues (Fig. 10.2). The delivery of protons or carbon ions to the target is achieved through two distinct methods, passive scattering and pencil beam scanning.

Passive scattering typically utilizes a two-stage scattering system to create a wide proton beam of a given diameter for treatment [24]. The first stage of the scattering system is constructed from lead whose thickness is specified by a set of lead wedges [25] and is

customizable for varying beam energies/ranges. After passing through this scatterer the proton beam is Gaussian in profile with a FWHM of a few centimeters. The second stage of the scattering system is a contoured Lexan and lead disk whose profile is designed to be energy/field size specific and generate a uniform proton beam of given diameter. The Lexan thickness of the second scattering foil is complimentary to that of the lead component to ensure the proton beam range uniformity is maintained across the entire beam area [26]. The SOBP is generated by a rotating Lexan wheel with varying thickness steps to superimpose multiple Bragg peaks of varying range. Using this method SOBPs can be created with 0.5–1.0 cm resolution. The radiation is conformed to the target volume laterally by an aperture, made from brass or Cerrobend, and in depth through the use of a beam-specific compensator or bolus that is typically made from a low Z material such as wax or Lexan.

In pencil beam scanning beam delivery applications [27], the pencil beam from the accelerator is used directly to deliver dose to the target with no scattering. Instead the pencil beam is magnetically scanned over the target volume [28, 29] similar to airbrushing. The unmodulated Bragg peak creates a high dose spot at a given position within the target. These high dose spots are then moved laterally using magnetic positioning to deliver dose to a layer of the target at a given depth. When the planned dose to that specific layer has been delivered, the energy of the beam is then changed at the accelerator and dose is delivered to the next layer. This method of dose delivery allows for dose to be delivered homogeneously or inhomogeneously to the target (often referred to as intensity modulated proton therapy or IMPT [30]) with it possible to shape the lateral, distal, and proximal boundaries of the dose delivery without the need for an aperture or compensator.

The two methods of proton delivery are complimentary in their clinical application. Passive scattering with an aperture allows for proton beam delivery with improved penumbra over pencil beam scanning delivery with no aperture. However, the downside can be creation of the aperture and the necessity for this in passive scattered proton delivery can impact deliverable field size. Pencil beam scanning can allow for the treatment of larger fields (the size is limited by the strength of the scanning magnets but is often 40×40 cm^2) and shaping of both the proximal and distal sides of the SOBP. The flexibility of pencil beam scanning to deliver inhomogeneous and complex dose distributions also has potential clinical benefit in some cases. However, it must be noted that care needs to be taken when treating moving targets with pencil beam scanning. As pencil beam scanning and IMPT relies on accurate placement of the high-dose beam spot in three-dimensional space, as governed by the treatment plan, it can be susceptible to dose delivery errors if motion is not minimized through the use of immobilization or beam delivery techniques such as gating. Movement of the target during beam delivery and incorrect placement of the beam spot can lead to hot/cold dose spots within the target and potential irradiation of nontarget tissue. Passive scattering is much less susceptible to such errors as the target is treated uniformly with time and the lateral, distal, and proximal dose margins are created during the treatment planning process to account for tumor motion that is evaluated using 4DCT and potentially minimized using immobilization.

10.6 Treatment Facilities

Proton and carbon ion therapy facilities are characterized by a large central accelerator that provides high-energy particles to multiple treatment rooms [25]. The central accelerator is typically either a synchrotron or cyclotron. Synchrotrons generate a pulsed beam of protons or heavier ions, the energy of which can be varied at the accelerator level to meet the needs of the treatment team. This method produces a very monoenergetic beam of ions with minimal energy spread, yet the rate of beam delivery is typically fixed. Cyclotrons on the other hand produce a continuous beam of single maximum ion energy. Lower energies that may be required for treatment are then generated by passing the

ion beam through a variable range shifter that is located in close proximity to the accelerator to minimize transportation of secondary radiations to the treatment room. Cyclotron produced ion beams are characterized by a beam with increased energy spread, yet the rate of beam delivery can be increased by varying the beam current in the accelerator. The treatment rooms can employ either an isocentric 360° gantry, limited arc, or gantry fixed beam delivery using either passive scattering or pencil beam delivery techniques. The patient is located and immobilized on a positioner with 3–6 degrees of freedom and is aligned for treatment using digital X-ray images compared to digitally reconstructed radiographs generated during the treatment planning process. Single-room proton therapy systems are also becoming available which utilize compact gantry mounted cyclotron accelerators. These systems typically use a reduced gantry arc of rotation and employ a robotic patient positioner to achieve a wide range of treatment angles.

10.7 Out-of-Field Dose

As a result of radiation interactions with the beam delivery system and the patient secondary radiations such as electrons, photons, and neutrons can be produced that go on to deposit unwanted out-of-field dose to the patient. Of these radiations, neutrons pose the greatest concern due to their increased relative biological effectiveness [31]. The amount of out-of-field dose delivered to the patient is dependent on many factors including beam delivery technique, incident proton energy, and incident beam area to collimated beam area ratio. The extent of out-of-field dose has been investigated by a number of groups at various institutions [32–39] and is typically of the order of mSv/Gy near the treatment field with an exponential fall off to μSv/Gy 5–10 cm from the field edge [32]. It is important to also note that the out-of-field dose delivered by proton beam delivery is comparable to or less than that delivered from head scatter, head leakage, and patient scatter during IMRT or arc-based photon treatments [40]. An additional factor that contributes to out-of-field dose in heavy ion therapy (i.e., carbon therapy) is fragmentation of the treatment particle producing radiations that may go on to deliver dose beyond the distal edge of the Bragg peak. This will be discussed further in the next section.

10.8 Carbon Therapy

The rationale behind using heavier ions (such as Carbon or Oxygen) in clinical treatment is motivated by multiple factors, many of which are similar to the ones discussed for protons including a narrower Bragg peak with improved peak-to-entrance dose ratio, sharper penumbra, and potentially lower integral dose. Heavier ions have the additional benefits of an increased linear energy transfer (LET) and subsequent increase in RBE, currently estimated at 3 [41] for carbon, over protons (1.1) and x-rays (1). The higher LET means that increasing amounts of the damage done by carbon beams is through direct damage rather than through a secondary free radical mechanism and thus carbon ions also have less dependence on oxygenation. The hope is that higher LET accelerated ions such as carbon will increase cell killing in those tumors with hypoxia and cells with high rates of sublethal repair and/or high radioresistance to low LET radiation.

There are, however, a number of factors that have hampered the clinical deployment of heavy ion therapy into regular clinical practice. The first and perhaps biggest hurdle is the facility cost and complexity. Accelerating and directing heavier ions require larger diameter accelerators and larger magnets, resulting in larger/heavier gantries. These considerations not only impact the footprint of the facility but also the engineering and design to achieve precision of alignment which in turn elevates cost. While heavy ions exhibit advantages in physical dose distribution due to their size, fragmentation of the primary ion to lighter fragments can lead to dose delivery beyond the distal edge of the Bragg peak. This can negatively impact the dose sparing of a

heavy ion beam especially beyond the distal edge. Finally, heavy ions can vary significantly in their biological effectiveness along the depth dose profile requiring biologically effective dose to be the parameter used in planning. The data used in computing biologically effective dose can either be experimental based [42] or model based such as by the local effect model (LEM) [43, 44]. While this enhanced biological effectiveness increases cell killing in those tumors with hypoxia and cells with high rates of sublethal repair and/or high radioresistance to low LET radiation, additional biological validation and clinical trials with varying fractionation will increase clinical confidence in the technique.

10.9 Future Directions

As particle therapy continues to evolve we are seeing key work being completed in technical development, phase III clinical trials, and increased patient access. Technical improvements are focused on widening the therapeutic window for large tumors and tumors in difficult locations, while further increasing the conformity of the dose delivery. Maturing clinical trials will begin to provide quantitative data on the benefits of particle therapy in relation to other treatment modalities. Finally, a wider availability of particle therapy, including smaller, self-contained, and less expensive proton centers will provide increasing patient access to the benefits afforded by proton and particle therapy.

The technical advances envisaged for particle therapy focus on expanding the range of tumors that can be treated. In part, this advancement is shared with photon therapy, in that reductions in the ITV and PTV allow for less normal tissue to be treated. Reductions in the ITV can occur through improvements to patient immobilization, gated beam delivery, and tumor tracking. The use of implanted fiducials aids tumor localization, however, requires an invasive procedure and dose perturbation by the implanted material. To address dose perturbation carbon-coated, stainless steel fiducials or water equivalent fiducials could be employed, however, the problem of an invasive procedure still exists in patients who oftentimes have coagulopathies. Advanced fiducial or surface imaging technology could be employed to track target motion and in conjunction with beam gating technology ensure that beam delivery only occurs when the target is properly located. Cone beam CT (CBCT) also provides a potential for volumetric analysis of target placement in the treatment room and can possibly be employed in adaptive therapy. In adaptive therapy applications the CBCT images could be used along with deformable image registration and pencil beam scanning beam delivery to replan treatments addressing concerns which arise with ascites and variation in water path length that can oftentimes render these patients unsuitable for proton and particle therapy.

The treatment of liver tumors with particle therapy, while growing, is only reaching its adolescence. Current reports in the literature encompass retrospective [10–12, 45–50] and phase II clinical trials [4–8] and the current time is exciting in that the first phase III data including protons is set to emerge through several studies. The first is a phase III trial from JMSPTRC showing favorable interim results of proton therapy versus transarterial chemoembolization [51]. The second, RTOG 1112, is actively encouraging treatment of patients in the SBRT and Sorafenib arm with proton therapy. Analysis from these trials will aid in quantifying the benefits of proton therapy in the treatment of liver tumors.

As the physical, biological, and clinical benefits are becoming defined, providing access to this technology will remain a key issue. Patients require multiple treatments given on a daily or frequent basis, necessitating proximity to a treatment center. Recently, we have seen a significant rise in the number of proton therapy centers worldwide as the benefits of this modality of treatment are realized and technology improves. The development of single room proton centers provides at least part of the answer in widening the availability of this technology to the patient population. As the number of proton centers continues to rise, patients are

experiencing increased access to this modality and the physical, biological, and clinical benefits this provides.

10.10 Conclusion

Particle therapy is an enticing choice in the treatment of liver tumors, due to its ability to spare what often is an already poorly functioning liver through the use of the Bragg peak. However, as detailed within this chapter, special consideration must be taken with patient selection, treatment planning, and delivery so the level of precision seen on treatment plans can be translated into a deliverable dose to the patient. As shown in the phase II trials these challenges are being successfully met and thus the role of particle therapy, and in particular proton therapy, for the treatment of liver tumors will expand. As more patients are treated, increasing data will become available from which informed decisions can be made on when to employ particle therapy in the treatment of liver tumors.

References

1. Wilson RR. Radiological use of fast protons. Radiology. 1946;47:487–91.
2. Suit HD. Protons to replace photons in external beam radiation therapy? Clin Oncol. 2003;15:S29–31.
3. Engelsman M, Schwarz M, Dong L. Physics controversies in proton therapy. Sem Radiat Oncol. 2013;23:88–96.
4. Bush DA, Kayali Z, Grove R, Slater JD. The safety and efficacy of high-dose proton beam radiotherapy for hepatocellular carcinoma: a phase 2 prospective trial. Cancer. 2011;117:3053–9.
5. Fukumitsu N, Sugahara S, Nakayama H, et al. A prospective study of hypofractionated proton beam therapy for patients with hepatocellular carcinoma. Int J Radiat Oncol Biol Phys. 2009;74:831–6.
6. Hong TS, Wo JY, Yeap BY, et al. Multi-institutional phase ii study of high-dose hypofractionated proton beam therapy in patients with localized, unresectable hepatocellular carcinoma and intrahepatic cholangiocarcinoma. J Clin Oncology: Official Journal of the American Society of Clinical Oncology. 2016;34:460–8.
7. Kawashima M, Furuse J, Nishio T, et al. Phase II study of radiotherapy employing proton beam for hepatocellular carcinoma. J Clin Oncol: Official Journal of the American Society of Clinical Oncology. 2005;23:1839–46.
8. Nakayama H, Sugahara S, Fukuda K, et al. Proton beam therapy for hepatocellular carcinoma located adjacent to the alimentary tract. Int J Radiat Oncol Biol Phys. 2011;80:992–5.
9. Gandhi SJ, Liang X, Ding X, et al. Clinical decision tool for optimal delivery of liver stereotactic body radiation therapy: photons versus protons. Pract Radiat Oncol. 2015;5:209–18.
10. Sugahara S, Oshiro Y, Nakayama H, et al. Proton beam therapy for large hepatocellular carcinoma. Int J Radiat Oncol Biol Phys. 2010;76:460–6.
11. Hata M, Tokuuye K, Sugahara S, et al. Proton beam therapy for hepatocellular carcinoma patients with severe cirrhosis. Strahlentherapie und Onkologie: Organ der Deutschen Rontgengesellschaft [et al]. 2006;182:713–20.
12. Hata M, Tokuuye K, Sugahara S, et al. Proton beam therapy for hepatocellular carcinoma with portal vein tumor thrombus. Cancer. 2005;104:794–801.
13. Berthelsen AK, Dobbs J, Kjellen E, et al. What's new in target volume definition for radiologists in ICRU Report 71? How can the ICRU volume definitions be integrated in clinical practice? Cancer Imaging: The Official Publication of the International Cancer Imaging Society. 2007;7:104–16.
14. Wroe AJ, Bush DA, Schulte RW, Slater JD. Clinical immobilization techniques for proton therapy. Technol Cancer Res Treat. 2015;14:71–9.
15. Wroe A, Bush D, Slater J. Immobilization considerations for proton radiation therapy. Technol Cancer Res Treat. 2013.
16. Keane FK, Hong TS. Charged particle therapy for hepatocellular carcinoma: a commentary on a recently published meta-analysis. Ann Transl Med. 2015;3:365.
17. Cheung J, Kudchadker RJ, Zhu XR, Lee AK, Newhauser WD. Dose perturbations and image artifacts caused by carbon-coated ceramic and stainless steel fiducials used in proton therapy for prostate cancer. Phys Med Biol. 2010;55:7135–47.
18. Rydhog JS, Mortensen SR, Larsen KR, et al. Liquid fiducial marker performance during radiotherapy of locally advanced non small cell lung cancer. Radiother Oncol: Journal of the European Society for Therapeutic Radiology and Oncology. 2016.
19. Yang M, Zhu XR, Park PC, et al. Comprehensive analysis of proton range uncertainties related to patient stopping-power-ratio estimation using the stoichiometric calibration. Phys Med Biol. 2012;57:4095–115.
20. Paganetti H. Range uncertainties in proton therapy and the role of Monte Carlo simulations. Phys Med Biol. 2012;57:R99–117.
21. Dawson LA, Normolle D, Balter JM, McGinn CJ, Lawrence TS, Ten Haken RK. Analysis of radiation-induced liver disease using the Lyman NTCP model. Int J Radiat Oncol Biol Phys. 2002;53:810–21.

22. Pan X, Zhang X, Li Y, Mohan R, Liao Z. Impact of using different four-dimensional computed tomography data sets to design proton treatment plans for distal esophageal cancer. Int J Radiat Oncol Biol Phys. 2009;73:601–9.
23. Paganetti H, Goitein M. Radiobiological significance of beamline dependent proton energy distributions in a spread-out Bragg peak. Med Phys. 2000;27:1119–26.
24. Koehler AM, Schneider RJ, Sisterson JM. Flattening of proton dose distributions for large-field radiotherapy. Med Phys. 1977;4:297–301.
25. Lesyna D. Facility overview for a proton beam treatment center. Technol Cancer Res Treat. 2007;6:41–8.
26. Wroe AJ, Schulte RW, Barnes S, McAuley G, Slater JD, Slater JM. Proton beam scattering system optimization for clinical and research applications. Med Phys. 2013;40.
27. Lomax AJ, Albertini F, Boehringer T, et al. Spot scanning proton therapy: treatment planning and treatment verification. Radiother Oncol. 2006;78:S21-S.
28. Pedroni E. The new proton scanning gantry of PSI: a system designed for IMPT delivery in the whole body including moving targets. Radiother Oncol. 2006;78:S71-S.
29. Pedroni E, Bohringer T, Coray A, et al. Initial experience of using an active beam delivery technique at PSI. Strahlenther Onkol. 1999;175:18–20.
30. Lomax A, Albertini F, Bolsi A, et al. Intensity modulated proton therapy at PSI: things we have learnt (and are still learning). Radiother Oncol. 2005;76:S54–5.
31. Hall EJ. Intensity-modulated radiation therapy, protons, and the risk of second cancers. Int J Radiat Oncol Biol Phys. 2006;65:1–7.
32. Wroe A, Clasie B, Kooy H, Flanz J, Schulte R, Rosenfeld A. Out-of-field dose equivalents delivered by passively scattered therapeutic proton beams for clinically relevant field configurations. Int J Radiat Oncol Biol Phys. 2009;73:306–13.
33. Wroe A, Rosenfeld A, Schulte R. Out-of-field dose equivalents delivered by proton therapy of prostate cancer. Med Phys. 2007;34:3449–56.
34. Jarlskog CZ, Lee C, Bolch WE, Xu XG, Paganetti H. Assessment of organ-specific neutron equivalent doses in proton therapy using computational whole-body age-dependent voxel phantoms. Phys Med Biol. 2008;53:693–717.
35. Zheng Y, Newhauser W, Fontenot J, Taddei P, Mohan R. Monte Carlo study of neutron dose equivalent during passive scattering proton therapy. Phys Med Biol. 2007;52:4481–96.
36. Fontenot JD, Zheng Y, Taddei P, Newhauser W. Stray radiation exposure during proton radiotherapy of the prostate: the influence of the patient on scatter and production. Med Phys. 2007;34:2507.
37. Zheng Y, Newhauser W, Fontenot J, Taddei P, Mohan R. Study of neutron exposure during passively scattered proton therapy. Med Phys. 2007;34:2549–50.
38. Moyers MF, Benton ER, Ghebremedhin A, Coutrakon G. Leakage and scatter radiation from a double scattering based proton beamline. Med Phys. 2008;35:128–44.
39. Schneider U, Agosteo S, Pedroni E, Besserer J. Secondary neutron dose during proton therapy using spot scanning. Int J Radiat Oncol Biol Phys. 2002;53:244–51.
40. Hauri P, Halg R, Besserer J, Schneider U. General dose model for stray dose calculation of static and intensity-modulated photon radiation. Med Phys. 2016;43:1955–67.
41. Kato H, Tsujii H, Miyamoto T, et al. Results of the first prospective study of carbon ion radiotherapy for hepatocellular carcinoma with liver cirrhosis. Int J Radiat Oncol Biol Phys. 2004;59:1468–76.
42. Kanai T, Endo M, Minohara S, et al. Biophysical characteristics of HIMAC clinical irradiation system for heavy-ion radiation therapy. Int J Radiat Oncol Biol Phys. 1999;44:201–10.
43. Scholz M, Kellerer AM, Kraft-Weyrather W, Kraft G. Computation of cell survival in heavy ion beams for therapy. The model and its approximation. Radiat Environ Biophys. 1997;36:59–66.
44. Elsasser T, Kramer M, Scholz M. Accuracy of the local effect model for the prediction of biologic effects of carbon ion beams in vitro and in vivo. Int J Radiat Oncol Biol Phys. 2008;71:866–72.
45. Chiba T, Tokuuye K, Matsuzaki Y, et al. Proton beam therapy for hepatocellular carcinoma: a retrospective review of 162 patients. Clin Cancer Res: An Official Journal of the American Association for Cancer Research. 2005;11:3799–805.
46. Hashimoto T, Tokuuye K, Fukumitsu N, et al. Repeated proton beam therapy for hepatocellular carcinoma. Int J Radiat Oncol Biol Phys. 2006;65:196–202.
47. Hata M, Tokuuye K, Sugahara S, et al. Proton beam therapy for hepatocellular carcinoma with limited treatment options. Cancer. 2006;107:591–8.
48. Lee SU, Park JW, Kim TH, et al. Effectiveness and safety of proton beam therapy for advanced hepatocellular carcinoma with portal vein tumor thrombosis. Strahlentherapie und Onkologie: Organ der Deutschen Rontgengesellschaft [et al]. 2014;190:806–14.
49. Nakayama H, Sugahara S, Tokita M, et al. Proton beam therapy for hepatocellular carcinoma: The University of Tsukuba experience. Cancer. 2009;115:5499–506.

50. Sugahara S, Nakayama H, Fukuda K, et al. Proton-beam therapy for hepatocellular carcinoma associated with portal vein tumor thrombosis. Strahlentherapie und Onkologie: Organ der Deutschen Rontgengesellschaft [et al]. 2009;185:782–8.

51. Bush DA, Smith JC, Slater JD, et al. Randomized clinical trial comparing proton beam radiation therapy with transarterial chemoembolization for hepatocellular carcinoma: results of an interim analysis. Int J Radiat Oncol*Biol*Phys. 2016;95:477–82.

Yttrium-90 Selective Internal Radiation Therapy

11

D. Thor Johnson, MD, PhD and Adam Leon Kesner, PhD

11.1 Introduction

Yttrium-90 (Y-90) selective internal radiation therapy (SIRT), also known as transarterial radioembolization (TARE), is one of the newer modalities of radiation therapy available. This therapy first became accessible in the United States following the FDA approval of Theraspheres (BTG International) in 1999 under a humanitarian device exemption largely based on a small observational study showing safety [1] and a second study showing improved survival in a cohort of HCC patients treated with Y-90 when treated with a dose greater than 80 Gy [http://www.accessdata.fda.gov/scripts/cdrh/cfdocs/cfhde/hde.cfm?id=H980006]. SIR-spheres (SirTex Medical) were approved through a different mechanism by the FDA (approval as a device, not a drug) in 2002 in the United States on the basis of an Australian trial involving 74 patients. This trial compared intra-arterial chemotherapy alone (floxuridine) with the same intra-arterial chemotherapy and a single administration of SIR-spheres in a population of patients with bi-lobar non-resectable liver metastases. The trial found improved partial and complete response rate for patients receiving SIR-Spheres, as assessed by tumor area on imaging (44% vs. 17.6%, $P = 0.01$) as well as increased time to progression for patients receiving SIR-Spheres in comparison to patients receiving chemotherapy alone when measured by either tumor areas (9.7 vs. 15.9 months, $P = 0.001$), tumor volumes (7.6 vs. 12.0 months, $P = 0.04$) or CEA levels (5.7 vs. 6.7 months, $P = 0.06$) [2]. The use of these devices has grown over the last two decades and Y-90 SIRT has become a significant part of the oncological armamentarium for the treatment of liver tumors.

11.2 General Principles

Yttrium 90 is a pure beta emitter, which decays to stable Zirconium-90 with a half-life of 64.1 h. The beta particles are emitted with a maximum and average energy of 2.27 and 0.93 meV, respectively. The average range of the beta particles in tissue is 2.5 mm with a maximum tissue penetration of 11 mm. Maximum range in air is approximately 10 m. With its 2.67-day half-life, 94% of the emissions/radiation dose will be delivered within 11 days of implantation. As with all beta emitters, secondary gamma rays are created via bremsstrahlung interaction of the principle electron emissions. These gamma rays are introduced in the vicinity of the isotope and are emitted with a spectrum of energies. Since a

D.T. Johnson (✉)
Department of Radiology, University of Colorado Denver, 8085 South Willow Court, Centennial, CO 80112, USA
e-mail: thor.johnson@ucdenver.edu

A.L. Kesner
Department of Radiology, University of Colorado, Anschutz Medical Campus, 12,700 E. 19th Avenue MC278, Aurora, CO 80206, USA
e-mail: adam.kesner@ucdenver.edu

J. Meyer and T.E. Schefter (eds.), *Radiation Therapy for Liver Tumors*,
DOI 10.1007/978-3-319-54531-8_11

portion of these gamma rays will traverse both shielding and the patient, they can be utilized for treatment verification, post administration imaging, and must be accounted for when considering the radiation safety aspect of clinical Y-90 use.

Both the SIR-Spheres and Theraspheres brands function by incorporating Y-90 isotope into small beads (microspheres), to deliver internal targeted radiation therapy. While similar in design and delivery mechanism, there are some significant differences between the devices as demonstrated in Table 11.1.

Use of a particular device is related to local IRB approval (for Theraspheres given the humanitarian device exemption status) and the specific training and preference of the treating physician. There is presently no clinical evidence supporting the consistent superiority of one type of Yttrium-90 over another. There are however delivery differences that may be useful to clinicians in particular circumstances.

Theraspheres have simpler preparation and delivery mechanisms. SIR-Spheres doses are prepared onsite before treatment, and readily allow users the flexibility to adjust doses the day of treatment and/or split doses for delivery into multiple arteries.

11.3 Radiation Dose

In distinction to external beam radiation, Y90 delivers Beta irradiation. Similar to gamma irradiation, beta radiation toxicity is related to DNA damage. The primary differences relate to continuous exposure during decay of Y90 versus fractionated dosing with external conformational beam radiation and the very low radius of activity of beta radiation in which the dose is strongly dependent on the distance from the microsphere to the tumor nucleus. This dose dramatically decreases at distances greater than 2.5 mm. This necessitates the spheres being directly infused into the tumor for effective dose delivery. 3D microdosimetry on tumor samples of a patient receiving SIRT have demonstrated that at 2 cm the tumor was entirely encompassed by the 100 Gy isodose line, with some portions of the tumor receiving doses of greater than 1000 Gy [3]. Given the fundamental differences in method of radiation dose administration, dose distribution, time course of radiation delivery, and even effective dose, comparing dosimetry between external beam radiation and Y90 presents many challenges.

Doses of 120 Gy have been consistently shown to be safe clinically in liver therapy with Y90, although doses as high as 150 Gy for lobar therapy are frequently safely prescribed. Doses as high as 500 Gy for radiation segmentectomy have also been utilized safely [4]. This is somewhat surprising, given the severe liver injury that can be induced by significantly smaller doses of radiation delivered via external beam irradiation although as previously stated the intrinsic differences of the modalities make direct comparison difficult. It is also of note that clinically effective radiation dose differs significantly between these modalities. This discrepancy is also not well delineated by the existing literature. Dose and dose rate effects are relatively well understood for Gamma radiation, but much less

Table 11.1 Comparison of the characteristics of the two available Y90 devices, theraspheres and sirspheres

Device	Therasphere	Sirsphere
Material	Glass with Y-90 imbedded	Resin with Y-90 bound to surface
Particle size	20–30 micron	20–60 micron
Embolic effect	Minimal to mild	Mild to moderate
Dose vials provided by manufacturer	3–20 GBq	3 GBq
Average particle radiation	2500 Bq	50 Bq
Specific gravity	3.6 g/mL	1.6 g/mL
Number of spheres per 3 GBq	1.2–8 million	40–80 million

so for Beta radiation. Similar physical absorbed doses from the different types of radiation may have significant differences in biological effect on hepatocytes. With SIRT treatments, the particles are delivered via the hepatic artery and, in both metastatic and primary liver disease there is significant heterogeneity of the hepatic arterial supply with asymmetry favoring tumors. Tumors, in general, derive the vast majority of their blood supply via the hepatic artery in addition to vessels induced by tumor angiogenesis through VEGF (also derived from the arteries). The hepatic parenchyma derives the minority of flow from the hepatic artery (approximately 25–35% of total blood flow) and the majority from the portal vein (65–75% of blood flow). Hepatocytes also derive approximately 50% of oxygen from the portal vein [5]. In addition vascular tone in the hepatic artery is controlled by vasoactive factors through contractile cells that are often absent in the disorganized arteries of hepatic malignancies. This flow asymmetry results in preferential arterial supply to the tumor relative to the normal parenchyma. In fact when evaluating dosimetery in a segmental delivery, 1214 Gy was delivered to the tumor and 210 Gy to the normal liver parenchyma [4]. In dosimetry assessments relative perfusion of hepatic tumors has varied between 10:1 and 1:1 clinically [6, 7]. This is likely to make a significant difference given the small area of effect of the beta particles released from Y-90. Embolic spheres are never smaller than 20 microns, and as such they are deposited in the hepatic arterioles proximal to the hepatic arterial-portal venous anastomoses (12–15 microns) well away from the central venules and the sinusoidal space, as pictured in Fig. 11.1.

This would result in primary deposition of radiation toward the inflow vessels and away from the central venule in normal tissue. As the pathology of RILD is related to central venule fibrosis and obliteration [8], this asymmetric distribution of short penetration beta radiation may explain some differences of RILD with SIRT compared to whole liver external beam irradiation.

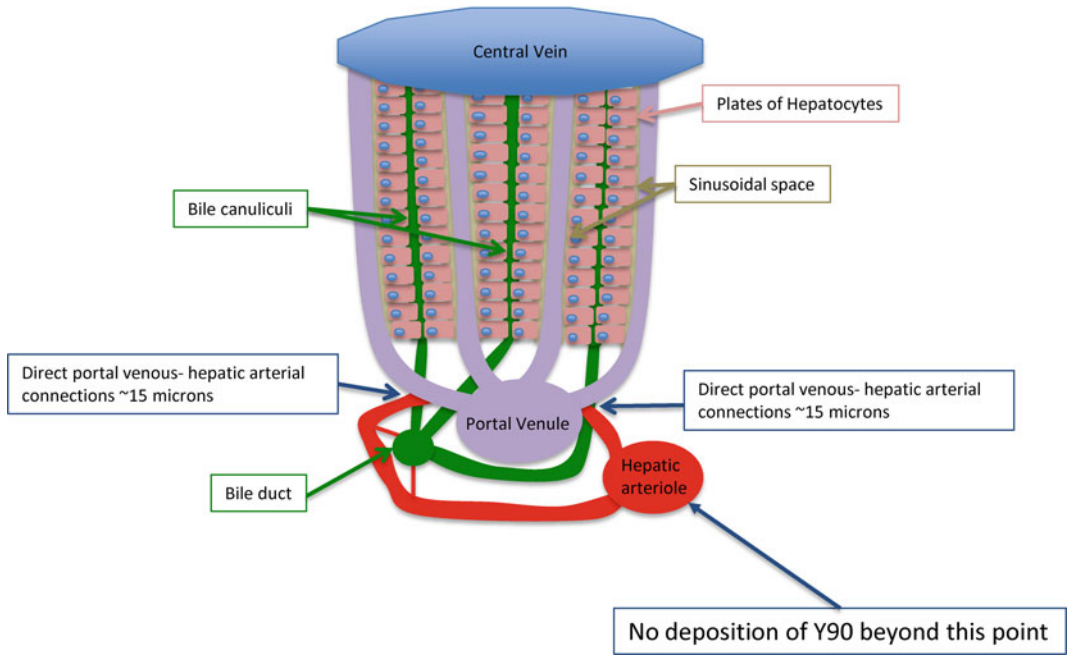

Fig. 11.1 Anatomy of the hepatic sinusoid

11.4 SIRT: Indications, Workup, and Treatment

11.4.1 Indications for SIRT

Patients who are considered potential candidates for SIRT include those with unresectable primary hepatic or metastatic cancer (liver dominant), and a life expectancy of at least 3 months. In metastatic colorectal cancer, SIRT has been given both with chemotherapy and alone primarily in the second line or salvage settings. There are competing therapies for the candidate group of patients (including SBRT, surgery, percutaneous ablation, bland embolization, chemotherapy, and transarterial chemoembolization), so the involvement of a multidisciplinary team is recommended to assure that only the patients in which SIRT is the most suitable treatment be offered the therapy.

11.4.2 Contraindications

There are several exclusions for SIRT. Shunting of spheres to the lungs is calculated pretreatment using a Tc^{99m} macro-aggregated albumin (MAA) nuclear scan. These scans can be used to derive an estimate of the radiation dose to the lungs that would likely result from a SIRT treatment. Theraspheres is contraindicated for a patient if their projected lung dose for is ≥ 30 Gy per treatment, or 50 Gy aggregate. SIR-Spheres dose reductions are recommended if lung shunt fractions are between 10 and 20%, and no treatment if higher than 20%. Additional contraindications include uncorrectable/unavoidable blood flow to the gastrointestinal tract from the liver, excessive tumor burden with limited hepatic reserve, elevated total bilirubin level (>2 mg/dL) in a non-cirrhotic patient, uncorrectable contrast allergy, uncorrectable coagulopathy, severe uncorrectable leukopenia (absolute neutrophil count less than 1000) [9]. Bevacizumab within 4 weeks of treatment is generally considered a contraindication due to increase in vascular complications from angiography; including thrombosis, poor wound healing, dissection, spasm, and pseudoaneurysm formation [10, 11]. Oxaliplatin is often dose-reduced to 60 mg/m^2 during the time surrounding Y-90 therapy due to decrease in patient tolerance in combination therapy with higher doses of Oxaliplatin [12]. Some institutions also consider history of sphincterotomy or cystic duct surgery to be a relative contraindication, however this is highly variable among practices. If there is significant portal hypertension, or liver decompensation in particular elevation of INR, embolization should be considered carefully. Patients with prior liver SIRT should be reviewed both for cumulative dose of radiation to the lungs (which should be less than 50 Gy total), as well as ability to tolerate more treatment.

11.4.3 Preprocedural Workup

Patients universally require pre-procedural high quality cross-sectional imaging. Either triple-phase MRI or CT is suitable as long as the institution is capable of performing volume assessment with the chosen modality. Tumor burden, vascular variants, presence or absence of portal vein thrombosis, and liver volumes should be assessed on imaging in preparation for the procedure. Complete laboratory work-up is necessary including LFTs, bilirubin, albumin, INR, WBC, and creatinine as close as possible to the proposed treatment date.

11.4.4 Procedural Detail

Prior to performing the delivery of radiation to the liver it is standard practice to obtain a TC^{99m} micro-aggregated albumin (MAA) mapping study. This is a combination of high quality angiography as well as the delivery of a diagnostic MAA nuclear medicine study. The MAA is injected in order to determine the proportion of particles that are likely to shunt through the tumor and into the lungs.

The patient is brought to the angiography suite and a 4–6 French sheath is placed in either the femoral artery (usually right) or the radial artery (usually left). The most common hepatic vascular anatomy is only present in only 55–65%

of patients and as such careful angiography is vital. Selective angiography is performed in the superior mesenteric artery, followed by the celiac artery. This is followed by careful assessment of the hepatic vessels including: assessment of the common hepatic, left gastric (to assess for accessory left hepatic arteries or a gastrohepatic trunk), the proper hepatic, the left hepatic, right hepatic, and right gastric arteries. In some cases subsegmental anatomy is assessed. In our IR suites, it is routine to perform dynamic contrast enhanced C-Arm CT of both the left and the right hepatic arteries to assess for vascular supply to extra-hepatic tissues. The most common extra-hepatic tissues include the stomach, duodenum, or anterior abdominal wall (through a variant artery called the falciform artery). Any vessel that supplies extra-hepatic tissue should be coil embolized in preparation for the procedure. Most practitioners also coil the right gastric (if present) and some coil the gastroduodenal artery routinely. This should be strongly considered if treatment plan includes whole liver treatment. It is important to discuss with transplant surgery if the patient is listed for liver transplant whether the GDA should be embolized or not, given differences in surgical technique among transplant surgeons. After the practitioner is comfortable that they have evaluated any potential anatomic obstacles to treatment, a microcatheter is positioned in the location of likely treatment with Y-90 and the patient has a small amount of TC^{99m} MAA infused into the liver. The patient is then transferred to nuclear medicine and imaged with a gamma camera. Institutions can do either planar or SPECT-imaging based on local preferences, with imaging recommended to occur within 1 h of injection to prevent falsely high positive shunt fraction related to free TC^{99m} [9]. There is however, greater accuracy in determining gastrointestinal shunting using SPECT-CT (96%) compared with planar imaging (72%) [13]. Furthermore, SPECT-CT has been shown to provide more accurate lung shunt fraction determinations, as compared to planar [14]. A shunt fraction is calculated by evaluating the lungs and liver and calculating the fraction of spheres that traverse the liver vessels and are ultimately trapped in the lungs. If a patient's shunt fraction is too high (see above), the procedure is most often canceled and an alternative therapy pursued.

Representative Celiac arteriogram and corresponding planar TC^{99m} scan are demonstrated in Figs. 11.2 and 11.3.

In the setting of HCC, it is possible that pretreatment with Sorafenib may normalize vascular supply to tumor enough to decrease shunt fraction and allow treatment [15]. Sorafenib has multiple molecular targets that affect tumor angiogenesis, and as such can affect the disorganized vessels of tumors that lead to high shunt fraction.

After obtaining shunt fraction the dose to be delivered is calculated on an individualized basis. Therasphere and SIR-Sphere products have different dose calculation protocols. Most notably, Therasphere stipulates dose calculations and prescriptions to be computed in units of absorbed dose (Gy). Alternatively, SIR-Spheres uses empirical or partitioned (personalized) models that provide prescriptions in units of activity (GBq).

11.4.5 Therasphere Dose Calculation

The recommended dose to the liver by Therasphere is between 80 and 150 Gy. The dose calculation for glass microspheres is based on target dose and the patient's liver mass (or treatment volume), which is calculated from volume assessment of preprocedural CT and MRI. This equation assumes a homogenous volume of distribution:

$$\text{Dose(Gy)} = \frac{50[\text{Injection Activity(GBq)}][1-F][1-R]}{\text{Liver Mass (kg)}}.$$

In this equation, dose is calculated as a scaled calibration of activity concentration in the liver. F represents the lung shunt fraction, and R is the expected residual waste (i.e. the amount of spheres expected to be retained within the delivery device and not delivered to the patient—generally set at 1%), and the two variables are

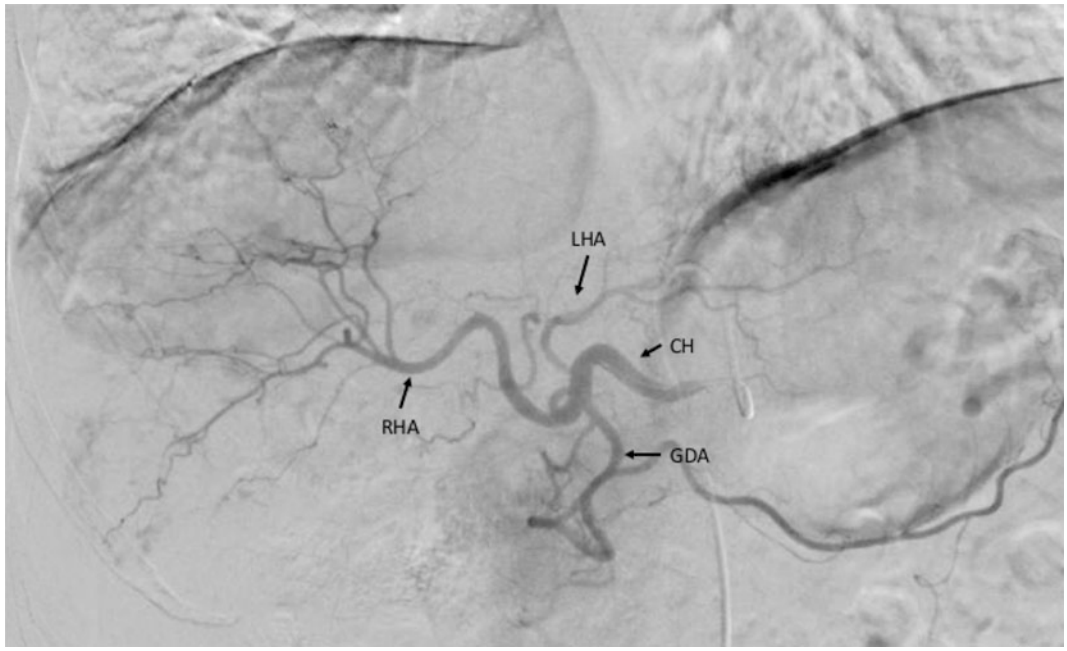

Fig. 11.2 The typical vascular pattern of a celiac angiogram in a patient being prepared for Y-90 treatment

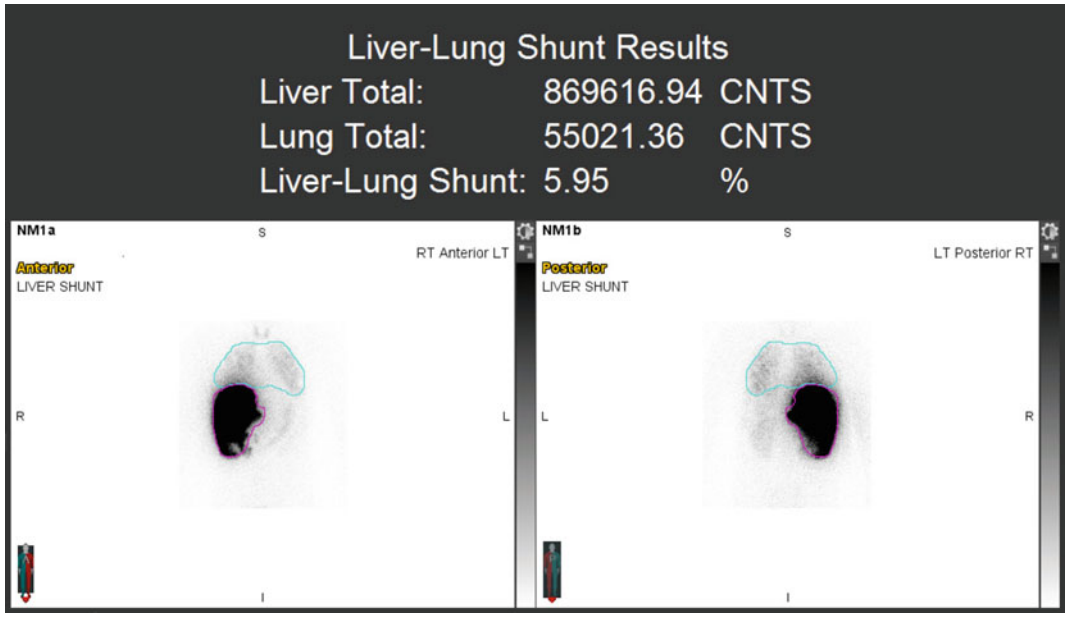

Fig. 11.3 Corresponding TC^{99m} scan from the same patient above during shunt study

used to scale the dose calculation. Determination of required activity for specific treatment is made using by rearranging the variables in the equation and solving for activity.

For example if we calculate the activity required to deliver a whole liver dose of 120 Gy to a patient with a 2 kg liver mass, 5% lung shunt fraction, and 1% anticipated residual waste, we find the required administration activity would be 5.1 GBq. If we know the treatment day and time, then we can use the Therasphere dose calculation tools to determine the vial that should be ordered (vials orders characterized by their Sunday 12 pm EST calibration). The manufacturer of Theraspheres (BTG plc, London, England) provides an online calculator that allows precise calculation of dose and order details with input of specific patient variables (https://www.btg-im.com/therasphere-idoc). Theraspheres allows for the possibility of using a dose calibrated within one or two weeks of the planned treatment date. This allows the user the option to use more or less particles to deliver the same absorbed radiation dose. Increasing the number of particles can be helpful with larger and more hypervascular tumors. The target dose for any given tumor has not been precisely defined aside from the early studies demonstrating that less than 80 Gy was inadequate therapy in HCC [7]; it is believed however that doses of 100–120 Gy offer a good balance between response rates and complications including hepatic fibrosis for standard users, although as stated previously, highly experienced clinicians have safely delivered segmental doses higher than 500 Gy.

11.4.6 SIR-Sphere Dose Calculation

Dosimetry principles are similar for resin microsphere dosimetry, but treatment planning and dose ordering are handled differently across vendors. The SIR-Sphere user's manual relies on the partition model for calculating the desired administration activity. This model has been approved by the FDA for SIR-Sphere treatment protocols, and the dose, as measured in Gy, is not directly calculated or considered. The partition model incorporates the body surface area (BSA), whole liver volume, and target region volume into its method of calculation (Sirtex user's manual, issued March 2002; pp 38–42). Users are encouraged to use vendor supplied worksheets, or their online calculator (http://apps01.sirtex.com/smac/). It is of note that the online calculator is not FDA cleared, but gives equivalent calculations as the vendor worksheet. There is an older empiric method of dose calculation, however this method demonstrates a worse side-effect profile than the BSA method and as such is no longer recommended except in cases in which BSI is significantly incorrect in estimating liver volume (significant hepatomegaly, prior hepatectomy).

Activity prepared for injection for a SIR-Sphere treatment can be calculated using the following equation:

$$\begin{aligned}&\text{Injection Activity (GBq)}\\&\quad = [(\text{BSA} - 0.2) + \text{Tumor Involvement}]\\&\qquad \times \%\ \text{Liver Treated.}\end{aligned}$$

Specific formulas for *BSA*, *Tumor Involvement*, and *% Liver Treated* may be found in the SIRTEX package insert.

The activity prescribed can be reduced if the hepatic function is compromised, however specific guidelines for dose reduction have not been assessed in clinical trials. Patients with poor function or those with very small tumor burden generally have dose reduced by 20–30% (not below 80 Gy for Theraspheres). SIRTEX also recommends dose reduction if shunt fraction is greater than 10% as discussed earlier.

11.5 Treatment Day

The patient is once again brought to the angiography suite and arterial puncture is repeated. Access to the celiac artery is once again obtained. Repeat hepatic angiography is performed as vessels that were embolized in preparation for Y-90 treatment can collateralize in the interval between planning angiography and treatment. After planning angiography, the Y-90

delivery apparatus is assembled and Y-90 is delivered. Theraspheres have a low enough number of particles, and smaller diameter of particles, and are expected to be delivered in full. For SIR-Spheres, the number of particles is high enough that stasis is sometime reached, and full delivery not possible. The NRC considers an administration outside of a ± 20% window of the intended prescription dose to be a misadministration classified as a reportable medical event. However, if stasis is identified during administration with angiography, it is acceptable/expected to cease administration, and a misadministration event does not need to be reported, regardless of the actual dose administered.

11.6 Follow-up

11.6.1 Post-Treatment Imaging and Dosimetry

TC^{99m}-MAA gamma imaging is used during SIRT treatment planning to calculate the appropriate Y-90 administration dose; the MAA is used as a surrogate for the Y-90 microspheres and its distribution is assumed to be representative of the Y-90 microsphere treatment deposition. This strategy has shown to be effective for patient specific treatment planning [16]. However, researchers have shown that there can be significant differences in the distribution of microspheres between the two procedures [17]. Accurate and localized dosimetry resulting from a SIRT treatment may be derived by directly imaging the Y-90 distributed in the body after the spheres have been implanted. 3D nuclear emission images may be obtained using either bremsstrahlung SPECT/CT, or PET/CT. PET is possible because the decay properties of Y-90 include a small percentage of positron emissions (32 positrons per million decays). This is a very low signal for imaging, but with long acquisition times and time-of-flight PET technology images can be generated. PET/CT is favored over SPECT/CT as it has better resolution and is more accurate for quantification.

Post-treatment direct radiation imaging allows for an accurate accounting of implanted sphere distribution from a SIRT treatment. The 3D Y-90 biodistribution images can be converted to 3D dose deposition maps using kernel convolution, and assessed for varying dosimetric characteristics. Ideally this type of analysis may provide additional insights into the treatment and/or direct clinicians toward favorable courses of action. However, present literature is still undeveloped in this area and remains an active topic of research. Post-treatment imaging/dosimetry is not required in vendor protocols. Initial studies have shown that using Y-90 imaging to calculate absorbed dose may be predictive of response [18]. Biodistribution characteristics like target volume sphere load and/or homogeneity of spheres may also be derived from imaging, and have been shown to correlate with partial or regional tumor response [18]. It has been suggested that Y-90 post treatment imaging may be useful for the consideration of secondary follow-up treatments [14], but the safety of multiple radioembolization treatments has not yet been established [19].

11.6.2 Follow-up Cross-Sectional Imaging

Patients generally return for clinical follow-up in one to three months, at which time symptoms are assessed and plans for continued therapy are discussed. If patients are receiving separate doses to the left and right (recommended based on increased safety profile) then the treatments should be scheduled at least one month apart. Multiphase CT doesn't adequately assess response until 2–3 months following therapy. MRI with high quality diffusion-weighted imaging can assess response at 1 month in the majority of cases. At one month the CT or MRI can actually look worse with increase in size of lesions and continued enhancement despite response (Fig. 11.4). In some cases there is continued improvement of the tumor response out to several months following completion of therapy. FDG- PET has been proposed as a

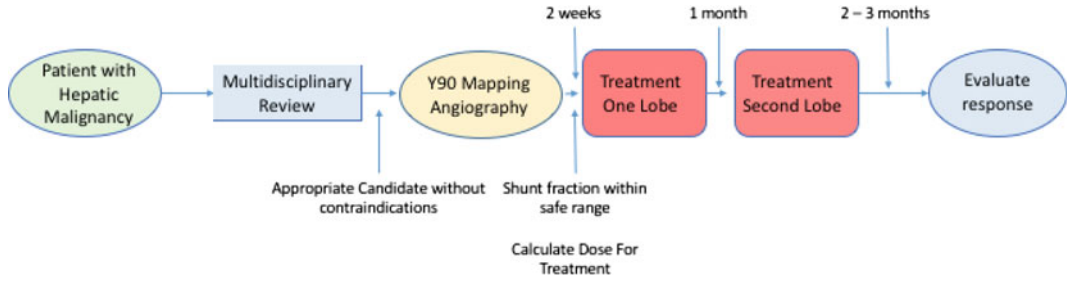

Fig. 11.4 General treatment algorithm

potential modality to follow treatment of Y-90 earlier than definitive changes by MRI, and is in fact comparable at 3 months following therapy [20] as well as predictive of response at 4 weeks in small series [21]. These results are promising but presently there is inadequate prospective data to include early PET as the modality of choice for monitoring of response to SIRT in any of the consensus guidelines [22].

General algorithm for patient treatment is diagramed in Fig. 11.4.

MRI images and corresponding pathological specimens are demonstrated in Fig. 11.5 for a patient treated with Theraspheres.

11.7 Complications

Complications are mild and generally self-limited. In the largest prospective randomized trial of SIR-Spheres complications greater than grade 3 were present in 13% more of CRC patients treated with both Y-90 and chemotherapy versus chemotherapy alone. There was a 1.3% increase in grade 5 toxicities over patients treated with chemotherapy alone. The most common adverse events attributable to Y-90 were fatigue, neutropenia, thrombocytopenia, ascites, and gastrointestinal ulcers. Other adverse

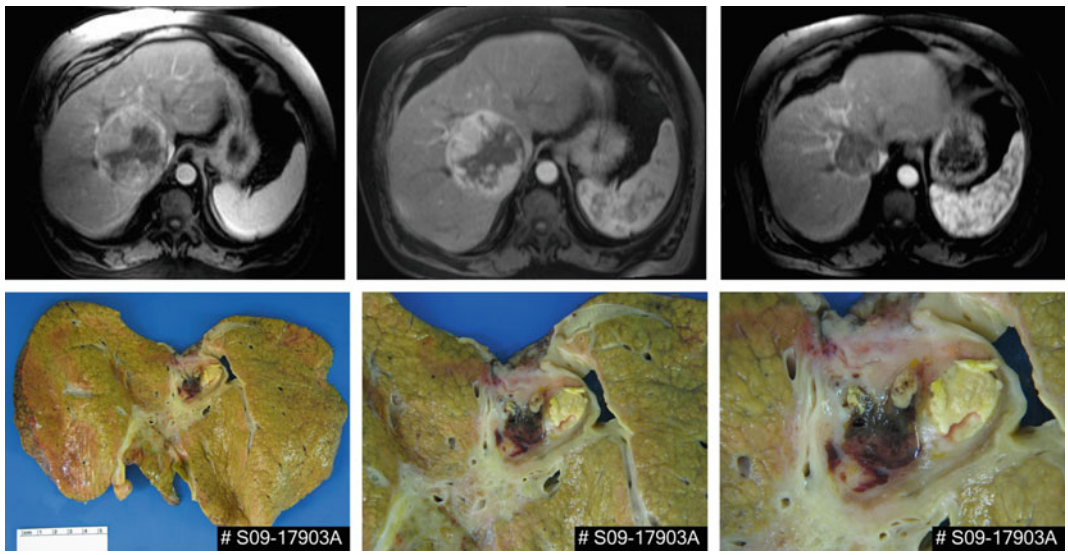

Fig. 11.5 Cirrhotic patient presenting with 9 cm HCC treated with 130 Gy dose to the right lobe of the liver. *First Panel*—Tumor at presentation, *Second Panel*—Tumor 6 weeks following single treatment, *Third Panel*—Tumor at 6 months now 5 cm without residual enhancement, *Lower panel* explant photos after patient underwent liver transplantation demonstrating significant fibrosis in the treatment site without viable tumor

events were not statistically significant [23]. In the largest meta-analysis of therapy with Theraspheres, up to 70% patients can be expected to experience post-radioembolization syndrome (PRS), which can include nausea, vomiting, fatigue, abdominal discomfort, and/or cachexia. PRS is generally less severe than the post-embolization syndrome of most other solid organ embolotherapies. Hospitalization is rarely required [24] and generally resolves within a month. The incidence of RILD is rare, ranging from 0 to 4%. RILD is defined in the Y90 literature the same as in the general radiotherapy literature as radioembolization literature in the classical sense- anicteric hepatomegaly and ascites related to fibrosis surrounding the central venules leading to outflow obstruction. This is increased in single session whole liver treatment (as was performed in the SIRFLOX trial), and in patients with either bilirubin greater than 2 or patients in whom the empiric method of dose calculation was utilized (SIR-Spheres).The incidence of biliary complications following Y-90 therapy was less than 10% by imaging. 1% of these patients required therapy for these complications [25]. Increased portal pressure (based on increase in size of spleen and increase in size of portal vein by imaging) has been demonstrated with whole liver treatment with Y-90 [26]. This complication does not occur with unilobar treatment, as there is generally hypertrophy of the contralateral lobe as the treated lobe develops fibrosis. Clinically significant findings of portal hypertension such as reduction of platelets <100,000 or variceal bleed are rare [26]. Preexisting portal hypertension or portal vein thrombosis from cirrhosis are not contraindications to treatment, as portal vein thrombosis is for transarterial chemoembolization. Radiation pneumonitis is generally only seen in patients with high lung shunt fractions. In an assessment of radiation pneumonitis in 403 Therasphere-treated patients 53 patients had a dose to the lungs greater than 30 Gy and follow-up imaging available. Ten of these patients had evidence of grade 1 radiation pneumonitis, none of which required treatment [27]. If standard dosimetry models are employed, the incidence of radiation pneumonitis should be less than 1% [27, 28]. GI ulceration occurs in less than 5% of cases related to unrecognized vascular supply to the bowel from the hepatic supply [24]. Transient lymphopenia is seen in the majority of cases treated with Theraspheres. No opportunistic infections have been reported as a result of lymphopenia [29].

11.8 Conclusion

The use of Y-90 SIRT is growing, and it is becoming an established treatment option for oncologic care in the liver for primary and metastatic liver cancer. In general, literature has demonstrated improved outcomes with the use of SIRT treatment and an acceptable complication profile when performed by experienced practitioners. Effective utilization of Y-90 requires a multidisciplinary team approach, careful patient selection, and meticulous angiographic workup/treatment. Y-90 therapy will continue to evolve as techniques are refined, and as several ongoing prospective randomized trials are completed.

References

1. Dancey JE, Shepherd FA, Paul K, et al. Treatment of nonresectable hepatocellular carcinoma with intrahepatic 90Y-microspheres. J Nucl Med. 2000;41:1673–81.
2. Gray B, Van Hazel G, Hope M, et al. Randomised trial of SIR-Spheres plus chemotherapy versus chemotherapy alone for treating patients with liver metastases from primary large bowel cancer. Ann Oncol. 2001;12:1711–20.
3. Kennedy AS, Nutting C, Coldwell D, Gaiser J, Drachenberg C. Pathologic response and microdosimetry of (90)Y microspheres in man: review of four explanted whole livers. Int J Radiat Oncol Biol Phys. 2004;60:1552–63.
4. Riaz A, Gates VL, Atassi B, et al. Radiation segmentectomy: a novel approach to increase safety and efficacy of radioembolization. Int J Radiat Oncol Biol Phys. 2011;79:163–71.
5. Tygstrup N, Winkler K, Mellemgaard K, Andreassen M. Determination of the hepatic arterial blood flow and oxygen supply in man by clamping the hepatic artery during surgery. J Clin Invest. 1962;41:447–54.

6. Gyves JW, Ziessman HA, Ensminger WD, et al. Definition of hepatic tumor microcirculation by single photon emission computerized tomography (SPECT). J Nucl Med. 1984;25:972–7.
7. Houle S, Yip TK, Shepherd FA, et al. Hepatocellular carcinoma: pilot trial of treatment with Y-90 microspheres. Radiology. 1989;172:857–60.
8. Fajardo LF, Colby TV. Pathogenesis of veno-occlusive liver disease after radiation. Arch Pathol Lab Med. 1980;104:584–8.
9. Kennedy A, Nag S, Salem R, et al. Recommendations for radioembolization of hepatic malignancies using yttrium-90 microsphere brachytherapy: a consensus panel report from the radioembolization brachytherapy oncology consortium. Int J Radiat Oncol Biol Phys. 2007;68:13–23.
10. Economopoulou P, Kotsakis A, Kapiris I, Kentepozidis N. Cancer therapy and cardiovascular risk: focus on bevacizumab. Cancer Manag Res. 2015;7:133–43.
11. Volk AM, Fritzmann J, Reissfelder C, Weber GF, Weitz J, Rahbari NN. Impact of Bevacizumab on parenchymal damage and functional recovery of the liver in patients with colorectal liver metastases. BMC Cancer. 2015;16:84.
12. Sharma RA, Van Hazel GA, Morgan B, et al. Radioembolization of liver metastases from colorectal cancer using yttrium-90 microspheres with concomitant systemic oxaliplatin, fluorouracil, and leucovorin chemotherapy. J Clin Oncol. 2007;25:1099–106.
13. Hamami ME, Poeppel TD, Muller S, et al. SPECT/CT with 99mTc-MAA in radioembolization with 90Y microspheres in patients with hepatocellular cancer. J Nucl Med. 2009;50:688–92.
14. Braat AJ, Smits ML, Braat MN, et al. (9)(0)Y Hepatic Radioembolization: An update on current practice and recent developments. J Nucl Med. 2015;56:1079–87.
15. Theysohn JM, Schlaak JF, Muller S, et al. Selective internal radiation therapy of hepatocellular carcinoma: potential hepatopulmonary shunt reduction after sorafenib administration. J Vasc Interv Radiol. 2012;23:949–52.
16. Lau WY, Kennedy AS, Kim YH, et al. Patient selection and activity planning guide for selective internal radiotherapy with yttrium-90 resin microspheres. Int J Radiat Oncol Biol Phys. 2012;82:401–7.
17. Wondergem M, Smits ML, Elschot M, et al. 99mTc-macroaggregated albumin poorly predicts the intrahepatic distribution of 90Y resin microspheres in hepatic radioembolization. J Nucl Med. 2013;54:1294–301.
18. Padia SA, Alessio A, Kwan SW, Lewis DH, Vaidya S, Minoshima S. Comparison of positron emission tomography and bremsstrahlung imaging to detect particle distribution in patients undergoing yttrium-90 radioembolization for large hepatocellular carcinomas or associated portal vein thrombosis. J Vasc Interv Radiol. 2013;24:1147–53.
19. Zarva A, Mohnike K, Damm R, et al. Safety of repeated radioembolizations in patients with advanced primary and secondary liver tumors and progressive disease after first selective internal radiotherapy. J Nucl Med. 2014;55:360–6.
20. Haug AR, Tiega Donfack BP, Trumm C, et al. 18F-FDG PET/CT predicts survival after radioembolization of hepatic metastases from breast cancer. J Nucl Med. 2012;53:371–7.
21. Sabet A, Meyer C, Aouf A, et al. Early post-treatment FDG PET predicts survival after 90Y microsphere radioembolization in liver-dominant metastatic colorectal cancer. Eur J Nucl Med Mol Imaging. 2015;42:370–6.
22. Annunziata S, Treglia G, Caldarella C, Galiandro F. The role of 18F-FDG-PET and PET/CT in patients with colorectal liver metastases undergoing selective internal radiation therapy with yttrium-90: a first evidence-based review. Sci World J. 2014;2014:879469.
23. van Hazel GA, Heinemann V, Sharma NK, et al. SIRFLOX: randomized phase III trial comparing first-line mFOLFOX6 (plus or minus Bevacizumab) versus mFOLFOX6 (plus or minus Bevacizumab) plus selective internal radiation therapy in patients with metastatic colorectal cancer. J Clin Oncol. 2016;34:1723–31.
24. Riaz A, Lewandowski RJ, Kulik LM, et al. Complications following radioembolization with yttrium-90 microspheres: a comprehensive literature review. J Vasc Interv Radiol 2009; 20:1121-30; quiz 31.
25. Atassi B, Bangash AK, Lewandowski RJ, et al. Biliary sequelae following radioembolization with yttrium-90 microspheres. J Vasc Interv Radiol. 2008;19:691–7.
26. Jakobs TF, Saleem S, Atassi B, et al. Fibrosis, portal hypertension, and hepatic volume changes induced by intra-arterial radiotherapy with 90yttrium microspheres. Dig Dis Sci. 2008;53:2556–63.
27. Salem R, Parikh P, Atassi B, et al. Incidence of radiation pneumonitis after hepatic intra-arterial radiotherapy with yttrium-90 microspheres assuming uniform lung distribution. Am J Clin Oncol. 2008;31:431–8.
28. Leung TW, Lau WY, Ho SK, et al. Radiation pneumonitis after selective internal radiation treatment with intraarterial 90yttrium-microspheres for inoperable hepatic tumors. Int J Radiat Oncol Biol Phys. 1995;33:919–24.
29. Salem R, Lewandowski RJ, Atassi B, et al. Treatment of unresectable hepatocellular carcinoma with use of 90Y microspheres (TheraSphere): safety, tumor response, and survival. J Vasc Interv Radiol. 2005;16:1627–39.

Interstitial Brachytherapy for Liver Tumors: Practical Issues

12

Michael R. Folkert, MD, PhD and Brian Hrycushko, PhD

12.1 Background

12.1.1 Concept of Interstitial Brachytherapy for Liver Lesions

While surgery is considered the standard of care for primary [1, 2] and metastatic liver lesions [3–6], the majority of patients are not surgical candidates due to medical comorbidities, a limited liver reserve or other anatomical barriers to resection. Alternative minimally invasive (e.g., radiofrequency and microwave thermal ablation, cryotherapy, irreversible electroporation, transarterial chemoembolization, radioembolization) and non-invasive (i.e., external beam radiation therapy) liver-directed therapies exist; however, efficacy may be limited by tumor size, location, and/or amount of functional liver reserve. External beam radiation therapies in particular are limited by functional liver reserve and liver tolerance to radiation, and while radioembolization (generally using ^{90}Y microspheres) has been proven beneficial for multiple or larger tumors, it is limited by vascular access, shunting, functional liver reserve, and often by prior radiation [7–12].

An alternative to these other liver-directed therapies (discussed in other chapters) is interstitial brachytherapy, generally using an ^{192}Ir high-dose-rate (HDR) afterloader source. Percutaneous interstitial HDR brachytherapy treatment directly irradiates the target lesion by placing a radiation source within the lesion under image-guidance. This therapy may avoid many anatomical constraints faced by thermal ablation techniques, as it is not limited by lesion size or by the presence of vascular/biliary structures. Unlike external beam radiotherapy, where the radiation beam must traverse healthy tissue in order to reach the tumor, brachytherapy techniques deliver the radiation from within the tumor. As a result, the dose to surrounding healthy tissues is greatly reduced with brachytherapy. This distinct characteristic of brachytherapy dose distributions is useful for the treatment of primary or metastatic liver lesions. The liver has been shown to have a significant dose-volume effect for toxicity; when the volume of irradiated liver increases, the dose tolerance for radiation induced liver disease decreases dramatically to levels where tumor eradication is unlikely to occur. For select patients with primary or metastatic liver lesions, HDR brachytherapy can provide for an aggressive focal irradiation with an ablative dose to the tumor and significant sparing of functional liver tissue.

M.R. Folkert (✉) · B. Hrycushko
Department of Radiation Oncology, Southwestern Medical Center, The University of Texas, 2280 Inwood Road, Dallas, TX 75390-9303, USA
e-mail: michaelr.folkert@utsouthwestern.edu

B. Hrycushko
e-mail: Brian.Hrycushko@utsouthwestern.edu

J. Meyer and T.E. Schefter (eds.), *Radiation Therapy for Liver Tumors*,
DOI 10.1007/978-3-319-54531-8_12

12.1.2 Interstitial Brachytherapy Physics

At its core, brachytherapy is the delivery of radiation with the source being placed close to or within the site to be treated. With an understanding that larger radiation dose leads to greater probability of cellular kill and tumor control, the main advantage of brachytherapy lies in the physical dose distribution surrounding the source. A high, ablative dose is concentrated in the immediate vicinity of the source followed by a rapid fall-off in dose with increasing distance. A geometric based inverse-square relationship with distance dominates the dose fall-off. Photon attenuation, especially at lower energy emissions, also contributes. Figure 12.1 shows the TG43-based radial dose function for different radionuclide sources [13–15], which accounts for absorption and scatter only and factors out the geometric fall-off in dose. These dose characteristics of radionuclide brachytherapy provide for the ultimate in radiation dose conformity with a large dose to the target and the ability to spare surrounding healthy tissues. In fact, with a variety of radioactive sources characterized by mode, energy, and half-life of decay, brachytherapy in theory can provide for the best radiation dose distribution. We note that this work will focus on the clinical use of image-guided HDR brachytherapy for liver cancer, but other brachytherapy procedures such as ^{125}I seed LDR brachytherapy [16–18] and microsphere-based radionuclide therapy using beta particle emitters [19–24] have been successfully used clinically.

High-dose-rate (HDR) brachytherapy dose delivery is provided with the assistance of an "afterloader," an automated device that handles the source rather than a human practitioner (Fig. 12.2). The development of afterloading technology was driven by the need to reduce the radiation exposure to staff involved in brachytherapy procedures. Afterloading involves the placing of catheters and applicators into or on the patient without the presence of the radioactive source. This improved brachytherapy treatments because more time could be spent on the geometric placement of applicators while considering dose characteristics of the source. HDR brachytherapy uses remote afterloading technology where the radioactive source is introduced with staff safely located outside the shielded treatment room. Image-guided treatment planning based on applicator placement along with a stepping source allows one to optimize the dose distribution in ways unachievable without remote afterloading technology. All current commercially available remote afterloading technology follow the same general principles of operation with a few distinct differences [25]. In general, a single ^{192}Ir or ^{60}Co source at the end of a cable is moved from a shielded safe to a planned position for a planned amount of time using a motor drive. The source drive mechanism then steps the source to different positions until all dwellings have been completed. The source is then retracted to the safe and directed by an indexer to the next channel. Several key safety features include operational interlocks to prevent accidental irradiation, emergency retract buttons, room door interlocks, and an emergency crank used to manually return the source in the event that other source retract mechanisms fail. Vendor specific applicators and possibly inter-vendor adapters can be purchased to go along with remote afterloaders to treat various disease sites.

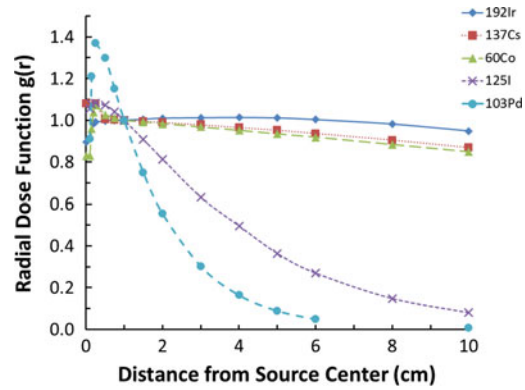

Fig. 12.1 AAPM TG43-based1 [13] radial dose function [g(r)] for various represented radionuclide sources based on a line source approximation (reproduced from tabulated values [14, 15]). This accounts for dose fall-off on the transverse plane due to photon scattering and attenuation only, and factors out the dominant geometry related dose fall-off

Fig. 12.2 Remote afterloader used for ^{192}Ir high-dose-rate interstitial brachytherapy techniques at our institution. The frame houses a shielded vault in which the ^{192}Ir source is stored; when used for treatment, the source is directed through one of the channels inserted into the head (*green* connectors)

Future directions for remote afterloading technology may include the use of multiple sources, as current models support several drive mechanisms, and possibly radionuclides with different decay characteristics and energy spectra, such as ^{169}Yb or ^{170}Tm [26, 27].

12.1.3 History of Interstitial Brachytherapy for Liver Tumors

Percutaneous HDR brachytherapy for liver lesions has a long history, having been performed under ultrasound guidance in the USA by Dritschilo et al. in the 1980's [28]. In their phase 1 pilot study, radiation dose was escalated from 8 to 50 Gy in a single treatment. Toxicities, consisting of transient elevations in liver chemistries and self-limited nausea and vomiting, were minimal. From personal communications with the corresponding author, challenges with this delivery technique included difficulties in ultrasound visualization of the tumor and in the percutaneous placement of multiple catheters to adequately cover the entire target region with a tumoricidal dose. Subsequently, Ricke and colleagues CT-guided percutaneous liver HDR brachytherapy.

12.2 Patient Selection

At our institution, all patients must undergo formal evaluation by the Liver and/or GI Tumor Program at UTSW so that they may be fairly informed of their treatment options including surgical resection, external beam radiation therapy, interventional ablative therapies, systemic therapies, and supportive care. Selection of the optimal interstitial brachytherapy candidate is similar to that of other focal techniques, such as thermal ablation or SBRT, with greater flexibility in terms of location, size, and number of lesions. The presence of vascular "heat sinks" and lesion size are less of a concern for interstitial brachytherapy than for thermal techniques, and lesion size/liver reserve is less of an issue for interstitial brachytherapy than for SBRT. It is possible that patients could have lesions that are too large or advanced to effectively treat, although primary lesions as large as 12 cm [29, 30] and metastatic lesions as large as 13.5 cm [31] in diameter have been successfully implanted in prospective studies. In these cases, radioembolization could be the preferred treatment. Patients with refractory coagulopathies would also be difficult to treat and noninvasive treatments such as stereotactic body radiation therapy may be the preferred treatment modality. Certain areas of the liver are of greater concern; lesions at the periphery of the liver in close contact with viscera may not be optimal for large single-fraction interstitial brachytherapy treatments.

Based on published prospective experiences by Mohnike et al. in patients with HCC [29], candidates for interstitial brachytherapy had

unresectable disease with 4 or fewer nodules, and the tumor margin had to be clearly defined on CT or MRI. Patients with Child-Pugh Class C hepatic impairment were ineligible; patients required a platelet count above 50,000, ECOG performance status 0–2 or Karnofsky Performance Status (KPS) >70, prothrombin time of at least 50%, and bilirubin <5 μmol/dL. Patients with ascites or portal vein occlusion were eligible. For patients with metastatic disease to the liver, where hepatic function is generally less compromised, Ricke et al. [31] used similar biochemical parameters, and excluded patients with ≥ 10 tumors, patients with more than 3 tumors ≥ 5 cm in diameter, or patients with more than 3 lesions with two or more lesions >3 cm in diameter.

Patient selection criteria for this procedure at our institution are shown in Table 12.1. For our purposes, patients should have the following: histologic or radiographic proof of a liver malignancy suitable for radiation therapy (i.e., no germ cell or hematological malignancies); CT, MR, or contrast-enhanced ultrasound (CEUS) defined lesions with lesion size ≥ 3 cm in maximum dimension, or lesion size ≥ 1 cm if treatment with thermal ablation techniques such as RFA would be compromised by proximity to nearby vascular/biliary structures, and predicted survival of >6 months. Patients who are ineligible for interstitial brachytherapy include patients with a history of prior irradiation or other treatment to the liver or abdomen who after brachytherapy treatment would have a cumulative dose to the liver or other normal tissues greater than the protocol defined constraints (Table 12.2); active peptic ulcer disease for lesions within 5 cm of the stomach; underlying hepatic cirrhosis with Child-Pugh class B9 or C hepatic impairment; patients with parahepatic extension of disease with direct non-liver visceral involvement, or patients with contraindications to general anesthesia. Additionally, interstitial brachytherapy is not recommended for patients with significant laboratory abnormalities, further summarized in Table 12.1.

12.3 Needle Placement, Treatment Planning, Quality Assurance, and Dose Delivery

12.3.1 Needle/Catheter Placement Technique

Percutaneous interstitial catheter implantation can be performed under analgesia/sedation (Midazolam & Fentanyl) and local anesthesia (Lidocaine), but general anesthesia is often preferred to avoid any risk of needle migration between placement and treatment delivery that would compromise optimal dose delivery. Patients undergo deep venous thrombosis prophylaxis and pain management throughout the course of treatment as per routine.

Based on a pre-planned distribution (see Sect. 12.3.2.2.3) or physician's discretion (and the lesion size, shape, and location), under image guidance (CT, fluoroscopic, and/or contrast-enhanced ultrasound), one or more large bore trochar puncture needles (generally 17-G) are placed at least 5 mm past the desired target. If using a pre-planned technique, a registration CT scan is acquired and fused with a planned needle distribution; pre-planned entry points and catheter trajectories are marked on the patient's skin, with or without a template grid. Verification of tumor location may be performed with iodinated intravenous contrast; additionally/alternatively, contrast-enhanced ultrasound (CEUS) may also be used to delineate the lesion and guide needle placement [32, 33]. Catheter entry locations depend on the geometry of the tumor and any anatomical limitations such as pleural space, stomach, or spinal cord restrictions. Placing needles past the lesion avoids target coverage issues resulting from anisotropy in the dose distribution near the distal end of the source.

For each planned catheter, the 17-G trochar puncture needle is exchanged over a stiff angiographic guide wire for a flexible 6-F catheter sheath using Seldinger's technique. The angiographic guide wire is removed, and a closed-end

Table 12.1 Patient selection

Anatomic criteria			
Size			
	CT, MR, or contrast-enhanced ultrasound (CEUS) defined lesions, with lesion size $\geq$3 cm in maximum dimension or lesion size $\geq$1 cm if treatment with thermal ablation techniques would be compromised by a proximity to vascular/biliary structures ("heat sink")		
Exclusion criteria			
Location			
	Parahepatic extension of disease with direct non-liver visceral involvement (Absolute contraindication)		
	Lesions within 5 cm of the stomach for patients with active peptic ulcer disease (Relative contraindication)		
Laboratory criteria	Factor	Ineligibility Threshold	
Serum chemistries			
	Albumin	<2.5	
	Alkaline Phosphatase	>5 X upper limits of normal (ULN)	
	ALT/AST	>5 X ULN	
	Total bilirubin	>5	
CBC (complete blood count)	*Note: only exclusion criteria if refractory to treatment*		
	Platelet count	<75,000/ml	
	Hgb level	<8 gm/dl	
	ANC	<500/ml	
Coagulation profile	*Note: only exclusion criteria if refractory to treatment*		
	INR	>2	
	PTT	>80	

Also includes patients who are on anticoagulation medication that may not be safely held for the procedure ($\geq$5 days for antiplatelet agents and warfarin; $\geq$24 h for low-molecular weight heparin formulations)

6-F afterloading catheter is introduced into the 6-F sheath. Upon completion of catheter placement, a post-implant non-enhanced or contrast-enhanced CT of the liver is acquired to verify the correct catheter positioning within the tumor and to acquire images for final 3-dimensional treatment planning. The length of needles outside the patient is recorded to verify if there is any movement before treatment.

12.3.2 Treatment Planning Principles

12.3.2.1 Dosimetric Goals

In the studies by Ricke and Mohnike et al. mentioned above, the dose to 2/3^{rds} of the liver was limited to no more than 5 Gy to reduce the risk of hepatotoxicity and radiation-induced liver damage. The stomach, duodenum, and colon were limited to a maximum dose of 15 Gy to 1 cc volume while the spinal cord was limited to a maximum dose of 8 Gy to 1 cc [29, 31]. At our institution, based in part on our experience with a single fraction SBRT approach, our adapted dosimetric treatment goals are summarized in Table 12.2.

12.3.2.2 Treatment Planning Technique

Treatment Catheters, Target, and Organ-at-Risk Delineation

CT-based planning for interstitial HDR brachytherapy is the brachytherapy planning

Table 12.2 Dosimetric criteria

Target/organ at risk	Goal	Special considerations
Clinical target volume (CTV)	Minimum peripheral dose of 25 Gy	
Liver	67% or 700 cc liver receives < 5 Gy	Assess both and apply whichever is more conservative
Esophagus	D1 cc < 15 Gy D5 cc < 12 Gy D10 cc < 9 Gy	Limit of 85 Gy in BED_{2Gy} equivalent including current and prior treatment to no more than 1 cc; minimum of 6 months between radiation treatment courses [36–38]
Stomach	D1 cc < 15 Gy D5 cc < 12 Gy D10 cc < 9 Gy	Proton-pump inhibitors prescribed if >1 cc of stomach/duodenum receives over 10 Gy Also limit of 85 Gy in BED_{2Gy} equivalent including current and prior treatment to no more than 1 cc; minimum of 6 months between radiation treatment courses [36–38]
Small bowel (duodenum, jejunum, ileum)	D1 cc < 15 Gy D5 cc < 12 Gy D10 cc < 9 Gy	Proton-pump inhibitors prescribed if >1 cc of stomach/duodenum receives over 10 Gy Also limit of 85 Gy in BED_{2Gy} equivalent including current and prior treatment to no more than 1 cc; minimum of 6 months between radiation treatment courses [36–38]
Large bowel (colon)	D1 cc < 15 Gy D5 cc < 12 Gy D10 cc < 9 Gy	Limit of 85 Gy in BED_{2Gy} equivalent including current and prior treatment to no more than 1 cc; minimum of 6 months between radiation treatment courses [36–38]
Spinal cord	D1 cc < 8 Gy	75 Gy in 2 Gy fractions BED_{2Gy} equivalent including current and prior treatment; minimum of 6 months between radiation treatment courses [35]
Kidney	D1 cc < 11 Gy D200 cc < 8.4 Gy	

For dosimetric purposes, BED_{2Gy} is the biologically effective dose (BED) in 2 Gy fractions, and is determined by the calculation: $BED_{2Gy} = nd(1 + d/\alpha/\beta)/(1 + 2/\alpha/\beta)$, where n number of fractions and d dose per fraction [35];
1. for spinal cord/cauda equina, α/β is the constant for spinal cord late effect and equals 2;
2. for esophagus/stomach/bowel late effect, $\alpha/\beta = 3$ [40–42]

technique of choice for the treatment of liver lesions unsuitable for surgery [29–31, 34–38]. Following catheter placement and verification, a contrast-enhanced CT image of the entire liver volume with 2 mm slice thickness is acquired. These images are sent to the treatment planning system where a 3D-based image plan can be generated. The treatment catheter is digitized in the treatment planning system by identifying the metal needles or a metal wire placed within close ended catheters at CT from the tip of the catheter to the exit location of the body. With catheter reconstruction, the physical tip of the implant needle is not the location of the first dwell location. The actual distance from the visualized tip to the first allowable dwell location must be determined from the vendor supplied instructions for use documentation and verified during commissioning. The correct measured length of the needle/transfer guide tube combination is input to the planning system. A previously acquired contrast enhanced liver MRI scan may be fused with the CT data set to help identify the CTV. The CTV is identified as visible borders and enhancing rim on the contrast-enhanced CT scan. All normal organs at risk, depending on target location, are then contoured (stomach, bowel, spinal cord, etc.) (Fig. 12.3).

Brachytherapy Dose Calculation and Optimization

Current HDR brachytherapy dose calculations are based on the AAPM TG43 formalism [13–15]. This formalism is based on the factorization

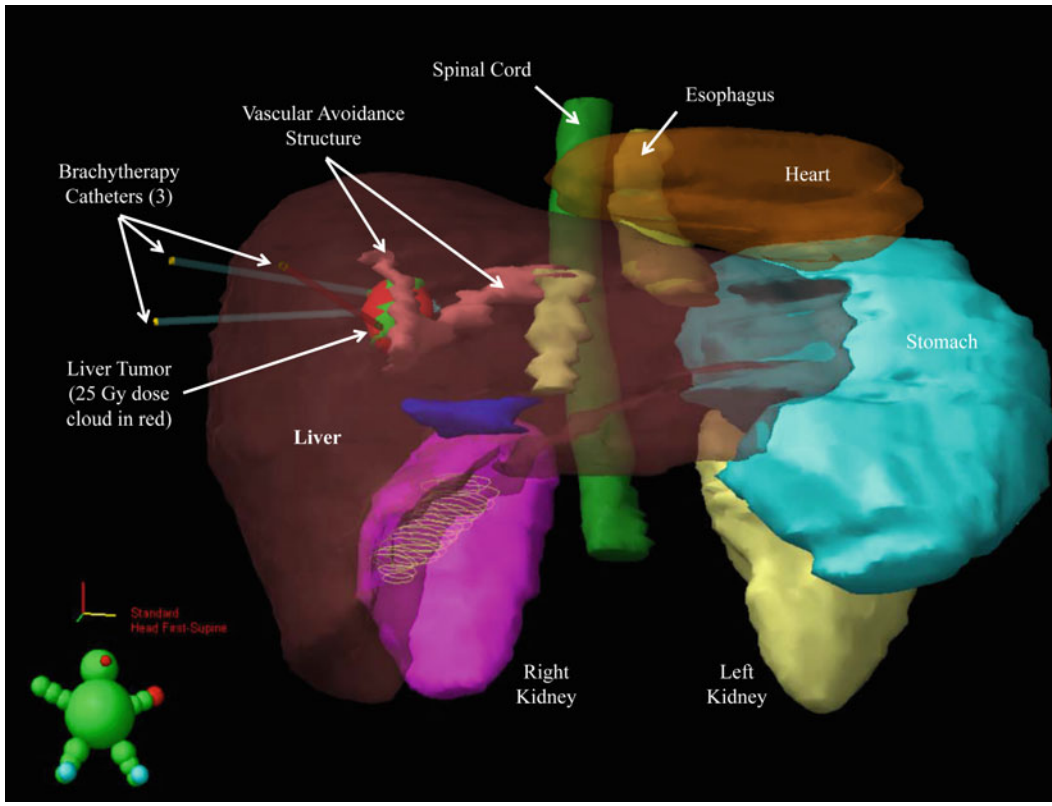

Fig. 12.3 3-dimensional representation of liver lesion (in *green*, with 25 Gy enclosing dose cloud in *red*) and organs at risk (OARs), with brachytherapy catheters in place. Note vascular avoidance structure designed to avoid adverse needle placement. (OARs: liver, *transparent maroon*; right kidney, *purple*; left kidney, *yellow*; stomach, *blue-green*; heart, *brown*; spinal cord, *green*; esophagus, tan; portal vein, *blue*; IVC, dun)

of measured and Monte Carlo generated tables of dose rate per unit source strength at distance from the source in a water medium. The factorization provides for improved accuracy in interpolation between table values by filtering out of the large dose gradients with the use of a geometry function. When applied correctly, the TG43 equations accurately reproduce the original dose rate tables. Dose calculations from the treatment planning system superpose the pre-calculated TG43 single source dose distributions for all dwell positions and dwell times. The TG43 based dose formalism has significantly improved standardization of dose calculations for brachytherapy and has allowed for practical intercomparison between treatment plans.

The TG43 dose calculation algorithm ignores the influence of tissue heterogeneities, applicator materials, and the patient geometry. This can result in incorrect dose calculations for HDR brachytherapy of liver lesions near lung tissue or close to the surface of the body. Superficially located tumors will have reduced scatter dose contribution compared to that calculated by the TG43 algorithm [39]. The TG43 algorithm also does not account for any attenuation from metal applicators or needles. Low energy brachytherapy sources are significantly affected by changes in atomic number (Z) due to the Z^3 dependence in the photoelectric cross section. For ^{125}I LDR seed brachytherapy contrast agents can significantly attenuate the emitted photons. Interseed attenuation has been shown to reduce the minimum peripheral dose depending on the seed distribution [40]. Just as external beam radiotherapy dose calculations have transitioned from

simple hand calculations in a homogeneous medium to complex heterogeneous medium dose calculations, brachytherapy is evolving to provide a more accurate dose assessment. With the underlying assumption that the true radiation dose distribution is strongly correlated with tumor control and normal tissue toxicity a more accurate and individualized dose calculation with state of the art dose algorithms will improve therapy outcomes. Several advanced dose algorithms exist, such as collapsed cone superposition convolution algorithms [41, 42] and solvers of the linear Boltzman transport equation (Monte Carlo-based algorithms [43, 44] and grid-based Boltzman solvers [45, 46]). The use of such algorithms, which take into account tissue and applicator heterogeneities in composition, is expected to significantly reduce the uncertainty in dose calculations. Challenges remain in how to adopt and commission model-based brachytherapy algorithms into a clinical setting. AAPM task group #186 [47] provides guidelines for validating such algorithms for heterogeneity and scatter effects and recommends reporting of TG43 and model-based algorithm dose metric results in a transitioning phase.

With the goal to deliver as high a dose as possible to the tumor and minimize dose to surrounding tissues, one needs to determine the best dwell positions and dwell times to obtain this dose distribution. In general, a dose distribution must be designed which satisfies the constraints and objectives determined by the user. Several optimization strategies exist in treatment planning to help in achieving these objectives and constraints in a timely manner. The simplest of optimization strategies in brachytherapy use forward-planned geometric or graphical optimization based on the experience of the planner [48, 49]. Most planners are more comfortable in designing their dose distributions by manually dragging isodose lines. More elegant optimization strategies use inverse optimization techniques to ideally converge towards a global optimum solution [50–55]. The planner defines objectives by determining restrictions on target volumes and normal tissues before optimization. (See Sect. 12.3.2.1 *Dosimetric Goals and Table 12.2 for our planning guidelines.*)

Prior to delivery, the length of each catheter is compared with values input into the treatment planning system. For multiple fraction treatments, CT scans are acquired for each fraction and fused with the initial planning CT image set to verify correct applicator position. Each catheter length is verified again prior to each treatment to prevent misadministration of the dose to the target.

Pre-planning Technique

Due to the importance of delivering a tumoricidal dose of radiation to the target lesion while at the same time limiting patient trauma, bleeding, and infection risk from needle placement, we utilize a pre-planned image-guided technique at our institution. The excellent local rates of 95% or more reported in the various German experiences for liver metastases were predicated on whether *an optimal dose distribution could be achieved*; i.e., 23–25 Gy to the periphery of the tumor for liver metastases. (Dosimetric analysis performed by Ricke et al. had demonstrated a dose response with improved local control at a minimum peripheral dose of $\sim$23 Gy to the target lesion [29, 31, 56]) An image-guided optimized and pre-planned catheter placement technique is by definition designed to facilitate optimal catheter placement to maximize the likelihood of achieving therapeutic goals.

Pre-planning determines whether it is possible to achieve dosimetry goals before the first needle is placed within the patient. To develop a pre-plan, an optimized dose distribution is generated prior to treatment by modeling one or more "virtual" catheters in the brachytherapy treatment planning system through a collaborative effort including the radiation oncologist, interventional radiologist, and medical physicist. These "virtual" catheters can be adjusted, taking the patient's anatomy into account, to achieve an optimal therapeutic plan. The image containing the "virtual" catheters (including the entry point

on the skin, trajectory, and terminal depth) is fused with the registration scan performed immediately prior to the patient's procedure and then used as a guide for placement of percutaneous interstitial treatment catheters. After all catheters are placed, a verification scan is performed, adjusted and re-optimized if necessary, and the patient can then be efficiently and accurately treated.

The primary goal of pre-planned and optimized image-guided needle placement is to ensure that an effective minimum peripheral dose is achieved for all patients to maximize treatment efficacy, while limiting radiation dose to healthy tissue to safe levels. Additionally, review of the toxicities of percutaneous interstitial brachytherapy for liver lesions demonstrates two primary themes; hemorrhage in the needle track and catheter track infection/abscess [56]. Both of these toxicities are a direct result of the mechanical trauma caused by the percutaneously placed needle, and are aggravated by the need to introduce more needles to achieve desired target coverage, or by adjusting and/or reintroducing the needle to achieve desired positioning. As such, a secondary goal for pre-planned optimization is to minimize the number of needles needed to achieve desired coverage, and to ensure that needles are initially placed in the optimal location.

12.3.3 HDR Interstitial Brachytherapy Quality Assurance (QA)

Quality assurance (QA) must be performed for every HDR brachytherapy treatment to eliminate errors as recommended in the AAPM TG-59 report [57]. and required by state and national regulations Prior to needle implantation, the positioning accuracy of the afterloader needs to be verified. Timer accuracy and machine interlocks should also be tested for the safety of the patient and staff. As the treatment plans are typically developed by a medical physicist under tight time constraints in a high-pressure environment they should be scrutinized by a second (backup) physicist when completed. A secondary dose calculation should be performed which verifies dose to calculation points. This checks that the correct source strength is also use in the plan. Patient specific QA should be performed before the treatment begins. It is important to verify the patient identity, the connections and length of catheters, and that the plan from the treatment planning system matches that which is to be delivered by the afterloader console. After completion of the treatment, the radiation levels of the patient and afterloader are to be measured with a survey meter and compared to pretreatment levels to verify the source has returned to the afterloader safe.

12.3.4 Treatment Delivery and Followup After the Procedure

Once QA has been performed and the plan has been reviewed and confirmed by the radiation oncologist, the percutaneously placed catheters will be connected to the HDR afterloading system and treatment will be delivered in a single fraction. After irradiation, the brachytherapy catheter(s) is/are removed; the 6-F sheath(s) is/are cautiously withdrawn, and the puncture channels are sealed with absorbable/resorbable thrombogenic material. The patient is then extubated and recovered. Observation is generally performed for a minimum of 2 h, with continuous ECG and hemodynamic monitoring.

Regular follow up visits will then generally be scheduled at 2 months (±2 weeks) and then at 3 month (±2 weeks) intervals; at our institution, patients are followed indefinitely, and all patients with primary liver tumors are followed in a centralized clinic. During these follow up visits, standard evaluations currently performed on all patients with primary or metastatic hepatic malignancies (physical examination and abdominal imaging at a minimum) are performed.

12.4 Advantages and Disadvantages of Interstitial Brachytherapy Relative to External Beam Radiation Therapy Techniques

HDR brachytherapy is potentially advantageous compared with external beam radiotherapy due to the source (a high-activity ^{192}Ir source) being placed directly within the tumor. Accordingly, a significantly greater ablative radiation dose is delivered within the tumor while the dose to surrounding healthy tissues is greatly reduced. This advantage is made visually apparent in Fig. 12.4. While the target lesion (red contour) is covered by the prescription dose (shown as blue line), the 50% isodose line (shown as purple line) covers a significantly lower volume of liver and other healthy tissues for HDR brachytherapy (Fig. 12.4, left) compared to that of stereotactic body external beam radiotherapy (SBRT; Fig. 12.4, right).

SBRT treatment planning strategies often aim to resemble the dose distributions characteristic to brachytherapy procedures. Conformal SBRT plans prescribe to a low isodose line to achieve a steep dose gradient outside the target [58, 59]. Prescribing dose in this manner inherently results in large dose heterogeneities; dose hot spots within solid tumors should enhance the tumoricidal effect and improve tumor control probability. It has been argued that centrally located dose hotspots within solid tumors are necessary in order to sterilize hypoxic and radioresistant tumor cells, although conclusive evidence is lacking. Several groups have compared SBRT to HDR brachytherapy treatment plans for gynecological [60–63] and prostate cancers [64, 65], with an overall trend of improved target coverage with external beam techniques at a cost of increased dose to surrounding organs at risk. Brachytherapy does have potential for improvement, and recent technology providing more freedom in source positioning has shown to improve target coverage [66, 67]. In the end, one of the most problematic consequences of extreme dose heterogeneities from SBRT and brachytherapy plans is the difficulty in interinstitutional comparison of planning practices and outcomes.

With highly heterogeneous and conformal dose distributions, brachytherapy seems fitting for the treatment primary and metastatic liver malignancies. An advantage of HDR brachytherapy, especially for liver tumors, is that the target is fixed to the catheters from which the source travels through. Any movement will occur both with the source and the target. One can

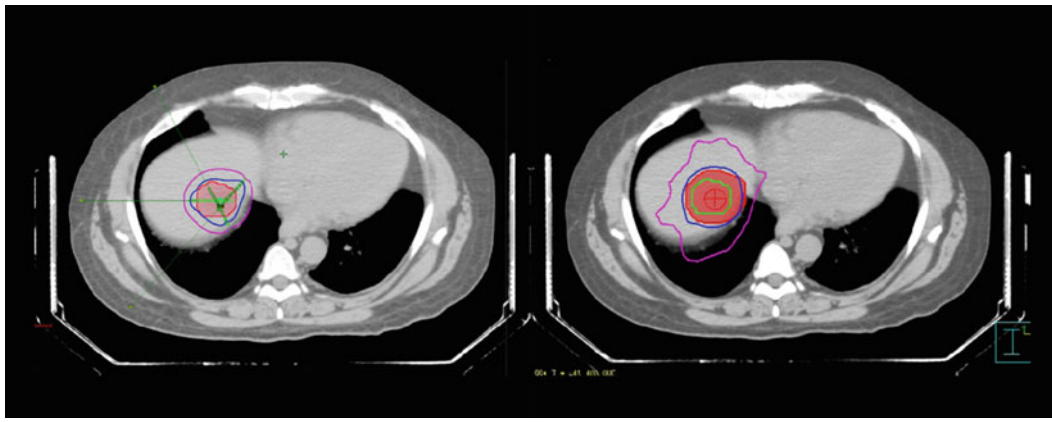

Fig. 12.4 HDR brachytherapy (*left*) and SBRT (*right*) plan comparison with the prescription (35 Gy) isodose line shown in *blue* and the 50% (17.5 Gy) isodose line shown in *purple*. Of note, the target volume (*red* contour) for external beam must be increased to account for setup variations and organ/patient motion. This is unnecessary for HDR brachytherapy. [Reprinted from [83]. With permission from Elsevier.]

effectively reduce or eliminate the PTV margins use in external beam radiation, which in turn reduces the radiation burden to surrounding tissues. The excellent normal tissue sparing and possibility for dose escalation may lead to improved local control rates. It is possible that charged particle techniques may serve to reduce the amount of healthy liver exposure to radiation relative to photon-based external beam radiation techniques [68]; this will be further explored in other sections of this book.

A major disadvantage of interstitial brachytherapy for liver lesions is the invasiveness of the treatment; patients with significant coagulopathies or issues with anesthesia will not be eligible for treatment. There is a risk of catheter displacement with any patient movement; this can be reduced but not eliminated with single-fraction treatments, and further reduced by maintaining patients under anesthesia for the entire procedure including dose delivery; the latter does increase risk of anesthesia complications.

12.5 Future Directions

Advances in medical robotics have led to the design of image-guided robotic-based brachytherapy systems with automatic needle insertion [69–73]. The aim is for more accurate placement of the needle through needle rotations, force modeling, and needle steering [74–77]. This has been primarily geared towards ultrasound-guided LDR prostate brachytherapy, however, it is justifiable to prevent geographic miss resulting from the large dose gradients characteristic to any brachytherapy procedure. Image-guided robotic liver brachytherapy is feasible based on a pre-plan optimized for ideal needle trajectories to maximize therapy efficacy while meeting normal tissue objectives and minimizing needle trauma. Additional research likely to impact liver brachytherapy practice centers on efficiency and speeding up the overall brachytherapy procedure. Automatic planning strategies using automatic catheter detection [78, 79] and organ or lesion segmentation [80–82] will speed up the treatment planning process and lessen the burden on the OR staff as well as the patient.

References

1. Chou FF, Sheen-Chen SM, Chen YS, Chen MC, Chen CL. Surgical treatment of cholangiocarcinoma. Hepatogastroenterology. 1997;44(15):760–5.
2. Farmer DG, Rosove MH, Shaked A, Busuttil RW. Current treatment modalities for hepatocellular carcinoma. Ann Surg. 1994;219(3):236–47.
3. Wei AC, Greig PD, Grant D, Taylor B, Langer B, Gallinger S. Survival after hepatic resection for colorectal metastases: a 10-year experience. Ann Surg Oncol. 2006;13(5):668–76.
4. Fong Y, Blumgart LH, Cohen AM. Surgical treatment of colorectal metastases to the liver. CA: Cancer J Clin. 1995;45(1):50–62.
5. Fong Y, Fortner J, Sun RL, Brennan MF, Blumgart LH. Clinical score for predicting recurrence after hepatic resection for metastatic colorectal cancer: analysis of 1001 consecutive cases. Ann Surg. 1999;230(3):309–318; discussion 318–321.
6. Scheele J, Stang R, Altendorf-Hofmann A, Paul M. Resection of colorectal liver metastases. World J Surg. 1995;19(1):59–71.
7. Kuvshinoff BW, Ota DM. Radiofrequency ablation of liver tumors: influence of technique and tumor size. Surgery. 2002;132(4):605–611; discussion 611–602.
8. Rhim H, Goldberg SN, Dodd GD, 3rd, et al. Essential techniques for successful radio-frequency thermal ablation of malignant hepatic tumors. Radiographics: a review publication of the Radiological Society of North America, Inc. 2001;21 Spec No: S17–35; discussion S36–19.
9. Wang X, Sofocleous CT, Erinjeri JP, et al. Margin size is an independent predictor of local tumor progression after ablation of colon cancer liver metastases. Cardiovasc Intervent Radiol. 2013;36(1):166–75.
10. Pan CC, Kavanagh BD, Dawson LA, et al. Radiation-associated liver injury. Int J Radiat Oncol Biol Phys. 2010;76(3 Suppl):S94–100.
11. Kennedy AS. Radiation oncology approaches in liver malignancies. American Society of Clinical Oncology educational book/ASCO. American Society of Clinical Oncology. Meeting. 2014;e150–155.
12. Kennedy A. Radioembolization of hepatic tumors. J Gastrointest Oncol. 2014;5(3):178–89.
13. Nath R, Anderson LL, Luxton G, Weaver KA, Williamson JF, Meigooni AS. Dosimetry of interstitial brachytherapy sources: recommendations of the AAPM radiation therapy committee task group no. 43. American Association of Physicists in Medicine. Med Phys. 1995;22(2):209–34.

14. Perez-Calatayud J, Ballester F, Das RK, et al. Dose calculation for photon-emitting brachytherapy sources with average energy higher than 50 keV: report of the AAPM and ESTRO. Med Phys. 2012;39(5):2904–29.
15. Rivard MJ, Coursey BM, DeWerd LA, et al. Update of AAPM task group no. 43 report: a revised AAPM protocol for brachytherapy dose calculations. Med Phys. 2004;31(3):633–74.
16. Martinez-Monge R, Nag S, Nieroda CA, Martin EW. Iodine-125 brachytherapy in the treatment of colorectal adenocarcinoma metastatic to the liver. Cancer. 1999;85(6):1218–25.
17. Lin ZY, Chen J, Deng XF. Treatment of hepatocellular carcinoma adjacent to large blood vessels using 1.5T MRI-guided percutaneous radiofrequency ablation combined with iodine-125 radioactive seed implantation. Eur J Radiol. 2012;81(11):3079–83.
18. Nag S, DeHaan M, Scruggs G, Mayr N, Martin EW. Long-term follow-up of patients of intrahepatic malignancies treated with iodine-125 brachytherapy. Int J Radiat Oncol Biol Phys. 2006;64(3):736–44.
19. Dezarn WA, Cessna JT, DeWerd LA, et al. Recommendations of the American Association of Physicists in Medicine on dosimetry, imaging, and quality assurance procedures for 90Y microsphere brachytherapy in the treatment of hepatic malignancies. Med Phys. 2011;38(8):4824–45.
20. Memon K, Lewandowski RJ, Riaz A, Salem R. Yttrium 90 microspheres for the treatment of hepatocellular carcinoma. Recent Results Cancer Res. 2013;190:207–24.
21. Raval M, Bande D, Pillai AK, et al. Yttrium-90 radioembolization of hepatic metastases from colorectal cancer. Front Oncol. 2014;4:120.
22. Gulec SA, Pennington K, Wheeler J, et al. Yttrium-90 microsphere-selective internal radiation therapy with chemotherapy (chemo-SIRT) for colorectal cancer liver metastases: an in vivo double-arm-controlled phase II trial. Am J Clin Oncol. 2013;36(5):455–60.
23. Fendler WP, Ilhan H, Paprottka PM, et al. Nomogram including pretherapeutic parameters for prediction of survival after SIRT of hepatic metastases from colorectal cancer. Eur Radiol. 2015;25(9):2693–700.
24. Vente MA, Wondergem M, van der Tweel I, et al. Yttrium-90 microsphere radioembolization for the treatment of liver malignancies: a structured meta-analysis. Eur Radiol. 2009;19(4):951–9.
25. Das R, Venselaar J. Comprehensive brachytherapy: physical and clinical aspects. In: Venselaar J, et al., editors. Comprehensive brachytherapy: physical and clinical aspects. Boca Raton, FL: CRC Press; 2013. p. 9–27.
26. Ballester F, Granero D, Perez-Calatayud J, Venselaar JL, Rivard MJ. Study of encapsulated 170Tm sources for their potential use in brachytherapy. Med Phys. 2010;37(4):1629–37.
27. Lymperopoulou G, Papagiannis P, Sakelliou L, Milickovic N, Giannouli S, Baltas D. A dosimetric comparison of 169Yb versus 192Ir for HDR prostate brachytherapy. Med Phys. 2005;32(12):3832–42.
28. Dritschilo A, Grant EG, Harter KW, Holt RW, Rustgi SN, Rodgers JE. Interstitial radiation therapy for hepatic metastases: sonographic guidance for applicator placement. AJR Am J Roentgenol. 1986;147(2):275–8.
29. Mohnike K, Wieners G, Schwartz F, et al. Computed tomography-guided high-dose-rate brachytherapy in hepatocellular carcinoma: safety, efficacy, and effect on survival. Int J Radiat Oncol Biol Phys. 2010;78(1):172–9.
30. Collettini F, Schnapauff D, Poellinger A, et al. Hepatocellular carcinoma: computed-tomography-guided high-dose-rate brachytherapy (CT-HDRBT) ablation of large (5–7 cm) and very large (>7 cm) tumours. Eur Radiol. 2012;22(5):1101–9.
31. Ricke J, Mohnike K, Pech M, et al. Local response and impact on survival after local ablation of liver metastases from colorectal carcinoma by computed tomography-guided high-dose-rate brachytherapy. Int J Radiat Oncol Biol Phys. 2010;78(2):479–85.
32. Kim TK, Khalili K, Jang HJ. Local ablation therapy with contrast-enhanced ultrasonography for hepatocellular carcinoma: a practical review. Ultrasonography. 2015;34(4):235–45.
33. Sparchez Z, Radu P, Kacso G, Sparchez M, Zaharia T, Al Hajjar N. Prospective comparison between real time contrast enhanced and conventional ultrasound guidance in percutaneous biopsies of liver tumors. Med Ultrason. 2015;17(4):456–463.
34. Collettini F, Singh A, Schnapauff D, et al. Computed-tomography-guided high-dose-rate brachytherapy (CT-HDRBT) ablation of metastases adjacent to the liver hilum. Eur J Radiol. 2013;82(10):e509–14.
35. Brinkhaus G, Lock JF, Malinowski M, et al. CT-guided high-dose-rate brachytherapy of liver tumours does not impair hepatic function and shows high overall safety and favourable survival rates. Ann Surg Oncol. 2014;21(13):4284–92.
36. Collettini F, Golenia M, Schnapauff D, et al. Percutaneous computed tomography-guided high-dose-rate brachytherapy ablation of breast cancer liver metastases: initial experience with 80 lesions. J Vasc Intervent Radiol: JVIR. 2012;23(5):618–26.
37. Geisel D, Collettini F, Denecke T, et al. Treatment for liver metastasis from renal cell carcinoma with computed-tomography-guided high-dose-rate brachytherapy (CT-HDRBT): a case series. World J Urol. 2013;31(6):1525–30.
38. Brinkhaus G, Lock JF, Malinowski M, et al. CT-guided high-dose-rate brachytherapy of liver tumours does not impair hepatic function and shows high overall safety and favourable survival rates. Ann Surg Oncol. 2014.
39. Pantelis E, Papagiannis P, Karaiskos P, et al. The effect of finite patient dimensions and tissue inhomogeneities on dosimetry planning of 192Ir HDR breast brachytherapy: a Monte Carlo dose

verification study. Int J Radiat Oncol Biol Phys. 2005;61(5):1596–602.
40. Mobit P, Badragan I. Dose perturbation effects in prostate seed implant brachytherapy with I-125. Phys Med Biol. 2004;49(14):3171–8.
41. Carlsson AK, Ahnesjo A. The collapsed cone superposition algorithm applied to scatter dose calculations in brachytherapy. Med Phys. 2000;27 (10):2320–32.
42. Tedgren AK, Ahnesjo A. Accounting for high Z shields in brachytherapy using collapsed cone superposition for scatter dose calculation. Med Phys. 2003;30(8):2206–17.
43. Chibani O, Williamson JF. MCPI: a sub-minute Monte Carlo dose calculation engine for prostate implants. Med Phys. 2005;32(12):3688–98.
44. Taylor RE, Yegin G, Rogers DW. Benchmarking brachydose: Voxel based EGSnrc Monte Carlo calculations of TG-43 dosimetry parameters. Med Phys. 2007;34(2):445–57.
45. Petrokokkinos L, Zourari K, Pantelis E, et al. Dosimetric accuracy of a deterministic radiation transport based 192Ir brachytherapy treatment planning system. Part II: Monte Carlo and experimental verification of a multiple source dwell position plan employing a shielded applicator. Med Phys. 2011;38 (4):1981–92.
46. Zhou C, Inanc F. Integral-transport-based deterministic brachytherapy dose calculations. Phys Med Biol. 2003;48(1):73–93.
47. Beaulieu L, Carlsson Tedgren A, Carrier JF, et al. Report of the task group 186 on model-based dose calculation methods in brachytherapy beyond the TG-43 formalism: current status and recommendations for clinical implementation. Med Phys. 2012;39 (10):6208–36.
48. Major T, Polgar C, Fodor J, Somogyi A, Nemeth G. Conformality and homogeneity of dose distributions in interstitial implants at idealized target volumes: a comparison between the Paris and dose-point optimized systems. Radiother Oncol. 2002;62(1):103–11.
49. Kestin LL, Jaffray DA, Edmundson GK, et al. Improving the dosimetric coverage of interstitial high-dose-rate breast implants. Int J Radiat Oncol Biol Phys. 2000;46(1):35–43.
50. Akimoto T, Katoh H, Kitamoto Y, Shirai K, Shioya M, Nakano T. Anatomy-based inverse optimization in high-dose-rate brachytherapy combined with hypofractionated external beam radiotherapy for localized prostate cancer: comparison of incidence of acute genitourinary toxicity between anatomy-based inverse optimization and geometric optimization. Int J Radiat Oncol Biol Phys. 2006;64(5):1360–6.
51. Alterovitz R, Lessard E, Pouliot J, Hsu IC, O'Brien JF, Goldberg K. Optimization of HDR brachytherapy dose distributions using linear programming with penalty costs. Med Phys. 2006;33(11):4012–9.
52. Hsu IC, Lessard E, Weinberg V, Pouliot J. Comparison of inverse planning simulated annealing and geometrical optimization for prostate high-dose-rate brachytherapy. Brachytherapy. 2004;3(3):147–52.
53. Jacob D, Raben A, Sarkar A, Grimm J, Simpson L. Anatomy-based inverse planning simulated annealing optimization in high-dose-rate prostate brachytherapy: significant dosimetric advantage over other optimization techniques. Int J Radiat Oncol Biol Phys. 2008;72(3):820–7.
54. Lahanas M, Baltas D, Giannouli S. Global convergence analysis of fast multiobjective gradient-based dose optimization algorithms for high-dose-rate brachytherapy. Phys Med Biol. 2003;48(5): 599–617.
55. Lahanas M, Baltas D, Zamboglou N. A hybrid evolutionary algorithm for multi-objective anatomy-based dose optimization in high-dose-rate brachytherapy. Phys Med Biol. 2003;48(3):399–415.
56. Ricke J, Wust P. Computed tomography-guided brachytherapy for liver cancer. Semin Radiat Oncol. 2011;21(4):287–93.
57. Kubo HD, Glasgow GP, Pethel TD, Thomadsen BR, Williamson JF. High dose-rate brachytherapy treatment delivery: Report of the AAPM Radiation Therapy Committee Task Group No. 59. Med Phys. 1998;25(4):375–403.
58. Ding C, Solberg TD, Hrycushko B, Xing L, Heinzerling J, Timmerman RD. Optimization of normalized prescription isodose selection for stereotactic body radiation therapy: conventional vs robotic linac. Med Phys. 2013;40(5):051705.
59. Oku Y, Takeda A, Kunieda E, et al. Analysis of suitable prescribed isodose line fitting to planning target volume in stereotactic body radiotherapy using dynamic conformal multiple arc therapy. Pract Radiat Oncol. 2012;2(1):46–53.
60. Jones R, Chen Q, Best R, Libby B, Crandley EF, Showalter TN. Dosimetric feasibility of stereotactic body radiation therapy as an alternative to brachytherapy for definitive treatment of medically inoperable early stage endometrial cancer. Radiat Oncol. 2014;9:164.
61. Cengiz M, Dogan A, Ozyigit G, et al. Comparison of intracavitary brachytherapy and stereotactic body radiotherapy dose distribution for cervical cancer. Brachytherapy. 2012;11(2):125–9.
62. Merrow C, deBoer S, Podgorsak MB. VMAT for the treatment of gynecologic malignancies for patients unable to receive HDR brachytherapy. J Appl Clin Med Phys. 2014;15(5):4839.
63. Georg D, Kirisits C, Hillbrand M, Dimopoulos J, Potter R. Image-guided radiotherapy for cervix cancer: high-tech external beam therapy versus high-tech brachytherapy. Int J Radiat Oncol Biol Phys. 2008;71(4):1272–8.
64. Fukuda S, Seo Y, Shiomi H, et al. Dosimetry analyses comparing high-dose-rate brachytherapy, administered as monotherapy for localized prostate cancer, with stereotactic body radiation therapy simulated using CyberKnife. J Radiat Res. 2014;55 (6):1114–21.

65. Spratt DE, Scala LM, Folkert M, et al. A comparative dosimetric analysis of virtual stereotactic body radiotherapy to high-dose-rate monotherapy for intermediate-risk prostate cancer. Brachytherapy. 2013;12(5):428–33.
66. Patil N, Chakraborty S, D'Souza D. Comparison of intracavitary brachytherapy and stereotactic body radiotherapy dose distribution for cervical cancer: in regard to Cengiz et al. Brachytherapy. 2013;12 (4):387.
67. Fokdal L, Sturdza A, Mazeron R, et al. Image guided adaptive brachytherapy with combined intracavitary and interstitial technique improves the therapeutic ratio in locally advanced cervical cancer: analysis from the retroEMBRACE study. Radiother Oncol. 2016.
68. Skinner HD, Hong TS, Krishnan S. Charged-particle therapy for hepatocellular carcinoma. Semin Radiat Oncol. 2011;21(4):278–86.
69. Fichtinger G, Burdette EC, Tanacs A, et al. Robotically assisted prostate brachytherapy with transrectal ultrasound guidance–phantom experiments. Brachytherapy. 2006;5(1):14–26.
70. Podder TK, Buzurovic I, Huang K, Showalter T, Dicker AP, Yu Y. Reliability of EUCLIDIAN: an autonomous robotic system for image-guided prostate brachytherapy. Med Phys. 2011;38(1):96–106.
71. Lin AW, Trejos AL, Mohan S, et al. Electromagnetic navigation improves minimally invasive robot-assisted lung brachytherapy. Comput Aided Surg. 2008;13(2):114–23.
72. Podder TK, Beaulieu L, Caldwell B, et al. AAPM and GEC-ESTRO guidelines for image-guided robotic brachytherapy: report of Task Group 192. Med Phys. 2014;41(10):101501.
73. Hungr N, Troccaz J, Zemiti N, Tripodi N. Design of an ultrasound-guided robotic brachytherapy needle-insertion system. Conf Proc IEEE Eng Med Biol Soc. 2009;2009:250–3.
74. Abolhassani N, Patel R, Moallem M. Control of soft tissue deformation during robotic needle insertion. Minim Invasive Ther Allied Technol. 2006; 15(3):165–76.
75. van den Bosch MR, Moman MR, van Vulpen M, et al. MRI-guided robotic system for transperineal prostate interventions: proof of principle. Phys Med Biol. 2010;55(5):N133–40.
76. Majewicz A, Marra SP, van Vledder MG, et al. Behavior of tip-steerable needles in ex vivo and in vivo tissue. IEEE Trans Biomed Eng. 2012; 59(10):2705–15.
77. Reed KB, Majewicz A, Kallem V, et al. Robot-Assisted Needle Steering. IEEE Robot Autom Mag. 2011;18(4):35–46.
78. Dise J, Liang X, Scheuermann J, et al. Development and evaluation of an automatic interstitial catheter digitization tool for adaptive high-dose-rate brachytherapy. Brachytherapy. 2015;14(5):619–25.
79. Poulin E, Racine E, Binnekamp D, Beaulieu L. Fast, automatic, and accurate catheter reconstruction in HDR brachytherapy using an electromagnetic 3D tracking system. Med Phys. 2015;42(3):1227–32.
80. Kardell M, Magnusson M, Sandborg M, Alm Carlsson G, Jeuthe J, Malusek A. Automatic segmentation of pelvis for brachytherapy of prostate. Radiat Prot Dosimetry. 2015.
81. Wu W, Zhou Z, Wu S, Zhang Y. Automatic liver segmentation on volumetric ct images using supervoxel-based graph cuts. Comput Math Methods Med. 2016;2016:9093721.
82. Afifi A, Nakaguchi T. Unsupervised detection of liver lesions in CT images. Conf Proc IEEE Eng Med Biol Soc. 2015;2015:2411–4.
83. Hrycushko BA, Meyer J, Sutphin P, et al. Dosimetric and economic comparison of interstitial high-dose-rate brachytherapy to stereotactic body radiation therapy for liver lesions. Brachytherapy. 2015;14(21):S101.

Part IV
Hepatocellular Carcinoma

13 Hepatocellular Carcinoma: Epidemiology, Basic Principles of Treatment, and Clinical Data

Amit G. Singal, MD, MS, Purva Gopal, MD, MS and Adam C. Yopp, MD

13.1 Epidemiology

Hepatocellular carcinoma (HCC) is the most common type of primary liver cancer and is the 5th most common cancer worldwide [1]. It is the 5th most common cancer in men and 7th most common cancer in women. HCC has a high mortality rate and is the 3rd leading cause of cancer-related death worldwide. There is geographic variation in HCC incidence worldwide, with the majority of cases occurring in developing countries (Fig. 13.1). Over 75% of HCC occur in Southeast Asian and sub-Saharan Africa, with incidence rates exceeding 20 per 100,000 persons. Hepatitis B virus (HBV) is the primary etiologic factor for HCC in these areas, accounting for >70% of HCC patients [2]. Southern European countries have intermediate-incidence rates, whereas the lowest incidence rates (<5 per 100,000 persons) are found in North America, South America, and Northern Europe. In these countries, hepatitis C virus (HCV)-associated cirrhosis is the most common etiologic factor, accounting for approximately 60% of HCC cases [1].

HCC incidence in several high- and intermediate-incidence areas appears to be stabilizing or falling [1]. In China and Taiwan, this decrease is related to implementation of HBV vaccination programs and higher rates of HBV treatment. In Japan and Southern Europe, the decrease may relate to an aging cohort of HCV-infected patients [3], as the peak incidence of HCV in these countries preceded that of the USA by 10–20 years [4]. In contrast, the number of HCC cases in low-incidence areas, such as the USA, is rising [5]. Over the ten-year period from 1995 to 2004, HCC had the largest increase in incidence among solid tumors in the USA [6]. The rising incidence of HCC is largely related to the high prevalence of advanced HCV infection and non-alcoholic steatohepatitis (NASH) [1, 7]. Given the 25–30 year lag between acquisition of HCV and the development of cirrhosis, many HCV-infected patients in the USA are now presenting with complications of cirrhosis; HCV-related HCC is anticipated to continue increasing over the next 20 years [4]. Similarly, the prevalence of NASH has increased in parallel with increasing rates of diabetes and obesity; therefore, NASH-related complications, including HCC, are anticipated to increase over the next several decades.

HCC continues to have a poor prognosis, with an incidence-to-mortality ratio that approaches 1, accounting for one of the fastest growing death rates among solid tumors. A large

A.G. Singal (✉)
Department of Internal Medicine, UT Southwestern Medical Center, 5959 Harry Hines Blvd, P.O. Box 1, Suite 420, Dallas, TX 75390, USA
e-mail: amit.singal@utsouthwestern.edu

P. Gopal
Department of Pathology, UT Southwestern Medical Center, Dallas, TX, USA

A.C. Yopp
Department of Surgery, UT Southwestern Medical Center, Dallas, TX, USA

J. Meyer and T.E. Schefter (eds.), *Radiation Therapy for Liver Tumors*,
DOI 10.1007/978-3-319-54531-8_13

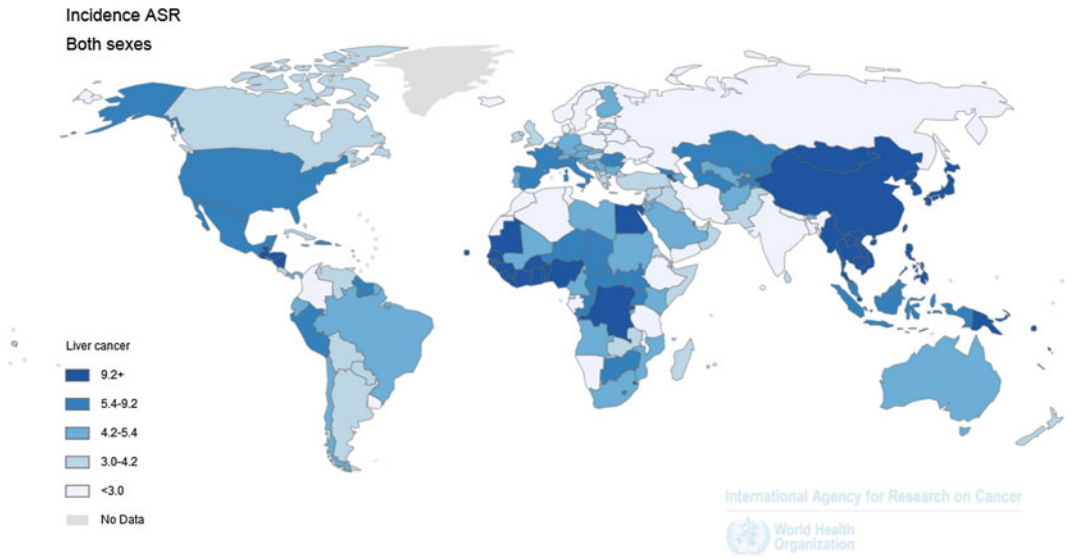

Fig. 13.1 Geographic variation in liver cancer incidence (age-standardized). [Reproduced with permission from Ferlay J, Soerjomataram I, Ervik M, Dikshit R, Eser S, Mathers C, Rebelo M, Parkin DM, Forman D, Bray, F. GLOBOCAN 2012 v1.0, Cancer Incidence and Mortality Worldwide: IARC CancerBase No. 11 [Internet]. Lyon, France: International Agency for Research on Cancer; 2013. Available from: http://globocan.iarc.fr, accessed on 29 April 2016.]

population-based study from the USA with >15,000 patients reported 3- and 5-year survival rates were 11 and 8%, respectively, in 1992–1993, compared to 18 and 13% in 1997–1999 [6]. Similarly, 5-year survival rates in Europe were 0.9–4.9% in the early 1980s, compared to 4.6–7.9% in the mid-1990s [8]. Whereas the prognosis for most solid cancers improved from 1994 to 2003, the mortality rate for HCC nearly doubled [1, 9]. The continued poor prognosis for HCC is largely driven by high rates of late-stage presentation, when curative options no longer exist [10–15].

13.2 Risk Factors

13.2.1 Hepatitis B

HBV infection is the most common risk factor for HCC worldwide. HCC risk among HBV-infected patients is related to the mode of HBV acquisition [16, 17]. People who live in HBV-endemic areas, such as Southeast Asia or Africa, typically acquire HBV infection at birth (vertical transmission), and over 90% of these people develop chronic HBV infection. HBV carriers without cirrhosis have an annual HCC incidence of approximately 0.5%, which increases to 1% in elderly patients [18, 19]. HCC surveillance is recommended in Asian males over age 40 and Asian women over age 50 even in the absence of cirrhosis [20]. Patients from Africa are at particularly high risk, potentially related to a synergistic effect of aflatoxin exposure, and surveillance is recommended at an earlier age [21]. HBV-infected patients who are exposed to aflatoxin have a relative risk of 59.4 (95% CI 16.6–212.0) for HCC compared to those with neither exposure [22]. In contrast, most people in the USA and Europe acquire HBV infection via intravenous drug use or sexual transmission (horizontal transmission) and most experience spontaneous resolution after an acute infection. Patients with chronic HBV via horizontal transmission are at low risk for HCC in the absence of cirrhosis. In fact, >90% of HBV-infected patients who develop HCC in the USA have underlying

cirrhosis [23]. Risk factors, including older age, co-infection with HCV, family history of HCC, HBV genotype, and high viral replication (high DNA levels and HBV eAg positivity) may identify subgroups who are at higher risk [24–28]. However, risk models with these variables have not been externally validated and are not ready for routine use in clinical practice [25, 26].

13.2.2 Hepatitis C

HCC can be attributed to HCV infection in approximately 60% of patients in the USA, Europe and Japan [1, 9]. HCC risk is increased 17-fold in HCV-infected patients compared to HCV-negative patients (OR 17.2, 95% CI 13.9–21.6) [29]; however, HCC risk is primarily limited to those with cirrhosis, with an annual incidence rate of 2–8% [30–32] and patients without cirrhosis are at a low risk for developing HCC [33, 34]. Several factors can moderate HCC risk in HCV-infected patients, including older age, male gender, alcohol use, and comorbid conditions such as HIV infection or diabetes [35, 36]. Although viral factors, such as genotype or viral load, do not correlate with HCC risk, successful treatment significantly reduces HCC risk among patients with HCV cirrhosis [37–39]. In patients with cirrhosis who achieve a sustained virologic response, the relative risk of HCC is only 0.27 (95% CI 0.19–0.39) [40].

13.2.3 Metabolic Syndrome and Non-alcoholic Steatohepatitis (NASH)

Several studies have linked HCC to the metabolic syndrome and its components. An analysis of SEER-Medicare demonstrated patients with metabolic syndrome have 2.1-fold increased odds (95% CI 2.0–2.3) of HCC compared to those without metabolic syndrome [41]. Similarly, a prospective study of >900,000 individuals found liver cancer mortality was 4.5-fold higher in men with BMI >35 and 1.7-fold higher in women with BMI >35 compared to normal weight individuals [42]. A meta-analysis found a pooled risk estimate of 2.4 (95% CI 1.9–2.8) among 17 case-control studies and 2.2 (95% CI 1.7–3.0) among 25 cohort studies for the association between diabetes and HCC [43]. The association between metabolic syndrome and HCC is likely driven by an increased risk of NASH as well as the direct carcinogenic potential of obesity [44]. Although it is clear NASH is a risk factor for HCC, this risk is lower than HCV-related cirrhosis. The highest HCC risk is seen among the subset of NASH patients with cirrhosis, although there are increasing reports of HCC developing in NASH patients in the absence of cirrhosis. Patients with NASH cirrhosis have cumulative HCC incidence rates of 2.4–12.8%, while NASH patients without cirrhosis have cumulative HCC mortality rates below 1% [45]. NASH cirrhosis is anticipated to be the major etiologic factor for HCC in the future as the prevalence of NASH continues increasing, in parallel with the obesity and diabetes epidemics [46].

13.2.4 Alcohol Abuse and Alcoholic Cirrhosis

Alcoholic cirrhosis is a well-recognized risk factor for HCC, and alcoholic liver disease has been reported as a contributing factor in nearly one-third of HCC cases [47–49]. However, HCC incidence rates in alcoholic cirrhosis may be overestimated given early studies predated routine HCV testing. A recent registry study from Denmark suggested HCC mortality rates may be less than 1% in alcoholic cirrhosis [50]; however, these results require external validation. Although HCC risk increases with daily alcohol intake of 40–60 grams/day [51, 52], it is unclear if lower alcohol levels increase HCC risk. An Italian case-control study with 464 HCC patients and 824 patients without liver disease found a linear increase in the odds of HCC with increasing alcohol intake, starting at 60 grams/day [53]. This study also suggested a synergistic effect between alcohol and viral hepatitis, as patients with both risk factors had a

twofold increased incidence of HCC compared to those with viral hepatitis alone. Outside of promoting the development of cirrhosis, there is little evidence for a direct carcinogenic effect of alcohol [48].

13.2.5 Cirrhosis Due to Other Causes

Regardless of cause, cirrhosis is the most important risk factor for HCC [20]. The most common etiologies of cirrhosis associated with HCC include HBV infection, HCV infection, alcohol, and NASH. Hemochromatosis, primary biliary cirrhosis, autoimmune hepatitis, and alpha-1 antitrypsin deficiency are less common causes and have prevalence rates of 1–8% among patients with HCC [54–56]. Of note, patients with cirrhosis due to genetic hemochromatosis are at markedly increased risk of HCC, with a relative risk of ~20.

13.2.6 Demographic Risk Factors

In most countries, HCC rarely occurs before age 40 and the highest age-specific rates are seen in those older than 70 years [24]. Male gender is also an independent risk factor for HCC, with 2–4 times higher rates in men than women [24]. The higher incidence rates in men may be related to differential exposure to risk factors, including viral hepatitis, alcohol, and obesity [1, 57]; however, available data do not fully explain observed differences in HCC rates and a potential role for sex hormones has been suggested [58]. There are also racial/ethnic differences in the distribution of HCC. Age-adjusted incidence rates are highest in Asians (10.8 per 100,000 person-years), followed by Hispanics (7.0 per 100,000 person-years), Blacks (6.3 per 100,000 person-years), and finally, non-Hispanic Whites (2.4 per 100,000 person-years) [59]. The largest increase in HCC incidence is noted among Hispanics, whereas the smallest increase is noted among Asians.

13.3 Pathogenesis

In the last several years, there have been important advances in our understanding of HCC pathogenesis and the critical oncogenic and tumor suppressor pathways involved. The dominant paradigm suggests carcinogenesis occurs through a multistep process resulting in the progression of normal cells through pre-neoplastic states into invasive cancers [60]. The key phenotypic characteristics of cancer cells are self-sufficiency in growth signals, insensitivity to growth-inhibitory signals, evasion of apoptosis, limitless replicative potential, sustained angiogenesis, and tissue invasion and metastasis. Although the acquisition of each characteristic is thought to be necessary for the development of a full neoplastic phenotype [61], the predominant required event is unconstrained cell proliferation. This "cancer platform" concept suggests the key events driving carcinogenesis include the simultaneous development of deregulated proliferation and reduced cell death. The subsequent development of invasion, angiogenesis, metastasis, and immune evasion are secondary to the development of unrestricted proliferation [62].

13.3.1 Receptor Tyrosine Kinase Pathways

The Ras mitogen-activated protein kinase (MAPK) and phosphatidylinositol 3-kinase (PI3K)-Akt kinase signaling pathways are activated by ligand binding and phosphorylation of several growth factor tyrosine kinase receptors, including the EGF receptors, the fibroblast growth factor (FGF) receptors, the hepatocyte growth factor (HGF) receptor c-met, the stem cell growth factor receptor c-kit, the PDGF receptor, and the vascular endothelial growth factor (VEGF) receptor [63]. The downstream consequences of activation of these receptors are multiple and include activation of the Grb2/Shc/SOS adapter molecule complex and downstream activation of the Ras/Raf/Erk 1/2

MAPK pathway, which results in activation of the AP-1 transcriptional activators c-fos and c-jun and consequent induction of transcription of genes that drive cell proliferation. Sorafenib is an example of an agent that blocks this pathway [64].

13.3.2 Wnt/β-Catenin Pathway

Wnts are secreted cysteine-rich glycoprotein ligands that act as ligands for the Frizzled family of cell surface receptors and activate receptor-mediated signaling pathways. The best-studied Wnt pathway activates β-catenin [65]. Activation of the Wnt pathway occurs in approximately 30–40% of HCC as a result of mutations in the β-catenin gene (12–26% of human HCC) and mutations in AXIN1 or AXIN2 (8–13% of human HCC) [66]. Wnts are involved in regulation of liver regeneration and in the maintenance and self-renewal of pluripotent stem cells and progenitor cells. Thus, they may play a role in the maintenance of the cancer stem cell compartment and are attractive targets for cancer therapy [67].

13.3.3 PI3Kinase/AKT/mTOR Pathway

Multiple cellular growth factors, including insulin, insulin-like growth factors, and cytokines such as interleukin-2, activate the PI3K family of enzymes, which produce the lipid second messenger phosphoinositol triphosphate (PIP3) and related second messengers. PIP3 in turn activates Akt/protein kinase B (PKB). Activated Akt phosphorylates several cellular target proteins, including the proapoptotic protein BAD and the mammalian target of rapamycin (mTOR) subfamily of proteins [68]. mTOR proteins in turn regulate the phosphorylation of p70 S6 kinase, a serine-threonine kinase, and the translational repressor protein PHAS-1/4E-BP. These factors coordinate translation of cell cycle regulatory proteins and promote cell cycle progression [69]. In one study, overexpression of phospho-mTOR was found in 15% of HCC tumors. mTOR phosphorylation was associated with increased expression of total p70 S6 kinase, which was found in 45% of HCC. In vitro experiments showed that rapamycin reduced p70 S6K phosphorylation and markedly inhibited proliferation of both HepG2 and Hep3B HCC cell lines. Rapamycin and other mTOR kinase inhibitors show significant activity against cancers with activated PI3K/Akt pathways [70] and are currently under investigation.

13.3.4 Angiogenic Pathways

Substances produced by cancer cells in response to local hypoxia or the interaction of the proliferating mass of cells with surrounding stromal tissue stimulate the growth of new blood vessels from the surrounding parenchyma into the tumor. Signaling pathways critical to the angiogenic process includes growth factor-mediated pathways such as VEGF and FGF receptor signaling as well as the nitric oxide signaling pathway. Hypoxia induces expression of hypoxia inducible factor 1 (HIF1) and insulin-like growth factor 2 (IGF2), both of which stimulate expression of VEGF and other growth factors [71]. HCCs are highly vascular and presumably dependent on active neoangiogenesis for their growth. In parallel with the increase in angiogenic stimuli, it has been shown that the expression of collagen XVIII, the precursor of the anti-angiogenic molecule endostatin, is decreased in larger and more vascular HCC [72].

13.3.5 Telomerase

Telomeres are specialized protein-DNA structures at the ends of chromosomes that contain long stretches of TTAGGG hexameric repeats. Telomeres prevent degradation of chromosome ends and end-to-end fusion with other chromosomes. Aging of somatic cells is associated with reduction in telomere length because of the inability of traditional DNA polymerases to replicate completely the end of the chromosomal DNA. In contrast, germ line and neoplastic cells

express telomerase, an enzyme that restores telomere length. There is progressive shortening of telomeres during progression from chronic hepatitis to cirrhosis and eventually to HCC [73, 74]. Hepatocarcinogenesis is characterized by the evolution of clones of hepatocytes with increased telomerase expression and an immortalized phenotype [75, 76]. Given that it is not expressed in normal cells, telomerase-targeted therapies will likely have minimal to no significant side effects and are an attractive target for drug development.

13.3.6 Stem Cells

The acquisition of stem cell-like properties in tumors is thought to regulate cellular self-renewal potential and promote cell proliferation [77]. The Bmi-1 signaling pathway may connect this "stemness feature" to tumorigenesis. Bmi-1 belongs to the Polycomb gene group (PcG) that is involved in maintaining target genes in their transcriptional state. The ability of Bmi-1 to immortalize cells by inducing telomerase activity and promote tumorigenesis through repression of the $p16^{INK4a}$ and $p19^{ARF}$ expression indicates the involvement of the Bmi-1 "stemness" function in neoplastic proliferation [78]. Bmi-1 overexpression may cause hepatocyte immortalization through suppression of p16 and activation of human telomerase [79]; however, the exact mechanistic role of Bmi-1 in HCC tumorigenesis is not clear.

13.4 Clinical Presentation and Early Detection

The clinical presentation of HCC is driven by the degree of hepatic reserve. In patients with cirrhosis, HCC can present with hepatic decompensation including ascites, hepatic encephalopathy, or jaundice [80]. Nearly 40% of patients have HCC as their first presentation of cirrhosis [15]. In those with adequate hepatic reserve, HCC is more likely to present with tumor-related symptoms including pain, weakness, weight loss, or a palpable mass on exam [80]. Small tumors are often asymptomatic, and HCC typically becomes symptomatic when it reaches 5–8 cm in diameter [81, 82]. Outside of elevated alpha fetoprotein (AFP) levels, laboratory findings are non-specific and more related to the underlying liver disease than HCC. Extrahepatic manifestations of HCC can result from distant metastases or a paraneoplastic syndrome. Osteoclastic destruction from bone metastases can present as pain, while other sites of metastases (lung, lymph nodes, adjacent abdominal viscera) are often asymptomatic [83]. Paraneoplastic symptoms, which can occur in advanced stage tumors and serve as a poor prognostic marker, include hyperlipidemia, hypoglycemia, and hypercalcemia [84].

13.4.1 Hepatocellular Carcinoma Surveillance

Since many patients with HCC are asymptomatic at an early stage, routine surveillance in patients with known cirrhosis is important (Table 13.1). In patients with chronic HBV, HCC surveillance is supported by a randomized controlled trial

Table 13.1 Populations in whom HCC risk is sufficiently high to warrant surveillance

Surveillance recommended
Asian male hepatitis B carriers over age 40
Asian female hepatitis B carriers over age 50
African Blacks with hepatitis B
Hepatitis B carriers with family history of HCC
Cirrhosis related to hepatitis B
Cirrhosis related to hepatitis C
Stage 4 primary biliary cirrhosis
Cirrhosis related to genetic hemochromatosis
Cirrhosis related to other etiologies
Surveillance benefits uncertain
Hepatitis B carriers younger than 40 (males) or 50 (females)
Hepatitis B carriers who contacted infection via horizontal transmission
Hepatitis C carriers without cirrhosis
Non-alcoholic fatty liver patients without cirrhosis

among 18,816 HBV carriers who were randomized to surveillance with abdominal ultrasound and the serum biomarker, AFP, every 6 months (n = 9,373) or no surveillance (n = 9,443) [85]. Of the 86 patients who developed HCC in the surveillance group, 45% were early stage, compared to none of the 67 patients who developed HCC in the no-surveillance group ($p < 0.01$). HCC-related mortality was significantly lower in those undergoing surveillance (83.2 vs. 131.5 per 100,000, $p < 0.01$), with a hazard ratio of 0.63 (95% CI 0.41–0.98). The potential benefit of surveillance in patients with cirrhosis has only been assessed in case-control and cohort studies. Although these studies have limitations including unmeasured confounders, possible selection bias, lead-time bias, and length-time bias, they have demonstrated a consistent association between HCC surveillance and higher rates of early tumor detection, curative treatment, and improved survival [86]. Surveillance with biannual ultrasound and AFP has been demonstrated to be cost-effective in patients with compensated cirrhosis in several decision analysis models, increasing mean life expectancy with cost-effectiveness ratios between $26,000 and $55,000 per QALY [87–89].

13.5 Diagnosis

13.5.1 Radiologic Diagnosis

Patients with an abnormal screening test require diagnostic evaluation to determine the presence or absence of HCC (Fig. 13.2). Radiological imaging has priority in the diagnostic evaluation of patients with suspected HCC since it can facilitate HCC diagnosis, without a need for biopsy (see below), and characterizes tumor burden simultaneously. Lesions <1 cm in diameter on ultrasound are rarely HCC, so follow-up with a repeat ultrasound in 3 months is sufficient [90, 91]. For lesions ≥1 cm, triple-phase CT or dynamic contrast-enhanced MRI should be performed. If the lesion's appearance is typical for HCC ("arterial enhancement and delayed washout"), this is sufficient for a diagnosis of HCC and no further investigation is needed (see discussion below). If the appearance is not typical

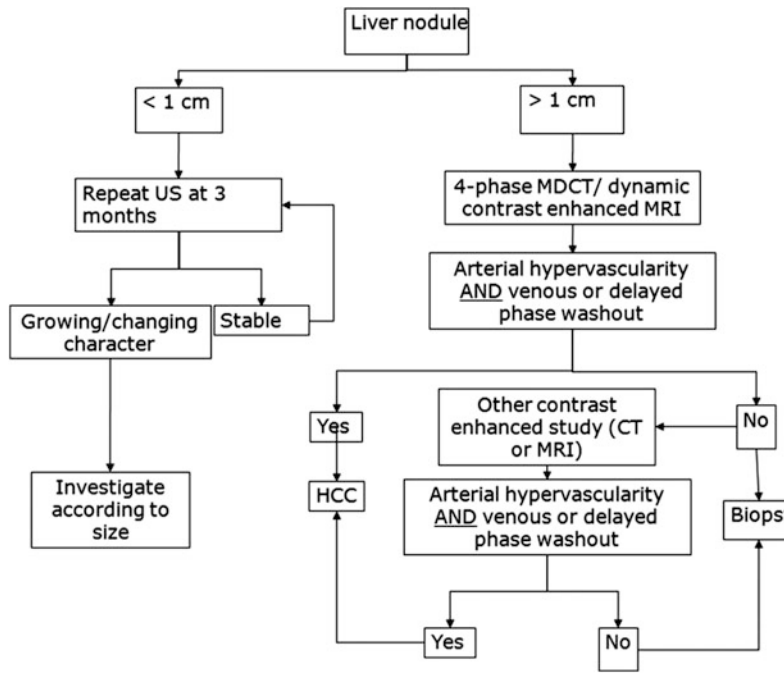

Fig. 13.2 Diagnostic algorithm (AASLD guidelines) for hepatocellular carcinoma. [Reprinted from Bruix J, Sherman M. Management of hepatocellular carcinoma: an update. Hepatology. 2011;53:1020–2. With permission from John Wiley and Sons]

for HCC, a second contrast-enhanced study or biopsy should be performed. Patients with a high suspicion for HCC but negative biopsy should be followed with serial contrast-enhanced imaging. If the lesion enlarges but remains atypical appearing, repeat biopsy can be considered. A study validating this approach found the first biopsy was positive in 70% of patients with HCC; however, up to 3 biopsies were required in some cases [92].

As noted above, patients with a positive surveillance test should be evaluated with triple-phase CT or contrast-enhanced MRI. Established protocols for CT and MRI define the amount and method of contrast administration, timing of the studies after contrast administration, and thickness of slices required for adequate resolution. Several studies have compared performance characteristics of CT and MRI as diagnostic modalities for HCC [100–103]. The sensitivity of MRI is 61–95% compared to 51–86% for triple-phase CT [104]. The role of other imaging modalities, including contrast-enhanced ultrasound, remains debated [105, 106]. Positron emission tomography has poor performance for HCC diagnosis and is not included in the diagnostic algorithm [107].

HCC lesions enhance more than the surrounding liver in the arterial phase and less than the hepatic parenchyma in the venous and delayed phases. Arterial enhancement is an essential characteristic of HCC but is non-specific, as it can be seen in other hypervascular hepatic lesions, such as hemangioma and focal nodular hyperplasia as well as some metastases [108, 109]. Delayed washout is the strongest predictor of HCC among those with an arterial-enhancing lesion (OR 61, 95% CI 3.8–73) [93]. The presence of arterial enhancement and delayed washout had a sensitivity of 89% and specificity of 96% for HCC. The phenomenon of "arterial enhancement and delayed washout" is related to the differential blood supply of the tumor compared to the surrounding liver [102, 110]. The liver obtains ~75% of its blood supply from the portal vein and the remainder from the hepatic artery. As a dysplastic nodule transitions to HCC, there is a gradual reduction in the portal blood supply to the nodule and an increase in arterial blood flow from hepatic artery branches through neoangiogenesis [111, 112]. In the arterial phase, HCC receive contrast-containing arterial blood, while arterial blood to the surrounding liver is diluted by venous blood without contrast. In the portal venous and delayed phases, HCC tumors do not receive any contrast given lack of a portal venous blood supply, while the surrounding liver receives portal blood with contrast.

Lesions between 1 and 2 cm demonstrate typical imaging characteristics less often than larger lesions and can pose the most difficulty for diagnosis. Many of these lesions are not malignant; however, some small HCC lesions can have aggressive behavior leading to vascular invasion and poor survival if not diagnosed early [93–96]. Although requiring one characteristic contrast-enhanced study to make a diagnosis of HCC in 1–2 cm lesions has a lower positive predictive value than requiring two studies, the positive predictive value still exceeds 90% [92, 97, 98]. Serste and colleagues validated this approach in a study among 74 patients with 1–2 cm nodules, of whom 47 had HCC [99]. The sensitivity and specificity of characteristic findings on one imaging study, for the detection of HCC or high-grade dysplatic nodules, was 96 and 100%, respectively, compared to 57 and 100% if characteristics findings were required on both studies. Liver biopsy provided an accurate diagnosis in the 21 (28%) patients with discordant imaging findings on CT and MRI. Chapter 2 describes the Liver Imaging Reporting and Data System (LI-RADS), which serves as a guideline for radiographic diagnosis of liver lesions, in more detail.

Although most HCC exhibit arterial enhancement and delayed washout, some HCC have an atypical presentation. For example, hypovascular HCC enhances less than the surrounding liver in both arterial and venous phase imaging [113, 114]. This appearance is related to immature neoangiogenesis and incompletely established arterial supply. As the lesion matures, the blood supply becomes more arterialized and it will usually exhibit characteristic features [115].

13.5.2 Histologic Diagnosis

Biopsy should be considered in patients with a suspicious liver mass whose appearance is not typical for HCC on contrast-enhanced imaging. Percutaneous biopsy has a sensitivity of 67–100% and specificity of 100% for HCC diagnosis [116–118]. In a study of >2000 biopsies, the most common complication was post-procedural bleeding, but this occurred in only 0.4% of patients [116]. Biopsy of HCC was initially reported to have a 2.7% incidence of needle tract tumor seeding [119]; however, use of a coaxial needle technique significantly reduces this risk [120].

Large HCC can often be diagnosed through imaging alone; however, smaller lesions are more likely to have non-characteristic imaging and may require biopsy to make a diagnosis. In the setting of cirrhosis, there is often a stepwise progression from cirrhotic regenerative nodule to dysplastic nodule to HCC. Some dysplastic nodules have concurrent foci of HCC at time of initial presentation, and one-third of high-grade dysplastic nodules will progress to HCC over a two-year follow-up period [121]. Dysplastic nodules can be classified as low-grade or high-grade, with the risk of HCC increasing with the degree of dysplasia. Malignant transformation rates are 25% in low-grade dysplastic nodules, compared to rates as high as 63% in high-grade dysplastic nodules; however, the latter figure may be difficult to interpret given high-grade dysplastic nodules can be difficult to distinguish from well-differentiated HCC [122, 123]. Not all dysplastic nodules will progress to HCC, as 15% of nodules can disappear on follow-up.

The International Consensus Group for Hepatocellular Neoplasia developed definitions for each of these lesions, leading to increased global standardization of nomenclature among pathologists [124]. Low-grade dysplastic nodules appear distinct from the surrounding liver and can be nodular appearing due to a peripheral fibrous scar. These nodules are characterized by a mild increase in cell density without cytologic atypia or architectural changes. Unpaired arteries can sometimes be present in small numbers [125]. High-grade dysplastic nodules are more likely to demonstrate a nodular appearance, although they lack a true capsule. High-grade dysplastic nodules are characterized by the presence of cytologic atypia and architectural changes, but the atypia is insufficient for a diagnosis of HCC. They often exhibit a combination of increased cell density, irregular trabeculae, small cell change, and unpaired arteries but should not have evidence of stromal invasion [126]. Immunostaining for keratins 7 or 19 may be used in difficult cases to differentiate stromal invasion versus ductular reaction and pseudo-invasion [127]; if present, the stains would support a diagnosis of HCC.

Early HCC are vaguely nodular and are characterized by a combination of histologic features including: (1) increased cell density more than two times that of the surrounding tissue, with an increased nuclear to cytoplasm ratio and irregular thin trabecular pattern, (2) varying numbers of intratumoral portal tracts, (3) pseudoglandular formation, (4) diffuse fatty change, and (5) unpaired arteries [125, 128, 129]. Features of HCC may be present diffusely throughout the lesion but may be restricted to only a portion of the nodule. Furthermore, all of these findings may be found in both early HCC and high-grade dysplastic nodules. Therefore, stromal invasion remains the most helpful feature to distinguish early HCC and high-grade dysplastic nodules. Figure 13.3 shows various histological features of HCC.

Staining for several biomarkers, including glypican-3 (GPC3), heat shock protein 70 (HSP70), and glutamine synthetase (GS), has been proposed to help distinguish HCC from high-grade dysplastic nodules [130–135]. GPC3 is an oncofetal protein that is expressed in 60–90% of HCC, although at lower rates around 50% in well-differentiated HCC. HSP70, a potent anti-apoptotic protein, is expressed in up to 80% of early HCC in resection specimens but less than 50% of cases on biopsy. GS, which correlates with beta-catenin mutations, has a stepwise increase in expression from precancerous to early and advanced HCC. GS expression has been

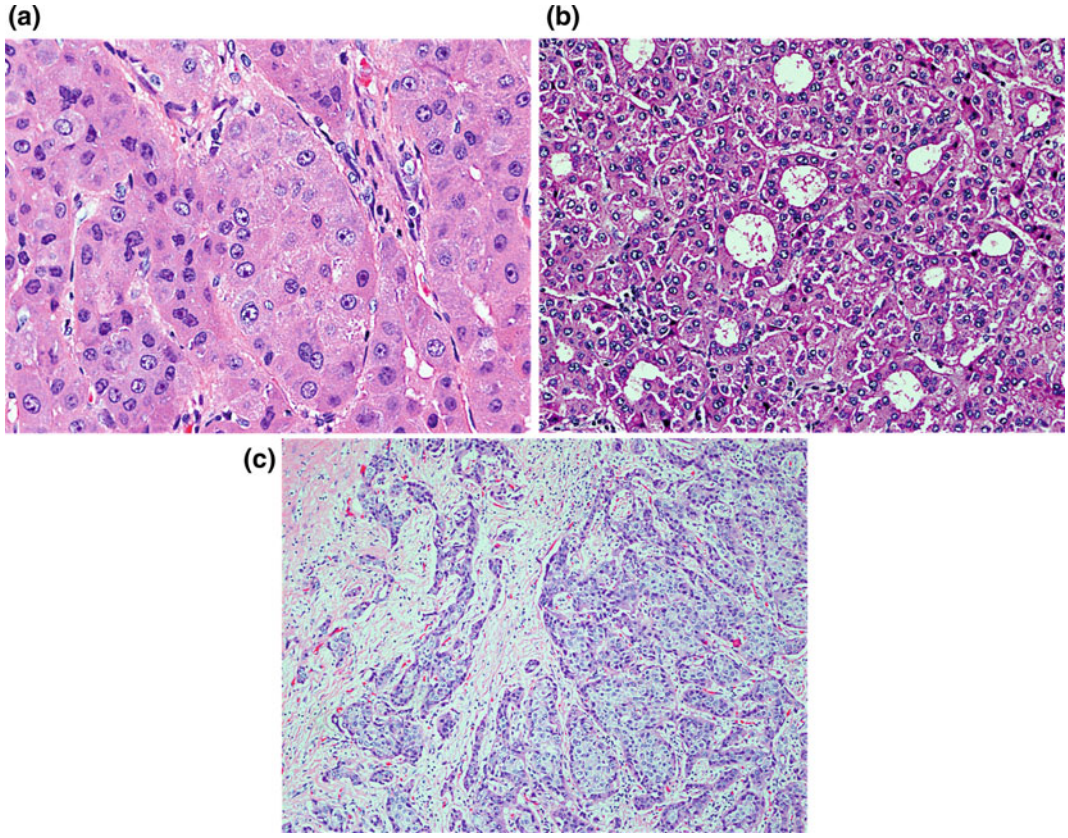

Fig. 13.3 Histologic characteristics of hepatocellular carcinoma including thickened hepatocyte cords (**a**), pseudoglandular formation (**b**), and stromal invasion (**c**)

reported in 13–70% of early HCC but only 10–15% of high-grade dysplastic nodules. The diagnostic accuracy of a panel of these 3 markers was assessed among a cohort of 186 patients with regenerative nodules (n = 13), low-grade dysplastic nodules (n = 21), high-grade dysplastic nodules (n = 50), very well-differentiated HCC (n = 17), well-differentiated HCC (n = 40), and poorly differentiated HCC (n = 35) [131]. When two markers were positive, the accuracy for HCC detection was 78.4%, with 100% specificity. This panel was subsequently prospectively validated among a cohort of 60 patients who underwent biopsy for liver nodules smaller than 2 cm [136]. When at least two of the markers were positive, the sensitivity and specificity were 60 and 100%, respectively; however, the panel only corrected 1 of 3 false positives using conventional pathology analysis. Although this panel appears promising, its clinical utility over conventional pathology has yet to be established.

Recent advances in genomics could provide novel tools to further improve HCC diagnosis. Application of real-time reverse transcription polymerase chain reaction has demonstrated differential expression of genes in high-grade dysplastic nodules and early HCC. For example, a 3-gene set including GPC3, survivin, and LYVE1 had a discriminatory accuracy of 94% between dysplastic nodules and early HCC [137].

13.6 Staging

One of the central factors driving prognosis in patients with HCC is tumor burden. In most solid tumors, staging is determined at time of surgery

and by pathologic examination of a resected specimen, leading to the Tumor Node Metastasis (TNM) classification [138]. However, the TNM staging system in HCC fails to account for the degree of liver dysfunction and patient performance status [139]—two important dimensions that cannot be ignored in patients with HCC. Several other staging systems have been proposed, including the Barcelona Clinic Liver Cancer (BCLC), Cancer of the Liver Italian Program (CLIP), and Japan Integrated Staging (JIS). Although there is not one universally accepted staging system, the BCLC (Fig. 13.4) may offer the most prognostic information because it includes an assessment of tumor burden, liver function, and patient performance status [139, 140] and has been endorsed by the American Association for the Study of Liver Diseases (AASLD) [141]. The prognostic ability of the BCLC has been validated in European, American, and Asian populations [139, 140, 142]. In a study comparing the prognostic ability of seven staging systems, the BCLC was found to have the best predictive power for survival [139]. Median survival for patients with BCLC stage D tumors was only ~5 months, which was significantly shorter than the 10-month median survival for those with BCLC stage C tumors ($p = 0.01$). Patients with BCLC stage B tumors had a median survival of ~27 months ($p = 0.04$ vs. BCLC stage C tumors) and BCLC stage A patients had a median survival >4 years ($p < 0.001$ vs. BCLC stage B). In addition to its strong prognostic ability, the BCLC is the only staging system that has been linked to an evidence-based treatment algorithm (Fig. 13.4). However, the validity of the BCLC staging system will need to be re-evaluated in the future with progress in both risk stratifications and treatment options.

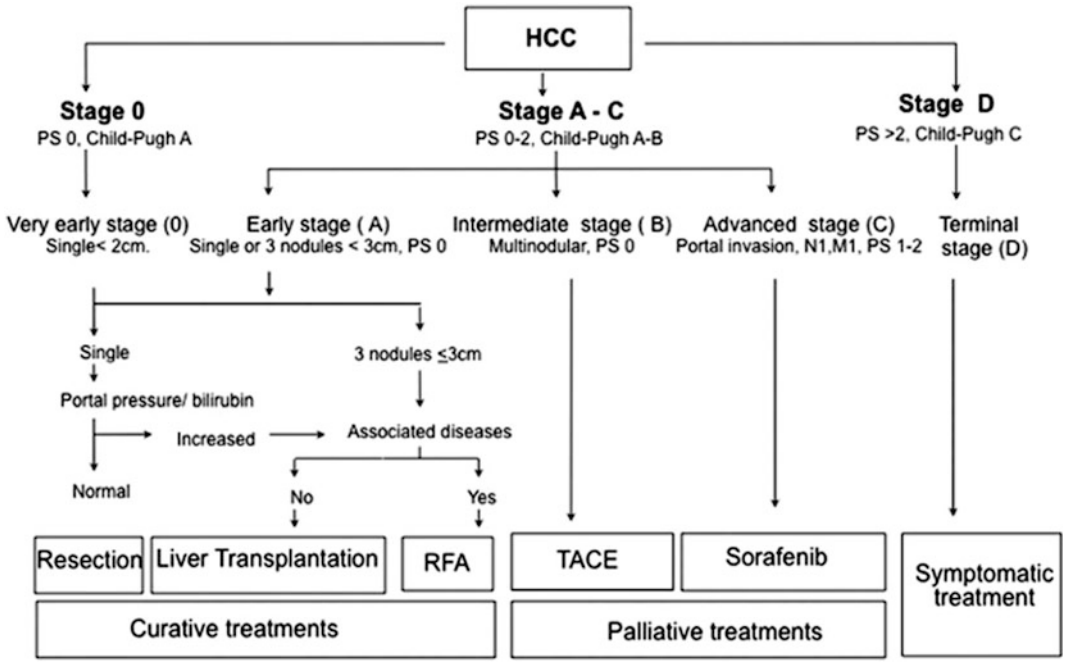

Fig. 13.4 Barcelona clinic liver cancer (BCLC) staging system for hepatocellular carcinoma [Reprinted from Bruix J, Sherman M. Management of hepatocellular carcinoma: an update. Hepatology. 2011;53:1020–2. With permission from John Wiley and Sons]

13.7 Treatment

There have been significant advances in HCC treatment over the past ten years, with improvements in technology and patient selection. Curative therapies include surgical resection, liver transplantation (LT), and locoregional ablative techniques such as radiofrequency ablation (RFA), microwave ablation (MWA), and stereotatic body radiation therapy (SBRT); each approach offers the chance of complete response and long-term survival. Palliative therapies, which typically slow tumor progression and prolong survival, include transarterial chemoembolization (TACE), transarterial radioembolization (TARE), and systemic chemotherapy.

13.7.1 Hepatic Resection

Surgical resection is the treatment of choice for non-cirrhotic patients with HCC. Despite more advanced tumor stage at diagnosis, HCC patients without cirrhosis are more likely to be resection candidates due to lower risk of liver failure [143]. Whereas >40% of HCC in Southeast Asia occurs in the absence of cirrhosis, this accounts for less than 10% of HCC in the USA [23, 144]. Consequently, widespread use of resection is limited in Western countries.

Patients with limited hepatic reserve are at risk for hepatic decompensation, so careful patient selection is crucial. Although perioperative mortality rates after resection have improved over time, hepatic decompensation occurs in 4–5% of patients [145, 146]. It is important to consider both quality and quantity of the future liver remnant (FLR) after resection. In patients with limited fibrosis, the risk of postoperative morbidity is low if FLR exceeds 30%; however, an FLR of 40% is typically required in patients with cirrhosis [147]. In patients with insufficient FLR, portal vein embolization (PVE) can be a useful adjunct to promote hypertrophy of the unaffected hepatic lobe [148, 149]. Quality of FLR is based on an assessment of hepatic function and degree of portal hypertension. Patients with Child Pugh A disease have significantly better survival after resection than patients with Child Pugh B or C disease [147, 150]. However, Child Pugh score alone has a floor effect and is unable to identify Child Pugh A patients at risk for postoperative liver failure. Five-year survival rates are only 25% in patients with portal hypertension and bilirubin >1 mg/dL, compared to 74% in patients without portal hypertension and normal bilirubin levels [151]. Whereas some studies have used invasive means, such as hepatic vein gradient greater than 10 mmHg, to define portal hypertension, others have used platelet count <100,000/mm^3 as a non-invasive surrogate marker [152–155].

The efficacy of surgical resection is also linked to tumor stage. Five-year survival rates are only 10% in patients with vascular invasion compared to 41–57% in those without vascular invasion. Similarly, patients with tumors <2 cm in diameter have 5-year survival rates of 54–93%, whereas those with 2–5 cm tumors have 38–53% 5-year survival rates, and those with tumors >5 cm have 5-year survival rates below 39% [156–159]. Although resection yields 5-year survival rates of nearly 70% (Table 13.2), it is limited by high tumor recurrence rates, as high as 50–70% after 5 years [160]. Early recurrences within 2 years are likely due to dissemination of the original tumor, whereas late recurrences after 2 years are more likely "de novo" HCC. Early recurrence risk is associated with tumor factors (pre-operative tumor stage), whereas viral factors (e.g., persistent HCV infection) and degree of liver dysfunction drive late recurrences [161, 162].

A Cochrane review found 12 randomized controlled trials assessing the role of adjuvant or neoadjuvant therapy with resection [163]. Lower recurrence rates were observed across studies, although only three reported significant reductions in recurrence. Overall, there is insufficient evidence for neoadjuvant or adjuvant regimens with resection. In contrast, several studies, including 5 randomized controlled trials, have demonstrated HCV treatment after resection or ablation (i.e., secondary prevention) significantly reduces HCC recurrence rates [164]. Patients

Table 13.2 Selected cohort studies of surgical resection for hepatocellular carcinoma

Reference	Number of patients	Proportion of patients with cirrhosis (%)	Proportion of patients with child pugh A status (%)	Overall survival
Itamoto [237]	136	100	77.2	70% at 5 years
Poon [238]	204	100	95.6	68% at 5 years
Taura [239]	293	56.7	87.4	61% at 5 years
Kamiyama [240]	321	39.3	96.6	74% at 5 years
Park [241]	213	100	100	69% at 5 years
Huang [242]	115	65.2	92.2	76% at 5 years
Sakaguchi [243]	111	70.3	83.8	78% at 5 years
Zhou [244]	1018	100	97.6	67% at 5 years

with SVR have HCC recurrence rates of approximately 35%, which is significantly lower than the 61% recurrence rate among non-responders ($p = 0.005$) [164].

13.7.2 Liver Transplantation (LT)

LT offers the unique ability to not only treat HCC, but also correct the underlying liver disease, thus minimizing the risk of tumor recurrence. In a landmark study, Mazzaferro and colleagues demonstrated long-term survival was possible in patients with limited tumor burden [165]. Among patients with one tumor <5 cm in diameter or 2–3 tumors each <3 cm in diameter and without portal vein invasion or extrahepatic metastases, 4-year survival rates of 85% were achieved. These criteria, known as the Milan criteria, form the basis of priority listing status for LT in the USA. When these criteria are applied in clinical practice, several studies show recurrence rates are less than 15% and 5-year survival rates approach 60–70% (Table 13.3) [166].

Strict selection criteria have been maintained given the need to obtain the maximum benefit from a limited number of available organs. However, some believe the Milan criteria may be too restrictive and have proposed expanding selection criteria to include patients with larger tumors [167–169]. For example, the University of California San Francisco (UCSF) criteria include patients with a single lesion <6.5 cm or 2–3 lesions, each <4.5 cm with a maximum tumor burden of 8.0 cm [170]. The benefit to patients beyond Milan criteria must be weighed against the harm from delaying transplantation in others on the waiting list. The harms of expanding selection criteria typically outweigh the benefits when 5-year post-transplant survival rates fall below 61% [171]. Although promising results have been reported from single-center cohort studies, patients exceeding Milan criteria have higher post-transplant mortality (HR 1.68, 95% CI 1.39–2.03) [172], with 5-year post-transplant survival rates of only 38% [173].

An alternative approach to expanding transplant criteria is downstaging larger tumors to Milan criteria using TACE, TARE, or local

Table 13.3 Selected cohort studies of liver transplantation for hepatocellular carcinoma

Reference	Number of patients	Transplant criteria	Recurrence rate	Overall survival
Mazzaferro [245]	60	Milan	7% at 4 years	75% at 4 years
Herrero [246]	47	Expanded criteria	13% at 5 years	79% at 5 years
Todo [247]	316	Expanded criteria	13% at 3 years	69% at 3 years
Pelletier [248]	2552	Milan	Not reported	65% at 5 years

Table 13.4 Selected cohort studies of local ablative therapy for hepatocellular carcinoma

Reference	Number of patients	Rate of local tumor progression	Overall survival
Lencioni [249]	206	10%	41% at 5 years
Tateishi [250]	319	9%	54% at 5 years
Chen [251]	256	Not reported	41% at 5 years
Choi [252]	570	12%	58% at 5 years
Livraghi [253]	216	1%	55% at 5 years
N'Kontchou [254]	235	12%	40% at 5 years

ablative therapy [174]. In a prospective study among 61 patients with T3 lesions, downstaging was successful in 43 (70%) patients [175]. The 4-year survival of the entire cohort was 69 and 92% in the 35 patients who underwent LT. This process theoretically selects tumors with more favorable biology that responds to downstaging treatments and would likely do well after LT [176]. Although few data compare the effectiveness of downstaging modalities, a single-center analysis with 86 patients suggested TARE outperforms TACE in terms of successful downstaging (58% vs. 31%, $p = 0.02$) and overall survival (35.7 vs. 18.7 months, $p = 0.18$) [177]. Further large prospective studies are needed to define the role and optimal technique for successful downstaging.

In regions with prolonged waiting times for LT, intrahepatic tumor growth, vascular invasion, or extrahepatic metastases may lead to dropout from the waiting list while awaiting an organ. In regions with waiting times exceeding 12 months, nearly 25% of HCC patients experience dropout [178, 179]. Accordingly, the proportion of LT recipients receiving "bridging therapy" while on the waiting list increased from 37.3% in 2003 to 58.1% in 2008 [180]. Although there is not any proven post-transplant survival advantage in treating HCC patients while awaiting LT, "bridging" therapy may reduce the risk of dropout [180, 181].

13.7.3 Local Ablative Therapies

Local ablation therapy is an alternative for patients with early HCC who are not eligible for resection or LT. RFA involves the use of electromagnetic energy deposition via a percutaneous probe to induce thermal injury to the tumor, leading to local coagulation necrosis [182]. Excellent long-term outcomes have been reported after RFA (Table 13.4) [183–185]. In a study among 1170 patients with HCC, complete tumor ablation was achieved in 99.4% after a median number of 2 RFA sessions [186]. Five- and ten-year survival rates were 60.2 and 27.3%, respectively; however, 74.8% of patients had recurrence within five years of the procedure.

Three RCTs demonstrated similar 3-year survival rates after percutaneous ablation and resection in patients with early HCC, although there was a consistent trend in improved disease-free survival after resection [187–189]. The choice between the treatments depends on local expertise and the risk of local recurrence and perioperative mortality [190]. A Markov model concluded resection is the best therapeutic option, except in cases where patients were older than 70 years, resection perioperative mortality exceeded 30%, negative margins were achieved in less than 60% of patients, or RFA could be performed at least 60% of time for recurrence [191].

A major limitation of RFA is its poor efficacy in large tumors, with a lower chance of complete necrosis in tumors exceeding 3 cm. Tumors >3 cm require repositioning of the electrode or multiple treatment sessions to obtain clear ablation margins. Lesions >5 cm only have 50% chance of complete response even with a more aggressive approach [192–194]. Accordingly, RFA yields 3- and 5-year survival rates of 84 and 65% for tumors <3 cm compared to 71 and 47%

in larger tumors ($p < 0.001$) [186]. TACE prior to RFA has been proposed to decrease HCC blood flow and heat dispersion to increase the size of RFA necrosis, although well-conducted randomized trials are still necessary [195]. Another limitation of RFA is an inability to treat some HCC due to tumor location. Subcapsular and surface HCC and those adjacent to the gallbladder are associated with higher rates of incomplete ablation and may be associated with higher complications rates [196–198]. Similarly, tumors adjacent to large vessels can have a 50% lower chance of complete response to RFA, as the vessel acts as a "heat sink" for the radiofrequency energy [199]. Finally, RFA is associated with potential adverse events including pleural effusion, peritoneal bleeding, and a 0.3% risk of procedure-related mortality [200–202].

MWA is an alternative therapy, involving ultrasound-guided placement of an electrode and microwave treatment to induce regional necrosis surrounding the HCC [203, 204]. MWA can overcome some limitations of RFA, achieving wider ablative zones, and avoiding heat sink effects [205]. A randomized trial comparing RFA and MWA among 72 patients found similar rates of complete response (96% vs. 89%, $p = 0.26$), residual foci of untreated disease (8.3% vs. 17.4%, $p = 0.20$), and complications (2.8% vs. 11.1%, $p = 0.36$); however, the number of required treatment sessions was significantly lower in the RFA group (1.1 vs. 2.4, $p < 0.001$) [206]. There have been advances in microwave ablation since this study, so repeat trials comparing RFA and MWA are needed. Other novel therapies, such as irreversible electroporation (IRE), have also shown promise as alternative techniques but further data are needed.

13.7.4 Transarterial Chemoembolization (TACE)

TACE involves selective delivery of intra-arterial chemotherapy into the tumor, followed by embolization with a goal of inducing tissue necrosis. TACE is a primary treatment for patients with preserved liver function (Child A or B) and tumors that are not amenable to surgical resection, LT, or local ablative therapies, in the absence of vascular invasion or distant metastases [207–209]. TACE carries a significant risk of hepatic ischemia in patients with hepatofugal blood flow and/or main portal vein thrombus. Although this has traditionally been considered a contraindication to TACE, subsequent reports have suggested this may be performed in select patients with preserved liver function [210, 211].

Objective response rates range between 16 and 60%, and fewer than 2% of patients achieve a complete response [207–209]. The residual tumor recovers its blood supply and continues to grow, necessitating repeated TACE treatments at regular intervals. TACE results in slower rates of tumor progression, which translates into lower rates of vascular invasion and distant metastases. A meta-analysis of randomized trials demonstrated a survival benefit for TACE in patients with intermediate stage tumors (Table 13.5).

Table 13.5 Selected randomized trials of TACE for hepatocellular carcinoma[a]

Reference	Number of patients	Proportion child A	Objective response rate (TACE vs. comparison arm)	2-year survival
Pelletier [255]	42	88%	33% vs. 0%	Not reported
GETCH [256]	96	91%	16% vs. 5%	38% vs. 26%
Bruix [257]	80	82%	55% vs. 0%	49% vs. 50%
Pelletier [258]	73	76%	9% vs. 2%	24% vs. 26%
Lo [259]	79	Not reported	11% vs. 1%	31% vs. 11%
Llovet [260]	75	70%	14% vs. 0%	63% vs. 27%

[a]*Note* Comparison arm was medical/conservative management in all studies except Pelletier et al. (1998), where the comparison arm was tamoxifen

TACE results in a significantly prolonged two-year survival of 63% compared to 27% with supportive care ($p < 0.001$) [209].

Although attempts are made to be as selective as possible, there is often injury to surrounding hepatic parenchyma resulting in post-embolization syndrome with pain, nausea, and low-grade fevers [212]. The post-embolization syndrome is usually self-limited to 48–72 h, and usually resolves with pain medications and hydration. The degree of side effects and risk of hepatic toxicity may be determined by the type and frequency of the TACE regimen, with high variability in procedural technique between centers. There is also variability in the choice of chemotherapeutic agent (doxorubicin alone vs. combination with mitomycin-C or 5-fluorouracil vs. bland embolization), embolizing agent (gel foam vs. microparticles), TACE re-treatment schedule (ranging from every 2 months to 6 months), and degree of selectivity (ranging from super-selective to lobar TACE).

The introduction of drug-eluting beads (DEB-TACE), which can be more embolic and maintain higher intratumor doxorubicin levels, may help reduce some heterogeneity between centers [213]. DEB-TACE involves embolic microspheres that sequester chemotherapeutic drugs, such as doxorubicin, and release them in a controlled and sustained fashion. A RCT among 212 patients with intermediate stage HCC found DEB-TACE had similar response rates to conventional TACE (27% vs. 22% complete response, 25% vs. 21% partial response) and similar treatment-related serious adverse effects rates (24% vs. 30%) [214]. However, the DEB-TACE group had lower rates of post-embolization liver toxicity and systemic doxyrubicin effects, such as alopecia. DEB-TACE was superior to bland embolization in an RCT among 84 patients, with higher complete response rates at 6 months (27% vs. 14%), lower recurrence rates at 12 months (46% vs. 78%), and significantly longer time-to-progression (42 weeks vs. 36 weeks, $p = 0.008$) [215]. A study of 104 patients treated with DEB-TACE validated its safety (9.6% major complication rate) and efficacy (median survival 48.6 months) [216].

13.7.5 Systemic Therapy

Several chemotherapeutic agents have been investigated as potential therapies for patients with advanced HCC who are not candidates for local therapy [217]. Studied agents included but are not limited to doxorubicin, tamoxifen, cisplatin, seocalcitol, and nolatrexed. However, these agents failed to demonstrate notable response rates or improvement in survival over best supportive care. In 2008, sorafenib, a multikinase inhibitor, was the first and only agent to date that has been shown to significantly improve survival benefit in patients with advanced HCC [218].

There have been two large randomized trials demonstrating a survival benefit with sorafenib (Table 13.6). The SHARP (Sorafenib Hepatocellular Carcinoma Assessment Randomized Protocol) trial was terminated early, after finding median survival improved from 7.9 months with placebo to 10.7 months with sorafenib (HR 0.58, 95% CI 0.45–0.74) [218]. Time-to-progression was significantly prolonged from 2.8 months in the placebo group to 5.5 months among those receiving sorafenib ($p < 0.001$). The majority of patients included in this trial had Child A cirrhosis (95%) and good performance status (92%)

Table 13.6 Selected randomized trials of sorafenib for hepatocellular carcinoma

Reference	Number of patients	Proportion child A (%)	Comparison arm	Objective response rate (sorafenib vs. comparison arm)	Median survival
Llovet [218]	602	97	Placebo	2% vs. 1%	10.7 vs. 7.9 months
Cheng [219]	226	97	Placebo	3% vs. 1%	6.5 vs. 4.2 months

with advanced tumors (53% extrahepatic spread and 70% vascular invasion). Another randomized trial with sorafenib in patients with advanced HCC was performed in Asia, in which there were significantly higher rates of patients with HBV infection [219]. Median survival was 6.5 months in the patients treated with sorafenib, compared to 4.2 months in those who received placebo (HR 0.68, 95% CI 0.50–0.93).

Sorafenib was well tolerated, with most adverse events being mild to moderate in nature. The most common grade 3–4 adverse events in both trials were hand-foot skin reaction (8–11%), diarrhea (6–8%), and fatigue (3–4%). Its tolerability has been confirmed in an interim analysis of GIDEON (Global Investigation of therapeutic Decisions in hepatocellular carcinoma and of its treatment with sorafeNib), a post-marketing study assessing the tolerability and outcomes of sorafenib in clinical practice. Although patients with Child B cirrhosis experience higher rates of serious adverse events (60% vs. 33%), the incidence of drug-related serious adverse events appears similar (16% vs. 10%) [220]. Patients with Child C cirrhosis or poor performance status are unlikely to significantly benefit from or tolerate systemic targeted therapy [221].

There have been several trials evaluating other targeted therapies for advanced HCC (Table 13.7). The anti-angiogenic agent sunitinib did not demonstrate superiority or non-inferiority compared to sorafenib as a first-line agent in a phase III study of 1,073 patients [222]. Similarly, brivanib showed promise in phase II studies; however, phase III trials failed to demonstrate improved survival compared to placebo [223, 224]. Although promising results have been seen for other agents in phase II studies, none have been confirmed to date in large phase III studies [225–231].

Recently, tumor markers are being incorporated into treatment selection for patients with advanced HCC who progressed or were intolerant to sorafenib. In a phase II study, tivantinib, a

Table 13.7 Potential novel agents for patients with advanced hepatocellular carcinoma

Agents	Phase study	Mechanism of action
First line		
Brivanib	III	Anti-angiogenic
Linifanib	II–III	Anti-angiogenic
Sorafenib + Erlotinib	III	Multikinase inhibitor and anti-angiogenic
Second line		
Ramucirumab	II–III	Anti-angiogenic
Bevacizumab	II	Anti-angiogenic
Cediranib Pazopanib Lenvatinib Lenalidomide Axitinib	I–II	Anti-angiogenic
Gefitinib Lapatinib Cetuximab	I–II	EGFR inhibitor
Everolimus	III	mTOR inhibitor
Sirolimus Temsirolimus	I–II	mTOR inhibitor
Tivatinib cabozantinib	II	Hepatocyte growth factor/c-MET inhibitor
Belinostat	I–II	Histone deacetylase inhibitor
STA-9090	I–II	HSP-90 inhibitor
Nivolumab	I–II	Immunotherapy

selective oral MET inhibitor, was not associated with improved overall survival among all-comers (HR 0.90, 95% CI 0.57–1.40); however, a survival benefit was noted in those with high MET expression (HR 0.38, 95% CI 0.18–0.82) [232]. A randomized phase III study evaluating tivantinib as a second-line agent among patients with high MET expression is now ongoing.

There is also increasing interest in immunotherapy for patients with advanced HCC. In a phase I/II study, nivolumab, a fully human IgG4 monoclonal antibody PD-L1 inhibitor, was evaluated as a second-line agent among 41 patients with advanced HCC who were intolerant or refusing sorafenib [233]. Among the 39 patients in whom response was assessed, 2 (5%) had a complete response and 7 (18%) had partial response; overall survival at 6 months was 72%.

13.7.6 Multidisciplinary Management of Hepatocellular Carcinoma

Treatment decisions for HCC have become increasingly complex with the availability of novel therapies and the growing use of multimodal and multiprovider treatments. Studies have shown high rates of treatment underuse, inappropriate treatment, and treatment delays in clinical practice [234, 235]. Appropriate treatment decisions, individualized for each patient, require the complementary expertise of multiple specialties. A multidisciplinary approach involving a team of hepatologists, surgeons, interventional radiologists, radiation oncologists, medical oncologists, and radiologists allow delivery of optimal treatment and have been associated with improved outcomes including rates of curative treatment, time-to-treatment, and overall survival [236].

13.8 Summary

HCC is the 3rd most common cause of cancer-related death worldwide and one of the most common causes of death in patients with cirrhosis. The highest HCC incidence rates are in Southeast Asia and Africa, related to HBV infection; however, these rates are declining with more widespread vaccination and treatment programs. Its incidence in the USA and Europe is rising due to hepatitis C infection and non-alcoholic fatty liver disease. HCC surveillance is recommended in high-risk populations to detect HCC at an early stage, when curative options exist. Radiologic imaging is the most important aspect in the diagnostic evaluation of patients with suspected HCC, as it can facilitate HCC diagnosis without a need for biopsy and provides determination of tumor burden. Although there is not one universally accepted staging system, the BCLC system is the most widely accepted and has been linked to a treatment algorithm. There are treatment options for most patients with any stage of HCC; however, treatment decisions must be individualized after accounting for factors such as degree of liver dysfunction and patient performance status.

References

1. El-Serag HB. Epidemiology of viral hepatitis and hepatocellular carcinoma. Gastroenterology. 2012; 142(1264–1273):e1.
2. Beasley R. Hepatitis B virus. The major etiology of hepatocellular carcinoma. Cancer. 1988;61:1942–56.
3. Umemura T, Ichijo T, Yoshizawa K, Tanaka E, Kiyosawa K. Epidemiology of hepatocellular carcinoma in Japan. J Gastroenterol. 2009;44(Suppl 19):102–7.
4. Tanaka Y, Hanada K, Mizokami M, Yeo AE, Shih JW, Gojobori T, Alter HJ. A comparison of the molecular clock of hepatitis C virus in the United States and Japan predicts that hepatocellular carcinoma incidence in the United States will increase over the next two decades. Proc Natl Acad Sci U S A. 2002;99:15584–9.
5. Ryerson AB, Eheman CR, Altekruse SF, Ward JW, Jemal A, Sherman RL, Henley SJ, Holtzman D, Lake A, Noone AM, Anderson RN, Ma J, Ly KN, Cronin KA, Penberthy L, Kohler BA. Annual report to the nation on the status of cancer, 1975–2012, featuring the increasing incidence of liver cancer. Cancer. 2016.
6. Altekruse SF, McGlynn KA, Reichman ME. Hepatocellular carcinoma incidence, mortality, and survival trends in the United States from 1975 to 2005. J Clin Oncol. 2009;27:1485–91.

7. El-Serag HB, Davila JA, Petersen NJ, McGlynn KA. The continuing increase in the incidence of hepatocellular carcinoma in the United States: an update. Ann Intern Med. 2003;139:817–23.
8. Capocaccia R, Sant M, Berrino F, Simonetti A, Santi V, Trevisani F. Hepatocellular carcinoma: trends of incidence and survival in Europe and the United States at the end of the 20th century. Am J Gastroenterol. 2007;102:1661–70; quiz 1660, 1671.
9. El-Serag HB. Hepatocellular carcinoma: recent trends in the United States. Gastroenterology. 2004;127:S27–34.
10. Davila JA, Henderson L, Kramer JR, Kanwal F, Richardson PA, Duan Z, El-Serag HB. Utilization of surveillance for hepatocellular carcinoma among hepatitis C virus-infected veterans in the United States. Ann Intern Med. 2011;154:85–93.
11. Davila JA, Morgan RO, Richardson PA, Du XL, McGlynn KA, El-Serag HB. Use of surveillance for hepatocellular carcinoma among patients with cirrhosis in the United States. Hepatology. 2010;52:132–41.
12. Singal AG, Nehra M, Adams-Huet B, Yopp AC, Tiro JA, Marrero JA, Lok AS, Lee WM. Detection of hepatocellular carcinoma at advanced stages among patients in the HALT-C trial: where did surveillance fail? Am J Gastroenterol. 2013;108:425–32.
13. Singal AG, Tiro JA, Gupta S. Improving hepatocellular carcinoma screening: applying lessons from colorectal cancer screening. Clin Gastroenterol Hepatol. 2013;11:472–7.
14. Singal AG, Yopp A, C SS, Packer M, Lee WM, Tiro JA. Utilization of hepatocellular carcinoma surveillance among American patients: a systematic review. J Gen Intern Med. 2012;27:861–7.
15. Singal AG, Yopp AC, Gupta S, Skinner CS, Halm EA, Okolo E, Nehra M, Lee WM, Marrero JA, Tiro JA. Failure rates in the hepatocellular carcinoma surveillance process. Cancer Prev Res (Phila). 2012;5:1124–30.
16. de Franchis R, Meucci G, Vecchi M, Tatarella M, Colombo M, Del Ninno E, Rumi MG, Donato MF, Ronchi G. The natural history of asymptomatic hepatitis B surface antigen carriers. Ann Intern Med. 1993;118:191–4.
17. Evans AA, Chen G, Ross EA, Shen FM, Lin WY, London WT. Eight-year follow-up of the 90,000-person Haimen City cohort: I. Hepatocellular carcinoma mortality, risk factors, and gender differences. Cancer Epidemiol Biomarkers Prev. 2002;11:369–76.
18. McMahon BJ, Alberts SR, Wainwright RB, Bulkow L, Lanier AP. Hepatitis B-related sequelae. Prospective study in 1400 hepatitis B surface antigen-positive Alaska native carriers. Arch Intern Med. 1990;150:1051–4.
19. Villeneuve JP, Desrochers M, Infante-Rivard C, Willems B, Raymond G, Bourcier M, Cote J, Richer G. A long-term follow-up study of asymptomatic hepatitis B surface antigen-positive carriers in Montreal. Gastroenterology. 1994;106:1000–5.
20. Bruix J, Sherman M. Management of hepatocellular carcinoma: an update. Hepatology. 2010;53:1–35.
21. Kew MC, Macerollo P. Effect of age on the etiologic role of the hepatitis B virus in hepatocellular carcinoma in blacks. Gastroenterology. 1988;94:439–42.
22. Qian GS, Ross RK, Yu MC, Yuan JM, Gao YT, Henderson BE, Wogan GN, Groopman JD. A follow-up study of urinary markers of aflatoxin exposure and liver cancer risk in Shanghai, People's Republic of China. Cancer Epidemiol Biomarkers Prev. 1994;3:3–10.
23. Yang JD, Kim WR, Coelho R, Mettler TA, Benson JT, Sanderson SO, Therneau TM, Kim B, Roberts LR. Cirrhosis is present in most patients with hepatitis B and hepatocellular carcinoma. Clin Gastroenterol Hepatol. 2011;9:64–70.
24. El-Serag HB, Rudolph KL. Hepatocellular carcinoma: epidemiology and molecular carcinogenesis. Gastroenterology. 2007;132:2557–76.
25. Yang HI, Sherman M, Su J, Chen PJ, Liaw YF, Iloeje UH, Chen CJ. Nomograms for risk of hepatocellular carcinoma in patients with chronic hepatitis B virus infection. J Clin Oncol. 2010;28:2437–44.
26. Yuen MF, Tanaka Y, Fong DY, Fung J, Wong DK, Yuen JC, But DY, Chan AO, Wong BC, Mizokami M, Lai CL. Independent risk factors and predictive score for the development of hepatocellular carcinoma in chronic hepatitis B. J Hepatol. 2009;50:80–8.
27. Yang HI, Lu SN, Liaw YF, You SL, Sun CA, Wang LY, Hsiao CK, Chen PJ, Chen DS, Chen CJ. Hepatitis B e antigen and the risk of hepatocellular carcinoma. N Engl J Med. 2002;347:168–74.
28. Chen CJ, Yang HI, Su J, Jen CL, You SL, Lu SN, Huang GT, Iloeje UH. Risk of hepatocellular carcinoma across a biological gradient of serum hepatitis B virus DNA level. JAMA. 2006;295:65–73.
29. Donato F, Boffetta P, Puoti M. A meta-analysis of epidemiological studies on the combined effect of hepatitis B and C virus infections in causing hepatocellular carcinoma. Int J Cancer. 1998;75:347–54.
30. Fattovich G, Giustina G, Degos F, Tremolada F, Diodati G, Almasio P, Nevens F, Solinas A, Mura D, Brouwer JT, Thomas H, Njapoum C, Casarin C, Bonetti P, Fuschi P, Basho J, Tocco A, Bhalla A, Galassini R, Noventa F, Schalm SW, Realdi G. Morbidity and mortality in compensated cirrhosis type C: a retrospective follow-up study of 384 patients. Gastroenterology. 1997;112:463–72.
31. Niederau C, Lange S, Heintges T, Erhardt A, Buschkamp M, Hurter D, Nawrocki M, Kruska L, Hensel F, Petry W, Haussinger D. Prognosis of chronic hepatitis C: results of a large, prospective cohort study. Hepatology. 1998;28:1687–95.

32. Sun CA, Wu DM, Lin CC, Lu SN, You SL, Wang LY, Wu MH, Chen CJ. Incidence and cofactors of hepatitis C virus-related hepatocellular carcinoma: a prospective study of 12,008 men in Taiwan. Am J Epidemiol. 2003;157:674–82.
33. Yoshida H, Shiratori Y, Moriyama M, Arakawa Y, Ide T, Sata M, Inoue O, Yano M, Tanaka M, Fujiyama S, Nishiguchi S, Kuroki T, Imazeki F, Yokosuka O, Kinoyama S, Yamada G, Omata M. Interferon therapy reduces the risk for hepatocellular carcinoma: national surveillance program of cirrhotic and noncirrhotic patients with chronic hepatitis C in Japan. IHIT Study Group. Inhibition of Hepatocarcinogenesis by Interferon Therapy. Ann Intern Med. 1999;131:174–81.
34. Lok AS, Seeff LB, Morgan TR, di Bisceglie AM, Sterling RK, Curto TM, Everson GT, Lindsay KL, Lee WM, Bonkovsky HL, Dienstag JL, Ghany MG, Morishima C, Goodman ZD. Incidence of hepatocellular carcinoma and associated risk factors in hepatitis C-related advanced liver disease. Gastroenterology. 2009;136:138–48.
35. Poynard T, Bedossa P, Opolon P. Natural history of liver fibrosis progression in patients with chronic hepatitis C. The OBSVIRC, METAVIR, CLINIVIR, and DOSVIRC groups. Lancet. 1997;349:825–32.
36. Thomas DL, Astemborski J, Rai RM, Anania FA, Schaeffer M, Galai N, Nolt K, Nelson KE, Strathdee SA, Johnson L, Laeyendecker O, Boitnott J, Wilson LE, Vlahov D. The natural history of hepatitis C virus infection: host, viral, and environmental factors. JAMA. 2000;284:450–6.
37. Braks RE, Ganne-Carrie N, Fontaine H, Paries J, Grando-Lemaire V, Beaugrand M, Pol S, Trinchet JC. Effect of sustained virological response on long-term clinical outcome in 113 patients with compensated hepatitis C-related cirrhosis treated by interferon alpha and ribavirin. World J Gastroenterol. 2007;13:5648–53.
38. Bruno S, Stroffolini T, Colombo M, Bollani S, Benvegnu L, Mazzella G, Ascione A, Santantonio T, Piccinino F, Andreone P, Mangia A, Gaeta GB, Persico M, Fagiuoli S, Almasio PL. Sustained virological response to interferon-alpha is associated with improved outcome in HCV-related cirrhosis: a retrospective study. Hepatology. 2007;45:579–87.
39. Veldt BJ, Heathcote EJ, Wedemeyer H, Reichen J, Hofmann WP, Zeuzem S, Manns MP, Hansen BE, Schalm SW, Janssen HL. Sustained virologic response and clinical outcomes in patients with chronic hepatitis C and advanced fibrosis. Ann Intern Med. 2007;147:677–84.
40. Singal AG, Volk ML, Jensen D, Di Bisceglie AM, Schoenfeld PS. A sustained viral response is associated with reduced liver-related morbidity and mortality in patients with hepatitis C virus. Clin Gastroenterol Hepatol. 2010;8:280–8, 288 e1.
41. Welzel TM, Graubard BI, Zeuzem S, El-Serag HB, Davila JA, McGlynn KA. Metabolic syndrome increases the risk of primary liver cancer in the United States: a study in the SEER-Medicare database. Hepatology. 2011;54:463–71.
42. Calle EE, Rodriguez C, Walker-Thurmond K, Thun MJ. Overweight, obesity, and mortality from cancer in a prospectively studied cohort of U.S. adults. N Engl J Med. 2003;348:1625–38.
43. Wang P, Kang D, Cao W, Wang Y, Liu Z. Diabetes mellitus and risk of hepatocellular carcinoma: a systematic review and meta-analysis. Diab Metab Res Rev. 2012;28:109–22.
44. Bugianesi E. Non-alcoholic steatohepatitis and cancer. Clin Liver Dis. 2007;11:191–207, x–xi.
45. White DL, Kanwal F, El-Serag HB. Association between nonalcoholic fatty liver disease and risk for hepatocellular cancer, based on systematic review. Clin Gastroenterol Hepatol. 2012;10(1342–1359):e2.
46. Starley BQ, Calcagno CJ, Harrison SA. Nonalcoholic fatty liver disease and hepatocellular carcinoma: a weighty connection. Hepatology. 2010;51:1820–32.
47. Adami HO, Hsing AW, McLaughlin JK, Trichopoulos D, Hacker D, Ekbom A, Persson I. Alcoholism and liver cirrhosis in the etiology of primary liver cancer. Int J Cancer. 1992;51:898–902.
48. Bagnardi V, Blangiardo M, La Vecchia C, Corrao G. A meta-analysis of alcohol drinking and cancer risk. Br J Cancer. 2001;85:1700–5.
49. Hassan MM, Hwang LY, Hatten CJ, Swaim M, Li D, Abbruzzese JL, Beasley P, Patt YZ. Risk factors for hepatocellular carcinoma: synergism of alcohol with viral hepatitis and diabetes mellitus. Hepatology. 2002;36:1206–13.
50. Jepsen P, Ott P, Andersen PK, Sorensen HT, Vilstrup H. Risk for hepatocellular carcinoma in patients with alcoholic cirrhosis: a danish nationwide cohort study. Ann Intern Med. 2012;156:841–7.
51. La Vecchia C. Alcohol and liver cancer. Eur J Cancer Prev. 2007;16:495–7.
52. Morgan TR, Mandayam S, Jamal MM. Alcohol and hepatocellular carcinoma. Gastroenterology. 2004;127:S87–96.
53. Donato F, Tagger A, Gelatti U, Parrinello G, Boffetta P, Albertini A, Decarli A, Trevisi P, Ribero ML, Martelli C, Porru S, Nardi G. Alcohol and hepatocellular carcinoma: the effect of lifetime intake and hepatitis virus infections in men and women. Am J Epidemiol. 2002;155:323–31.
54. Elmberg M, Hultcrantz R, Ekbom A, Brandt L, Olsson S, Olsson R, Lindgren S, Loof L, Stal P, Wallerstedt S, Almer S, Sandberg-Gertzen H, Askling J. Cancer risk in patients with hereditary hemochromatosis and in their first-degree relatives. Gastroenterology. 2003;125:1733–41.

55. Jones DE, Metcalf JV, Collier JD, Bassendine MF, James OF. Hepatocellular carcinoma in primary biliary cirrhosis and its impact on outcomes. Hepatology. 1997;26:1138–42.
56. Propst T, Propst A, Dietze O, Judmaier G, Braunsteiner H, Vogel W. Prevalence of hepatocellular carcinoma in alpha-1-antitrypsin deficiency. J Hepatol. 1994;21:1006–11.
57. Anthony JC, Echeagaray-Wagner F. Epidemiologic analysis of alcohol and tobacco use. Alcohol Res Health. 2000;24:201–8.
58. Yu MW, Chang HC, Chang SC, Liaw YF, Lin SM, Liu CJ, Lee SD, Lin CL, Chen PJ, Lin SC, Chen CJ. Role of reproductive factors in hepatocellular carcinoma: impact on hepatitis B- and C-related risk. Hepatology. 2003;38:1393–400.
59. El-Serag HB, Lau M, Eschbach K, Davila J, Goodwin J. Epidemiology of hepatocellular carcinoma in Hispanics in the United States. Arch Intern Med. 2007;167:1983–9.
60. Thorgeirsson SS, Grisham JW. Molecular pathogenesis of human hepatocellular carcinoma. Nat Genet. 2002;31:339–46.
61. Hanahan D, Weinberg RA. The hallmarks of cancer. Cell. 2000;100:57–70.
62. Green DR, Evan GI. A matter of life and death. Cancer Cell. 2002;1:19–30.
63. Roberts LR, Gores GJ. Hepatocellular carcinoma: molecular pathways and new therapeutic targets. Semin Liver Dis. 2005;25:212–25.
64. Strumberg D, Richly H, Hilger RA, Schleucher N, Korfee S, Tewes M, Faghih M, Brendel E, Voliotis D, Haase CG, Schwartz B, Awada A, Voigtmann R, Scheulen ME, Seeber S. Phase I clinical and pharmacokinetic study of the Novel Raf kinase and vascular endothelial growth factor receptor inhibitor BAY 43-9006 in patients with advanced refractory solid tumors. J Clin Oncol. 2005;23:965–72.
65. You L, He B, Xu Z, Uematsu K, Mazieres J, Fujii N, Mikami I, Reguart N, McIntosh JK, Kashani-Sabet M, McCormick F, Jablons DM. An anti-Wnt-2 monoclonal antibody induces apoptosis in malignant melanoma cells and inhibits tumor growth. Cancer Res. 2004;64:5385–9.
66. Giles RH, van Es JH, Clevers H. Caught up in a Wnt storm: Wnt signaling in cancer. Biochim Biophys Acta. 2003;1653:1–24.
67. Willert K, Brown JD, Danenberg E, Duncan AW, Weissman IL, Reya T, Yates JR 3rd, Nusse R. Wnt proteins are lipid-modified and can act as stem cell growth factors. Nature. 2003;423:448–52.
68. Singh R, Czaja MJ. Capitalizing on AKT signaling to inhibit hepatocellular carcinoma cell proliferation. Cancer Biol Ther. 2005;4:1419–21.
69. Tanaka S, Arii S. Molecularly targeted therapy for hepatocellular carcinoma. Cancer Sci. 2009;100:1–8.
70. Chan S. Targeting the mammalian target of rapamycin (mTOR): a new approach to treating cancer. Br J Cancer. 2004;91:1420–4.
71. Maxwell PH, Dachs GU, Gleadle JM, Nicholls LG, Harris AL, Stratford IJ, Hankinson O, Pugh CW, Ratcliffe PJ. Hypoxia-inducible factor-1 modulates gene expression in solid tumors and influences both angiogenesis and tumor growth. Proc Natl Acad Sci U S A. 1997;94:8104–9.
72. Musso O, Rehn M, Theret N, Turlin B, Bioulac-Sage P, Lotrian D, Campion JP, Pihlajaniemi T, Clement B. Tumor progression is associated with a significant decrease in the expression of the endostatin precursor collagen XVIII in human hepatocellular carcinomas. Cancer Res. 2001;61:45–9.
73. Miura N, Horikawa I, Nishimoto A, Ohmura H, Ito H, Hirohashi S, Shay JW, Oshimura M. Progressive telomere shortening and telomerase reactivation during hepatocellular carcinogenesis. Cancer Genet Cytogenet. 1997;93:56–62.
74. Stewart SA, Weinberg RA. Telomerase and human tumorigenesis. Semin Cancer Biol. 2000;10:399–406.
75. Kojima H, Yokosuka O, Imazeki F, Saisho H, Omata M. Telomerase activity and telomere length in hepatocellular carcinoma and chronic liver disease. Gastroenterology. 1997;112:493–500.
76. Nagao K, Tomimatsu M, Endo H, Hisatomi H, Hikiji K. Telomerase reverse transcriptase mRNA expression and telomerase activity in hepatocellular carcinoma. J Gastroenterol. 1999;34:83–7.
77. Pardal R, Clarke MF, Morrison SJ. Applying the principles of stem-cell biology to cancer. Nat Rev Cancer. 2003;3:895–902.
78. Dimri GP, Martinez JL, Jacobs JJ, Keblusek P, Itahana K, Van Lohuizen M, Campisi J, Wazer DE, Band V. The Bmi-1 oncogene induces telomerase activity and immortalizes human mammary epithelial cells. Cancer Res. 2002;62:4736–45.
79. Effendi K, Mori T, Komuta M, Masugi Y, Du W, Sakamoto M. Bmi-1 gene is upregulated in early-stage hepatocellular carcinoma and correlates with ATP-binding cassette transporter B1 expression. Cancer Sci. 2010;101:666–72.
80. Trevisani F, D'Intino PE, Caraceni P, Pizzo M, Stefanini GF, Mazziotti A, Grazi GL, Gozzetti G, Gasbarrini G, Bernardi M. Etiologic factors and clinical presentation of hepatocellular carcinoma. Differences between cirrhotic and noncirrhotic Italian patients. Cancer. 1995;75:2220–32.
81. Trevisani F, De NS, Rapaccini G, Farinati F, Benvegnu L, Zoli M, Grazi GL, Del PP, Di N, Bernardi M. Semiannual and annual surveillance of cirrhotic patients for hepatocellular carcinoma: effects on cancer stage and patient survival (Italian experience). Am J Gastroenterol. 2002;97:734–44.

82. Yuen MF, Cheng CC, Lauder IJ, Lam SK, Ooi CG, Lai CL. Early detection of hepatocellular carcinoma increases the chance of treatment: Hong Kong experience. Hepatology. 2000;31:330–5.
83. Natsuizaka M, Omura T, Akaike T, Kuwata Y, Yamazaki K, Sato T, Karino Y, Toyota J, Suga T, Asaka M. Clinical features of hepatocellular carcinoma with extrahepatic metastases. J Gastroenterol Hepatol. 2005;20:1781–7.
84. Luo JC, Hwang SJ, Wu JC, Lai CR, Li CP, Chang FY, Chiang JH, Lui WY, Chu CW, Lee SD. Clinical characteristics and prognosis of hepatocellular carcinoma patients with paraneoplastic syndromes. Hepatogastroenterology. 2002;49:1315–9.
85. Zhang BH, Yang BH, Tang ZY. Randomized controlled trial of screening for hepatocellular carcinoma. J Cancer Res Clin Oncol. 2004;130: 417–22.
86. Singal AG, Pillai A, Tiro J. Early detection, curative treatment, and survival rates for hepatocellular carcinoma surveillance in patients with cirrhosis: a meta-analysis. PLoS Med. 2014;11:e1001624.
87. Sarasin FP, Giostra E, Hadengue A. Cost-effectiveness of screening for detection of small hepatocellular carcinoma in western patients with Child-Pugh class a cirrhosis. Am J Med. 1996;101:422–34.
88. Arguedas MR, Chen VK, Eloubeidi MA, Fallon MB. Screening for hepatocellular carcinoma in patients with hepatitis C cirrhosis: a cost-utility analysis. Am J Gastroenterol. 2003;98:679–90.
89. Lin OS, Keeffe EB, Sanders GD, Owens DK. Cost-effectiveness of screening for hepatocellular carcinoma in patients with cirrhosis due to chronic hepatitis C. Aliment Pharmacol Ther. 2004;19:1159–72.
90. Iwasaki M, Furuse J, Yoshino M, Ryu M, Moriyama N, Mukai K. Sonographic appearances of small hepatic nodules without tumor stain on contrast-enhanced computed tomography and angiography. J Clin Ultrasound. 1998;26:303–7.
91. Jeong YY, Mitchell DG, Kamishima T. Small (<20 mm) enhancing hepatic nodules seen on arterial phase MR imaging of the cirrhotic liver: clinical implications. AJR Am J Roentgenol. 2002;178:1327–34.
92. Forner A, Vilana R, Ayuso C, Bianchi L, Sole M, Ayuso JR, Boix L, Sala M, Varela M, Llovet JM, Bru C, Bruix J. Diagnosis of hepatic nodules 20 mm or smaller in cirrhosis: prospective validation of the noninvasive diagnostic criteria for hepatocellular carcinoma. Hepatology. 2008;47:97–104.
93. Marrero JA, Hussain HK, Nghiem HV, Umar R, Fontana RJ, Lok AS. Improving the prediction of hepatocellular carcinoma in cirrhotic patients with an arterially-enhancing liver mass. Liver Transpl. 2005;11:281–9.
94. Mueller GC, Hussain HK, Carlos RC, Nghiem HV, Francis IR. Effectiveness of MR imaging in characterizing small hepatic lesions: routine versus expert interpretation. AJR Am J Roentgenol. 2003;180:673–80.
95. Shimizu A, Ito K, Koike S, Fujita T, Shimizu K, Matsunaga N. Cirrhosis or chronic hepatitis: evaluation of small (< or = 2-cm) early-enhancing hepatic lesions with serial contrast-enhanced dynamic MR imaging. Radiology. 2003;226:550–5.
96. Taouli B, Goh JS, Lu Y, Qayyum A, Yeh BM, Merriman RB, Coakley FV. Growth rate of hepatocellular carcinoma: evaluation with serial computed tomography or magnetic resonance imaging. J Comput Assist Tomogr. 2005;29:425–9.
97. Leoni S, Piscaglia F, Golfieri R, Camaggi V, Vidili G, Pini P, Bolondi L. The impact of vascular and nonvascular findings on the noninvasive diagnosis of small hepatocellular carcinoma based on the EASL and AASLD criteria. Am J Gastroenterol. 2010;105:599–609.
98. Sangiovanni A, Manini MA, Iavarone M, Romeo R, Forzenigo LV, Fraquelli M, Massironi S, Della Corte C, Ronchi G, Rumi MG, Biondetti P, Colombo M. The diagnostic and economic impact of contrast imaging techniques in the diagnosis of small hepatocellular carcinoma in cirrhosis. Gut. 2010;59:638–44.
99. Serste T, Barrau V, Ozenne V, Vullierme MP, Bedossa P, Farges O, Valla DC, Vilgrain V, Paradis V, Degos F. Accuracy and disagreement of computed tomography and magnetic resonance imaging for the diagnosis of small hepatocellular carcinoma and dysplastic nodules: role of biopsy. Hepatology. 2012;55:800–6.
100. Burrel M, Llovet JM, Ayuso C, Iglesias C, Sala M, Miquel R, Caralt T, Ayuso JR, Sole M, Sanchez M, Bru C, Bruix J. MRI angiography is superior to helical CT for detection of HCC prior to liver transplantation: an explant correlation. Hepatology. 2003;38:1034–42.
101. Kang BK, Lim JH, Kim SH, Choi D, Lim HK, Lee WJ, Lee SJ. Preoperative depiction of hepatocellular carcinoma: ferumoxides-enhanced MR imaging versus triple-phase helical CT. Radiology. 2003;226:79–85.
102. Krinsky GA, Lee VS. MR imaging of cirrhotic nodules. Abdom Imaging. 2000;25:471–82.
103. Rode A, Bancel B, Douek P, Chevallier M, Vilgrain V, Picaud G, Henry L, Berger F, Bizollon T, Gaudin JL, Ducerf C. Small nodule detection in cirrhotic livers: evaluation with US, spiral CT, and MRI and correlation with pathologic examination of explanted liver. J Comput Assist Tomogr. 2001;25:327–36.
104. Stoker J, Romijn MG, de Man RA, Brouwer JT, Weverling GJ, van Muiswinkel JM, Zondervan PE, Lameris JS, Ijzermans JN. Prospective comparative study of spiral computer tomography and magnetic

resonance imaging for detection of hepatocellular carcinoma. Gut. 2002;51:105–7.
105. Gaiani S, Celli N, Piscaglia F, Cecilioni L, Losinno F, Giangregorio F, Mancini M, Pini P, Fornari F, Bolondi L. Usefulness of contrast-enhanced perfusional sonography in the assessment of hepatocellular carcinoma hypervascular at spiral computed tomography. J Hepatol. 2004;41:421–6.
106. Quaia E, Calliada F, Bertolotto M, Rossi S, Garioni L, Rosa L, Pozzi-Mucelli R. Characterization of focal liver lesions with contrast-specific US modes and a sulfur hexafluoride-filled microbubble contrast agent: diagnostic performance and confidence. Radiology. 2004;232:420–30.
107. Teefey SA, Hildeboldt CC, Dehdashti F, Siegel BA, Peters MG, Heiken JP, Brown JJ, McFarland EG, Middleton WD, Balfe DM, Ritter JH. Detection of primary hepatic malignancy in liver transplant candidates: prospective comparison of CT, MR imaging, US, and PET. Radiology. 2003;226:533–42.
108. Kelekis NL, Semelka RC, Worawattanakul S, de Lange EE, Ascher SM, Ahn IO, Reinhold C, Remer EM, Brown JJ, Bis KG, Woosley JT, Mitchell DG. Hepatocellular carcinoma in North America: a multiinstitutional study of appearance on T1-weighted, T2-weighted, and serial gadolinium-enhanced gradient-echo images. AJR Am J Roentgenol. 1998;170:1005–13.
109. Willatt JM, Hussain HK, Adusumilli S, Marrero JA. MR Imaging of hepatocellular carcinoma in the cirrhotic liver: challenges and controversies. Radiology. 2008;247:311–30.
110. Shinmura R, Matsui O, Kobayashi S, Terayama N, Sanada J, Ueda K, Gabata T, Kadoya M, Miyayama S. Cirrhotic nodules: association between MR imaging signal intensity and intranodular blood supply. Radiology. 2005;237:512–9.
111. Efremidis SC, Hytiroglou P. The multistep process of hepatocarcinogenesis in cirrhosis with imaging correlation. Eur Radiol. 2002;12:753–64.
112. Matsui O. Imaging of multistep human hepatocarcinogenesis by CT during intra-arterial contrast injection. Intervirology. 2004;47:271–6.
113. Hyodo T, Murakami T, Imai Y, Okada M, Hori M, Kagawa Y, Kogita S, Kumano S, Kudo M, Mochizuki T. Hypovascular nodules in patients with chronic liver disease: risk factors for development of hypervascular hepatocellular carcinoma. Radiology. 2013;266:480–90.
114. Takayasu K, Arii S, Sakamoto M, Matsuyama Y, Kudo M, Ichida T, Nakashima O, Matsui O, Izumi N, Ku Y, Kokudo N, Makuuchi M. Clinical implication of hypovascular hepatocellular carcinoma studied in 4,474 patients with solitary tumour equal or less than 3 cm. Liver Int. 2013;33:762–70.
115. Madan K, Kudo M, Fukuta N. Multistep progression from a hypovascular nodule to a nodule-in-nodule type hepatocellular carcinoma in hepatitis C-related cirrhosis. Indian J Gastroenterol. 2008;27:176.
116. Buscarini L, Fornari F, Bolondi L, Colombo P, Livraghi T, Magnolfi F, Rapaccini GL, Salmi A. Ultrasound-guided fine-needle biopsy of focal liver lesions: techniques, diagnostic accuracy and complications. A retrospective study on 2091 biopsies. J Hepatol. 1990;11:344–8.
117. Hertz G, Reddy VB, Green L, Spitz D, Massarani-Wafai R, Selvaggi SM, Kluskens L, Gattuso P. Fine-needle aspiration biopsy of the liver: a multicenter study of 602 radiologically guided FNA. Diagn Cytopathol. 2000;23:326–8.
118. Wang P, Meng ZQ, Chen Z, Lin JH, Ping B, Wang LF, Wang BH, Liu LM. Diagnostic value and complications of fine needle aspiration for primary liver cancer and its influence on the treatment outcome-a study based on 3011 patients in China. Eur J Surg Oncol. 2008;34:541–6.
119. Silva MA, Hegab B, Hyde C, Guo B, Buckels JA, Mirza DF. Needle track seeding following biopsy of liver lesions in the diagnosis of hepatocellular cancer: a systematic review and meta-analysis. Gut. 2008;57:1592–6.
120. Maturen KE, Nghiem HV, Marrero JA, Hussain HK, Higgins EG, Fox GA, Francis IR. Lack of tumor seeding of hepatocellular carcinoma after percutaneous needle biopsy using coaxial cutting needle technique. AJR Am J Roentgenol. 2006;187:1184–7.
121. Kobayashi M, Ikeda K, Hosaka T, Sezaki H, Someya T, Akuta N, Suzuki F, Suzuki Y, Saitoh S, Arase Y, Kumada H. Dysplastic nodules frequently develop into hepatocellular carcinoma in patients with chronic viral hepatitis and cirrhosis. Cancer. 2006;106:636–47.
122. Borzio M, Borzio F, Croce A, Sala M, Salmi A, Leandro G, Bruno S, Roncalli M. Ultrasonography-detected macroregenerative nodules in cirrhosis: a prospective study. Gastroenterology. 1997;112:1617–23.
123. Borzio M, Fargion S, Borzio F, Fracanzani AL, Croce AM, Stroffolini T, Oldani S, Cotichini R, Roncalli M. Impact of large regenerative, low grade and high grade dysplastic nodules in hepatocellular carcinoma development. J Hepatol. 2003;39:208–14.
124. Pathologic diagnosis of early hepatocellular carcinoma: a report of the international consensus group for hepatocellular neoplasia. Hepatology. 2009;49:658–64.
125. Park YN, Yang CP, Fernandez GJ, Cubukcu O, Thung SN, Theise ND. Neoangiogenesis and sinusoidal "capillarization" in dysplastic nodules of the liver. Am J Surg Pathol. 1998;22:656–62.
126. Watanabe S, Okita K, Harada T, Kodama T, Numa Y, Takemoto T, Takahashi T. Morphologic studies of the liver cell dysplasia. Cancer. 1983;51:2197–205.

127. Park YN, Kojiro M, Di Tommaso L, Dhillon AP, Kondo F, Nakano M, Sakamoto M, Theise ND, Roncalli M. Ductular reaction is helpful in defining early stromal invasion, small hepatocellular carcinomas, and dysplastic nodules. Cancer. 2007;109: 915–23.
128. Hytiroglou P. Morphological changes of early human hepatocarcinogenesis. Semin Liver Dis. 2004;24:65–75.
129. Hytiroglou P, Park YN, Krinsky G, Theise ND. Hepatic precancerous lesions and small hepatocellular carcinoma. Gastroenterol Clin North Am. 2007;36:867–87, vii.
130. Capurro M, Wanless IR, Sherman M, Deboer G, Shi W, Miyoshi E, Filmus J. Glypican-3: a novel serum and histochemical marker for hepatocellular carcinoma. Gastroenterology. 2003;125:89–97.
131. Di Tommaso L, Destro A, Seok JY, Balladore E, Terracciano L, Sangiovanni A, Iavarone M, Colombo M, Jang JJ, Yu E, Jin SY, Morenghi E, Park YN, Roncalli M. The application of markers (HSP70 GPC3 and GS) in liver biopsies is useful for detection of hepatocellular carcinoma. J Hepatol. 2009;50:746–54.
132. Di Tommaso L, Franchi G, Park YN, Fiamengo B, Destro A, Morenghi E, Montorsi M, Torzilli G, Tommasini M, Terracciano L, Tornillo L, Vecchione R, Roncalli M. Diagnostic value of HSP70, glypican 3, and glutamine synthetase in hepatocellular nodules in cirrhosis. Hepatology. 2007;45:725–34.
133. Garrido C, Gurbuxani S, Ravagnan L, Kroemer G. Heat shock proteins: endogenous modulators of apoptotic cell death. Biochem Biophys Res Commun. 2001;286:433–42.
134. Libbrecht L, Severi T, Cassiman D, Vander Borght S, Pirenne J, Nevens F, Verslype C, van Pelt J, Roskams T. Glypican-3 expression distinguishes small hepatocellular carcinomas from cirrhosis, dysplastic nodules, and focal nodular hyperplasia-like nodules. Am J Surg Pathol. 2006;30:1405–11.
135. Midorikawa Y, Ishikawa S, Iwanari H, Imamura T, Sakamoto H, Miyazono K, Kodama T, Makuuchi M, Aburatani H. Glypican-3, overexpressed in hepatocellular carcinoma, modulates FGF2 and BMP-7 signaling. Int J Cancer. 2003;103:455–65.
136. Tremosini S, Forner A, Boix L, Vilana R, Bianchi L, Reig M, Rimola J, Rodriguez-Lope C, Ayuso C, Sole M, Bruix J. Prospective validation of an immunohistochemical panel (glypican 3, heat shock protein 70 and glutamine synthetase) in liver biopsies for diagnosis of very early hepatocellular carcinoma. Gut. 2012;61:1481–7.
137. Llovet JM, Chen Y, Wurmbach E, Roayaie S, Fiel MI, Schwartz M, Thung SN, Khitrov G, Zhang W, Villanueva A, Battiston C, Mazzaferro V, Bruix J, Waxman S, Friedman SL. A molecular signature to discriminate dysplastic nodules from early hepatocellular carcinoma in HCV cirrhosis. Gastroenterology. 2006;131:1758–67.
138. Fleming ID. AJCC/TNM cancer staging, present and future. J Surg Oncol. 2001;77:233–6.
139. Marrero JA, Fontana RJ, Barrat A, Askari F, Conjeevaram HS, Su GL, Lok AS. Prognosis of hepatocellular carcinoma: comparison of 7 staging systems in an American cohort. Hepatology. 2005;41:707–16.
140. Cillo U, Vitale A, Grigoletto F, Farinati F, Brolese A, Zanus G, Neri D, Boccagni P, Srsen N, D'Amico F, Ciarleglio FA, Bridda A, D'Amico DF. Prospective validation of the barcelona clinic liver cancer staging system. J Hepatol. 2006;44:723–31.
141. Bruix J, Sherman M. Management of hepatocellular carcinoma: an update. Hepatology. 2011;53:1020–2.
142. Chen CH, Hu FC, Huang GT, Lee PH, Tsang YM, Cheng AL, Chen DS, Wang JD, Sheu JC. Applicability of staging systems for patients with hepatocellular carcinoma is dependent on treatment method–analysis of 2010 Taiwanese patients. Eur J Cancer. 2009;45:1630–9.
143. Trevisani F, Frigerio M, Santi V, Grignaschi A, Bernardi M. Hepatocellular carcinoma in non-cirrhotic liver: a reappraisal. Dig Liver Dis. 2010;42:341–7.
144. Bismuth H, Majno PE. Hepatobiliary surgery. J Hepatol. 2000;32:208–24.
145. Poon RT, Fan ST, Lo CM, Liu CL, Lam CM, Yuen WK, Yeung C, Wong J. Improving perioperative outcome expands the role of hepatectomy in management of benign and malignant hepatobiliary diseases: analysis of 1222 consecutive patients from a prospective database. Ann Surg. 2004;240:698–708; discussion 708–10.
146. Simons JP, Ng SC, Hill JS, Shah SA, Zhou Z, Tseng JF. In-hospital mortality from liver resection for hepatocellular carcinoma: a simple risk score. Cancer. 2010;116:1733–8.
147. Farges O, Malassagne B, Flejou JF, Balzan S, Sauvanet A, Belghiti J. Risk of major liver resection in patients with underlying chronic liver disease: a reappraisal. Ann Surg. 1999;229:210–5.
148. de Graaf W, van Lienden KP, van den Esschert JW, Bennink RJ, van Gulik TM. Increase in future remnant liver function after preoperative portal vein embolization. Br J Surg. 2011;98:825–34.
149. Farges O, Belghiti J, Kianmanesh R, Regimbeau JM, Santoro R, Vilgrain V, Denys A, Sauvanet A. Portal vein embolization before right hepatectomy: prospective clinical trial. Ann Surg. 2003;237:208–17.
150. Cucchetti A, Ercolani G, Vivarelli M, Cescon M, Ravaioli M, La Barba G, Zanello M, Grazi GL, Pinna AD. Impact of model for end-stage liver disease (MELD) score on prognosis after hepatectomy for hepatocellular carcinoma on cirrhosis. Liver Transpl. 2006;12:966–71.
151. Llovet JM, Fuster J, Bruix J. Intention-to-treat analysis of surgical treatment for early

hepatocellular carcinoma: resection versus transplantation. Hepatology. 1999;30:1434–40.
152. Bruix J, Castells A, Bosch J, Feu F, Fuster J, Garcia-Pagan JC, Visa J, Bru C, Rodes J. Surgical resection of hepatocellular carcinoma in cirrhotic patients: prognostic value of preoperative portal pressure. Gastroenterology. 1996;111:1018–22.
153. Ishizawa T, Hasegawa K, Kokudo N, Sano K, Imamura H, Beck Y, Sugawara Y, Makuuchi M. Risk factors and management of ascites after liver resection to treat hepatocellular carcinoma. Arch Surg. 2009;144:46–51.
154. Stremitzer S, Tamandl D, Kaczirek K, Maresch J, Abbasov B, Payer BA, Ferlitsch A, Gruenberger T. Value of hepatic venous pressure gradient measurement before liver resection for hepatocellular carcinoma. Br J Surg. 2011;98:1752–8.
155. Taketomi A, Kitagawa D, Itoh S, Harimoto N, Yamashita Y, Gion T, Shirabe K, Shimada M, Maehara Y. Trends in morbidity and mortality after hepatic resection for hepatocellular carcinoma: an institute's experience with 625 patients. J Am Coll Surg. 2007;204:580–7.
156. Ikai I, Arii S, Kojiro M, Ichida T, Makuuchi M, Matsuyama Y, Nakanuma Y, Okita K, Omata M, Takayasu K, Yamaoka Y. Reevaluation of prognostic factors for survival after liver resection in patients with hepatocellular carcinoma in a Japanese nationwide survey. Cancer. 2004;101:796–802.
157. Arii S, Yamaoka Y, Futagawa S, Inoue K, Kobayashi K, Kojiro M, Makuuchi M, Nakamura Y, Okita K, Yamada R. Results of surgical and nonsurgical treatment for small-sized hepatocellular carcinomas: a retrospective and nationwide survey in Japan. The liver cancer study group of Japan. Hepatology. 2000;32:1224–9.
158. Zhou XD, Tang ZY, Yang BH, Lin ZY, Ma ZC, Ye SL, Wu ZQ, Fan J, Qin LX, Zheng BH. Experience of 1000 patients who underwent hepatectomy for small hepatocellular carcinoma. Cancer. 2001;91:1479–86.
159. Kianmanesh R, Regimbeau JM, Belghiti J. Selective approach to major hepatic resection for hepatocellular carcinoma in chronic liver disease. Surg Oncol Clin N Am. 2003;12:51–63.
160. Poon RT. Optimal initial treatment for early hepatocellular carcinoma in patients with preserved liver function: transplantation or resection? Ann Surg Oncol. 2007;14:541–7.
161. Poon RT, Fan ST, Ng IO, Lo CM, Liu CL, Wong J. Different risk factors and prognosis for early and late intrahepatic recurrence after resection of hepatocellular carcinoma. Cancer. 2000;89:500–7.
162. Portolani N, Coniglio A, Ghidoni S, Giovanelli M, Benetti A, Tiberio GA, Giulini SM. Early and late recurrence after liver resection for hepatocellular carcinoma: prognostic and therapeutic implications. Ann Surg. 2006;243:229–35.
163. Samuel M, Chow PK, Chan Shih-Yen E, Machin D, Soo KC. Neoadjuvant and adjuvant therapy for surgical resection of hepatocellular carcinoma. Cochrane Database Syst Rev. 2009;CD001199.
164. Singal AK, Freeman DH Jr, Anand BS. Meta-analysis: interferon improves outcomes following ablation or resection of hepatocellular carcinoma. Aliment Pharmacol Ther. 2010;32:851–8.
165. Mazzaferro V, Regalia E, Doci R, Andreola S, Pulvirenti A, Bozzetti F, Montalto F, Ammatuna M, Morabito A, Gennari L. Liver transplantation for the treatment of small hepatocellular carcinomas in patients with cirrhosis. N Engl J Med. 1996;334:693–9.
166. Onaca N, Davis GL, Jennings LW, Goldstein RM, Klintmalm GB. Improved results of transplantation for hepatocellular carcinoma: a report from the international registry of hepatic tumors in liver transplantation. Liver Transpl. 2009;15:574–80.
167. Duffy JP, Sis A, Benjamin E, Watson M, Farmer DG, Ghobrial RM, Lipshutz G, Yersiz H, Lu DS, Lassman C, Tong MJ, Hiatt JR, Busuttil RW. Liver transplantation criteria for hepatocellular carcinoma should be expanded: a 22-year experience with 467 patients at UCLA. Ann Surg. 2007;246:502–9; discussion 509–11.
168. Onaca N, Davis GL, Goldstein RM, Jennings LW, Klintmalm GB. Expanded criteria for liver transplantation in patients with hepatocellular carcinoma: a report from the international registry of hepatic tumors in liver transplantation. Liver Transpl. 2007;13:391–9.
169. Yao FY, Xiao L, Bass NM, Kerlan R, Ascher NL, Roberts JP. Liver transplantation for hepatocellular carcinoma: validation of the UCSF-expanded criteria based on preoperative imaging. Am J Transpl. 2007;7:2587–96.
170. Yao FY, Ferrell L, Bass NM, Watson JJ, Bacchetti P, Venook A, Ascher NL, Roberts JP. Liver transplantation for hepatocellular carcinoma: expansion of the tumor size limits does not adversely impact survival. Hepatology. 2001;33:1394–403.
171. Volk ML, Vijan S, Marrero JA. A novel model measuring the harm of transplanting hepatocellular carcinoma exceeding Milan criteria. Am J Transpl. 2008;8:839–46.
172. Mazzaferro V, Bhoori S, Sposito C, Bongini M, Langer M, Miceli R, Mariani L. Milan criteria in liver transplantation for hepatocellular carcinoma: an evidence-based analysis of 15 years of experience. Liver Transpl. 2011;17(Suppl 2):S44–57.
173. Pelletier SJ, Fu S, Thyagarajan V, Romero-Marrero C, Batheja MJ, Punch JD, Magee JC, Lok AS, Fontana RJ, Marrero JA. An intention-to-treat analysis of liver transplantation for hepatocellular carcinoma using organ procurement transplant network data. Liver Transpl. 2009;15:859–68.

174. Parikh ND, Waljee AK, Singal AG. Downstaging hepatocellular carcinoma: a systematic review and pooled analysis. Liver Transpl. 2015;21:1142–52.
175. Yao FY, Kerlan RK Jr, Hirose R, Davern TJ 3rd, Bass NM, Feng S, Peters M, Terrault N, Freise CE, Ascher NL, Roberts JP. Excellent outcome following down-staging of hepatocellular carcinoma prior to liver transplantation: an intention-to-treat analysis. Hepatology. 2008;48:819–27.
176. Yao FY. Expanded criteria for hepatocellular carcinoma: down-staging with a view to liver transplantation–yes. Semin Liver Dis. 2006;26:239–47.
177. Lewandowski RJ, Kulik LM, Riaz A, Senthilnathan S, Mulcahy MF, Ryu RK, Ibrahim SM, Sato KT, Baker T, Miller FH, Omary R, Abecassis M, Salem R. A comparative analysis of transarterial downstaging for hepatocellular carcinoma: chemoembolization versus radioembolization. Am. J. Transpl. 9:1920–8.
178. Maddala YK, Stadheim L, Andrews JC, Burgart LJ, Rosen CB, Kremers WK, Gores G. Drop-out rates of patients with hepatocellular cancer listed for liver transplantation: outcome with chemoembolization. Liver Transpl. 2004;10:449–55.
179. Vitale A, Boccagni P, Brolese A, Neri D, Srsen N, Zanus G, Pagano D, Pauletto A, Bonsignore P, Scopelliti M, D'Amico FE, Ometto G, Polacco M, Burra P, Gambato M, Feltracco P, Romano A, Cillo U. Progression of hepatocellular carcinoma before liver transplantation: dropout or liver transplantation? Transpl Proc. 2009;41:1264–7.
180. Thuluvath PJ, Guidinger MK, Fung JJ, Johnson LB, Rayhill SC, Pelletier SJ. Liver transplantation in the United States, 1999–2008. Am J Transpl. 2010;10:1003–19.
181. Lesurtel M, Mullhaupt B, Pestalozzi BC, Pfammatter T, Clavien PA. Transarterial chemoembolization as a bridge to liver transplantation for hepatocellular carcinoma: an evidence-based analysis. Am J Transpl. 2006;6:2644–50.
182. Lencioni R, Crocetti L. Radiofrequency ablation of liver cancer. Tech Vasc Interv Radiol. 2007;10:38–46.
183. Choi D, Lim HK, Rhim H, Kim YS, Lee WJ, Paik SW, Koh KC, Lee JH, Choi MS, Yoo BC. Percutaneous radiofrequency ablation for early-stage hepatocellular carcinoma as a first-line treatment: long-term results and prognostic factors in a large single-institution series. Eur Radiol. 2007;17:684–92.
184. Tateishi R, Shiina S, Teratani T, Obi S, Sato S, Koike Y, Fujishima T, Yoshida H, Kawabe T, Omata M. Percutaneous radiofrequency ablation for hepatocellular carcinoma. An analysis of 1000 cases. Cancer. 2005;103:1201–9.
185. N'Kontchou G, Mahamoudi A, Aout M, Ganne-Carrie N, Grando V, Coderc E, Vicaut E, Trinchet JC, Sellier N, Beaugrand M, Seror O. Radiofrequency ablation of hepatocellular carcinoma: long-term results and prognostic factors in 235 Western patients with cirrhosis. Hepatology. 2009;50:1475–83.
186. Shiina S, Tateishi R, Arano T, Uchino K, Enooku K, Nakagawa H, Asaoka Y, Sato T, Masuzaki R, Kondo Y, Goto T, Yoshida H, Omata M, Koike K. Radiofrequency ablation for hepatocellular carcinoma: 10-year outcome and prognostic factors. Am J Gastroenterol. 2012;107:569–77; quiz 578.
187. Chen MS, Li JQ, Zheng Y, Guo RP, Liang HH, Zhang YQ, Lin XJ, Lau WY. A prospective randomized trial comparing percutaneous local ablative therapy and partial hepatectomy for small hepatocellular carcinoma. Ann Surg. 2006;243:321–8.
188. Huang GT, Lee PH, Tsang YM, Lai MY, Yang PM, Hu RH, Chen PJ, Kao JH, Sheu JC, Lee CZ, Chen DS. Percutaneous ethanol injection versus surgical resection for the treatment of small hepatocellular carcinoma: a prospective study. Ann Surg. 2005;242:36–42.
189. Lu MD, Kuang M, Liang LJ, Xie XY, Peng BG, Liu GJ, Li DM, Lai JM. Li SQ [Surgical resection versus percutaneous thermal ablation for early-stage hepatocellular carcinoma: a randomized clinical trial]. Zhonghua Yi Xue Za Zhi. 2006;86:801–5.
190. Cho YK, Rhim H, Noh S. Radiofrequency ablation versus surgical resection as primary treatment of hepatocellular carcinoma meeting the Milan criteria: a systematic review. J Gastroenterol Hepatol. 2011;26:1354–60.
191. Molinari M, Helton S. Hepatic resection versus radiofrequency ablation for hepatocellular carcinoma in cirrhotic individuals not candidates for liver transplantation: a Markov model decision analysis. Am J Surg. 2009;198:396–406.
192. Iannitti DA, Dupuy DE, Mayo-Smith WW, Murphy B. Hepatic radiofrequency ablation. Arch Surg. 2002;137:422–6; discussion 427.
193. Pompili M, Mirante VG, Rondinara G, Fassati LR, Piscaglia F, Agnes S, Covino M, Ravaioli M, Fagiuoli S, Gasbarrini G, Rapaccini GL. Percutaneous ablation procedures in cirrhotic patients with hepatocellular carcinoma submitted to liver transplantation: assessment of efficacy at explant analysis and of safety for tumor recurrence. Liver Transpl. 2005;11:1117–26.
194. Mulier S, Ni Y, Jamart J, Ruers T, Marchal G, Michel L. Local recurrence after hepatic radiofrequency coagulation: multivariate meta-analysis and review of contributing factors. Ann Surg. 2005;242:158–71.
195. Veltri A, Moretto P, Doriguzzi A, Pagano E, Carrara G, Gandini G. Radiofrequency thermal ablation (RFA) after transarterial chemoembolization (TACE) as a combined therapy for unresectable non-early hepatocellular carcinoma (HCC). Eur Radiol. 2006;16:661–9.
196. Kim SW, Rhim H, Park M, Kim H, Kim YS, Choi D, Lim HK. Percutaneous radiofrequency

ablation of hepatocellular carcinomas adjacent to the gallbladder with internally cooled electrodes: assessment of safety and therapeutic efficacy. Korean J Radiol. 2009;10:366–76.
197. Komorizono Y, Oketani M, Sako K, Yamasaki N, Shibatou T, Maeda M, Kohara K, Shigenobu S, Ishibashi K, Arima T. Risk factors for local recurrence of small hepatocellular carcinoma tumors after a single session, single application of percutaneous radiofrequency ablation. Cancer. 2003;97:1253–62.
198. Llovet JM, Vilana R, Bru C, Bianchi L, Salmeron JM, Boix L, Ganau S, Sala M, Pages M, Ayuso C, Sole M, Rodes J, Bruix J. Increased risk of tumor seeding after percutaneous radiofrequency ablation for single hepatocellular carcinoma. Hepatology. 2001;33:1124–9.
199. Lu DS, Yu NC, Raman SS, Limanond P, Lassman C, Murray K, Tong MJ, Amado RG, Busuttil RW. Radiofrequency ablation of hepatocellular carcinoma: treatment success as defined by histologic examination of the explanted liver. Radiology. 2005;234:954–60.
200. Livraghi T, Solbiati L, Meloni MF, Gazelle GS, Halpern EF, Goldberg SN. Treatment of focal liver tumors with percutaneous radio-frequency ablation: complications encountered in a multicenter study. Radiology. 2003;226:441–51.
201. Shiina S, Teratani T, Obi S, Sato S, Tateishi R, Fujishima T, Ishikawa T, Koike Y, Yoshida H, Kawabe T, Omata M. A randomized controlled trial of radiofrequency ablation with ethanol injection for small hepatocellular carcinoma. Gastroenterology. 2005;129:122–30.
202. Giorgio A, Tarantino L, de Stefano G, Coppola C, Ferraioli G. Complications after percutaneous saline-enhanced radiofrequency ablation of liver tumors: 3-year experience with 336 patients at a single center. AJR Am J Roentgenol. 2005;184:207–11.
203. Seki T, Wakabayashi M, Nakagawa T, Itho T, Shiro T, Kunieda K, Sato M, Uchiyama S, Inoue K. Ultrasonically guided percutaneous microwave coagulation therapy for small hepatocellular carcinoma. Cancer. 1994;74:817–25.
204. Sato M, Watanabe Y, Ueda S, Iseki S, Abe Y, Sato N, Kimura S, Okubo K, Onji M. Microwave coagulation therapy for hepatocellular carcinoma. Gastroenterology. 1996;110:1507–14.
205. Boutros C, Somasundar P, Garrean S, Saied A, Espat NJ. Microwave coagulation therapy for hepatic tumors: review of the literature and critical analysis. Surg Oncol. 2010;19:e22–32.
206. Shibata T, Iimuro Y, Yamamoto Y, Maetani Y, Ametani F, Itoh K, Konishi J. Small hepatocellular carcinoma: comparison of radio-frequency ablation and percutaneous microwave coagulation therapy. Radiology. 2002;223:331–7.
207. A comparison of lipiodol chemoembolization and conservative treatment for unresectable hepatocellular carcinoma. Groupe d'Etude et de Traitement du Carcinome Hepatocellulaire. N Engl J Med. 1995;332:1256–61.
208. Bruix J, Llovet JM. Two decades of advances in hepatocellular carcinoma research. Semin Liver Dis. 2010;30:1–2.
209. Llovet JM, Real MI, Montana X, Planas R, Coll S, Aponte J, Ayuso C, Sala M, Muchart J, Sola R, Rodes J, Bruix J. Arterial embolisation or chemoembolisation versus symptomatic treatment in patients with unresectable hepatocellular carcinoma: a randomised controlled trial. Lancet. 2002;359:1734–9.
210. Chung GE, Lee JH, Kim HY, Hwang SY, Kim JS, Chung JW, Yoon JH, Lee HS, Kim YJ. Transarterial chemoembolization can be safely performed in patients with hepatocellular carcinoma invading the main portal vein and may improve the overall survival. Radiology. 2011;258:627–34.
211. Yamada R, Sato M, Kawabata M, Nakatsuka H, Nakamura K, Takashima S. Hepatic artery embolization in 120 patients with unresectable hepatoma. Radiology. 1983;148:397–401.
212. Pomoni M, Malagari K, Moschouris H, Spyridopoulos TN, Dourakis S, Kornezos J, Kelekis A, Thanos L, Chatziioanou A, Hatjimarkou I, Marinis A, Koskinas J, Kelekis D. Post embolization syndrome in doxorubicin eluting chemoembolization with DC bead. Hepatogastroenterology. 2012;59:820–5.
213. Varela M, Real MI, Burrel M, Forner A, Sala M, Brunet M, Ayuso C, Castells L, Montana X, Llovet JM, Bruix J. Chemoembolization of hepatocellular carcinoma with drug eluting beads: efficacy and doxorubicin pharmacokinetics. J Hepatol. 2007;46:474–81.
214. Lammer J, Malagari K, Vogl T, Pilleul F, Denys A, Watkinson A, Pitton M, Sergent G, Pfammatter T, Terraz S, Benhamou Y, Avajon Y, Gruenberger T, Pomoni M, Langenberger H, Schuchmann M, Dumortier J, Mueller C, Chevallier P, Lencioni R. Prospective randomized study of doxorubicin-eluting-bead embolization in the treatment of hepatocellular carcinoma: results of the PRECISION V study. Cardiovasc Intervent Radiol. 2010;33:41–52.
215. Malagari K, Pomoni M, Kelekis A, Pomoni A, Dourakis S, Spyridopoulos T, Moschouris H, Emmanouil E, Rizos S, Kelekis D. Prospective randomized comparison of chemoembolization with doxorubicin-eluting beads and bland embolization with BeadBlock for hepatocellular carcinoma. Cardiovasc Intervent Radiol. 2010;33:541–51.
216. Burrel M, Reig M, Forner A, Barrufet M, de Lope CR, Tremosini S, Ayuso C, Llovet JM, Real MI, Bruix J. Survival of patients with hepatocellular carcinoma treated by transarterial

chemoembolisation (TACE) using drug eluting beads. Implications for clinical practice and trial design. J Hepatol. 2012;56:1330–5.
217. Zhu AX. Systemic treatment of hepatocellular carcinoma: dawn of a new era? Ann Surg Oncol. 2010;17:1247–56.
218. Llovet JM, Ricci S, Mazzaferro V, Hilgard P, Gane E, Blanc JF, de Oliveira AC, Santoro A, Raoul JL, Forner A, Schwartz M, Porta C, Zeuzem S, Bolondi L, Greten TF, Galle PR, Seitz JF, Borbath I, Haussinger D, Giannaris T, Shan M, Moscovici M, Voliotis D, Bruix J. Sorafenib in advanced hepatocellular carcinoma. N Engl J Med. 2008;359:378–90.
219. Cheng AL, Kang YK, Chen Z, Tsao CJ, Qin S, Kim JS, Luo R, Feng J, Ye S, Yang TS, Xu J, Sun Y, Liang H, Liu J, Wang J, Tak WY, Pan H, Burock K, Zou J, Voliotis D, Guan Z. Efficacy and safety of sorafenib in patients in the Asia-Pacific region with advanced hepatocellular carcinoma: a phase III randomised, double-blind, placebo-controlled trial. Lancet Oncol. 2009;10:25–34.
220. Lencioni R, Fau-Kudo M, Kudo M, Fau-Ye SL, Ye Sl, Fau-Bronowicki JP, Bronowicki Jp, Fau-Chen XP, Chen Xp, Fau-Dagher L, Dagher L, Fau-Furuse J, Furuse J, Fau-Geschwind JF, Geschwind Jf, Fau-Ladron de Guevara L, Ladron de Guevara L, Fau-Papandreou C, Papandreou C, Fau-Sanyal AJ, Sanyal Aj, Fau-Takayama T, Takayama T, Fau-Yoon SK, Yoon Sk, Fau-Nakajima K, Nakajima K, Fau-Cihon F, Cihon F, Fau-Heldner S, Heldner S, Fau-Marrero JA, Marrero JA. First interim analysis of the GIDEON (Global Investigation of therapeutic decisions in hepatocellular carcinoma and of its treatment with sorafeNib) non-interventional study. Int J Clin Pract. 2012;66 (7):675–83.
221. Worns MA, Weinmann A, Pfingst K, Schulte-Sasse C, Messow CM, Schulze-Bergkamen H, Teufel A, Schuchmann M, Kanzler S, Duber C, Otto G, Galle PR. Safety and efficacy of sorafenib in patients with advanced hepatocellular carcinoma in consideration of concomitant stage of liver cirrhosis. J Clin Gastroenterol. 2009;43:489–95.
222. Cheng A, Kang YK, Lin D, et al. Phase III trial of sunitinib (Su) versus sorafenib (So) in advanced hepatocellular carcinoma (HCC). J Clin Oncol. 2011;29S:Abstract 4000.
223. Finn RS, Kang YK, Mulcahy M, Polite BN, Lim HY, Walters I, Baudelet C, Manekas D, Park JW. Phase II, open-label study of brivanib as second-line therapy in patients with advanced hepatocellular carcinoma. Clin Cancer Res. 2012;18:2090–8.
224. Park JW, Finn RS, Kim JS, Karwal M, Li RK, Ismail F, Thomas M, Harris R, Baudelet C, Walters I, Raoul JL. Phase II, open-label study of brivanib as first-line therapy in patients with advanced hepatocellular carcinoma. Clin Cancer Res. 2011;17:1973–83.
225. Ang C, O'Reilly EM, Abou-Alfa GK. Targeted agents and systemic therapy in hepatocellular carcinoma. Recent Results Cancer Res. 2013;190:225–46.
226. Kaseb AO, Garrett-Mayer E, Morris JS, Xiao L, Lin E, Onicescu G, Hassan MM, Hassabo HM, Iwasaki M, Deaton FL, Abbruzzese JL, Thomas MB. Efficacy of bevacizumab plus erlotinib for advanced hepatocellular carcinoma and predictors of outcome: final results of a phase II trial. Oncology. Volume 82. Switzerland: Basel. 2012;67–74.
227. O'Neil BH, Goff LW, Kauh JS, Strosberg JR, Bekaii-Saab TS, Lee RM, Kazi A, Moore DT, Learoyd M, Lush RM, Sebti SM, Sullivan DM. Phase II study of the mitogen-activated protein kinase 1/2 inhibitor selumetinib in patients with advanced hepatocellular carcinoma. J Clin Oncol. 2011;29:2350–6.
228. Philip PA, Mahoney MR, Holen KD, Northfelt DW, Pitot HC, Picus J, Flynn PJ, Erlichman C. Phase 2 study of bevacizumab plus erlotinib in patients with advanced hepatocellular cancer. Cancer. 2012;118:2424–30.
229. Siegel AB, Cohen EI, Ocean A, Lehrer D, Goldenberg A, Knox JJ, Chen H, Clark-Garvey S, Weinberg A, Mandeli J, Christos P, Mazumdar M, Popa E, Brown RS Jr, Rafii S, Schwartz JD. Phase II trial evaluating the clinical and biologic effects of bevacizumab in unresectable hepatocellular carcinoma. J Clin Oncol. 2008;26:2992–8.
230. Thomas MB, Morris JS, Chadha R, Iwasaki M, Kaur H, Lin E, Kaseb A, Glover K, Davila M, Abbruzzese J. Phase II trial of the combination of bevacizumab and erlotinib in patients who have advanced hepatocellular carcinoma. J Clin Oncol. 2009;27:843–50 (United States).
231. Siegel AB, Cohen EI, Ocean A, Lehrer D, Goldenberg A, Knox JJ, Chen H, Clark-Garvey S, Weinberg A, Mandeli J, Christos P, Mazumdar M, Popa E, Brown RS, Jr., Rafii S, Schwartz JD. Phase II trial evaluating the clinical and biologic effects of bevacizumab in unresectable hepatocellular carcinoma. J Clin Oncol. 2008;26:2992–8 (United States).
232. Santoro A, Rimassa L, Borbath I, Daniele B, Salvagni S, Van Laethem JL, Van Vlierberghe H, Trojan J, Kolligs FT, Weiss A, Miles S, Gasbarrini A, Lencioni M, Cicalese L, Sherman M, Gridelli C, Buggisch P, Gerken G, Schmid RM, Boni C, Personeni N, Hassoun Z, Abbadessa G, Schwartz B, Von Roemeling R, Lamar ME, Chen Y, Porta C. Tivantinib for second-line treatment of advanced hepatocellular carcinoma: a randomised, placebo-controlled phase 2 study. Lancet Oncol. 2013;14:55–63.
233. El-Khoueiry AB, Melero I, Crocenzi T, Welling T, Yau TC. Phase I/II safety and antitumor activity of nivolumab in patients with advanced hepatocellular carcinoma (HCC): CA209–040. J Clin Oncol. 2015;33:LBA101.

234. Singal AG, Waljee AK, Patel N, Chen EY, Tiro JA, Marrero JA, Yopp AC. Therapeutic delays lead to worse survival among patients with hepatocellular carcinoma. J Natl Compr Canc Netw. 2013;11:1101–8.
235. Tan D, Yopp A, Beg MS, Gopal P, Singal AG. Meta-analysis: underutilisation and disparities of treatment among patients with hepatocellular carcinoma in the United States. Aliment Pharmacol Ther. 2013;38:703–12.
236. Yopp AC, Mansour JC, Beg MS, Arenas J, Trimmer C, Reddick M, Pedrosa I, Khatri G, Yakoo T, Meyer JJ, Shaw J, Marrero JA, Singal AG. Establishment of a multidisciplinary hepatocellular carcinoma clinic is associated with improved clinical outcome. Ann Surg Oncol. 2014;21:1287–95.
237. Itamoto T, Nakahara H, Tashiro H, Ohdan H, Hino H, Ochi M, et al. Indications of partial hepatectomy for transplantable hepatocellular carcinoma with compensated cirrhosis. Am J Surg. 2005;189:167–72.
238. Poon RT, Fan ST, Lo CM, Liu CL, Wong J. Difference in tumor invasiveness in cirrhotic patients with hepatocellular carcinoma fulfilling the Milan criteria treated by resection and transplantation: impact on long-term survival. Ann Surg. 2007;245:51–8.
239. Taura K, Ikai I, Hatano E, Yasuchika K, Nakajima A, Tada M, et al. Influence of coexisting cirrhosis on outcomes after partial hepatic resection for hepatocellular carcinoma fulfilling the Milan criteria: an analysis of 293 patients. Surgery. 2007;142:685–94.
240. Kamiyama T, Nakanishi K, Yokoo H, Kamachi H, Tahara M, Suzuki T, et al. Recurrence patterns after hepatectomy of hepatocellular carcinoma: implication of Milan criteria utilization. Ann Surg Oncol. 2009;16:1560–71.
241. Park YK, Kim BW, Wang HJ, Kim MW. Hepatic resection for hepatocellular carcinoma meeting Milan criteria in child–turcotte–pugh class a patients with cirrhosis. Transpl Proc. 2009;41:1691–7.
242. Huang J, Yan L, Cheng Z, Wu H, Du L, Wang J, et al. A randomized trial comparing radiofrequency ablation and surgical resection for HCC conforming to the Milan criteria. Ann Surg. 2010;252:903–12.
243. Sakaguchi T, Suzuki S, Morita Y, Oishi K, Suzuki A, Fukumoto K, et al. Impact of the preoperative des-gamma-carboxy prothrombin level on prognosis after hepatectomy for hepatocellular carcinoma meeting the Milan criteria. Surg Today. 2010;40:638–45.
244. Zhou J, Wang Z, Qiu SJ, Huang XW, Sun J, Gu W, et al. Surgical treatment for early hepatocellular carcinoma: comparison of resection and liver transplantation. J Cancer Res Clin Oncol. 2010;136:1453–60.
245. Mazzaferro V, Regalia E, Doci R, Andreola S, Pulvirenti A, Bozzetti F, Montalto F, Ammatuna M, Morabito A, Gennari L. Liver transplantation for the treatment of small hepatocellular carcinomas in patients with cirrhosis. N Engl J Med. 1996;334:693–9.
246. Herrero JI, Sangro B, Quiroga J, Pardo F, Herraiz M, Cienfuegos JA, Prieto J. Influence of tumor characteristics on the outcome of liver transplantation among patients with liver cirrhosis and hepatocellular carcinoma. Liver Transpl. 2001;7:631–6.
247. Todo S, Furukawa H, Japanese Study Group on Organ Transplantation. Living donor liver transplantation for adult patients with hepatocellular carcinoma: experience in Japan. Ann Surg. 2004;240:451–9.
248. Pelletier SJ1, Fu S, Thyagarajan V, Romero-Marrero C, Batheja MJ, Punch JD, Magee JC, Lok AS, Fontana RJ, Marrero JA. An intention-to-treat analysis of liver transplantation for hepatocellular carcinoma using organ procurement transplant network data. Liver Transpl. 2009 Aug;15(8):859–68.
249. Lencioni R, Cioni D, Crocetti L, et al. Early-stage hepatocellular carcinoma in patients with cirrhosis: long-term results of percutaneous image-guided radiofrequency ablation. Radiology. 2005;234:961–7.
250. Tateishi R, Shiina S, Teratani T, et al. Percutaneous radiofrequency ablation for hepatocellular carcinoma. An analysis of 1000 cases. Cancer. 2005;103:1201–9.
251. Chen MH, Yan K, Yang W, et al. Long term (5 years) outcome of radiofrequency ablation for hepatocellular carcinoma in 256 cases. Beijing Da Xue Xue Bao. 2005;37:671–2.
252. Choi D, Lim HK, Rhim H, et al. Percutaneous radiofrequency ablation for early-stage hepatocellular carcinoma as a first-line treatment: long-term results and prognostic factors in a large single-institution series. Eur Radiol. 2007;17:684–92.
253. Livraghi T, Meloni F, Di Stasi M, et al. Sustained complete response and complications rates after radiofrequency ablation of very early hepatocellular carcinoma in cirrhosis: Is resection still the treatment of choice? Hepatology. 2008;47:82–9.
254. N'Kontchou G, Mahamoudi A, Aout M, et al. Radiofrequency ablation of hepatocellular carcinoma: long-term results and prognostic factors in 235 Western patients with cirrhosis. Hepatology. 2009;50:1475–83.
255. Pelletier G, Roche A, Ink O, Anciaux ML, Derhy S, Rougier P, Lenoir C, et al. A randomized trial of hepatic arterial chemoembolization in patients with unresectable hepatocellular carcinoma. J Hepatol. 1990;11:181–4.
256. Group d'Etude et de Traitment du Carcinome Hépatocellulaire. A comparison of lipiodol chemoembolization and conservative treatment for unresectable hepatocellular carcinoma. N Engl J Med. 1995;332:1256–61.

257. Bruix J, Llovet JM, Castells A, Montana X, Bru C, Ayuso MC, Vilana R, et al. Transarterial embolization versus symptomatic treatment in patients with advanced hepatocellular carcinoma: results of a randomized, controlled trial in a single institution. Hepatology. 1998;27:1578–83.
258. Pelletier G, Ducreux M, Gay F, Luboinski M, Hagege H, Dao T, Van Steenbergen W, et al. Treatment of unresectable hepatocellular carcinoma with lipiodol chemoembolization: a multicenter randomized trial. J Hepatol. 1998;29:129–34.
259. Lo CM, Ngan H, Tso WK, Liu CL, Lam CM, Poon RT, Fan ST, et al. Randomized controlled trial of transarterial lipiodol chemoembolization for unresectable hepatocellular carcinoma. Hepatology. 2002;35:1164–71.
260. Llovet JM, Real MI, Montana X, Planas R, Coll S, Aponte J, Ayuso C, et al. Arterial embolisation or chemoembolisation versus symptomatic treatment in patients with unresectable hepatocellular carcinoma: a randomized controlled trial. Lancet. 2002;359:1734–9.

Radiation Therapy for Hepatocellular Carcinoma: Clinical Data

14

Erqi L. Pollom, MD, Yushen Qian, MD, Julie L. Koenig, BS, Albert C. Koong, MD, PhD and Daniel T. Chang, MD

Abbreviations	
BCLC	Barcelona clinic liver cancer
BED	Biological effective dose
EBRT	External beam radiotherapy
FACT-Hep	Functional assessment of cancer therapy—Hepatobiliary cancer
FFLP	Freedom from local progression
iBR	Interstitial brachytherapy
HCC	Hepatocellular carcinoma
HDR	High-dose-rate
GI	Gastrointestinal
MTD	Maximum tolerated dose
NTCP	Normal tissue complication probability
PMH	Princess Margaret hospital
PVT	Portal vein thrombus

E.L. Pollom · Y. Qian · D.T. Chang (✉)
Department of Radiation Oncology,
Stanford Healthcare, 875 Blake Wilbur Drive,
MC 5847, Stanford, CA 94305-5847, USA
e-mail: dtchang@stanford.edu

E.L. Pollom
e-mail: erqiliu@stanford.edu

Y. Qian
e-mail: yushenq@stanford.edu

J.L. Koenig
Stanford University School of Medicine,
566 Arguello Way, Stanford, CA 94305, USA
e-mail: jlkoenig@stanford.edu

A.C. Koong
Radiation Oncology, Stanford University,
300 Pasteur Drive, Stanford, CA 94305, USA
e-mail: akoong@stanford.edu

J. Meyer and T.E. Schefter (eds.), *Radiation Therapy for Liver Tumors*,
DOI 10.1007/978-3-319-54531-8_14

TARE	Transarterial radioembolization
RBE	Relative biological effectiveness
REILD	TARE-induced liver disease
RFA	Radiofrequency ablation
RILD	Radiation induced liver disease
RT	Radiotherapy
SBRT	Stereotactic body radiotherapy
SABR	Stereotactic ablative radiotherapy
TACE	Transarterial chemoembolization
TTP	Time to progression

14.1 Introduction

The burden of liver cancer is growing, with liver cancer deaths increasing at the highest rate of all cancers among both men and women [1]. Hepatocellular carcinoma (HCC), the most common primary liver cancer, represents a distinct clinical challenge because of its unique etiology, natural history, sensitivity to local therapies, and specific disease management guidelines and algorithms [2]. Historically, the role of radiation therapy in the treatment of unresectable HCC was limited due to low radiation tolerance of the whole liver and perceived radioresistance of HCC. However, better understanding of liver tolerance and recent advances in radiation planning and delivery technology have facilitated the safe delivery of higher and more effective doses. As a noninvasive treatment modality, radiation can target lesions that may not be amenable to other local-regional therapies due to tumor size, number, location, or the presence of vascular invasion. The promising results with early experiences of fractionated, conformal radiotherapy have led to the development of more dose-escalated regimens through stereotactic body radiotherapy (SBRT) and charged particle therapy. Radiation can also be delivered to HCC lesions using brachytherapy and trans-arterial radioembolization techniques. Finally, there are exciting possibilities with combining these various radiation approaches with other regional and systemic treatment modalities for improved efficacy.

14.2 Clinical Applications

The general treatment strategy for HCC is based on overall size of the tumor, number of tumor nodules, underlying liver function, and general health of the patient. Surgery, either through resection or liver transplantation, is curative; yet less than a third of patients with HCC are eligible candidates [3]. Therefore, a number of liver-directed therapies are available for organ-confined disease. Inoperable patients are typically managed with local-regional therapies including radiofrequency ablation (RFA) and transarterial chemoembolization (TACE). However, these modalities may not be appropriate under certain scenarios that may represent opportunities for radiation therapy to establish a role. For instance, larger tumors are associated with high rates of local recurrence after RFA [4, 5]. In addition, RFA may not be suitable for tumors adjacent to the liver edge or visceral organs, due to the risk of diaphragmatic injury [6] and intraperitoneal seeding [7], and is associated with high recurrence rates for lesions near large blood vessels due to the heat sink effect [8]. In addition to tumor size, the presence of portal vein thrombus can be a relative contraindication for TACE.

Figure 13.4 shows the Barcelona Clinic Liver Cancer staging system, which provides a guideline for various therapies [9]. Though radiotherapy is not included, there is growing literature that it may play an important role in the management of this disease. For early stage disease,

radiotherapy could be used as bridge therapy for patients awaiting liver transplant. For intermediate-stage disease, radiation can have an ablative role in definitive treatment or for possible tumor downstaging for transplant or resection eligibility. In the advanced setting, radiation can be an important treatment option for palliation. This chapter provides a summary of the clinical data for radiation therapy, including fractionated external beam radiation therapy (EBRT), stereotactic body radiotherapy (SBRT), particle therapy, brachytherapy, and radioembolization, and discusses results of radiation in various clinical scenarios.

14.3 Radiation Modalities

14.3.1 Fractionated External Beam Radiotherapy

Historically, external beam radiation did not play a major role for definitive treatment of intrahepatic tumors because of concerns for radiation-associated liver disease (RILD). However, advances in imaging techniques, three-dimensional radiation planning, respiratory motion management, and image-guided radiotherapy, as well as improved understanding of radiation-associated liver toxicity through the development of the normal tissue complication probability (NTCP) model have led to renewed interest in radiotherapy in HCC. Table 14.1 summarizes select EBRT clinical series.

The University of Michigan demonstrated in a series of prospective studies [10–13] that high dose, fractionated conformal radiation could be delivered to focal liver lesions using an NTCP model to maximize dose on an individual basis [14]. Patients were treated with 60–90 Gy in 1.5 Gy fractions twice daily with concurrent hepatic artery floxuridine, with the radiation dose based on the amount of normal liver that could be spared without exceeding a 5–20% risk of RILD. The median survival of patients treated on this study was 15.2 months, which was superior compared to historical controls. At a median follow-up of 26 months in living patients, there was 21% grade 3 toxicity, 9% grade 4 toxicity, and one treatment-related death due to RILD associated with this intense regimen. Total dose was the only predictor of survival, as patients receiving ≥ 75 Gy (upper quartile) had a better median survival of 23.9 months compared to those receiving <75 Gy (median survival 14.9 months). In addition, the pattern of failure observed in the trial was primarily local, which, along with the finding that survival was dose-dependent, suggested that there was potential for improved outcomes through further intensification of local therapy.

A phase II trial from France subsequently reported promising results with high-dose three-dimensional radiotherapy (66 Gy in 33 fractions) in Child–Pugh A/B cirrhotic patients with small HCCs who were not eligible for surgical treatment [15]. Twenty patients (80%) had a complete response, three patients (12%) had a partial response, and two patients (8%) had stable disease after treatment. At a median follow-up of 29 months, local control was 78%, with the majority of recurrences occurring outside of the irradiated volume. While Child–Pugh A patients tolerated treatment well, with 19% developing asymptomatic grade 3 toxicities, Child–Pugh B patients experienced more toxicity, with 22% developing grade 4 toxicities.

Numerous studies have also been published from Asia, where the incidence of HCC is higher, demonstrating the feasibility and efficacy of radiation dose-escalation in the treatment of HCC. In a large multicenter, retrospective series from Korea, 398 patients were treated with a median biological effective dose (BED), assuming α/β ratio of 10 Gy, of 53.1 Gy (range 4.2–124.8 Gy). The majority of patients had Child–Pugh A cirrhosis (73.9%) while 22.1% of patients had Child–Pugh B cirrhosis. The median survival time of all patients was 12 months. There was no grade 3 or higher toxicity. Higher doses were also associated with improved 2-year survival rate in this series: 31% for patients who received ≥ 53.1 Gy versus 22% for those who received lower doses [16]. In a retrospective series from China, 128 patients with unresectable HCC were treated with hypofractionated 3D-conformal radiotherapy to 40–60 Gy

with 3–5 Gy per fraction. The majority of patients had Child–Pugh A cirrhosis (84.4%) while 15.6% of patients had Child–Pugh B cirrhosis. Median overall survival was 20 months, and overall survival was 65% at 1 year, 43% at 2 years, and 33% at 3 years. Late gastrointestinal (GI) toxicity grade 3 or above occurred in 3% of patients, and 15% of patients experienced RILD [17]. Tumor size and Child–Pugh Class were independent predictors of survival.

14.3.2 Stereotactic Body Radiotherapy

The promising results of fractionated conformal radiotherapy renewed interest in further dose-escalation, which was enabled by the development of SBRT, also known as stereotactic ablative radiotherapy (SABR). SBRT allows the delivery of ablative doses of radiation, with rapid dose fall-off at the periphery of the target. Early experience with this highly conformal technique demonstrated excellent local control and toxicity rates as well as acceptable impact on quality of life.

SBRT for the treatment of intrahepatic malignancies was first reported in 1995 by Blomgren et al. [18]. at the Karolinska Institute, Stockholm, where the stereotactic radiosurgery experience for treating brain tumors was adapted to treat extracranial targets. There has since been accumulating clinical experience with SBRT

Table 14.1 Select clinical series for fractionated external beam radiotherapy for hepatocellular carcinoma and other liver malignancies

Authors	Patients	Tumor diameter/volume (tumor number)	Dose/fraction size	Objective response rate (%)	Overall survival	Toxicity $\geq$G3 (%)
Ben-Josef et al. [11]	128 /Liver Malignancies	–	Median 60.75 Gy / 1.5 Gy BID (40–90 Gy)	52	Median 15.8 months; 3 year 17%	35
Mornex et al. [15]	27 (16 CP-A/11 CP-B) /HCC only	Single tumor $\leq$5cm (22); 2 tumors $\leq$3 cm (5)	66 Gy /2 Gy	92	41% at 29 months	41
Liu et al. [103]	44 (32 CP-A/12 CP-B) /HCC only	<5 cm (16); 5–10 cm (16); >10 cm (12)	Median 50.4 Gy (39.6–60) Gy / 1.8 Gy	61.4	Median 15.2 month; 1 year 61%; 2 year 40%	0
Liang et al. [17]	128(108 CP-A/20 CP-B) /HCC only	<125 mL (29), 125–1000 (87), >1000 (12)	Median 53.6 Gy (40 + 60 Gy)/ Median 4.88 Gy (3–5 Gy)	55	Median 20 months, 1 year 65%, 2 year 43%	3
Kim et al. [104]	70 /HCC only	<8 cm (37), $\geq$8 cm (33)	Median 54 Gy (44–54 Gy) /2–3 Gy	54.3	Median 10.8 months, 1 year 43.1%, 2 year 17.6%	12.9
Oh et al. [105]	40 (36 CP-A/4 CP-B) /HCC only	<5 cm (18), $\geq$5 cm (22)	Median 54 Gy (30–54 Gy) /Median 3 Gy (2.5–5) Gy	62.8	1 year 72%, 2 year 45.6%	0
Seong et al. [16]	398 (294 CP-A/88 CP-B)/HCC only	Median 6.2 cm	Median 45 Gy/Median 1.5 Gy	–	Median 12 months, 2 year 27.9%	–

Abbreviations: *CP* Child–Pugh, *HCC* Hepatocellular carcinoma, *G3* Grade 3

demonstrating sustained response in the majority of treated patients, even for large tumors. Several prospective and retrospective studies have shown excellent 1-year and 2-year local control in the 70–90% range with low toxicity (Table 14.2). A phase I dose-escalation study from Indiana University to determine the maximum tolerated dose of SBRT in selected patients with primary HCC showed that SBRT to doses up to 48 Gy in three fractions is safe in select Child–Pugh class A patients with HCC [19]. They reported their updated experience in 2011 [20] with treating Child–Pugh class A patients to a median of 48 Gy in three fractions and Child–Pugh class B patients to 40 Gy in five fractions, based on the results from their phase I dose-escalation trial. They reported 2-year local control, progression-free survival, and overall survival of 90, 48, and 67%, respectively. Eventually, 23 patients underwent transplant, with a median time to transplant of 7 months. There were no grade 3 or higher non-hematologic toxicities.

The Princess Margaret Hospital (PMH) developed a protocol using an individualized six-fraction SBRT dose–allocation approach similar to that from the University of Michigan, in which the prescribed tumor dose was determined based on the effective volume of normal liver irradiated, with encouraging phase I results [21, 22]. In an updated analysis of the completed phase I and II PMH studies, Bujold et al. reported a total of 102 Child–Pugh A HCC patients who were ineligible for local-regional therapies and treated with SBRT to a median dose 36 Gy in six fractions [23] Despite the fact that 55% of patients had portal vein thrombosis, 12% of patients had extrahepatic disease, and 52% of patients had received prior therapies, clinical outcomes were impressive with one-year local control of 87% and median overall survival of 17 months. Also of note, despite the large tumor sizes included in this study (median gross tumor volume of 117 cc and median diameter of the largest lesion of 7.2 cm), tumor size and volume did not correlate with local control or overall survival. Minimum dose to the planning target volume correlated with local control on univariate analysis only ($p = 0.02$). Grade 3 and higher toxicity was seen in 36% of patients.

14.3.2.1 Comparison with Other Modalities

Given these promising results, SBRT has rapidly become an accepted local therapy for treating patients with HCC. Until recently, there has not been any evidence directly comparing SBRT with other local treatment options for inoperable HCC, such as RFA. Local ablation is considered first-line treatment for localized HCC not suitable for surgery [2]. RFA induces coagulative necrosis of tumor through thermal ablation and is the preferred technique for treating small HCC lesions [24–26]. However, RFA is an invasive procedure, often requiring general anesthesia, and control rates for larger lesions are suboptimal [27, 28]. A recent retrospective study from the University of Michigan demonstrated improved local control for SBRT relative to RFA, particularly for larger lesions. In this series, 224 patients with inoperable HCC were treated with either RFA (161 patients, 249 tumors) or SBRT (63 patients, 83 tumors). SBRT dose used ranged from 27–60 Gy in 3–5 fractions. Freedom from local progression (FFLP) was defined as absence of progressive of disease within or at PTV margin or ablation zone. Repeat RFA was allowed, and tumors requiring multiple RFAs for residual disease were not counted as failure until after all tumors were successfully treated. One and 2-year FFLP for tumors treated for RFA were 83.6 and 80.2%, respectively, while 1- and 2-year FFLP for tumors treated with SBRT were 97.4 and 83.8%, respectively. For tumors that were 2 cm in diameter or larger, RFA was associated with significantly worse local control compared to RFA (hazard ratio for local progression 3.35, $p = 0.025$). Acute grade 3 and higher complications occurred after 11 and 5% of RFA and SBRT treatments, respectively ($p = 0.31$). There was no difference in overall survival between patients treated with SBRT or RFA. Based on these results, the authors recommended that SBRT be the preferred treatment for larger lesions.

Table 14.2 Select SBRT series

Authors	Patients	No. lesions (No. of patients)	Dose/fractions	Median diameter or volume	Local control	Overall survival	Toxicity ≥G3
Andolino et al. [20]	60 (36 CP-A/24 CP-B)	1(51), 2(7), 3(2)	30–48 Gy/3 – CP-A 40 Gy/5 – CP-B	3.1 cm	2 year 90%	2 year 67%	35%
Bibault et al. [106]	75 (67 CP-A/8 CP-B)	–	40–45 Gy/3	3.7 cm	1 year 89.8%	1 year 78.5%, 2 year 50.4%	6.6% had decompensated cirrhosis
Bujold et al. [23]	102 (all CP-A)	1(40), >1 (62)	Median 36 Gy/6 (24–54 Gy)	7.2 cm	1 year 87%	Median 17 months	36%
Cardenes et al. [19]	17 (6 CP-A/11 CP-B)	1(12), 2(2), 3(3)	36–48 Gy/3	4 cm	100%	1 year 75%, 2 year 60%	18%
Huertas et al. [107]	77 (66 CP-A/11 CP-B)	1(67), 2(10)	45 Gy/3	2.4 cm	1 year 99%	1 year 81.8%, 2 year 56.6%	4% RILD, 1 grade 5 toxicity from hematemesis
Jang et al. [108]	82 (74 CP-A/8 CP-B)	1(71), 2(9), 3(2)	33–60 Gy/3	3.0 cm	2 year 87%	2 year 63%	9.8%
Kang et al. [109]	47 (41 CP-A/6 CP-B)	1(39), 2(7), 3(1)	42–60 Gy/3	2.9 cm	2 year 94.6%	2 year 68.7%	10%
Kwon et al. [110]	42 (38 CP-A/4 CP-B)	1(27), >1 (15)	30–39 Gy/3	15.4 cc	1 year 72%	1 year 93%	2%
Sanuki et al. [111]	185 (158 CP-A/27 CP-B)	1(185)	35–40 Gy/5	2.7 cm (35 Gy group) 2.4 cm (40 Gy group)	3 year 91%	3 year 70%	13%
Seo et al. [112]	38 (34 CP-A/4 CP-B)	–	30–57 Gy/3	40.5 cc	1 year 78%	1 year 69%	0%
Tse et al. [21]	31 (all CP-A)	–	Median 30.6 Gy (24–54 Gy)/6	173 cc (9–1913 cc)	1 year 65%	1 year 85%	29%
Wahl et al. [113]	63 57 CP-A/24 CP-B/2 CP-C[a])	83 lesions among 63 patients	27–60 Gy/3–5	2.2 cm	1 year 97.5%	1 year 74%	5%
Yamashita et al. [114]	79 (67 CP-A/9 CP-B/1 CP-C/2 unknown)	1(79)	40–60 Gy/4–10	2.7 cm	18% had local progression	2 year 53%	4.6%
Yoon et al. [115]	93 (69 CP-A/24 CP-B)	1(83), 2(10)	30–60 Gy/3–4	2.0 cm	3 year 92%	1 year 86%	6.5% hepatic toxicity

Abbreviations: *CP* Child–Pugh, *No.* Number, and *G3* Grade 3
[a]Breakdown per lesion as reported in the paper

These same investigators also conducted a similar retrospective study comparing 125 patients receiving SBRT with 85 patients who received TACE [29]. The 1- and 2-year LC with SBRT was 96.5 and 91% compared to 47 and 23% for TACE ($p < 0.001$). In addition, the 1- and 2-year freedom from hepatic progression for SBRT was 56.5 and 27% compared to 36 and 11% for TACE ($p < 0.001$).

14.3.2.2 Toxicity

Through precisely targeting tumors and minimizing dose to normal liver, SBRT has not been associated with increased rates of radiation-induced liver disease compared to fractionated, conformal radiotherapy despites its high doses. Patient selection is important, however, as a recent phase I/II study demonstrated increased grade III/IV liver toxicity in Child–Pugh class B patients [30]. In this study, 38 Child–Pugh class A patients and 21 Child–Pugh class B patients were treated with SBRT to 24–48 Gy in three fractions. While only 11% of the Child–Pugh class A patients experienced $\geq$ grade III liver toxicity, 38% of the Child–Pugh class B patients experienced $\geq$ grade III liver toxicity. The investigators found that the volume of liver receiving doses as low as 2.5 Gy to be correlated with developing toxicity in Child–Pugh class B patients. Additionally, there are additional toxicity concerns unique to SBRT given that its safety is predicated on avoiding organs at risk in the delivery of ablative doses of radiation. Gastrointestinal ulceration and perforation as well as hepatobiliary toxicity, including biliary obstruction and stricture, have been reported in patients treated with SBRT for liver lesions [31–34]. Bae et al. found V25 > 20 cc and maximum point dose of 35 and 38 Gy (over three fractions) predicted for severe gastroduodenal toxicity. Similarly, Osmundson et al. found a dose-dependent relationship between hepatobiliary toxicity and the volume of the central hepatobiliary tract treated with SBRT, and recommended dose constraints for the central hepatobiliary tract of V40 (in five fractions) < 21 cm and V37 < 24 cm. Extra caution is warranted when SBRT is combined with new biologic and anti-angiogenic agents. Multiple reports have reported unanticipated toxicities arising after the combination of SBRT and angiogenesis-targeting agents, particularly of late luminal gastrointestinal toxicities [35]. Significant toxicity including grade 3 and grade 4 bowel toxicities and tumor rupture was recently reported in a phase I trial from Princess Margaret Hospital with the use of concurrent sorafenib and SBRT among patients with Child–Pugh Class A HCC [36]. Additionally, half of the patients in the high effective irradiated liver volume group had worsening of Child–Pugh liver function class. Based on these results, the authors recommended against concurrent SBRT with sorafenib outside a clinical trial.

Although the majority of the clinical reports of SBRT have highlighted its excellent local control and toxicity rates, SBRT can also offer potential favorable impact on the dimension of quality of life as well. SBRT is a noninvasive outpatient therapy, requires minimal pre-medication, and involves a limited number of treatments that may be more convenient and appealing for patients.

In 2008, Mendez Romero et al. prospectively assessed the impact of SBRT on the quality of life of 28 patients with liver tumors (19 had liver metastases, 9 had HCC) using the EQ-5D index, EQ-5D VAS and European Organization for Research and Treatment of Cancer Quality of Life Questionnaire Core-30 (QLQ C-30) global health status instruments at time points of directly before and 1, 3, and 6 months after treatment, with high response rates (70–100% across all time points) [37]. They found that quality of life was not significantly influenced by treatment with SBRT, and that patients maintained pretreatment level quality of life in the six months period after treatment.

Klein et al. subsequently published their quality of life outcomes that were collected prospectively over a ten-year period from 222 patients treated with SBRT for liver cancer, about half of whom had HCC [38]. The majority of HCC patients had Child–Pugh A liver function and received 24–60 Gy in six fractions. Quality of life was assessed using the QLQ-C30 and/or Functional Assessment of Cancer Therapy—

Hepatobiliary Cancer (FACT-Hep, version 4) questionnaires at baseline and 1, 3, 6, and 12 months after treatment. They found that liver SBRT temporarily worsened appetite and fatigue at one month but that this recovered by three months. Patients with small tumors 6 cm or less in diameter did not experience a clinically significant decline in QOL at any time point. Overall quality of life was unchanged for all patients.

Although these quality of life results compare favorably to other treatment approaches, including resection, RFA and TACE, for HCC, [39–42] no direct comparisons have yet been published. Health-related quality of life in HCC is understudied, but is increasingly recognized as an important endpoint, and should be an important factor in the treatment decision for patients and their physicians.

14.3.3 Particle Therapy

Given the need to limit radiation dose to the liver in patients with HCC due to underlying liver disease and decreased functional reserve, the dosimetric characteristics of heavy particle radiotherapy, such as protons, are appealing. The Bragg peak phenomenon results in decreased integral dose to the uninvolved portion of the liver. Thus, proton therapy is ideal for safe dose-escalation to tumors in located in critical, radiosensitive organs.

Most of the published clinical experiences of proton therapy are retrospective series predominantly from Asia. One of the first clinical series of proton therapy for treating HCC was reported from the University of Tsukuba in Japan [43]. In this series, 162 patients with 192 HCCs lesions were treated from 1985–1998 with proton radiotherapy to a median dose of 72 Cobalt Gray Equivalent (CGE) in 16 fractions (50–88 in 10–24 fractions). The median tumor size was 3.8 cm (ranging from 1.5–14.5 cm), 25 patients (15%) had portal vein tumor thrombus, and 72 patients (44%) had Child–Pugh Class B and C cirrhosis. Overall survival and local control at five years were 23.5 and 86.9%, respectively. Only 3% of the patients experienced grade 2 or higher late toxicity. There was no treatment discontinuation due to liver toxicity and no treatment-related deaths.

Several prospective single-institution proton series have also reported five year local control of 81–88% and five year overall survival of 25–39% [44–47] (Table 14.3). In a phase II trial at Loma Linda, 76 patients (22 patients had Child–Pugh A, 36 patients had Child–Pugh B, 18 patients had Child–Pugh C cirrhosis) were treated

Table 14.3 Select prospective studies of charged particle therapy for hepatocellular carcinoma

Authors	Patients	Particle	Dose/fractions	PVT (%)	Local control	Survival	Toxicity ≥G3 (%)
Bush et al. [46, 47]	76 (47% CP-B, 24% CP-C)	P	63 GyE/15	5	2 year 75%	18.4 months (median)	0
Fukumitsu et al. [45]	51 (20% CP-B, 0% CP-C)	P	66 GyE/10	0	3 year 94.5%	5 year 39%	2
Kawashima et al. [44]	30 (33% CP-B, 0% CP-C)	P	76 GyE/20	40	2 year 96%	3 year 62%	40
Kato et al. [116]	24 (33% CP-B, 0% CP-C)	C	49.5–79. GyE/15	58	1 year 92%, 5 year 81%	5 year 25%	26
Hong et al. [52]	44 (32 CP-A, 9 CP-B, 3 no cirrhosis)	P	58.0 GyE/15	29.5	2 year 94.8%	1 year 76.5%	2.3

Abbreviations: *P* Proton, *C* Carbon, *CP* Child–Pugh Class, *PVT* portal vein thrombosis, *G3* Grade 3, *GyE* Gray equivalent

to 63 Gy in 15 fractions. Of these patients, 18 eventually underwent a liver transplant; 6 (33%) of these patients had a complete response and 7 (39%) had microscopic residual disease. Median progression-free and overall survival was 36 and 18 months, respectively. No grade 3 or higher toxicity was reported. Because of these promising results, Loma Linda conducted a randomized trial comparing transarterial chemoembolization and proton beam radiotherapy with the primary endpoint of progression-free survival [48]. Interim analysis results showed a trend toward improved 2-year progression-free survival (48 vs. 31%, $p = 0.06$) with proton beam. There were also significantly fewer hospitalization days after proton treatment compared to TACE (166 vs. 24 days, $p < 0.001$). The 2-year overall survival for all patients was 59%, and was not significantly different between treatment groups.

Other particles including carbon ions have also been explored in the treatment of HCC. Carbon ion therapy has the additional advantage over proton therapy of a narrower penumbra, increased relative biological effectiveness (RBE), and lower oxygen enhancement ratio (OER). Thus, carbon ion beams are expected to provide a beneficial dose distribution that leads to improved therapeutic ratio, more so than with proton beam. A phase I–II trial from Japan delivered 49.5–79.6 GyE in 15 fractions using carbon ions to 24 patients (16 had Child–Pugh A and 8 had Child–Pugh B cirrhosis), and reported 5-year local control of 81% and 5 year overall survival of 25%. One patient had a grade 3 early skin reaction while five patients experienced grade 3 early hematological toxicity and three patients experienced late grade 3 hematological toxicity. Others have also reported the safety and effectiveness of hypofractionated carbon treatment (52.8 GyE in four fractions) [49]. However, longer follow-up is required to ensure that these large doses per fraction do not result in increased late toxicity.

The excellent conformality of particle therapy is particularly advantageous in situations where there is high risk of developing toxicity with radiation. For example, many patients with portal venous thrombosis have poor functional liver reserve but need large volumes of their liver irradiated. Hata et al. reported treating 12 patients who had tumor thrombus in the main trunk or major branches of the portal vein with a total of 50–72 Gy in 10–22 fractions using protons [50]. They reported 2-year progression-free survival of 67%, and no grade 3 or higher toxicity. Two patients were alive with no evidence of disease at 4.3 and 6.4 years after therapy. Another proton series of 35 patients with HCC portal venous thrombosis were treated with 50–72 CGE with local control rates of over 45% at 2 years. Only three patients developed severe acute toxicity [51]. Recently, a multi-institutional phase II trial of proton therapy for unresectable HCC and intrahepatic cholangiocarcinoma treated tumors to a mean dose of 58 GyE in 15 fractions [52]. With this regimen, the results showed a very promising 2-year local control of 94.8% for HCC despite nearly 30% of patients having vascular thrombus.

The Tsukuba proton radiotherapy group has also reported on the efficacy and safety of HCC retreatment for either progressive or synchronous HCC lesions in a series of 27 patients with 68 total lesions [53]. The median interval was 24 months between the first and second course of treatment and median dose delivered was 72 Gy in 16 fractions and 66 Gy in 16 fractions for the first course and rest of the courses, respectively. The 5-year local control rate and overall survival were 87.8 and 56%, respectively. One patient with Child–Pugh Class B and another patient with Child–Pugh Class C cirrhosis experienced acute hepatic failure.

While the reported clinical experience with proton and carbon ion therapy have been associated with some of the best outcomes so far, particularly for patients who are at high risk of hepatic insufficiency with radiation, particle therapy is an expensive technology available at few facilities worldwide. Additionally, there is increasing evidence demonstrating comparable clinical efficacy and safety with photon SBRT. Further comparative evaluation of particle therapy is needed to determine whether its theoretical advantage translates into a clinically significant advantage over other less expensive and more

accessible therapies, and if so, which patient subgroups could benefit most from this treatment modality.

14.3.4 Radioembolization

Trans-arterial radioembolization [TARE, also known as selective internal radiation therapy (SIRT)], involves injection of radioactive microspheres for delivery of internal radiation. The microspheres are loaded with a radioactive compound, such as Yttrium-90 (Y-90), which is a beta-emitter with a short half-life (2.67 days) and limited tissue penetration (average 2.5 mm, maximum 11 mm). Selective catheter-based administration of Y-90 microspheres via the hepatic artery preferentially delivers high-dose radiation to the tumor-associated capillary bed while sparing normal liver tissue, allowing for delivery of doses up to 50–150 Gy [54, 55] without developing the clinical complications of conventional external beam radiotherapy [56]. In contrast to TACE, the dominant mechanism of occlusion is microvascular rather than macrovascular occlusion, and tumor necrosis is believed to be predominantly a result of radiation rather than ischemia [57]. Two common commercial microspheres available are TheraSphere®, made of glass, and SIR-Spheres, made of resin; although they differ in several characteristics including the activity per microsphere and number of microspheres typically injected in a treatment, clinical outcomes are similar between the two [58]. In the United States, FDA has approved the use of Sir-Spheres for treatment of unresectable colorectal cancer metastases to the liver, and the use of TheraSphere® for treatment of unresectable HCC under a Humanitarian Device Exemption provision.

TARE has traditionally been used in clinical practice for patients with advanced-stage HCC, patients felt to be poor candidates for TACE, early stage patients as a bridge to liver transplantation, or for palliation of non-ablatable tumors. Long-term survival outcomes support the safety and efficacy of TARE for patients with HCC, including those with advanced disease and limited treatment options. Salem et al. analyzed outcomes of 291 patients (526 treatments) treated with Y-90 as part of a single-center prospective longitudinal cohort study, and reported response rates of 42 and 57% based on WHO and EASL criteria, respectively [59]. The overall time to tumor progression (TTP) was 7.9 months, with median survival of 17.2 months for Child–Pugh class A, and 7.7 months for Child–Pugh class B disease. In 108 consecutive patients (159 treatments) with advanced HCC and liver cirrhosis treated with Y-90 microspheres, Hilgard et al. reported a 40% response rate by EASL criteria, time-to-progression of 10.0 months, and median survival of 16.4 months [60]. The most common side effect was a grade 1/2 transient fatigue syndrome. Sangro et al. conducted a European multicenter retrospective analysis on prognostic factors driving survival in patients treated with TARE using Y-90 microspheres [61]. The majority of patients were Child–Pugh class A (82.5%), had underlying cirrhosis (78.5%), but many had multinodular disease (75.9%) and/or portal vein occlusion (13.5% branch, 9.8% main). Median overall survival of all patients was 12.8 months, which varied by Barcelona Clinic Liver Cancer (BCLC) staging—(BCLC A, 24.4 months; BCLC B, 16.9 months; BCLC C, 10.0 months). Tumor burden and liver function were predictive of survival within the context of BCLC staging. Treatment was well tolerated with the majority of adverse events (fatigue, nausea/vomiting, and abdominal pain) being mild.

While two randomized controlled trials established TACE as the standard of care in BCLC intermediate-stage disease [62, 63], demonstrating a survival benefit for TACE compared with conservative management with best supportive care, there has been few published randomized evidence comparing TARE and TACE. A phase II randomized trial comparing TACE and TARE showing improved time to progression with TARE compared to TACE (median >26 vs 6.8 months, $p = 0.007$), but no difference in overall survival (18.6 vs. 17.7 months, $p = 0.99$) [64]. Nonrandomized, retrospective analyses have attempted to compare outcomes of patients with HCC treated with

TACE or TARE [65–67]. Salem et al. reported less toxicity and longer time to tumor progression (13.3 months vs. 8.4 months) with TARE compared with TACE [66]. El Fouly et al. conducted a prospective non-randomized controlled trial comparing TARE with TACE for patients intermediate-stage HCC, and found no differences in median survival and time-to-progression despite higher tumor burden in the TARE cohort, as well as significantly higher rate of adverse event and hospitalization time in the TACE cohort [68]. The pilot study SIRTACE was the first to compare single session TARE with multi-session TACE for unresectable HCC. Both modalities were well tolerated without any significant differences in health-related quality of life. Local control was similar with best overall response rate for target lesions of 13.3 and 30.8%, and disease control rates of 73.3 and 76.9% for TACE and TARE, respectively [69], suggesting that TARE may be an appropriate alternative option for patients who are eligible for TACE. Three ongoing randomized controlled trials are further evaluating TARE versus TACE for patients with intermediate-stage HCC (NCT00956930, NCT01381211, NCT02004210).

A particular setting where TARE may have an advantage over TACE is in the presence of main portal vein thrombus, which is a relative contraindication for the latter. Because TARE's effect is mainly through radiation damage and not through embolic ischemia, the risk of liver damage is decreased. A study by Mazzaferro et al. showed that overall survival (13 vs. 18 months) and time to progression (7 vs. 13 months) was not significantly different between patients with portal vein thrombus and without portal vein thrombus treated with TARE [70]. In the study by Salem et al., the median overall survival of patients with portal vein thrombus and Child–Pugh A cirrhosis treated with TARE was 10.7 months, which compares favorably to the 8.9 months median overall survival reported in the SHARP trial for patients with portal vein thrombus and/or extrahepatic disease treated with sorafenib alone [59, 71].

TARE is generally well tolerated with a favorable safety profile. Large series have reported mild procedure related symptoms including fatigue, abdominal pain, nausea, vomiting, and low grade fever that occur in about 20–60% of patients [59–62], and rates of grade 3/4 biliary toxicity are under 10% [72]. Sangro et al. have reported on TARE-induced liver disease (REILD), a hepatic sinusoidal obstruction syndrome appearing 4–8 weeks after TARE, characterized by jaundice, mild ascites, and moderate increase in gamma-glutamyl transpeptidase and alkaline phosphatase in the absence of tumor progression or bile duct occlusion [73]. Gil-Alzugaray et al. have shown that use of a comprehensive treatment protocol that includes an algorithm for individualized activity calculations reduces the incidence of severe REILD from 13.3 to 2.2% [74].

While the majority of evidence supporting the use of TARE in HCC has been based on retrospective or non-randomized prospective studies, the favorable outcomes in local control and toxicity profiles have generated renewed interest into the use of TARE upfront in intermediate-stage HCC patients whom traditionally would have been treated with TACE.

14.3.5 Interstitial Brachytherapy

Interstitial high-dose-rate (HDR) brachytherapy (iBT) is a technique that currently remains investigational for HCC. iBT uses an iridium-92 (Ir-92) source which is temporarily inserted through a needle catheter placed under CT guidance in order to deliver a locally ablative dose of radiation [75]. Dritschilo et al. studied the feasibility of and safety of ultrasonography directed interstitial brachytherapy for treatment of hepatic metastases. In the six patients who were treated, treatment was well tolerated, and a partial response or stable disease was observed in all six patients. The authors determined that doses of 50 Gy, with potential to ablate metastatic tumor deposits, could be safely delivered in a single fraction to tumors up to 25 mL without

clinically significant toxicity in follow-up evaluations at 2–6 months [76]. The authors also reported feasibility results of a separate pilot study where 11 patients with multiple liver metastases (2–11 separate tumors, with median diameter 6 cm) were treated with sonographically guided iBT with doses of 20 Gy to the periphery of the target volume in a single treatment. Treatment was well tolerated, with median hospitalization of eight days, with no radiation related complications on follow-up at 18 months [77]. Ricke et al. studied CT-guided iBT to treat liver metastases in combination with thermal ablation or as standalone treatment [78]. In this Phase I–II study, 37 patients with 38 liver lesions with mean tumor size 4.6 cm were treated with either brachytherapy alone or in combination, with 6-month local control rates of 73 and 87% for combined modality treatment and brachytherapy alone, respectively. The rate of severe complications was 5% [78].

Mohnike et al. prospectively analyzed outcomes in 83 patients with 140 HCC lesions who underwent CT-guided iBT with Ir-192. The average diameter of a patient's largest lesion was 5.8 cm, and 52% of patients had multiple lesions. Median time-to-progression and overall survival were 10.4 and 19.4 months, respectively. Perioperative and 30-day mortality were 1.2 and 4.9%, respectively [79]. These results compared favorably to historical controls. In another analysis from the same authors, 192 patients with 296 lesions of primary and secondary liver malignancies were treated with iBT, and the rate of major complications was below 5%, with the most common being grade 3/4 bleeding (1.46%), formation of liver abscess (1.17%), and GI ulcer formation (0.87%) [80].

iBT has also been evaluated as an alternative to TACE to bridge patients with HCC to liver transplantation. Denecke et al. retrospectively analyzed 20 patients who received CT-guided brachytherapy prior to transplantation, and compared their outcomes to matched patients who received TACE before transplantation. Recurrence rates for iBT and TACE at 1 year (10% vs. 14%) and 3 years (10% vs. 30%) favored iBT, and iBT was found to have higher rates of tumor necrosis [81], suggesting that this modality may be an alternative bridging modality, especially for patients unsuitable for TACE.

iBT for HCC is an emerging modality for patients with lesions that are large or in close proximity to large vessels. Local control and survival outcomes compare favorably with historical controls, with low incidence of serious adverse events. There is also early evidence that iBT may be an alternative to TACE to bridge patients to transplantation. Further randomized prospective investigation is warranted to establish iBT as a local treatment modality in such clinical

14.3.6 Radiation Treatment for Patients with Vascular Invasion

Portal vein or inferior vena cava tumor thrombus is a common finding in patients with advanced HCC, with 44–62.8% of patients with HCC found to have vascular invasion at autopsy [82, 83]. Vascular invasion can result in tumor dissemination and portal vein hypertension, resulting in ascites, hematemesis, and encephalopathy, and is associated with a poor prognosis, with a median survival of 2–4 months with best supportive care [84]. These patients are often unsuitable for TACE, due to concern for ischemic liver damage, and have few treatment options. Charged particle and photon therapy has been shown to be effective for treating HCC associated with vascular invasion, and eventual recanalization of the portal vein has been reported. Kim et al. reported an objective response rate of the portal vein thrombus (PVT) of 45.8% in 59 patients with HCC and PVT treated with 30–54 Gy at 2–3 Gy per fraction [85]. They found a dose-response relationship, with doses $\geq$58 Gy associated with a response rate of 54.6% versus a response rate of 20.7% in those treated with lower doses. Responders had a median survival of 10.7 months while non-responders had a response rate of 5.3 months ($p = 0.05$). Another study of conformal, fractionated radiotherapy reported a PVT response rate of 44.7% and also

found that doses 58 Gy or higher as well as PVT size (<30 mm) were significant factors for tumor response [86]. In a retrospective review of 97 patients, Nakazawa et al. showed that fractionated conformal radiation was associated with improved survival compared to sorafenib in patients who have unresectable HCC with PVT, and recommended that radiation be first-line therapy in these patients [87]. Heavy particle therapy and SBRT have similarly been associated with improved local control and survival in these patients [50, 51, 88]. Radiation can be also be used in combination with TACE, with the objective of shrinking portal vein and inferior vena cava tumor thrombus and improving portal blood flow, allowing for subsequent treatment with TACE and potentially even allowing for consideration for liver transplant. Table 14.4 summarizes select clinical series of TACE used in combination with radiation. As such, radiation has an important role in the subset of HCC patients with PVT. Figure 14.1 shows an example of a tumor with portal vein invasion that was successfully treated with SBRT, allowing reconsidering of liver transplant.

14.3.7 Bridge to Transplant

Although liver transplantation is a curative treatment option for patients with unresectable HCC, up to 20% of patients on the waitlist will drop out due to tumor progression [89]. Local-regional therapy, such as TACE, RFA, and ethanol injection, is often used as a bridge treatment for patients with HCC waiting for liver transplantation in order to try to downstage tumors or prevent tumor progression and improve post-transplant survival. Particle therapy, SBRT and interstitial brachytherapy, as

Table 14.4 Select clinical series of combination therapy with transarterial chemobolization and radiation

Authors	Patients	Tumor diameter/volume	Dose/Fraction size	Portal vein thrombosis (%)	Objective response rate (%)	Overall survival	Toxicity ≥G3
Seong et al. [117]	30 (no CP-C)	Mean 8.95 cm	Mean 44 Gy/1.8 Gy	37	63.3	1 year 67%	0%
Guo et al. [118]	50 (48 CP-A, 2 CP-B)	Median 144 cm^3	Mean 43 Gy/2 Gy	22	18	1 year 60%	20% (2 cases of RILD that led to death)
Yamada et al. [119]	19 (13 CP-A, 5 CP-B, 1 CP-C)	Mean 5.2 cm	60 Gy/2 Gy	37	58	1 year 41%	37% patients had deterioration of CP score
Koo et al.	42 (26 CP-A, 16 CP-B)	Mean 10 cm	40–48 Gy/2.5–4 Gy	45	43	1 year 48%	0%
Yoon et al. [120]	412 (264 CP-A, 148 CP-B)	Median 9.5 cm	Median 40 Gy/2–5 Gy	100	39.6	1 year 43%	10.4%
Xu et al. [121]	140 (137 CP-A, 3 CP-B)	Median 7.8 cm	Median 44 Gy/2 Gy	19	19.2	1 year 66%	3 cases of RILD (2 led to death)
Tazawa et al. [121]	24 (12 CP-A, 8 CP-B, 4 CP-C)	Mean 63.3 cm^3	50 Gy/2 Gy	100	50	1 year 73%	13%

Abbreviations: *CP* Child–Pugh, *G3* Grade 3

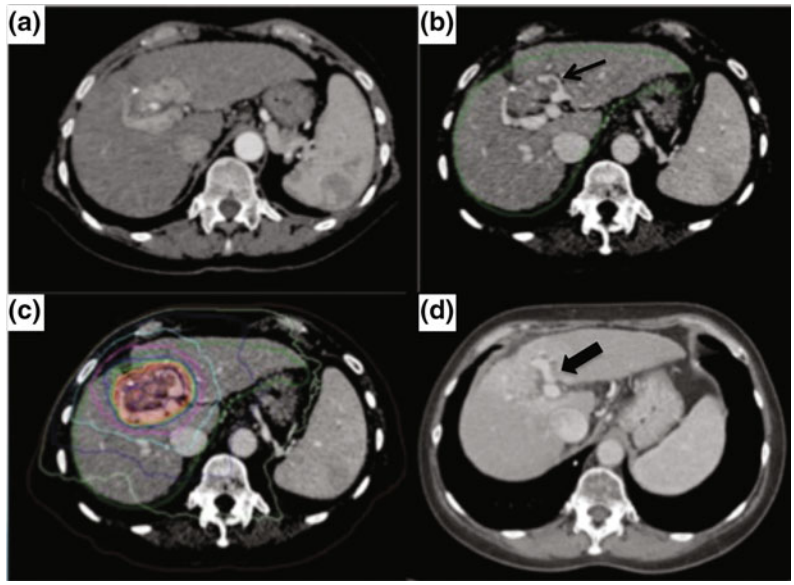

Fig. 14.1 A patient with central hepatocellular carcinoma and portal vein invasion who was treated with stereotactic body radiotherapy (SBRT). Panel **a** and **b** show the enhancing tumor with portal vein invasion (*thin arrow*). Panel **c** shows the treatment plan. Panel **d** shows a normalized portal vein with no residual portal vein invasion (*thick arrow*). Patient underwent a liver transplant 3 years after SBRT and is currently disease-free 2 years after transplant

discussed above, have also been shown to be advantageous in select patients who are not eligible for TACE or RFA due to treatment intolerance or tumor location in order to bridge the gap between HCC diagnosis and curative liver transplantation. O'Connor et al. reported using SBRT in 10 patients with 11 lesions (2.5–5.5 cm) who either failed or were ineligible for other local therapies [90]. Median dose used was 51 Gy (range 33–54 Gy) in three fractions. SBRT was well tolerated, and all 10 patients ultimately underwent successful orthotopic liver transplant with a median time from SBRT to transplant of 3.7 months. Explant pathology revealed a complete pathological response in 3 (27%) of the 11 tumors and only small, millimetric foci of viable HCC with otherwise extensive necrosis in three of the remaining lesions. At last reported follow-up, all patients were alive and disease-free, with no post-transplant recurrences. Facciuto et al. also reported 27 patients with 39 lesions who were treated with SBRT using 24–36 Gy in 2–4 fractions [91]. Seventeen patients went on to achieve liver transplantation, with a mean wait time from SBRT to liver transplant of four months. Of the 22 pathologically evaluated lesions, 14% had a complete response (100% tumor necrosis), 23% had a partial response (30–99% tumor necrosis), and 63% had no response (0–29% tumor necrosis). The use of conformal radiation has not been reported to increase operative complications, and may prove to be a useful treatment option for well-selected patients with HCC who on are the transplant waitlist and are not candidates for other local therapies.

14.3.8 Palliation

Although best supportive care is generally recommended for patients with terminal stage HCC, many of these patients develop discomfort due to metastatic lesions or disease burden in the liver. Radiotherapy can play an important role in providing effective palliation these patients. Radiation with doses from 12.5 to 50 Gy has been shown to achieve pain relief in 73% of treated

lesions [92]. Low-dose whole liver radiotherapy (8 Gy in one fraction) has been shown to improve symptoms from diffuse liver involvement in 50% of patients at 1 month after treatment with minimal toxicity [93].

14.4 Combination Therapy and Future Directions

Despite high rates of local control achieved with radiotherapy, patients with HCC are at high risk of regional and systemic progression. Thus, there is motivation to combine radiation with regional and systemic therapy to improve outcomes.

TACE is a hepatic artery directed therapy that has some tumor specificity, as hepatic tumors derive most of their blood supply from the hepatic artery while the majority of blood supply to the liver parenchyma comes from the portal vein. TACE has demonstrated a positive survival impact in large, multifocal tumors unsuitable for surgery and ablation [62, 63, 94, 95], and has become standard of care for unresectable disease. However, the ablative effect of TACE is limited, and combining radiation with TACE has been explored as a means of improving local control. Radiation can be delivered first, to improve the effectiveness of subsequent TACE in the setting of portal vein thrombosis, as described above, or alternatively, it can be delivered after TACE as consolidation to target residual disease. Multiple retrospective studies have shown that the combination of TACE and radiation improves response rate and survival over TACE alone in patients with large HCC and/or PVT, as summarized in Table 14.4. A meta-analysis of 17 trials and 1476 patients with unresectable HCC showed that the combination of TACE and radiation was better than TACE alone in terms of survival and tumor response, without any increase in toxicity [96].

Sorafenib is an oral multikinase inhibitor with antiproliferative and antiangiogenic effects, and has been shown to improve survival in patients with advanced HCC compared to placebo in two randomized controlled trials [71, 97]. Nevertheless, the majority of these patients eventually experience progression of disease and die of liver failure, prompting further investigations to improve clinical outcomes by combining sorafenib with local therapy. Preclinical studies have suggested improved outcome with combining a variety of anti-angiogenic agents with radiation. Dawson et al. conducted a phase I study of patients with advanced HCC with SBRT and concurrent sorafenib [98]. Sorafenib was delivered 7 days before SBRT, during SBRT, and after SBRT. Two of three patients with an effective irradiated liver volume of 30–60% treated to 30 and 33 Gy in six fractions with concurrent sorafenib (400 mg daily) developed GI toxicity. Thus, sorafenib was de-escalated to 200 mg po daily. In the three patients who had a low effective liver volume irradiated (<30%) and received concurrent sorafenib (400 mg daily), none experienced dose limiting toxicity. This regimen is currently being compared to SBRT alone in RTOG 1112 (https://www.rtog.org/ClinicalTrials/ProtocolTable/StudyDetails.aspx?study=1112).

Similarly, SORAMIC is a prospective randomized phase 2 study comparing combined modality treatment of Y-90 TARE and sorafenib versus sorafenib alone for unresectable intermediate or advanced HCC. An interim safety analysis demonstrated the combined modality arm was as well tolerated as sorafenib alone, with no significant differences found in the number of total and grade 3 and above adverse events [99]. Further study of overall survival of advanced HCC patients treated with TARE plus sorafenib versus sorafenib alone is being investigated by ongoing phase III clinical trial "Efficacy Evaluation of TheraSphere in Patients With Inoperable Liver Cancer (STOP-HCC)" [NCT01556490]. It is worth noting that three randomized trials testing adjuvant sorafenib following resection, ablation, or TACE, showed no improvement in survival [100–102]. Thus, further investigation,

such as RTOG 1112, is needed to clarify the benefit of combining radiation therapy with sorafenib.

14.5 Conclusion

There has been increased interest and experience with using radiation for the treatment of HCC, and published studies have shown excellent outcome with acceptable toxicity profile. Local control rates for SBRT and charged particle in particular approach and even exceed 90% in multiple series. Although refinements in radiation delivery techniques have enabled tumoricidal doses to be delivered safely, better understanding of normal tissue tolerance and proper patient selection is crucial. Further prospective and randomized comparative effectiveness studies as well as quality-of-life studies are needed to inform the integration of radiotherapy into treatment guidelines.

References

1. Ryerson AB, Eheman CR, Altekruse SF, et al. Annual Report to the Nation on the Status of Cancer, 1975–2012, featuring the increasing incidence of liver cancer. Cancer. 2016.
2. European Association For The Study Of The L, European Organisation For R, Treatment Of C. EASL-EORTC clinical practice guidelines: management of hepatocellular carcinoma. J Hepatol. 2012;56:908–943.
3. Belghiti J, Kianmanesh R. Surgical treatment of hepatocellular carcinoma. HPB: Official J Int Hepato Pancreato Biliary Assoc. 2005;7:42–9.
4. Lam VW, Ng KK, Chok KS, et al. Risk factors and prognostic factors of local recurrence after radiofrequency ablation of hepatocellular carcinoma. J Am Coll Surg. 2008;207:20–9.
5. Sherman M, Burak K, Maroun J, et al. Multidisciplinary Canadian consensus recommendations for the management and treatment of hepatocellular carcinoma. Curr Oncol. 2011;18:228–40.
6. Head HW, Dodd GD 3rd, Dalrymple NC, et al. Percutaneous radiofrequency ablation of hepatic tumors against the diaphragm: frequency of diaphragmatic injury. Radiology. 2007;243:877–84.
7. Stigliano R, Marelli L, Yu D, Davies N, Patch D, Burroughs AK. Seeding following percutaneous diagnostic and therapeutic approaches for hepatocellular carcinoma. What is the risk and the outcome? Seeding risk for percutaneous approach of HCC. Cancer Treat Rev. 2007;33:437–47.
8. Goldberg SN, Hahn PF, Tanabe KK, et al. Percutaneous radiofrequency tissue ablation: does perfusion-mediated tissue cooling limit coagulation necrosis? J Vasc Interv Radiol. 1998;9:101–11.
9. Bruix J, Sherman M. Management of hepatocellular carcinoma: an update. Hepatology. 2011;53:1020–2.
10. McGinn CJ, Ten Haken RK, Ensminger WD, Walker S, Wang S, Lawrence TS. Treatment of intrahepatic cancers with radiation doses based on a normal tissue complication probability model. J Clin Oncol. 1998;16:2246–52.
11. Ben-Josef E, Normolle D, Ensminger WD, et al. Phase II trial of high-dose conformal radiation therapy with concurrent hepatic artery floxuridine for unresectable intrahepatic malignancies. J Clin Oncol. 2005;23:8739–47.
12. Dawson LA, McGinn CJ, Normolle D, et al. Escalated focal liver radiation and concurrent hepatic artery fluorodeoxyuridine for unresectable intrahepatic malignancies. J Clin Oncol. 2000;18:2210–8.
13. Robertson JM, Lawrence TS, Andrews JC, Walker S, Kessler ML, Ensminger WD. Long-term results of hepatic artery fluorodeoxyuridine and conformal radiation therapy for primary hepatobiliary cancers. Int J Radiat Oncol Biol Phys. 1997;37:325–30.
14. Dawson LA, Normolle D, Balter JM, McGinn CJ, Lawrence TS, Ten Haken RK. Analysis of radiation-induced liver disease using the Lyman NTCP model. Int J Radiat Oncol Biol Phys. 2002;53:810–21.
15. Mornex F, Girard N, Beziat C, et al. Feasibility and efficacy of high-dose three-dimensional-conformal radiotherapy in cirrhotic patients with small-size hepatocellular carcinoma non-eligible for curative therapies–mature results of the French Phase II RTF-1 trial. Int J Radiat Oncol Biol Phys. 2006;66:1152–8.
16. Seong J, Lee IJ, Shim SJ, et al. A multicenter retrospective cohort study of practice patterns and clinical outcome on radiotherapy for hepatocellular carcinoma in Korea. Liver Int. 2009;29:147–52.
17. Liang SX, Zhu XD, Lu HJ, et al. Hypofractionated three-dimensional conformal radiation therapy for primary liver carcinoma. Cancer. 2005;103:2181–8.
18. Blomgren H, Lax I, Naslund I, Svanstrom R. Stereotactic high dose fraction radiation therapy of extracranial tumors using an accelerator. Clinical experience of the first thirty-one patients. Acta Oncol. 1995;34:861–70.
19. Cardenes HR, Price TR, Perkins SM, et al. Phase I feasibility trial of stereotactic body radiation therapy for primary hepatocellular carcinoma. Clin Transl Oncol. 2010;12:218–25.
20. Andolino DL, Johnson CS, Maluccio M, et al. Stereotactic body radiotherapy for primary

hepatocellular carcinoma. Int J Radiat Oncol Biol Phys. 2011;81:e447–53.
21. Tse RV, Hawkins M, Lockwood G, et al. Phase I study of individualized stereotactic body radiotherapy for hepatocellular carcinoma and intrahepatic cholangiocarcinoma. J Clin Oncol. 2008;26:657–64.
22. Dawson LA, Eccles C, Craig T. Individualized image guided iso-NTCP based liver cancer SBRT. Acta Oncol. 2006;45:856–64.
23. Bujold A, Massey CA, Kim JJ, et al. Sequential phase I and II trials of stereotactic body radiotherapy for locally advanced hepatocellular carcinoma. J Clin Oncol. 2013;31:1631–9.
24. Shiina S, Teratani T, Obi S, et al. A randomized controlled trial of radiofrequency ablation with ethanol injection for small hepatocellular carcinoma. Gastroenterology. 2005;129:122–30.
25. Lin SM, Lin CJ, Lin CC, Hsu CW, Chen YC. Randomised controlled trial comparing percutaneous radiofrequency thermal ablation, percutaneous ethanol injection, and percutaneous acetic acid injection to treat hepatocellular carcinoma of 3 cm or less. Gut. 2005;54:1151–6.
26. Shiina S, Tateishi R, Arano T, et al. Radiofrequency ablation for hepatocellular carcinoma: 10-year outcome and prognostic factors. Am J Gastroenterol. 2012;107:569–577; quiz 578.
27. Mazzaferro V, Battiston C, Perrone S, et al. Radiofrequency ablation of small hepatocellular carcinoma in cirrhotic patients awaiting liver transplantation: a prospective study. Ann Surg. 2004;240:900–9.
28. Lu DS, Yu NC, Raman SS, et al. Radiofrequency ablation of hepatocellular carcinoma: treatment success as defined by histologic examination of the explanted liver. Radiology. 2005;234:954–60.
29. Sapir E, Tao Y, Schipper M, Bazzi L, et al. Stereotactic body radiotherapy as an alternative to transarterial chemoembolization (TACE) for hepatocellular carcinoma (HCC). Presented at 2016 ASCO Annual Meeting. Abstract #4087.
30. Lasley FD, Mannina EM, Johnson CS, et al. Treatment variables related to liver toxicity in patients with hepatocellular carcinoma, Child-Pugh class A and B enrolled in a phase 1–2 trial of stereotactic body radiation therapy. Pract Radiat Oncol. 2015;5:e443–9.
31. Bae SH, Kim MS, Cho CK, et al. Predictor of severe gastroduodenal toxicity after stereotactic body radiotherapy for abdominopelvic malignancies. Int J Radiat Oncol Biol Phys. 2012;84:e469–74.
32. Hoyer M, Roed H, Traberg Hansen A, et al. Phase II study on stereotactic body radiotherapy of colorectal metastases. Acta Oncol. 2006;45:823–30.
33. Shaffer JL, Osmundson EC, Visser BC, Longacre TA, Koong AC, Chang DT. Stereotactic body radiation therapy and central liver toxicity: a case report. Pract Radiat Oncol. 2015;5:282–5.
34. Osmundson EC, Wu Y, Luxton G, Bazan JG, Koong AC, Chang DT. Predictors of toxicity associated with stereotactic body radiation therapy to the central hepatobiliary tract. Int J Radiat Oncol Biol Phys. 2015;91:986–94.
35. Pollom EL, Deng L, Pai RK, et al. Gastrointestinal toxicities with combined antiangiogenic and stereotactic body radiation therapy. Int J Radiat Oncol Biol Phys. 2015;92:568–76.
36. Brade AM, Ng S, Brierley J, et al. Phase 1 trial of sorafenib and stereotactic body radiation therapy for hepatocellular carcinoma. Int J Radiat Oncol Biol Phys. 2016;94:580–7.
37. Mendez Romero A, Wunderink W, van Os RM, et al. Quality of life after stereotactic body radiation therapy for primary and metastatic liver tumors. Int J Radiat Oncol Biol Phys. 2008;70:1447–52.
38. Klein J, Dawson LA, Jiang H, et al. Prospective longitudinal assessment of quality of life for liver cancer patients treated with stereotactic body radiation therapy. Int J Radiat Oncol Biol Phys. 2015;93:16–25.
39. Eid S, Stromberg AJ, Ames S, Ellis S, McMasters KM, Martin RC. Assessment of symptom experience in patients undergoing hepatic resection or ablation. Cancer. 2006;107:2715–22.
40. Salem R, Gilbertsen M, Butt Z, et al. Increased quality of life among hepatocellular carcinoma patients treated with radioembolization, compared with chemoembolization. Clin Gastroenterol Hepatol. 2013;11(1358–1365):e1351.
41. Huang G, Chen X, Lau WY, et al. Quality of life after surgical resection compared with radiofrequency ablation for small hepatocellular carcinomas. Br J Surg. 2014;101:1006–15.
42. Toro A, Pulvirenti E, Palermo F, Di Carlo I. Health-related quality of life in patients with hepatocellular carcinoma after hepatic resection, transcatheter arterial chemoembolization, radiofrequency ablation or no treatment. Surg Oncol. 2012;21:e23–30.
43. Chiba T, Tokuuye K, Matsuzaki Y, et al. Proton beam therapy for hepatocellular carcinoma: a retrospective review of 162 patients. Clin Cancer Res. 2005;11:3799–805.
44. Kawashima M, Furuse J, Nishio T, et al. Phase II study of radiotherapy employing proton beam for hepatocellular carcinoma. J Clin Oncol. 2005;23:1839–46.
45. Fukumitsu N, Sugahara S, Nakayama H, et al. A prospective study of hypofractionated proton beam therapy for patients with hepatocellular carcinoma. Int J Radiat Oncol Biol Phys. 2009;74:831–6.
46. Bush DA, Kayali Z, Grove R, Slater JD. The safety and efficacy of high-dose proton beam radiotherapy for hepatocellular carcinoma: a phase 2 prospective trial. Cancer. 2011;117:3053–9.
47. Bush DA, Hillebrand DJ, Slater JM, Slater JD. High-dose proton beam radiotherapy of

hepatocellular carcinoma: preliminary results of a phase II trial. Gastroenterology. 2004;127:S189–93.
48. Bush DA, Smith JC, Slater JD, et al. Randomized clinical trial comparing proton beam radiation therapy with transarterial chemoembolization for hepatocellular carcinoma: results of an interim analysis. Int J Radiat Oncol Biol Phys. 2016;95:477–82.
49. Imada H, Kato H, Yasuda S, et al. Comparison of efficacy and toxicity of short-course carbon ion radiotherapy for hepatocellular carcinoma depending on their proximity to the porta hepatis. Radiother Oncol. 2010;96:231–5.
50. Hata M, Tokuuye K, Sugahara S, et al. Proton beam therapy for hepatocellular carcinoma with portal vein tumor thrombus. Cancer. 2005;104:794–801.
51. Sugahara S, Nakayama H, Fukuda K, et al. Proton-beam therapy for hepatocellular carcinoma associated with portal vein tumor thrombosis. Strahlenther Onkol. 2009;185:782–8.
52. Hong TS, Wo JY, Yeap BY, et al. Multi-Institutional Phase II study of high-dose hypofractionated proton beam therapy in patients with localized, unresectable hepatocellular carcinoma and intrahepatic cholangiocarcinoma. J Clin Oncol. 2016;34:460–8.
53. Hashimoto T, Tokuuye K, Fukumitsu N, et al. Repeated proton beam therapy for hepatocellular carcinoma. Int J Radiat Oncol Biol Phys. 2006;65:196–202.
54. Andrews JC, Walker SC, Ackermann RJ, Cotton LA, Ensminger WD, Shapiro B. Hepatic radioembolization with Yttrium-90 containing glass microspheres: preliminary results and clinical follow-Up. J Nucl Med. 1994;35:1637–44.
55. Dancey JE, Shepherd FA, Paul K, et al. Treatment of nonresectable hepatocellular carcinoma with intrahepatic 90Y-microspheres. J Nucl Med. 2000;41:1673–81.
56. Liapi E. Geschwind J-FH. Intra-Arterial therapies for hepatocellular carcinoma: where do we stand? Ann Surg Oncol. 2010;17:1234–46.
57. Kulik LM, Carr BI, Mulcahy MF, et al. Safety and efficacy of 90Y radiotherapy for hepatocellular carcinoma with and without portal vein thrombosis. Hepatology. 2008;47:71–81.
58. Sangro B, Iñarrairaegui M, Bilbao JI. Radioembolization for hepatocellular carcinoma. J Hepatol. 56: 464–73.
59. Salem R, Lewandowski RJ, Mulcahy MF, et al. Radioembolization for hepatocellular carcinoma using Yttrium-90 microspheres: a comprehensive report of long-term outcomes. Gastroenterology. 2010;138:52–64.
60. Hilgard P, Hamami M, Fouly AE, et al. Radioembolization with yttrium-90 glass microspheres in hepatocellular carcinoma: european experience on safety and long-term survival. Hepatology. 2010;52:1741–9.
61. Sangro B, Carpanese L, Cianni R, et al. Survival after Yttrium-90 resin microsphere radioembolization of hepatocellular carcinoma across Barcelona clinic liver cancer stages: a European evaluation. Hepatology. 2011;54:868–78.
62. Llovet JM, Real MI, Montaña X, et al. Arterial embolisation or chemoembolisation versus symptomatic treatment in patients with unresectable hepatocellular carcinoma: a randomised controlled trial. Lancet. 2002;359:1734–9.
63. Lo C-M, Ngan H, Tso W-K, et al. Randomized controlled trial of transarterial lipiodol chemoembolization for unresectable hepatocellular carcinoma. Hepatology. 2002;35:1164–71.
64. Salem R, Gordon AC, Mouli S, et al. Y90 radioembolization significantly prolongs time to progression compared with chemoembolization in patients with hepatocellular carcinoma. Gastroenterology. 2016 Dec; 151(6):1155–1163.e2.
65. Lance C, McLennan G, Obuchowski N, et al. comparative analysis of the safety and efficacy of transcatheter arterial chemoembolization and Yttrium-90 radioembolization in patients with unresectable hepatocellular carcinoma. J Vasc Interv Radiol. 2011;22:1697–705.
66. Salem R, Lewandowski RJ, Kulik L, et al. Radioembolization results in longer time-to-progression and reduced toxicity compared with chemoembolization in patients with hepatocellular carcinoma. Gastroenterology. 2011;140:497–507. e492.
67. Moreno-Luna LE, Yang JD, Sanchez W, et al. Efficacy and safety of transarterial radioembolization versus chemoembolization in patients with hepatocellular carcinoma. Cardiovasc Intervent Radiol. 2012;36:714–23.
68. El Fouly A, Ertle J, El Dorry A, et al. In intermediate stage hepatocellular carcinoma: radioembolization with Yttrium 90 or chemoembolization? Liver Int. 2015;35:627–35.
69. Kolligs FT, Bilbao JI, Jakobs T, et al. Pilot randomized trial of selective internal radiation therapy vs. chemoembolization in unresectable hepatocellular carcinoma. Liver Int. 2015;35:1715–21.
70. Mazzaferro V, Sposito C, Bhoori S, et al. Yttrium-90 radioembolization for intermediate-advanced hepatocellular carcinoma: a phase 2 study. Hepatology. 2013;57:1826–37.
71. Llovet JM, Ricci S, Mazzaferro V, et al. Sorafenib in advanced hepatocellular carcinoma. N Engl J Med. 2008;359:378–90.
72. Atassi B, Bangash AK, Lewandowski RJ, et al. Biliary sequelae following radioembolization with yttrium-90 microspheres. J Vasc Interv Radiol. 2008;19:691–7.
73. Sangro B, Gil-Alzugaray B, Rodriguez J, et al. Liver disease induced by radioembolization of liver tumors. Cancer. 2008;112:1538–46.

74. Gil-Alzugaray B, Chopitea A, Iñarrairaegui M, et al. Prognostic factors and prevention of radioembolization-induced liver disease. Hepatology. 2013;57:1078–87.
75. Mohnike K, Wieners G, Pech M, et al. Image-guided interstitial high-dose-rate brachytherapy in hepatocellular carcinoma. Dig Dis. 2009;27:170–4.
76. Dritschilo A, Grant EG, Harter KW, Holt RW, Rustgi SN, Rodgers JE. Interstitial radiation therapy for hepatic metastases: sonographic guidance for applicator placement. AJR Am J Roentgenol. 1986;147:275–8.
77. Dritschilo A, Harter KW, Thomas D, et al. Intraoperative radiation therapy of hepatic metastases: technical aspects and report of a pilot study. Int J Radiat Oncol Biol Phys. 1988;14:1007–11.
78. Ricke J, Wust P, Stohlmann A, et al. CT-guided interstitial brachytherapy of liver malignancies alone or in combination with thermal ablation: phase I–II results of a novel technique. Int J Radiat Oncol Biol Phys. 2004;58:1496–505.
79. Mohnike K, Wieners G, Schwartz F, et al. Computed tomography–guided high-dose-rate brachytherapy in hepatocellular carcinoma: safety, efficacy, and effect on survival. Int J Radiat Oncol Biol Phys. 2010;78:172–9.
80. Mohnike K, Wolf S, Damm R, et al. Radioablation of liver malignancies with interstitial high-dose-rate brachytherapy. Strahlentherapie und Onkologie. 2016:1–9.
81. Denecke T, Stelter L, Schnapauff D, et al. CT-guided interstitial brachytherapy of hepatocellular carcinoma before liver transplantation: an equivalent alternative to transarterial chemoembolization? Eur Radiol. 2015;25:2608–16.
82. Pirisi M, Avellini C, Fabris C, et al. Portal vein thrombosis in hepatocellular carcinoma: age and sex distribution in an autopsy study. J Cancer Res Clin Oncol. 1998;124:397–400.
83. Kalogeridi MA, Zygogianni A, Kyrgias G, et al. Role of radiotherapy in the management of hepatocellular carcinoma: a systematic review. World J Hepatol. 2015;7:101–12.
84. Llovet JM, Bustamante J, Castells A, et al. Natural history of untreated nonsurgical hepatocellular carcinoma: rationale for the design and evaluation of therapeutic trials. Hepatology. 1999;29:62–7.
85. Kim DY, Park W, Lim DH, et al. Three-dimensional conformal radiotherapy for portal vein thrombosis of hepatocellular carcinoma. Cancer. 2005;103:2419–26.
86. Toya R, Murakami R, Baba Y, et al. Conformal radiation therapy for portal vein tumor thrombosis of hepatocellular carcinoma. Radiother Oncol. 2007;84:266–71.
87. Nakazawa T, Hidaka H, Shibuya A, et al. Overall survival in response to sorafenib versus radiotherapy in unresectable hepatocellular carcinoma with major portal vein tumor thrombosis: propensity score analysis. BMC Gastroenterol. 2014;14:84.
88. Xi M, Zhang L, Zhao L, et al. Effectiveness of stereotactic body radiotherapy for hepatocellular carcinoma with portal vein and/or inferior vena cava tumor thrombosis. PLoS ONE. 2013;8:e63864.
89. Shah SA, Cleary SP, Tan JC, et al. An analysis of resection vs transplantation for early hepatocellular carcinoma: defining the optimal therapy at a single institution. Ann Surg Oncol. 2007;14:2608–14.
90. O'Connor JK, Trotter J, Davis GL, Dempster J, Klintmalm GB, Goldstein RM. Long-term outcomes of stereotactic body radiation therapy in the treatment of hepatocellular cancer as a bridge to transplantation. Liver Transpl. 2012;18:949–54.
91. Facciuto ME, Singh MK, Rochon C, et al. Stereotactic body radiation therapy in hepatocellular carcinoma and cirrhosis: evaluation of radiological and pathological response. J Surg Oncol. 2012;105:692–8.
92. Seong J, Koom WS, Park HC. Radiotherapy for painful bone metastases from hepatocellular carcinoma. Liver Int. 2005;25:261–5.
93. Soliman H, Ringash J, Jiang H, et al. Phase II trial of palliative radiotherapy for hepatocellular carcinoma and liver metastases. J Clin Oncol. 2013;31:3980–6.
94. Llovet JM, Bruix J. Systematic review of randomized trials for unresectable hepatocellular carcinoma: chemoembolization improves survival. Hepatology. 2003;37:429–42.
95. Marelli L, Stigliano R, Triantos C, et al. Transarterial therapy for hepatocellular carcinoma: which technique is more effective? a systematic review of cohort and randomized studies. Cardiovasc Intervent Radiol. 2006;30:6–25.
96. Meng MB, Cui YL, Lu Y, et al. Transcatheter arterial chemoembolization in combination with radiotherapy for unresectable hepatocellular carcinoma: a systematic review and meta-analysis. Radiother Oncol. 2009;92:184–94.
97. Cheng AL, Kang YK, Chen Z, et al. Efficacy and safety of sorafenib in patients in the Asia-Pacific region with advanced hepatocellular carcinoma: a phase III randomised, double-blind, placebo-controlled trial. Lancet Oncol. 2009;10:25–34.
98. Dawson L, Brade A, Cho C, Kim J. Phase I Study of Sorafenib and SBRT for advanced hepatocellular carcinoma. MA: American Society for Therapeutic Radiology and Oncology Boston; 2012.
99. Ricke J, Bulla K, Kolligs F, et al. Safety and toxicity of radioembolization plus Sorafenib in advanced hepatocellular carcinoma: analysis of the European multicentre trial SORAMIC. Liver Int. 2015;35:620–6.
100. Bruix J, Takayama T, Mazzaferro V, et al. Adjuvant sorafenib for hepatocellular carcinoma after resection or ablation (STORM): a phase 3, randomised,

double-blind, placebo-controlled trial. Lancet Oncol. 2015;16:1344–54.
101. Lencioni R, Llovet JM, Han G, et al. Sorafenib or placebo plus TACE with doxorubicin-eluting beads for intermediate stage HCC: The SPACE trial. J Hepatol. 2016;64:1090–8.
102. Meyer T, Fox R, Ma YT et al. A randomized placebo-controlled, double-blinded, phase III trial evaluating sorafenib in combination with transarterial chemoembolisation (TACE) in patients with unresectable hepatocellular carcinoma (HCC). Proceedings of the 2016 ASCO Annual Meeting; 2016 June 3–7; Chicago, IL. Abstract 4018.
103. Liu M-T, Li S-H, Chu T-C, et al. Three-dimensional conformal radiation therapy for unresectable hepatocellular carcinoma patients who had failed with or were unsuited for transcatheter arterial chemoembolization. Jpn J Clin Oncol. 2004;34:532–9.
104. Kim TH, Kim DY, Park J-W, et al. Three-dimensional conformal radiotherapy of unresectable hepatocellular carcinoma patients for whom transcatheter arterial chemoembolization was ineffective or unsuitable. Am J Clin Oncol. 2006;29:568–75.
105. Oh D, Lim DH, Park HC, et al. Early three-dimensional conformal radiotherapy for patients with unresectable hepatocellular carcinoma after incomplete transcatheter arterial chemoembolization: a prospective evaluation of efficacy and toxicity. Am J Clin Oncol. 2010;33:370–5.
106. Bibault JE, Dewas S, Vautravers-Dewas C, et al. Stereotactic body radiation therapy for hepatocellular carcinoma: prognostic factors of local control, overall survival, and toxicity. PLoS ONE. 2013;8:e77472.
107. Huertas A, Baumann AS, Saunier-Kubs F, et al. Stereotactic body radiation therapy as an ablative treatment for inoperable hepatocellular carcinoma. Radiother Oncol. 2015;115:211–6.
108. Jang WI, Kim MS, Bae SH, et al. High-dose stereotactic body radiotherapy correlates increased local control and overall survival in patients with inoperable hepatocellular carcinoma. Radiat Oncol. 2013;8:250.
109. Kang JK, Kim MS, Cho CK, et al. Stereotactic body radiation therapy for inoperable hepatocellular carcinoma as a local salvage treatment after incomplete transarterial chemoembolization. Cancer. 2012;118:5424–31.
110. Kwon JH, Bae SH, Kim JY, et al. Long-term effect of stereotactic body radiation therapy for primary hepatocellular carcinoma ineligible for local ablation therapy or surgical resection. Stereotactic radiotherapy for liver cancer. BMC Cancer. 2010;10:475.
111. Sanuki N, Takeda A, Oku Y, et al. Stereotactic body radiotherapy for small hepatocellular carcinoma: a retrospective outcome analysis in 185 patients. Acta Oncol. 2014;53:399–404.
112. Seo YS, Kim MS, Yoo SY, et al. Preliminary result of stereotactic body radiotherapy as a local salvage treatment for inoperable hepatocellular carcinoma. J Surg Oncol. 2010;102:209–14.
113. Wahl DSM, Tao Y, Pollom E, Caoili E, Lawrence T, Schipper M, Feng M. Outcomes after stereotactic body radiotherapy or radiofrequency ablation for hepatocellular carcinoma. J Clin Oncol. 2015.
114. Yamashita H, Onishi H, Murakami N, et al. Survival outcomes after stereotactic body radiotherapy for 79 Japanese patients with hepatocellular carcinoma. J Radiat Res. 2015;56:561–7.
115. Yoon SM, Lim YS, Park MJ, et al. Stereotactic body radiation therapy as an alternative treatment for small hepatocellular carcinoma. PLoS ONE. 2013;8:e79854.
116. Kato H, Tsujii H, Miyamoto T, et al. Results of the first prospective study of carbon ion radiotherapy for hepatocellular carcinoma with liver cirrhosis. Int J Radiat Oncol Biol Phys. 2004;59:1468–76.
117. Seong J, Keum KC, Han KH, et al. Combined transcatheter arterial chemoembolization and local radiotherapy of unresectable hepatocellular carcinoma. Int J Radiat Oncol Biol Phys. 1999;43:393–7.
118. Guo WJ, Yu EX, Liu LM, et al. Comparison between chemoembolization combined with radiotherapy and chemoembolization alone for large hepatocellular carcinoma. World J Gastroenterol. 2003;9:1697–701.
119. Yamada K, Izaki K, Sugimoto K, et al. Prospective trial of combined transcatheter arterial chemoembolization and three-dimensional conformal radiotherapy for portal vein tumor thrombus in patients with unresectable hepatocellular carcinoma. Int J Radiat Oncol Biol Phys. 2003;57:113–9.
120. Yoon SM, Lim YS, Won HJ, et al. Radiotherapy plus transarterial chemoembolization for hepatocellular carcinoma invading the portal vein: long-term patient outcomes. Int J Radiat Oncol Biol Phys. 2012;82:2004–11.
121. Tazawa J, Maeda M, Sakai Y, et al. Radiation therapy in combination with transcatheter arterial chemoembolization for hepatocellular carcinoma with extensive portal vein involvement. J Gastroenterol Hepatol. 2001;16:660–5.

Part V

Intrahepatic and Hilar Cholangiocarcinoma

15 Intrahepatic and Hilar Cholangiocarcinomas: Epidemiology, Basic Principles of Treatment, and Clinical Data

S. Lindsey Davis, MD

15.1 Background

The general term cholangiocarcinoma refers to any cancer arising from bile duct epithelium, though is further defined by anatomic location. Those cholangiocarcinomas that occur in the bile ducts within the hepatic parenchyma are considered intrahepatic tumors, while those that occur from the junction of the left and right hepatic ducts to the common bile duct are considered extrahepatic. Extrahepatic cholangiocarcinomas are further categorized, with those cancers occurring at or near the junction of the left and right hepatic ducts considered hilar cholangiocarcinomas or Klatskin tumors, and those distal to the confluence to just above the ampulla of Vater considered distal cholangiocarcinomas (Fig. 15.1). Gallbladder and ampullary cancers are considered separate entities [1]. It is thought that the hilar tumors make up the largest proportion of cholangiocarcinomas, followed by extrahepatic and then intrahepatic tumors [2]. The following Chap. 16 will review the epidemiology, risk factors, diagnosis, molecular pathogenesis, staging, and treatment of intrahepatic and hilar cholangiocarcinomas.

S. Lindsey Davis (✉)
Division of Medical Oncology, Department of Medicine, University of Colorado Anschutz Medical Campus, Mail Stop 8117, 12801 East 17th Avenue, Room 8125, Aurora, CO 80045, USA
e-mail: Sarah.Davis@ucdenver.edu

15.2 Epidemiology

The most recent assessment of cholangiocarcinoma in the USA according to SEER data reports that there were 11,296 patients (6036 men and 5260 women) with intrahepatic cholangiocarcinoma between the years 2000 and 2011. According to this data, the incidence of intrahepatic cholangiocarcinoma in the USA is 1.6 cases per 100,000 per year, with a prevalence of 15.88 per million persons. This incidence clearly increases with age and is highest in patients 80 years of age and older. When evaluated according to race/ethnic group, the incidence is higher in Asian and Hispanic populations as compared to non-Hispanic white and black populations [3].

Interestingly, the most recent estimates of intrahepatic cholangiocarcinoma incidence have significantly increased as compared to past SEER data, which demonstrated an incidence of 0.32 cases per 100,000 between 1975 and 1979, and 0.85 per 100,000 between 1995 and 1999 [4]. Given improvements in the diagnosis of cholangiocarcinoma in the USA since the 1970s, it is possible that some of this increase is related to increased detection of intrahepatic cholangiocarcinoma rather than a true increase in incidence. However, data evaluating this possibility has shown no trend toward a diagnosis of smaller tumors or earlier stage disease, and no increase in the degree of microscopic confirmation of disease, as may be expected in the case of improved diagnosis [4]. Furthermore, an increase related to

J. Meyer and T.E. Schefter (eds.), *Radiation Therapy for Liver Tumors*,
DOI 10.1007/978-3-319-54531-8_15

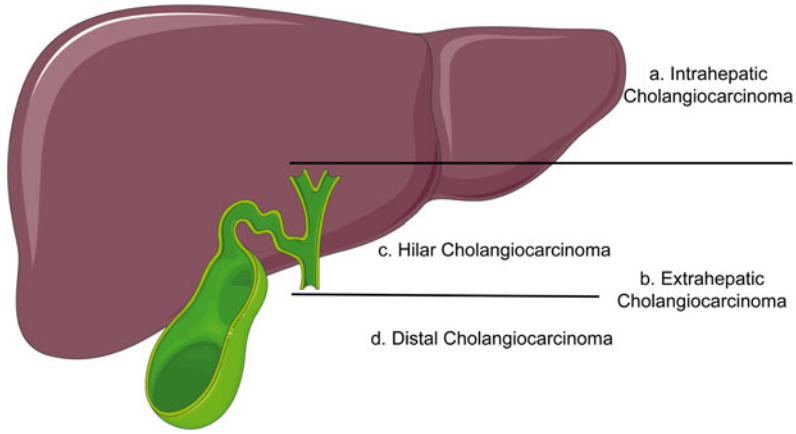

Fig. 15.1 Cholangiocarcinoma classification: **a** Intrahepatic cholangiocarcinoma: tumors in the bile ducts within the hepatic parenchyma **b** Extrahepatic cholangiocarcinoma: tumors from the junction of the *left* and *right* hepatic ducts to the common bile duct. **c** Hilar cholangiocarcinoma: at or near the junction of the *left* and *right* hepatic ducts. **d** Distal cholangiocarcinoma: distal to the confluence to just above the ampulla of Vater [Figure created using graphics from http://www.servier.com/Powerpoint-image-bank and PowerPoint. With permission from Creative Commons (https://creativecommons.org/licenses/by/3.0/)]

increased detection of disease would be expected to plateau over time [3], which has not been seen according to most recent SEER data.

The true incidence of hilar cholangiocarcinoma is more difficult to assess, as it has been categorized as both intrahepatic and extrahepatic cholangiocarcinoma according to varied International Classification of Diseases for Oncology (ICD-O) coding schemes [5]. In addition, since hilar cholangiocarcinoma should be categorized as extrahepatic based on its anatomic involvement of the hepatic duct bifurcation, the incidence and prevalence data for intrahepatic cholangiocarcinoma may be falsely elevated by the inclusion of this subset, explaining some of the increase in its incidence described above. One study evaluating SEER registry data from 1973 to 2002 estimated that the misclassification of hilar cholangiocarcinomas led to overreporting of intrahepatic cholangiocarcinoma by 13% and underreporting of extrahepatic cholangiocarcinoma by 15%. However, even after the exclusion of hilar cholangiocarcinoma from the intrahepatic subset, the incidence of intrahepatic cholangiocarcinoma in the USA still increased between the years 1992 and 2000 [5].

A similar evaluation was undertaken in England and Wales, yielding comparable results. In addition, the latter study noted that there is no ICD code available for the term "hilar cholangiocarcinoma," only for Klatskin tumors, leading to further confusion as the two terms are generally not used interchangeably for tumor registration purposes. Furthermore, the study identified that tumors that are not specifically classified beyond the term "cholangiocarcinoma" are most often categorized as intrahepatic cholangiocarcinoma by tumor registries [6]. According to this data, it is clearly very difficult to identify the true incidence of hilar cholangiocarcinoma.

Worldwide, cholangiocarcinoma as a whole represents about 10–25% of primary liver cancers, with incidence rates estimated between 0.3 and 1.5 per 100,000 in most Western countries as well as many Eastern Asian nations. However, cholangiocarcinoma represents the most common cause of cancer in men in Thailand, and the third most common cause in women, with incidence rates of 33.4 per 100,000 and 12.3 per 100,000, respectively, between 1998 and 2000 [7]. Though the same caveats of classification apply, the trend of increasing incidence of intrahepatic cholangiocarcinoma in the USA has also been seen in various European and Asian countries [8–10].

15.3 Risk Factors

A variety of risk factors have been found to contribute to the development of cholangiocarcinoma. Of these, liver fluke infection and biliary tract disorders associated with chronic inflammation are the best established.

Liver fluke infections have been most closely linked to cholangiocarcinoma risk in endemic areas of Asia, specifically Thailand, which explains at least a portion of the significant disease burden in this country. The liver fluke *Opisthorchis viverrini* is most closely associated with cholangiocarcinoma risk, though *Clonorchis sinensis* has also been implicated. Infection in humans occurs through ingestion of raw or undercooked fish serving as hosts. After ingestion, the parasites move from the duodenum to the biliary tree where they mature and can survive for over 10 years. The link between liver fluke infection and cholangiocarcinoma is thought to be chronic inflammation and associated tissue and DNA damage induced in the setting of this chronic infection, though additional host and environmental factors likely contribute [11]. Efforts to reduce the burden of liver fluke infections in endemic areas such as northeast Thailand are ongoing, with a significant decrease in such infections documented in an approximately 20-year period of attempted parasite control through education and treatment with the anti-helminthic agent praziquantel. An associated decrease in cholangiocarcinoma incidence has yet to be observed in these areas, though work to strengthen prevention programs is ongoing [12].

Another well-defined risk factor for cholangiocarcinoma is primary sclerosing cholangitis (PSC), which is associated with an estimated 7–9% incidence of cholangiocarcinoma. Various studies evaluating the risk of cholangiocarcinoma in PSC have determined that approximately half of cholangiocarcinomas diagnosed in this patient population are found within the first year of PSC diagnosis [13]. Chronic inflammation is thought to be the primary pathogenic feature leading to increased risk of cholangiocarcinoma in PSC, and as of yet, no additional factors have been identified as reliable predictors of cholangiocarcinoma in this population. There are no clear guidelines for screening for cholangiocarcinoma in PSC, though a combination of imaging, ERCP, and Ca 19-9 monitoring is generally accepted [14].

Bile duct cysts have also been identified as an underlying risk factor for the development of cholangiocarcinoma, with an incidence of 10–30% documented in adult patients. Highest risk has been associated with type I and type IV cysts, with an ongoing risk of developing cholangiocarcinoma remaining even after cyst excision. Higher concentrations and stasis of bile acids due to cysts, as well as reflux of pancreatic enzymes and amylase in the bile ducts, are thought to contribute to malignant transformation in these patients [15]. Given the association of malignancy with bile duct cysts, surgical resection is generally recommended for these lesions [16].

Through similar processes of biliary obstruction and bile stasis leading to chronic inflammation, hepatolithiasis has also been identified as a risk factor for cholangiocarcinoma. Though rare in Western countries, the prevalence of hepatolithiasis has been documented at up to 47% in parts of Asia [17], with cholangiocarcinoma identified in up to 10% of patients with intrahepatic stones [18].

In addition to these well-documented risk factors for cholangiocarcinoma, recent studies have suggested that cirrhosis and viral hepatitis B and C may also be associated with an increased risk of developing intrahepatic cholangiocarcinoma. Three meta-analyses have evaluated the risk of hepatitis B and cholangiocarcinoma, all focusing on intrahepatic disease. All three demonstrated an increased risk of intrahepatic cholangiocarcinoma, with documented relative risk of 3.42 (95% CI, 2.46–43.74) [19] and odds ratio of 5.45 (95% CI, 3.19–9.63) [20] and 3.17 (95% CI, 1.88–5.34) [21], respectively. One study also evaluated overall risk of cholangiocarcinoma in patients with hepatitis B infection and found a relative risk of 2.66 (95% CI, 1.97–3.60) [19]. A greater association with Asian

versus Western populations was not consistently demonstrated across these three meta-analyses.

An increased risk of cholangiocarcinoma in patients with hepatitis C has also been documented in a recent meta-analysis, with an odds ratio of 5.44 (95% CI, 2.72–10.89). In a pooled risk assessment of intrahepatic and extrahepatic diseases, the risk was greater in the intrahepatic subset (OR-3.38, 95% CI, 2.72–4.21) as compared to extrahepatic (OR = 1.75, 95% CI, 1.00–3.05). In addition, this risk seemed to be more pronounced in North America than Asia (pooled OR = 6.48 vs. 2.01) [22].

Other potential risk factors for the development of cholangiocarcinoma include diabetes, obesity, and alcohol use, though these associations have not been as widely studied and associations are less strong [23]. In addition, there are some hereditary cancer syndromes with which cholangiocarcinoma is thought to be associated, including hereditary non-polyposis colorectal cancer (HNPCC) syndrome [24] and BAP1 hereditary cancer predisposition syndrome [25].

15.4 Diagnosis

Due to its anatomic location, cholangiocarcinoma can be difficult to clearly appreciate by imaging and access by biopsy, making diagnosis challenging, especially in the early stages of the disease. In addition, presenting symptoms are often non-specific, including such complaints as fatigue, weight loss, and generalized abdominal pain, without features isolating to the biliary tree. Painless jaundice can be associated with hilar cholangiocarcinoma, though is uncommon in patients with primary intrahepatic disease [26]. Multiple modalities are often required to make the diagnosis of cholangiocarcinoma, as will be detailed below.

15.4.1 Laboratory Testing

Though the CA 19-9 tumor biomarker is often used to trend disease activity in patients with known cholangiocarcinoma, its use as a diagnostic tool is limited. This is largely due to elevations of CA 19-9 in the setting of biliary obstruction and inflammation from any cause, as well as the fact that CA 19-9 may also be elevated in a variety of other malignancies, including primary pancreatic cancer. The sensitivity and specificity of CA 19-9 for the diagnosis of cholangiocarcinoma range widely between studies, though in one assessment of 322 patients with biliary tract disease, the sensitivity and specificity of CA 19-9 were 77.6% and 83% in patients without cholangitis or cholestasis, while in patients with either of these conditions, sensitivity and specificity decreased to 74% and 41.5%, respectively [27]. Also of note, approximately 10% of individuals are not capable of producing CA 19-9 due to lack of Lewis antigen [28].

Various studies have attempted to combine serum biomarkers in hopes of improving test specificity. One such trial identified the combination of an elevated CA 19-9 and elevated alkaline phosphatase level as most specific out of a panel of serum makers, with diagnostic accuracy reaching 95% in their study set of approximately 170 patients [29]. Additional potential biomarkers to aid in cholangiocarcinoma are under investigation, though none are yet validated for clinical use [26].

15.4.2 Imaging

Various imaging studies are often utilized in the workup of cholangiocarcinoma, including multiphasic contrast-enhanced computed tomography (CT) and magnetic resonance imaging (MRI). Unlike hepatocellular carcinoma, such studies are not generally considered to be diagnostic of cholangiocarcinoma, though they can help to guide further testing. Though positron-emission tomography (PET) may be helpful for the assessment of the nodal and metastatic involvement of disease in some scenarios [30], it is rarely useful in the diagnosis of cholangiocarcinoma, especially in early-stage disease. Magnetic resonance cholangiopancreatography (MRCP) can be helpful in the

diagnosis of hilar lesions, with sensitivity and specificity similar to those of more invasive methods such as endoscopic retrograde cholangiography (ERCP) [31].

The limitations of using imaging to diagnose cholangiocarcinoma are largely related to difficulties in distinguishing bile duct cancers from other intrahepatic and biliary processes, both malignant and benign. Small intrahepatic cholangiocarcinoma lesions can be difficult to differentiate from hepatocellular carcinoma in the setting of underlying cirrhosis. A study of gadolinium-based contrast-enhanced MRI was performed in 71 patients with intrahepatic cholangiocarcinoma and 612 patients with hepatocellular carcinoma, all with underlying cirrhosis. When pathologic specimens were compared to imaging findings, stable and progressive contrast enhancement was demonstrated in significantly more intrahepatic cholangiocarcinomas, while classic contrast washout in delayed phases was demonstrated in a greater proportion of hepatocellular carcinomas. However, given some overlap in imaging findings between the two malignancies, these imaging characteristics are not considered diagnostic of intrahepatic cholangiocarcinoma [32].

The utility of the Liver Imaging Reporting and Data System (LI-RADS) v2014—developed to assist in the classification of hepatic lesions in patients at risk of hepatocellular carcinoma—has been assessed for utility in the diagnosis of intrahepatic mass-forming cholangiocarcinomas by gadoxetic acid-enhanced MRI. In a retrospective review of 35 pathologically confirmed intrahepatic cholangiocarcinomas in patients with cirrhosis or chronic hepatitis B, approximately 80% were correctly assigned according to the LI-RADS algorithm, though up to 11% were incorrectly diagnosed as HCC [33]. This again suggests that current imaging protocols are not sufficient for the diagnosis of cholangiocarcinoma.

Hilar cholangiocarcinoma can be difficult to distinguish from the benign autoimmune condition known as immunoglobulin G4 (IgG4)-associated cholangitis by imaging. Specific characteristics have been identified to help differentiate these two processes, with cholangiocarcinoma more commonly associated with strictures longer than 12 mm, asymmetric areas of narrowing, indistinct margins, and venous hyperenhancement. In contrast, multifocal biliary strictures, significant thickening of the bile duct wall, smooth margins, visible lumen, late arterial hyperenhancement, and homogeneous delayed phase hyperenhancement are more commonly associated with IgG4-associated cholangitis [34]. However, additional testing including IgG4 levels [35], ratios to total IgG or IgG1 [34], and histologic evaluation are necessary to rule out IgG4-associated cholangitis in most cases.

15.4.3 Endoscopy

While of minimal utility in the diagnosis of intrahepatic cholangiocarcinoma, ERCP and endoscopic ultrasound (EUS) can be very useful in the diagnosis of hilar cholangiocarcinoma, especially in settings where a tumor mass or stricture is not clearly visible on standard imaging. In this setting, ERCP and EUS can be both diagnostic and therapeutic, providing an opportunity for visual assessment and biopsy as well as dilation and stent placement for strictures.

If tissue sampling by ERCP is performed, there is a significant chance that pathologic assessment of brushing and biopsy results will be inconclusive, with the sensitivity of such testing ranging from 20 to 60% [36]. New endoscopic technology has emerged that may help improve diagnostic accuracy. Probe-based confocal laser endomicroscopy (pCLE) is a technique that utilizes a specialized probe and fluorescein contrast to provide real-time visualization of the epithelial and subepithelial tissue of suspicious biliary strictures to assist in making the diagnosis of malignancy [37]. A prospective study of pCLE with ERCP applied to indeterminate biliary strictures in 112 patients demonstrated a sensitivity of 89% and specificity of 82%, as

compared to tissue sampling alone with a sensitivity of 56% and specificity of 100% [38].

15.4.4 Percutaneous Biopsy

There are concerns that percutaneous biopsy of a mass suspicious for cholangiocarcinoma increases the risk of tumor seeding and ultimately tumor spread. This concern is based on retrospective data demonstrating a significant increase in peritoneal metastasis in patients with hilar cholangiocarcinoma who underwent diagnostic percutaneous FNA biopsy prior to liver transplant. Of note, only six of 191 patients had a diagnostic FNA biopsy pre-transplant, although five of these six patients (83%) later developed peritoneal metastasis. None of nine patients with FNA biopsies that were negative for adenocarcinoma developed peritoneal disease, and only 8% of the patients who did not undergo biopsy were found to have peritoneal spread [39]. A second retrospective analysis of 67 patients with extrahepatic cholangiocarcinoma treated with percutaneous transhepatic biliary drainage (PTBD) prior to resection demonstrated a 6% incidence of catheter tract metastasis [40].

Concerns of seeding based on these data are primarily relevant to patients with localized disease being considered for a curative treatment. Given these patients will ultimately undergo surgical resection or transplantation, biopsy for tissue diagnosis is often deferred in this setting in hopes of mitigating the potential risk of seeding. However, biopsy should still be pursued in those patients who will be treated upfront with chemotherapy or radiation.

15.4.5 Pathologic Assessment

Though pathologic assessment is required to make the diagnosis of cholangiocarcinoma (Fig. 15.2), as noted above, obtaining sufficient biopsy tissue for histologic diagnosis is often limited by tumor location and paucicellular character [41]. The sensitivity of cytologic diagnosis for cholangiocarcinoma has been improved upon with the integration of fluorescence in situ hybridization (FISH) testing of biliary duct brushings (Fig. 15.3) [42]. The combination of cytology and polysomy per FISH further increases the diagnostic sensitivity (58%) above and beyond either modality alone (cytology, 21%; FISH 47%) [43]. Testing for polysomy by FISH is now considered a standard diagnostic tool, especially in cases where cytology alone is inconclusive for diagnosis.

15.5 Molecular Pathogenesis

As may be assumed from the risk factors associated with the development of cholangiocarcinoma, inflammation is thought to be the key driver of pathogenesis in this malignancy. In addition, activation of signaling pathways related to these inflammatory processes is considered an associated contributor.

Oxidative stress has been identified as a likely mediator of inflammatory carcinogenesis in cholangiocarcinoma, as evidenced by the identification of oxidized biomolecules in cholangiocarcinoma tissues [44], and activation of anti-apoptosis pathways in cholangiocyte cells exposed to such molecules [45]. Generation of such molecules has been related to activation by pro-inflammatory cytokines in chronic inflammatory states and is thought to cause direct damage to DNA and proteins [46]. In addition, inflammatory activation of cyclooxygenase-2 (COX-2) expression has been linked to activation of the epidermal growth factor receptor (EGFR) and downstream pathways associated with cancer cell growth and invasion [47].

It is thought that clonal expansion of those cells that are able to survive under oxidative stress conditions ultimately leads to malignant transformation to cholangiocarcinoma. Studies of cholangiocyte cell lines resistant to hydrogen peroxide demonstrated a higher proliferation rate, pseudopodia formation, loss of cell-to-cell adhesion, and increased expression of DNA methyltransferase-1, supporting this hypothesis [44].

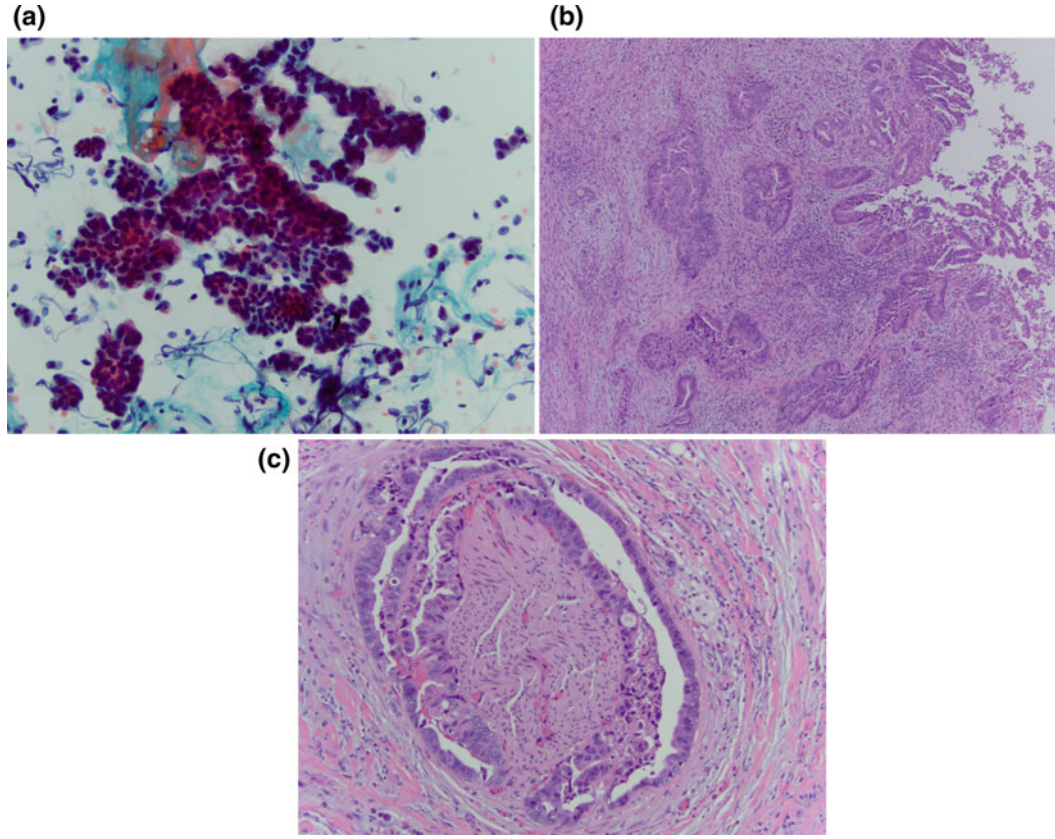

Fig. 15.2 Histologic diagnosis of cholangiocarcinoma: **a** Cytologic specimen consistent with adenocarcinoma by pap stain at 20×. **b**. H&E tissue specimen demonstrating high-grade dysplasia at the bile duct surface (*right edge*) with infiltrating adenocarcinoma (*center*) at 4×. **c** Classic finding of perineural invasion on H&E tissue specimen at 10×. [Courtesy of Dr. Kalpana Devaraj, University of Colorado, Anschutz Medical Campus]

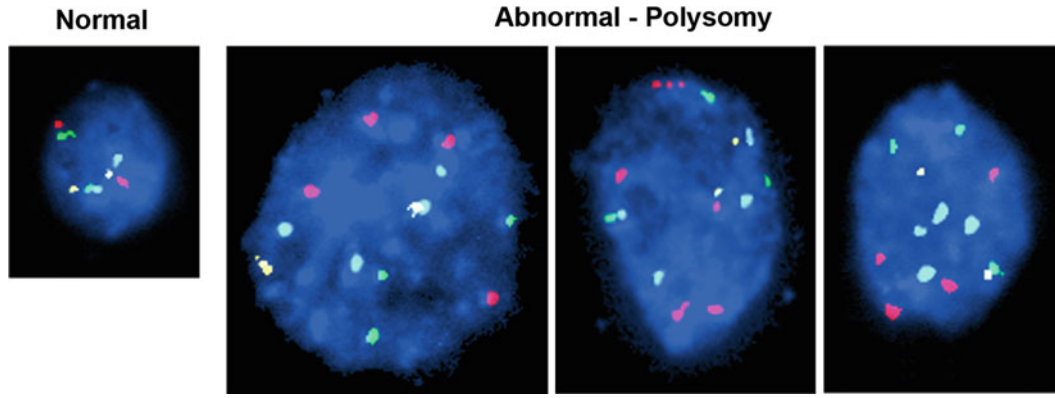

Fig. 15.3 Bile duct brushing fluorescence in situ hybridization: Each color corresponds to a probe specific for the centromere of a particular chromosome. A normal cell compared to malignant cholangiocarcinoma cells demonstrating polysomy; three or more copies of at least two of four probes. [Courtesy of Colorado Genetics Laboratory, University of Colorado, Anschutz Medical Campus]

Interestingly, it has recently been determined that in the setting of intrahepatic disease, these processes of cholangiocarcinoma development may affect not only cholangiocytes as precursor cells, but also mature hepatocytes. This concept is supported by the malignant transformation of mature hepatocytes into intrahepatic cholangiocarcinoma cells in the setting of overexpression of activated Notch1 and AKT in preclinical models [48, 49]. Similar studies have confirmed biliary epithelial cells as a progenitor of intrahepatic cholangiocarcinoma as well [50], indicating this subset of cholangiocarcinoma may originate from various cell types, and that Notch pathway activation plays an important role in cholangiocarcinoma pathogenesis.

Somatic mutations associated with aberrant cell signaling have also been associated with cholangiocarcinoma pathogenesis. Recent advances in molecular profiling through next-generation sequencing have led to the identification of distinct profiles for intrahepatic and extrahepatic diseases [51–53]. While mutations in *KRAS*, *CDKN2B* (responsible for cell cycle regulation), and *ARID1A* (associated with chromatin remodeling) are documented with some frequency in both intrahepatic and extrahepatic cholangiocarcinomas, *IDH1/2* mutations and *FGFR1-3* fusions and amplifications are most often found in intrahepatic disease [53]. In addition, extrahepatic cholangiocarcinoma is associated with a higher frequency of *TP53* and *ERBB2* mutation [52]. As these studies did not distinguish hilar disease in their analyses, the genetic profile of this cholangiocarcinoma subtype remains unclear at this time.

In addition to these molecular alterations, ROS kinase fusions have been documented in 9% of resected cholangiocarcinomas [54]. Though reported in a small study limited to 23 Chinese patients, this finding remains of interest given the targetable nature of this mutation with existing therapies. Targeting of this and other molecular aberrations identified in both intrahepatic and extrahepatic diseases is currently being evaluated in clinical trials.

15.6 Basic Principles of Staging

15.6.1 Intrahepatic Cholangiocarcinoma

The staging of intrahepatic cholangiocarcinoma has evolved in recent years, moving away from staging systems based on hepatocellular carcinoma toward a unique system designed to provide a more specific prognostic assessment. This transition has resulted in the development of four proposed systems: Okabayashi et al. [55], Liver Cancer Study Group of Japan (LCSGJ) [56], Nathan et al. [57], and AJCC/UICC 7th Edition (Table 15.1) [58]. Though generally similar, the four systems differ on the specific prognostic factors used to determine tumor stage. While all four include tumor number, vascular invasion, and lymph node metastases as key determinants, the LCSGJ system also incorporates tumor size and serosal invasion, the Nathan et al. [59] system includes extrahepatic extension, and the AJCC classification system involves periductal and visceral peritoneal invasion. A comparison of these four systems has been performed in 163 patients with intrahepatic cholangiocarcinoma, with only the AJCC system found to significantly correlate stage with clinical outcome in this study [60]. Still, none of the staging systems addresses resectability, which significantly affects outcome and prognosis as the only curative treatment for this malignancy.

15.6.2 Hilar Cholangiocarcinoma

The Bismuth–Corlette classification (Fig. 15.4) has long been used to categorize hilar cholangiocarcinoma based on the extent of hepatic ductal involvement in order to better guide surgical management. Hilar cholangiocarcinomas are divided into four types according to this system: Type I, tumor below the confluence of the left and right hepatic ducts; Type II, tumor reaching the confluence; Type III, tumor occluding the common hepatic and either the right hepatic ducts (Type IIIa) or left hepatic

Table 15.1 AJCC/UICC staging for intrahepatic and hilar cholangiocarcinomas

	Intrahepatic cholangiocarcinoma	Hilar cholangiocarcinoma
Primary tumor		
T1	Solitary tumor without vascular invasion	Tumor confined to the bile duct, extension up to the muscle layer or fibrous tissue
T2a	Solitary tumor with vascular invasion	Tumor invades beyond the wall of the bile duct to surrounding adipose tissue
T2b	Multiple tumors, with or without vascular invasion	Tumor invades adjacent hepatic parenchyma
T3	Tumor perforating the visceral peritoneum or involving extrahepatic structures through direct invasion	Tumor invades unilateral branches of the portal vein or hepatic artery
T4	Tumor with periductal invasion	Tumor invades main portal vein or its branches bilaterally; or the common hepatic artery; or the second-order biliary radicals bilaterally; or unilateral second-order biliary radicals with contralateral portal vein or hepatic artery involvement
Regional lymph nodes		
N0	No regional lymph node metastasis	No regional lymph node metastasis
N1	Regional lymph node metastasis	Regional lymph node metastasis (including nodes along the cystic duct, common bile duct, hepatic artery, and portal vein)
N2	–	Metastasis to periaortic, pericaval, superior mesenteric artery, and/or celiac artery lymph nodes
Distant metastasis		
M0	No distant metastasis	No distant metastasis
M1	Distant metastasis	Distant metastasis
Stage		
I	T1N0M0	T1N0M0
II	T2N0M0	T2N0M0
III	T3N0M0	–
IIIA	–	T3N0M0
IIIB	–	T1–3N1M0
IVA	T4N0M0, T1–4N1M0	T4N0–1M0
IVB	T1–4N0–1M1	T1–4N2M0, T1–4N0–2M1

ducts (Type IIIb); Type IV, tumor that involves the confluence and both right and left hepatic ducts or tumors that are multicentric [61]. As this classification does not take prognostic factors into consideration, it is not truly a staging system, but rather a descriptive tool useful in determining management.

A separate AJCC/UICC staging system has been developed for hilar cholangiocarcinoma in the 7th Edition (Table 15.1) [58]. This is a significant change from prior AJCC systems in which hilar cholangiocarcinoma was staged as distal cholangiocarcinoma. The current staging system takes into account depth of bile duct invasion, hepatic extension, portal vein and hepatic artery involvement, and nodal and distant metastasis, though does not assess factors important in determining resectability, which are closely tied to disease stratification and outcomes.

Since the current AJCC system does not assess these determinants of resection, additional staging systems for hilar cholangiocarcinoma

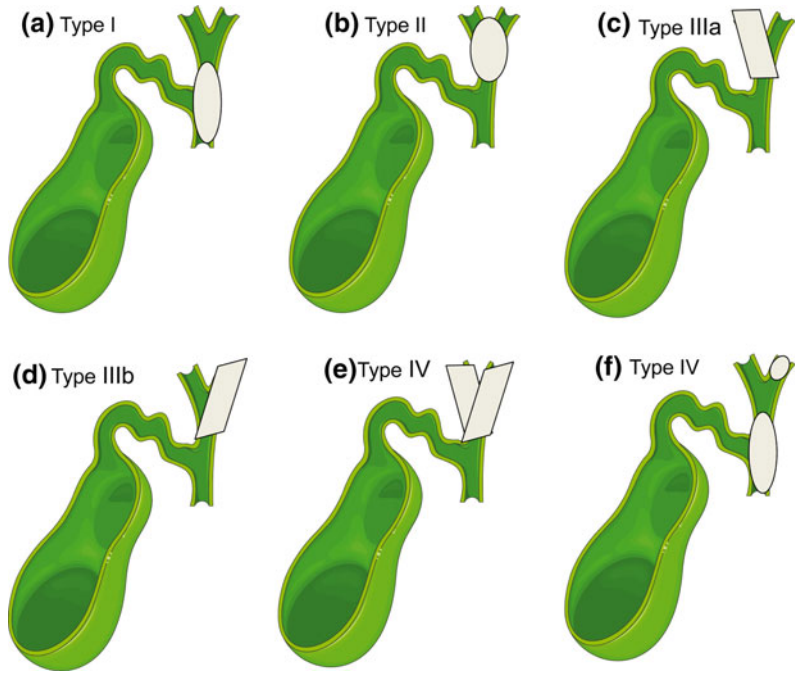

Fig. 15.4 Bismuth–Corlette classification: **a** Type I, tumor below the confluence of the *left* and *right* hepatic ducts; **b** Type II, tumor reaching the confluence; **c** Type IIIa, tumor occluding the common hepatic and the *right* hepatic ducts; **d** Type IIIb tumor occluding the common hepatic and the *left* hepatic ducts; **e** Type IV, tumor that involves the confluence and both *right* and *left* hepatic ducts; or **f**. Type IV, multicentric tumors [Figure created using graphics from http://www.servier.com/Powerpoint-image-bank and PowerPoint. With permission from Creative Commons (https://creativecommons.org/licenses/by/3.0/)]

that incorporate such have been proposed. The Memorial Sloan Kettering Cancer Center (MSKCC) system was the first of this type. This system assigns patients with hilar cholangiocarcinoma to one of the three *T*-stages according to the extent of ductal involvement by tumor, presence or absence of portal vein involvement, and presence or absence of hepatic lobar atrophy. Though in the original study the resectability rate ($p < 0.00001$, odds ratio = 0.21 [0.13–0.35]) and R0 resection rate ($p < 0.00001$, odds ratio = 0.3 [0.18–0.5]) were shown to decrease with increasing *T*-stage, and *T*-stage correlated with overall survival [62], later assessment of overall survival according to MSKCC stage in a unique patient data set did not confirm these findings [63]. Limiting factors of this system include lack of assessment of arterial involvement as well as nodal or distant metastatic disease.

A new classification system that takes into account features from each of these previously developed systems has been proposed by the International Cholangiocarcinoma Group for the Staging of Perihilar Cholangiocarcinoma. This system uses the extent of bile duct involvement, tumor size and growth type, portal vein and hepatic artery involvement, liver remnant volume, underlying hepatic disease, and lymph node and distant metastases as factors for determining the stage. The new system remains to be validated, though the group has created an online registry to help achieve this goal [64].

Overall, there have been significant improvements in the systems designed to stage cholangiocarcinoma in recent years, namely creating staging systems specific to the clearly unique entities of intrahepatic and hilar disease. However, there is still a need for a staging system that

can accurately provide a pre-surgical assessment of prognosis. Such a system has been proposed for hilar cholangiocarcinoma, though validation is ongoing.

15.7 Treatment of Localized Disease

As the only confirmed curative intervention for the treatment of cholangiocarcinoma, surgical intervention in the form of resection, or in select cases liver transplant, should be considered in all patients with localized disease. Unfortunately, many patients are not candidates for such therapy. Locoregional therapies may provide some benefit in this setting, as will be described.

15.7.1 Surgery

Achieving the goal of complete resection with negative microscopic margins (R0) for intrahepatic cholangiocarcinoma often requires a very extensive surgery, frequently with extended hepatectomy and extrahepatic bile duct reconstruction [65, 66]. Even in patients in whom complete resection is achieved, the risk of recurrence is high, reported in 45–60% of patients [66–68]. Similarly, overall survival rates following resection of intrahepatic cholangiocarcinoma are low, with most documented at or below 50% at 5 years [67–71].

Similarly, complex surgical resection, often with biliary and/or vascular reconstruction, is generally required for the surgical management of hilar cholangiocarcinoma. Recent studies have estimated postoperative mortality associated with resection of hilar cholangiocarcinoma at 1.4–10.7%, with variability according to geographic location [72–74]. These rates have significantly improved over the last number of years, along with survival rates following surgical resection. Unfortunately, these still remain low for a curative intent surgery, with five-year survival estimates ranging from 25.5–38.1% [72, 74, 75]. This is largely related to high rates of recurrent disease despite aggressive surgical intervention, with rates documented around 55% according to recent assessments [72, 75].

Studies of adjuvant chemotherapy following surgical resection have been performed in hopes of decreasing recurrence rates and improving overall survival. Unfortunately, such an advantage has not been clearly demonstrated in clinical trials, with the largest study evaluating periampullary cancers, including 96 patients with cholangiocarcinoma, showing no statistically significant survival benefit with either 5-fluorouracil (5-FU) or gemcitabine chemotherapy as compared with observation alone following surgery [76]. Ongoing clinical trials are evaluating the use of alternative chemotherapy regimens in the adjuvant setting, including gemcitabine and cisplatin in the international ACTICCA-1 trial (ClinicalTrials.gov, NCT02170090), gemcitabine and oxaliplatin in the French PRODIGE-12 trial (ClinicalTrials.gov, NCT01313377), and capecitabine in the British BILCAP trial (ClinicalTrials.gov, NCT00363584). The use of radiation therapy in the adjuvant setting will be discussed elsewhere.

15.7.2 Liver Transplant

Unfortunately, many patients with intrahepatic cholangiocarcinoma have unresectable disease due to size or location of tumor, or due to underlying cirrhotic liver disease. As such, liver transplantation has been considered as a potential treatment modality, though such practice is not widely accepted due to lack of supporting evidence. Retrospective studies have evaluated small cohorts of patients with unresectable intrahepatic cholangiocarcinoma treated with liver transplantation, with overall survival ranging from 26 to 50% at 4–5 years post-transplant [77–80]. Given the variability in patient selection procedures and neoadjuvant and adjuvant therapies included in these studies, no reliable conclusions regarding the benefit of liver transplantation in this setting can be drawn. A recent retrospective study of liver transplantation for intrahepatic cholangiocarcinoma in Spain identified a subset of patients with single

tumors <2 cm who may benefit from this approach, with a five-year overall survival of 73% in a small cohort of eight patients. This data suggests that transplant may still be appropriate for the treatment of unresectable intrahepatic cholangiocarcinoma in a subpopulation of patients [81], though this remains to be proven in prospective clinical trials.

For many patients with hilar cholangiocarcinoma, tumor resection is not possible due to the anatomic location of the lesion. A protocol of liver transplantation in combination with neoadjuvant chemoradiation in such patients with stage I/II disease has been implemented at the Mayo Clinic and has been associated with improved survival as well as lower recurrence rates as compared to patients treated with resection. The neoadjuvant therapy utilized in this protocol is multifaceted, consisting of, first, chemoradiation (4500 cGy in 30 fractions) with 5-FU chemotherapy, followed by a 2000–3000 cGy endoluminal intracavitary brachytherapy boost with iridium-192, and finally a course of 5-FU therapy continued as tolerated until the time of transplantation. Of the 38 patients treated according to this protocol in the original Mayo Clinic study, one-, three-, and 5-year survival rates were 92, 82, and 82%, as compared to 82, 48, and 21% in the 26 patients who underwent resection. The recurrence rate was also lower in the transplant group at 13% as compared to 27% in the resection group [82]. This approach has been further evaluated at 12 US liver transplant centers, with a recurrence-free survival rate of 65% at 5 years in patients meeting United Network for Organ Sharing (UNOS) criteria of tumor mass <3 cm, no prior transperitoneal tumor biopsy, and no metastatic disease [83]. Based on these results, liver transplantation should be considered in all patients with localized hilar cholangiocarcinoma that is not amenable to surgical resection. A French study is currently underway to compare transplantation to resection in the setting of resectable hilar cholangiocarcinoma (clinicaltrials.gov; NCT02232932).

15.7.3 Locoregional Therapies

Unfortunately, for many patients with localized cholangiocarcinoma, neither surgical resection nor transplantation is an option. In this subset of patients, locoregional therapies may be considered, though randomized trials to provide information on the benefit of such are lacking. Included amongst these therapies are radiofrequency ablation (RFA), transarterial embolization (bland embolization, chemoembolization, and radioembolization), transarterial chemoinfusion, and radiation therapy. Radioembolization and radiation therapy for the treatment of cholangiocarcinoma will be addressed elsewhere.

15.7.3.1 Ablation

Radiofrequency ablation for the treatment of intrahepatic cholangiocarcinoma has been evaluated in small series of patients with effective ablation documented in over 90% of tumors $\leq$3 cm in size [84–90]. Associated overall survival ranges from 27.4 to 38.5 months in these studies, many of which include patients with recurrent disease following primary surgical intervention [77, 84, 85, 90].

The use of traditional percutaneous or intraoperative RFA for the treatment of hilar cholangiocarcinoma is often limited by tumor location and anatomy. In such patients, ERCP-directed RFA has recently been established as a feasible therapy [91–93]. This approach is similar to that utilized for photodynamic therapy (PDT), an ablation technique utilizing a specific wavelength of light emitted by an ERCP probe to locally activate a systemically administered photosensitizer, with the goal of inducing cell apoptosis. Various studies of this method have demonstrated a significant improvement in overall survival when PDT was combined with stenting as compared to stenting alone [94–96]. In a small population of patients with mostly hilar cholangiocarcinoma, ERCP-directed RFA was compared to PDT, with overall survival of 9.6 versus 7.5 months, which was not statistically significantly different ($p = 0.799$) [97].

15.7.3.2 Chemoembolization

Chemoembolization, due to the nature of the procedure, is only applicable to the treatment of intrahepatic cholangiocarcinoma lesions. One retrospective study in patients with intrahepatic disease compared 72 patients who underwent transarterial chemoembolization (TACE) with cisplatin to 83 patients who received supportive care. Overall survival was significantly longer in the treatment group at 12.2 months as compared to 3.3 months in the supportive care group ($p < 0.001$), and 23% of patients treated with TACE had documented tumor regression [98]. A meta-analysis of 14 studies of transarterial therapies for the treatment of unresectable cholangiocarcinoma documented a median survival from the time of diagnosis of 15.6 months, with stable disease as the most common treatment outcome. These studies were varied in agents utilized for both chemotherapy and embolization, with two studies evaluating intra-arterial chemotherapy alone, which limits the comparison [99]. A subsequent study evaluated 115 patients treated with four different TACE regimens: (1) mitomycin C, (2) gemcitabine, (3) mitomycin C and gemcitabine, and (4) mitomycin C, gemcitabine, and cisplatin. No statistically significant difference in survival was noted according to chemotherapy protocol in this study, with median overall survival of 13 months documented [100].

Combining chemoembolization with systemic chemotherapy seems to provide a more profound benefit. In one study, the combination of systemic chemotherapy with chemoembolization was associated with a significantly longer overall survival of 28 months versus 16 months in patients who were treated with chemoembolization alone (hazard ratio (HR), 1.94; 95% confidence interval (CI), 1.13–3.33; $p = 0.02$) [101].

Chemoembolization utilizing drug-eluting beads (DEB-TACE) has also been evaluated in the treatment of intrahepatic cholangiocarcinoma. In a small study, nine patients with unresectable intrahepatic cholangiocarcinoma were treated with TACE using oxaliplatin-eluting microspheres in addition to systemic chemotherapy with gemcitabine and oxaliplatin, with outcomes compared with 11 patients treated with chemotherapy alone. The overall survival of the patients treated with DEB-TACE in addition to chemotherapy was significantly longer at 30 months, as compared to 12.7 months in those patients treated with systemic chemotherapy alone ($p = 0.004$). Another small study has retrospectively compared DEB-TACE with irinotecan-eluting beads to both standard TACE using mitomycin C and lipiodol with gelfoam embolization and systemic chemotherapy with gemcitabine and oxaliplatin. Overall survival in the DEB-TACE group was 11.7 months, which was similar to that of 11.0 months in the systemic chemotherapy group, but superior to that of 5.7 months in patients treated with standard TACE [102]. However, a retrospective review of 198 patients with intrahepatic cholangiocarcinoma treated with TACE, DEB-TACE, bland embolization, or radioembolization identified no difference in median overall survival according to the type of liver-directed therapy [103].

15.7.3.3 Transarterial Chemoinfusion

Transarterial chemoinfusion, or intra-arterial administration of chemotherapy to intrahepatic lesions without associated embolization, has also been evaluated in small studies of intrahepatic cholangiocarcinoma. Intra-arterial infusion of gemcitabine, mitomycin C, and 5-fluorouracil alone and in combination with adriamycin, epirubicin, mitomycin C, cisplatin, and interferon have been determined feasible with reasonable side effect profile. Response rates and overall survival in these small studies of varied agents ranged from 7.7 to 64% and 11.3–22.8 months, respectively [104–108]. In a recent meta-analysis comparing outcomes from studies of transarterial chemoinfusion, TACE, DEB-TACE, and radioembolization, transarterial chemoinfusion had the highest median overall survival and response rate, though also the highest rate of grade III–IV toxicity [109].

15.8 Systemic Therapy for Cholangiocarcinoma

Unfortunately, many patients with cholangiocarcinoma are not candidates for local therapies. In those patients for whom hepatic disease extent or metastatic spread preclude such treatment, systemic therapy is considered. The recommended chemotherapy regimen for such patients is based on data from the Advanced Biliary Cancer (ABC)-02 study. In this trial, 410 patients with locally advanced or metastatic intrahepatic or extrahepatic cholangiocarcinoma, gallbladder cancer, or ampullary cancer were randomized to treatment with gemcitabine 1000 mg/m2 and cisplatin 25 mg/m2 days 1 and 8 of a 21-day cycle, or gemcitabine 1000 mg/m2 days 1, 8, and 15 of a 28-day cycle. Patients in the gemcitabine/cisplatin group had a median overall survival of 11.7 months, as compared to 8.1 months in the single-agent gemcitabine group (HR, 0.64; 95% CI, 0.52–0.80; $p < 0.001$). Progression-free survival was similarly improved in the combination chemotherapy arm at 8.0 months as compared to 5.0 months in the gemcitabine group (HR, 0.63; 95% CI, 0.51–0.77; $p < 0.001$). Though the majority of patients in this study had a diagnosis of cholangiocarcinoma (58.8%), only 80 patients (20%) had intrahepatic disease and 57 (14%) had hilar cholangiocarcinoma. There was no difference in treatment effect according to tumor type in subset analysis [110].

There is no standard therapy for the treatment of advanced or metastatic cholangiocarcinoma in the second-line setting and beyond [111], though many ongoing studies evaluating systemic therapy for cholangiocarcinoma are hoping to change this. The majority of these studies are focused on biologically targeted agents. One area of particular interest for the treatment of intrahepatic cholangiocarcinoma is in drugs targeting mutated isocitrate dehydrogenase (IDH) proteins. In cancers with mutations in IDH1 or 2, cells produce D-2-hydroxyglutarate (2-HG), which has been shown to prevent hepatocyte differentiation and promote cell proliferation and survival, ultimately leading to the development of intrahepatic cholangiocarcinoma [112].

Based on this data, as well as the identification of IDH mutations in 15–29% of intrahepatic cholangiocarcinomas [113–116], clinical studies of IDH1 inhibitors are currently underway to assess potential activity in human patients. In a phase 1 clinical trial of novel IDH1 inhibitor AG-120 in patients with advanced, IDH1-mutant solid tumors (NCT02073994), preliminary efficacy results are significant for a clinical benefit rate of 43% in patients with cholangiocarcinoma [117]. Additional studies are planned to further assess the clinical activity of AG-120 in this disease. Other IDH inhibitors are also being evaluated in IDH-mutant patients, including those with cholangiocarcinoma, in early phase clinical trials; IDH1 inhibitor IDH305 (NCT02381886) and pan-IDH inhibitor AG-881 (NCT02481154).

Fibroblast growth factor receptor (FGFR) 2 fusions are also a target of interest for the treatment of intrahepatic cholangiocarcinoma. Such translocations have been identified in 6–45% of patients with intrahepatic cholangiocarcinoma according to varied detection methods including FISH, exome sequencing, and whole transcriptome sequencing [118–122]. The fusion of FGFR2 to respective partners leads to the activation of intracellular signaling pathways that ultimately lead to cellular growth and proliferation [123]. Targeting FGFR in cholangiocarcinoma is being further investigated in a phase 2 study of the pan-FGFR inhibitor BGJ398. Interim data is significant for a response rate of 14% and disease control rate of 82% in 22 evaluable patients with FGFR-altered cholangiocarcinoma [124].

15.9 Conclusion

In summary, cholangiocarcinoma is a relatively rare malignancy worldwide, with the exception of a few Asian countries, most notably Thailand.

Identifying the true incidence and prevalence of intrahepatic and hilar cholangiocarcinomas is difficult due to variable classification systems, though the incidence of intrahepatic cholangiocarcinoma does seem to be increasing in the USA and many other countries. Risk factors associated with the development of cholangiocarcinoma are related to chronic inflammation of the biliary tree through processes such as liver fluke infection and primary sclerosing cholangitis. On the molecular level, oxidative stress is a likely mediator of inflammatory carcinogenesis. Advances in molecular profiling have better defined the molecular landscape of cholangiocarcinoma and further distinguished intrahepatic disease and extrahepatic disease as unique processes. Diagnosis of both intrahepatic and hilar cholangiocarcinoma generally requires multiple modalities including laboratory tests, imaging studies, and often endoscopic procedures and biopsy, though in the case of localized disease, biopsy may be deferred until after surgical intervention to decrease the risk of tumor seeding. The staging systems for cholangiocarcinoma have recently been improved through the creation of unique systems specific to intrahepatic, hilar, and extrahepatic disease, though there is still a need for a validated staging system that can accurately provide a pre-surgical assessment of prognosis. As the only confirmed curative intervention for the treatment of cholangiocarcinoma, the feasibility of resection should be determined for all patients, and liver transplantation should be considered for patients with hilar disease in whom resection is not an option. Locoregional therapies may provide some benefit to patients with localized disease who are not surgical candidates. Patients with metastatic cholangiocarcinoma may benefit from combination chemotherapy with gemcitabine and cisplatin, though prognosis remains poor. Studies of therapies targeting IDH1 mutations and FGFR fusions are underway in hopes of improving outcomes in this patient population.

References

1. Nakeeb A, Pitt HA, Sohn TA, Coleman J, Abrams RA, Piantadosi S, et al. Cholangiocarcinoma. A spectrum of intrahepatic, perihilar, and distal tumors. Ann surg. 1996;224(4):463–73; discussion 73–5. PubMed PMID: 8857851. Pubmed Central PMCID: 1235406.
2. DeOliveira ML, Cunningham SC, Cameron JL, Kamangar F, Winter JM, Lillemoe KD, et al. Cholangiocarcinoma: Thirty-one-year experience with 564 patients at a single institution. Ann surg. 2007 245(5):755–62. PubMed PMID: 17457168. Pubmed Central PMCID: 1877058.
3. Mosadeghi S, Liu B, Bhuket T, Wong RJ. Sex-specific and race/ethnicity-specific disparities in cholangiocarcinoma incidence and prevalence in the U.S.: An updated analysis of the 2000–2011 surveillance, epidemiology, and end results registry. Hepatology research: The official journal of the Japan Society of Hepatology. 2015 Oct 28. PubMed PMID: 26508039.
4. Shaib YH, Davila JA, McGlynn K, El-Serag HB. Rising incidence of intrahepatic cholangiocarcinoma in the United States: A true increase? J Hepatol. 2004;40(3):472–7 PubMed PMID: 15123362.
5. Welzel TM, McGlynn KA, Hsing AW, O'Brien TR, Pfeiffer RM. Impact of classification of hilar cholangiocarcinomas (Klatskin tumors) on the incidence of intra and extrahepatic cholangiocarcinoma in the United States. J Natl Cancer Inst. 2006;98 (12):873–5 PubMed PMID: 16788161.
6. Khan SA, Emadossadaty S, Ladep NG, Thomas HC, Elliott P, Taylor-Robinson SD, et al. Rising trends in cholangiocarcinoma: Is the ICD classification system misleading us? J Hepatol. 2012;56(4):848–54 PubMed PMID: 22173164.
7. Sripa B, Pairojkul C. Cholangiocarcinoma: lessons from Thailand. Curr Opin Gastroenterol. 2008;24 (3):349–56. PubMed PMID: 18408464. Pubmed Central PMCID: 4130346.
8. Alvaro D, Crocetti E, Ferretti S, Bragazzi MC, Capocaccia R, committee AC. Descriptive epidemiology of cholangiocarcinoma in Italy. Digestive and liver disease: Official journal of the Italian Society of Gastroenterology and the Italian Association for the Study of the Liver. 2010;42(7):490–5. PubMed PMID: 20022823.
9. von Hahn T, Ciesek S, Wegener G, Plentz RR, Weismuller TJ, Wedemeyer H, et al. Epidemiological trends in incidence and mortality of hepatobiliary cancers in Germany. Scand J Gastroenterol. 2011;46(9):1092–8 PubMed PMID: 21692710.

10. Utada M, Ohno Y, Tamaki T, Sobue T, Endo G. Long-term trends in incidence and mortality of intrahepatic and extrahepatic bile duct cancer in Japan. J Epidemiol/Jpn Epidemiol Assoc. 2014;24 (3):193–9. PubMed PMID: 24614916. Pubmed Central PMCID: 4000766.
11. Sithithaworn P, Yongvanit P, Duenngai K, Kiatsopit N, Pairojkul C. Roles of liver fluke infection as risk factor for cholangiocarcinoma. J Hepato-Biliary-Pancreat Sci. 2014;21(5):301–8 PubMed PMID: 24408775.
12. Khuntikeo N, Loilome W, Thinkhamrop B, Chamadol N, Yongvanit P. A comprehensive public health conceptual framework and strategy to effectively combat cholangiocarcinoma in Thailand. PLoS Negl Trop Dis. 2016 Jan;10(1):e0004293. PubMed PMID: 26797527. Pubmed Central PMCID: 4721916.
13. Chapman R, Fevery J, Kalloo A, Nagorney DM, Boberg KM, Shneider B, et al. Diagnosis and management of primary sclerosing cholangitis. Hepatology. 2010;51(2):660–78 PubMed PMID: 20101749.
14. Folseraas T, Boberg KM. Cancer risk and surveillance in primary sclerosing cholangitis. Clin Liver Dis. 2016;20(1):79–98 PubMed PMID: 26593292.
15. Soreide K, Korner H, Havnen J, Soreide JA. Bile duct cysts in adults. Br J Surg. 2004;91(12):1538–48 PubMed PMID: 15549778.
16. Soares KC, Kim Y, Spolverato G, Maithel S, Bauer TW, Marques H, et al. Presentation and clinical outcomes of choledochal cysts in children and adults: A multi-institutional analysis. JAMA Surg. 2015;150 (6):577–84 PubMed PMID: 25923827.
17. Tazuma S. Gallstone disease: Epidemiology, pathogenesis, and classification of biliary stones (common bile duct and intrahepatic). Best Pract Res Clin Gastroenterol. 2006;20(6):1075–83 PubMed PMID: 17127189.
18. Chijiiwa K, Ichimiya H, Kuroki S, Koga A, Nakayama F. Late development of cholangiocarcinoma after the treatment of hepatolithiasis. Surg, Gynecol Obstet. 1993;177(3):279–82 PubMed PMID: 8395085.
19. Li M, Li J, Li P, Li H, Su T, Zhu R, et al. Hepatitis B virus infection increases the risk of cholangiocarcinoma: a meta-analysis and systematic review. J Gastroenterol Hepatol. 2012;27(10):1561–8 PubMed PMID: 22694354.
20. Palmer WC, Patel T. Are common factors involved in the pathogenesis of primary liver cancers? A meta-analysis of risk factors for intrahepatic cholangiocarcinoma. J Hepatol. 2012 Jul;57(1):69–76. PubMed PMID: 22420979. Pubmed Central PMCID: 3804834.
21. Zhou Y, Zhao Y, Li B, Huang J, Wu L, Xu D, et al. Hepatitis viruses infection and risk of intrahepatic cholangiocarcinoma: evidence from a meta-analysis. BMC Cancer. 2012;12:289. PubMed PMID: 22799744. Pubmed Central PMCID: 3411483.
22. Li H, Hu B, Zhou ZQ, Guan J, Zhang ZY, Zhou GW. Hepatitis C virus infection and the risk of intrahepatic cholangiocarcinoma and extrahepatic cholangiocarcinoma: Evidence from a systematic review and meta-analysis of 16 case-control studies. World J Surg Oncol. 2015;13:161. PubMed PMID: 25903488. Pubmed Central PMCID: 4419416.
23. Razumilava N, Gores GJ. Cholangiocarcinoma. Lancet. 2014 Jun 21;383(9935):2168–79. PubMed PMID: 24581682. Pubmed Central PMCID: 4069226.
24. Mecklin JP, Jarvinen HJ, Virolainen M. The association between cholangiocarcinoma and hereditary nonpolyposis colorectal carcinoma. Cancer. 1992;69(5):1112–4 PubMed PMID: 1310886.
25. Pilarski R, Cebulla CM, Massengill JB, Rai K, Rich T, Strong L, et al. Expanding the clinical phenotype of hereditary BAP1 cancer predisposition syndrome, reporting three new cases. Genes, Chromosom, Cancer. 2014 Feb;53(2):177–82. PubMed PMID: 24243779. Pubmed Central PMCID: 4041196.
26. Brandi G, Venturi M, Pantaleo MA, Ercolani G, Gico. Cholangiocarcinoma: Current opinion on clinical practice diagnostic and therapeutic algorithms: A review of the literature and a long-standing experience of a referral center. Digestive and liver disease: Official journal of the Italian Society of Gastroenterology and the Italian Association for the Study of the Liver. 2016 Mar;48 (3):231–41. PubMed PMID: 26769568.
27. Kim HJ, Kim MH, Myung SJ, Lim BC, Park ET, Yoo KS, et al. A new strategy for the application of CA19-9 in the differentiation of pancreaticobiliary cancer: Analysis using a receiver operating characteristic curve. Am J Gastroenterol. 1999;94 (7):1941–6 PubMed PMID: 10406263.
28. Narimatsu H, Iwasaki H, Nakayama F, Ikehara Y, Kudo T, Nishihara S, et al. Lewis and secretor gene dosages affect CA19-9 and DU-PAN-2 serum levels in normal individuals and colorectal cancer patients. Can Res. 1998;58(3):512–8 PubMed PMID: 9458099.
29. Pattanapairoj S, Silsirivanit A, Muisuk K, Seubwai W, Cha'on U, Vaeteewoottacharn K, et al. Improve discrimination power of serum markers for diagnosis of cholangiocarcinoma using data mining-based approach. Clin Biochem. 2015;48 (10–11):668–73 PubMed PMID: 25863112.
30. Jiang L, Tan H, Panje CM, Yu H, Xiu Y, Shi H. Role of 18F-FDG PET/CT Imaging in Intrahepatic Cholangiocarcinoma. Clin Nucl Med. 2016;41 (1):1–7 PubMed PMID: 26402131.
31. Vogl TJ, Schwarz WO, Heller M, Herzog C, Zangos S, Hintze RE, et al. Staging of Klatskin tumours (hilar cholangiocarcinomas): comparison of MR cholangiography, MR imaging, and endoscopic retrograde cholangiography. Eur Radiol. 2006;16(10):2317–25 PubMed PMID: 16622690.

32. Huang B, Wu L, Lu XY, Xu F, Liu CF, Shen WF, et al. Small intrahepatic cholangiocarcinoma and hepatocellular carcinoma in cirrhotic livers may share similar enhancement patterns at multiphase dynamic MR imaging. Radiology. 2016;14:151205 PubMed PMID: 27077381.
33. Joo I, Lee JM, Lee SM, Lee JS, Park JY, Han JK. Diagnostic accuracy of liver imaging reporting and data system (LI-RADS) v2014 for intrahepatic mass-forming cholangiocarcinomas in patients with chronic liver disease on gadoxetic acid-enhanced MRI. J Magn Reson imaging: JMRI. 2016 Apr 18. PubMed PMID: 27087012.
34. Zen Y, Kawakami H, Kim JH. IgG4-related sclerosing cholangitis: All we need to know. J Gastroenterol. 2016;51(4):295–312 PubMed PMID: 26817943.
35. Du S, Liu G, Cheng X, Li Y, Wang Q, Li J, et al. Differential diagnosis of immunoglobulin G4-associated cholangitis from cholangiocarcinoma. J Clin Gastroent. 2016 Mar 11. PubMed PMID: 26974756.
36. De Bellis M, Sherman S, Fogel EL, Cramer H, Chappo J, McHenry L Jr, et al. Tissue sampling at ERCP in suspected malignant biliary strictures (Part 1). Gastrointest Endosc. 2002;56(4):552–61 PubMed PMID: 12297773.
37. Wani S, Shah RJ. Probe-based confocal laser endomicroscopy for the diagnosis of indeterminate biliary strictures. Curr Opin Gastroenterol. 2013;29 (3):319–23 PubMed PMID: 23507916.
38. Slivka A, Gan I, Jamidar P, Costamagna G, Cesaro P, Giovannini M, et al. Validation of the diagnostic accuracy of probe-based confocal laser endomicroscopy for the characterization of indeterminate biliary strictures: results of a prospective multicenter international study. Gastrointest Endosc. 2015;81(2):282–90 PubMed PMID: 25616752.
39. Heimbach JK, Sanchez W, Rosen CB, Gores GJ. Trans-peritoneal fine needle aspiration biopsy of hilar cholangiocarcinoma is associated with disease dissemination. HPB: The official journal of the International Hepato Pancreato Biliary Association. 2011 May;13(5):356–60. PubMed PMID: 21492336. Pubmed Central PMCID: 3093648.
40. Sakata J, Shirai Y, Wakai T, Nomura T, Sakata E, Hatakeyama K. Catheter tract implantation metastases associated with percutaneous biliary drainage for extrahepatic cholangiocarcinoma. World J Gastroenterol. 2005 Nov 28;11(44):7024–7. PubMed PMID: 16437610. Pubmed Central PMCID: 4717048.
41. Rizvi S, Gores GJ. Pathogenesis, diagnosis, and management of cholangiocarcinoma. Gastroenterology. 2013 Dec;145(6):1215–29. PubMed PMID: 24140396. Pubmed Central PMCID: 3862291.
42. Barr Fritcher EG, Kipp BR, Halling KC, Clayton AC. Fishing for pancreatobiliary tract malignancy in endoscopic brushings enhances the sensitivity of routine cytology. Cytopathology: official journal of the British Society for Clinical Cytology. 2014 Jul 30. PubMed PMID: 25073411.
43. Gonda TA, Glick MP, Sethi A, Poneros JM, Palmas W, Iqbal S, et al. Polysomy and p16 deletion by fluorescence in situ hybridization in the diagnosis of indeterminate biliary strictures. Gastrointest Endosc. 2012;75(1):74–9 PubMed PMID: 22100297.
44. Thanan R, Techasen A, Hou B, Jamnongkan W, Armartmuntree N, Yongvanit P, et al. Development and characterization of a hydrogen peroxide-resistant cholangiocyte cell line: A novel model of oxidative stress-related cholangiocarcinoma genesis. Biochem Biophys Res Commun. 2015;464(1):182–8 PubMed PMID: 26100205.
45. Jusakul A, Loilome W, Namwat N, Techasen A, Kuver R, Ioannou GN, et al. Anti-apoptotic phenotypes of cholestan-3β,5α,6β-triol-resistant human cholangiocytes: Characteristics contributing to the genesis of cholangiocarcinoma. J Steroid Biochem Mol Biol. 2013 Nov;138:368–75. PubMed PMID: 23959098. Pubmed Central PMCID: 3825754.
46. Tamir S, Burney S, Tannenbaum SR. DNA damage by nitric oxide. Chem Res Toxicol. 1996 Jul-Aug;9 (5):821–7. PubMed PMID: 8828916.
47. Han C, Wu T. Cyclooxygenase-2-derived prostaglandin E2 promotes human cholangiocarcinoma cell growth and invasion through EP1 receptor-mediated activation of the epidermal growth factor receptor and Akt. J Biol Chem. 2005;280(25):24053–63 PubMed PMID: 15855163.
48. Fan B, Malato Y, Calvisi DF, Naqvi S, Razumilava N, Ribback S, et al. Cholangiocarcinomas can originate from hepatocytes in mice. J Clin Invest. 2012 Aug;122(8):2911–5. PubMed PMID: 22797301. Pubmed Central PMCID: 3408746.
49. Sekiya S, Suzuki A. Intrahepatic cholangiocarcinoma can arise from Notch-mediated conversion of hepatocytes. J Clin Invest. 2012 Nov;122 (11):3914–8. PubMed PMID: 23023701. Pubmed Central PMCID: 3484442.
50. Guest RV, Boulter L, Kendall TJ, Minnis-Lyons SE, Walker R, Wigmore SJ, et al. Cell lineage tracing reveals a biliary origin of intrahepatic cholangiocarcinoma. Cancer Res. 2014 Feb 15;74 (4):1005–10. PubMed PMID: 24310400. Pubmed Central PMCID: 3929349.
51. Churi CR, Shroff R, Wang Y, Rashid A, Kang HC, Weatherly J, et al. Mutation profiling in cholangiocarcinoma: prognostic and therapeutic implications. PLoS One. 2014;9(12):e115383. PubMed PMID: 25536104. Pubmed Central PMCID: 4275227.
52. Holcombe RF XJ, Pishvaian MJ, et al, editor Tumor profiling of biliary tract carcinomas to reveal distinct molecular alterations and potential therapeutic targets. Gastrointestinal Cancer Symposium; 2015; San Francisco: Journal of Clinical Oncology.

53. Ross JS WK, Catenacci DVT, et al, editor Comprehensive genomic profiling of biliary tract cancers to reveal tumor-specific differences and genomic alterations. Gastrointestinal Cancers Symposium; 2015; San Francisco, CA: Journal of Clinical Oncology.
54. Gu TL, Deng X, Huang F, Tucker M, Crosby K, Rimkunas V, et al. Survey of tyrosine kinase signaling reveals ROS kinase fusions in human cholangiocarcinoma. PLoS One. 2011;6(1):e15640. PubMed PMID: 21253578. Pubmed Central PMCID: 3017127.
55. Okabayashi T, Yamamoto J, Kosuge T, Shimada K, Yamasaki S, Takayama T, et al. A new staging system for mass-forming intrahepatic cholangiocarcinoma: Analysis of preoperative and postoperative variables. Cancer. 2001;92(9):2374–83 PubMed PMID: 11745293.
56. Yamasaki S. Intrahepatic cholangiocarcinoma: macroscopic type and stage classification. J Hepato-Biliary-Pancreat Surg. 2003;10(4):288–91 PubMed PMID: 14598147.
57. Nathan H, Aloia TA, Vauthey JN, Abdalla EK, Zhu AX, Schulick RD, et al. A proposed staging system for intrahepatic cholangiocarcinoma. Ann Surg Oncol. 2009;16(1):14–22 PubMed PMID: 18987916.
58. American Joint Committee on Cancer: AJCC Cancer Staging Maual. Edge S, editor. New York: Springer; 2009.
59. Bartella I, Dufour JF. Clinical Diagnosis and Staging of Intrahepatic Cholangiocarcinoma. J Gastrointest Liver Dis: JGLD. 2015;24(4):481–9 PubMed PMID: 26697575.
60. Farges O, Fuks D, Le Treut YP, Azoulay D, Laurent A, Bachellier P, et al. AJCC 7th edition of TNM staging accurately discriminates outcomes of patients with resectable intrahepatic cholangiocarcinoma: By the AFC-IHCC-2009 study group. Cancer. 2011;117(10):2170–7 PubMed PMID: 21523730.
61. Bismuth H, Corlette MB. Intrahepatic cholangioenteric anastomosis in carcinoma of the hilus of the liver. Surg Gynecol Obstet. 1975;140(2):170–8 PubMed PMID: 1079096.
62. Jarnagin WR, Fong Y, DeMatteo RP, Gonen M, Burke EC, Bodniewicz BJ, et al. Staging, resectability, and outcome in 225 patients with hilar cholangiocarcinoma. Ann Surg. 2001 Oct;234(4):507–17; discussion 17-9. PubMed PMID: 11573044. Pubmed Central PMCID: 1422074.
63. Zervos EE, Osborne D, Goldin SB, Villadolid DV, Thometz DP, Durkin A, et al. Stage does not predict survival after resection of hilar cholangiocarcinomas promoting an aggressive operative approach. Am J Surg. 2005;190(5):810–5 PubMed PMID: 16226963.
64. Deoliveira ML, Schulick RD, Nimura Y, Rosen C, Gores G, Neuhaus P, et al. New staging system and a registry for perihilar cholangiocarcinoma. Hepatology. 2011;53(4):1363–71 PubMed PMID: 21480336.
65. Sotiropoulos GC, Bockhorn M, Sgourakis G, Brokalaki EI, Molmenti EP, Neuhauser M, et al. R0 liver resections for primary malignant liver tumors in the noncirrhotic liver: a diagnosis-related analysis. Dig Dis Sci. 2009;54(4):887–94 PubMed PMID: 18712480.
66. Endo I, Gonen M, Yopp AC, Dalal KM, Zhou Q, Klimstra D, et al. Intrahepatic cholangiocarcinoma: Rising frequency, improved survival, and determinants of outcome after resection. Ann Surg. 2008;248(1):84–96 PubMed PMID: 18580211.
67. Choi SB, Kim KS, Choi JY, Park SW, Choi JS, Lee WJ, et al. The prognosis and survival outcome of intrahepatic cholangiocarcinoma following surgical resection: Association of lymph node metastasis and lymph node dissection with survival. Ann Surg Oncol. 2009;16(11):3048–56 PubMed PMID: 19626372.
68. Yamamoto M, Takasaki K, Otsubo T, Katsuragawa H, Katagiri S. Recurrence after surgical resection of intrahepatic cholangiocarcinoma. J Hepato-Biliary-Pancreatic Surg. 2001;8(2):154–7 PubMed PMID: 11455472.
69. Uenishi T, Kubo S, Yamazaki O, Yamada T, Sasaki Y, Nagano H, et al. Indications for surgical treatment of intrahepatic cholangiocarcinoma with lymph node metastases. J Hepato-Biliary-Pancreatic Surg. 2008;15(4):417–22 PubMed PMID: 18670844.
70. Paik KY, Jung JC, Heo JS, Choi SH, Choi DW, Kim YI. What prognostic factors are important for resected intrahepatic cholangiocarcinoma? J Gastroenterol Hepatol. 2008;23(5):766–70 PubMed PMID: 17868336.
71. Ohtsuka M, Ito H, Kimura F, Shimizu H, Togawa A, Yoshidome H, et al. Results of surgical treatment for intrahepatic cholangiocarcinoma and clinicopathological factors influencing survival. Br J Surg. 2002;89(12):1525–31 PubMed PMID: 12445060.
72. Nuzzo G, Giuliante F, Ardito F, Giovannini I, Aldrighetti L, Belli G, et al. Improvement in perioperative and long-term outcome after surgical treatment of hilar cholangiocarcinoma: Results of an Italian multicenter analysis of 440 patients. Arch Surg. 2012;147(1):26–34 PubMed PMID: 22250108.
73. Farges O, Regimbeau JM, Fuks D, Le Treut YP, Cherqui D, Bachellier P, et al. Multicentre European study of preoperative biliary drainage for hilar cholangiocarcinoma. Br J Surg. 2013;100(2):274–83 PubMed PMID: 23124720.
74. Nagino M, Ebata T, Yokoyama Y, Igami T, Sugawara G, Takahashi Y, et al. Evolution of surgical treatment for perihilar cholangiocarcinoma: a single-center 34-year review of 574 consecutive resections. Ann Surg. 2013;258(1):129–40 PubMed PMID: 23059502.

75. Kang MJ, Jang JY, Chang J, Shin YC, Lee D, Kim HB, et al. Actual Long-Term Survival Outcome of 403 Consecutive Patients with Hilar Cholangiocarcinoma. World J Surg. 2016 May 20. PubMed PMID: 27206402.
76. Neoptolemos JP, Moore MJ, Cox TF, Valle JW, Palmer DH, McDonald AC, et al. Effect of adjuvant chemotherapy with fluorouracil plus folinic acid or gemcitabine vs observation on survival in patients with resected periampullary adenocarcinoma: the ESPAC-3 periampullary cancer randomized trial. JAMA, J Am Med Assoc. 2012;308(2):147–56 PubMed PMID: 22782416.
77. Fu BS, Zhang T, Li H, Yi SH, Wang GS, Xu C, et al. The role of liver transplantation for intrahepatic cholangiocarcinoma: a single-center experience. Eur Surg Res Euro chirurgische Forschung Recherches chirurgicales europeennes. 2011;47 (4):218–21 PubMed PMID: 22041581.
78. Sotiropoulos GC, Kaiser GM, Lang H, Molmenti EP, Beckebaum S, Fouzas I, et al. Liver transplantation as a primary indication for intrahepatic cholangiocarcinoma: A single-center experience. Transpl Proc. 2008;40(9):3194–5 PubMed PMID: 19010231.
79. Casavilla FA, Marsh JW, Iwatsuki S, Todo S, Lee RG, Madariaga JR, et al. Hepatic resection and transplantation for peripheral cholangiocarcinoma. J Am Coll Surg. 1997 Nov;185(5):429–36. PubMed PMID: 9358085. Pubmed Central PMCID: 2958518.
80. Robles R, Figueras J, Turrion VS, Margarit C, Moya A, Varo E, et al. Spanish experience in liver transplantation for hilar and peripheral cholangiocarcinoma. Ann Surg. 2004 Feb;239(2):265–71. PubMed PMID: 14745336. Pubmed Central PMCID: 1356221.
81. Sapisochin G, Rodriguez de Lope C, Gastaca M, Ortiz de Urbina J, Suarez MA, Santoyo J, et al. "Very early" intrahepatic cholangiocarcinoma in cirrhotic patients: should liver transplantation be reconsidered in these patients? Am J Transplant: official J Am Soc Transplant Am Soc Transplant Surg. 2014;14(3):660–7 PubMed PMID: 24410861.
82. Rea DJ, Heimbach JK, Rosen CB, Haddock MG, Alberts SR, Kremers WK, et al. Liver transplantation with neoadjuvant chemoradiation is more effective than resection for hilar cholangiocarcinoma. Ann Surg. 2005 Sep;242(3):451–8; discussion 8-61. PubMed PMID: 16135931. Pubmed Central PMCID: 1357753.
83. Darwish Murad S, Kim WR, Harnois DM, Douglas DD, Burton J, Kulik LM, et al. Efficacy of neoadjuvant chemoradiation, followed by liver transplantation, for perihilar cholangiocarcinoma at 12 US centers. Gastroenterology. 2012 Jul;143 (1):88–98 e3; quiz e14. PubMed PMID: 22504095. Pubmed Central PMCID: 3846443.
84. Kim JH, Won HJ, Shin YM, Kim KA, Kim PN. Radiofrequency ablation for the treatment of primary intrahepatic cholangiocarcinoma. AJR Am J Roentgenol. 2011;196(2):W205–9 PubMed PMID: 21257864.
85. Kim JH, Won HJ, Shin YM, Kim PN, Lee SG, Hwang S. Radiofrequency ablation for recurrent intrahepatic cholangiocarcinoma after curative resection. Eur J Radiol. 2011;80(3):e221–5 PubMed PMID: 20950977.
86. Chiou YY, Hwang JI, Chou YH, Wang HK, Chiang JH, Chang CY. Percutaneous ultrasound-guided radiofrequency ablation of intrahepatic cholangiocarcinoma. Kaohsiung J Med Sci. 2005;21(7):304–9 PubMed PMID: 16089307.
87. Carrafiello G, Lagana D, Cotta E, Mangini M, Fontana F, Bandiera F, et al. Radiofrequency ablation of intrahepatic cholangiocarcinoma: preliminary experience. Cardiovasc Intervent Radiol. 2010;33(4):835–9 PubMed PMID: 20411389.
88. Haidu M, Dobrozemsky G, Schullian P, Widmann G, Klaus A, Weiss H, et al. Stereotactic radiofrequency ablation of unresectable intrahepatic cholangiocarcinomas: a retrospective study. Cardiovasc Intervent Radiol. 2012;35(5):1074–82 PubMed PMID: 22006031.
89. Giorgio A, Calisti G, G DES, Farella N, A DIS, Amendola F, et al. Radiofrequency ablation for intrahepatic cholangiocarcinoma: retrospective analysis of a single centre experience. Anticancer Res. 2011 Dec;31(12):4575–80. PubMed PMID: 22199333.
90. Butros SR, Shenoy-Bhangle A, Mueller PR, Arellano RS. Radiofrequency ablation of intrahepatic cholangiocarcinoma: feasability, local tumor control, and long-term outcome. Clin Imaging. 2014 Jul-Aug;38(4):490–4. PubMed PMID: 24637151.
91. Steel AW, Postgate AJ, Khorsandi S, Nicholls J, Jiao L, Vlavianos P, et al. Endoscopically applied radiofrequency ablation appears to be safe in the treatment of malignant biliary obstruction. Gastrointest Endosc. 2011;73(1):149–53 PubMed PMID: 21184881.
92. Figueroa-Barojas P, Bakhru MR, Habib NA, Ellen K, Millman J, Jamal-Kabani A, et al. Safety and efficacy of radiofrequency ablation in the management of unresectable bile duct and pancreatic cancer: a novel palliation technique. J Oncol. 2013;2013:910897. PubMed PMID: 23690775. Pubmed Central PMCID: 3649248.
93. Alis H, Sengoz C, Gonenc M, Kalayci MU, Kocatas A. Endobiliary radiofrequency ablation for malignant biliary obstruction. Hepatobiliary Pancreat Dis Int: HBPD INT. 2013;12(4):423–7 PubMed PMID: 23924501.
94. Ortner ME, Caca K, Berr F, Liebetruth J, Mansmann U, Huster D, et al. Successful photodynamic therapy for nonresectable cholangiocarcinoma: a randomized prospective study. Gastroenterology. 2003;125(5):1355–63 PubMed PMID: 14598251.

95. Cheon YK, Lee TY, Lee SM, Yoon JY, Shim CS. Longterm outcome of photodynamic therapy compared with biliary stenting alone in patients with advanced hilar cholangiocarcinoma. HPB: official J Int Hepato Pancreato Biliary Assoc. 2012 Mar;14 (3):185–93. PubMed PMID: 22321037. Pubmed Central PMCID: 3371201.
96. Lee TY, Cheon YK, Shim CS, Cho YD. Photodynamic therapy prolongs metal stent patency in patients with unresectable hilar cholangiocarcinoma. World J Gastroenterol. 2012 Oct 21;18 (39):5589–94. PubMed PMID: 23112552. Pubmed Central PMCID: 3482646.
97. Strand DS, Cosgrove ND, Patrie JT, Cox DG, Bauer TW, Adams RB, et al. ERCP-directed radiofrequency ablation and photodynamic therapy are associated with comparable survival in the treatment of unresectable cholangiocarcinoma. Gastrointest Endosc. 2014;80(5):794–804 PubMed PMID: 24836747.
98. Park SY, Kim JH, Yoon HJ, Lee IS, Yoon HK, Kim KP. Transarterial chemoembolization versus supportive therapy in the palliative treatment of unresectable intrahepatic cholangiocarcinoma. Clin Radiol. 2011;66(4):322–8 PubMed PMID: 21356394.
99. Edwards ARJ. Transarterial therapies for unresectable cholangiocarcinoma: a meta-analysis. J Vasc Interv Radiol. 2012;23:S101.
100. Vogl TJ, Naguib NN, Nour-Eldin NE, Bechstein WO, Zeuzem S, Trojan J, et al. Transarterial chemoembolization in the treatment of patients with unresectable cholangiocarcinoma: Results and prognostic factors governing treatment success. J Int du cancer. 2012;131(3):733–40 PubMed PMID: 21976289.
101. Kiefer MV, Albert M, McNally M, Robertson M, Sun W, Fraker D, et al. Chemoembolization of intrahepatic cholangiocarcinoma with cisplatinum, doxorubicin, mitomycin C, ethiodol, and polyvinyl alcohol: a 2-center study. Cancer. 2011;117 (7):1498–505 PubMed PMID: 21425151.
102. Kuhlmann JB, Euringer W, Spangenberg HC, Breidert M, Blum HE, Harder J, et al. Treatment of unresectable cholangiocarcinoma: conventional transarterial chemoembolization compared with drug eluting bead-transarterial chemoembolization and systemic chemotherapy. Eur J Gastroenterol Hepatol. 2012;24(4):437–43 PubMed PMID: 22261548.
103. Hyder O, Marsh JW, Salem R, Petre EN, Kalva S, Liapi E, et al. Intra-arterial therapy for advanced intrahepatic cholangiocarcinoma: a multi-institutional analysis. Ann Surg Oncol. 2013;20(12):3779–86 PubMed PMID: 23846786.
104. Tanaka N, Yamakado K, Nakatsuka A, Fujii A, Matsumura K, Takeda K. Arterial chemoinfusion therapy through an implanted port system for patients with unresectable intrahepatic cholangiocarcinoma–initial experience. Eur J Radiol. 2002;41 (1):42–8 PubMed PMID: 11750151.
105. Vogl TJ, Schwarz W, Eichler K, Hochmuth K, Hammerstingl R, Jacob U, et al. Hepatic intraarterial chemotherapy with gemcitabine in patients with unresectable cholangiocarcinomas and liver metastases of pancreatic cancer: a clinical study on maximum tolerable dose and treatment efficacy. J Cancer Res Clin Oncol. 2006;132(11):745–55 PubMed PMID: 16858591.
106. Shitara K, Ikami I, Munakata M, Muto O, Sakata Y. Hepatic arterial infusion of mitomycin C with degradable starch microspheres for unresectable intrahepatic cholangiocarcinoma. Clin Oncol. 2008;20(3):241–6 PubMed PMID: 18222071.
107. Yashima Y, Sato S, Kawai T, Sugimoto T, Sato T, Kanda M, et al. Intraarterial 5-fluorouracil and interferon therapy is safe and effective for nonresectable biliary tract adenocarcinoma. Hep Intl. 2015;9(1):142–8 PubMed PMID: 25788388.
108. Inaba Y, Arai Y, Yamaura H, Sato Y, Najima M, Aramaki T, et al. Phase I/II study of hepatic arterial infusion chemotherapy with gemcitabine in patients with unresectable intrahepatic cholangiocarcinoma (JIVROSG-0301). Am J Clin Oncol. 2011;34 (1):58–62 PubMed PMID: 20177362.
109. Boehm LM, Jayakrishnan TT, Miura JT, Zacharias AJ, Johnston FM, Turaga KK, et al. Comparative effectiveness of hepatic artery based therapies for unresectable intrahepatic cholangiocarcinoma. J Surg Oncol. 2015;111(2):213–20 PubMed PMID: 25176325.
110. Valle J, Wasan H, Palmer DH, Cunningham D, Anthoney A, Maraveyas A, et al. Cisplatin plus gemcitabine versus gemcitabine for biliary tract cancer. New Engl J Med. 2010;362(14):1273–81 PubMed PMID: 20375404.
111. Rogers JE, Law L, Nguyen VD, Qiao W, Javle MM, Kaseb A, et al. Second-line systemic treatment for advanced cholangiocarcinoma. J Gastrointest Oncol. 2014 Dec;5(6):408–13. PubMed PMID: 25436118. Pubmed Central PMCID: 4226829.
112. Saha SK, Parachoniak CA, Ghanta KS, Fitamant J, Ross KN, Najem MS, et al. Mutant IDH inhibits HNF-4alpha to block hepatocyte differentiation and promote biliary cancer. Nature. 2014 Sep 4;513 (7516):110–4. PubMed PMID: 25043045. Pubmed Central PMCID: 4499230.
113. Goyal L, Govindan A, Sheth RA, Nardi V, Blaszkowsky LS, Faris JE, et al. Prognosis and Clinicopathologic Features of Patients With Advanced Stage Isocitrate Dehydrogenase (IDH) Mutant and IDH Wild-Type Intrahepatic Cholangiocarcinoma. Oncologist. 2015 Sep;20 (9):1019–27. PubMed PMID: 26245674. Pubmed Central PMCID: 4571807.

114. Grassian AR, Pagliarini R, Chiang DY. Mutations of isocitrate dehydrogenase 1 and 2 in intrahepatic cholangiocarcinoma. Curr Opin Gastroenterol. 2014;30(3):295–302 PubMed PMID: 24569570.
115. Borger DR, Tanabe KK, Fan KC, Lopez HU, Fantin VR, Straley KS, et al. Frequent mutation of isocitrate dehydrogenase (IDH)1 and IDH2 in cholangiocarcinoma identified through broad-based tumor genotyping. Oncologist. 2012;17(1):72–9. PubMed PMID: 22180306. Pubmed Central PMCID: 3267826.
116. Kipp BR, Voss JS, Kerr SE, Barr Fritcher EG, Graham RP, Zhang L, et al. Isocitrate dehydrogenase 1 and 2 mutations in cholangiocarcinoma. Hum Pathol. 2012;43(10):1552–8 PubMed PMID: 22503487.
117. Burris H MI, Maher E, et al. The first reported results of AG-120, a first-in-class, potent inhibitor of the IDH1 mutant protein, in a Phase I study of patients with advanced IDH1-mutant solid tumors, including glimoas. Mol Cancer Ther. 2015;14(12, Suppl 2):Abstract PL04–5.
118. Graham RP, Barr Fritcher EG, Pestova E, Schulz J, Sitailo LA, Vasmatzis G, et al. Fibroblast growth factor receptor 2 translocations in intrahepatic cholangiocarcinoma. Hum Pathol. 2014;45 (8):1630–8 PubMed PMID: 24837095.
119. Arai Y, Totoki Y, Hosoda F, Shirota T, Hama N, Nakamura H, et al. Fibroblast growth factor receptor 2 tyrosine kinase fusions define a unique molecular subtype of cholangiocarcinoma. Hepatology. 2014;59(4):1427–34 PubMed PMID: 24122810.
120. Ross JS, Wang K, Gay L, Al-Rohil R, Rand JV, Jones DM, et al. New routes to targeted therapy of intrahepatic cholangiocarcinomas revealed by next-generation sequencing. Oncologist. 2014 Mar;19(3):235–42. PubMed PMID: 24563076. Pubmed Central PMCID: 3958461.
121. Sia D, Losic B, Moeini A, Cabellos L, Hao K, Revill K, et al. Massive parallel sequencing uncovers actionable FGFR2-PPHLN1 fusion and ARAF mutations in intrahepatic cholangiocarcinoma. Nat Commun. 2015;6:6087 PubMed PMID: 25608663.
122. Nakamura H, Arai Y, Totoki Y, Shirota T, Elzawahry A, Kato M, et al. Genomic spectra of biliary tract cancer. Nat Genet. 2015;47(9):1003–10 PubMed PMID: 26258846.
123. Wu YM, Su F, Kalyana-Sundaram S, Khazanov N, Ateeq B, Cao X, et al. Identification of targetable FGFR gene fusions in diverse cancers. Cancer Discovery. 2013 Jun;3(6):636–47. PubMed PMID: 23558953. Pubmed Central PMCID: 3694764.
124. Javle M SR, Zhu A, et al. A phase 2 study of BGJ398 in patients with advanced or metastatic FGFR-altered cholangiocarcinoma who failed or are intolerant to platinum-based chemotherapy. J Clin Oncol. 2016;34(4_suppl):abstr 335.

Radiation Therapy for Intrahepatic and Hilar Cholangiocarcinoma: Clinical Data

16

Sagar A. Patel, MD, Florence K. Keane, MD and Theodore S. Hong, MD

16.1 Introduction

Cholangiocarcinomas are rare malignancies arising from intrahepatic and extrahepatic bile ducts and characterized by early nodal and distant metastases. They are divided into three categories based on anatomic location of origin within the biliary system: intrahepatic, hilar, and extrahepatic. Each likely demonstrates a distinct biology and pattern of progression, as reflected by individual staging systems for each class [1]. The hilar variant remains the most common type of cholangiocarcinoma; however, the incidence of intrahepatic cholangiocarcinoma (IHC) continues to rise in the USA [2, 3]. Complete surgical resection remains the optimal treatment modality; however, there is a high rate of both local relapse and distant relapse [4–8]. Long-term survival is poor because of late presentation of disease and limited therapies.

S.A. Patel
Harvard Radiation Oncology Program, Harvard Medical School, Boston, MA, USA

F.K. Keane
Department of Radiation Oncology, Massachusetts General Hospital, Boston, MA, USA

T.S. Hong (✉)
Department of Radiation Oncology, Massachusetts General Hospital, 55 Fruit Street, Boston, MA 02115, USA
e-mail: tshong1@partners.org; TSHONG1@mgh.harvard.edu

16.2 Background

16.2.1 Adjuvant Therapy

High rates of recurrence despite resection provide the rationale for exploring adjuvant local and systemic therapies. Although adjuvant therapy is widely used and often recommended in guidelines, the survival benefit of any adjuvant strategy has never been proven in prospective, randomized trials. With relatively few patients resectable at presentation, it is difficult to complete a large randomized adjuvant trial powered to show improvements in overall survival. However, in patients who are able to undergo surgical resection, lymph node involvement, residual disease, positive margins, and vascular invasion are all associated with worse prognosis [9, 10]. As IHC is typically confined to the liver and systemic chemotherapy has traditionally had limited efficacy, there has been growing interest in locoregional therapy. Furthermore, before the recently published ABC-02 trial [11], there was a lack of consensus regarding the optimal chemotherapy regimen that could be extrapolated for use in the adjuvant setting. The literature, as a result, consists mainly of single institutional series and registry analyses, and the data on the value of adjuvant therapy are mixed.

Historically, the use of radiation therapy in the adjuvant setting was more favored for distal extrahepatic lesions [12], perhaps due to concern over hepatic tolerance and resulting inability to deliver tumoricidal doses for intrahepatic and

J. Meyer and T.E. Schefter (eds.), *Radiation Therapy for Liver Tumors*,
DOI 10.1007/978-3-319-54531-8_16

perihilar tumors. Therefore, much of the available data include a heterogeneous mix of patients with intra- and extrahepatic cholangiocarcinoma, including gallbladder cancer. In 2012, Horgan et al. published a meta-analysis [13] of 20 published institutional and registry studies to explore the impact of adjuvant therapy on survival for biliary tract cancers (tumors of the gallbladder and intrahepatic, perihilar, and distal bile duct). These studies incorporated over 6700 patients, and approximately 27% received adjuvant therapy. Notably, only one study within the meta-analysis included patients with intrahepatic tumors. The majority of patients with margin-negative, node-positive disease received either chemotherapy or chemoradiotherapy, while the majority with margin-positive, node-negative disease received radiation therapy alone. Regardless, there was a near-significant improvement in overall survival with the addition of any adjuvant therapy compared to surgery (OR 0.74, $p = 0.06$); there were no differences in outcomes with the use of adjuvant therapy in gallbladder and bile duct tumors. Patients receiving adjuvant chemotherapy (OR 0.39, 95% CI 0.23–0.66) or chemoradiotherapy (OR 0.61, 95% CI 0.38–0.99) derived greater benefit than those treated with radiotherapy alone (OR 0.98, 95% CI 0.67–1.43). Furthermore, a major benefit of adding adjuvant therapy was observed in node-positive (OR 0.49, 95% CI 0.30–0.80) and margin-positive disease (OR 0.36, 95% CI 0.19–0.68).

Only a minority of patients in this meta-analysis had intrahepatic disease. Smaller institutional series have demonstrated an improvement in outcomes in those with IHC receiving adjuvant therapy. A retrospective review of 90 patients with resected intrahepatic cholangiocarcinoma with involved regional lymph nodes treated at Fudan University between 1998 and 2008 found that median survival was 19.1 months in the 24 patients who received adjuvant radiotherapy compared with 9.5 months in the 66 patients who did not receive radiotherapy [14]. A series of 373 patients treated between 1977 and 2001 at Chang Gung Memorial Hospital reported improved median overall survival in the 63 patients receiving radiotherapy compared to those patients who did not receive radiotherapy (11.7 months vs. 6.25 months, $p = 0.0197$) [15]. These reports are limited by their retrospective nature and the fact that many of the patients did not receive systemic chemotherapy.

16.2.2 Definitive/Palliative Therapy

Resectability rates for intrahepatic cholangiocarcinoma have modestly increased over time, due in part to more aggressive operative strategies and expanded criteria for resectability. Yet, approximately 70% of patients are unresectable at diagnosis due to the presence of multiple intrahepatic tumors, vascular invasion, and/or nodal or distant metastases [16]. For these patients, median survival is low, ranging from 2.3 to 9 months [16, 17]. Chemotherapy is the mainstay of treatment for these patients, with the ABC-02 randomized controlled trial demonstrating an improvement in overall survival from 8.1 to 11.7 months in patients with metastatic or unresectable cholangiocarcinoma who received gemcitabine and cisplatin over patients receiving gemcitabine alone [11].

Radiotherapy has also been employed in patients with unresectable disease. A retrospective study of 84 patients with intrahepatic cholangiocarcinoma treated at Fudan University in China demonstrated improvements in overall survival in 35 patients receiving radiotherapy with or without trans-arterial chemoembolization (TACE) compared with 49 patients who received supportive care and/or TACE without radiotherapy. Patients were treated to 30–60 Gy in 1.8–2 Gy/fraction, with 86% of patients receiving ≥ 50 Gy. One-year survival was 38.5% versus 16.4%, and median overall survival was 9.5 months versus 5.1 months ($p = 0.0003$) in the radiotherapy and no-radiotherapy groups, respectively. There was one case of radiation-induced liver disease (RILD), which progressed to hepatic failure [18, 19].

Similarly, a SEER analysis of 3839 IHC patients who did not undergo resection found a

median survival of 7 months compared to 3 months in patients who did and did not receive radiotherapy, respectively. While this report was retrospective in a population-based database and did not report on receipt of chemotherapy, it did provide suggestion of a benefit from radiotherapy in patients who could not receive surgery [20].

However, conventional radiotherapy doses have been shown to be insufficient for disease control, with most patients experiencing local progression as the first site of disease after treatment [21]. Treatment is often limited by a compromised underlying hepatic function of patients, placing them at higher risk for associated toxicities, including RILD. Hepatic tissue tolerance within a traditionally poor patient substrate resulted in a very restricted therapeutic window with historical doses given the high risk of liver injury; however, the feasibility of delivering tumoricidal dose was obtained with modern techniques of radiation delivery. The use of these advanced techniques provided impressive local control benefits that translated into prolonged survival, rivaling that of resection, without an increase in toxicity. Thus, the role of radiation in the management of primary liver tumors, especially intrahepatic cholangiocarcinoma, is rapidly rising.

16.3 Radiotherapy: Dose-Escalation and Results with Advanced Treatments

The bulk of the data on the use of radiotherapy in intrahepatic cholangiocarcinoma are limited to small prospective trials or retrospective reviews of individual center experiences. Much of the data are extrapolated from larger studies of patients that include hepatocellular carcinoma (HCC).

16.3.1 Three-Dimensional Conformal Radiotherapy

The development of three-dimensional conformal radiotherapy (3D-CRT) enabled more targeted delivery of radiation while avoiding surrounding normal tissue. Furthermore, dose-volume histograms (DVH) provided the opportunity to study potential dose predictors of toxicity [22]. Initial series of toxicity in the era of 3D-CRT were based on retrospective reports. More refined models of the interaction between radiotherapy dose, treatment volume, and toxicity were subsequently developed. A Phase I/II dose-escalation study of radiotherapy with concurrent hepatic arterial fluorodeoxyuridine enrolled 43 patients with either primary or metastatic liver tumors (18 with IHC, 9 with HCC, and 16 with colorectal metastases to the liver). Radiotherapy dose was calculated based on a maximum 10% complication risk of RILD as per the Lyman normal tissue complication probability (NTCP) model. This model assumes a sigmoid relationship between dose of uniform radiation to an organ and the probability of a complication [23]. Patients were treated to a median dose of 58.5 Gy in 1.5 Gy twice-daily fractions. The median overall survival of patients with hepatobiliary tumors was 11 months, and there was improved overall and progression-free survival for all patients receiving over 70 Gy compared with patients receiving less than 70 Gy [24, 25]. There was one case of grade 3 RILD, which resolved with supportive care. In the 18 patients with intrahepatic cholangiocarcinoma, the median survival was 16.4 months for patients treated with more than 70 Gy versus 11 months for those treated with less than 70 Gy.

The refined NTCP model described above was subsequently used in a Phase II trial of hyperfractionated 3DCRT with concurrent hepatic arterial chemotherapy [26]. A total of 128 patients (47 with liver metastases, 46 with cholangiocarcinoma, and 35 with hepatocellular carcinoma) were prescribed doses of radiation according to a maximum 10–15% risk of RILD. Of note, the model was adjusted for patients with primary hepatobiliary versus metastatic tumors based on previous data showing differences in liver tolerance in patients with primary hepatobiliary disease. Median survival was 13.3 months in patients with cholangiocarcinoma, which was superior to historical controls.

On multivariate analysis, tumor dose $\geq$75 Gy was associated with improved overall survival (23.9 months vs. 14.9 months, $p < 0.01$). These early data demonstrated both the feasibility and importance of dose-escalated conformal radiotherapy to achieve tumor control.

16.3.2 Feasibility and Benefit of Dose-Escalation

Tao et al. [27] recently reported a series of patients with intrahepatic cholangiocarcinoma treated with dose-escalated radiotherapy between 2002 and 2014. About 89% of patients received chemotherapy prior to RT. Radiation doses ranged from 35 to 100 Gy (median 58.05 Gy) in 3–30 fractions (median biologic equivalent dose (BED), assuming $\alpha/\beta = 10$, of 80.5 Gy, range 43.75–180 Gy). For the entire cohort, three-year overall survival (OS) was 44%. There was a significant difference in both overall survival and local control based on BED. For patients treated with doses corresponding to a BED >80.5 Gy, three-year OS was 73% versus 38% for patients who received doses corresponding to BED <80.5 Gy ($p = 0.017$). Three-year local control was 78% in the dose-escalated cohort versus 45% for those receiving lower doses ($p = 0.04$). This finding was independent of primary tumor size.

Dose-escalated radiotherapy was achieved with three-dimensional conformal intensity-modulated radiation therapy with 6 megavoltage photons or passive scatter proton beam techniques. For patients who received 50.4 Gy or more, motion control and image guidance were implemented in two ways. For some cases, a fiducial-based kilovoltage image-guided soft tissue alignment during deep inspiration breath-hold was used to minimize doses to the liver, bile duct, and GI mucosa. In other cases, an internal target volume was created, and patients were treated during free breathing with kilovoltage image-guided alignment to bone. In selected larger tumors receiving >50.4 Gy, gross tumor volume was treated with a simultaneous integrated boost (SIB); a central SIB of 75 Gy in 15 fractions or 100 Gy in 25 fractions was delivered to the center of the tumor via this technique.

This analysis demonstrated that using high radiation doses with a moderately hypofractioned approach to treat inoperable IHC improves local control, thereby resulting in a substantial survival benefit for patients. Modern techniques of radiotherapy including stereotactic delivery and charged particle therapy have enabled the ability to reach optimal tumoricidal doses for cholangiocarcinoma while still respecting normal tissue tolerances. Both will be discussed in more detail.

16.3.3 Stereotactic Body Radiotherapy

Stereotactic body radiotherapy (SBRT) is a radiation delivery modality which employs immobilization, motion control, and multiple conformal beams to deliver high doses of radiotherapy to a target volume with rapid dose falloff. The high dose per fraction of SBRT is thought to result in an ablative effect on the tumor, potentially through vascular damage. However, the precise mechanism of SBRT-induced cell death remains to be determined [28–31].

Stereotactic radiotherapy was first employed to treat intracranial lesions as early as the 1950s [32], but it was not used for extracranial sites until the 1990s [33, 34] given the challenges of patient immobilization, target definition, and intrafractional tracking for extracranial sites.

16.3.3.1 SBRT in Intrahepatic Cholangiocarcinoma

The feasibility and safety of SBRT in the treatment of liver tumors was initially assessed in patients with metastatic hepatic lesions, primarily from colorectal adenocarcinoma [35–38], with local control at one year ranging from 71 to 95%. The use of SBRT since expanded to include both primary and metastatic tumors confined to the liver.

A Phase I dose-escalation study of SBRT in 41 patients with unresectable HCC or IHC at Princess Margaret Hospital included ten patients

with IHC [39]. Patients were treated within three predefined liver effective volume (Veff) strata, with three dose-escalation levels within each strata based on a 5, 10, or 20% risk of toxicity. With the exception of low accrual to the low V_{eff} strata, all risk levels within each strata were assessed. The median dose delivered was 36 Gy (range 24–54 Gy) in six fractions. The median survival in patients with IHC was 15 months, and one-year overall survival was 38%. There was no grade 4/5 toxicity or radiation-induced liver disease, although two patients with IHC did have transient biliary obstruction, presumably due to radiation edema. One patient experienced a gastrointestinal bleed, and one patient developed a small bowel obstruction due to tumor progression. Finally, seven patients had a decline in liver function, from Child-Pugh Class A to Child-Pugh Class B, presumably due to progression of baseline hepatic disease.

Several small Phase I or II studies and retrospective reviews of SBRT for hepatic lesions have included small numbers of patients with IHC (Table 16.1). There have been no randomized trials on the use of SBRT in IHC.

16.3.4 Charged Particle Therapy

Charged particle therapy, including protons and carbon ions, represents a potential technique for increasing the dose to a tumor while minimizing damage to the surrounding hepatic parenchyma. Protons have a distinct physical advantage over standard photon-based radiation. Photons deposit energy along the beam path beyond the tumor; this exit dose often leads to unwanted radiation exposure to uninvolved hepatic parenchyma, thereby increasing the risk of RILD as it is mediated by the dose delivered and volume of liver irradiated [23, 51]. In contrast, protons have minimal exit dose, which provides a theoretical clinical benefit by allowing escalation to tumoricidal doses without compromising normal tissue. There are no randomized data on the use of charged particle therapy versus photon therapy for HCC or IHC. This modality, however, has been used effectively in the treatment of individual patients with IHC, often with dramatic shrinkage of the primary lesion (Fig. 16.1).

Recently, a multi-institutional Phase II study was completed utilizing high-dose, hypofractionated proton beam therapy for localized, unresectable HCC and IHC [50]. Of the 83 evaluable patients, 44 had HCC and 39 had IHC; almost 90% of the IHC patients had no evidence of cirrhosis. For IHC patients, 34 (87%) had one lesion, three (8%) had two lesions, and two (5%) had three lesions. The median dose delivered was 58.0 GyE in 15 fractions. The average dose received by liver tissue not involved by tumor for all patients was 21.4 GyE (range 3.2–29.5 GyE). In the entire cohort, only four patients experienced at least one grade 3 treatment-related toxicity. One of the 44 HCC patients developed grade 3 thrombocytopenia; of the 39 IHC patients, one developed liver failure and ascites, one developed a stomach ulcer, and one was found to have hyperbilirubinemia. Three of the 83 patients (3.6%) had worsening Child-Turcotte-Pugh (CTP) score: two patients from A to B at three months and one patient from A to B at six months. There were no grade 4 or 5 treatment-related toxicities. In terms of efficacy, only four patients developed local progression within two years of follow-up; two-year local control rate was 94% for patients with either HCC or IHC; however, recurrence beyond two years only occured in patients with IHC, specifically in four additional patients. Notably, all patients who experienced local progression had received less than 60 GyE. For patients with IHC, the median progression-free survival was 8.4 months, median overall survival was 22.5 months, and two-year overall survival was 46.5%. The impressive results of this study, especially when compared with historical data using conventionally fractionated RT for IHC, have recognized high-dose, hypofractionated proton beam therapy as an attractive modality for inoperable intrahepatic tumors, especially those that are too large for the extreme hypofractionation associated with SBRT (Table 16.1).

Table 16.1 Use of high-dose radiotherapy in the treatment of intrahepatic cholangiocarcinoma

Author, year of publication	Study design	# of IHC pts	Tumor size (cm^3)	Mode of RT delivery	Total dose (Gy)	# Fx	One-year LC	One-year OS	Toxicity
Liu et al. [40]	Retrospective	6	8.8 (0.2–222.4)	3D-conformal SBRT	20–50	3–5	93%[a]	81%[a]	None for IHC pts
Ibarra et al. [41]	Retrospective	11	80.2 (30.6–818.5)	SBRT, Cyberknife, or linac-based	22–50	1–10	50%	45%	7 with grade 3 toxicities
Lanciano et al. [42]	Retrospective	4	60.9 (2.29–316)	SBRT, Cyberknife	36–60	3	92%[a]	73%[a]	None for IHC pts
Barney et al. [43]	Retrospective	6	16–412.4	IMRT or 3D-conformal SBRT	55 (45–60)	3 or 5	100%	73%	1 w/Gr. 3 biliary stenosis; 1 w/Gr. 5 liver failure[a]
Dewas et al. [44]	Retrospective	6	63 (36–112)	SBRT, Cyberknife	45 (29–45)	3 or 4	100%	NR%	NR
Goyal et al. [45]	Retrospective	3	384 (80–818)	SBRT, Cyberknife	34 (24–45)	1–3	82% at 8 mos	NR	None
Goodman et al. [46]	Phase I	5	32 (0.8–146.6)	SBRT, Cyberknife	18–30	1	77%[a]	71.4%[b]	None for IHC pts
Kopek et al. [47]	Prospective	1	32 (9–205)	SBRT, linac-based	45	3	84%[a]	Median 10.6 mos[a]	21 w/Gr 3 elevation in liver enzymes, 6 w/GI bleed[a]
Tse et al. [39]	Phase I	10	172 (10–465)	SBRT, linac-based	36 (24–54)	6	65%	58%	2 w/transient biliary obstruction, 2 w/decline to CP B
Wulf et al. [48]	Retrospective	1	53 (9–516)	SBRT, linac-based	26–37.5	1–3	100%	60%	No grade 3
Herfarth et al. [49]	Phase I/II	3	10	SBRT, linac-based	14–26	1	71%[c]	72%[c]	None
Blomgren et al. [34]	Retrospective	1	67	SBRT, microtron, or linac-based	63	3	14 mos median	11 mos median	NR
Tao et al. [27]	Retrospective	79	198 (12–966)	3D-conformal, IMRT, or proton	58.05 (35–100)	28 (15–30)	81% at 1 yr 45% at 2 yrs	87% at 1 yr 61% at 2 yrs	7 w/biliary stenosis requiring stent[d]
Hong et al. [50]	Phase II	39	133.7 (3.7–599.7)	Proton	58 (15–67.5)	15	94.1% at 2 yrs	69.7% at 1 yr 46.5% at 2 yrs	3 w/Gr 3 liver failure, hyperbilirubinemia, gastric ulcer

Abbreviations: *SBRT* Stereotactic body radiotherapy; *HC* Intrahepatic cholangiocarcinoma; *RT* Radiotherapy; *Fx* Fractions of radiotherapy; *LC* Local control; *OS* Overall survival; *NR* Not reported; *CP B* Child-Pugh Class B cirrhosis; *GI* Gastrointestinal; *pts* Patients

[a]Includes entire cohort in study

[b]Includes two patients with HCC

[c]Includes 56 patients with metastatic lesions

[d]Unclear if due to radiation-induced biliary toxicity or tumor progression

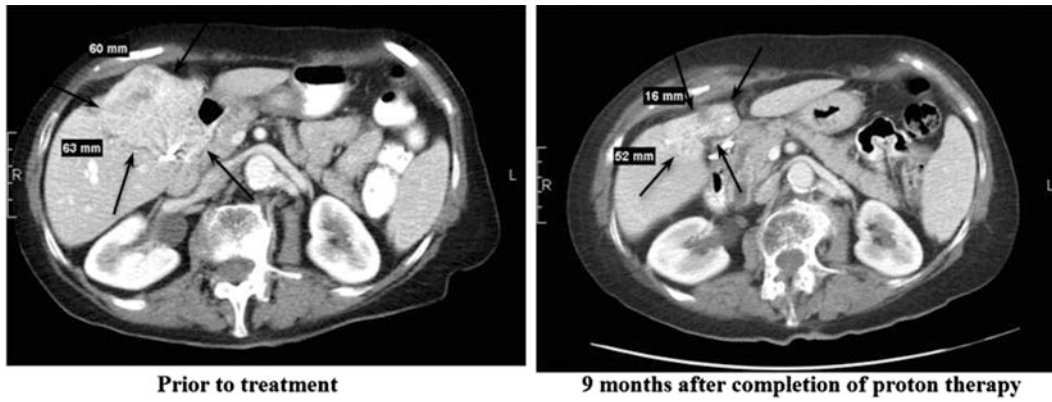

Fig. 16.1 Axial CT slices of an intrahepatic cholangiocarcinoma lesion before and after completion of proton therapy

Fig. 16.2 Schema for NRG GI001 trial

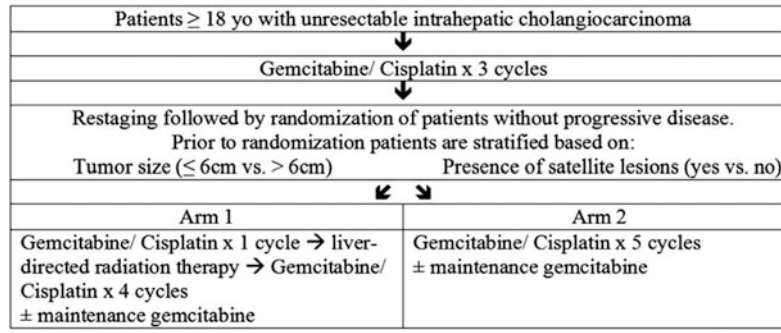

16.4 Future Directions

Given the encouraging results seen with the addition of radiation therapy for localized, unresectable IHC, the NRG Oncology Group has developed a Phase III trial of gemcitabine and cisplatin with or without liver-directed radiotherapy to determine the impact of radiotherapy on outcomes in patients receiving optimal systemic therapy. Patients will receive three cycles of gemcitabine and cisplatin, followed by restaging and stratification based on tumor size ($\leq$ 6 cm vs. >6 cm) and the presence or absence of satellite lesions. Patients will then be randomized to liver-directed radiotherapy and additional gemcitabine and cisplatin versus gemcitabine and cisplatin alone (Fig. 16.2). Selection of the prescription dose is to be based on the mean liver dose.

16.5 Neoadjuvant Therapy with Transplantation for Hilar Cholangiocarcinoma

Cholangiocarcinoma arising at the hepatic duct bifurcation (i.e., hilar cholangiocarcinoma) characteristically arises in patients with primary sclerosing cholangitis (PSC). These patients, similar to those with severe cirrhosis, are usually not candidates for the extensive resection that would be needed to obtain negative margins. Despite the rare incidence of cholangiocarcinoma overall, patients with PSC are at significantly higher risk with incidence reported from 4 to 20%, and majority are hilar (i.e., Klatskin tumor) [52, 53]. Liver transplantation was studied as an alternative for those patients with localized disease who were not candidates for extensive resection. Initial outcomes were poor due to high incidence of

locoregional dissemination and recurrence [54, 55]. Due to the potentially long waiting time for organ transplantation, neoadjuvant therapy with radiation and concurrent chemotherapy was proposed in order to obtain local control and decrease risk of regional recurrence following transplant [55, 56]. The University of Nebraska and the Mayo Clinic have demonstrated that excellent survival can be achieved for highly selected patients with early stage hilar cholangiocarcinoma treated with aggressive neoadjuvant therapy leading to liver transplantation.

The University of Nebraska initially studied this multimodal technique; seventeen patients with hilar cholangiocarcinoma, all presenting with obstructive cholangitis, were treated between 1987 and 2000 with chemotherapy (daily 5-FU 300 mg/m^2) and intraluminal bile duct brachytherapy (iridium-192 6000 cGy delivered over 55–60 h) while awaiting liver transplantation. Patients were only eligible if maximal tumor dimension was 2 cm without radiographic extrahepatic disease or intra/extrahepatic metastasis. The basis for these guidelines was the fact that the iridium wires used for radiotherapy had a penetration of 1 cm; therefore, tumors greater than 2 cm in diameter may not achieve optimal dose at the periphery. Notably, nine patients had PSC and/or ulcerative colitis, and three patients had decompensated cirrhosis. The most significant complication between chemoradiation and surgery was recurrent episodes of cholangitis. Eleven patients were free of complications or tumor progression precluding surgery and underwent transplantation (median waiting time 87 days, range 15–792). The median survival was 25 months for the patients who underwent liver transplantation; five of these patients (45%) remained free of tumor recurrence 2.8–14.5 years after transplant [58].

In 1993, the Mayo Clinic also initiated a protocol for unresectable hilar cholangiocarcinoma due to extent of disease and/or underlying liver disease. All patients were treated with neoadjuvant radiation (4000–4500 cGy by external beam, followed by 2000–3000 cGy intraluminal brachytherapy with iridium-192) and chemotherapy (concurrent bolus 5-FU with external beam and protracted venous infusion 5-FU with brachytherapy, which continued until surgery) followed by liver transplantation. This protocol differed with the additional use of external beam radiotherapy. Eligible patients had a maximal tumor diameter of 3 cm without evidence of intra/extrahepatic metastasis. The initial publication [57] presented the first 19 patients, for which 11 patients had no evidence of progression at the time of surgery and completed the protocol. With a median follow-up of 44 months, only one patient who completed the protocol developed tumor relapse. Since this publication, over 130 additional patients with unresectable hilar cholangiocarcinoma have been enrolled, and 90 patients have been reported to have favorable findings at the time of transplant. Five-year actuarial survival for all patients that began neoadjuvant therapy is 55%, and five-year survival after transplant is 71% [59].

16.6 Conclusion

The development of modern radiotherapy techniques has facilitated the incorporation of radiotherapy into the treatment of intrahepatic cholangiocarcinoma, specifically by allowing for dose-escalation to tumor without increasing toxicity or the risk of radiation-induced liver disease. In the unresectable setting, the ability to achieve tumoricidal dose for primary cholangiocarcinoma has led to significant improvements in local control, translating into a survival benefit for patients, which is in some instances comparable to those historically reported after resection. Through the use of modern techniques, including SBRT and proton therapy, liver-directed radiotherapy has become effective and feasible. Further study is needed to determine its full potential in the treatment of IHC, as well as the optimal integration of radiotherapy with chemotherapy.

References

1. Edge S, Byrd D, Compton C, et al., editors. AJCC cancer staging manual. New York: Springer; 2010.
2. Shaib YH, Davila JA, McGlynn K, El-Serag HB. Rising incidence of intrahepatic cholangiocarcinoma in the United States: a true increase? J Hepatol. 2004;40:472–7.
3. Shaib Y, El-Serag HB. The epidemiology of cholangiocarcinoma. Semin Liver Dis. 2004;24:115–25.
4. Hasegawa S, Ikai I, Fujii H, et al. Surgical resection of hilar cholangiocarcinoma: analysis of survival and postoperative complications. World J Surg. 2007;31:1256.
5. Jarnagin WR, Ruo L, Little SA, et al. Patterns of initial disease recurrence after resection of gallbladder carcinoma and hilar cholangiocarcinoma: implications for adjuvant therapeutic strategies. Cancer. 2003;98:1689.
6. Maithel SK, Gamblin TC, Kamel I, et al. Multidisciplinary approaches to intrahepatic cholangiocarcinoma. Cancer. 2013;119:3929–42.
7. Spolverato G, Vitale A, Cuchetti A, et al. Can hepatic resection provide a long-term cure for patients with intrahepatic cholangiocarcinoma? Cancer. 2015;121:3998–4006.
8. Mavros MN, Economopoulos KP, Alexiou VG, et al. Treatment and prognosis for patients with intrahepatic cholangiocarcinoma: systematic review and meta-analysis. JAMA Surg. 2014;149:565–74.
9. Guglielmi A, et al. Intrahepatic cholangiocarcinoma: prognostic factors after surgical resection. World J Surg. 2009;33:1247–54.
10. Shimada K, et al. Clinical impact of the surgical margin status in hepatectomy for solitary mass-forming type intrahepatic cholangiocarcinoma without lymph node metastases. J Surg Oncol. 2007;96:160–5.
11. Valle J, et al. Cisplatin plus gemcitabine versus gemcitabine for biliary tract cancer. N Engl J Med. 2010;362:1273–81.
12. Nelson JW, Ghafoori AP, Willett CG, et al. Concurrent chemoradiotherapy in resected extrahepatic cholangiocaricinoma. Int J Radiat Oncol Biol Phys. 2011;81:189.
13. Horgan AM, Amir E, Walter T, et al. Adjuvant therapy in the treatment of biliary tract cancer: a systematic review and meta-analysis. J Clin Oncol. 1934;2012:30.
14. Jiang W, et al. Benefit of radiotherapy for 90 patients with resected intrahepatic cholangiocarcinoma and concurrent lymph node metastases. J Cancer Res Clin Oncol. 2010;136:1323–31.
15. Jan YY, Yeh CN, Yeh TS, Chen TC. Prognostic analysis of surgical treatment of peripheral cholangiocarcinoma: two decades of experience at Chang Gung memorial hospital. W J Gastroenterol. 2005;11:1779–84.
16. Endo I, et al. Intrahepatic cholangiocarcinoma: rising frequency, improved survival, and determinants of outcome after resection. Ann Surg. 2008;248:84–96.
17. Ohtsuka M, et al. Results of surgical treatment for intrahepatic cholangiocarcinoma and clinicopathological factors influencing survival. Br J Surg. 2002;89:1525–31.
18. Chen YX, et al. Determining the role of external beam radiotherapy in unresectable intrahepatic cholangiocarcinoma: a retrospective analysis of 84 patients. BMC Cancer. 2010;10:492.
19. Zeng ZC, et al. Consideration of the role of radiotherapy for unresectable intrahepatic cholangiocarcinoma: a retrospective analysis of 75 patients. Cancer J. 2006;12:113–22.
20. Shinohara ET, Mitra N, Guo M, Metz JM. Radiation therapy is associated with improved survival in the adjuvant and definitive treatment of intrahepatic cholangiocarcinoma. Int J Radiat Oncol Biol Phys. 2008;72:1495–501.
21. Crane CH, Macdonald KO, Vauthey JN, et al. Limitations of conventional doses of chemoradiation for unresectable biliary cancer. Int J Radiat Oncol Biol Phys. 2002;53:969–74.
22. Ben-Josef E, Lawrence TS. Radiotherapy for unresectable hepatic malignancies. Semin Radiat Oncol. 2005;15:273–8.
23. Dawson LA, et al. Analysis of radiation-induced liver disease using the Lyman NTCP model. Int J Radiat Oncol Biol Phys. 2002;53:810–21.
24. McGinn CJ, et al. Treatment of intrahepatic cancers with radiation doses based on a normal tissue complication probability model. J Clin Oncol. 1998;16:2246–52.
25. Dawson LA, et al. Escalated focal liver radiation and concurrent hepatic artery fluorodeoxyuridine for unresectable intrahepatic malignancies. J Clin Oncol. 2000;18:2210–8.
26. Ben-Josef E, et al. Phase II trial of high-dose conformal radiation therapy with concurrent hepatic artery floxuridine for unresectable intrahepatic malignancies. J Clin Oncol. 2005;23:8739–47.
27. Tao R, Krishnan S, Bhosale PR, et al. Ablative radiotherapy doses lead to a substantial prolongation of survival in patients with inoperable intrahepatic cholangiocarcinoma: a retrospective dose response analysis. J Clin Oncol. 2016;34:129–226.
28. Park C, Papiez L, Zhang S, Story M, Timmerman RD. Universal survival curve and single fraction equivalent dose: useful tools in understanding potency of ablative radiotherapy. Int J Radiat Oncol Biol Phys. 2008;70:847–52.
29. Song CW, et al. Radiobiology of stereotactic body radiation therapy/stereotactic radiosurgery and the linear-quadratic model. Int J Radiat Oncol Biol Phys. 2013;87:18–9.
30. Brown JM, Carlson DJ, Brenner DJ. The tumor radiobiology of SRS and SBRT: are more than the 5

Rs involved? Int J Radiat Oncol Biol Phys. 2014;88:254–62.
31. Song CW, Kim MS, Cho LC, Dusenbery K, Sperduto PW. Radiobiological basis of SBRT and SRS. Int. J Clin Oncol. 2014;19(4):570–8.
32. Leksell L. The stereotaxic method and radiosurgery of the brain. Acta Chir Scand. 1951;102:316–9.
33. Lax I, Blomgren H, Näslund I, Svanström R. Stereotactic radiotherapy of malignancies in the abdomen. Methodological aspects. Acta Oncol. 1994;33:677–83.
34. Blomgren H, Lax I, Näslund I, Svanström R. Stereotactic high dose fraction radiation therapy of extracranial tumors using an accelerator. Clinical experience of the first thirty-one patients. Acta Oncol. 1995;34:861–70.
35. Méndez Romero A, et al. Stereotactic body radiation therapy for primary and metastatic liver tumors: a single institution phase I-II study. Acta Oncol. 2006;45:831–7.
36. van der Pool AEM, et al. Stereotactic body radiation therapy for colorectal liver metastases. Br J Surg. 2010;97:377–82.
37. Rusthoven KE, et al. Multi-institutional phase I/II trial of stereotactic body radiation therapy for liver metastases. J Clin Oncol. 2009;27:1572–8.
38. Lee MT, et al. Phase I study of individualized stereotactic body radiotherapy of liver metastases. J Clin Oncol. 2009;27:1585–91.
39. Tse RV, et al. Phase I study of individualized stereotactic body radiotherapy for hepatocellular carcinoma and intrahepatic cholangiocarcinoma. J Clin Oncol. 2008;26:657–64.
40. Liu E, et al. Stereotactic body radiation therapy for primary and metastatic liver tumors. Transl Oncol. 2013;6:442–6.
41. Ibarra RA, et al. Multicenter results of stereotactic body radiotherapy (SBRT) for non-resectable primary liver tumors. Acta Oncol. 2012;51:575–83.
42. Lanciano R, et al. Stereotactic body radiation therapy for patients with heavily pretreated liver metastases and liver tumors. Front Oncol. 2012;2:23.
43. Barney MB, Olivier KR, Miller RC, Haddock MG. Clinical outcomes and toxicity using stereotactic body radiotherapy (SBRT) for advanced cholangiocarcinoma. Radiat Oncol. 2012;7:67.
44. Dewas S, et al. Prognostic factors affecting local control of hepatic tumors treated by Stereotactic Body Radiation Therapy. Radiat Oncol. 2012;7:166.
45. Goyal K, et al. Cyberknife stereotactic body radiation therapy for nonresectable tumors of the liver: preliminary results. HPB Surg. 2010;pii:309780.
46. Goodman KA, et al. Dose-escalation study of single-fraction stereotactic body radiotherapy for liver malignancies. Int J Radiat Oncol Biol Phys. 2010;78:486–93.
47. Kopek N, Holt MI, Hansen AT, Høyer M. Stereotactic body radiotherapy for unresectable cholangiocarcinoma. Radiother Oncol. 2010;94:47–52.
48. Wulf J, et al. Stereotactic radiotherapy of primary liver cancer and hepatic metastases. Acta Oncol. 2006;45:838–47.
49. Herfarth KK, et al. Stereotactic single-dose radiation therapy of liver tumors: results of a phase I/II trial. J Clin Oncol. 2001;19:164–70.
50. Hong TS, Wo JY, Beow YY, et al. A multi-institutional phase II study of high dose hypofractionated proton beam therapy in patients with localized, unresectable hepatocellular carcinoma and intrahepatic cholangiocarcinoma. J Clin Oncol. 2016;34:460–8.
51. Emami B, et al. Tolerance of normal tissue to therapeutic irradiation. Int J Radiat Oncol Biol Phys. 1991;21:109–22.
52. Ahrendt SA, Cameron JL, Pitt HA. Current management of patients with perihilar cholangiocarcinoma. Adv Surg. 1996;30:427–52.
53. Rosen CB, Nagomey DM, Wiesner RH, et al. Cholangiocarcinoma complicating primary sclerosing cholangitis. Ann Surg. 1991;213:21–5.
54. Iwatsuki S, Todo S, Marsh JW, et al. Treatment of hilar cholangiocarcinoma (Klatskin tumors) with hepatic resection transplantation. J Am Coll Surg. 1998;187:358–64.
55. Goldstein RM, Stone M, Tillery GW, et al. Is liver transplantation indicated for cholangiocarcinoma? Am J Surg. 1993;166:768–71.
56. McMasters KM, Tuttle TM, Leach SD, et al. Neoadjuvant chemoradiation for extrahepatic cholangiocarcinoma. Am J Surg. 1997;174:605–8.
57. DeVreede I, Steers JL, Burch PA, et al. Prolonged disease-free survival after orthotopic liver transplantation plus adjuvant chemoirradiation for cholangiocarcinoma. Liver Transpl. 2000;6:309–16.
58. Sudan D, DeRoover A, Chinnakotla S, et al. Radiochemotherapy and transplantation allow long-term survival for nonresectable hilar cholangiocarcinoma. Am J Transplant. 2002;2:774–9.
59. Rosen CB, Heimbach JK, Gores GJ. Surgery for cholangiocarcinoma: the role of liver transplantion. HPB. 2008;10:186–9.

Part VI
Liver Metastases

Liver Metastases: Basic Principles of Treatment and Clinical Data

17

Matthew R. Porembka, MD and Michael A. Choti, MD

17.1 Introduction

Liver metastases are frequently encountered in the care of patients with gastrointestinal malignancy. Historically, the presence of liver disease was thought to represent an incurable problem limiting treatment options to palliative chemotherapy. However, recent advancements in the treatment of patients with gastrointestinal malignancy have facilitated curative liver directed therapies including resection, ablation, and intra-arterial therapies of metastasis. Specifically, advancements in clinical imaging have allowed for more accurate assessment of disease burden. Modern systemic chemotherapies demonstrate higher and more durable response rates. Liver surgery for metastases has become safe and routine procedures secondary to the evolution of surgical and anesthetic techniques. This chapter will review the surgical options for the treatment of liver metastases including resection, ablation, and arterial-based therapies. Although, curative liver metastasectomy has been described for numerous indications, colorectal cancer and neuroendocrine liver metastases are the most frequent indications for intervention and this chapter will focus on these two indications.

17.2 Surgery in the Treatment of Colorectal Cancer Liver Metastases

Despite an increased emphasis on screening and prevention, colorectal cancer (CRC) remains the third most commonly diagnosed cancer in the United States [1]. Over 135,000 new cases will have been diagnosed in 2014 and approximately 49,000 patients will die of their disease [1]. Among those patients diagnosed with CRC, about half will develop metastases. The liver is the most common organ affected by metastatic disease and is often the only site of metastatic disease. Approximately, 30% of patients will have liver only metastases at the time of presentation or recurrence, accounting for about 30,000 patients per year in the Unites States [2, 3]. It is now accepted that without surgical management, median survival is limited and 5-year survival is rare. Systemic chemotherapy for metastatic colorectal cancer has significantly improved over the last two decades with response rates typically exceeding 50%. In trials looking at chemotherapy alone, median survival is about 2 years, but 5-year survival remains uncommon and long-term cure is rare [4].

The majority of data which drives the use of colorectal liver metastasectomy is based on

M.R. Porembka (✉) · M.A. Choti
Department of Surgery, University of Texas Southwestern Medical Center,
5323 Harry Hines Blvd, Dallas
TX 75390-8548, USA
e-mail: matthew.porembka@utsouthwestern.edu

M.A. Choti
e-mail: michael.choti@utsouthwestern.edu

J. Meyer and T.E. Schefter (eds.), *Radiation Therapy for Liver Tumors*,
DOI 10.1007/978-3-319-54531-8_17

retrospective studies, many of which are limited by small numbers and selection bias. However, complete resection has been repeatedly associated with prolonged survival compared with patients not undergoing surgical therapy with 5-year overall survival exceeding 50%. Although these favorable results could reflect favorable patient selection, comparison between series of chemotherapy and surgery over the last four decades demonstrates dramatically different results in favor of surgical resection. The argument for hepatic resection is further strengthened by the fact that patients are cured by surgery at a rate similar to that of some primary non-metastatic malignancies.

17.3 Results of Liver Resection for Colorectal Metastases

Liver resection, when performed by experienced surgeons at high volume centers, is safe with reported perioperative mortality of 1% [5–8]. Although operative mortality should be uncommon, significant complications have been reported in up to 30% of patients [8–10]. The morbidity associated specifically with liver resection includes hemorrhage, perihepatic abscess, bile leak and/or fistula, pleural effusion, and hepatic failure. The long-term survival reported following hepatic resection with curative intent for metastatic colorectal cancer has improved significantly in the last decade. While older series report 5-year survival rates of 25–40% [11], more contemporary series report 5-year survival in excess of 50% and durable cure in some patients [6, 12, 13]. Large multi-institutional collective series demonstrate trends in improved long-term outcome [7, 10, 13–15] (Table 17.1).

Despite aggressive surgical resection and modern systemic chemotherapy, the majority of patients will recur and succumb to their disease. Numerous risk stratification tools have been developed to assist in patient selection for liver metastasectomy to identify patients that are likely to experience long-term disease control [16]. Pathologic features of the primary tumor appear to correlate with long-term outcome following liver resection. Both nodal status and histologic grade of the primary tumor are associated with poorer outcome following liver resection in several reported series [6, 7, 13]. The first clinical risk score was published by Fong et al. in 1999 and highlighted high risk features associated with poor outcome [7]. Factors including number of metastasis, disease-free interval less than 12 months, node-positive primary tumor, largest tumor greater than 5 cm, and CEA greater than 200 were associated with decreased survival. Patients with increased numbers of risk factors had a progressively worse survival. These findings have been supported by multiple other studies [6, 7, 13]. Even though this risk score was developed before the implementation of modern chemotherapy, it demonstrated that well selected patients, even those with multifocal and bilobar disease, could derive long-term survival benefit with surgery.

Technical factors related to surgery can also impact patient outcomes and prognosis. It is well accepted that margin status is associated with survival, although it is not always possible to predict final margin status based on preoperative imaging. Most series have demonstrated that positive surgical resection margin is associated with higher risk of local recurrence and poor long-term survival [6, 17, 18]. It has been postulated that the inferior long-term outcome associated with a histologic positive margin is less related to local recurrence, but that the presence of a positive margin is a surrogate marker for more aggressive tumor biology. The optimal width of the negative surgical margin, however, remains controversial. Some investigators have reported an improved survival when clearance margins were one centimeter or greater [19] while others have shown no differences, provided the margin is grossly negative [17, 20]. The perceived inability to achieve a negative margin based on preoperative imaging should not preclude resection as patients with close margins can still experience survival benefit after surgical resection. The type of resection performed does not appear to affect long-term recurrence rates, independent of margin status [6, 7, 13].

Table 17.1 Large series reporting short- and long-term outcomes after curative intent surgical therapy for colorectal liver metastases

Authors (year published)	Number	Mortality (%)	Morbidity (%)	5-year disease-free survival (%)	5-year overall survival (%)
Nordlinger et al. (1996) [14]	1568	2	23	15	28
Fong et al. (1999) [7]	1001	3	31	–	37
Malik et al. (2007) [10]	700	3	30	31	45
De Jong et al. (2009) [15]	1669	–	–	30	47
House et al. (2010) [13]	1600	2	44	27–33	37–51

Extrahepatic disease, even when isolated and resectable, is associated with unfavorable prognosis following liver resection of colorectal metastases [7, 11]. Direct extension into adjacent structures and locoregional recurrence should not be considered extrahepatic disease and is not a contraindication to resection. However, concomitant hepatic and extrahepatic metastasectomy is controversial. Pulmonary metastases represent the second most frequent metastasis in patients with colorectal cancer. About 5–10% of patients who present with metastatic disease will have both liver and lung metastases. Similar to liver resection for isolated hepatic metastasis, studies have reported favorable long-term survival rates after resection of localized pulmonary disease [21]. In highly selected patients, favorable 5-year survival rates in excess of 30% have been reported for patients undergoing combined lung and liver resection [22, 23]. Although prognosis following resection of pulmonary and liver metastasis does not appear to be affected by synchronous versus metachronous presentation, the presence of multiple pulmonary metastases (>3) was significantly associated with worse disease specific survival [24].

17.4 Ablative Therapies in CRLM

Although surgical resection may afford the only potential for cure in patients with hepatic metastases, many patients may not be candidates for surgical resection for a variety of reasons. Novel methods for local ablation have been developed with a goal of increasing the number of patients eligible for local, potentially curative therapy. There are two classifications of ablative therapies: thermal and nonthermal. Nonthermal technologies include chemical ablation with ethanol or acetic acid instillation and irreversible electroporation. Thermal ablative technology includes radiofrequency ablation (RFA), cryoablation, and microwave ablation (MWA).

Thermal ablation is the most commonly used ablative technology used to treat CLRM. With this technique, a needle-probe is inserted within the selected tumor under image guidance and electric current is employed to generate heat, resulting in interstitial thermal destruction. Ablation can be performed laparoscopically, percutaneously, or through an open laparotomy. Careful planning of the ablation area is necessary to achieve complete destruction of the target lesion. Tumor size as well as location can preclude effective ablation with curative intent. Tumor sizes larger than 3–4 cm are associated with an increased incidence of local recurrence [25]. Similarly, tumors near major vascular structures such as the vena cava are more difficult to achieve long-term local control with ablation. A major contraindication for thermal ablation is small tumors in close proximity to central biliary structures which result in severe and complicated biliary stricture.

The optimal method for evaluating the efficacy of ablation using imaging modalities is not well defined. Given the local changes associated

with ablation, it is sometimes difficult to discriminate between postoperative change and tumor recurrence. Hypoattenuating lesions may persist for months to years despite complete tumor destruction. Although contrast CT and MRI are useful for post ablation surveillance, MRI may be more sensitive for detecting viable tumor or early recurrence given [26, 27]. In most cases, a local recurrence is characterized by an increase in the lesion size on serial scans, evidence of new areas of contrast enhancement, or areas of restricted diffusion.

There are no published randomized controlled trials examining the efficacy of ablation in CRLM compared to resection or between ablation modalities. Data is largely based on single-center, single-arm, retrospective studies [28]. Local recurrence rates published in the literature range from less than 10% to as high as 40 to 50% [28–30]. Survival benefit associated with ablation is variable and inconsistent with some studies have reported 5-year survival of less than 20% following ablation whereas other studies have reported 5-year survival rates in the range of 40% or more [28]. In most cases, survival is similar between RFA and MWA (Table 17.2). However, RFA has been associated with higher local recurrence rates, which may be secondary to limitations of the technology or patient selection. In a single institution study of 254 similar patients comparing RFA to MWA, patients undergoing MWA were observed to have a lower rate of ablation sight recurrence comparted to RFA (6% vs. 20%, respectively). The only factor that was significantly associated with local recurrence on multivariable analysis was treatment with RFA [41]. This finding was supported by a systematic review of outcomes of thermal ablation which demonstrated a higher risk of local recurrence for RFA (10–31%) compared to MWA (5–13%) [42]. Several studies have attempted to compare the outcome of resection to ablation with a majority of studies demonstrating inferior disease-free and overall survival of RFA compared with resection. More recently, Shibata et al. reported a prospective trial comparing MWA to resection which demonstrated similar survival [40]. At present, although early studies support the use of ablation in selected patients, it should be considered an adjunctive therapy to resection as high-quality data is not available to make informed conclusions.

17.5 Hepatic Artery Chemotherapy for CLRM

Hepatic-directed therapy in the management of metastatic colorectal cancer is a well-established therapy that includes hepatic arterial infusion

Table 17.2 Comparison of thermal ablation techniques in the treatment of colorectal liver metastases

Author	Year	N	Method	Survival (%)			Complications (%)	Local Recurrence (%)
				1 year	3 year	5 year		
Veltri [31]	2008	122	RFA	79	38	22	1.1	26.3
Solbiati [32]	2012	99	RFA	98	69	25	2.0	6.9
Siperstein [33]	2007	234	RFA	–	20	18	–	–
Kennedy [34]	2013	130	RFA	94	50	29	1.5	9.2
Hammill [35]	2011	113	RFA	87	52	33	1.8	2.6
Berber [36]	2008	68	RFA	–	35	30	2.9	–
Groeschl [37]	2014	198	MWA	45	17	–	–	6
Liang [38]	2003	21	MWA	91	46	–	0	14
Ogata [39]	2008	32	MWA	–	–	32	–	–
Shibata [40]	2000	14	MWA	71	57	14	14	–

RFA radiofrequency ablation, *MWA* microwave ablation

pumps and conventional transarterial chemoembolization. Hepatic artery chemotherapy exploits the dual blood supply of the liver. Although most hepatocytes are supplied by the portal venous system, hepatic tumors are primarily supplied by the hepatic arterial system [43]. Direct infusion of chemotherapy into the hepatic arterial system delivers high doses of chemotherapy directly to the tumor while limiting systemic toxicity.

Transarterial chemoembolization with irinotecan-loaded drug-eluting beads (DEBIRI) in combination with capecitabine has been studied in a prospective, single-center study and found to be technically feasible and safe. In this small study of 23 patients with liver-dominant disease that was refractory to chemotherapy, DEBIRI was well tolerated and resulted in overall disease control in 60% of patients with a progression free and overall survival of 4 and 7.3 months, respectively [44].

Hepatic artery infusion chemotherapy (HAI) delivers a constant infusion of chemotherapy into the hepatic arterial supply through an implantable subcutaneous pump. Fluorodeoxiuridine (FUDR), which is an active metabolite of 5-FU that is rapidly metabolized within the liver on the first pass, is the most commonly used regional chemotherapeutic agents [45].

The efficacy of HAI chemotherapy has been extensively studied for various indications including: (1) first line therapy with HAI alone, (2) second line therapy consisting of HAI with systemic therapy, and (3) downstaging of initially unresectable disease with HAI therapy. Ten randomized clinical trials have been performed evaluating the efficacy of HAI as a first line therapy in unresectable CRLM. The trials span a three-decade period and display significant heterogeneity in terms of trial design and implantation and are limited by inadequate sample sizes, crossover study designs, or inadequately administered systemic chemotherapy. A meta-analysis pooled all available data and demonstrated superior response rates associated with HAI (43%) compared to systemic therapy (18%, $p < 0.0001$). Although there was a trend toward an overall survival advantage favoring HAI chemotherapy (15.9 months) over systemic therapy (12.4 months), the difference was not significant (hazard ratio 0.90, 95% CI 0.76–1.07). Aggregate evaluation of these data suggests improved response rate with HAI chemotherapy alone (without systemic therapy) that does not translate into a survival advantage [46, 47].

Outcomes of patients with unresectable CRLM who progress on first line chemotherapy are poor with median overall survival less than 12 months [48]. Although first line trials failed to demonstrate survival advantage associated with HAI, encouraging findings such as delayed hepatic progression and superior response rates motivated subsequent investigations of HAI chemotherapy in combination with systemic chemotherapy. The combination of systemic 5-FU/LV with HAI FUDR compared to 5-FU/LV alone was investigated in a randomized trial of 84 patients. No survival difference benefit was observed by the addition of HAI FUDR (1-year OS, 46%) compared to 5-FU alone (53%). However, patients treated with combination therapy experienced increased toxicity [49]. Subsequently, the introduction of modern systemic agents including oxaliplatin and irinotecan spurred several phase I studies investigating the role of HAI FUDR with these newer agents. Results were consistent among these smaller trials and demonstrated no increase in toxicities associated with the addition of HAI FUDR to systemic irinotecan, oxaliplatin/irinotecan, or oxaliplatin/5-FU. In this cohort of heavily pretreated patients, the addition to HAI FUDR to modern systemic chemotherapy was associated with impressive response rates (HAI FUDR/irinotecan 74%, HAI FUDR/FOLFOX 87%, HAI FUDR/irinotecan/oxaliplatin 90%) and median overall survival (HAI FUDR/irinotecan 17.2 months, HAI FUDR/FOLFOX 22 months, HAI FUDR/irinotecan/oxaliplatin 36 months). In addition, 18% of patients in the HAI FUDR/irinotecan group that previously failed oxaliplatin were converted to resectable disease [50, 51].

The finding of durable response rates in patients who have failed multiple lines of chemotherapy prompted studies focusing on the ability of HAI FUDR to downstage patients with initially unresectable disease to facilitate definitive resection. The MSKCC group prospectively evaluated the efficacy of HAI FUDR/irinotecan/oxaliplatin

in 49 patients with unresectable CRLM. Nearly all patients had bilobar disease (98%) and 73% had greater than 5 tumors. Overall response rate was 92%, complete response was observed in 8%, and 47% was converted to resectable disease. Of those patients undergoing resection, median disease-free survival was 7.6 months. In a large retrospective review of 373 with unresectable disease treated with HAI FUDR and systemic chemotherapy, 25% of patients converted to resectable disease; median overall survival of patient receiving resection was 59 months [52]. Although well controlled studies evaluating HAI FUDR in combination with modern systemic therapy are lacking, the limited data available demonstrates dramatic response rates in heavily pretreated patients which facilitates conversion to resection in 25% of patients. Additional prospective randomized controlled trials are needed to validate these promising results.

17.6 Treatment of Neuroendocrine Liver Metastases

Neuroendocrine tumors (NET) are rare tumors that are often slow growing. Approximately, 70% arise from the gastrointestinal tract and have the capability to produce hormones resulting in significant symptoms that negatively impact quality of life. These tumors have a predilection for metastasis to the liver and the majority of patients will die of liver failure. The approach to surgical intervention in patient with NET metastases is considerably different that of CRLM owing to the unique tumor biology of NET and need to control hormonal syndromes that negatively impact quality of life.

The pattern of metastasis in NET is predominantly to the liver with frequent multifocal lesions that are numerous and bilobar leaving only a minority of patients eligible for complete resection. However, unlike CRLM, complete resection is not required to extend survival and obtain symptom control. It is believed that liver directed therapies are underused owing to the lack of understanding to NET biology and failure to refer to surgeons for evaluation.

Prospective data in the treatment of NET liver metastasis is lacking. The majority of data that drives the use of aggressive surgical management of NET is based on retrospective series that are often not well controlled owing to the rarity of the tumors. Most series are surgical in nature, suffer from selection bias, and results are compared to historical controls obtained in a time prior to modern tumor classification, imaging, and modern therapies. Although the data must be interpreted with caution, there is evidence supporting the aggressive management of NET to obtain control of hepatic disease as well as symptoms that have failed nonoperative management.

There are several major differences between the treatment of NET liver metastasis and other cancers. First, margin negative resection is not required. NET is well encapsulated tumors that do not infiltrate the hepatic parenchyma allowing them to be easily enucleated. Multiple series have demonstrated no difference in survival outcomes between R0 and R1 resections. Although favored, complete resection of hepatic and extrahepatic disease is not required. Surgical debulking of the majority of liver disease has been associated with similar survival outcomes as patients with complete resection.

Surgical debulking has been advocated to control hormonal syndromes and prolong survival. The first series of debulking was published in 1990 which demonstrated improved symptom control when at least 90% of grossly visible tumor was removed [53]. Subsequently, Sarmiento et al. published their large retrospective experience detailing 170 patients with carcinoid and pancreatic NET who underwent debulking of at least 90% of grossly visible hepatic disease [54]. A variety of patients were explored including those with unknown primaries and extrahepatic disease. The majority of patients had extensive disease with bilobar metastases (67%); only 44% had complete resection of all known disease and 96% of the remainder had residual disease in the liver. In those patients with functional primary tumors, 96% had improvement or complete relief of their symptoms. Symptom control rates were durable with a median symptom free interval of

45.5 months and a recurrence rate of 59% at 5 years. Nearly all patients had recurrence of disease or symptoms (84% at 5 years and 95% at 10 years). Debulking resulted in a 5- and 10-year overall survival rate of 61 and 35%, respectively. There was no difference between symptom control, recurrence, or survival between pancreatic and nonpancreatic primary tumors. The authors compared their results to historical controls which demonstrated a 5-year overall survival rate of 30–40% and median survival of 24–48 months. Likewise, similar series confirm these findings and that positive margins are not associated with worse recurrence free or overall survival [55].

A large multiinstitutional review recently aggregated the experience of eight international centers and detailed the surgical treatment of 339 patients undergoing debulking for NET [56]. The disease burden was similar to that published in previous series with 60% having bilobar disease requiring hepatic resection (78%), ablation (3%), or resection and ablation (19%). Incomplete resection was performed in 19% of patients. In this group, recurrence at 5 years was nearly universal at 94%. Median survival was 125 months with 5-year and 10-year overall survival rates of 74 and 51%, respectively. Patients with functional tumors and gross negative resections (R0/R1) derived the most benefit from surgery. Decreased survival was associated with synchronous liver metastasis, extrahepatic disease, and nonfunctional tumors on multivariate analysis.

Other series have attempted to determine clinical risk factors associated with prognosis. In patients with expanded indications for surgical debulking which included extrahepatic disease and a lower threshold of gross tumor debulking (70%), age was the only prognostic factor which correlated to time to liver progression [57]. Median time to liver progression was 71.6 months for the entire cohort. However, patients less than 50 years of age demonstrated shorter disease-free interval (39 months) compared to patients older than 50 (median not reached). Time to progression was not associated with number of tumors resected, metastasis grade, type of hepatic resection, thoroughness of debulking, or the presence of extrahepatic disease. Five-year disease specific survival was 90% and liver failure was the sole case of all disease-related deaths. Survival was also associated with age with patients younger than 50 years old demonstrating a 5-year survival of 73%; the survival rated in older patients was 97%. Although there may be a biologic basis driving this finding, the survival difference suggests an inherent selection bias between the groups or that older patients are more likely to succumb from non-neoplastic disease compared to younger patients.

Given the multifocal nature of NET liver metastasis, formal resection of all disease is sometime not possible and adjunctive therapies to resection are sometimes needed. Ablation and arterial-based therapies are useful in the treatment of these patients. The use of ablation alone for the treatment of NET metastasis is limited as multiple ablations at a single setting can be difficult. There is also an increased risk of incomplete ablation for tumors greater than 5 cm. In series where ablation was performed as an isolated procedure, symptom relief appeared to be similar to resection with approximately 65% of patient demonstrating decreased tumor markers and 75% having subjective improvement in symptoms [58, 59]. There is no useful survival data regarding ablation as a sole treatment. The greatest utility of ablation is as an adjunct to resection to maximize the effectiveness of debulking and to avoid resection of unnecessary parenchyma, which is associated increased perioperative morbidity and mortality.

Intra-arterial therapies are frequently used in the treatment of NET liver metastases. Intra-arterial treatments include occlusion of the hepatic arteries (bland embolization) or embolization of the hepatic artery with concurrent infusion of chemotherapy (chemoembolization) or radioactive particles (radioembolization). Radioembolization is beyond the scope of this chapter and will be included elsewhere. These therapies are often directed to symptom treatment and usually reserved for patients who are not candidates for surgical resection.

Several series have compared bland embolization and chemoembolization. In general, carcinoid tumors demonstrated higher response rates compared to pancreatic primaries (67% vs. 35%) and significantly higher median survival (33 months vs. 23 months) [60]. Although the incidence of toxicity is similar between bland and chemoembolization, there appears to be little advantage in chemoembolization over bland embolization in terms of response rates and survival [61].

The comparison of treatment modalities is not well studied. In an effort to determine the optimal treatment strategy for patient with NET liver metastases, a large, multi-institutional retrospective review compared treatment modalities with patient characteristics. Selection bias was clearly evident among patient groups as inferior survival was observed in the embolization group suggesting more advanced disease that was not amenable to surgery. Propensity scores were used to match patients across clinicopathologic criteria including tumor type, bilobar disease, liver tumor involvement, extrahepatic disease, and clinical symptoms. In this study, surgery was associated with greater benefit for symptomatic patients with greater than 25% liver involvement compared to intra-arterial therapy. Median survival was 81 months for surgery compared to 51 months for intra-arterial therapy. Conversely, there was no advantage for surgery in asymptomatic patients with less than 25% liver involvement as median survival times were not statistically significant (16.7 months vs. 18.5 months, respectively) [56].

17.7 Summary

Surgical therapies for hepatic metastases have been shown to be increasingly safe and effective therapy, resulting in more frequent and aggressive application of this local approach. An understanding of underlying disease biology, comprehensive preoperative staging, and thorough patient risk stratification is necessary to appropriate select patients for therapy. The indications for and use of local therapies to treat of hepatic metastases continue to expand as systemic chemotherapy improves.

References

1. Siegel RL, Miller KD, Jemal A. Cancer statistics. CA Cancer J Clin. 2015;65(1):5–29.
2. Weiss L, Grundmann E, Torhorst J, Hartveit F, Moberg I, Eder M, et al. Haematogenous metastatic patterns in colonic carcinoma: an analysis of 1541 necropsies. J Pathol. 1986;150(3):195–203.
3. Ohlsson B, Pålsson B. Follow-up after colorectal cancer surgery. Acta Oncol. 2003;42(8):816–26.
4. Gallagher DJ, Kemeny N. Metastatic colorectal cancer: from improved survival to potential cure. Oncology. 2010;78(3–4):237–48.
5. Choti MA, Bowman HM, Pitt HA, Sosa JA, Sitzmann JV, Cameron JL, et al. Should hepatic resections be performed at high-volume referral centers? J Gastrointest Surg. 1998;2(1):11–20.
6. Choti MA, Sitzmann JV, Tiburi MF, Sumetchotimetha W, Rangsin R, Schulick RD, et al. Trends in long-term survival following liver resection for hepatic colorectal metastases. Ann Surg. 2002;235(6):759–66.
7. Fong Y, Fortner J, Sun RL, Brennan MF, Blumgart LH. Clinical score for predicting recurrence after hepatic resection for metastatic colorectal cancer: analysis of 1001 consecutive cases. Ann Surg. 1999;230(3):309–18–discussion318–21.
8. Kingham TP, Correa-Gallego C, D'Angelica MI, Gonen M, Dematteo RP, Fong Y, et al. Hepatic parenchymal preservation surgery: decreasing morbidity and mortality rates in 4,152 resections for malignancy. J Am Coll Surg. 2015;220(4):471–9.
9. Farid SG, Aldouri A, Morris-Stiff G, Khan AZ, Toogood GJ, Lodge JPA, et al. Correlation between postoperative infective complications and long-term outcomes after hepatic resection for colorectal liver metastasis. Ann Surg. 2010;251(1):91–100.
10. Malik HZ, Prasad KR, Halazun KJ, Aldoori A, Al-Mukhtar A, Gomez D, et al. Preoperative prognostic score for predicting survival after hepatic resection for colorectal liver metastases. Ann Surg. 2007;246(5):806–14.
11. Scheele J, Stangl R, Altendorf-Hofmann A. Hepatic metastases from colorectal carcinoma: impact of surgical resection on the natural history. Br J Surg. 1990;77(11):1241–6.
12. Tomlinson JS, Jarnagin WR, Dematteo RP, Fong Y, Kornprat P, Gonen M, et al. Actual 10-year survival after resection of colorectal liver metastases defines cure. J Clin Oncol. 2007;25(29):4575–80.
13. House MG, Ito H, Gonen M, Fong Y, Allen PJ, Dematteo RP, et al. Survival after hepatic resection for metastatic colorectal cancer: trends in outcomes for

1,600 patients during two decades at a single institution. J Am Coll Surg. 2010;210(5):744–52–752–5.
14. Nordlinger B, Guiguet M, Vaillant JC, Balladur P, Boudjema K, Bachellier P, et al. Surgical resection of colorectal carcinoma metastases to the liver. A prognostic scoring system to improve case selection, based on 1568 patients. Association Française de Chirurgie. Cancer. 1996;77(7):1254–62.
15. de Jong MC, Pulitano C, Ribero D, Strub J, Mentha G, Schulick RD, et al. Rates and patterns of recurrence following curative intent surgery for colorectal liver metastasis: an international multi-institutional analysis of 1669 patients. Ann Surg. 2009;250(3):440–8.
16. Bilchik AJ, Poston G, Adam R, Choti MA. Prognostic variables for resection of colorectal cancer hepatic metastases: an evolving paradigm. J Clin Oncol. 2008;26(33):5320–1.
17. Pawlik TM, Scoggins CR, Zorzi D, Abdalla EK, Andres A, Eng C, et al. Effect of surgical margin status on survival and site of recurrence after hepatic resection for colorectal metastases. Ann Surg. 2005;241(5):715–22–discussion722–4.
18. Are C, Gonen M, Zazzali K, Dematteo RP, Jarnagin WR, Fong Y, et al. The impact of margins on outcome after hepatic resection for colorectal metastasis. Ann Surg. 2007;246(2):295–300.
19. Hughes KS, Rosenstein RB, Songhorabodi S, Adson MA, Ilstrup DM, Fortner JG, et al. Resection of the liver for colorectal carcinoma metastases. A multi-institutional study of long-term survivors. Dis Colon Rectum. 1988;31(1):1–4.
20. Nuzzo G, Giuliante F, Ardito F, Vellone M, Giovannini I, Federico B, et al. Influence of surgical margin on type of recurrence after liver resection for colorectal metastases: a single-center experience. Surgery. 2008;143(3):384–93.
21. Inoue M, Ohta M, Iuchi K, Matsumura A, Ideguchi K, Yasumitsu T, et al. Benefits of surgery for patients with pulmonary metastases from colorectal carcinoma. Ann Thorac Surg. 2004;78(1):238–44.
22. Neeff H, Hörth W, Makowiec F, Fischer E, Imdahl A, Hopt UT, et al. Outcome after resection of hepatic and pulmonary metastases of colorectal cancer. J Gastrointest Surg. 2009;13(10):1813–20.
23. Headrick JR, Miller DL, Nagorney DM, Allen MS, Deschamps C, Trastek VF, et al. Surgical treatment of hepatic and pulmonary metastases from colon cancer. Ann Thorac Surg. 2001;71(3):975–9–discussion979–80.
24. Mineo TC, Ambrogi V, Tonini G, Bollero P, Roselli M, Mineo D, et al. Longterm results after resection of simultaneous and sequential lung and liver metastases from colorectal carcinoma. J Am Coll Surg. 2003;197(3):386–91.
25. van Duijnhoven FH, Jansen MC, Junggeburt JMC, van Hillegersberg R, Rijken AM, van Coevorden F, et al. Factors influencing the local failure rate of radiofrequency ablation of colorectal liver metastases. Ann Surg Oncol. 2006;13(5):651–8.
26. Kuehl H, Antoch G, Stergar H, Veit-Haibach P, Rosenbaum-Krumme S, Vogt F, et al. Comparison of FDG-PET, PET/CT and MRI for follow-up of colorectal liver metastases treated with radiofrequency ablation: initial results. Eur J Radiol. 2008;67(2):362–71.
27. Schraml C, Clasen S, Schwenzer NF, Koenigsrainer I, Herberts T, Claussen CD, et al. Diagnostic performance of contrast-enhanced computed tomography in the immediate assessment of radiofrequency ablation success in colorectal liver metastases. Abdom Imaging. 2008;33(6):643–51.
28. Wong SL, Mangu PB, Choti MA, Crocenzi TS, Dodd GD, Dorfman GS, et al. American Society of Clinical Oncology 2009 clinical evidence review on radiofrequency ablation of hepatic metastases from colorectal cancer. J Clin Oncol. 2010;28(3):493–508.
29. Gleisner AL, Choti MA, Assumpcao L, Nathan H, Schulick RD, Pawlik TM. Colorectal liver metastases: recurrence and survival following hepatic resection, radiofrequency ablation, and combined resection-radiofrequency ablation. Arch Surg. 2008;143(12):1204–12.
30. Ruers TJM, Joosten JJ, Wiering B, Langenhoff BS, Dekker HM, Wobbes T, et al. Comparison between local ablative therapy and chemotherapy for non-resectable colorectal liver metastases: a prospective study. Ann Surg Oncol. 2007;14(3):1161–9.
31. Veltri A, Sacchetto P, Tosetti I, Pagano E, Fava C, Gandini G. Radiofrequency ablation of colorectal liver metastases: small size favorably predicts technique effectiveness and survival. Cardiovasc Intervent Radiol. 2008;31(5):948–56.
32. Solbiati L, Ahmed M, Cova L, Ierace T, Brioschi M, Goldberg SN. Small liver colorectal metastases treated with percutaneous radiofrequency ablation: local response rate and long-term survival with up to 10-year follow-up. Radiology. 2012;265(3):958–68.
33. Siperstein AE, Berber E, Ballem N, Parikh RT. Survival after radiofrequency ablation of colorectal liver metastases: 10-year experience. Ann Surg. 2007;246(4):559–65–discussion565–7.
34. Kennedy TJ, Cassera MA, Khajanchee YS, Diwan TS, Hammill CW, Hansen PD. Laparoscopic radiofrequency ablation for the management of colorectal liver metastases: 10-year experience. J Surg Oncol. 2013;107(4):324–8.
35. Hammill CW, Billingsley KG, Cassera MA, Wolf RF, Ujiki MB, Hansen PD. Outcome after laparoscopic radiofrequency ablation of technically resectable colorectal liver metastases. Ann Surg Oncol. 2011;18(7):1947–54.
36. Berber E, Tsinberg M, Tellioglu G, Simpfendorfer CH, Siperstein AE. Resection versus laparoscopic radiofrequency thermal ablation of solitary colorectal liver metastasis. J Gastrointest Surg. 2008;12(11):1967–72.

37. Groeschl RT, Pilgrim CHC, Hanna EM, Simo KA, Swan RZ, Sindram D, et al. Microwave ablation for hepatic malignancies: a multiinstitutional analysis. Ann Surg. 2014;259(6):1195–200.
38. Liang P, Dong B, Yu X, Yang Y, Yu D, Su L, et al. Prognostic factors for percutaneous microwave coagulation therapy of hepatic metastases. AJR Am J Roentgenol. 2003;181(5):1319–25.
39. Ogata Y, Uchida S, Hisaka T, Horiuchi H, Mori S, Ishibashi N, et al. Intraoperative thermal ablation therapy for small colorectal metastases to the liver. Hepatogastroenterology. 2008;55(82–83):550–6.
40. Shibata T, Niinobu T, Ogata N, Takami M. Microwave coagulation therapy for multiple hepatic metastases from colorectal carcinoma. Cancer. 2000; 89(2):276–84.
41. Correa-Gallego C, Fong Y, Gonen M, D'Angelica MI, Allen PJ, DeMatteo RP, et al. A Retrospective Comparison of Microwave Ablation vs. Radiofrequency Ablation for Colorectal Cancer Hepatic Metastases. Ann Surg Oncol. 2014;21(13):1–6.
42. Pathak S, Jones R, Tang JMF, Parmar C, Fenwick S, Malik H, et al. Ablative therapies for colorectal liver metastases: a systematic review. Colorectal Dis. 2011;13(9):e252–65.
43. Ackerman NB, Hodgson WB. Vascular patterns of liver tumors and their consequences for different therapeutic approaches. Recent Results Cancer Res. 1986;100:248–55.
44. Iezzi R, Marsico VA, Guerra A, Cerchiaro E, Cassano A, Basso M, et al. Trans-arterial chemoembolization with irinotecan-loaded drug-eluting beads (debiri) and capecitabine in refractory liver prevalent colorectal metastases: a phase ii single-center study. Cardiovasc Intervent Radiol. 2015;38(6):1523–31.
45. Kemeny NE. Regional chemotherapy of colorectal cancer. Eur J Cancer. 1995;31A(7–8):1271–6.
46. Meta-Analysis Group in Cancer, Piedbois P, Buyse M, Kemeny N, Rougier P, Carlson R, et al. Reappraisal of hepatic arterial infusion in the treatment of nonresectable liver metastases from colorectal cancer. J Natl Cancer Inst. 1996;88(5):252–258.
47. Mocellin S, Pilati P, Lise M, Nitti D. Meta-analysis of hepatic arterial infusion for unresectable liver metastases from colorectal cancer: the end of an era? J Clin Oncol. 2007;25(35):5649–54.
48. Kemeny N. The management of resectable and unresectable liver metastases from colorectal cancer. Curr Opin Oncol. 2010;22(4):364–73.
49. Allen-Mersh TG, Glover C, Fordy C, Mathur P, Quinn H. Randomized trial of regional plus systemic fluorinated pyrimidine compared with systemic fluorinated pyrimidine in treatment of colorectal liver metastases. Eur J Surg Oncol. 2000;26(5):468–73.
50. Kemeny N, Jarnagin W, Paty P, Gonen M, Schwartz L, Morse M, et al. Phase I trial of systemic oxaliplatin combination chemotherapy with hepatic arterial infusion in patients with unresectable liver metastases from colorectal cancer. J Clin Oncol. 2005;23(22):4888–96.
51. Kemeny N, Gonen M, Sullivan D, Schwartz L, Benedetti F, Saltz L, et al. Phase I study of hepatic arterial infusion of floxuridine and dexamethasone with systemic irinotecan for unresectable hepatic metastases from colorectal cancer. J Clin Oncol. 2001;19(10):2687–95.
52. Ammori JB, Kemeny NE, Fong Y, Cercek A, Dematteo RP, Allen PJ, et al. Conversion to complete resection and/or ablation using hepatic artery infusional chemotherapy in patients with unresectable liver metastases from colorectal cancer: a decade of experience at a single institution. Ann Surg Oncol. 2013;20(9):1–7.
53. McEntee GP, Nagorney DM, Kvols LK, Moertel CG, Grant CS. Cytoreductive hepatic surgery for neuroendocrine tumors. Surgery. 1990;108(6):1091–6.
54. Sarmiento JM, Heywood G, Rubin J, Ilstrup DM, Nagorney DM, Que FG. Surgical treatment of neuroendocrine metastases to the liver: a plea for resection to increase survival. J Am Coll Surg. 2003;197(1):29–37.
55. Glazer ES, Tseng JF, Al-Refaie W, Solorzano CC, Liu P, Willborn KA, et al. Long-term survival after surgical management of neuroendocrine hepatic metastases. HPB (Oxford). 2010;12(6):427–33.
56. Mayo SC, de Jong MC, Bloomston M, Pulitano C, Clary BM, Reddy SK, et al. Surgery versus intra-arterial therapy for neuroendocrine liver metastasis: a multicenter international analysis. Ann Surg Oncol. 2011;18(13):3657–65.
57. Graff-Baker AN, Sauer DA, Pommier SJ, Pommier RF. Expanded criteria for carcinoid liver debulking: Maintaining survival and increasing the number of eligible patients. Surgery. 2014;156 (6):1369–76–discussion1376–7.
58. Berber E, Flesher N, Siperstein AE. Laparoscopic radiofrequency ablation of neuroendocrine liver metastases. World J Surg. 2002;26(8):985–90.
59. Mazzaglia PJ, Berber E, Milas M, Siperstein AE. Laparoscopic radiofrequency ablation of neuroendocrine liver metastases: a 10-year experience evaluating predictors of survival. Surgery. 2007; 142(1):10–9.
60. Gupta S, Johnson MM, Murthy R, Ahrar K, Wallace MJ, Madoff DC, et al. Hepatic arterial embolization and chemoembolization for the treatment of patients with metastatic neuroendocrine tumors: variables affecting response rates and survival. Cancer. 2005;104(8):1590–602.
61. Ruutiainen AT, Soulen MC, Tuite CM, Clark TWI, Mondschein JI, Stavropoulos SW, et al. Chemoembolization and bland embolization of neuroendocrine tumor metastases to the liver. J Vasc Interv Radiol. 2007;18(7):847–55.

Radiation Therapy for Liver Metastases: Clinical Data

18

Morten Høyer, MD, PhD

18.1 Radiotherapy of Liver Metastases

Cancer confined to the primary tumor site and to the locoregional lymph nodes is usually considered curable when treated with surgery or radiation therapy. Immunotherapy, i.e. for metastatic melanoma may lead to long lasting remission, but in most cases of widespread metastatic cancer in adult patients, the treatment options are limited to cytotoxic therapy with the intention to prolong life for incurable patients. Hellman and Weichselbaum suggested that cancer progression is a multistep process with a state of oligometastases between the stages of purely localized stage and the stage of widely metastatic disease [1]. Patients with oligometastatic cancer may potentially be cured or may obtain long lasting remission if both the primary cancer and the metastases are treated aggressively.

The European Society for Medical Oncology (ESMO) consensus guidelines 2016 for management of metastatic colorectal cancer ranks SBRT as equivalent to radiofrequency ablation (RFA) and other ablation techniques in patients with inoperable oligometastases and recommends that the appropriate ablative tool from the "toolbox" based on patients and cancer-related characteristics should be chosen on the individual patient [2]. However, most MTDs still consider radiation therapy for patients where no other local ablation therapy is possible. The efficacy in terms of improvement of survival of surgery or other local ablative therapies of oligometastases has not been proven and no randomized trial has compared the efficacy of surgery, thermal ablation and radiation therapy. A matched comparative analysis of 60 patients treated for CRC liver metastases with either RFA or robotic SBRT showed the longest disease-free survival in patients treated with SBRT. However, there was a trend for longer overall survival in the RFA group, which did not reach a statistically significant level [3]. Trials comparing different modalities like surgery or RFA and radiation succumb to poor accrual. An example is the RAS study (NCT01233544) randomizing CRC liver metastasis patients between RFA and SBRT that unfortunately was terminated because of poor accrual.

Although there is no proven benefit from local therapy of metastases, there are substantial numbers of cohort studies supporting that selected patients may have a favorable prognosis when the liver metastases are treated locally, even without receiving systemic therapy.

18.2 Radiotherapy with or Without Systemic Antineoplastic Therapy

Delaying the progression of the cancer and thereby allowing a delay of onset or avoidance of systemic antineoplastic therapy is often an

M. Høyer (✉)
Danish Center for Particle Therapy,
Aarhus University Hospital, Palle Juul-Jensen's
Boulevard 99, 8000 Aarhus N, Denmark
e-mail: hoyer@aarhus.rm.dk

J. Meyer and T.E. Schefter (eds.), *Radiation Therapy for Liver Tumors*,
DOI 10.1007/978-3-319-54531-8_18

argument for radiation therapy of metastases. There are no randomized trials evaluating the effect of systemic therapy in addition to radiation therapy for liver metastases, but there is also no evidence for omission of systemic therapy. Two published randomized trials have explored the effect of addition of systemic therapy to the surgical resection of colorectal carcinoma (CRC) liver metastases. They both found that chemotherapy improved the progression-free or disease-free survival [4, 5]. In the largest retrospective cohort study of patients treated with SBRT for metastases both pre- and post-SBRT chemotherapy was related to improved overall survival, thus supporting the effect of addition of systemic therapy [6]. Of 321 oligometastatic patients included in this analysis, 201 patients (66%) were treated for liver metastases.

A local therapy such as SBRT may potentially benefit patients who have more widely disseminated metastatic cancer that does not necessarily meet the definition of oligometastasis. By combining locally ablative therapy with systemic therapy, there is potential to prolong progression-free survival and overall survival. A study of 24 patients with non-small cell lung cancer where erlotinib was combined with consolidative SBRT of the detectable metastatic lesions. This resulted in progression free and overall survival rates of 15 and 20 months, respectively, in patients who had failed platinum-based chemotherapy with no more than six metastases [7]. EGFR mutation was not part of the routine work-up for this study and none of 13 patients in whom the analysis was done had an EGFR mutation. The outcome of this study is better than expected when compared to similar patient cohorts treated with erlotinib alone. Consolidative local ablation combined with systemic antineoplastic therapy for metastatic cancer, as well as local therapy for metastatic oligoprogression where remaining metastatic lesions are controlled by systemic therapy may be important areas for future clinical research.

The addition of chemotherapy to whole-liver radiation therapy (WLRT) has been explored in the past. Most often, fluoro-deoxyuridine or 5-fluorouracil was used to enhance the response rates. No modern chemotherapy regimens have been tested together with WLRT. Chemotherapeutic drugs did not seem to improve the objective or symptomatic responses when comparing to studies where WLRT was given alone [8–11].

18.3 Pattern of Practice in Radiation Therapy for Liver Metastases

With steadily improving systemic therapies, we expect to see an increasing number of patients with oligometastases to the liver [12]. A substantial proportion may be eligible for radiation therapy. A large survey on the use of SBRT targeting individual radiation oncologists had 1007 responses [13]. It showed a marked increase in the use of SBRT for metastases. Sixty-one percent used SBRT for treatment of patients with 1–3 metastases; 75% for treatment of metastases to the liver. In a survey targeting centers with an active program on radiation therapy for metastases, 69 of 80 responders (86%) treated metastases to the liver with radiation therapy [14]. Fifty had an active liver SBRT program. Fewer used WLRT for palliation of liver metastasis related symptoms. Thirty-two responders (40%) treated more than five patients with WLRT per year.

18.4 3-D Conformal X-Ray Therapy

The Ann Arbor group treated 22 patients with CRC liver metastases with conventional 3-D conformal radiation therapy (CRT) and concomitant intra-arterial hepatic chemotherapy (fluoro-deoxyuridine). With total doses of 48–73 Gy in 1.5–1.65 Gy given twice a day, the response rate was 50%. However, only 25% of the patients were without hepatic progression within 1 year [15]. In a risk-adapted NTCP-based dose-escalation study from the Ann Arbor on CRT of primary and secondary liver cancer using a median total dose of 60.75 Gy (range, 40–90 Gy), 1.5 Gy twice daily and concomitant fluoro-deoxyuridine, the response rate for CRC patients

was 60% [16, 17]. The patients included in this study had a large tumor burden with median tumor size of 10 × 10 × 8 cm. The median survival time for these patients was 17 months and radiation dose above 60.75 Gy was associated with favorable survival for the entire study group.

In general, response rates after CRT are high, but local control rates are lower than what is seen after the high-dose-per-fraction and high total dose radiation therapy associated with SBRT. However, CRT studies are not directly comparable to SBRT studies, as patient selection is different, generally including larger metastases in CRT cohorts. CRT, with the possibility of integration of IGRT and IMRT, is most useful in selected cases where SBRT is not possible, e.g., when the target is close to the bowel.

18.5 Stereotactic Body Radiation Therapy

SBRT was developed on the principles of stereotactic brain radiosurgery, and initial attempts were performed using a fixed body frame for patient immobilization and with image guidance primarily based on simple mega-voltage portal imaging to deliver 1–6 large fractions of radiation to a malignant tumor outside the brain. The first paper on clinical results of SBRT was published by a research group from the Karolinska Institute, Stockholm in 1995 [18] and since then the technique has evolved dramatically and it is now one of the important cornerstones in modern radiation oncology.

The early publication from Stockholm reported a local control rate of treated tumors that was much higher than expected, but a large number of publications confirm the high probability of local control after hypofractionated radiotherapy with high biological equivalent doses. Table 18.1 gives the results of the prospective and the largest retrospective cohort studies in SBRT for liver metastases [6, 19–31]. Most reports of local control rates are in the range 80–100%. A few studies report lower local control rates, i.e., the study by de Vin with a local control of 33%. This study included patients with a broad range of metastasis sites with liver metastases accounting for only 25% of the cases.

A number of studies have reported a dose-response effect with higher local control probability with the use of high biological equivalent doses [6, 21, 27, 28]. In a pooled analysis from three North-American centers, the actuarial local control rates were 86 and 42% at 1-year with doses of above and below BED_{10Gy} of 75 Gy, respectively [27]. In the study from Denmark, the overall 2 years local recurrence rate was 13% and the rate was considerably reduced with BED_{10Gy} over 100 Gy (hazard ratio 0.34) [6].

It has been claimed that liver metastases may be radio-resistant compared to metastases at other sites. The control rate of metastases is often lower in liver compared to lung, but it is unclear whether this relates to differences in radiosensitivity or to differences in radiation techniques. Lower control rates for CRC metastases were found is some studies [27, 32], but not in others [6, 21]. In the Danish study, the local relapse probability for metastases was higher in the liver compared to other sites, possibly explained by differences in radiosensitivity or by poorer imaging for target contouring of metastases to the liver compared to other sites [6].

Currently, there is no randomized phase III data to support the efficacy of SBRT for liver metastases, although a British randomized phase III trial (CORE) is expected to start recruiting patents with breast cancer oligometastases to conventional (systemic) therapy versus the same therapy plus SBRT for the detectable metastases (NCT02759783). The survival of patients in nonrandomized SBRT-studies depends in part on how well they are selected. However, studies of large cohorts of patients with metastatic cancer treated with SBRT have reported favorable survival rates even in negatively selected patients who were not eligible for surgery or radiofrequency ablation (Table 18.1).

Milano et al. found that patients with metastatic breast cancer to the liver and other sites of the body had a favorable survival compared to patients with metastatic cancer of other origin [33]. Fode et al. found a median overall survival of 6.1 year for breast cancer patients [6]. Due to

Table 18.1 Results from prospective and large retrospective studies of SBRT for liver metastases

Author; year	Design	Pts with liver metastases	Frx × dose	m-FU mts	Local control 2-years (%)	Survival 1-, 2-years (%)	Severe morbidity
Schefter 2005 [19]	Phase I	18	3 × 12–20 Gy	NR	NR	NR	None
Katz 2007 [20]	Retrospect	69	5 × 10 Gy	14.5	57	68, 24	None
McCammon 2009 [21]	Retrospect	81/141[a]	3 × 12 Gy 3 × 16 Gy 3 × 20 Gy	8.2	89 59 8	NR	8 grade ≥3: pneumonitis, dermatitis, soft-tissue inflammation/fibrosis, vertebral fracture
Rusthoven 2009 [23]	Phase I/II	47	3 × 12–20 Gy	16	92	77, 30	1 grade 3: soft-tissue necrosis
Lee 2009 [24]	Phase I	68	6 × 4.6–10 Gy	11	71 (1-yr)	79, 41 (3 yr)	7 grade ≥3: thrombocytes[b], hepatic[b], gastritis, lethargy, nausea
Goodman 2010 [26]	Phase I	19	1 × 18–30 Gy	17	75	62, 49	2 grade ≥3: duodenal ulceration, bowel obstruction
Rule 2010 [25]	Phase I	27	3 × 10 Gy 5 × 10 Gy 5 × 12 Gy	20	56 89 100	90, 50 78, 67 75, 56	1 grade 3: hepatic[b]
Van der Pool 2010 [22]	Retrospect	20	3 × 10–12.5 Gy	26	74	100, 74	3 grade 3: hepatic[b] and lethargy
Chang 2011 [27]	Retrospect	65	2–3 × 20 Gy	55	38 (2–yr)	77, 45	Acute: 2 grade 3 hepatic[b] Late: 4 grade 3 hepatic[a] and gastritis
Comito 2014 [28]	Phase II	42	4 × 12 Gy – 3 × 25 Gy	24	80	80, 65	None
De Vin 2014 [29]	Retrospect	77/309[a]	10 × 4–5 Gy	12	33	32 (3-yr)	NR
Fode 2015 [6]	Retrospect	225/321[a]	3 × 15–22.5	29	LR: 13	80, 58	Acute: 11 grade ≥3: hepatic[b], nausea pain, gastritis, skin, deterioration of performance status Late: 3 grade ≥3: gastritis and skin
Scorsetti 2015 [30]	Phase II	42	3 × 25 Gy	24	91	81, 65	No grade ≥3
Meyer 2016 [31]	Phase I	14	1 × 35–40 Gy	30	100	85, 78	No grade ≥3

m-FU median follow-up; *NR* not reported; *LR* local recurrence in competitive risk analysis
[a]Mixed patient material included other than liver metastasis patients
[b]Biochemical tests

the low number of patients, the survival of breast cancer patients in the Fode study was not statistically different from other patients' survival. Katz et al. did not find the histological type influenced survival of the patients [20]. It seems obvious that some cancer types have a more indolent and less aggressive clinical appearance and for some cancer types there are several lines of systemic antineoplastic therapies that may affect the survival. Lack of differences in survival between tumor types may be a result of the patient selection.

Because of the limited knowledge on prognostic factors related to SBRT of patients with liver metastases, there is no consensus on the criteria to select patients. There is therefore considerable heterogeneity in patient and cancer characteristics among the published studies. Only few studies have patients numbers that are sufficient for assessment of prognostic factors. Cumulative GTV smaller than 3 cm was related to long overall survival in a study of patients with lung and liver metastases [28]. A large retrospective cohort study of patients primarily with liver metastases, but also some with lung and other metastatic sites, found that WHO performance status 0–1, solitary metastasis, size of largest metastasis under 3 cm, metachronous metastasis and pre-SBRT chemotherapy were related to favorable survival in a multivariate analysis [6].

SBRT of liver tumors is generally tolerated well. However, the esophagus, the stomach, the duodenum, and the large bowel should be considered in the selection of patients and in the treatment planning process because of their limited tolerance to radiation and the risk of severe adverse effects when they are exposed to large radiation doses. The liver tolerates large doses to relatively large volumes as long as a sufficient volume of liver is spared. Gastritis, gastric- or intestinal ulceration, chronic skin reaction, rib fracture, and hepatic failure seldom occur as late effects after SBRT for liver metastases [6].

There is growing use of SBRT for treatment of liver metastases. The results of prospective phase I/II trials and retrospective cohort studies are encouraging, but we are still missing high level evidence to prove its efficacy.

18.6 Particle Therapy with Protons and Carbon Ions

Due to their physical properties, protons and heavier ions have considerable potential in radiation therapy for primary and secondary liver tumors. The sparing is most prominent in volumes of normal tissue receiving the low-to-intermediate radiation dose. Because of the relatively low radiation tolerance of the liver, liver cancer patients are obvious candidates for particle therapy, especially if issues related to interplay effects and immature image guidance can be managed. A treatment planning study compared intensity modulated proton therapy (IMPT) and photons based intensity modulated radiation therapy (IMRT) in stereotactic body radiation therapy (SBRT) for liver tumors [34]. The study used a dose escalation risk-adapted prescription policy where the highest possible tumor dose was applied, provided that dose volume constraints to organs at risk were met. In 10 patients tested, there was sparing of normal liver tissue with protons compared to photons. With the highest dose level, the median V_{15Gy} was reduced by 32% with use of IMPT. Nine of 10 cases could be treated at the highest dose level using IMPT whereas only two cases met this constraint at the highest dose level and six at the lowest dose level with use of IMRT. Other treatment planning studies report similar positive findings [35].

There are a number of published studies on proton and carbon-ion therapy of hepatocellular carcinoma (see Chap. 14). The particle therapy experience in treatment of metastases is limited to few case-reports and it does not allow for conclusions on the efficacy in treatment of oligometastases. Fortunately, a dose escalation study giving 3 × 12–20 Gy by use of passive scattering protons is actively recruiting patients with liver metastases at Loma Linda University (NCT01697371).

18.7 Radioembolization

Radioembolization or selective internal radiation therapy (SIRT) involves intra-hepatic administration of microspheres containing Yttrium-90 (^{90}Y). The primary aims of radioembolization are to delay cancer progression and to improve survival. Studies of radioembolization without systemic antineoplastic therapy showed response rates of 35–75% in patients with CRC liver metastases (Table 18.2). When combined with systemic chemotherapy, the overall response rates increased to 76–91% [36, 37]. Two small randomized trials compared the combination of radioembolization and chemotherapy to chemotherapy alone in patients with CRC liver metastases [38, 39]. They both found improved response rates and progression-free survival and one study found improved survival in the SIRT arm. The large SIRFLOX study randomized 530 patients with mCRC liver-predominant disease referred for first-line chemotherapy between FOLFOX (±bevacizumab) chemotherapy and SIRT versus FOLFOX alone [40]. In this well-powered study the two arms had similar progression-free survival, but SIRT considerably delayed the progression in the liver by almost 8 months. Results of a similar multicenter study, the randomized FOXFIRE study, are also awaited [41].

In cohort studies of neuroendocrine tumors, radioembolization resulted in favorable response rates of 63–90% [42, 43]. Both of these studies report favorable median survival for this patient group.

Relatively common adverse effects are flu-like symptoms, moderate pain, gastro-intestinal symptoms, and neutropenia, whereas complications such as radiation induced liver disease (RILD), radiation cholangitis, vascular injury, infection/liver abscess, radiation pneumonitis, and gastric perforation occur less frequently. Grade III–IV toxicities in terms of intestinal ulceration, neutropenia, and transient hepatotoxicity were observed in a phase I study of combined radioembolization and FOLFOX chemotherapy in patients with CRC liver metastases [44].

18.8 Interstitial Brachytherapy for Liver Metastases

CT-guided interstitial brachytherapy with insertion of needles and use of afterloading technique with Iridium-192 has been used in highly specialized centers as a salvage of patients with liver tumors who are unsuitable for RFA and SBRT. Catheters are inserted to achieve target doses of 20 Gy or higher. There are reports of cohort studies describing successful control of even very large liver tumors over 10 cm in diameter and with doses exceeding 20 Gy the local control rates most often exceeds 70–90% [45].

The 2-year local control rate was 81% in a retrospective cohort study of 80 patients with 179 inoperable colorectal liver metastases treated with interstitial brachytherapy [46]. Local progression was significantly related to the size of the metastasis with control rates of 87 and 59% for lesions smaller than or larger than 40 mm, respectively. The survival rate at 3 years after treatment for liver metastases was 41%. In a phase II study of 41 patients with metastatic breast cancer, the local control was 87% and overall survival 60% 2 years after interstitial brachytherapy for liver metastases [47].

Metastases in the hilum of the liver has been considered a relative contraindication for brachytherapy, but a recent publication describes the successful ablation of metastases with a distance of less than 5 mm to the common bile duct or hepatic bifurcation with only 4 of 34 (12%) lesions recurring after CT-guided brachytherapy [48].

A matched pair-analysis of patients (18 patients with 36 liver metastases) who had received interstitial laser therapy or brachytherapy for metastases smaller than 50 mm in diameter concluded that brachytherapy was associated to a higher local control probability compared to laser therapy [49].

With the purpose of improving local control in the liver, interesting approaches include the combination of brachytherapy with either hepatic artery infusion of chemotherapy or laser induced thermotherapy. The combination of regional hepatic artery chemotherapy and brachytherapy

Table 18.2 Results from randomized and large cohort studies of radioembolization (SIRT) for liver metastases

Author; year	Design	Treatment	Primary cancer	Number	m-FU (mts.)	Response rate [CR+PR] (%)	Survival 1-, 2-years (%)	Severe morbidity
Stubbs 2006 [36]	Cohort	SIRT	CRC	100	11	75	48, 18	9 severe, 2 deaths
Kennedy 2006 [37]	Multicenter cohort	SIRT	CRC	208	13	35	45% at 1 year in responders	11% grade $\geq$ 3 1 death (pulm. embolus)
Sharma 2007 [44]	Phase I	Chemo+SIRT	CRC	20	NR	90	NR	5 grade $\geq$ 3
Gray 2001 [38]	Randomized	HAC+SIRT HAC	CRC	74	42	44 18 $P = 0.03$	72, 39 68, 29 NS	23 grade $\geq$ 3 23 grade $\geq$ 3
van Hazel 2004 [39]	Randomized phase II	Chemo+SIRT Chemo	CRC	21	NR	91 0 $P < 0.001$	70, 52 50, 10 $P = 0.02$	13 grade $\geq$ 3 5 grade $\geq$ 3
van Hazel 2016 [40]	Randomized phase III	Chemo+SIRT Chemo	CRC	530	NR	76 68 NS	NR (delayed progression in liver)	83% grade $\geq$ 3 73% grade $\geq$ 3
Rhee 2008 [42]	Multicenter cohort	SIRT	NET	42	NR	54 (Theraspheres)	70, 48 (Theraspheres)	3 grade 3 (serologic)
Kennedy 2008 [43]	Multicenter cohort	SIRT	NET	148	42	63	85, 75	33% grade $\geq$ 3

m-FU median follow-up; *CR* complete remission; *PR* partial regression; *NR* not reported; *NS* no significant difference
NET neuroendocrine tumor; *HAC* hepatic artery chemotherapy

in CRC liver metastases tested in a phase II study resulted in local control and overall survival rates that are similar to those observed after brachytherapy alone and the sequence between the two treatments did not influence the results [50]. The combination of laser therapy and brachytherapy in a phase I–II study resulted in a local control rate comparable to the rate observed after brachytherapy alone. However, the two groups of patients who received or did not receive laser therapy were not identical [51].

Major complications are rare, but liver failure, ulceration of the stomach and duodenum, bleeding in the liver or thoracic wall have been observed after 5% of the procedures and pleural effusion and risible pain and nausea may relatively frequently occur after brachytherapy of the liver [47].

Brachytherapy is a highly efficient ablation therapy for liver metastases. Local control rates are in the range of 70–90%, but severe complications may occur and brachytherapy should be limited to experienced centers.

18.9 Low-Dose Whole-Liver Radiation Therapy

Low-dose whole-liver radiation therapy (WLRT) may be used for palliation for patients with incurable primary or secondary liver cancer with the primary focus on reducing pain and other cancer-related symptoms (Fig. 18.1). Pain relief ranges from 55 to 80% in studies using WLRT alone [8, 52–56]. The relatively low radiation tolerance of the liver is the main reason for the relatively sparse use of WLRT. However, WLRT seems to be safe with less than 5% risk of radiation induced liver disease (RILD) as long as total ED_{2Gy} to the whole liver is kept below 33 Gy and in most of cases RILD resolves within 1–2 months [57]. Early on, the focus of WLRT was on improvement of disease control and overall survival with intensifying radiation dose and combining with systemic therapy. However, most patients treated with WLRT are end-stage cancer patients with short survival expectation and no other effective treatment options available. The relevant endpoints to report nowadays are therefore symptom relief and quality of life.

The Radiation Therapy Oncology Group (RTOG) pilot study used dose-fractionation schedules ranging from 21 to 30 Gy in 7–19 fractions to treat 109 patients [53]. Response in terms of partial or complete symptom control was observed for abdominal pain, nausea and vomiting, ascites, anorexia, abdominal distension, jaundice, and night sweats/fever, with complete response rates for individual symptoms up to 34% and improvement in performance status in 25% of the patients. Leibel et al. found an 80% response rate for pain (complete in 54%) and improved performance status in 28% [8]. Pain relief occurred quickly and had a median duration of 13 weeks.

Systemic or regional chemotherapy with fluoro-deoxyuridine or 5-fluorouracil used in addition to WLRT did not improve the objective or symptomatic responses when tested in randomized clinical trials [8–11].

Most experience on WLRT is based on normo- or hyperfractionation, but a prospective Australian study used a hypofractionated palliative schedule of 2 × 5 Gy in two consecutive days in a cohort of 28 patients [52]. At 2 months after treatment, 53–66% of individual symptoms present at base-line improved. Pain relief was observed in 65% at 2 weeks and 53% of the patients surviving at 10 weeks still recorded a pain response. A newly published Canadian phase II study using a single fraction WLRT schedule of 8 Gy to the tumor-bearing part (majority) of the liver or the whole liver was performed on 41 patients of whom 20 had metastases and 21 had primary liver cancer [57]. The patients were also examined with the EORTC QLQ-C30 and FACT-hep quality of life and symptom scores. On average, 48% experienced improvement in cancer-related symptoms at 1-month post treatment. Pain was the most frequent base-line symptom and it improved in 26% of the patients, insomnia improved in 50% and nausea and vomiting in 26%. In 26% of the patients, overall global health also improved.

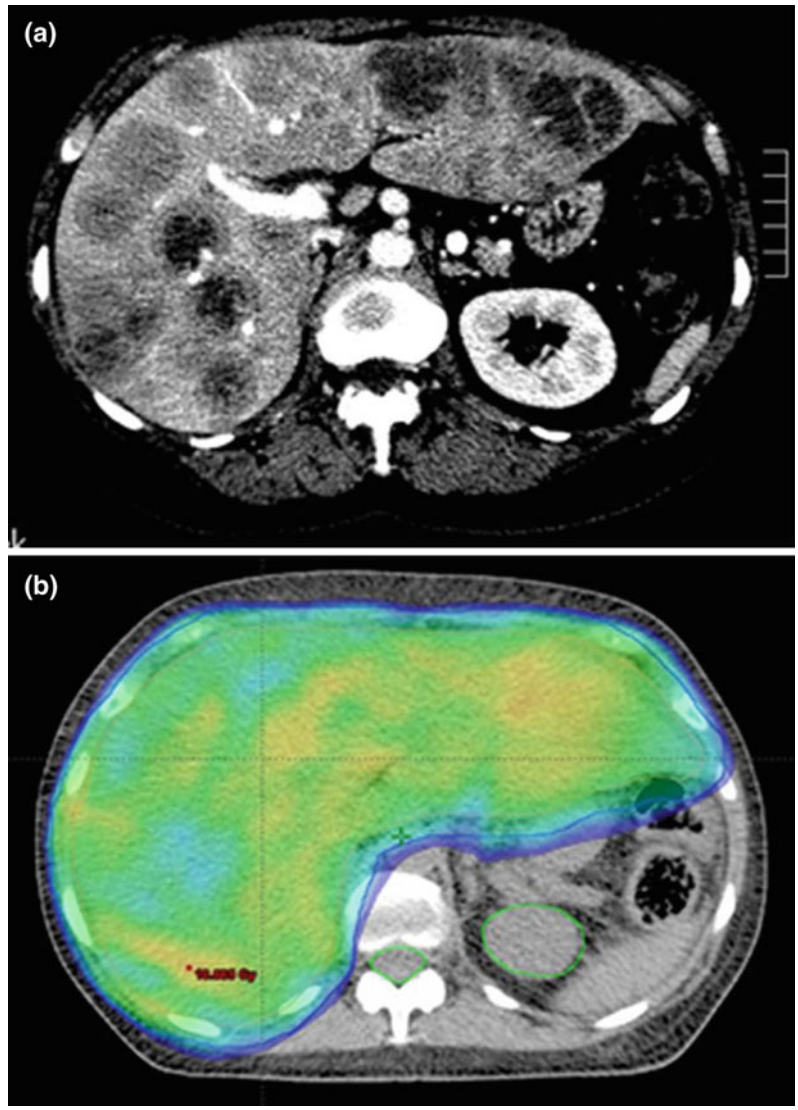

Fig. 18.1 Multiple breast cancer metastasis to the liver (**a**) and a treatment plan for 2 × 5 Gy whole-liver radiation therapy for palliation (**b**)

With an increasing number of systemic therapies available for patients with metastatic cancer, the need for palliative WLRT is declining. However, we consider WLRT as an option for patients suffering with symptoms from liver metastases and it is considerably underused. Clinical studies have shown considerable palliative effect after low-dose palliative WLRT, with pain relief in 26–80% of the patients and improvement of quality of life in a proportion of the patients.

References

1. Hellman S, Weichselbaum RR. Oligometastases. J Clin Oncol. 1995;13(1):8–10.
2. van Cutsem E, Cervantes A, Adam R, van Krieken JH, Aderka D et al. ESMO consensus guidelines for the management of patients with metastatic colorectal cancer. Ann Oncol Epub. 2016 Jul 5.
3. Stintzing S, Grothe A, Hendrich S, Hoffmann RT, Heinemann V, Rentsch M, et al. Percutaneous radiofrequency ablation (RFA) or robotic

radiosurgery (RRS) for salvage treatment of colorectal liver metastases. Acta Oncol. 2013;52(5):971–7.
4. Portier G, Elias D, Bouche O, Rougier P, Bosset JF, Saric J, et al. Multicenter randomized trial of adjuvant fluorouracil and folinic acid compared with surgery alone after resection of colorectal liver metastases: FFCD ACHBTH AURC 9002 trial. J Clin Oncol. 2006;24(31):4976–82.
5. Nordlinger B, Sorbye H, Glimelius B, Poston GJ, Schlag PM, Rougier P, et al. Perioperative FOLFOX4 chemotherapy and surgery versus surgery alone for resectable liver metastases from colorectal cancer (EORTC 40983): long-term results of a randomised, controlled, phase 3 trial. Lancet Oncol. 2013;14(12):1208–15.
6. Fode MM, Hoyer M. Survival and prognostic factors in 321 patients treated with stereotactic body radiotherapy for oligo-metastases. Radiother Oncol. 2015;114(2):155–60.
7. Iyengar P, Kavanagh BD, Wardak Z, Smith I, Ahn C, Gerber DE, et al. Phase II trial of stereotactic body radiation therapy combined with erlotinib for patients with limited but progressive metastatic non-small-cell lung cancer. J Clin Oncol. 2014;32(34):3824–30.
8. Leibel SA, Pajak TF, Massullo V, Order SE, Komaki RU, Chang CH, et al. A comparison of misonidazole sensitized radiation therapy to radiation therapy alone for the palliation of hepatic metastases: results of a radiation therapy oncology group randomized prospective trial. Int J Radiat Oncol Biol Phys. 1987;13(7):1057–64.
9. Webber BM, Soderberg CH Jr, Leone LA, Rege VB, Glicksman AS. A combined treatment approach to management of hepatic metastasis. Cancer. 1978;42(3):1087–95.
10. Rotman M, Kuruvilla AM, Choi K, Bhutiani I, Aziz H, Rosenthal J, et al. Response of colo-rectal hepatic metastases to concomitant radiotherapy and intravenous infusion 5 fluorouracil. Int J Radiat Oncol Biol Phys. 1986;12(12):2179–87.
11. Lawrence TS, Dworzanin LM, Walker-Andrews SC, Andrews JC, Ten Haken RK, Wollner IS, et al. Treatment of cancers involving the liver and porta hepatis with external beam irradiation and intraarterial hepatic fluorodeoxyuridine. Int J Radiat Oncol Biol Phys. 1991;20(3):555–61.
12. Hoyer M, Swaminath A, Bydder S, Lock M, Mendez RA, Kavanagh B, et al. Radiotherapy for liver metastases: a review of evidence. Int J Radiat Oncol Biol Phys. 2012;82(3):1047–57.
13. Pan H, Simpson DR, Mell LK, Mundt AJ, Lawson JD. A survey of stereotactic body radiotherapy use in the United States. Cancer. 2011;117(19):4566–72.
14. Lock MI, Hoyer M, Bydder SA, Okunieff P, Hahn CA, Vichare A, et al. An international survey on liver metastases radiotherapy. Acta Oncol. 2012;51(5):568–74.
15. Robertson JM, Lawrence TS, Walker S, Kessler ML, Andrews JC, Ensminger WD. The treatment of colorectal liver metastases with conformal radiation therapy and regional chemotherapy. Int J Radiat Oncol Biol Phys. 1995 May 15;32(2):445–50.
16. Dawson LA, McGinn CJ, Normolle D, Ten Haken RK, Walker S, Ensminger W, et al. Escalated focal liver radiation and concurrent hepatic artery fluorodeoxyuridine for unresectable intrahepatic malignancies. J Clin Oncol. 2000;18(11):2210–8.
17. Ben-Josef E, Normolle D, Ensminger WD, Walker S, Tatro D, Ten Haken RK, et al. Phase II trial of high-dose conformal radiation therapy with concurrent hepatic artery floxuridine for unresectable intrahepatic malignancies. J Clin Oncol. 2005;23(34):8739–47.
18. Blomgren H, Lax I, Naslund I, Svanstrom R. Stereotactic high dose fraction radiation therapy of extracranial tumors using an accelerator. Clinical experience of the first thirty-one patients. Acta Oncol. 1995;34(6):861–70.
19. Schefter TE, Kavanagh BD, Timmerman RD, Cardenes HR, Baron A, Gaspar LE. A phase I trial of stereotactic body radiation therapy (SBRT) for liver metastases. Int J Radiat Oncol Biol Phys. 2005;62(5):1371–8.
20. Katz AW, Carey-Sampson M, Muhs AG, Milano MT, Schell MC, Okunieff P. Hypofractionated stereotactic body radiation therapy (SBRT) for limited hepatic metastases. Int J Radiat Oncol Biol Phys. 2007;67(3):793–8.
21. McCammon R, Schefter TE, Gaspar LE, Zaemisch R, Gravdahl D, Kavanagh B. Observation of a dose-control relationship for lung and liver tumors after stereotactic body radiation therapy. Int J Radiat Oncol Biol Phys. 2009;73(1):112–8.
22. van der Pool AE, Mendez RA, Wunderink W, Heijmen BJ, Levendag PC, Verhoef C, et al. Stereotactic body radiation therapy for colorectal liver metastases. Br J Surg. 2010;97(3):377–82.
23. Rusthoven KE, Kavanagh BD, Burri SH, Chen C, Cardenes H, Chidel MA, et al. Multi-institutional phase I/II trial of stereotactic body radiation therapy for lung metastases. J Clin Oncol. 2009;27(10):1579–84.
24. Lee MT, Kim JJ, Dinniwell R, Brierley J, Lockwood G, Wong R, et al. Phase I study of individualized stereotactic body radiotherapy of liver metastases. J Clin Oncol. 2009;27(10):1585–91.
25. Rule W, Timmerman R, Tong L, Abdulrahman R, Meyer J, Boike T, et al. Phase I dose-escalation study of stereotactic body radiotherapy in patients with hepatic metastases. Ann Surg Oncol. 2011;18(4):1081–7.
26. Goodman KA, Wiegner EA, Maturen KE, Zhang Z, Mo Q, Yang G, et al. Dose-escalation study of single-fraction stereotactic body radiotherapy for liver malignancies. Int J Radiat Oncol Biol Phys. 2010;78(2):486–93.

27. Chang DT, Swaminath A, Kozak M, Weintraub J, Koong AC, Kim J, et al. Stereotactic body radiotherapy for colorectal liver metastases: a pooled analysis. Cancer. 2011;117(17):4060–9.
28. Comito T, Cozzi L, Clerici E, Campisi MC, Liardo RL, Navarria P, et al. Stereotactic Ablative Radiotherapy (SABR) in inoperable oligometastatic disease from colorectal cancer: a safe and effective approach. BMC Cancer. 2014;14:619.
29. de Vin T, Engels B, Gevaert T, Storme G, De RM. Stereotactic radiotherapy for oligometastatic cancer: a prognostic model for survival. Ann Oncol. 2014;25 (2):467–71.
30. Scorsetti M, Comito T, Tozzi A, Navarria P, Fogliata A, Clerici E, et al. Final results of a phase II trial for stereotactic body radiation therapy for patients with inoperable liver metastases from colorectal cancer. J Cancer Res Clin Oncol. 2015;141:543–53.
31. Meyer J, Foster RD, Lev-Cohain N, Yokoo T, Dong Y, Schwarz RE, et al. A phase I dose-escalation trial of single-fraction stereotactic radiation therapy for liver metastases. Ann Surg Oncol. 2016;23:218–24.
32. Binkley MS, Trakul N, Jacobs LR, von ER, Le QT, Maxim PG, et al. Colorectal Histology Is Associated with an increased risk of local failure in lung metastases treated with stereotactic ablative radiation therapy. Int J Radiat Oncol Biol Phys. 2015 Aug 1; 92(5):1044–52.
33. Milano MT, Katz AW, Zhang H, Okunieff P. Oligometastases treated with stereotactic body radiotherapy: long-term follow-up of prospective study. Int J Radiat Oncol Biol Phys. 2012;83 (3):878–86.
34. Petersen JB, Lassen Y, Hansen AT, Muren LP, Grau C, Hoyer M. Normal liver tissue sparing by intensity-modulated proton stereotactic body radiotherapy for solitary liver tumours. Acta Oncol. 2011;50(6):823–8.
35. Gandhi SJ, Liang X, Ding X, Zhu TC, Ben-Josef E, Plastaras JP, et al. Clinical decision tool for optimal delivery of liver stereotactic body radiation therapy: photons versus protons. Pract Radiat Oncol. 2015;5 (4):209–18.
36. Stubbs RS, O'Brien I, Correia MM. Selective internal radiation therapy with 90Y microspheres for colorectal liver metastases: single-centre experience with 100 patients. ANZ J Surg. 2006; 76(8):696–703.
37. Kennedy AS, Coldwell D, Nutting C, Murthy R, Wertman DE Jr, Loehr SP, et al. Resin 90Y-microsphere brachytherapy for unresectable colorectal liver metastases: modern USA experience. Int J Radiat Oncol Biol Phys. 2006;65(2):412–25.
38. Gray B, Van HG, Hope M, Burton M, Moroz P, Anderson J, et al. Randomised trial of SIR-Spheres plus chemotherapy vs. chemotherapy alone for treating patients with liver metastases from primary large bowel cancer. Ann Oncol. 2001;12(12): 1711–20.
39. van Hazel G, Blackwell A, Anderson J, Price D, Moroz P, Bower G, et al. Randomised phase 2 trial of SIR-Spheres plus fluorouracil/leucovorin chemotherapy versus fluorouracil/leucovorin chemotherapy alone in advanced colorectal cancer. J Surg Oncol. 2004;88(2):78–85.
40. van Hazel GA, Heinemann V, Sharma NK, Findlay MP, Ricke J, Peeters M, et al. SIRFLOX: Randomized phase III trial comparing first-line mFOLFOX6 (plus or minus bevacizumab) versus mFOLFOX6 (plus or minus bevacizumab) plus selective internal radiation therapy in patients with metastatic colorectal cancer. J Clin Oncol. 2016;34(15):1723–31.
41. Dutton SJ, Kenealy N, Love SB, Wasan HS, Sharma RA. FOXFIRE protocol: an open-label, randomised, phase III trial of 5-fluorouracil, oxaliplatin and folinic acid (OxMdG) with or without interventional Selective Internal Radiation Therapy (SIRT) as first-line treatment for patients with unresectable liver-only or liver-dominant metastatic colorectal cancer. BMC Cancer. 2014;14:497.
42. Rhee TK, Lewandowski RJ, Liu DM, Mulcahy MF, Takahashi G, Hansen PD, et al. 90Y Radioembolization for metastatic neuroendocrine liver tumors: preliminary results from a multi-institutional experience. Ann Surg. 2008;247(6):1029–35.
43. Kennedy AS, Dezarn WA, McNeillie P, Coldwell D, Nutting C, Carter D, et al. Radioembolization for unresectable neuroendocrine hepatic metastases using resin 90Y-microspheres: early results in 148 patients. Am J Clin Oncol. 2008;31(3):271–9.
44. Sharma RA, van Hazel GA, Morgan B, Berry DP, Blanshard K, Price D, et al. Radioembolization of liver metastases from colorectal cancer using yttrium-90 microspheres with concomitant systemic oxaliplatin, fluorouracil, and leucovorin chemotherapy. J Clin Oncol. 2007;25(9):1099–106.
45. Ricke J, Wust P. Computed tomography-guided brachytherapy for liver cancer. Semin Radiat Oncol. 2011;21(4):287–93.
46. Collettini F, Lutter A, Schnapauff D, Hildebrandt B, Puhl G, Denecke T, et al. Unresectable colorectal liver metastases: percutaneous ablation using CT-guided high-dose-rate brachytherapy (CT-HDBRT). Rofo. 2014;186(6):606–12.
47. Wieners G, Mohnike K, Peters N, Bischoff J, Kleine-Tebbe A, Seidensticker R, et al. Treatment of hepatic metastases of breast cancer with CT-guided interstitial brachytherapy - a phase II-study. Radiother Oncol. 2011;100(2):314–9.
48. Collettini F, Singh A, Schnapauff D, Powerski MJ, Denecke T, Wust P, et al. Computed-tomography-guided high-dose-rate brachytherapy (CT-HDRBT) ablation of metastases adjacent to the liver hilum. Eur J Radiol. 2013;82(10):e509–14.
49. Pech M, Wieners G, Kryza R, Dudeck O, Seidensticker M, Mohnike K, et al. CT-guided brachytherapy (CTGB) versus interstitial laser ablation (ILT) of colorectal liver metastases: an intraindividual matched-pair analysis. Strahlenther Onkol. 2008;184(6):302–6.

50. Wieners G, Pech M, Hildebrandt B, Peters N, Nicolaou A, Mohnike K, et al. Phase II feasibility study on the combination of two different regional treatment approaches in patients with colorectal "liver-only" metastases: hepatic interstitial brachytherapy plus regional chemotherapy. Cardiovasc Interv Radiol. 2009;32(5):937–45.
51. Ricke J, Wust P, Stohlmann A, Beck A, Cho CH, Pech M, et al. CT-guided interstitial brachytherapy of liver malignancies alone or in combination with thermal ablation: phase I-II results of a novel technique. Int J Radiat Oncol Biol Phys. 2004; 58(5):1496–505.
52. Bydder S, Spry NA, Christie DR, Roos D, Burmeister BH, Krawitz H, et al. A prospective trial of short-fractionation radiotherapy for the palliation of liver metastases. Australas Radiol. 2003;47(3):284–8.
53. Borgelt BB, Gelber R, Brady LW, Griffin T, Hendrickson FR. The palliation of hepatic metastases: results of the radiation therapy oncology group pilot study. Int J Radiat Oncol Biol Phys. 1981;7(5):587–91.
54. Sherman DM, Weichselbaum R, Order SE, Cloud L, Trey C, Piro AJ. Palliation of hepatic metastasis. Cancer. 1978;41(5):2013–7.
55. Russell AH, Clyde C, Wasserman TH, Turner SS, Rotman M. Accelerated hyperfractionated hepatic irradiation in the management of patients with liver metastases: results of the RTOG dose escalating protocol. Int J Radiat Oncol Biol Phys. 1993;27 (1):117–23.
56. Ben-Josef E, Lawrence TS. Radiotherapy for unresectable hepatic malignancies. Semin Radiat Oncol. 2005;15(4):273–8.
57. Soliman H, Ringash J, Jiang H, Singh K, Kim J, Dinniwell R, et al. Phase II trial of palliative radiotherapy for hepatocellular carcinoma and liver metastases. J Clin Oncol. 2013;31(31):3980–6.

Part VII

Perspectives on Multidisciplinary Management

Multidisciplinary Model for Liver Tumors

19

Cheryl Meguid, DNP and Tracey E. Schefter, MD

19.1 Introduction

Liver malignancy is the epitome of complexity and thus represents the sine qua non for multidisciplinary care. Optimal outcomes demand the coordinated involvement of numerous specialties including interventional radiology, hepatology, liver transplant surgery, surgical oncology, medical oncology, and radiation oncology as well as supportive services. Multidisciplinary management is becoming more widely utilized in many healthcare centers today, as the focus of health care is developing into a more patient-centered approach, in which a patient's treatment plan is customized for them. The patient-centered approach is recognized as a quality measure in health care because of the proven benefit in terms of communication and coordination of care. Most importantly, the patient experience is improved, but there are many downstream effects, including better relationships among providers and improved adherence to treatment plans [1–5].

The multidisciplinary concept for patients with cancer has been established for decades, where historically, the primary focus has been discussion of a patient's diagnosis and treatment to date, with the goal of establishing a unified plan from a panel of specialists. This approach, however, is often presented in an ad hoc tumor board-type setting in which the onus is on the individual specialty providers to select cases for discussion and the information may or may not be relayed to the patient. This scenario has often resulted in fragmented and biased patient care, as well as a lack of communication between providers and with patients.

A modern, more formalized approach is a clinic and conference combination in real time. The patient is fully evaluated over a one- or two-day period. In this model, all necessary radiographic and/or laboratory testing and history and physical examination are completed in a half day and then presented to the multidisciplinary team. After presentation and discussion in conference, patients are seen by the providers to discuss treatment options and recommendations. Often, these patients then have group consultations by a team of support services. Support services include registered dieticians, social workers, smoking cessation specialists, financial counselors, integrative medicine specialists, and genetic counselors [1].

C. Meguid (✉)
Department of Surgical Oncology, University of Colorado Hospital, 12631 E. 17th Ave, 6th floor, MS C313, Aurora, CO 80045, USA
e-mail: Cheryl.meguid@ucdenver.edu

T.E. Schefter
Department of Radiation Oncology, University of Colorado Comprehensive Cancer Center, 1665 Aurora Ct, Suite 1032 MS F-706, Aurora, CO 80045, USA
e-mail: Tracey.schefter@ucdenver.edu

J. Meyer and T.E. Schefter (eds.), *Radiation Therapy for Liver Tumors*,
DOI 10.1007/978-3-319-54531-8_19

19.2 Benefits to Patients, Providers, and Hospital/Institution

The multidisciplinary approach for patients with malignancies has been shown to be beneficial to both patients and providers, as well as the institution [2–5].

19.2.1 Benefits to Patients

Patients benefit considerably from a multidisciplinary approach. The one- or two-day streamlined model is appreciated by all patients but especially those traveling long distances who otherwise would have had to make several trips for consultations with various providers. Often, there is a change in diagnosis or stage and/or detection of other abnormalities on review of radiographic imaging or pathology, sometimes also resulting in alteration of treatment recommendations previously offered from another facility. By combining provider visits, patients are only charged one facility fee, limiting costs otherwise associated with multiple clinic visits to various specialists. Documentation of the multidisciplinary conference recommendations and treatment plan is done in the electronic medical record (EMR), which often does not happen in a traditional tumor board setting, and if it does, it has the potential for bias. EMRs are becoming more readily available to view throughout multiple healthcare systems, and this is especially helpful to community providers who refer to larger facilities for treatment advice. The multidisciplinary model has been shown to increase accuracy of initial staging and also has been associated with improved survival for some cancers [1, 3, 6, 7]. Discussion of a patient's initial treatment plan may avoid certain setbacks, such as procedures which may exclude future treatment options. An example of this is percutaneous biliary drain placement disqualifying subsequent liver transplant at some institutions.

19.2.2 Benefits to Providers

Providers also benefit greatly from a multidisciplinary model. One of the most important items to note is that providers have a designated period for discussion, as this is often not the case during conventional consultations. When discussing a patient's case with different specialists in the same setting, there is improved communication and a better understanding of selection criteria for the vast array of liver-directed and systemic therapy options. Additionally, having a designated coordinator benefits referring providers because there is a consistent point of contact to relay the multidisciplinary team recommendations. It is our policy to bring all new liver tumor cases through the liver multidisciplinary clinic which minimizes physician bias in the treatment plan and often provides more than one option for the patient. The dynamic real time discussion between specialists confers learning opportunities for all, especially students, residents, and those in fellowship training [8]. For providers practicing in remote and rural settings, discussion of patients with cancer enhances implementation of multidisciplinary management [9].

In the one- or two-day model described earlier, the patient's clinical workup is completed that day (if not otherwise prior to the appointment), and therefore, the providers have all the information necessary to make treatment recommendations. Many multidisciplinary conferences offer continuing medical education (CME) credits, which is an added benefit to providers [1].

By having such an efficient model for care, there is also the potential to free up time for specialists to see more patients and/or be more productive with research.

19.2.3 Benefits to the Program

During the multidisciplinary evaluation, several treatment options are discussed for each patient.

One major benefit to the multidisciplinary program is including research coordinators in the discussion of each patient's plan for screening and participation into clinical trials. Starting a new program is also a good opportunity to start a database to track metrics such as growth (clinical or procedural), demographic information, referral sources, and items that may be used for research purposes, such as change in diagnosis and/or change in treatment recommendations.

19.2.4 Benefits to the Hospital/ Institution

There are many benefits to the hospital or institution in supporting multidisciplinary programs. Patients brought through the multidisciplinary clinic often undergo review of outside pathology and additional radiographic testing, either for restaging after treatment or to establish a diagnosis. These both result in significant downstream revenue for the hospital.

19.3 Key Components to Successful Multidisciplinary Care

There are some key elements that are important for maintaining a successful multidisciplinary program. What follows is an approach we have implemented at the University of Colorado:

- Buy-in from Administration and Physicians: Early on, it is important to establish commitment from participating providers, as they are vital to the success of the multidisciplinary program. A delegate from each specialty should participate each week, and by having a rotating schedule, it is not overly onerous for an individual provider. By having all disciplines represented, patients are guaranteed to get a comprehensive evaluation and personalized recommendations. Having hospital administration buy-in is also essential to the success of the multidisciplinary program, as they determine the hospital resources and funding. Salary support for the program coordinator and provision of food is essential in our experience.
- Designated Program Coordinator: Hiring a designated coordinator to run the multidisciplinary clinic is one of the most important factors in running a successful program. The coordinator ideally is an Advanced Practice Provider (APP) (Nurse Practitioner (NP) or Physician Assistant (PA)) who has the education and medical background to effectively screen and triage patients to determine whether a patient is appropriate to bring through a multidisciplinary program. APPs can determine whether further workup is needed prior to review by the multidisciplinary team, and this can be scheduled during the same MD evaluation. This provides the most efficient care from the perspective of the patient as well as providers. By reviewing outside records ahead of time, redundant testing is avoided. Having a designated coordinator as a main point of contact is beneficial for patients who have a hard time navigating the healthcare system. This is also useful for referring providers and for maintaining communication during treatment.
- Scheduling logistics: Figuring out scheduling logistics for the multidisciplinary program is essential prior to the clinic starting. Establishing the day, time, and location of the conference early on will help participating providers clear their schedules so they can fully participate and avoid the frustration that comes with having to be several places at the same time. The schedule the patients follow on the day of the clinic will differ based on the particular disease, but a thoughtful workflow must be configured. Two examples of clinics with differing scheduling needs are as follows:
  - *Pancreas and Biliary Multidisciplinary Clinic*: This is a good example of a one-day clinic visit. Patients undergo necessary diagnostic radiographic and laboratory testing first thing in the morning, followed by a history and physical examination and meeting with support services. The patient is presented at the

multidisciplinary conference and then meets with all of the specialists who might be involved in their care.

– *Esophageal and Gastric Multidisciplinary Clinic*: Most patients with esophageal malignancies routinely need an endoscopic ultrasound (EUS) to determine cancer staging. In this circumstance, it makes sense for a two-day clinic, as the patients require sedation for the procedure. On the first day, the patient undergoes necessary radiographic/laboratory testing, history and physical examination, and EUS. The multidisciplinary conference is held early on the second day, and the patients then have a consultation with all the providers who will be involved in their care.

In order to have these clinics run efficiently each week, it is important for all of the participating departments—for example, in the above examples—radiology, laboratory, clinic area, and endoscopy, to understand how the flow of the day for the patient will be. It is especially helpful to reserve "slots" in radiology to guarantee availability so that the program coordinators can quickly add on a last-minute patient should they need to. Creating a patient flow template is useful to help prevent scheduling confusion. One example used at our institution is shown in Table 19.1.

- Weekly Handout: The coordinator should develop a handout that lists each patient to be discussed and seen that day. A detailed description of the patient's clinical course to date should be included, such as pertinent past medical and surgical history, radiology, laboratory, endoscopy, and pathology reports. This handout is helpful for the multidisciplinary providers to refer to when a patient is being presented in conference. Emailing the handout the day before the conference may also be especially helpful to the pathologists and radiologists scheduled to host the multidisciplinary conference so that they may prepare ahead of time.
- Marketing: As mentioned earlier, an aggressive marketing campaign can help attract patients to the healthcare facility promoting the multidisciplinary clinic. A strong Webpage presence is important, as more patients today are utilizing the Internet to determine where to undergo treatment of their disease. The Webpage should clearly list the multidisciplinary coordinator and a contact phone number as this makes it much simpler for patients to navigate the healthcare system. If the healthcare facility specializes in the treatment of that disease with specialty services, such as robotic or laparoscopic approaches, and endoscopy procedures such as endoscopic mucosal resections (EMR), interventional radiology procedures, or localized radiation therapy, this should be advertised as well. Emphasizing that the patients are evaluated by multiple providers over a one- or two-day visit is essential on all marketing tools for the multidisciplinary program.

Table 19.1 Patient flow template

Time	Patient 1	Patient 2	Patient 3	Patient 4	Patient 5	Patient 6
7:30–11:30	CT: 07:30 Check-In 08:00 Scan	CT: 07:50 Check-In 08:20 Scan	Lab: 07:30	Lab: 08:00	Lab: 08:15	Lab: 08:30
	H&P: 08:30	H&P: 09:00	CT: 08:10 Check-In 08:40 Scan	CT: 08:30 Check-In 09:00 Scan	CT: 08:50 Check-In 09:20 Scan	CT: 09:10 Check-In 09:40 Scan
	Lab: 10:00	Lab: 10:00	H&P: 09:00	H&P: 10:00	H&P: 103:0	H&P: 10:30
11:30–12:00	Consultation with support services					
12:00–13:00	Patient lunch/multidisciplinary conference					
13:00–16:00	Consultation with specialists					

- Community Outreach: Physicians promoting the multidisciplinary programs should be encouraged to take part in presentations or outreach discussions with prospective referring physicians and practice groups. Participation in local or national support group events helps promote recognition of the multidisciplinary program within the community and/or region.
- Data Collection: The initiation of a program is an excellent opportunity to collect data for future research, such as volume growth, clinic visits, surgeries, and procedures. Metrics frequently noted to increase with implementation of a multidisciplinary program are change in diagnosis and change in treatment recommendations from outside institutions; therefore, this information should be documented as well.

19.4 Review of Literature

Presently, there is limited available literature regarding the multidisciplinary approach for liver tumors. One such report by Park et al. for unresectable hepatocellular carcinoma (HCC) describes a lack of scientific evidence for multidisciplinary management. Ward and colleagues, however, reported the importance of a multidisciplinary approach in treating patients with liver lesions, most often HCC, cholangiocarcinoma, or colorectal cancer metastasis as they found this to be the best method in both the preoperative and postoperative setting. Similarly, Venkatesh et al. concluded that patients with liver masses require multidisciplinary collaboration for efficient characterization and management. Jacobson reports that evidence comparing cancer care delivered in a multidisciplinary versus traditional settings is scant; however, unsupported benefits include having the ability to make a more accurate evaluation of patient information, greater standardization, and adherence to evidence-based care and improved cancer outcomes. Yopp et al. also support the multidisciplinary approach for HCC patients. They found that patients evaluated in their HCC multidisciplinary clinic had a median survival of 13.2 months compared to 4.8 months noted in patients prior to MDC establishment [7, 10–13].

When looking at other disease types, there are some publications noting the impact multidisciplinary programs have had on change in initial diagnosis, as review from a multidisciplinary team can find discrepancies during radiology, endoscopy, and/or pathology review of disease type and/or cancer staging. Also noted in the literature is finding a change in outside treatment recommendations, which can include decision for surgical resectability, radiation therapy, interventional radiology procedures, chemotherapy options, and eligibility into clinical trials [14, 15].

At the University of Colorado Hospital, we found that 27% of patients evaluated in a multidisciplinary program for gastrointestinal (GI) cancers had a change in diagnosis. This includes a radiographic or endoscopic change resulting in a stage change, a radiographic change resulting in a change in clinical diagnosis, and/or a change in pathology diagnosis. This group also reported a 28% change in treatment recommendation from outside providers in patients participating in their GI multidisciplinary clinics [16]. van Hagen et al. report a 34.5% change in treatment recommendation for patients with GI malignancies participating in their multidisciplinary program. Schmidt et al. describe a 26% change in treatment recommendation for esophageal cancer patients and a 40% change in treatment recommendation for lung cancer patients reviewed in their multidisciplinary clinic. Pawlik et al. found a 24% change in recommended management based on evaluation from the multidisciplinary team on patients with pancreatic cancer [17–19].

In other studies looking at the benefit of multidisciplinary care of patients, Bumm et al. found that treatment recommendations from the multidisciplinary team for patients with esophageal cancer were put into practice more than 95% of the time. Gardner et al. observed improved patient access to consultations and shorter time to initial treatment with the establishment of a multidisciplinary program for patients with

pancreatic adenocarcinoma undergoing neoadjuvant therapy. Litton et al. noted that 98% of patients participating in their breast multidisciplinary clinic rated their overall experience as "excellent" and that physicians also credited improved communications and increased efficiency in this approach. Wilson et al. stated that implementation of a multidisciplinary team increased the number of patients reviewed and the proportion reviewed within 2 weeks of diagnosis [20–23].

19.5 Case Report

As described above, there are many benefits of a multidisciplinary approach for patients who require multimodality therapy. At the University of Colorado Hospital, the Liver and Neuroendocrine Tumor (NET) Multidisciplinary Clinic (Liver MDC) sees complex patients with diagnoses such as HCC, metastatic tumors to the liver, liver metastasis with unknown primary cancer, neuroendocrine carcinomas, and cholangiocarcinomas. The majority of these patients come through the multidisciplinary clinic more than once for restaging evaluation after each treatment. Here is an example of a patient seen through Liver MDC:

Patient presentation

61 y/o female with a history of hypothyroidism and BRCA2 carrier, who presented to her local ER with acute onset right sided abdominal pain and increasing fatigue. Past surgical history negative, former 10 pack year smoking history. Physical examination was unremarkable. Laboratory results noted an elevated Alk Phos at 145 U/L.

Patient workup

- ***August 16, 2015 Abdominal Ultrasound***: heterogeneous echotexture of the right hepatic lobe, raising the possibility of large hepatic mass.
- ***August 16, 2015 CT***: 13.5 × 12.2 × 7.8 cm heterogeneously enhancing mass identified within the liver. The mass involves the anterior segment of the right lobe and the medial segment of the left lobe. No evidence of metastatic disease.
- ***August 20, 2015 Liver Multidisciplinary Clinic evaluation***: Abnormal laboratory results: Alk Phos 323 U/L and CA 19-9 1171.6 u/mL. Other tumor markers included AFP of 5.3 ng/mL and CEA 0.9 ng/mL. Multidisciplinary team felt she was not a surgical candidate due to bilobar disease and recommended initiating treatment with chemotherapy. She was referred for IR-guided liver biopsy to confirm tissue diagnosis.
- ***August 31, 2016 IR-guided liver biopsy***
- ***Pathology****: Adenocarcinoma consistent with pancreaticobiliary primary. Immunohisotchemical studies show strong positive expression for CK7 and CK19, weakly positive expression for CK20, and negative expression for CDX2 and HepPar, which supports clinical impression of adenocarcinoma of pancreaticobiliary origin.*
- ***September 10, 2016 port placed***

Patient treatment

- ***September 17, 2015 Neoadjuvant therapy initiated***: gemcitabine and cisplatin (day 1, 8 every 21 days). Cycle 2 started 10/15/15. Cycle 3 started 11/5/15. Tolerated well with some fatigue and nausea.
- ***November 11, 2015 CA 19-9***: ***899.0*** **u/mL**
- ***November 19, 2015 CT***: slightly decreased size and enhancement of infiltrative mass consistent with intrahepatic cholangiocarcinoma, now measuring 11.8 × 7.3 cm. Mass involves segments 1, 4, 5, 6, 8 and possibly segment 3. Pulmonary thromboembolic disease within segmental right lower lobe pulmonary arteries.
- ***November 19, 2015 Liver Multidisciplinary Clinic evaluation***: Multidisciplinary team felt she was still not a surgical candidate. Recommended continuing with cycle 4 of gemcitabine and cisplatin and then pursue treatment with localized therapy. Patient met with medical oncology, radiation oncology,

and interventional radiology and was presented with localized therapy options including chemoradiation versus selective internal radiation embolization (SIRT). Given the size of the lesion, we felt SIRT with Yttrium-90 would give her the best benefit. Lovenox initiated.

- ***December 2, 2015 CA 19-9***: ***678*** **u/mL**
- ***December 3, 2015 cycle 4 started***: Gemcitabine and cisplatin
- ***December 21, 2015 Nuclear Medicine Hepatic Artery Perfusion Scan***: The percent of shunting from the liver to the lungs is 3.7%
- ***January 5, 2016 SIRT with Yttrium-90 to right lobe***: Target volume 482 cc right posterior segments 6/7; 351 cc right anterior segments 5/8, and target dose 120 Gy
- ***January 3, 2016 SIRT with Yttrium-90 to left lobe***: Target volume 786 cc and target dose 120 Gy
- ***March 10, 2016 CT:*** Mild decrease in size and enhancement of large intrahepatic mass, measuring 11.1 × 6.2 cm. Arterial enhancing normal size portacaval node, suspicious for metastasis.
- ***May 12, 2016 CT:*** Mild decrease in size and enhancement of large intrahepatic mass, now 10.3 × 6.0 cm, likely representing therapeutic response. Unchanged atypical arterial enhancing normal size portacaval node requires continued attention of follow-up.
- ***May 12, 2016 Liver Multidisciplinary Clinic evaluation***: Patient continues to not be a surgical candidate. Multidisciplinary recommendation was to follow up with interventional radiology for radiation segmentectomy and referral to hepatology for formal transplant evaluation (for live donor transplant).

During the course of this patient's treatment, she was evaluated and seen by surgical oncology, medical oncology, radiation oncology, and interventional radiology. Having her come through the multidisciplinary clinic proved to be the most efficient way to coordinate her care.

19.6 Conclusion

Patients with complex malignancies are now routinely being diagnosed and treated by a multidisciplinary team consisting of surgeons, medical oncologists, radiation oncologists, gastroenterologists, and interventional radiologists. The multidisciplinary approach to care has been shown to be beneficial for both patients and providers and should be utilized whenever possible to allow patients the most comprehensive evaluation from a team of specialists for their disease.

References

1. Meguid C, Ryan CE, Edil BH, Schulick RD, Gajdos C, Boniface M, et al. Establishing a framework for building multidisciplinary programs. J Multidiscip Healthc. 2015;8:519–26.
2. Chang JH, Vines E, Bertsch H, Fraker DL, Czerniecki BJ, Rosato EF, et al. The impact of a multidisciplinary breast cancer center on recommendations for patient management: The University of Pennsylvania experience. Cancer. 2001;91(7):1231–7.
3. Fleissig A, Jenkins V, Catt S, Fallowfield L. Multidisciplinary teams in cancer care: are they effective in the UK? Lancet Oncol. 2006;7(11):935–43.
4. Gabel M, Hilton NE, Nathanson SD. Multidisciplinary breast cancer clinics. Do they work? Cancer. 1997;79(12):2380–4.
5. Page AJ, Cosgrove D, Elnahal SM, Herman JM, Pawlik TM. Organizing a multidisciplinary clinic. Chin Clin Oncol. 2014;3(4):43.
6. Elnahal SM, Moningi S, Wild AT, Dholakia AS, Hodgin M, Fan KY, et al. Improving safe patient throughput in a multidisciplinary oncology clinic. Physician Leadersh J. 2015;2(2):56–60, 2, 4–5.
7. Yopp AC, Mansour JC, Beg MS, Arenas J, Trimmer C, Reddick M, et al. Establishment of a multidisciplinary hepatocellular carcinoma clinic is associated with improved clinical outcome. Ann Surg Oncol. 2014;21(4):1287–95.
8. Siegel GW, Biermann JS, Chugh R, Jacobson JA, Lucas D, Feng M, et al. The multidisciplinary management of bone and soft tissue sarcoma: an essential organizational framework. J Multidiscip Healthc. 2015;8:109–15.
9. Charara RN, Kreidieh, FY, Farhat RA, Al-Feghali KA, Khoury KE, Haydar A, Nassar L, Berjawi G, Shamseddine A, El Saghir NS. Practice and impact of multidisciplinary tumor boards on patient management: a prospective study. J Glob Oncol. 2016. doi:10.1200/JGO.2016.004960 [Epub ahead of print].

10. Park HC, Seong J, Tanaka M, Zeng ZC, Lim HY, Guan S, et al. Multidisciplinary management of nonresectable hepatocellular carcinoma. Oncology. 2011;81(Suppl 1):134–40.
11. Venkatesh SK, Chandan V, Roberts LR. Liver masses: a clinical, radiologic, and pathologic perspective. Clin Gastroenterol Hepatol. 2014;12 (9):1414–29.
12. Ward TJ, Madoff DC, Weintraub JL. Interventional radiology in the multidisciplinary management of liver lesions: pre- and postoperative roles. Semin Liver Dis. 2013;33(3):213–25.
13. Jacobson JO. Multidisciplinary cancer management: a systems-based approach to deliver complex care. J Oncol Pract. 2010;6(6):274–5.
14. Newman EA, Guest AB, Helvie MA, Roubidoux MA, Chang AE, Kleer CG, et al. Changes in surgical management resulting from case review at a breast cancer multidisciplinary tumor board. Cancer. 2006;107(10):2346–51.
15. Petty JK, Vetto JT. Beyond doughnuts: tumor board recommendations influence patient care. J Cancer Educ. 2002;17(2):97–100.
16. Meguid C, Schulick RD, Schefter TE, Lieu CH, Boniface M, Williams N, et al. The multidisciplinary approach to GI cancer results in change of diagnosis and management of patients. Multidisciplinary care impacts diagnosis and management of patients. Ann Surg Oncol. 2016;23(12):3986–90.
17. van Hagen P, Spaander MC, van der Gaast A, van Rij CM, Tilanus HW, van Lanschot JJ, et al. Impact of a multidisciplinary tumour board meeting for upper-GI malignancies on clinical decision making: a prospective cohort study. Int J Clin Oncol. 2013;18 (2):214–9.
18. Schmidt HM, Roberts JM, Bodnar AM, Kunz S, Kirtland SH, Koehler RP, et al. Thoracic multidisciplinary tumor board routinely impacts therapeutic plans in patients with lung and esophageal cancer: a prospective cohort study. Ann Thorac Surg. 2015;99 (5):1719–24.
19. Pawlik TM, Laheru D, Hruban RH, Coleman J, Wolfgang CL, Campbell K, et al. Evaluating the impact of a single-day multidisciplinary clinic on the management of pancreatic cancer. Ann Surg Oncol. 2008;15(8):2081–8.
20. Bumm R, Feith M, Lordick F, Herschbach P, Siewert JR. Impact of multidisciplinary tumor boards on diagnosis and treatment of esophageal cancer. Eur Surg. 2007;39(3):136–40.
21. Gardner TB, Barth RJ, Zaki BI, Boulay BR, McGowan MM, Sutton JE, et al. Effect of initiating a multidisciplinary care clinic on access and time to treatment in patients with pancreatic adenocarcinoma. J Oncol Pract. 2010;6(6):288–92.
22. Litton G, Kane D, Clay G, Kruger P, Belnap T, Parkinson B. Multidisciplinary cancer care with a patient and physician satisfaction focus. J Oncol Pract. 2010;6(6):e35–7.
23. Wilson EE, Thompson SK, Bull J, Jones B, Price T, Devitt PG, et al. Improving care for patients with oesophageal and gastric cancer: impact of a statewide multidisciplinary team. ANZ J Surg. 2016;86(4): 270–3.

Part VIII
Future Directions

Radiation Therapy for Liver Tumors: Future Directions

20

Eric A. Mellon, MD, PhD, Gilbert Murimwa, MSc and Sarah E. Hoffe, MD

Abbreviations

RT	Radiotherapy
HCC	Hepatocellular
IHCC	Intrahepatic Cholangiocarcinoma
SBRT	Stereotactic Body Radiation Therapy
SABR	Stereotactic Ablative Radiation Therapy
RILD	Radiation-Induced Liver disease
FLR	Future liver remnant
NAFLD	Nonalcoholic fatty liver disease
NASH	Nonalcoholic steatohepatitis
CASH	Chemotherapy-associated steatohepatitis
ICG	Indocyanine green
SPECT	Single-photon emission computed tomography
MRI	Magnetic Resonance Imaging
miRNA	MicroRNA
RSI	Radiosensitivity index
CRC	Those colorectal
OS	Overall survival

E.A. Mellon (✉)
Department of Radiation Oncology,
University of Miami Miller School of Medicine
Sylvester Comprehensive Cancer Center,
1475 NW 12th Ave, Miami, FL 33136, USA
e-mail: eric.mellon@med.miami.edu

G. Murimwa
University of South Florida Morsani College of Medicine, Tampa, FL, USA

S.E. Hoffe
Department of Radiation Oncology,
Moffitt Cancer Center, 12902 Magnolia Drive,
Tampa, FL 33612, USA
e-mail: Sarah.Hoffe@moffitt.org

J. Meyer and T.E. Schefter (eds.), *Radiation Therapy for Liver Tumors*,
DOI 10.1007/978-3-319-54531-8_20

BED	Biologically effective dose
GTV	Gross tumor volume
TACE	Transarterial chemoembolization
TARE	Transarterial radioembolization
SIRT	Selective Internal Radiation Therapy
PFS	Progression-free survival
VTR	Virtual Tumor Resection
RFA	Radiofrequency Ablation

20.1 Introduction

The future of radiotherapy (RT) for liver tumors requires innovative technologies that expand RT applications, ultimately with validation in practice-changing clinical trials. Over the last 30 years, a strong foundation built on advanced imaging and computerized techniques has been developed to support a new role for RT in the treatment of patients with limited hepatic metastases as well as primary hepatocellular (HCC) and intrahepatic cholangiocarcinoma (IHCC), evolving from whole liver radiation to high dose partial liver radiation to stereotactic body radiation therapy (SBRT) [1, 2]. Indeed, at present, these advances have expanded the tumor ablation portfolio beyond the treatments offered by interventional radiologists and surgical oncologists such that small tumors can now be successfully ablated with stereotactic ablative radiation therapy (SABR) [3–8]. Yet, despite the tremendous progress demonstrating the safety and efficacy of radiation to the liver, significant questions still revolve around defining the optimal place of RT within the loco-regional liver treatment sandbox, inviting level 1 evidence to best select patients for RT with the most effective treatment dose, fractionation, and technique. In this review, we will explore some of these unanswered questions and potential future strategies.

20.2 Adaptive RT Based on Hepatic Function

Historically, whole liver radiation was reserved for palliative indications due to the relatively low liver tolerance limiting dose delivery and the potential for radiation-induced liver disease (RILD), an occasionally fatal syndrome that can occur from two weeks to four months following RT completion [9]. Data from these early studies with conventional 2 Gy fractionation also showed the contributing role of the patient's hepatic function, demonstrating a 5% risk at 5 years of RILD of 28 Gy for primary HCC and 32 Gy for metastases [10]. Through the lens of our modern liver experience, we now realize the significance of these early findings, with multiple investigators basing modern high dose delivery on a normal tissue complication probability model that can individualize prescription dose to minimize the risk of RILD [11, 12]. Unique to the liver is its significant capacity for regeneration, essential to surgeons when they calculate the future liver remnant [13–15], since, in patients with well-preserved liver function, an adequate future liver remnant (FLR) of at least 25% is necessary to avoid liver failure, but, in patients with impaired liver function, a FLR of up to 40% should be maintained.

Some techniques may allow for reduction of the volume of normal liver irradiated, such as

protons (discussed later) or MRI-guided radiotherapy. Compared with other integrated image guidance modalities, MRI for patient setup improves visualization of soft-tissue anatomy for patient and tumor position verification which may allow for reduction in margins and improved uninvolved liver sparing [16, 17]. MRI also provides near real-time visualization of moving liver tumors simultaneously with radiation therapy [18]. As the tumor can be visualized daily, there is also potential for volumetric daily anatomic and functional data to dynamically guide tailored field and volume adaptation during the course of care [19, 20].

The underlying health of the patient's liver is important to quantify for radiation treatment planning. Globally, in addition to the development of virally mediated dysfunction and carcinogenesis, there has also been a rising incidence of nonalcoholic fatty liver disease (NAFLD) [21], which is estimated to affect one billion individuals worldwide [22]. Among those patients with NAFLD, 30% will eventually develop nonalcoholic steatohepatitis (NASH) [23], with 15–25% of these patients ultimately progressing to cirrhosis. Moreover, in the metastatic setting, many patients are referred after progression of multiple lines of systemic chemotherapy which can result in chemotherapy-associated liver injury [24] and chemotherapy associated steatohepatitis (CASH) [25].

The future question, then, is how we can systematically integrate individual data about the patient's liver function into our treatment planning to minimize toxicity. Clinical data for HCC has been based on the Child-Pugh classification [26, 27] but more objective scoring systems with standard albumin and bilirubin lab values that avoid the subjective coding of encephalopathy and ascites may be more appropriate for RT, with the ALBI criteria [28] worthy of such future validation. Imaging methods of liver functional assessment are being developed using SPECT and MRI [29, 30] as well as with compounds that are excreted in bile such as indocyanine green (ICG) [31], that can measure liver function with significant dosimetric implications.

Our lung radiation oncology colleagues have developed techniques to integrate ventilation-perfusion patient data into treatment planning [32] to guide beam selection and enhance the therapeutic ratio; so future strategies for liver RT may be able to do the same to foster safer dose escalation. Additional data in the lung cancer setting also suggest that changes in the levels of circulating microRNA (miRNA), a type of RNA regulating gene expression, may help discriminate response to antitumor therapy [33]. Within the treatment of NAFLD, miRNAs are emerging as potential serum biomarkers to evaluate the status of disease severity [34], and recent data also suggests miRNAs have a role in the modulation of key cellular pathways that control the response to RT [35]. Future liver radiotherapy trials may thus consider evaluation of miRNAs to study whether their measurement can guide the response to the therapy of both the tumor as well as the normal liver tissue. Moreover, functional patient-centric data captured during the course of radiotherapy may drive adaptive treatment, such that early indicators of hepatic tolerance can be recognized and treatment fields adjusted before permanent damage can occur [36].

20.3 Adaptive RT Based on Intra-tumoral and Response Heterogeneity

Central to the oncologic RT dose prescription is the perceived radiosensitivity of the intended target and nearby normal tissues juxtaposed with the anticipated dose for local control. Prospective dosing may soon have more predictive reliability based on the multigene expression model of tumor radiosensitivity known as the radiosensitivity index (RSI) [37], which has been clinically validated in multiple patient cohorts across disease sites [38]. Recent data from this model suggests that the RSI differs not only between the primary site and metastasis, with the metastasis slightly more radioresistant, but also with the location of the metastatic site potentially influencing dose consideration since metastases

in the liver were found to be more radioresistant than the lung or lymph nodes [39]. Clinically, this is consistent with reports of SBRT for metastatic colorectal cancer (CRC) to the liver requiring higher doses for local control, with a recent pooled analysis correlating the importance of total dose, dose per fraction, and biologically equivalent dose (BED) [40].

Within tumors metastatic to the liver, current data [41] has reported significant intra-tumoral and inter-tumoral heterogeneity which can influence outcomes. Indeed, in a study reported by Sveen et al. [42], those metastatic colorectal (CRC) tumors involving the liver with a high degree of intra-individual genetic heterogeneity had worse 3-year overall survival (OS) of 18% versus 66% in those with lower heterogeneity. Furthermore, Stremitzer et al. [43] have shown that genetic variations within genes involved in immune responses and checkpoints are associated with outcome in patients with resected colorectal liver metastasis, showing significant differences in 3-year OS rate and the rates of extrahepatic recurrence. Other data suggest that the molecular heterogeneity that drives lesion-specific tumor responses can be measured with serial circulating tumor DNA measurements [44], suggesting serum biomarkers may aid in the development of a new adaptive RT paradigm.

Despite the emerging molecular heterogeneity data, with standard RT practice we generally deliver a uniform dose to the tumor and do not purposefully account for intrinsic cellular differences, either during or at the initiation of treatment. In the last decade, substantial progress in digital imaging has ushered in a new process of quantitatively extracting mineable features from a patient's individual radiology data to reveal a tumor's intrinsic pathophysiology, heralding the start of a new field called radiomics. When such mineable data from digital imaging is combined with genomic patient information, the resulting correlations form the basis of radiogenomics. With the novel analyses now available with the patient's individual imaging data, this may signal a new era of personalized intra-tumoral dosing, catalyzed by the potential to incorporate discrete quantitative features regarding prognosis, response, and distinct tumor habitats from CT, MR, and PET data (see Fig. 20.1) [45]. These extractable data have the potential to be adapted for each individual patient by analyzing the initial pretreatment imaging as well as the daily RT cone beam images to direct the dosing trajectory of the therapy. Historically, the radiation prescription is set prior to initiation of therapy based on the tumor characteristics of histology and stage but these innovative techniques may lead to a shift in RT dosing with a dynamic approach that is modified based on quantitative analysis of daily tumor response. Significant intra-tumoral heterogeneity has been reported for early stage

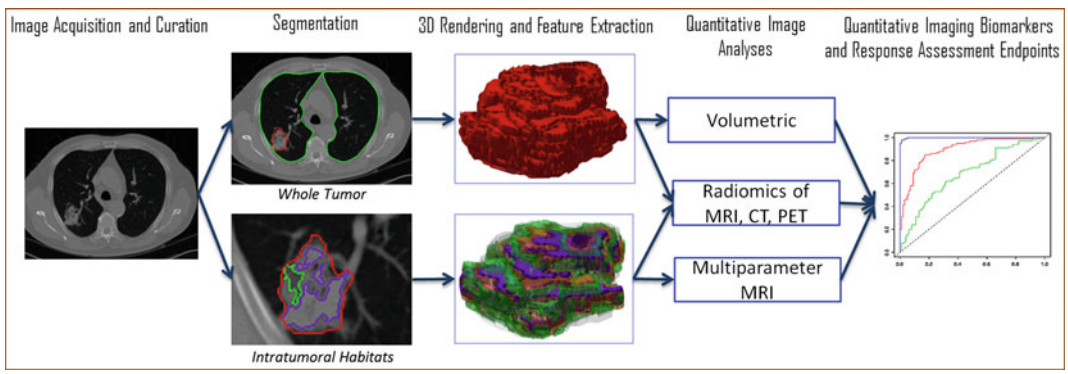

Fig. 20.1 Radiomic extraction process for imaging biomarker quantification and response assessment. [Courtesy of Olya Stringfield, PhD (Department of Cancer Imaging and Metabolism, Moffitt Cancer Center, Tampa, FL) and Robert Gillies, PhD (Department of Cancer Imaging and Metabolism as well as Department of Radiology, Moffitt Cancer Center, Tampa, FL)]

lung cancers by Grove et al. [46], with evidence that these radiomic features are strongly predictive of clinical outcome, and MRI tumor heterogeneity noted on prostate cancer images has been significantly correlated with pathologic Gleason score [47]. Data are now emerging for the significance of liver imaging heterogeneity as well, with a study of HCC patients noted to have correlative imaging phenotypes with response to doxorubicin, suggesting that a radiomics signature can improve the choice of therapeutic agent [48].

With the proliferation of MRI-guided radiation therapy, increased interest is expected in functional MRI information about the tumor microenvironment. These MRI tools have the future potential to guide initial RT treatment design, with higher dose targeting of MRI specified tumor sub-volumes. Diffusion-weighted MR Imaging (DWI) is perhaps the most frequently discussed technique applied to cancer radiotherapy [49]. DWI changes are observed during a course of SBRT, with increased apparent diffusion coefficient values (suggestive of increased necrosis) correlating with higher RT doses and improved response [50]. DWI also estimates HCC and liver metastasis necrosis due to transcatheter arterial embolization (TACE) [51, 52]. Perfusion-weighted MR Imaging (PWI), typically performed with gadolinium contrast, also estimates HCC necrosis [53]. In vivo MR spectroscopy (MRS) can also be applied to measure the levels of metabolites within the liver and liver cancers [54]. In particular, Phosphorus-31 MRS probes energy metabolism by detecting naturally occurring ^{31}P (no tracer required) to compare levels of phosphorus containing compounds. Acute responses to therapy for liver cancers have long been observed with ^{31}P MRS [55–57]. Based on the potential intra-tumoral changes indicative of response that can be identified during a course of therapy, intra-treatment MRI scans may guide future adaptive paradigms, allowing dose escalation of poorly responding sub-volumes and potential de-escalation of responding regions. A wide range of additional techniques to probe the tumor microenvironment with MR are available, of which many have an as yet undefined role in human liver cancer [58].

The future question is thus whether such differential dose prescription should be considered at treatment initiation and adapted to response during treatment. Recent studies have noted molecular differences between cells in the tumor core versus the periphery [59], with cancer cells at the tumor–host interface found to have invasion-promoting phenotypes in distinction to those cells in the center of the tumor exhibiting more supportive tissue characteristics. Moreover, vascularity has been reported as lower in the center versus the tumor edge and the lymphocytic immune response capacity has trended towards higher in the tumor edge, which may be of significant relevance as one of the most central future questions is how best to differentially exploit these intra-tumoral differences to enhance the immunomodulatory effort of SBRT in order to foster the greatest infiltration of immune effector cells and pro-inflammatory cytokines [60]. Thus, it may not be just how to enhance geographic RT-induced cell killing but also geographic RT-induced immune modulation that optimizes both local control and the potential for systemic RT mediated control as well. Further study is therefore needed to quantify the intra-tumoral radiosensitivity differences of liver tumors to optimize radiation dose assignments, with some data from other sites suggesting feasibility of directing higher doses to regions of increased radioresistance [61]. Crane and Koay advocate for a heterogeneous approach to achieve ablative doses, recommending a biologically effective dose (BED) of 140 Gy to the hypoxic core of the tumor while allowing up to 90% gross tumor volume (GTV) coverage of the portion of tumor adjacent to the radiosensitive GI tract [62].

In the future, mathematical models may also help predict radiation response to aid optimization of RT fractionation [63]. The newly defined proliferation saturation index (PSI) is defined as the ratio of the tumor volume to the host-influenced tumor carrying capacity. The carrying

capacity predicts the maximum volume of tumor cells that can be supported by the current in vivo tumor environment that is influenced by the status of the degree of oxygenation, nutrient availability, acidity, and immune state. Work to date suggests that integration of the PSI from the patient-specific imaging data available prior to treatment can determine the most appropriate fractionation schedule for the individual patient, a novel concept since current practice is to determine fractionation by the tumor type and stage. To date, the PSI has shown utility in retrospective treatment cohorts; future prospective work may validate PSI as a patient-specific tool to determine how data from imaging can be used to most appropriately select the ideal fractionation schedule for the individual patient in the specific tumor environmental milieu at the time of RT.

20.4 Strategies Combining RT with Other Agents

To date, SBRT studies have focused on outcomes with RT as the sole treatment modality. A major question for the future is how to augment the efficacy of RT with other modalities. In HCC, data have established the role of RT in targeting the tumor thrombus so that other treatments such as trans-arterial chemoembolization (TACE) or conformal RT can treat the larger volume disease [64–67]. In fact, a meta-analysis of 17 trials with nearly 1500 patients showed improved survival with TACE plus RT versus TACE alone [68]. Recently, Brade et al. [69] have reported a phase I trial of the oral multikinase inhibitor sorafenib before, during and after SBRT for HCC, noting that significant toxicity was observed with concurrent administration. In this study, there were significant grade ≥ 3 toxicities of those patients who had larger liver volumes irradiated with investigators noting complications such as GI bleeding, tumor rupture, thrombocytopenia, and increased liver enzymes. Given the toxicity of concurrent sorafenib and SBRT, the role of sequential combination therapy with SBRT delivered first followed by sorafenib is being tested by the Radiation Therapy Oncology Group Trial 1112. Investigators from the University of Michigan have noted that when radiation is delivered with trans-arterial radioembolization (TARE) using yttrium-90 microspheres for HCC, there is low dose rate radiation synergy with systemic therapy agents [70], with encouraging responses seen in patients treated concurrently with gemcitabine.

With respect to liver metastases, little data exist on the role of concurrent radiosensitizers with SBRT, yet three prospective studies are evaluating the efficacy of Selective Internal Radiation Therapy (SIRT) in conjunction with first line FOLFOX chemotherapy versus chemotherapy alone for metastatic colorectal cancer. So far, available data from the SIRFLOX study has shown an improvement in hepatic progression-free survival (PFS) but further data is awaited to determine whether the increased hepatic control will translate into a survival benefit [71]. The role of concurrent radiosensitizing chemotherapy with liver SBRT awaits future trials.

One emerging role for future exploration is the potential synergy with liver SBRT and immunotherapy [72]. This is particularly exciting in the highly immunogenic liver since it houses the majority of the body's macrophages. Patients with primary HCC liver cancer are excellent candidates for possible immunotherapy trials given that HCC is a cancer induced by inflammation [73] and adjuvant HCC randomized studies have shown a reduced risk of cancer recurrence with immunotherapy [74–76]. Current evidence has shown that RT may indeed improve the tumor immunologic response by eliciting antigen release from necrotic tumor cells and thereby forming an in situ vaccine [77]. Interest in combining RT with immunotherapy unites not only the potential for improved local anti-tumor response but also the potential for a systemic RT-induced, immune-mediated response distant from the irradiated site termed the abscopal effect. Significant implications for patients with liver tumors can be derived from the work by Golden et al. [78], whereby patients with metastatic solid tumors on single agent chemotherapy or hormonal therapy received RT of 35 Gy in ten fractions to one metastatic site

in combination with granulocyte-macrophage colony-stimulating factor (GM-CSF) with a subsequent targeting of a second metastatic site; results showed objective measurement of abscopal responses in 26.8% (11/41) of patients. Studies are ongoing to explore the combination of SBRT to the liver with immune agents, such as the initial work by Duffy et al. [79]. They have combined AMP 224, which binds to programmed death-1 immune checkpoint (PD-1), with SBRT to sites of CRC liver metastasis to determine if such a strategy can improve not only local control but also potential survival. This fusion protein, AMP 224, is composed of the extracellular domain of the Programmed Death-Ligand 2 and the Fc region of human IgG and not only functions as a PD-1 inhibitor but initial studies also suggest that it may deplete PD-1 highly expressed *T*-cells. The latest update from this work with escalated radiation doses of 8 Gy × 1 and 8 Gy × 3 has shown safety and feasibility but no objective responses, so much future work remains to be done. There is thus a new possible direction to expand the role of SBRT into the non-oligometastatic setting to improve systemic disease control by irradiation of a local liver site in combination with immunotherapy.

Future trials will also be able to explore the radiosensitivity differences between SBRT for virally versus nonvirally mediated tumors, since extrapolation from viral-associated cancers in other sites has shown higher radiosensitivity with lower doses [80, 81]. Data in the radioembolization setting suggest that virally associated HCC liver tumors have worse extrahepatic control [82]. Future trials of liver SBRT are needed to determine if the underlying carcinogenic etiology drives different patterns of local and distant disease control which could have important immunotherapy treatment implications.

20.5 RT for Larger Liver Tumor Burden?

Recent trials of SBRT for metastatic liver tumors have typically excluded more than five lesions and those located within 2 cm of the hepatic hilum [83, 84] and SBRT trials for primary liver cancer have generally restricted the size criteria to <7 cm [3, 85]. Investigators from the Princess Margaret Hospital, however, have included larger tumors and individualized the dose based on meeting NTCP criteria [86, 87]. Patients with primary liver cancers present with locally advanced disease and often have significant underlying liver dysfunction that makes them unsuitable for other therapies, thus future trials may explore the role of RT in the specific case of more extensive disease, potentially in combination with immunotherapy agents.

The question becomes how best to optimize the dose fractionation schedule for the individual patient based on underlying liver volume and function, tumor histology, size and number of lesions, tumor location, and history of prior therapies such as TACE, TARE, or systemic chemotherapy. In the future, pretreatment biopsies of the non-tumor bearing liver may be routinely indicated to help inform the patient's baseline liver functional status to guide personalized RT dosing. Higher dose per fraction trials have been delivered in a single fraction to 5–6 fractions to 15 fractions, with no prospective evaluation to date of how best to optimize such therapy. Future trials integrating validated radiomic signatures can help answer the issue of how best to personalize the dose to achieve the highest local control while minimizing the normal tissue toxicity based on the patient's individual functional data.

Another future strategy may be to expand the indications for RT to improve conversion to surgery with negative margins (R0 resection). With the advanced imaging technologies now available, virtual tumor resection (VTR) may become a potential strategy to estimate the extent of volumetric resection [88] and the width of the surgical margin. In a study of 113 patients with HCC, the estimated margin was compared to the actual margin in the specimen using a detailed three-dimensional (3D) CT scan based simulation, predicting the liver margin accurately with a difference of 1.6 mm [89]. If liver surgeons were able to incorporate VTR into the routine preoperative planning of liver resection, there may be

an expanded indication for neoadjuvant RT approaches, potentially to increase the likelihood of R0 resection or to ablate a small tumor in a part of the liver not ideally suited for surgery.

20.6 Future Role of Particle Therapy for Liver Tumors?

The potential of proton therapy for liver cancers is attractive with respect to the Bragg peak effect and its attendant ability to limit the low dose volume to hepatic tissue, thereby limiting the amount of normal liver irradiated [90, 91]. However, technical considerations in proton delivery to moving liver tumors have posed challenges. Recent data now suggests that effective respiratory gating systems are reproducible and offer great promise [92, 93]. Adding to the promise of proton therapy is the potential of increasing tumor cell kill by combining therapy with nanoparticles, which may hold a future role as radiosensitizers if some of the safety challenges can be overcome [94].

Emerging prospective trial data may quantify the benefit of protons in the treatment of liver cancers. For example, interim results have been reported for a prospective trial of proton radiotherapy compared to TACE as a bridging therapy to transplant for newly diagnosed HCC [95]. For the 69 patients randomized, proton therapy compared with TACE demonstrated a trend towards improved 2-year local tumor control (88% vs. 45%, $p = 0.06$) and progression-free survival (48% vs. 31%) as well as a reduction in hospitalization (24 vs. 113 total days, $p < 0.001$). Increasing doses of proton radiotherapy have recently been shown to be necessary to control intrahepatic cholangiocarcinoma (ICC) [4]. A prospective multi-institutional phase II study of 15 fractions of proton radiotherapy to a maximum of 67.5 Gy equivalent for unresectable HCC and ICC was recently reported demonstrating 2-year local control of 94.8% for HCC and 94.1% for ICC [96]. Since SBRT is less costly and more widely available, future work should define which patients benefit the most from proton radiotherapy.

Carbon ion radiotherapy is an emerging particle therapy that demonstrates a Bragg peak and induces cytotoxicity with less dependence on tumor oxygenation [97]. This implies that carbon ion therapy may have a unique role in hypovascular lesions such as many liver metastases, cholangiocarcinomas, and rare tumors such as sarcoma and teratoma. A comparative study of 343 patients treated on 8 proton therapy protocols and 4 carbon therapy protocols for HCC, an often hypervascular tumor, demonstrated equivalent 5-year local control (90.2% and 93%) and 5-year overall survival (38% and 36.3%) [98].

20.7 Value Considerations

Within the multidisciplinary management options for patients with liver tumors, surgical resection has been considered the gold standard based on the long-term outcome data [99]. However, with the healthcare shift toward greater scrutiny of quality and value [100], future trials may escalate the prioritization of liver SBRT based as an option due to the noninvasive delivery with low rates of toxicity, especially given the aging US population. In patients with HCC, retrospective data suggests that SBRT may be as effective as RFA [3]. To date, studies that have evaluated RFA versus SBRT for CRC liver metastases have shown that RFA is more cost effective [101] but prospective comparisons in patients with higher comorbid conditions have not been performed, especially relevant since RFA can be associated with injuries to the bile ducts, blood vessels, GI tract with perforation and lung collapse [102]. Thus, now that data has shown that SBRT is effective for small lesions with minimal complications, innovative clinical trials are needed to determine how best to match this tool to the most appropriate patient population.

20.8 Conclusion

SBRT as sole treatment modality for patients with liver tumors has shown excellent rates of local control with minimal toxicity. Future studies are needed to determine the optimal

patient selection for SBRT and the best personalized approach to precisely define the dose, fractionation, and anticipated response of the individual patient's tumor while maintaining liver function. New biological information from the field of radiomics may inform a new paradigm of heterogeneous dosimetry for liver tumors. Expanded indications for SBRT await validation from trials exploring the addition of concurrent radiosensitizing and immune modulating agents, suggesting that there may be a role for SBRT to enhance systemic as well as local response. Finally, prospective comparison of SBRT with other local modalities is needed to define the optimal position of SBRT within the multidisciplinary loco-regional liver treatment pathway.

References

1. Wo JY, Dawson LA, Zhu AX, Hong TS. An emerging role for radiation therapy in the treatment of hepatocellular carcinoma and intrahepatic cholangiocarcinoma. Surg Oncol Clin N Am. 2014;23(2):353–68.
2. Dawson LA. Overview: where does radiation therapy fit in the spectrum of liver cancer local-regional therapies? Semin Radiat Oncol. 2011;21(4):241–6.
3. Wahl DR, Stenmark MH, Tao Y, Pollom EL, Caoili EM, Lawrence TS, et al. Outcomes after stereotactic body radiotherapy or radiofrequency ablation for hepatocellular carcinoma. J Clin Oncol. 2016;34(5):452–9.
4. Tao R, Krishnan S, Bhosale PR, Javle MM, Aloia TA, Shroff RT, et al. Ablative radiotherapy doses lead to a substantial prolongation of survival in patients with inoperable intrahepatic cholangiocarcinoma: a retrospective dose response analysis. J Clin Oncol: official J Am Soc Clin Oncol. 2016;34(3):219–26.
5. Rule W, Timmerman R, Tong L, Abdulrahman R, Meyer J, Boike T, et al. Phase I dose-escalation study of stereotactic body radiotherapy in patients with hepatic metastases. Ann Surg Oncol. 2011;18(4):1081–7.
6. Loo BW, Chang JY, Dawson LA, Kavanagh BD, Koong AC, Senan S, et al. Stereotactic ablative radiotherapy: what's in a name? Pract Radiat Oncol. 2011;1(1):38–9.
7. Timmerman RD, Bizekis CS, Pass HI, Fong Y, Dupuy DE, Dawson LA, et al. Local surgical, ablative, and radiation treatment of metastases. CA Cancer J Clin. 2009;59(3):145–70.
8. Rusthoven KE, Kavanagh BD, Cardenes H, Stieber VW, Burri SH, Feigenberg SJ, et al. Multi-institutional phase I/II trial of stereotactic body radiation therapy for liver metastases. J Clin Oncol. 2009;27(10):1572–8.
9. Dawson LA, Ten Haken RK, Lawrence TS. Partial irradiation of the liver. Semin Radiat Oncol. 2001;11(3):240–6.
10. Dawson LA, Ten Haken RK. Partial volume tolerance of the liver to radiation. Semin Radiat Oncol. 2005;15(4):279–83.
11. Dawson LA, Eccles C, Craig T. Individualized image guided iso-NTCP based liver cancer SBRT. Acta Oncol. 2006;45(7):856–64.
12. Dawson LA, Normolle D, Balter JM, McGinn CJ, Lawrence TS, Ten Haken RK. Analysis of radiation-induced liver disease using the Lyman NTCP model. Int J Radiat Oncol Biol Phys. 2002;53(4):810–21.
13. Tanaka K, Shimada H, Matsuo K, Ueda M, Endo I, Togo S. Remnant liver regeneration after two-stage hepatectomy for multiple bilobar colorectal metastases. Eur J Surg Oncol. 2007;33(3):329–35.
14. Hemming AW, Reed AI, Howard RJ, Fujita S, Hochwald SN, Caridi JG, et al. Preoperative portal vein embolization for extended hepatectomy. Ann Surg. 2003;237(5):686–91; discussion 91–3.
15. Goh BK. Measured versus estimated total liver volume to preoperatively assess the adequacy of future liver remnant: which method should we use? Ann Surg. 2015;262(2):e72.
16. Noel CE, Parikh PJ, Spencer CR, Green OL, Hu Y, Mutic S, et al. Comparison of onboard low-field magnetic resonance imaging versus onboard computed tomography for anatomy visualization in radiotherapy. Acta Oncol. 2015;54(9):1474–82.
17. Mutic S, Dempsey JF. The ViewRay system: magnetic resonance-guided and controlled radiotherapy. Semin Radiat Oncol. 2014;24(3):196–9.
18. Wojcieszynski AP, Rosenberg SA, Brower JV, Hullett CR, Geurts MW, Labby ZE, et al. Gadoxetate for direct tumor therapy and tracking with real-time MRI-guided stereotactic body radiation therapy of the liver. Radiother Oncol: J Euro Soc Ther Radiol Oncol. 2016;118(2):416–8.
19. Acharya S, Fischer-Valuck BW, Kashani R, Parikh P, Yang D, Zhao T, et al. Online magnetic resonance image guided adaptive radiation therapy: first clinical applications. Int J Radiat Oncol Biol Phys. 2016;94(2):394–403.
20. Green O, Hu Y, Noel C, Olsen J, Mutic S. Observation of radiation-induced tissue signal intensity changes with the first commercial MRI-guided IMRT system. Int J Radiat Oncol Biol Phys. 2012;84(3):S758–9.
21. Hossain N, Kanwar P, Mohanty SR. A comprehensive updated review of pharmaceutical and nonpharmaceutical treatment for NAFLD. Gastroenterol Res Pract. 2016;2016:7109270.

22. Loomba R, Sanyal AJ. The global NAFLD epidemic. Nat Rev Gastroenterol Hepatol. 2013;10 (11):686–90.
23. Jahn D, Rau M, Wohlfahrt J, Hermanns HM, Geier A. Non-alcoholic steatohepatitis: from pathophysiology to novel therapies. Dig Dis. 2016;34 (4):356–63.
24. Robinson SM, Wilson CH, Burt AD, Manas DM, White SA. Chemotherapy-associated liver injury in patients with colorectal liver metastases: a systematic review and meta-analysis. Ann Surg Oncol. 2012;19(13):4287–99.
25. Vauthey JN, Pawlik TM, Ribero D, Wu TT, Zorzi D, Hoff PM, et al. Chemotherapy regimen predicts steatohepatitis and an increase in 90-day mortality after surgery for hepatic colorectal metastases. J Clin Oncol. 2006;24(13):2065–72.
26. Child CG, Turcotte JG. Surgery and portal hypertension. Major Probl Clin Surg. 1964;1:1–85.
27. Pugh RN, Murray-Lyon IM, Dawson JL, Pietroni MC, Williams R. Transection of the oesophagus for bleeding oesophageal varices. Br J Surg. 1973;60(8):646–9.
28. Johnson PJ, Berhane S, Kagebayashi C, Satomura S, Teng M, Reeves HL, et al. Assessment of liver function in patients with hepatocellular carcinoma: a new evidence-based approach-the ALBI grade. J Clin Oncol. 2015;33(6):550–8.
29. Wang H, Feng M, Frey KA, Ten Haken RK, Lawrence TS, Cao Y. Predictive models for regional hepatic function based on 99mTc-IDA SPECT and local radiation dose for physiologic adaptive radiation therapy. Int J Radiat Oncol Biol Phys. 2013;86(5):1000–6.
30. Cao Y, Wang H, Johnson TD, Pan C, Hussain H, Balter JM, et al. Prediction of liver function by using magnetic resonance-based portal venous perfusion imaging. Int J Radiat Oncol Biol Phys. 2013;85(1):258–63.
31. Hemming AW, Scudamore CH, Shackleton CR, Pudek M, Erb SR. Indocyanine green clearance as a predictor of successful hepatic resection in cirrhotic patients. Am J Surg. 1992;163(5):515–8.
32. McGuire SM, Marks LB, Yin FF, Das SK. A methodology for selecting the beam arrangement to reduce the intensity-modulated radiation therapy (IMRT) dose to the SPECT-defined functioning lung. Phys Med Biol. 2010;55(2):403–16.
33. Ponomaryova AA, Morozkin ES, Rykova EY, Zaporozhchenko IA, Skvortsova TE, Dobrodeev A, et al. Dynamic changes in circulating miRNA levels in response to antitumor therapy of lung cancer. Exp Lung Res. 2016;42(2):95–102.
34. Baffy G. MicroRNAs in Nonalcoholic Fatty Liver Disease. J Clin Med. 2015;4(12):1977–88.
35. Mueller AK, Lindner K, Hummel R, Haier J, Watson DI, Hussey DJ. MicroRNAs and Their Impact on Radiotherapy for Cancer. Radiat Res. 2016.
36. Stenmark MH, Cao Y, Wang H, Jackson A, Ben-Josef E, Ten Haken RK, et al. Estimating functional liver reserve following hepatic irradiation: adaptive normal tissue response models. Radiother Oncol. 2014;111(3):418–23.
37. Eschrich S, Zhang H, Zhao H, Boulware D, Lee JH, Bloom G, et al. Systems biology modeling of the radiation sensitivity network: a biomarker discovery platform. Int J Radiat Oncol Biol Phys. 2009;75 (2):497–505.
38. Torres-Roca JF. A molecular assay of tumor radiosensitivity: a roadmap towards biology-based personalized radiation therapy. Per Med. 2012;9 (5):547–57.
39. Ahmed KA, Fulp WJ, Berglund AE, Hoffe SE, Dilling TJ, Eschrich SA, et al. Differences Between Colon Cancer Primaries and Metastases Using a Molecular Assay for Tumor Radiation Sensitivity Suggest Implications for Potential Oligometastatic SBRT Patient Selection. Int J Radiat Oncol Biol Phys. 2015;92(4):837–42.
40. Chang DT, Swaminath A, Kozak M, Weintraub J, Koong AC, Kim J, et al. Stereotactic body radiotherapy for colorectal liver metastases: a pooled analysis. Cancer. 2011;117(17):4060–9.
41. Jesinghaus M, Pfarr N, Endris V, Kloor M, Volckmar AL, Brandt R, et al. Genotyping of colorectal cancer for cancer precision medicine: results from the IPH Center for Molecular Pathology. Genes Chromosom Cancer. 2016;55(6):505–21.
42. Sveen A, Loes IM, Alagaratnam S, Nilsen G, Holand M, Lingjaerde OC, Sorbye H, Berg KCG, Horn A, Angelsen JH, Knappskog S. Intra-individual genetic heterogeneity among liver metastases in metastatic colorectal cancer. ASCO Ann Meet Proc 2016;34(4 suppl):555.
43. Stremitzer S, Stintzing S, Heinemann V, Zhang W, Yang D, Ning Y, Sunakawa Y, Sebio A, Yamauchi S, Matsusaka S, Parekh A . Variations in Y chromosome-related genes and clinical outcome in metastatic colorectal cancer. ASCO Ann Meet Proc 2015;33(3 suppl):634.
44. Russo M, Siravegna G, Blaszkowsky LS, Corti G, Crisafulli G, Ahronian LG, et al. Tumor Heterogeneity and Lesion-Specific Response to Targeted Therapy in Colorectal Cancer. Cancer Discov. 2016;6(2):147–53.
45. Gillies RJ, Kinahan PE, Hricak H. Radiomics: images are more than pictures, they are data. Radiology. 2016;278(2):563–77.
46. Grove O, Berglund AE, Schabath MB, Aerts HJ, Dekker A, Wang H, et al. Quantitative computed tomographic descriptors associate tumor shape complexity and intratumor heterogeneity with prognosis in lung adenocarcinoma. PLoS ONE. 2015;10 (3):e0118261.
47. Wibmer A, Hricak H, Gondo T, Matsumoto K, Veeraraghavan H, Fehr D, et al. Haralick texture analysis of prostate MRI: utility for differentiating

non-cancerous prostate from prostate cancer and differentiating prostate cancers with different Gleason scores. Eur Radiol. 2015;25(10):2840–50.
48. Kuo MD, Gollub J, Sirlin CB, Ooi C, Chen X. Radiogenomic analysis to identify imaging phenotypes associated with drug response gene expression programs in hepatocellular carcinoma. J Vasc Interv Radiol. 2007;18(7):821–31.
49. Tsien C, Cao Y, Chenevert T. Clinical applications for diffusion magnetic resonance imaging in radiotherapy. Semin Radiat Oncol. 2014;24(3):218–26.
50. Eccles CL, Haider EA, Haider MA, Fung S, Lockwood G, Dawson LA. Change in diffusion weighted MRI during liver cancer radiotherapy: preliminary observations. Acta Oncol. 2009;48(7):1034–43.
51. Kamel IR, Bluemke DA, Ramsey D, Abusedera M, Torbenson M, Eng J, et al. Role of diffusion-weighted imaging in estimating tumor necrosis after chemoembolization of hepatocellular carcinoma. AJR Am J Roentgenol. 2003;181(3):708–10.
52. Buijs M, Vossen JA, Hong K, Georgiades CS, Geschwind JF, Kamel IR. Chemoembolization of hepatic metastases from ocular melanoma: assessment of response with contrast-enhanced and diffusion-weighted MRI. AJR Am J Roentgenol. 2008;191(1):285–9.
53. Mannelli L, Kim S, Hajdu CH, Babb JS, Clark TW, Taouli B. Assessment of tumor necrosis of hepatocellular carcinoma after chemoembolization: diffusion-weighted and contrast-enhanced MRI with histopathologic correlation of the explanted liver. AJR Am J Roentgenol. 2009;193(4):1044–52.
54. ter Voert EG, Heijmen L, van Laarhoven HW, Heerschap A. In vivo magnetic resonance spectroscopy of liver tumors and metastases. World J Gastroenterol. 2011;17(47):5133–49.
55. Maris JM, Evans AE, McLaughlin AC, D'Angio GJ, Bolinger L, Manos H, et al. 31P nuclear magnetic resonance spectroscopic investigation of human neuroblastoma in situ. New Engl J Med. 1985;312(23):1500–5.
56. Meyerhoff DJ, Karczmar GS, Valone F, Venook A, Matson GB, Weiner MW. Hepatic cancers and their response to chemoembolization therapy. Quantitative image-guided 31P magnetic resonance spectroscopy. Invest Radiol. 1992;27(6):456–64.
57. Dixon RM. NMR studies of phospholipid metabolism in hepatic lymphoma. NMR Biomed. 1998;11(7):370–9.
58. Matsuo M, Matsumoto S, Mitchell JB, Krishna MC, Camphausen K. Magnetic resonance imaging of the tumor microenvironment in radiotherapy: perfusion, hypoxia, and metabolism. Semin Radiat Oncol. 2014;24(3):210–7.
59. Lloyd MC, Cunningham JJ, Bui MM, Gillies RJ, Brown JS, Gatenby RA. Darwinian dynamics of intratumoral heterogeneity: not solely random mutations but also variable environmental selection forces. Cancer Res. 2016.
60. Finkelstein SE, Timmerman R, McBride WH, Schaue D, Hoffe SE, Mantz CA, et al. The confluence of stereotactic ablative radiotherapy and tumor immunology. Clin Dev Immunol. 2011;2011:439752.
61. Clausen MM, Hansen AE, Lundemann M, Hollensen C, Pommer T, Munck Af Rosenschöld P, et al. Dose painting based on tumor uptake of Cu-ATSM and FDG: a comparative study. Radiat Oncol. 2014;9:228.
62. Crane CH, Koay EJ. Solutions that enable ablative radiotherapy for large liver tumors: Fractionated dose painting, simultaneous integrated protection, motion management, and computed tomography image guidance. Cancer. 2016.
63. Prokopiou S, Moros EG, Poleszczuk J, Caudell J, Torres-Roca JF, Latifi K, et al. A proliferation saturation index to predict radiation response and personalize radiotherapy fractionation. Radiat Oncol. 2015;10:159.
64. Bujold A, Massey CA, Kim JJ, Brierley J, Cho C, Wong RK, et al. Sequential phase I and II trials of stereotactic body radiotherapy for locally advanced hepatocellular carcinoma. J Clin Oncol: official J Am Soc Clin Oncol. 2013;31(13):1631–9.
65. Lin CS, Jen YM, Chiu SY, Hwang JM, Chao HL, Lin HY, et al. Treatment of portal vein tumor thrombosis of hepatoma patients with either stereotactic radiotherapy or three-dimensional conformal radiotherapy. Jpn J Clin Oncol. 2006;36(4):212–7.
66. Yoon SM, Lim YS, Won HJ, Kim JH, Kim KM, Lee HC, et al. Radiotherapy plus transarterial chemoembolization for hepatocellular carcinoma invading the portal vein: long-term patient outcomes. Int J Radiat Oncol Biol Phys. 2012;82(5):2004–11.
67. Rim CH, Yang DS, Park YJ, Yoon WS, Lee JA, Kim CY. Effectiveness of high-dose three-dimensional conformal radiotherapy in hepatocellular carcinoma with portal vein thrombosis. Jpn J Clin Oncol. 2012;42(8):721–9.
68. Meng MB, Cui YL, Lu Y, She B, Chen Y, Guan YS, et al. Transcatheter arterial chemoembolization in combination with radiotherapy for unresectable hepatocellular carcinoma: a systematic review and meta-analysis. Radiother Oncol. 2009;92(2):184–94.
69. Brade AM, Ng S, Brierley J, Kim J, Dinniwell R, Ringash J, et al. Phase 1 trial of sorafenib and stereotactic body radiation therapy for hepatocellular carcinoma. Int J Radiat Oncol Biol Phys. 2016;94(3):580–7.
70. Cuneo KC, Davis MA, Feng MU, Novelli PM, Ensminger WD, Lawrence TS. Low dose rate radiosensitization of hepatocellular carcinoma in vitro and in patients. Transl Oncol. 2014;7(4):472–8.

71. van Hazel GA, Heinemann V, Sharma NK, Findlay MP, Ricke J, Peeters M, et al. SIRFLOX: Randomized phase III trial comparing first-line mFOLFOX6 (Plus or Minus Bevacizumab) versus mFOLFOX6 (Plus or Minus Bevacizumab) plus selective internal radiation therapy in patients with metastatic colorectal cancer. J Clin Oncol. 2016;34 (15):1723–31.
72. Zeng J, Harris TJ, Lim M, Drake CG, Tran PT. Immune modulation and stereotactic radiation: improving local and abscopal responses. Biomed Res Int. 2013;2013:658126.
73. Tsuchiya N, Sawada Y, Endo I, Uemura Y, Nakatsura T. Potentiality of immunotherapy against hepatocellular carcinoma. World J Gastroenterol. 2015;21(36):10314–26.
74. Kuang M, Peng BG, Lu MD, Liang LJ, Huang JF, He Q, et al. Phase II randomized trial of autologous formalin-fixed tumor vaccine for postsurgical recurrence of hepatocellular carcinoma. Clin Cancer Res. 2004;10(5):1574–9.
75. Takayama T, Sekine T, Makuuchi M, Yamasaki S, Kosuge T, Yamamoto J, et al. Adoptive immunotherapy to lower postsurgical recurrence rates of hepatocellular carcinoma: a randomised trial. Lancet. 2000;356(9232):802–7.
76. Peng BG, Liang LJ, He Q, Kuang M, Lia JM, Lu MD, et al. Tumor vaccine against recurrence of hepatocellular carcinoma. World J Gastroenterol. 2005;11(5):700–4.
77. Grass GD, Krishna N, Kim S. The immune mechanisms of abscopal effect in radiation therapy. Curr Probl Cancer. 2016;40(1):10–24.
78. Golden EB, Chhabra A, Chachoua A, Adams S, Donach M, Fenton-Kerimian M, et al. Local radiotherapy and granulocyte-macrophage colony-stimulating factor to generate abscopal responses in patients with metastatic solid tumours: a proof-of-principle trial. Lancet Oncol. 2015;16 (7):795–803.
79. Duffy AG, Makarova-Rusher OV, Pratt D, Kleiner DE, Fioravanti S, Walker M, Carey S, Figg WD, Steinberg SM, Anderson V, Levy E. A pilot study of AMP-224, a PD-L2 Fc fusion protein, in Combination with stereotactic body radiation therapy (SBRT) in patients with metastatic colorectal cancer. In ASCO Ann Meet Proc 2016;34 (4 suppl):560.
80. Kimple RJ, Smith MA, Blitzer GC, Torres AD, Martin JA, Yang RZ, et al. Enhanced radiation sensitivity in HPV-positive head and neck cancer. Cancer Res. 2013;73(15):4791–800.
81. Lee J, Poon I, Balogh J, Tsao M, Barnes E. A review of radiotherapy for merkel cell carcinoma of the head and neck. J Skin Cancer. 2012;2012:563829.
82. Frakes JM, Abuodeh Y, Naghavi A, Friedman M, Kim RD, Kothari N, El-Haddad G, Kis B, Biebel B, Sweeney J, Choi J. Viral hepatitis associated hepatocellular carcinoma outcomes with Y-90 radioembolization. ASCO Ann Meet Proc. 2016;34(4 suppl):414.
83. Meyer JJ, Foster RD, Lev-Cohain N, Yokoo T, Dong Y, Schwarz RE, et al. A phase I dose-escalation trial of single-fraction stereotactic radiation therapy for liver metastases. Ann Surg Oncol. 2016;23(1):218–24.
84. Zamboglou C, Messmer MB, Becker G, Momm F. Stereotactic radiotherapy in the liver hilum. Basis for future studies. Strahlenther Onkol. 2012;188 (1):35–41.
85. Sterzing F, Brunner TB, Ernst I, Baus WW, Greve B, Herfarth K, et al. Stereotactic body radiotherapy for liver tumors: principles and practical guidelines of the DEGRO Working Group on Stereotactic Radiotherapy. Strahlenther Onkol. 2014;190(10):872–81.
86. Tse RV, Hawkins M, Lockwood G, Kim JJ, Cummings B, Knox J, et al. Phase I study of individualized stereotactic body radiotherapy for hepatocellular carcinoma and intrahepatic cholangiocarcinoma. J Clin Oncol. 2008;26(4):657–64.
87. Lee MT, Kim JJ, Dinniwell R, Brierley J, Lockwood G, Wong R, et al. Phase I study of individualized stereotactic body radiotherapy of liver metastases. J Clin Oncol. 2009;27(10):1585–91.
88. Lang H, Radtke A, Hindennach M, Schroeder T, Frühauf NR, Malagó M, et al. Impact of virtual tumor resection and computer-assisted risk analysis on operation planning and intraoperative strategy in major hepatic resection. Arch Surg. 2005;140 (7):629–38; discussion 38.
89. Yamanaka J, Saito S, Fujimoto J. Impact of preoperative planning using virtual segmental volumetry on liver resection for hepatocellular carcinoma. World J Surg. 2007;31(6):1249–55.
90. Skinner HD, Hong TS, Krishnan S. Charged-particle therapy for hepatocellular carcinoma. Semin Radiat Oncol. 2011;21(4):278–86.
91. Wang X, Krishnan S, Zhang X, Dong L, Briere T, Crane CH, et al. Proton radiotherapy for liver tumors: dosimetric advantages over photon plans. Med Dosim: official J Am Assoc Med Dosim. 2008;33(4):259–67.
92. Hong TS, DeLaney TF, Mamon HJ, Willett CG, Yeap BY, Niemierko A, et al. A prospective feasibility study of respiratory-gated proton beam therapy for liver tumors. Pract Radiat Oncol. 2014;4(5):316–22.
93. De Ruysscher D, Sterpin E, Haustermans K, Depuydt T. Tumour movement in proton therapy: solutions and remaining questions: a review. Cancers (Basel). 2015;7(3):1143–53.
94. Chetty IJ, Martel MK, Jaffray DA, Benedict SH, Hahn SM, Berbeco R, et al. Technology for innovation in radiation oncology. Int J Radiat Oncol Biol Phys. 2015;93(3):485–92.
95. Bush DA, Smith JC, Slater JD, Volk ML, Reeves ME, Cheng J, et al. Randomized clinical trial comparing proton beam radiation therapy with

transarterial chemoembolization for hepatocellular carcinoma: results of an interim analysis. Int J Radiat Oncol Biol Phys. 2016;95(1):477–82.
96. Hong TS, Wo JY, Yeap BY, Ben-Josef E, McDonnell EI, Blaszkowsky LS, et al. Multi-institutional phase II study of high-dose hypofractionated proton beam therapy in patients with localized, unresectable hepatocellular carcinoma and intrahepatic cholangiocarcinoma. J Clin Oncol: official J Am Soc Clin Oncol. 2016;34(5):460–8.
97. Schardt D, Elsässer T, Schulz-Ertner D. Heavy-ion tumor therapy: Physical and radiobiological benefits. Rev Mod Phys. 2010;82(1):383.
98. Komatsu S, Fukumoto T, Demizu Y, Miyawaki D, Terashima K, Sasaki R, et al. Clinical results and risk factors of proton and carbon ion therapy for hepatocellular carcinoma. Cancer. 2011;117 (21):4890–904.
99. Tomlinson JS, Jarnagin WR, DeMatteo RP, Fong Y, Kornprat P, Gonen M, et al. Actual 10-year survival after resection of colorectal liver metastases defines cure. J Clin Oncol. 2007;25 (29):4575–80.
100. Porter ME. What is value in health care? N Engl J Med. 2010;363(26):2477–81.
101. Kim H, Gill B, Beriwal S, Huq MS, Roberts MS, Smith KJ. Cost-effectiveness analysis of stereotactic body radiation therapy compared with radiofrequency ablation for inoperable colorectal liver metastases. Int J Radiat Oncol Biol Phys. 2016.
102. Wong SL, Mangu PB, Choti MA, Crocenzi TS, Dodd GD, Dorfman GS, et al. American society of clinical oncology 2009 clinical evidence review on radiofrequency ablation of hepatic metastases from colorectal cancer. J Clin Oncol. 2010;28(3):493–508.

Index

Note: Page numbers followed by *f* and *t* indicate figures and tables respectively

J. Meyer and T.E. Schefter (eds.), *Radiation Therapy for Liver Tumors*,
DOI 10.1007/978-3-319-54531-8